Medical Radiology
Diagnostic Imaging

M.F. Reiser
H. Hricak
M. Knauth

Giovanni Maconi
Gabriele Bianchi Porro
Editors

Ultrasound of the Gastrointestinal Tract

Second Edition

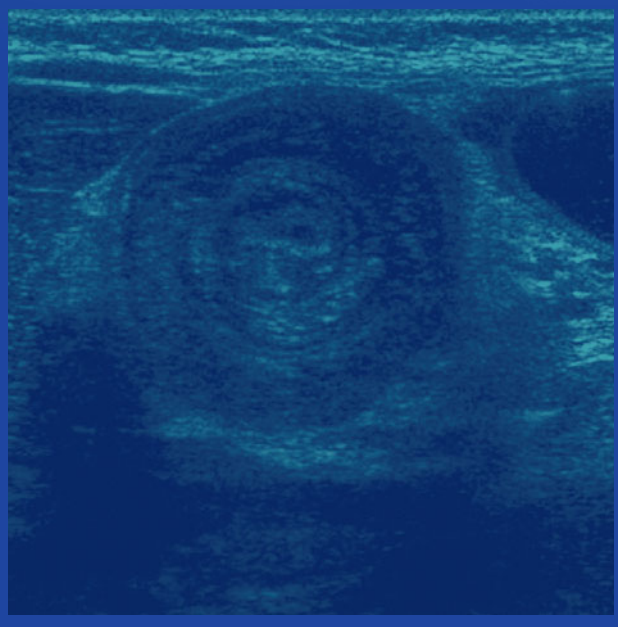

Springer

EXTRA MATERIALS
extras.springer.com

Medical Radiology

Diagnostic Imaging

For further volumes:
http://www.springer.com/series/4354

Giovanni Maconi • Gabriele Bianchi Porro
Editors

Ultrasound of the Gastrointestinal Tract

Second Edition

Springer

Editors
Giovanni Maconi
Gastroenterology Unit
Department of Biomedical and Clinical Sciences,
Luigi Sacco University Hospital
Milan
Italy

Gabriele Bianchi Porro
Centro Diagnostico Italiano
Milan
Italy

Additional material to this book can be downloaded from http://extras.springer.com/

ISSN 0942-5373
ISBN 978-3-642-31982-2 ISBN 978-3-642-31983-9 (eBook)
DOI 10.1007/978-3-642-31983-9
Springer Heidelberg New York Dordrecht London

Library of Congress Control Number: 2013940959

Foreword

The first edition of 'Ultrasound of the Gastrointestinal Tract' was most enthusiastically received by the readers of "Medical Radiology—Diagnostic Imaging". Ultrasound technology has made and continues to make steady progress, and our knowledge and expertise in this field are constantly expanding. Therefore, the series editors approached Giovanni Maconi and Gabriele Bianchi Porro and encouraged them to take over the endeavor of a second edition. We are very pleased that they agreed and that the second edition of this important book can now be presented. This is a truly comprehensive book, covering the whole spectrum of pathological conditions involving the gastrointestinal tract and addressing the established as well as novel techniques of ultrasound imaging, such as functional and 3D ultrasound, contrast agents and intraoperative ultrasound, elastography, and transperineal ultrasound.

Dedicated chapters elucidate the normal anatomy and the general methods of ultrasound examination, with the various clinical entities organized according to the prominent clinical presentations: acute abdomen, chronic inflammatory bowel diseases, infections, and neoplasm. In a separate chapter, procedures and technical developments including intravenous contrast-enhanced bowel ultrasound, oral contrast-enhanced bowel ultrasound, assessment of motor function and functional ultrasound of the gastrointestinal tract, 3D intestinal ultrasound, elastography, and other new advances in GI ultrasonography and transcutaneous gastrointestinal biopsy as well as transperineal ultrasound are described.

Distinguished scientists from all over the world contributed the book's well-structured and concise chapters, which include the etiology, clinical presentation and the value, and different imaging modalities for the diagnosis and management of patients with diseases of the gastrointestinal tract. We are confident that this book will be a great source of information for all those involved in the care of patients with GI diseases.

Munich

Maximilian F. Reiser

Preface

Seven years ago we published the first edition of 'Ultrasound of the Gastrointestinal Tract'. In order to update the content of the textbook, 2 years ago we agreed to write a second edition; now we are pleased to present the result of our work.

The two reasons which led us to do it were the large international success of the former edition, which sold out, and the wide appreciation of its comprehensive content and of its high-quality images, which proved to be very useful in daily practice.

New images, videos, and scientific data were inserted into the original chapters, which already provided a comprehensive overview of sonographic imaging and of its usefulness and limits in detecting acute and chronic gastrointestinal diseases, such as appendicitis, diverticulitis, obstruction, malabsorption, inflammatory and infectious bowel diseases, neoplasm, and hernias.

Completely, new chapters on techniques of investigation and on anatomy of the normal gastrointestinal tract and new topics, like rare inflammatory disorders, vasculitis, cystic fibrosis, amyloidosis and graft versus host disease, were added; finally, specific chapters were devoted to epiploic appendagitis and intestinal endometriosis.

However, every single chapter was meant to help the abdominal sonographer interpret incidental findings of the gastrointestinal tract and provide useful information for as many as possible problems in patients with abdominal complaints.

The book also considers specific technical developments and applications of gastrointestinal ultrasound such as functional and 3D ultrasound, contrast agents, operative ultrasound, sonoelastography of the gastrointestinal tract and transperineal sonography, which may become of increasing importance in the near future.

These applications may expand the use of gastrointestinal ultrasound, increasing its indications and accuracy in acute and chronic inflammatory, organic and functional disorders. In addition to that, gastrointestinal ultrasound still is a noninvasive, inexpensive, wide available and repeatable procedure, and a valid aid to select and carry out more expensive and invasive examinations.

We sincerely hope that the book will encounter the same interest and success of the previous edition and will still be a useful and insightful tool both for sonographers specialized in radiology, gastroenterology, internal medicine and surgery, and for many physicians with an interest in sonography or specifically in intestinal sonography.

The editors of this issue would like to thank the Series' Editor, Prof. Maximilian F. Reiser, for his valuable suggestions and assistance and all the authors who have accepted to so remarkably update or rewrite their contributions. We are also grateful with Sarah Boscu McGill for the English revision of most manuscripts of the book.

A most sincere word of gratitude goes to Corinna Schaefer of Springer-Verlag for her great, constant, patience, and untiring efforts in helping us to collect and edit the manuscripts; her devotion deserves special recognition.

Last, but not least, a special word of thanks goes to our families for all their encouragement and support.

We hope the readers will share our enthusiasm for the interesting and rapidly developing matter of ultrasound and will enjoy our textbook.

Giovanni Maconi
Gabriele Bianchi Porro

Contents

Contributors

Cristina Bezzio Gastroenterology Unit, Department of Biomedical and Clinical Sciences, "L. Sacco" University Hospital, Milan, Italy

Elena Bolzacchini Gastroenterology Unit, Department of Biomedical and Clinical Sciences, "L. Sacco" University Hospital, Milan, Italy

S. Boopathy Vijayaraghavan SONOSCAN Ultrasonic Scan Centre, Coimbatore, Tamil Nadu, India

Gabriella Carnevale First Department of Medicine, Fondazione IRCCS Policlinico San Matteo, University of Pavia, Pavia, Italy

Luigi Castellano Department of Internal Medicine and Gastroenterology, Ultrasonography Section II University, Naples, Italy

Etienne Danse Department of Radiology, Université Catholique de Louvain, St-Luc University Hospital, Brussels, Belgium

Ilario de Sio Department of Internal Medicine and Gastroenterology, Ultrasonography Section II University, Naples, Italy

Christoph Dietrich Caritas Krankenhaus, Bad Mergentheim, Germany

Elena Ercole Gastroenterology Division, Inflammatory Bowel Disease Centre, Turin, Italy

Francesco Esposito Radiology Unit, Azienda Ospedaliera, Naples, Italy

Mirella Fraquelli Seconda Divisione, Gastroenterologia IRCCS Fondazione Cà Granda Ospedale Maggiore Policlinico di Milano, Università degli Studi di Milano, Milan, Italy

Federica Furfaro Gastroenterology Unit, Department of Biomedical and Clinical Sciences, "L. Sacco" University Hospital, Milan, Italy

Daphne Geukens University Hospital Center, Charleroi, Belgium

Odd Helge Gilja Department of Medicine, National Center for Ultrasound in Gastroenterology, Haukeland University Hospital, Bergen, Norway

Norbert Gritzmann Gruppenpraxis für Radiologie, Vienna, Austria

Ken Haruma Division of Gastroenterology, Department of Internal Medicine, Kawasaki Medical School, Kurashiki-city, Okayama, Japan

Jiro Hata Department of Clinical Pathology and Laboratory Medicine, Kawasaki Medical School, Kurashiki-city, Okayama, Japan

Trygve Hausken Section of Gastroenterology, National Centre for Ultrasound in Gastroenterology, Haukeland University Hospital, Institute of Medicine, University of Bergen, Bergen, Norway

Roald Flesland Havre Institute of Medicine, University of Bergen and National Centre for Ultrasound in Gastroenterology, Department of Medicine, Haukeland University Hospital, Bergen, Norway

Hiroshi Imamura Department of Clinical Pathology and Laboratory Medicine, Kawasaki Medical School, Kurashiki-city, Okayama, Japan

Stefan Klein III. Medizinischen Klinik, Universitätsmedizin Mannheim, Mannheim, Germany

Dong Ho Lee Department of Radiology, Kyung Hee University Hospital, Dongdaemun-gu, Seoul, Korea

Francesco P. G. Leone Gynaecology Unit, Department of Biomedical and Clinical Sciences, "L. Sacco" University Hospital, Milan, Italy

Jae Hoon Lim Department of Radiology and Center for Imaging Science, Samsung Medical Center, Sungkyunkwan University School of Medicine, Seoul, Kangnam-ku, Korea

Carmelina Loguercio Department of Internal Medicine and Gastroenterology, II University, Naples, Italy

Giovanni Maconi Chair of Gastroenterology, Department of Clinical Sciences, "L. Sacco" University Hospital, Milan, Italy

Noriaki Manabe Department of Clinical Pathology and Laboratory Medicine, Kawasaki Medical School, Kurashiki-city, Okayama, Japan

Michela Monteleone Gastroenterology Unit, Department of Biomedical and Clinical Sciences, Milan, Italy

Marco Niosi Department of Internal Medicine and Gastroenterology, Ultrasonography Section II University, Naples, Italy

Caterina Rigazio Gastroenterology Division, Inflammatory Bowel Disease Centre, Turin, Italy

Doris Schacherer Department of Internal Medicine I, University of Regensburg, Regensburg, Germany

Luciano Tarantino Interventional Ultrasound Unit, Department of Medicine, S. Giovanni di Dio Hospital, Frattamaggiore, Naples, Italy

Fulvia Terracciano Gastroenterology Unit, Ultrasonographic Section Casa Sollievo della Sofferenza, S. Giovanni Rotondo, Foggia, Italy

Luigi Maria Vitale Department of Internal Medicine and Gastroenterology, Ultrasonography Section II University, Naples, Italy

Bowel Ultrasound: Investigation Technique and Normal Findings

Giovanni Maconi, Caterina Rigazio, and Elena Ercole

Contents

Abstract

Ultrasonographic examination of the gastrointestinal tract is currently employed in many suspected acute and chronic inflammatory conditions, for purely diagnostic purposes and the follow-up of well-known gastrointestinal diseases. Improvement in ultrasonographic technology and investigation techniques of the gastrointestinal tract have overcome to a great extent all impediments and prejudices in using bowel ultrasound for the assessment of digestive diseases. Nowadays, it is possible to assess accurately the main features of the intestinal wall such as its thickness, echo pattern, vascularity, flexibility and motility, to evaluate the diameter and intraluminal content of the bowel and peri-intestinal changes, such as lymph nodes and the status of mesenteric fat. Acknowledgment of these ultrasonographic findings makes it now possible to suspect or detect various gastrointestinal diseases, and improve and speed up diagnostic process of several conditions.

1 Introduction

Nowadays, abdominal ultrasound is an integral part of the decision making process in patients with abdominal disorders. Whether ultrasound examination is performed by clinicians or radiologists, it is usually the first imaging procedure which directly follows the history and physical examination in patients with symptoms or clinical signs suggesting abdominal disease.

The main advantages of using ultrasound as the first diagnostic imaging modality in abdominal disorders may be the shortening of time needed for achieving an accurate diagnosis, avoiding unnecessary, costly or even risky procedures with a positive fall-out in terms of the saving of financial resources.

G. Maconi (✉)
Chair of Gastroenterology, Department of Biomedical and Clinical Sciences, "L. Sacco" University Hospital, Via G. B. Grassi, 74, 20157 Milan, Italy
e-mail: giovanni.maconi@unimi.it

C. Rigazio · E. Ercole
Gastroenterology Division, Inflammatory Bowel Disease Centre, AO Ordine Mauriziano, Turin, Italy

G. Maconi and G. Bianchi Porro (eds.), *Ultrasound of the Gastrointestinal Tract*, Medical Radiology. Diagnostic Imaging,
DOI: 10.1007/174_2013_824, © Springer-Verlag Berlin Heidelberg 2013
Published Online: 9 March 2013

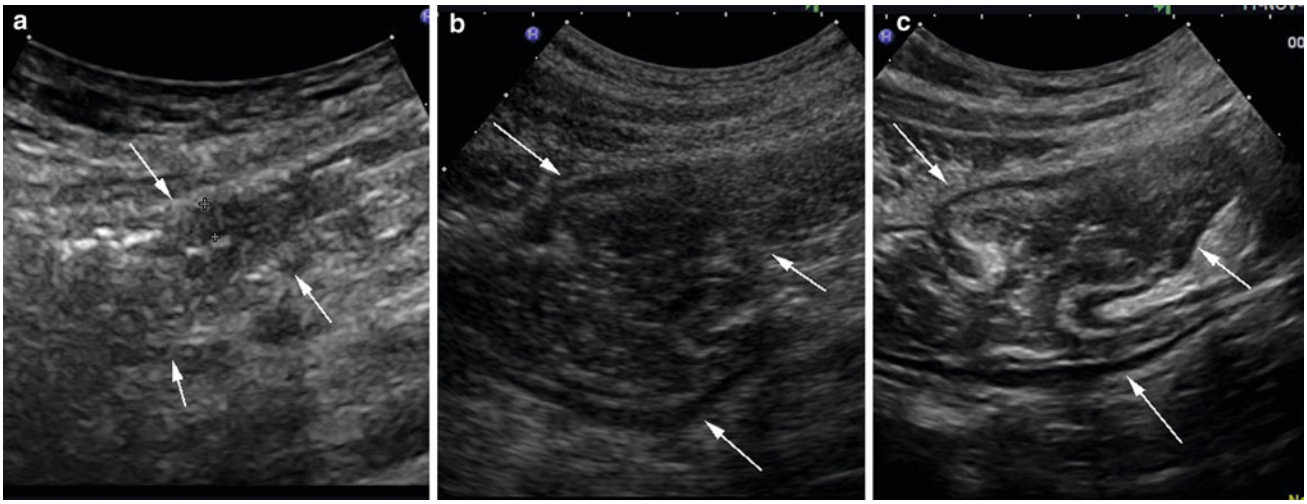

Fig. 1 Normal ileocecal anastomosis in a Crohn's disease patient. Comparison of convex 3.5–5 MHz probe (**a**), fundamental imaging (FI) with high resolution 4–8 MHz microcovex probe (**b**) and tissue harmonic imaging (THI) with the same high resolution probe (**c**). Although the bowel wall is detectable in all these setting, using higher frequency and switching from FI to THI the delineation of outer contours of the bowel (*arrows*), the bowel wall echo pattern and mesenteric fat became much more delineated

Of course, in order to obtain the maximum integration of available ultrasonographic information into the patient's management, the clinician should have appropriate knowledge of this procedure.

Unlike parenchymatous abdominal organs, the digestive tract has for a long time been considered unsuitable for exploration by ultrasound, even though the first study showing the potential effectiveness of this technique for bowel examination dates back to the 1970s (Hauser et al. 1974; Daggett 1974; Lutz and Petzoldt 1976).

In recent years, to a great extent, technology has overcome all impediments and prejudices in using bowel ultrasound for the assessment of several digestive diseases. Thanks to its non-invasiveness, ready availability, repeatability and accuracy, ultrasonographic examination of the gastrointestinal tract is currently employed in many suspected acute and chronic inflammatory conditions, not only for purely diagnostic purposes, but also for the management and follow-up of well-known gastrointestinal diseases.

2 Investigation Technique

Sonographic investigation of the gastrointestinal tact is performed using conventional ultrasonographic probes. Bowel examination should begin with a convex 3.5–5 MHz probe, to have an overview of the gastrointestinal tract, in particular when the examination is part of the abdominal ultrasound. Then, for a detailed visualisation of bowel wall a 4–13 MHz high resolution linear of microconvex array should be used, because lower frequencies are useful for the examination of deep abdominal structures and higher frequencies for superficial parts.

Appropriate setting of the instrument is important for a successful examination. In particular, the focus and gain of the instrument should be adjusted to allow adequate penetration and to optimise image resolution. When available, tissue harmonic imaging (THI) should be used since it is significantly better than fundamental imaging for the depiction of the features of the wall, the luminal contents and peri-intestinal findings, such as free fluid, mesenteric lymph nodes and mesenteric fat changes (Fig. 1) (Rompel et al. 2006). If possible, specific pre-setting for each probe should be prepared, to be used in different clinical and anatomical contexts (e.g. normal and oversize patients, paediatrics, perianal disease).

For routine ambulatory examinations, it is preferable to perform the bowel ultrasound in a fasting condition. In fact, meal and feeding states may increase intraluminal gas and may hamper the evaluation of some abnormal functional features of the stomach, such as delayed gastric emptying. Also the intake of a large quantity of liquid meals and water just before bowel ultrasound should be avoided. In some instances, this may mimic partial small bowel obstruction (e.g. due to adhesions) and malabsorption (e.g. coeliac disease) hampering a correct diagnosis and the exclusion of these conditions. However, the fasting state is not mandatory (e.g. in acute abdomen, bowel ultrasound may be of value despite feeding condition).

Routine bowel evaluation of patients with chronic (or not acute) abdominal symptoms, usually should be systematically performed, e.g. starting from hypogastrium or left iliac fossa (i.e. from the sigmoid colon) and than continued to examine the colon, terminal ileum, appendix, small bowel, up to the stomach. However, other examination sequences may be valid provided the whole gut is assessed. On the

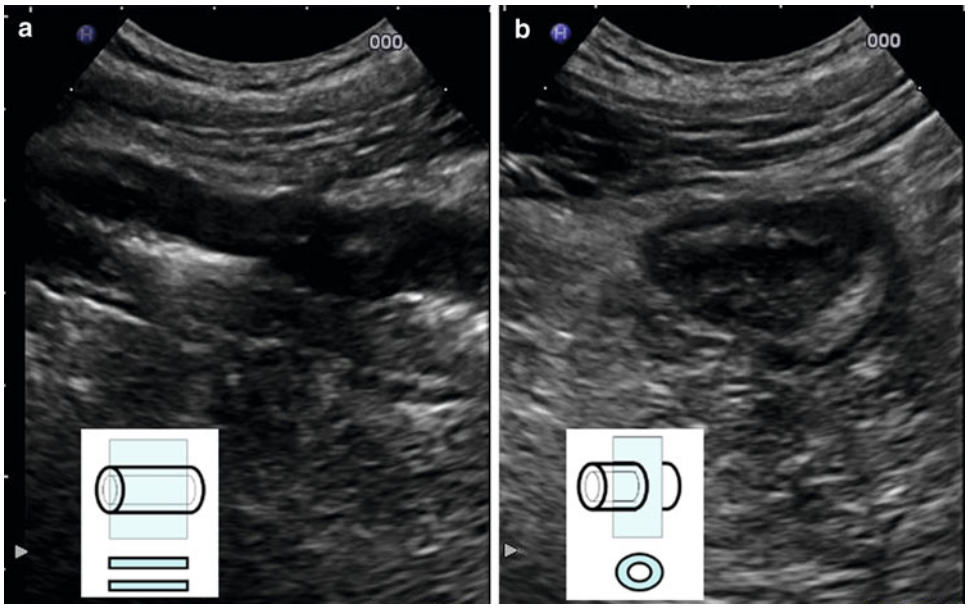

Fig. 2 Graphic representations and sonographic images of longitudinal (**a**) and transversal (**b**) sections of the terminal ileum in Crohn's disease patient

contrary, in acute setting, in particular when a well-localised abdominal pain is present, bowel examination should start form the maximum tenderness area complained of by the patient, possibly with the help of the patient, who may put the probe just over the tenderness point. However, even in the acute setting, the bowel examination should assess all parts of the gastrointestinal tract.

In the event of suboptimal visualisation of the bowel wall due to the presence of gas, graded compression of the investigated gastrointestinal segment may help to shift intraluminal gas and thereby to improve visualisation of posterior parts of the bowel, in particular for the anatomical structures in the lower quadrants of the abdomen such as appendix, terminal ileum, caecum and sigmoid colon (Bluth et al. 1979). The patients are examined in supine position but, if necessary, they may be turned on the left or right side or put in an upright position, to move the bowel and its content, to avoid the interference of gas and optimise the visualisation of the features of bowel walls.

3 Normal Bowel Wall

The main features of the bowel walls to be assessed by ultrasound include: thickness, echo pattern, vascularity, flexibility and motility. These features depend in turn on the stretching and diameter of the hollow organs, which are associated with the content and presence of peristalsis that vary site-by-site in the gut. Probe frequency and grade of pressure wield by operators are other relevant parameters that may influence the ultrasonographic aspect of the gut.

Irrespective of the segment examined, as the gastrointestinal tract is a "tube", ultrasound generally shows a "target" sign when the bowel segment is scanned transversally and as a "track" when it is scanned longitudinally (Fig. 2).

3.1 Bowel Echo Pattern

Echo pattern and thickening are the most important features of the bowel wall, and those commonly considered to detect the diseases of the gut.

Under good conditions of visualisation, the ultrasonographic aspect of the normal bowel wall is stratified, with five layers of different echogenicity. Each layer marks the boundary between two different histological structures. Starting from inside, the first layer is the interface between the lumen (hyperechoic) and the mucosa (tenuously hypoechoic). Between the mucosa and muscolaris propria (both hypoechoic) stands the submucosa (hyperechoic). The muscularis propria is limited by the last layer (hyperechoic), the serous (Fig. 3). Indeed, the wall layers and histology are not exactly matching, and the ultrasonographic image is not "the tissue" but rises from the resolution of different interfaces and reverberation artefacts (Bolondi et al. 1986; Kimmey et al. 1989; Nylund et al. 2008). However, their correspondence is used in the staging of some diseases and loss of stratification, when one or more layers are missing, is suspected or considered a sign of disease.

3.2 Bowel Thickness

The thickness of the bowel wall is regarded as the main ultrasonographic feature of the gut. Among the features of the bowel wall, this is the only quantitative parameter, and almost all studies reported only this value as the criterion to assess the presence of a gastrointestinal disease.

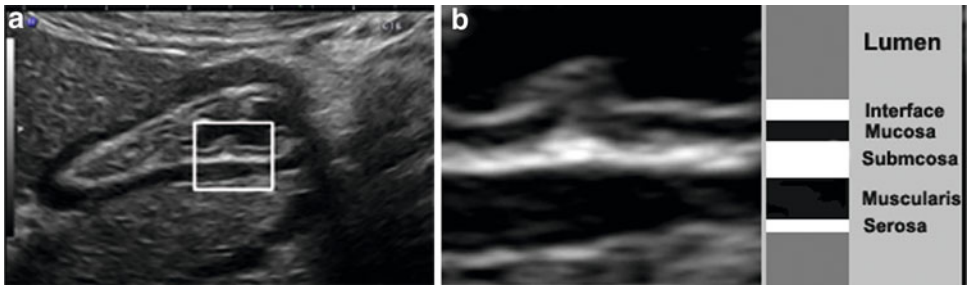

Fig. 3 Transversal section of gastric antrum (**a**) and detail of the normal wall (**b**) showing five layers, with different echogenicity

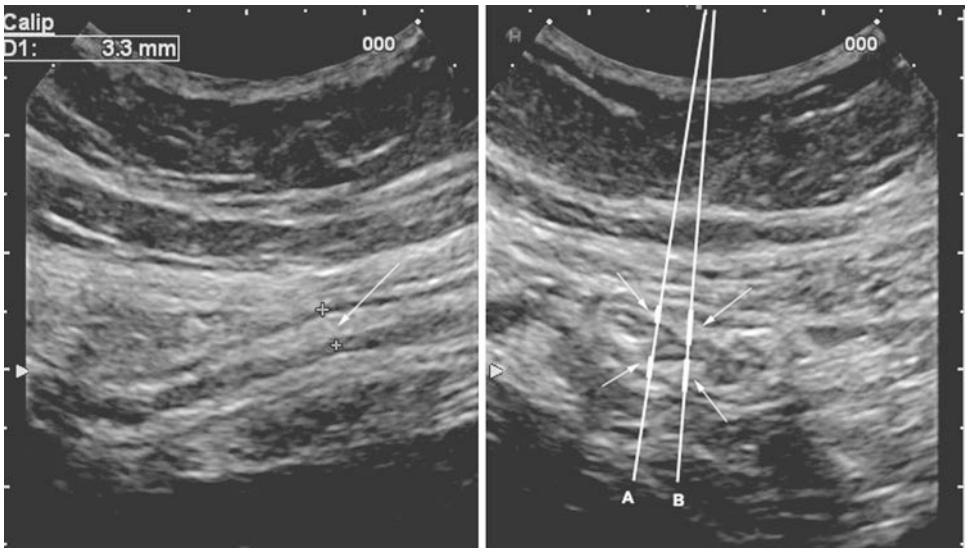

Fig. 4 Longitudinal (*left side*) and transverse (*right side*) sonographic section of the sigmoid colon in patient with quiescent ulcerative colitis. Because of the presence of mucosal folds, clearly appreciable of in the transverse section, the thickening of the bowel wall (*arrows*) in the lungitudinal section may vary according to the angle of insonation (A or B) of the loop

The measurement of wall thickness should be taken using the transducer with as high a frequency as possible, preferable 5 MHz or more or with the transducer that allows to distinguishing different layers of the wall. In fact, the measure of the thickening should be taken from the external hyperechoic layer, corresponding to the serosa, to the internal hyperechoic layer representing the interface between the mucosa and intestinal content. Only when these two interfaces are simultaneously visible in a perpendicular scan of the loop, the measurement should be considered appropriate. Since the dorsal part of the gastrointestinal tract is frequently difficult to image using transabdominal ultrasound, the measurements should be obtained from the anterior wall and repeated in that segment, both in longitudinal and transverse section, avoiding haustration and mucosal folds (e.g. in the colon; Fig. 4) and segments with spasms or contractions of the loop (e.g. in the small bowel and stomach; Fig. 5) to avoid overestimation of the thickness.

The thickness of normal gastrointestinal walls varies according to the anatomical segment, age, weight and, to some extent, to the fed/fasting state, being thicker in the sigmoid and ileum and usually increasing with age, weight and in feeding state (Nylund et al. 2012). It may also vary depending on the frequency of the transducer and the use of oral contrast agents. In fact, measurements with high frequency probes and with the use of contrast agents show thinner wall thickening (Pallotta et al. 1999; Nylund et al. 2012). However, despite normal wall thickness has been assessed as not above 2 mm, most studies and meta-analyses set the cut-off for bowel diseases (in particular for inflammatory diseases) between 3 and 4 mm (Fraquelli et al. 2005; Horsthuis et al. 2008). However, the gastric wall is usually thicker and may be up to 5–6 mm (Rapaccini et al. 1988).

3.3 Bowel Diameter and Intraluminal Contents

The diameter of the bowel and its content vary according to the site, the fasting/feeding state and bowel function.

Normal bowel loops usually show diameter <25 mm in the small bowel and <50 mm in the colon, even when luminal contrast agents are used. Although these values have been suggested as the cut-off for bowel intestinal obstruction, they may be valid also for other diseases and pathological conditions such as coeliac disease,

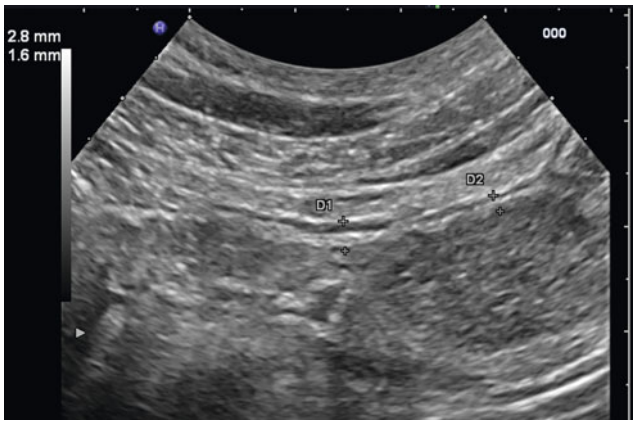

Fig. 5 Longitudinal section of terminal ileum, showing different bowel wall thickening (D1 and D2) due to the peristaltic contraction

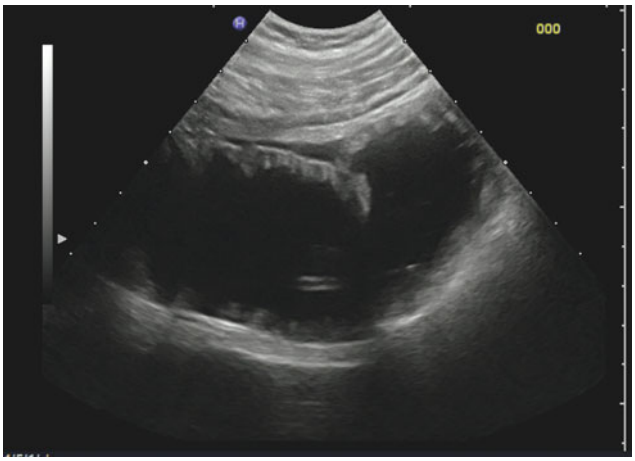

Fig. 6 Longitudinal scan of jejunal bowel loop, in dynamic ileus, with liquid content. Both external and internal profiles of the wall are well delineated

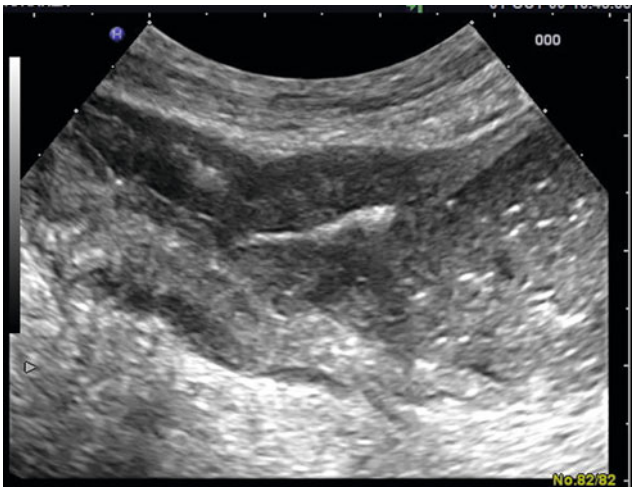

Fig. 7 Longitudinal scan of a dilated ileal loop in a patient with stricturing Crohn's disease. Bowel walls are well delineated by the semiliquid content characterised by liquids mixed with solid and gaseous components

malabsorption, intestinal infectious and inflammatory diseases, pseudo-obstruction and other abnormalities of bowel peristalsis.

As far as the intraluminal content is concerned, empty gut appears in longitudinal section as a thin hyperechoic line that represents the interface between the two mucosas that face each other. Otherwise, when content is gaseous, reverberation artefacts ("ring down" artefacts or "comet tail" artefacts) can hide the bowel wall distal to the probe and only the most superficial wall can be properly studied. The gradual compression of the loop can move the gas making it possible to examine the distal wall better.

The liquid content appears anechoic, the superficial and the distal wall are both displayable and the internal profile of the mucosa as well is usually clearly appreciable (Fig. 6). For this reason, luminal contrast media for ultrasonography such as SICUS (Small Intestinal Contrast UltraSound) are used to emphasise the issues described above (see "Oral Contrast-Enhanced Bowel Ultrasound").

Liquids mixed with a solid or gaseous component appear as corpuscular media. Its ultrasonographic image consists in spots with different sizes and echogenicity and if peristalsis is slow it is possible to distinguish levels in the content (Fig. 7).

The solid component may be appreciated with a stone-like aspect or as a dark solid mass with posterior shadowing (Fig. 8). Such content is usually observed in the colon, in particular in constipated patients, and sometimes in patients with bowel obstruction just proximally to the stenotic segment (the so called "fecal sign").

3.4 Bowel Wall Vascularity

The assessment of vascularity of bowel walls and intestinal lesions is part of the sonographic evaluation of intestinal diseases. Colour or power Doppler sonography and contrast-enhanced sonography may be used to estimate the perfusion of bowel abnormalities and show neovascularisation and hyperaemia occurring in inflammatory bowel diseases and neoplastic lesions. The assessment of hypervascularity is therefore a useful adjunct to B-mode assessment to suggest the inflammatory or neoplastic nature of an intestinal lesion.

Also the spectral analysis of Doppler signals of arteries supplying the gastrointestinal tract (coeliac trunk, superior and inferior mesenteric arteries) and the vessels draining the intestine has been used to estimate bowel perfusion and assess the activity of inflammatory bowel disease, but data about the accuracy (e.g. sensitivity and specificity) of this method in evaluating the activity of the diseases is still

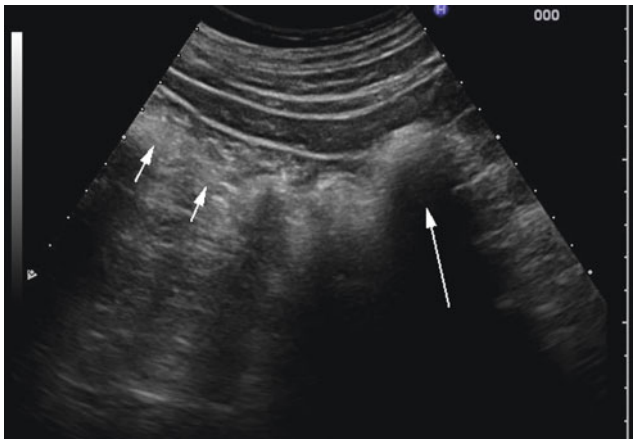

Fig. 8 Longitudinal scan of a colonic loop with solid (*long arrows*) and gaseous (*short arrows*) content

lacking. On the other hand, the only detection of corpuscular movement into the vessels can provide an estimation of the vascular bed of a tissue. On this regard, power and colour Doppler can usually assess the perfusion in vessels of 100 μm in width, with blood flow up to 1 mm/sec. Vascular perfusion in capillaries and vessels with diameter < 20 μm, can be assessed only using contrast-enhanced ultrasound ("Intravenous Contrast-enhanced Bowel Ultrasound"). These methods can be routinely employed to characterised lesions previously detected by conventional B-mode ultrasound.

3.5 Elasticity and Peristalsis

The assessment of bowel elasticity and peristalsis is a subjective, though important part of bowel examination. Although subjective, the estimate of compressibility of the bowel, namely the change in shape of the transverse section of the bowel under gentle compression with the probe, can be used to differentiate inflamed appendix from the bowel and, to some extent, to discriminate between a normal bowel wall from inflamed or neoplastic bowel segments and between inflammatory from fibrotic strictures in Crohn's disease. However, the assessment of this property of the bowel remains subjective and influenced by the depth of the loop in the abdomen. Advances have been made in the sonographic assessment of stiffness of several tissues and organs, including bowel, by means of sonoelastography ("Imaging of Tissue Elasticity in Gastrointestinal Disorders"). This technique may provide quantitative and qualitative estimates of tissue stiffness. It actually represents a promising tool to characterise the gastrointestinal lesions, but its use in routine practice is not recommended so far.

The assessment and quantification of bowel peristalsis may be difficult and subjective, although useful in several intestinal diseases. Increased small bowel peristalsis has been frequently described in coeliac disease and acute mechanic bowel obstruction, while dynamic ileus is characterised by absence of peristaltic movements (see "Coeliac Disease" and "Intestinal Obstruction"). However, the precise definition of "increased peristalsis" as well as the accuracy of bowel ultrasound in the assessment of bowel movement in fasting and feeding state is still lacking.

References

Hauser JB, Stanley RJ, Geisse G (1974) The ultrasound findings in an obstructed afferent loop. J Clin Ultrasound 2:287–289

Daggett PR (1974) Ultrasound in the assessment of intestinal motility. Br J Clin Pract 28:207–208

Lutz HT, Petzoldt R (1976) Ultrasonic patterns of space occupying lesions of the stomach and the intestine. Ultrasound Med Biol 2:129–132

Rompel O, Huelsse B, Bodenschatz K, Reutter G, Darge K (2006) Harmonic US imaging of appendicitis in children. Pediatr Radiol 36:1257–1264

Bluth EI, Merrit CR, Sullivan MA (1979) Ultrasonic evaluation of the stomach, small bowel and colon. Radiology 133:677–80

Bolondi L, Casanova P, Santi V, Caletti G, Barbara L, Labò G (1986) The sonographic appearance of the normal gastric wall: an in vitro study. Ultrasound Med Biol 12:991–998

Kimmey MB, Martin RW, Haggitt RC, Wang KY, Franklin DW, Silverstein FE (1989) Histologic correlates of gastrointestinal ultrasound images. Gastroenterology 96:433–441

Nylund K, Leh S, Immervoll H et al (2008) Crohn's disease: Comparison of in vitro ultrasonographic images and histology. Scand J Gastroenterol 43:719–726

Pallotta N, Baccini F, Corazziari E (1999) Contrast ultrasonography of the normal small bowel. Ultrasound in Med & Biol 25:1335–1340

Nylund K, Hausken T, Odegaard S, Eide GE, Gilja OH (2012) Gastrointestinal wall thickness measured with transabdominal ultrasonography and its relationship to demographic factors in healthy subjects. Ultraschall Med. In press

Fraquelli M, Colli A, Casazza G et al (2005) Role of US in detection of Crohn disease: meta-analysis. Radiology 236:95–101

Horsthuis K, Bipat S, Bennink RJ, Stoker J (2008) Inflammatory bowel disease diagnosed with US, MR, scintigraphy, and CT: meta-analysis of prospective studies. Radiology 247:64–79

Rapaccini GL, Aliotta A, Pompili M et al (1988) Gastric wall thickness in normal and neoplastic subjects: a prospective study performed by abdominal ultrasound. Gastrointest Radiol 13:197–199

Normal Gastrointestinal Tract

Caterina Rigazio, Elena Ercole, and Giovanni Maconi

Contents

Abstract

Transcutaneous sonography allows the evaluation of almost all tracts of the gut. The main characteristics of the gastrointestinal tract, in particular the features of its wall, intraluminal content, and extraintestinal findings, may be assessed from the upper esophagus to the rectum, with the exception of the intrathoracic esophagus, which is not accessible to the transcutaneous ultrasound beam. This chapter describes technical approaches to intestinal ultrasound examination and main ultrasonographic findings of the normal gastrointestinal tract.

1 Introduction

Transcutaneous sonography allows the evaluation of almost all tracts of the gut, from the upper esophagus to the anus. However, parts of the gastrointestinal tract, such as the intrathoracic esophagus, are not accessible to the transcutaneous ultrasound beam and others such as gastric fundus, duodenojejunal junction, left colonic flexure, and distal sigmoid colon, are not systematically and completely evaluable, mainly due to the presence of gas or patient constitution.

Evaluation of the gastrointestinal tract should be performed taking into account the main characteristics of the bowel wall, its intraluminal content, and extraintestinal findings like lymph nodes and mesenteric fat.

Ultrasound is a dynamic and repeatable tool, which experienced sonographers usually employs using variable technical approaches to overcome the main limitations due to gas and patient constitution. Progressive bowel compression of the air-containing organ, changing the patients position, water administration, or oral luminal contrast agents can be used to assess or to improve the visualization of all parts of the gastrointestinal tract.

C. Rigazio · E. Ercole
Gastroenterology Division, Inflammatory Bowel Disease Centre, AO Ordine Mauriziano, Turin, Italy

G. Maconi (✉)
Department of Clinical Sciences, "L. Sacco" University Hospital, Via G. B. Grassi, 74, 20157 Milan, Italy
e-mail: giovanni.maconi@unimi.it

G. Maconi and G. Bianchi Porro (eds.), *Ultrasound of the Gastrointestinal Tract*, Medical Radiology. Diagnostic Imaging,
DOI: 10.1007/174_2013_800, © Springer-Verlag Berlin Heidelberg 2013
Published Online: 13 March 2013

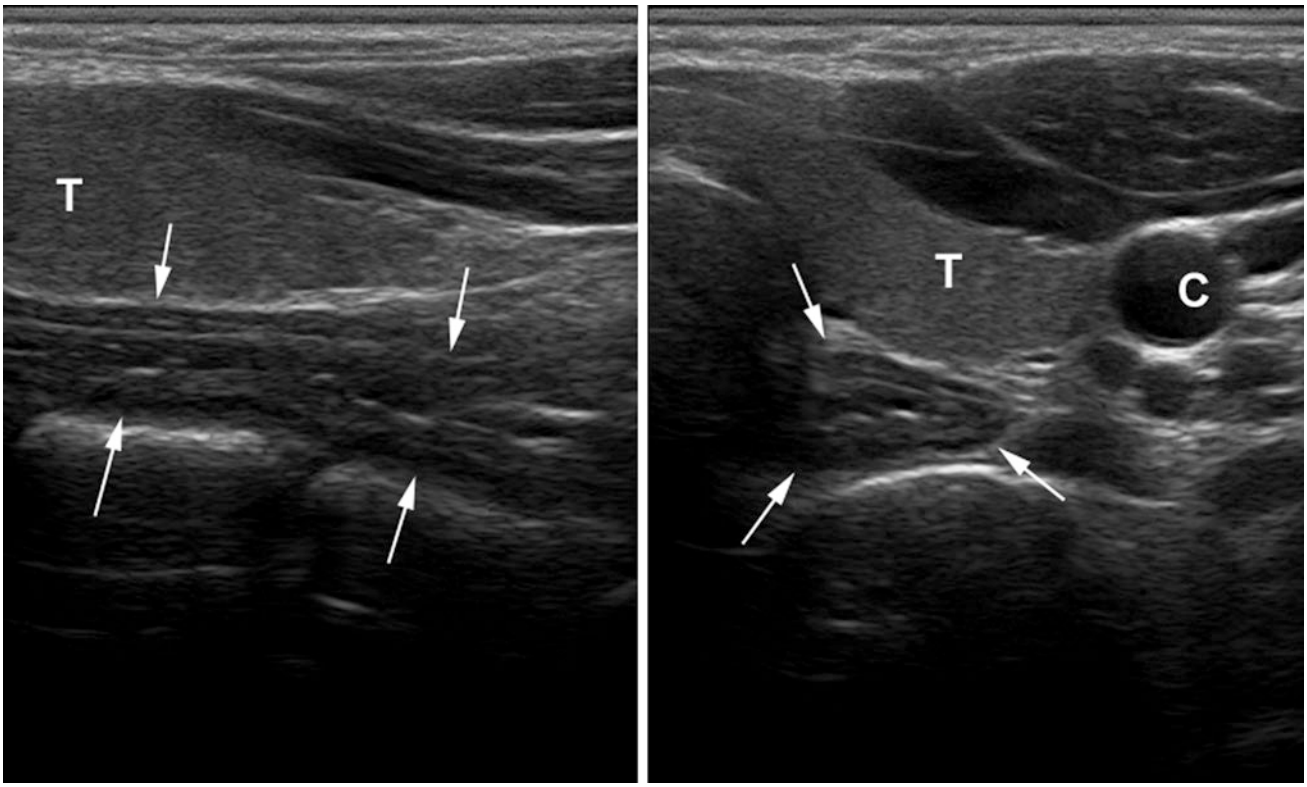

Fig. 1 Longitudinal (*left side*) and transverse (*right side*) scanning of cervical esophagus (*arrows*). *T* Thyroid, *C* Carotid artery

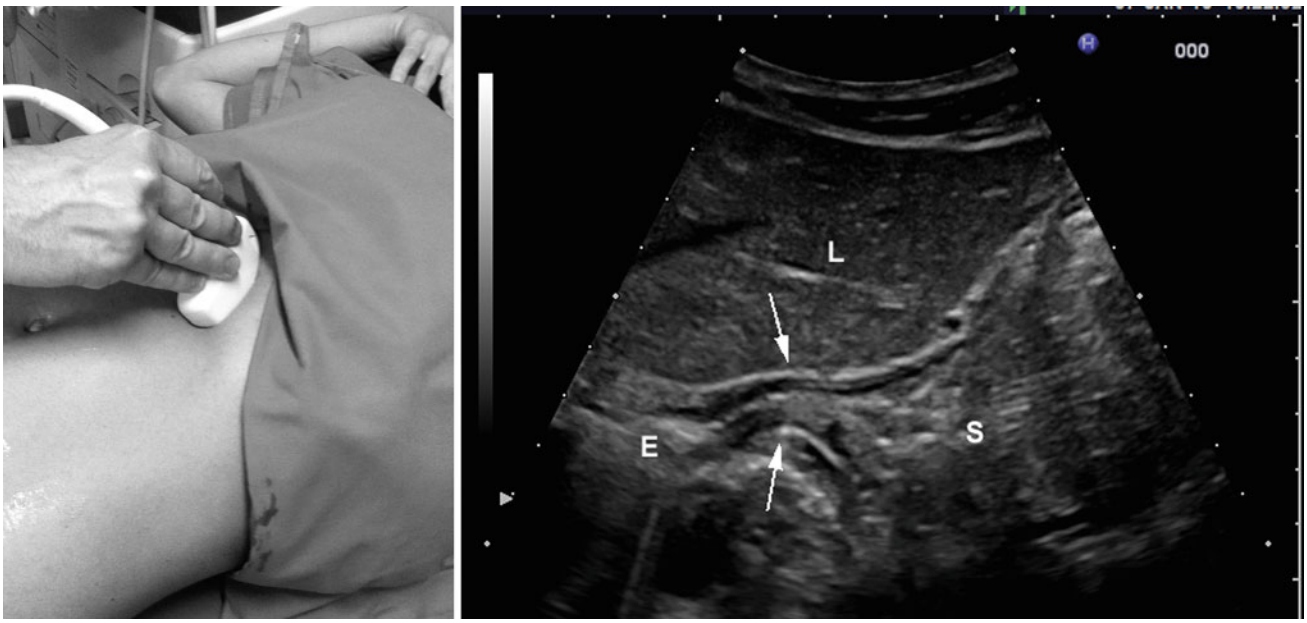

Fig. 2 Ascending subcostal scanning (*left side*) and corresponding ultrasonographic image (*right side*) of the terminal esophagus (*E*) and gastric cardia (*arrows*). *L* liver, *S* fundus of the stomach

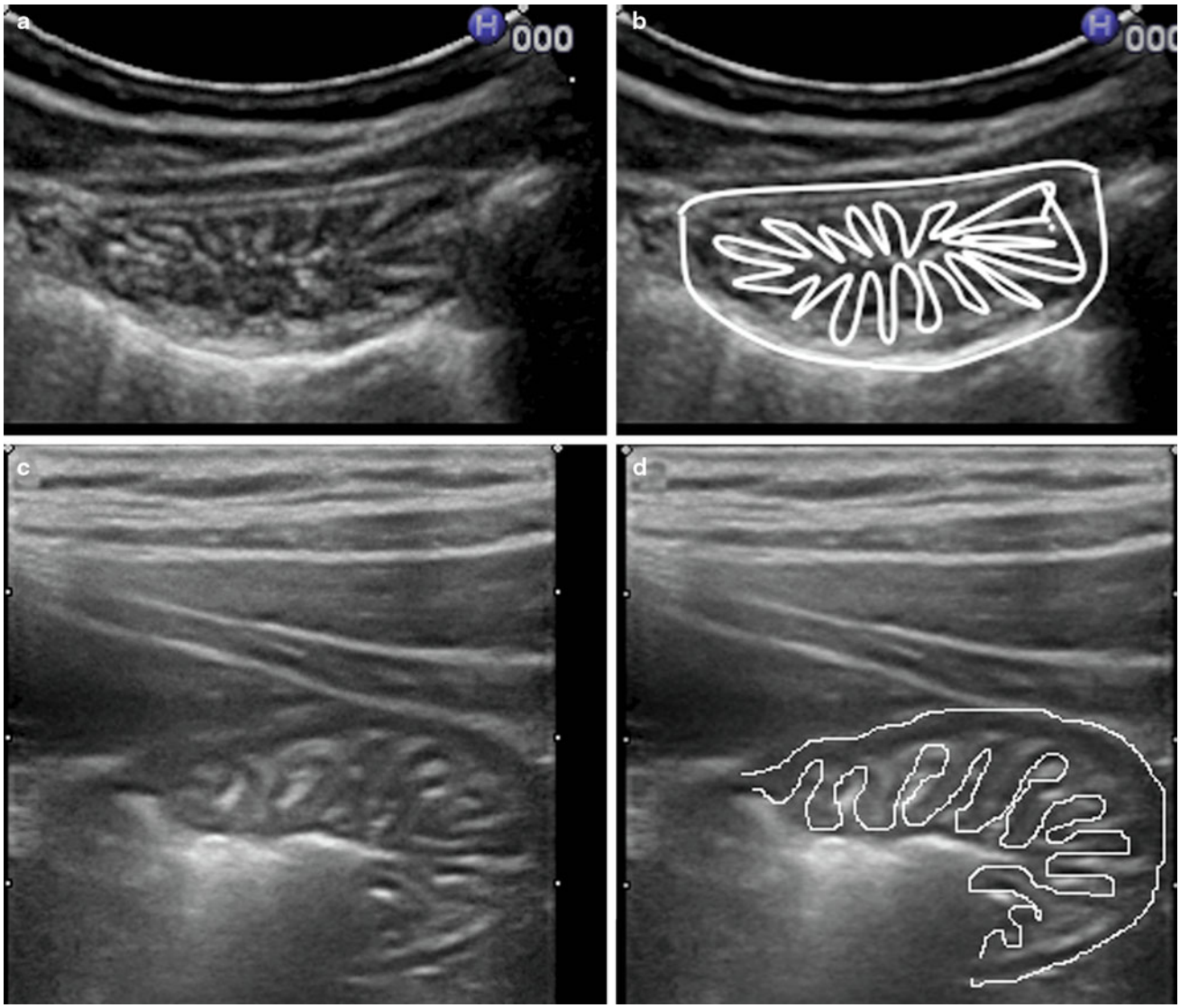

Fig. 3 Transversal scans (**a, c**) with schematic representations (**b, d**) of the gastric fundus showing gastric folds appearing as "carthweel" image

2 Esophagus

Transcutaneous ultrasound examination of the esophagus can be performed on the cervical and sub-diaphragmatic segment only. In fact, an acoustic window for the adequate scanning of the intrathoracic segment is lacking. The best diagnostic accuracy of the whole part can be reached using endoscopic ultrasound.

Cervical esophagus is pointed out by scanning the neck on the left side of the midline with a linear probe. It is 2–3 cm deep, behind the thyroid left lobe, postero-laterally to the trachea, prior to the long muscle of the neck, and to the osseous plan designed by the transverse processes of cervical vertebrae. It has a "target" appearance in transversal scans and it is tubular looking in longitudinal scans. The lumen is generally collapsed and becomes noticeable when the salivary bolus is passing through (Fig. 1).

Terminal esophagus is sub-diaphragmatic and can be examined by scanning sagittally the epigastrium or from the left paramedian site in ascending subcostal scans: the esophagus and the esophageal gastric junction are posterior to the left hepatic lobe, anterior to the osseous plan, and to the abdominal aorta (Fig. 2).

3 Stomach

The stomach may be studied with 3.5–13 MHz convex or linear probes. The gastric wall is multilayered, and its thickness up to 7 mm, depending on its functional state (contraction or relaxation, stretching). To better visualize

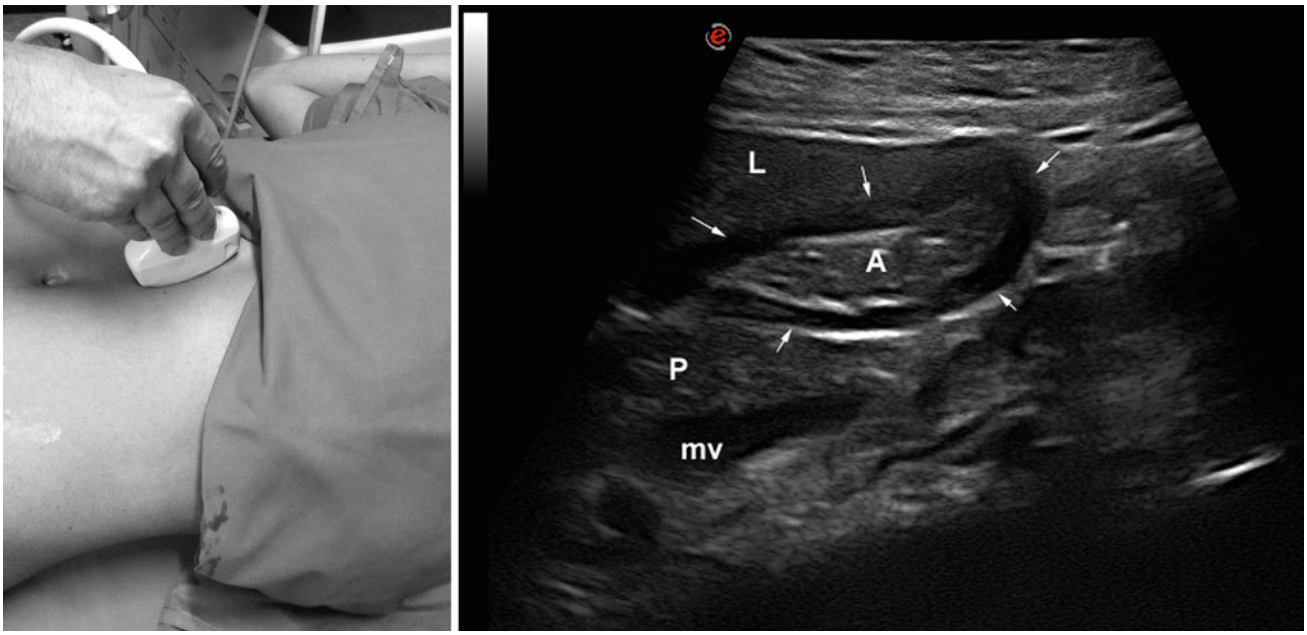

Fig. 4 Transversal scanning (*left side*) and corresponding ultrasonographic image (*right side*) of the gastric antrum (*A*) that is well demarcated by the thickened muscular layer (*arrows*). *L* liver, *P* pancreas, *mv* mesenteric vein

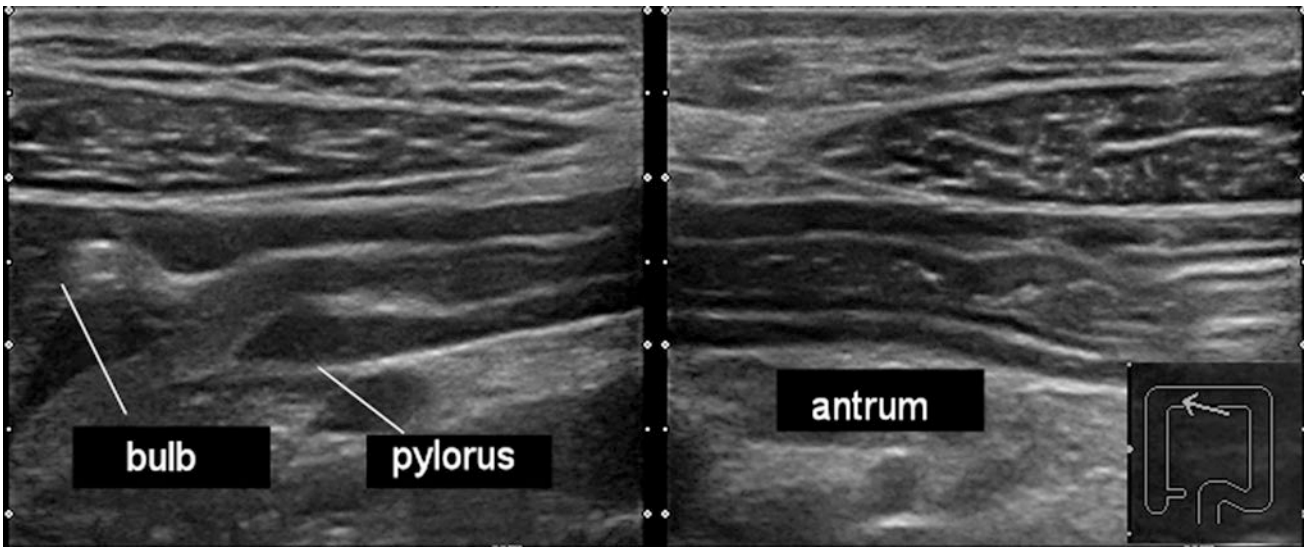

Fig. 5 Longitudinal scan on the long axis of stomach. On the *left side* it is well evident to the ogival shape of the thickened muscular layer of pylorus and the duodenal bulb. On the *right side* the antrum

the gastric wall, the intake of a small quantity of water just before the examination can be convenient.

Fundus and gastric body can be difficult to look over because they are deep-seated and frequently filled with gas so that there is an obstacle to the passage of the ultrasound beam. Fundus and body can be imaged by scanning sagittally the epigastrium or using ascending subcostal scans from the left side, keeping the probe parallel to the axis of the costal arch. They are placed medially to the left hepatic lobe, before the tail of the pancreas and laterally to the spleen. Changing the patient position can be useful to better study the fundus and gastric body. Depending on the stretching of the organ and on its content, gastric folds can be seen as introflections of the gastric wall, scanning the organ transversally to its major axis ("carthweel" image), or as stratified structures parallel to the gastric wall using longitudinal scans (Fig. 3).

The antrum and the pyloric region can be more easily examined because they are superficial (some details can be studied with a linear probe as well). They can be detected

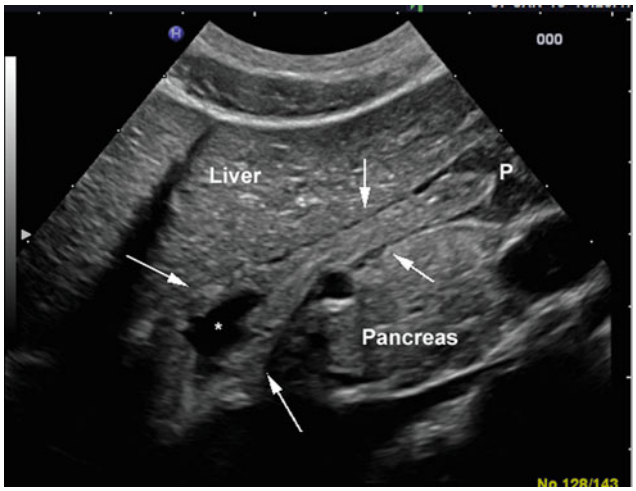

Fig. 6 Longitudinal scan of the bulb and descending duodenum (*arrows*) with liquid content (*asterisk*). *P* pylorus

with epigastric transversal and sagittal scans below the left hepatic lobe prior to the pancreatic body and the spleno-portal venous axis (Fig. 4). The pylorus can be distinguished from the antrum for its particular morphology and the greater thickness of its muscular layer (Fig. 5). Transabdominal ultrasonography may assess the anatomical variants of an operated stomach, which should be acknowledged because they can be mistaken for disorders of the small intestine or of the transverse colon. When a total gastrectomy has been performed a tubular structure, which is the terminal esophagus anastomosed to a jejunal loop, can be highlighted at the site of the stomach. In case of partial gastrectomy only the gastric stump anastomosed to jejunal loops is detectable.

4 Duodenum

The duodenum is divided into four parts each of them different for morphology, location, and relationship with the abdominal organs.

To the right of the pylorus, the duodenal bulb can be seen as a tubular structure with a thin wall and a mainly gaseous content, strongly echogenic under fasting conditions. It can be found below the left hepatic lobe, medial to the gallbladder, in front the cephalic portion of the pancreas and to the gastric antrum.

The second portion of the duodenum (descending duodenum) is antero-medial to the right kidney, lateral to the inferior vena cava and posterior to the gallbladder (Fig. 6). When the lumen is stretched by fluids, duodenal folds are recognizable as small fingerlike protrusions on the luminal site. Under the same conditions it is possible (rarely) to detect the papilla of Vater as a small (<1 cm) round structure protruding into the lumen.

The duodenal third portion has a very deep, horizontal course. It is difficult to visualize because of its seat and its lumen, normally collapsed. It can be searched with axial scans in the epi-mesogastrium before the aorto-caval plan, posteriorly to the superior mesenteric vessels.

The fourth duodenal portion (ascending) and the angle of Treitz are difficult to detect because they are located behind the stomach and frequently the gaseous content of the fundus and body is interposed. These structures can be detected with transverse scans of the epigastrium, behind the gastric antrum and before the pancreatic body and tail.

5 Small Intestine

Ultrasonography of the small intestine takes place in two stages. Usually it includes an overview scanning with the convex probe and a subsequent optimization of the details with linear or microconvex high frequency probes. The echogenicity of the wall is multilayered and the regular wall thickness, using high-resolution probes, with a slight degree of compression and in the absence of peristaltic contractions, is ≤4 mm.

Small intestine loops have increased mobility due to the peristalsis, the breathing, and the induced mobility due to the compression brought about by the probe, compared with other intestinal loops.

Mobility and compressibility of the loops are important characteristics, both in the functional study of small intestine and looking for pathological patterns. They may change in inflammatory or malignant bowel diseases and in the postsurgical adhesions syndrome.

The proper identification of the various sections of the jejunum and ileum is inaccurate for the lack of fixed landmarks but it is possible using topographic criteria and relying on the frequency of *valvulae conniventes* and of the peristaltic activity. Only the jejunum, at the Treitz level, and the terminal ileum have fixed, easily recognizable landmarks because they are located at the extremities of the mesenteric root.

The proximal jejunal loops are observed in the left hypochondrium. They have well-represented folds, frequently liquid content and active peristalsis (14 contractions per minute). Proceeding toward the terminal ileum, to the right iliac fossa, the ileal loops are detectable in the meso-ipogastrium and in the lower right quadrants. The folds became rarer until they disappear and peristaltic activity slows to seven contractions per minute (Fig. 7).

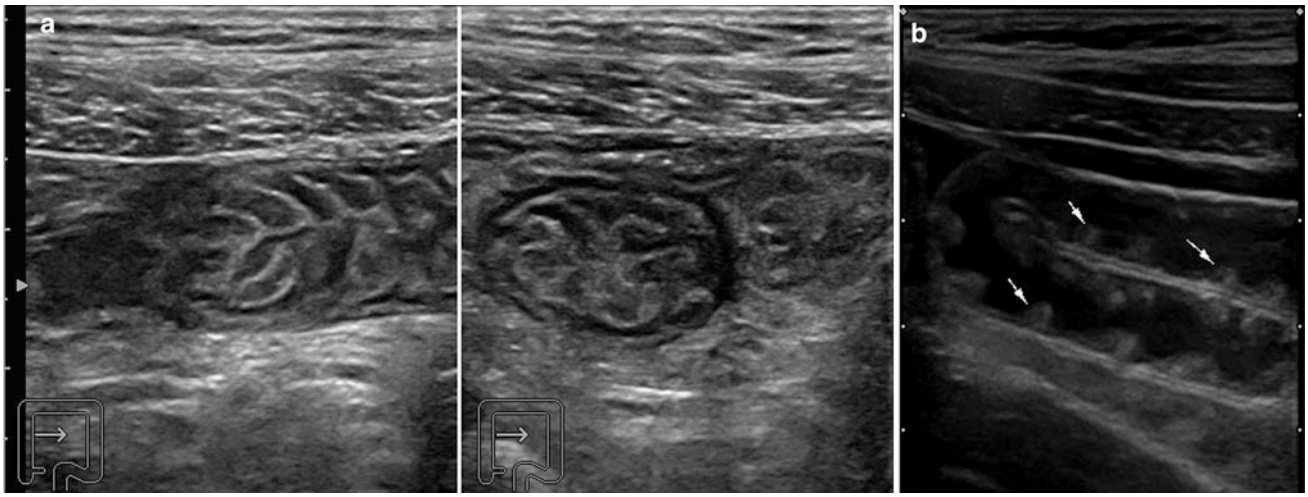

Fig. 7 **a** Longitudinal (*left*) and transverse (*right*) sections of a jejunal loop. Note the numerous folds give a "comb like" aspect. **b** Proximal ileal loop filled with liquid. The folds (*arrows*) are less represented and rare than in jejunum

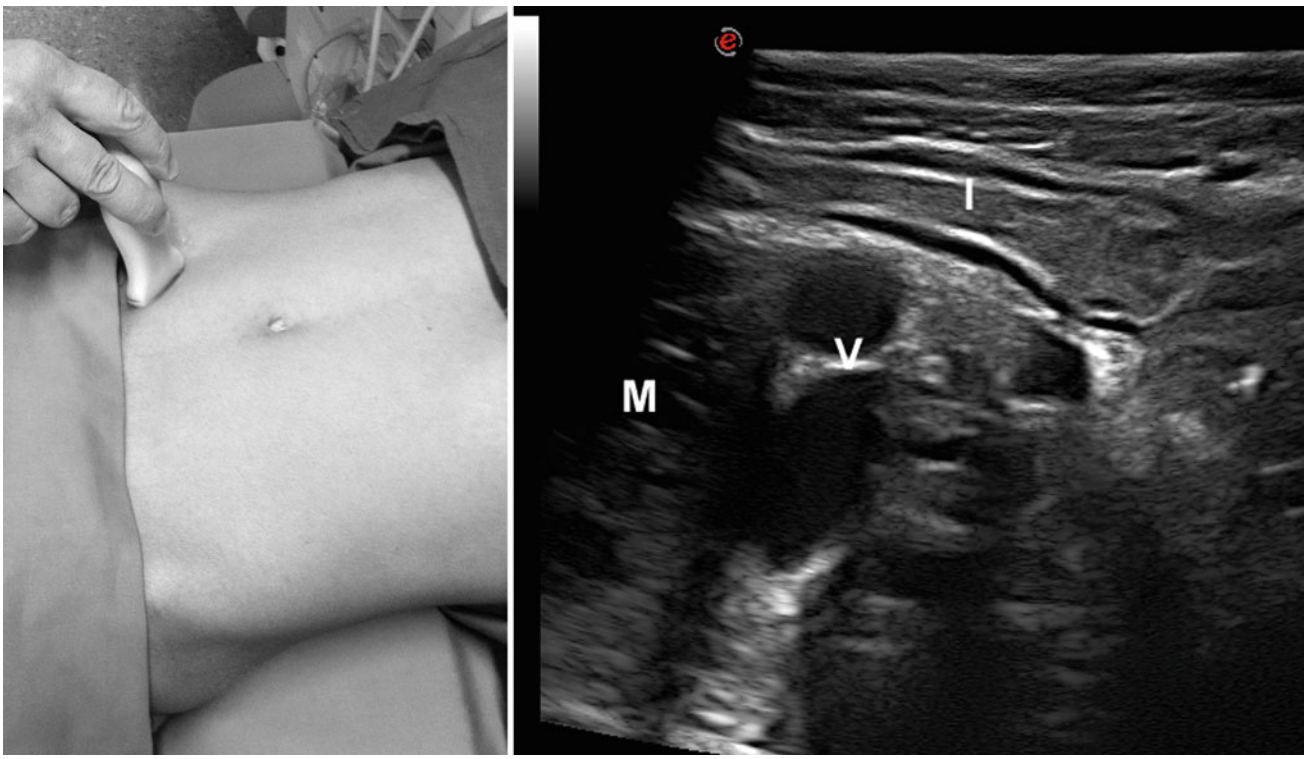

Fig. 8 Longitudinal/oblique scanning of the right iliac fossa (*left side*) and corresponding ultrasonographic image (*right side*) showing the terminal ileum (*I*). The ileum is detectable over the iliopsoas muscle (*M*) and iliac vessels (*V*)

The terminal ileum is easily detectable in the right iliac fossa antero-medially to the iliopsoas muscle and to the iliac vessels (Fig. 8, Video). It runs horizontally from the cecum for a short distance lowering caudally. Scanning longitudinally to its axis it is a tubular structure while in cross-sections it is a target image. It is possible to observe liquid–gas contents passing through the ileocecal valve to the colon.

6 Appendix

It is neither easy nor common in normal conditions to visualize the appendix. It may be detected using high-resolution probes and delicate maneuvering of gradual compression to move the ileal loops and the cecum in order to reduce the

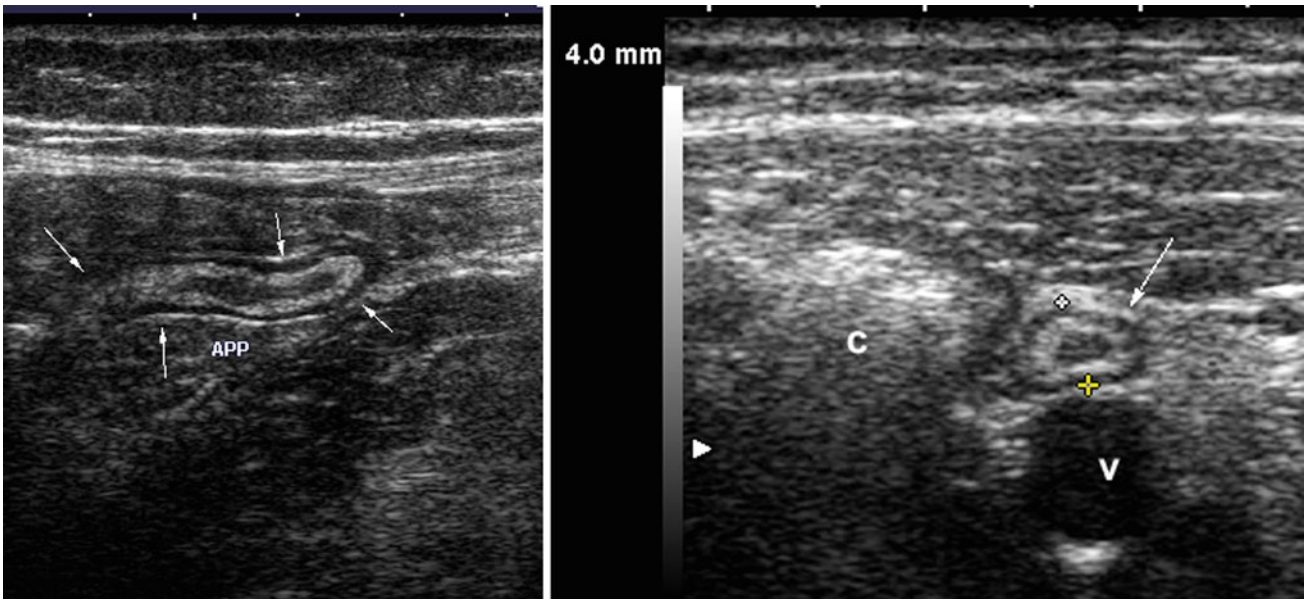

Fig. 9 Longitudinal (*left*) and transversal (*right*) sections of the normal appendix (*arrows*). *C* cecum, *V* iliac vein

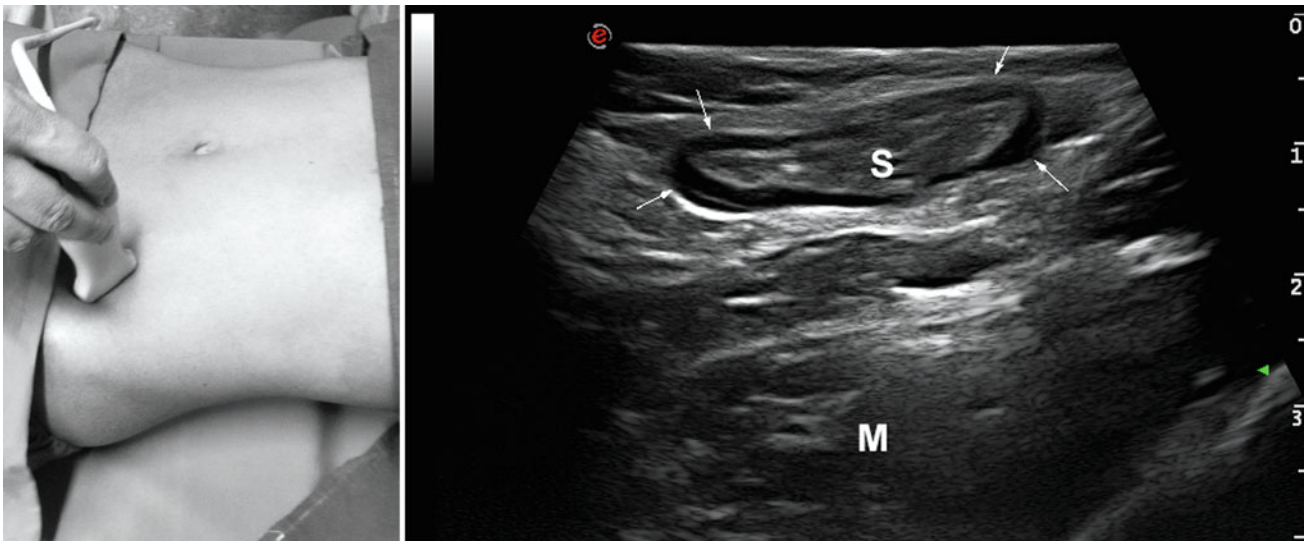

Fig. 10 Oblique scanning of the left iliac fossa (*left side*) and corresponding ultrasonographic image (*right side*) showing the sigmoid colon (*S*). Note the slight thickening of the muscularis propria. *M* iliopsoas muscle

artifacts due to their gaseous content. The appendix, when visible, is located in correspondence to the right iliac fossa, in front of the iliopsoas muscle, and posterior to the cecum and the terminal ileum. Since its site is susceptible to individual variability it can be useful, when looking for it, to change the patient's decubitus (left side) and to empty the bladder. The normal appendix appears as a thin tubular structure with stratified walls. It is mobile and easily compressible, its diameter ≤6 mm (Fig. 9) (see "Acute Appendicitis and Appendiceal Mucocele").

7 Colon

The distal sigmoid colon and the rectum are difficult to examine because of their deeper site. The colon differs from the small bowel for the characteristic haustra that determine its wavy, polycylic shape. The echo structure of the colon wall is multilayered with a clear representation of the mucosa, submucosa, and the muscular layer. Under the

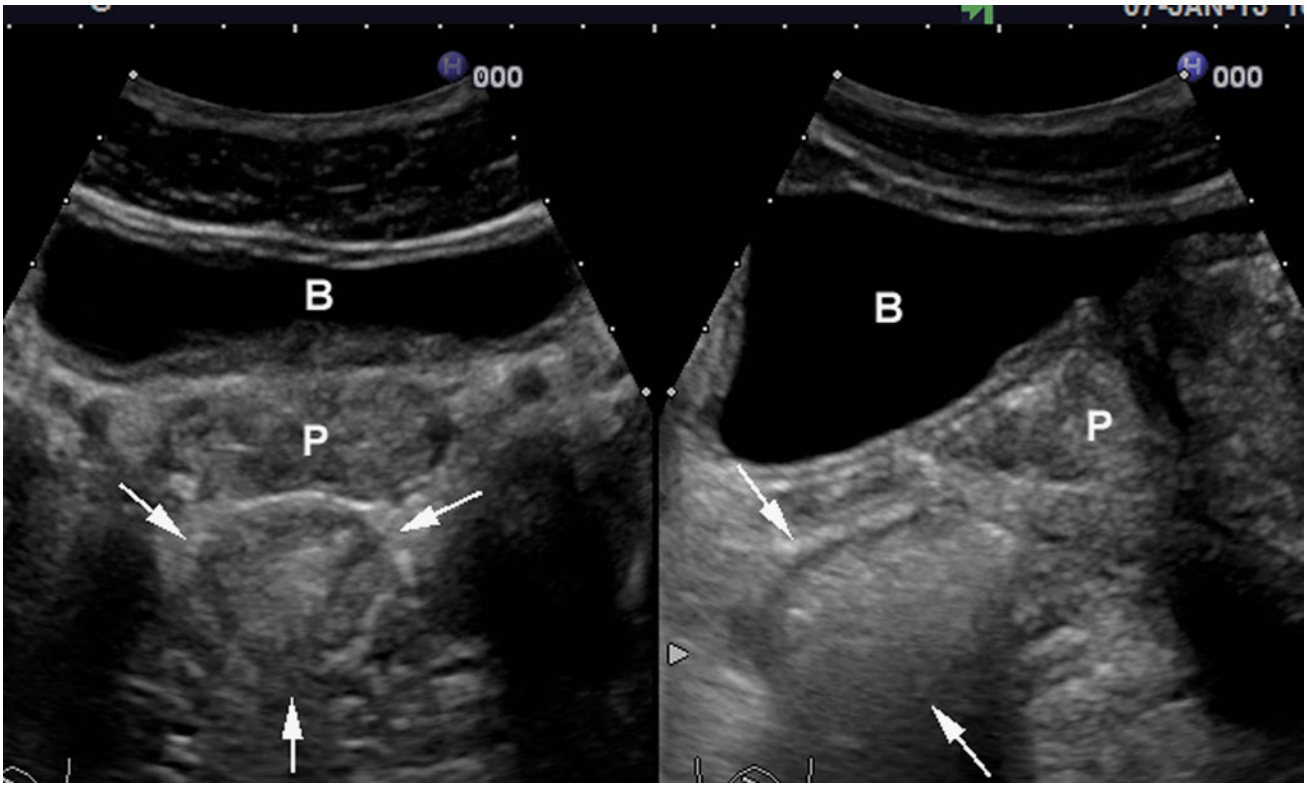

Fig. 11 Transversal (*left*) and longitudinal (*right*) scans of the rectum (*arrows*). It is observed behind the prostate (*P*) and the bladder (*B*)

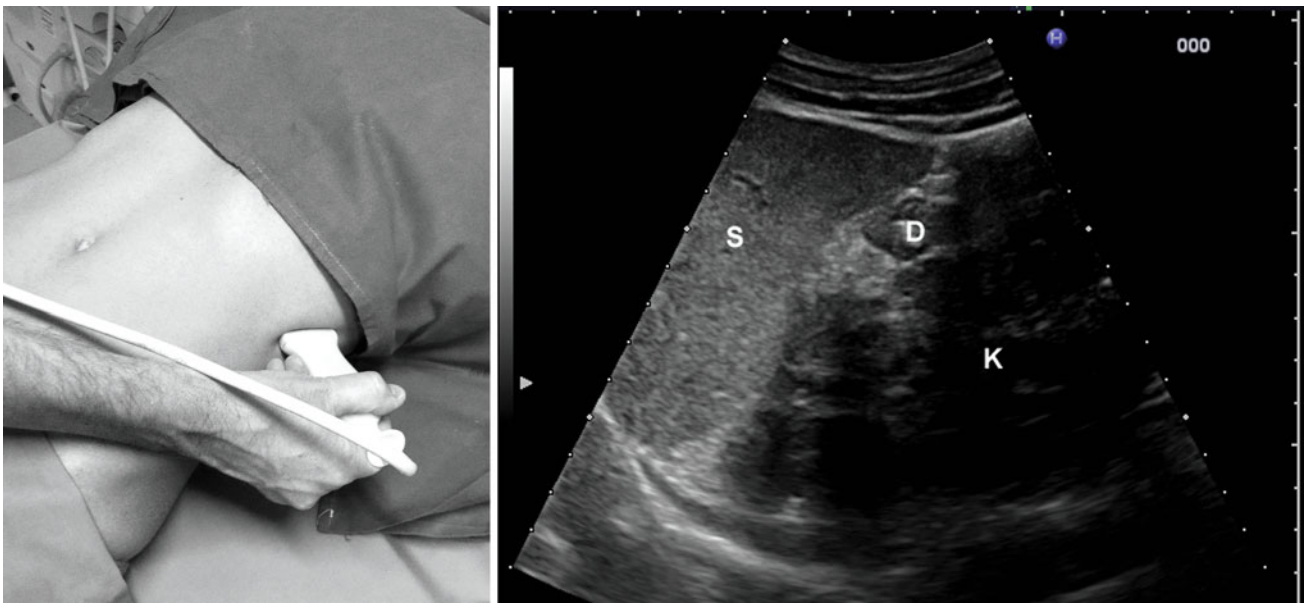

Fig. 12 Transversal scanning (*left side*) and corresponding ultrasonographic image (*right side*) of the splenic flexure of the colon (*D*) that is detectable with intercostals left side scans, between the spleen (*S*) and the kidney (*K*)

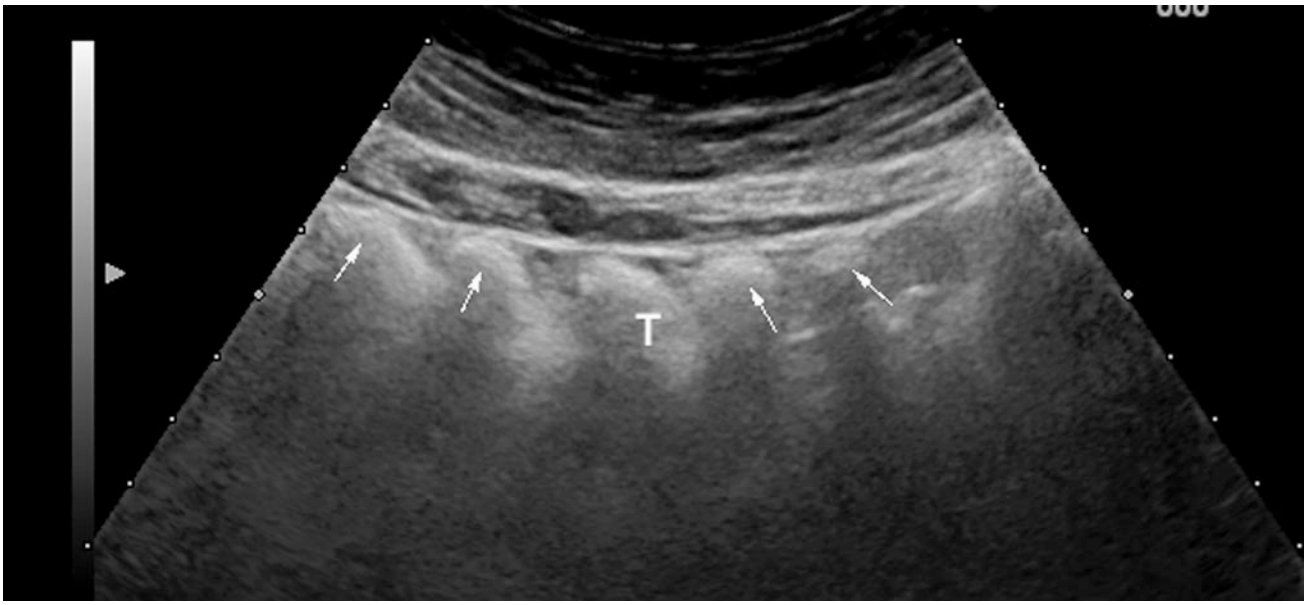

Fig. 13 Longitudinal scan of the transverse colon (*T*). Haustra coli (*arrows*), typically filled with gas, are well represented by an *undulating line*

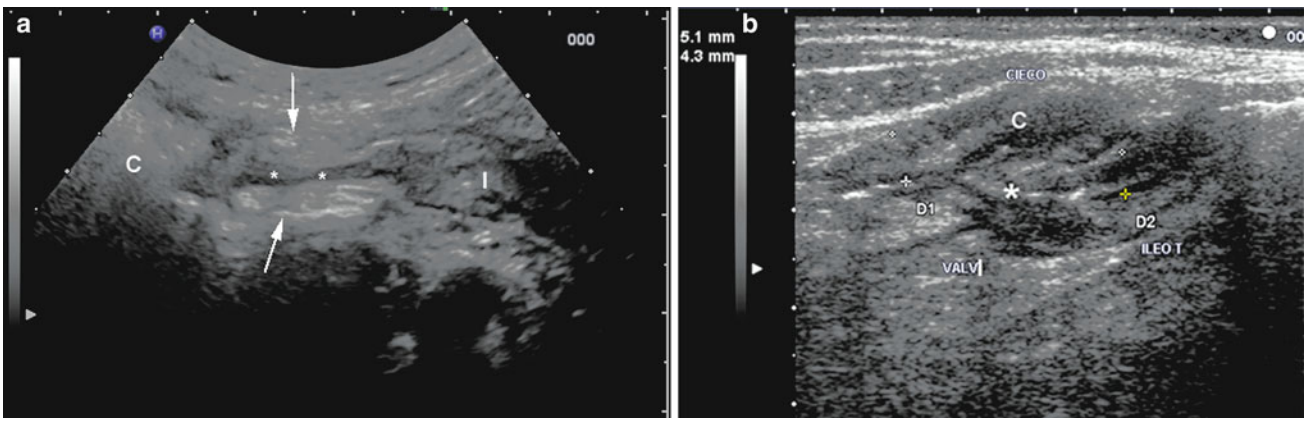

Fig. 14 Longitudinal scan of the ileocecal valve (*asterisk* and *arrows*) protruding in the cecum (*C*) in normal condition (**a**) and in a Crohn's disease patient (**b**). *I* terminal ileum

same conditions given for the small intestine the normal wall thickness is ≤4 mm. Due to the hypertrophy of the muscular layer, in the absence of concomitant alterations of parietal echo structure or of the surrounding structures, the sigma's thickness may be normal up to 5 mm (Fig. 10).

The rectum is even thicker and it is considered normal up to 7 mm. The urinary bladder repletion can facilitate the identification of the rectum, posterior to the prostate in males and to the uterus in women (Fig. 11).

The sigma is normally located in the left iliac fossa, in front of the psoas muscle, laterally and posterior to the bladder. The frequent absence of endoluminal contents helps the exploration of both the bowel walls (distal and proximal to the probe). In case of dolicocolon, the sigma can be found in the hypogastrium and in the right iliac fossa as well. If the sigma is located in the right iliac fossa and especially if the echopattern is altered it can be difficult to distinguish it from the distal and terminal ileum. Compared to the ileum, the sigma has a more gassy content, lower peristaltic activity and hypertrophy of the muscular layer.

The descending colon can be seen along the left side, and posterior up to the splenic flexure that is detectable between the spleen and the kidney (Fig. 12). Sometimes, it can be examined with intercostal left side scans or subcostal scans in the left hypochondrium.

The transverse colon can be observed with longitudinal scans below the gastric antrum. It generally runs transverse to the upper abdominal quadrants. The transverse colon wall proximal to the probe (anterior wall) shows a typical undulating aspect, due to the haustra coli. The

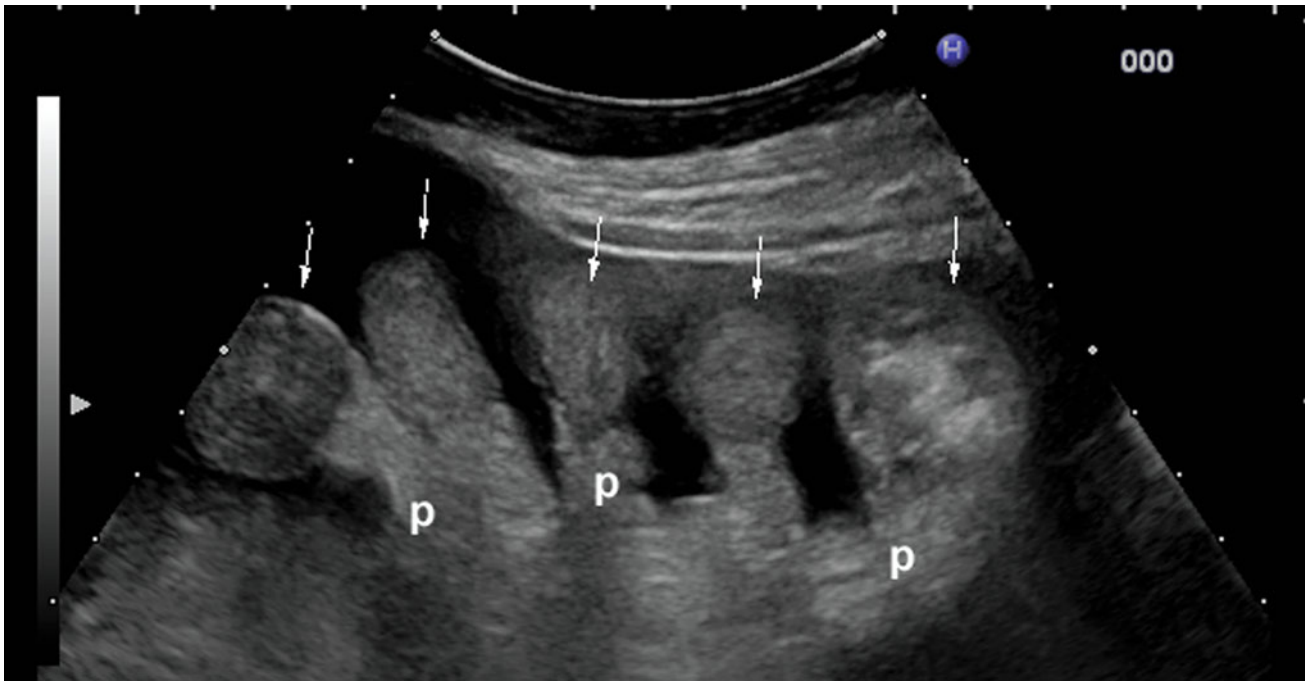

Fig. 15 Shape of intestinal loops (*arrows*) and mesenteric pedicles (*p*), emphasized by free fluid into the abdomen

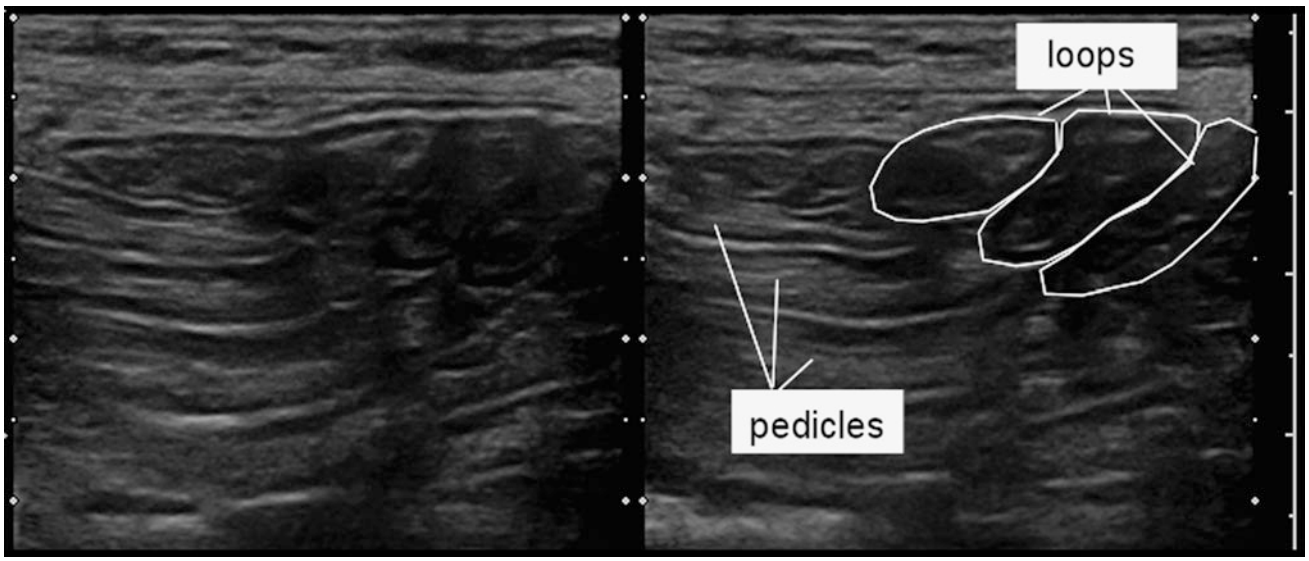

Fig. 16 Ultrasonographic images with schematic representation (*right*) of mesenteric pedicles: mildly hypoechoic parallel layers separated by thin hyperechoic strips. On the *right side* of them, ileal loops can be seen as "target" like images

other wall, distal to the probe (posterior wall), is often hidden by the gaseous content (Fig. 13). The hepatic flexure appears below and medial to the liver, in front of the right kidney.

Similarly to the transverse colon, the ascending colon has an undulating profile and is frequently distended by feces. The ascending colon is detected along the right side, down to the right iliac fossa, where the cecum is located. When the

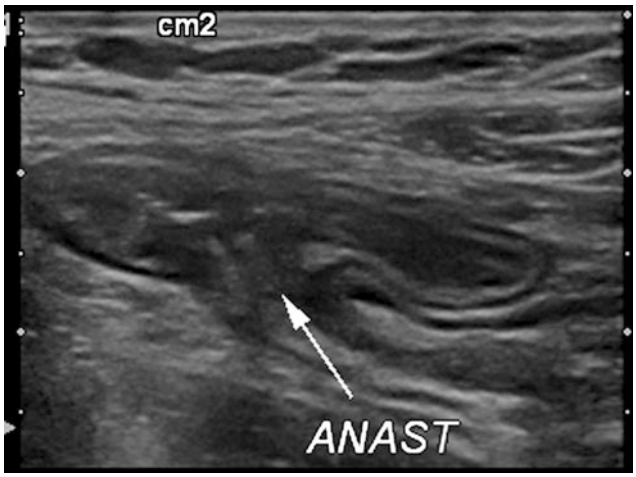

Fig. 17 Ileo-colonic anastomosis. Frequently the ileal cul-de-sac (*C*) is short and the anastomosis appearance is "T" like

cecum content is mainly liquid the ileocecal valve can be detected as a rounded, gently hyperechoic structure protruding into the lumen, crossed by a thin hypoechoic line, that is the transition between the ileum and the cecum (Fig. 14).

8 Mesentery

The mesentery is sonographically represented by mildly hypoechoic parallel layers, 7–12 mm in thickness, containing small vessels and defined by hyperechoic strips (separation planes containing small amounts of peritoneal fluids). These structures are the mesenteric pedicles and are more evident in patients with greater fat accumulation or if ascites is present (Fig. 15). The beginning of the mesentery appears with transverse and sagittal scans along the middle part of the proximal superior mesenteric artery and vein. The small intestine loops are at its extremities (Fig. 16).

The hyperechogenicity of perivisceral areas contrasts the echogenicity of the loops and improves the definition of their external profile. The greater thickness of these structures in obese patients can limit the exploration of deeper parts of the abdomen, leading less expert operators to misdiagnosis. The risk of confusing the stratified image of the mesentery with the "track" image of the collapsed bowel loops can be prevented by protracting the observation until peristalsis is shown, or by using more scans, mutually orthogonal, that should point out, on the loops only, the typical "target" image. The examination of perivisceral areas also allows the detection of mesenteric reactive or metastatic lymph nodes and complications such as free fluids or abscesses in inflammatory processes.

9 The Bowel After Surgery

Bowel ultrasound is frequently performed in the followup of inflammatory bowel diseases, in particular after surgery, occurring in up to 70 % of Crohn's disease patients and in 5–10 % of patients with ulcerative colitis.

The most frequent intervention in Crohn's disease is the resection of the terminal ileum and cecal pole. In these cases the ileo-ascending anastomosis, more often latero-lateral, can be detected as a point of relative hypomotility of the bowel in the right iliac fossa in front of the iliopsoas muscle with transverse or oblique ascending scans.

Ileal and colonic segments run paired for a short distance showing, in longitudinal scans, a "double track" image. Starting from this point it is possible to follow the neo-terminal ileum medially and the colonic slope laterally and upward (Fig. 17).

In the outcomes of further resections or more extended hemicolectomy the ileum-transverse anastomosis has similar appearance. It can be found in the right upper quadrant, in ascending subcostal scans or at the right side on the transverse umbilical line.

Tighten ileal stenosis can be conservatively treated by surgery with a plastic enlargement (strictureplasty). Depending on the severity and the extension of the stenosis the strictureplasty can be realized with longitudinal incision and transverse suture according to Mikulicz or Finney's method (similar to pyloroplasty) or with side-to-side strictureplasty. With this technique, the proximal intestinal loop is moved over the distal one in a side-to-side fashion ensuring that stenotic areas of one loop are placed adjacent to dilated areas of the other loop.

While performing intestinal ultrasound, the strictureplasty must be looked for in every abdominal sector using transverse scans from top to bottom and from the left to the right side. When regular it is detected as a short increased size intestinal tract producing slight discontinuity in the peristalsis.

Part I

Actue Abdomen

Acute Appendicitis and Appendiceal Mucocele

Norbert Gritzmann

Contents

Abstract

Appendicitis is a common cause for acute abdomen. The typical sonographic signs of acute appendicitis are presented. Also, CT and MR in the assessment of appendicitis are analysed. The main gastrointestinal, urological and gynaecological differential diagnoses are discussed. The clinical and ultrasound features of appendical mucoceles are presented.

1 Introduction

Appendicitis is a common disease in each period of life. Most frequently appendicitis occurs in children and adolescents. Histologically serous, phlegmonous, ulcerous and perforated forms are differentiated. These forms usually reveal thickening and enlargement of the tubular organ, whereas chronic or neurogenic forms do not alter the size of the appendix; therefore, neither can usually be diagnosed by imaging.

2 Clinical Evaluation of Acute Appendicitis

The clinical assessment of the painful right lower quadrant still is the cornerstone in the diagnosis of acute appendicitis. Important signs for acute appendicitis are pain at the Mc Burney's point, axillary-rectal difference of the temperature. In laboratory testing, signs of acute inflammation are present. The C reactive protein (CRP) is usually elevated, leukocytosis is often present. Clinical evaluation usually gives significant hints for pathology in the right lower quadrant; in rare cases, the appendix may even lie on the left side (Akbulut et al. 2010). However, specificity in diagnosing acute appendicitis is limited. Of all surgically treated appendices, 30–50 % do not reveal acute appendicitis in histology. The accuracy in clinical evaluation of acute appendicitis is especially low in young women and older patients (Ueberrueck et al. 2004; Strouse 2010).

N. Gritzmann (✉)
Gruppenpraxis für Radiologie,
Esslinger Hauptstr. 89, Vienna, Austria
e-mail: norbert.gritzmann@gmail.com

G. Maconi and G. Bianchi Porro (eds.), *Ultrasound of the Gastrointestinal Tract*, Medical Radiology. Diagnostic Imaging,
DOI: 10.1007/174_2012_657, © Springer-Verlag Berlin Heidelberg 2012
Published Online: 22 July 2012

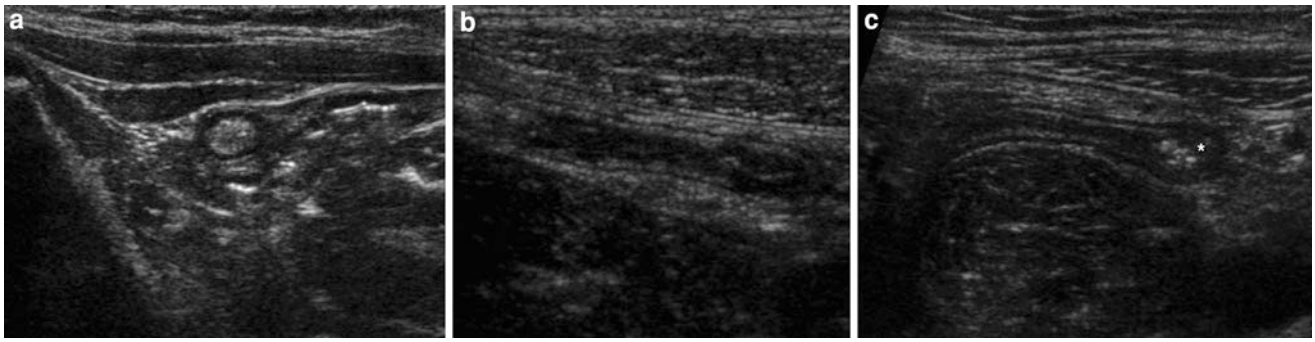

Fig. 1 Normal appendix. **a** Transverse section **b** longitudinal section **c** longitudinal section with a variable amount of air within the tip (*asterisk*)

Table 1 Sonographic signs of acute appendicitis

Antero-posterior (a.p.) diameter of 6 mm or more (Fig. 2), in some cases with lymphatic hyperplasia the a.p. diameter is greater than 6 mm (Rettenbacher et al. 2002)
Round configuration in the transverse section (Fig. 2) (Rettenbacher et al. 2001, 2002, 2003).
Missing compressibility (Puylaert 1986a)
Alteration of the periappendical fat (Fig. 3) (Noguchi et al. 2005; Lee et al. 2009)
Missing gas in the appendix (Rettenbacher et al. 2000)
Hypervascularisation of the appendix in colour Doppler (Fig. 4)
Moderately enlarged lymph nodes.
Pain directly above the appendix, with obstruction (Puylaert 1986a)
Faecolith in the appendix, with obstruction (Fig. 5)
Localised effusion

3 Diagnostic Methods

The main goal of imaging methods is to diagnose appendicitis quickly with high accuracy, non-invasive, cost effective methods and to provide differential diagnosis without laparotomy (Puylaert 1986a, Abu-Yousef 2001).

3.1 Sonography

In 1986, Puylaert published a groundbreaking study about the diagnosis of acute appendicitis using sonography with the graded compression technique.

Sonography is used mainly due to the good availability and the fact that no radiation is used. First of all, diagnosing appendicitis needs sufficient skill and expertise in the performance of gastrointestinal ultrasound. Different compression techniques are used to visualise the appendix (Lee et al. 2005).

Usually, the abdomen and the retroperitoneum are examined with the 3.5-MHz transducer. Then the caecum, which usually contains gas, is localised. Most often the appendix originates caudal to Bauhin's valve. The position of the appendix is highly variable. Retro-coecal position or a position within the small pelvis may be found.

The appendix is a blind ending tubular structure (Fig. 1). Normally, the appendix is compressible with an ovoid configuration in the transverse section. The antero-posterior diameter normally is < 6 mm. Compared with the terminal ileum no peristalsis is visualised in the normal appendix. In a study by Rettenbacher et al. (1997), it could be shown that the normal appendix is localised sonographically in 50–70 % of cases.

Frequently, a high-resolution transducer is used to visualise the appendix during graded compression. In many cases, the appendiceal region can be seen with transabdominal 7.5 MHz transducers. The use of colour or power Doppler may be useful; however, the use of colour Doppler methods is not mandatory.

Ultrasound contrast media have been used for the detection of hypervascularisation (INCESU et al. 2004). Harmonic imaging today is the standard technique in the abdomen. The main advantage is the higher signal-to-noise ratio, but the depth of penetration is lower with this technique. Recently, elastography has also been used in diagnosing of acute appendicitis (Kapoor et al. 2010); however, its exact role has to be established (Table 1).

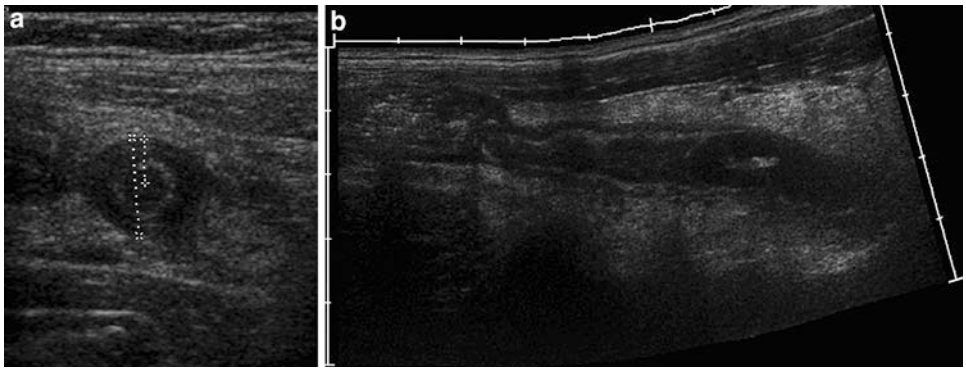

Fig. 2 Acute appendicitis. **a** In transverse section the appendix is round and measures 12 mm in diameter. **b** Longitudinal panoramic section

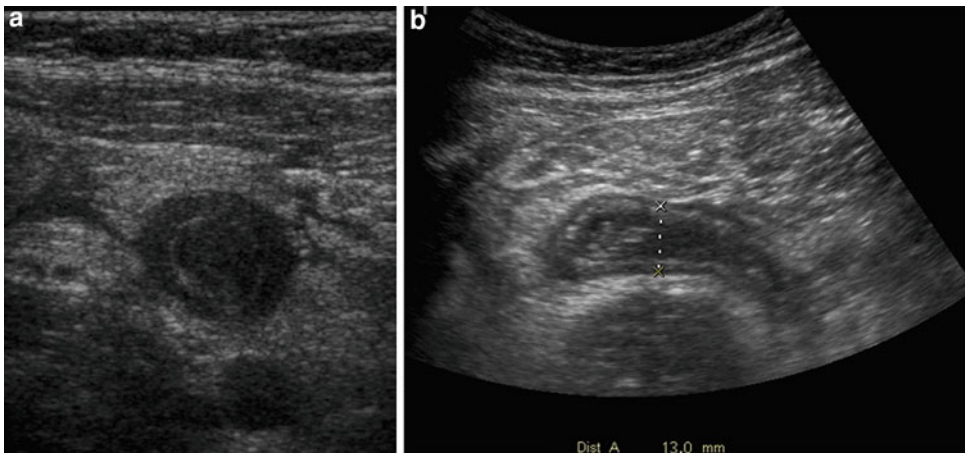

Fig. 3 **a** Transverse section in appendicitis. The appendix is enlarged and reveals echogenic alteration of the surrounding fat. **b** Longitudinal sonographic section of a blind ending tubular structure in the right lower quadrant. Acute appendicitis was found operatively. The appendix is dilated up to 13 mm in transverse diameter. The wall of the inflamed appendix is thickened too

In difficult to scan patients and in women, also a transrectal or transvaginal approach may visualise appendiceal region and appendicitis (Figs. 2–6).

If severe complications, such as significant perforation (Fig. 7) or abscess formation (Fig. 8), are present, the appendix often cannot be visualised as the origin of the inflammation. In these cases, CT should be performed in order to completely delineate the inflammation and to visualise a safe path for a transabdominal drainage; however, the drainage can be performed under US real time guidance.

The accuracy of sonography in diagnosing appendicitis varies between 70 and 95 % depending on the study (Chan et al. 2005; Kessler et al. 2004; Lee et al. 2005; Puylaert 1986a; Rettenbacher et al. 2002; van Breda Vriesman et al. 2003). In the present author's opinion, accuracies over 90 % can be achieved if sonography is performed by an experienced team (Gritzmann et al. 2002).

It is generally accepted that, sonography should be performed in clinically questionable cases, in order to reduce the high rate of false-negative appendectomies; however, in clinically highly suspicious cases the incidence of acute appendicitis was only about 70 %; therefore, it was advocated that sonography be performed in all cases with pain in the right lower quadrant (Rettenbacher et al. 2002). In rare cases the appendix may show an inflammed diverticel (Macheiner et al. 1999).

An acute appendicitis can be excluded if the normal appendix can be completely displayed and/or a differential diagnosis that explains the clinical findings can be found.

3.2 Computed Tomography

In the United States computed tomography (CT) is the preferred method in the evaluation of acute appendicitis (Rao et al. 1997); however, CT provides significant radiation doses to the patients.

CT can be performed only in the region of the painful right lower quadrant if it is preceded by sonography. This is a way to reduce radiation in young patients. Modern multi-detector scanners can visualise the abdomen at low doses using modes with a high spatial resolution. The main advantage of CT is that the operator dependency is lower than with sonography. Furthermore, the normal appendix can be seen in a higher percentage than with sonography. In European institutions, CT is often used as a problem-solving investigation if sonography fails to give a clear diagnosis (van Breda Vriesman et al. 2003). In the United States CT is more

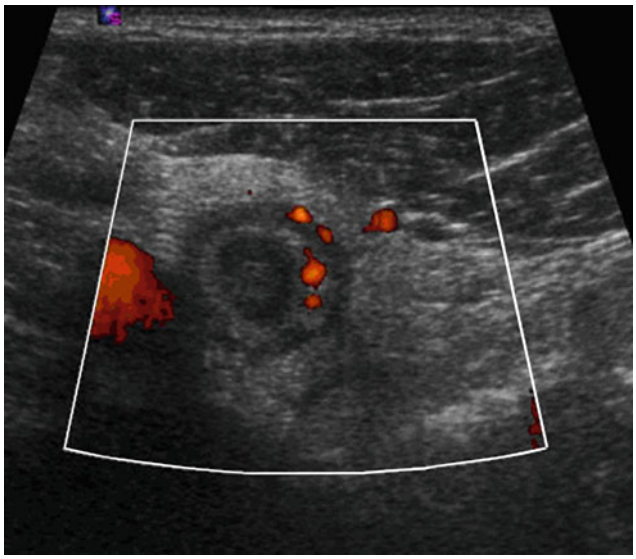

Fig. 4 Transverse section in appendicitis with hyperaemia and thickened wall surrounded by echogenic, hyperemic fat

frequently used as primary investigation (Frush and Frush 2009; Gaitini et al. 2008).

After oral application of water-soluble contrast media, perithyplitic abscesses or bowel loop abscesses are usually better delineated by CT.

3.3 Magnetic Resonance

Magnetic resonance imaging (MRI) is also used to diagnose acute appendicitis (Hörmann et al. 1998; Birchard et al. 2005; Tkacz et al. 2009; Leeuwenburgh et al. 2010). With fast sequences the lower abdomen can be imaged within seconds (for instance HASTE sequence). The prompt availability is a prerequisite for diagnosing acute appendicitis. The accuracy is reported to be comparable to that of CT (Hörmann et al. 1998); however, its relative high costs enable only MRI as a problem-solving investigation.

In the future this may change; however, up to now, MRI is not a primary standard imaging in the diagnosis of acute appendicitis.

4 Differential Diagnosis

The differential diagnosis can be divided into intestinal (Table 2), gynaecological, urological and diseases of other compartments (mainly abdominal wall, psoas muscle, gallbladder, pancreas).

Table 2 Intestinal differential diagnoses of acute appendicitis

Infectious ileocolitis
Lymphadenitis mesenterica
Invagination
Volvulus
Right-sided diverticulitis, sigmoid diverticulitis
Appendix diverticulitis, perforation or inflammation of diverticula of the small bowel
Meckel's diverticulum (complications)
Crohn's disease and ulcerative colitis
Tumour (perforated)
Ileocaecal tuberculosis
Ischaemia of the small bowel
Appendagitis, omental necrosis

4.1 Intestinal Differential Diagnosis

Most often infectious ileocoecitis is found (Puylaert 1986b; Tarantino et al. 2003). Sonographically the cecum and/or the terminal ileum are moderately thickened. The cecum shows hyperhaustration. Most often enlarged painful regional lymph nodes are found. The most frequent microbes are *Yersinia, Campylobacter* or *Salmonella* (Puylaert et al. 1988). Appendix can be reactively enlarged by these diseases.

When examining children, in the event of a painful lower quadrant, invagination of the small bowel has to be considered. The sonographic picture is typical. A double-layer intussusception can be visualised. With adults, tumours causing invagination have to be excluded. Furthermore, complications of a Meckel's diverticulum (inflammation, bleeding) have to be taken into account (Baldisserotto et al. 2003). Another differential diagnosis when examining children is a volvulus (Patino and Munden 2004). In this condition, the mesenteric vessels show a whirlpool sign.

In adults, diverticulitis of the ascending colon or cecum is an important conservatively managed disease (Wada et al. 1990). Also diverticulitis of the sigmoid colon can be right sided or projected on the right side (Hollerweger et al. 2001). The diverticula on the right side usually are true diverticula, which are often large.

Furthermore, a (perforated) tumour of the colon should be considered.

Crohn's disease is a frequent transmural chronic inflammation of the bowel. Usually, segmental thickening of the small bowel is seen. Also other parts of the bowel, appendix included (Fig. 9), can be involved. Due to the transmural inflammation the surrounding fat is frequently affected. Most times the inflamed fat gets more echogenic.

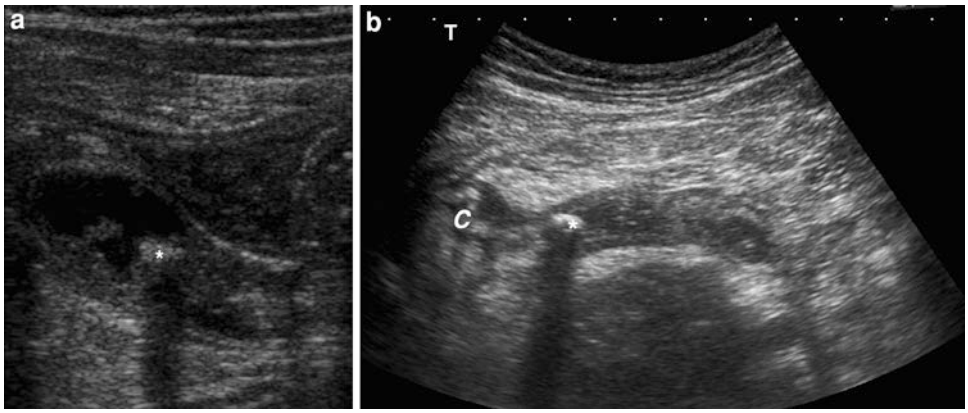

Fig. 5 **a** Obstructed appendix with faecoliths (*astrerisk*) and inflammatory content. **b** Longitudinal sonographic section in a thickened and dilated appendix. Faecoliths (*astrerisk*) is visualised in the proximal part of the appendix. The cecal pole *(arrows)* shows a concomitant inflammation. The surrounding fat is more echogenic due to edema

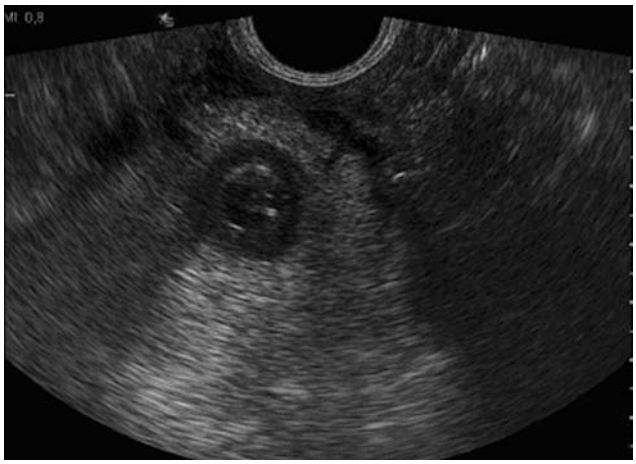

Fig. 6 Transrectal sonography displaying acute appendicitis with echogenic fat reaction

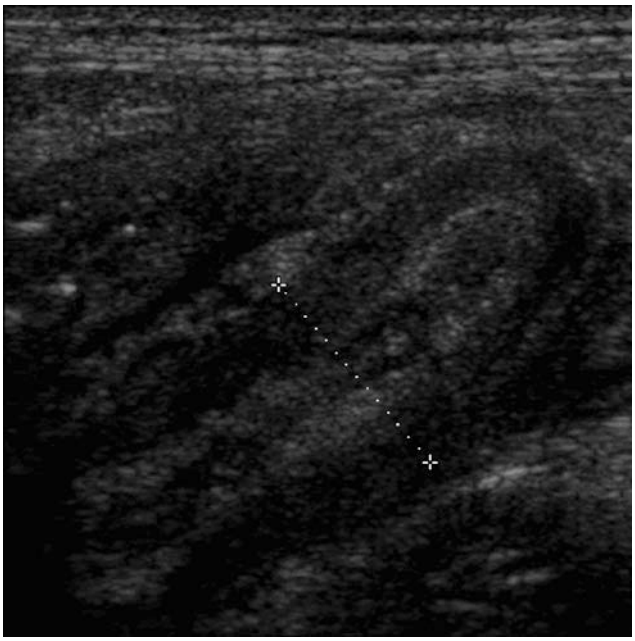

Fig. 7 Longitudinal section of an acute perforated appendicitis

Fistulas are often found. In chronic forms, frequently fibrous stenosis is present with dilation of the oral segments showing fluid-filled bowel loops. Ulcerative colitis is a rare differential diagnoses for appendicitis, since the disease is predominantly left sided.

Another rare disease in the right lower quadrant is tuberculosis of the ileo-caecal region (Portielje et al. 1995).

Appendagitis and omental infarction are further differential diagnoses to acute appendicits. In appendagitis, an inflammation torsion or necrosis of the epiploic appendices is present. Sonographically, an ovoid alteration of the pericolonic fat is seen. Usually, the echogenic altered fat is fixed to the ventral peritoneum, whereas the other bowel loops show normal breathing motility with regard to the peritoneum (Hollerweger et al. 2002; van Breda Vriesman et al. 2001).

In colour Doppler, the altered epiploic appendix reveals no vascularisation, whereas the surrounding fat may be hypervascularised (Grattan-smith et al. 2002). Usually, CT is additionally performed to verify this relatively rare diagnosis. Appendagitis is treated conservatively. Surgery can be avoided in this self-limiting disease.

4.2 Gynaecological Differential Diagnosis

Inflammation of the ovaries is a common differential diagnosis. This diagnosis is made when witnessing a combination of clinical and transvaginal sonographic signs. The most important sign is the pain above the ovary during examination. In a tubo-ovarial abscess, cystoid-hypoechogenic tubular structures can be found in transvaginal sonography. Furthermore, differential diagnoses are ruptured adnexal cysts, torque cysts or cysts with bleeding. All these pathologies may clinically mimic acute appendicitis.

The most important gynaecological differential diagnosis is ectopic pregnancy. In ruptured tubal gestation, a haematoma is seen in the adnexal region together with free intraperitoneal fluid. In the uterus a small pseudogestational sac can be depicted.

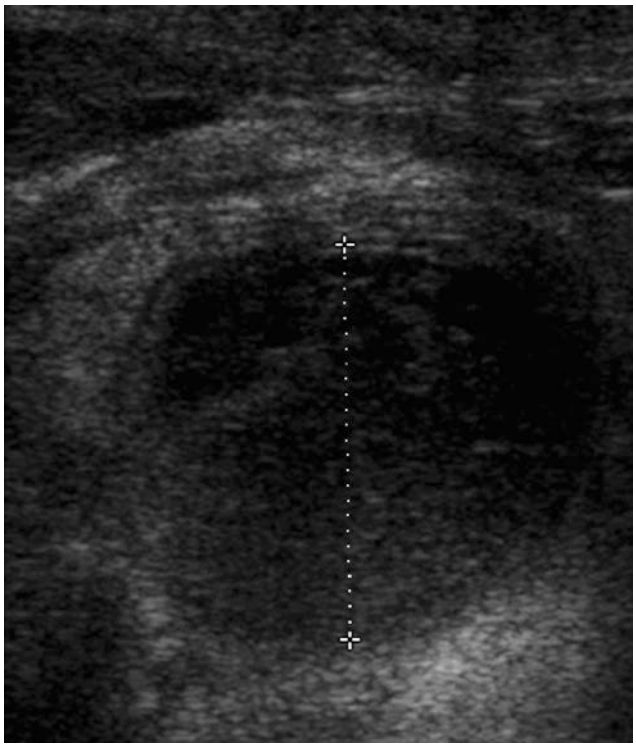

Fig. 8 Perithyplitic abscess. The appendix can not be displayed anymore

Transvaginal sonography is mainly used to diagnose gynaecological pathologies.

When the appendix is deeply situated in the small pelvis, transvaginal sonography may depict appendicitis too (Molander et al. 2002).

4.3 Urological Differential Diagnosis

Inflammation of the urinary tract may mimic appendicitis.

A stone in the right ureter may be a cause of right lower abdominal pain.

In acute renal colic, the collecting system may not be dilated. Colour Doppler sonography can be used to diagnose the acute obstruction. Furthermore, a careful search for perirenal fluid at the poles of the kidney should be performed.

Ureter stones are typically located at the three physiological narrowings. Usually, the stone is localised in the intramural part of the ureter, just proximal to the ostium. These stones can be diagnosed with transabdominal and transrectal or transvaginal sonography.

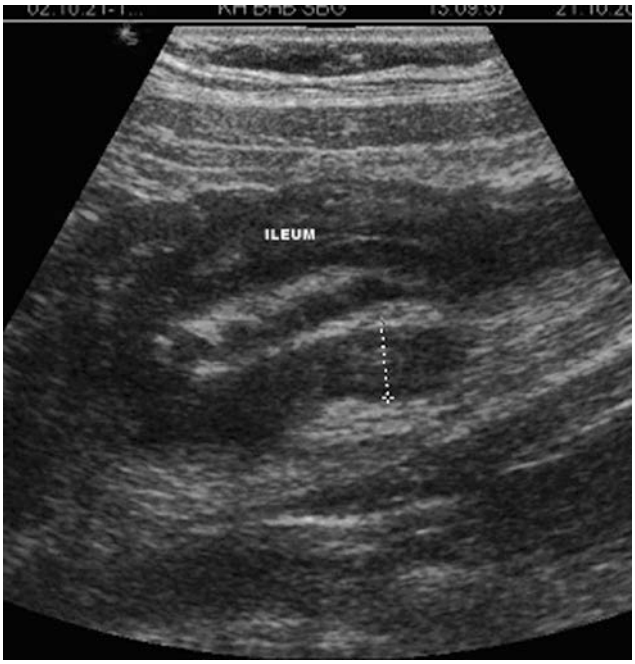

Fig. 9 Thickening of the appendix in Crohn's disease. The terminal ileum is thickened too

4.4 Diseases of Other Compartments

Haematomas of the abdominal wall may mimic acute appendicitis (OH et al. 2010). These cystoid lesions may be easily assessed with high-resolution transducers. They reveal no breathing mobility. Typically, these lesions are ovoid or spindle shaped.

Haematomas or abscesses may also be present in the psoas muscle. In these diseases, the psoas muscle is enlarged and reveals pressure tenderness.

Either CT/or MRI should be performed in order to rule out acute spondylodiscitis.

Acute cholecystitis may be caudally situated and may mimic appendicitis clinically. In rare cases, necrotic pancreatitis may be misinterpreted clinically.

In rare cases, dissecting or rupturing aneurysms of the retroperitoneal vessels may cause right lower quadrant pain.

5 Mucocele of the Appendix

Mucoceles of the appendix are relatively rare lesions. They vary considerably in size. Giant lesions up to 25 cm can be present. The large lesions are most often caused by mucus-producing tumours like cystadenoma or cystadenocarcinoma

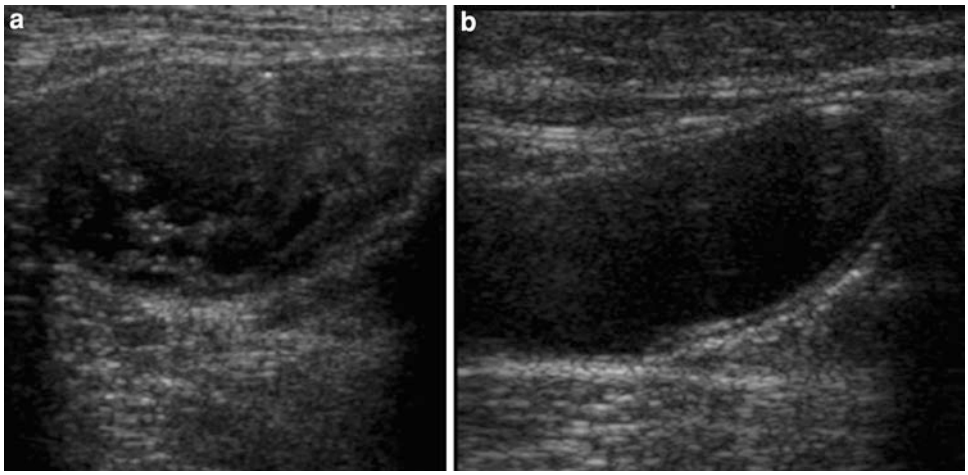

Fig. 10 Mucocele of the appendix. **a** Cystoid lesion in the region of the appendix with an onion skin structure. **b** Appendiceal mucocele appearing as a cystoid enlargement of the appendix

(Karakaya et al. 2008). Later, can rupture and produce a *Pseudomyxoma peritoneii*. Small non-neoplastic lesions are found incidentally during imaging.

Sonographically, mucoceles are cystoid or hypoechogenic lesions. An onionskin appearance has been described (Fig. 10; Dgani et al. 2002; Caspi et al. 2004). This echogenicity is thought to be caused by viscosity differences of the mucus. Colour Doppler is used to exclude vascularisation in the lesion. In *Pseudomyxoma peritoneii,* encapsulated cystoid lesions are found in the peritoneum.

6 Conclusion

Sonography is the first-line imaging method for diagnosing acute appendicitis. Experienced investigators have an accuracy of more than 90 %.

Sonography can diagnose many conservatively managed diseases.

Sonography can reduce the high rate of false-positive clinical examinations concerning acute appendicitis. It has to be stated that, exclusion of appendicitis can only be made sonographically if the normal appendix can be seen in its full length and/or other differential diagnoses can be depicted that explains the clinical symptoms. Mucoceles are rare cystoid lesions of the appendix. They exhibit a typical onion-skin-sign structure caused by mucus. In large mucoceles a tumour causes this lesion.

References

Abu-Yousef MM (2001) Ultrasonography of the right lower quadrant. Ultrasound Q 17:211–225

Akbulut S, Caliskan A, Ekin A, Yagmur Y (2010) Left-sided acute appendicitis with situs inversus totalis: review of 63 published cases and report of two cases. J Gastrointest Surg 14:1422–1428

Baldisserotto M, Maffazzoni DR, Dora MD (2003) Sonographic findings of Meckel's diverticulitis in children. AJR Am J Roentgenol 180:425–428

Birchard KR, Brown MA, Hyslop WB et al (2005) MRI of acute abdominal and pelvic pain in pregnant patients. AJR Am J Roentgenol 184:452–458

Caspi B, Cassif E, Auslender R et al (2004) The onion skin sign: a specific Sonographic marker of appendiceal mucocele. J Ultrasound Med 23:117–121

Chan I, Bicknell SG, Graham M (2005) Utility and diagnostic accuracy of sonography in detecting appendicitis in a community hospital. AJR Am J Roentgenol 184:1809–1812

Dgani S, Shapiro I, Leibovitz Z, Ohel G (2002) Songraphic appearance of appendiceal mucocele. Ultrasound Obstet Gynecol 19:99–101

Frush DP, Frush KS (2009) Oldham KT Imaging of acute appendicitis in children: EU versus U.S.… or US versus CT? A North American perspective. Pediatr Radiol 39:500–505

Gaitini D, Beck-Razi N, Mor-Yosef D et al (2008) Diagnosing acute appendicitis in adults: accuracy of color Doppler sonography and MDCT compared with surgery and clinical follow-up. AJR Am J Roentgenol 190:1300–1306

Grattan-Smith JD, Blews DE, Brand T (2002) Omental infarction in pediatric patients: sonographic and CT findings. AJR Am J Roentgenol 178:1537–1539

Gritzmann N, Hollerweger A, Macheiner P, Rettenbacher T (2002) Transabdominal sonography of the gastrointestinal tract. Eur Radiol 12:1748–1761

Hollerweger A, Macheiner P, Rettenbacher T et al (2001) Colonic diverticulitis: diagnostic value and appearance of inflamed diverticula-sonographic evaluation. Eur Radiol 11:1956–1963

Hollerweger A, Macheiner P, Rettenbacher T, Gritzmann N (2002) Primary epiploic appendagitis: sonographic findings with CT correlation. J Clin Ultrasound 30:481–495

Hörmann M, Paya K, Eibenberger K et al (1998) MR imaging in children with nonperforated acute appendicitis: value of unenhanced MR imaging in sonographically selected cases. AJR Am J Roentgenol 171:467–470

Incesu L, Yazicioglu AK, Selcuk MB, Ozen N (2004) Contrast-enhanced power Doppler US in the diagnosis of acute appendicitis. Eur J Radiol 50:201–209

Kapoor A, Kapoor A, Mahajan G (2010) Real-time elastography in acute appendicitis. J Ultrasound Med 29:871–877

Karakaya K, Barut F, Emre AU et al (2008) Appendiceal mucocele: case reports and review of current literature. World J Gastroenterol 14:2280–2283

Kessler N, Cyteval C, Gallix B et al (2004) Appendicitis: evaluation of sensitivity, specificity, and predictive values of US, Doppler US, and laboratory findings. Radiology 230:472–478

Lee JH, Jeong YK, Park KB et al (2005) Operator-dependent techniques for graded compression sonography to detect the appendix and diagnose acute appendicitis. AJR Am J Roentgenol 184:91–97

Lee MW, Kim YJ, Jeon HJ, Park SW, Jung SI, Yi JG (2009) Sonography of acute right lower quadrant pain: importance of increased intraabdominal fat echo. AJR Am J Roentgenol 192:174–179

Leeuwenburgh MM, Lamäris W, van Randen A, Bossuyt PM, Boermeester MA, Stoker J, OPTIMAP study group (2010) Optimizing imaging in suspected appendicitis (OPTIMAP-study): a multicenter diagnostic accuracy study of MRI in patients with suspected acute appendicitis. Study Protocol. BMC Emerg Med 10:19

Macheiner P, Rettenbacher T, Hollerweger A, Gritzmann N (1999) Diverticulitis of the appendix vermiformis: ultrasonographic appearance. Ultraschall Med 20:115–117

Molander P, Paavonen J, Sjoberg J et al (2002) Transvaginal sonography in the diagnosis of acute appendicitis. Ultrasound Obstet Gynecol 20:496–501

Noguchi T, Yoshimitsu K, Yoshida M (2005) Periappendiceal hyperechoic structure on sonography: a sign of severe appendicitis. J Ultrasound Med 24:323–327

Oh JH, Kim TH, Cha SJ, Kim SH (2010) Rectus sheath hematoma caused by non-contact strenuous exercise mimicking acute appendicitis. J Emerg Med 39:e117–e119

Patino MO, Munden MM (2004) Utility of the sonographic whirlpool sign in diagnosing midgut volvulus in patients with atypical clinical presentations. J Ultrasound Med 23:397–401

Portielje JE, Lohle PN, van der Werf SD, Puylaert JB (1995) Ultrasound and abdominal tuberculosis. Lancet 346:379–380

Puylaert JB (1986a) Acute appendicitis: US evaluation using graded compression. Radiology 158:355–360

Puylaert JB (1986b) Mesenteric adenitis and acute terminal ileitis: US evaluation using graded compression. Radiology 161:691–695

Puylaert JB, Lalisang RI, van der Werf SD, Doornbos L (1988) Campylobacter ileocolitis mimicking acute appendicitis: differentiation with graded-compression US. Radiology 166:737–740

Rao PM, Rhea JT, Novelline RA (1997) Sensitivity and specificity of the individual CT signs of appendicitis: experience with 200 appendiceal CT examinations. J Comput Assist Tomogr 21:686–692

Rettenbacher T, Hollerweger A, Macheiner P, Gritzmann N (1997) Ultrasonography of the normal vermiform appendix. Ultraschall Med 18:139–142

Rettenbacher T, Hollerweger A, Macheiner P et al (2000) Presence or absence of gas in the appendix: additional criteria to rule out or confirm acute appendicitis-evaluation with US. Radiology 214:183–187

Rettenbacher T, Hollerweger A, Macheiner P et al (2001) Outer diameter of the vermiform appendix as a sign of acute appendicitis: evaluation at US. Radiology 218:757–762

Rettenbacher T, Hollerweger A, Gritzmann N et al (2002) Appendicitis: should diagnostic imaging be performed if the clinical presentation is highly suggestive of the disease? Gastroenterology 123:992–998

Rettenbacher T, Hollerweger A, Macheiner P et al (2003) Ovoid shape of the vermiform appendix: a criterion to exclude acute appendicitis–evaluation with US. Radiology 226:95–100

Strouse PJ (2010) Pediatric appendicitis: an argument for US. Radiology 255:8–13

Tarantino L, Giorgio A, de Stefano G et al (2003) Acute appendicitis mimicking infectious enteritis: diagnostic value of sonography. J Ultrasound Med 22:945–950

Tkacz JN, Anderson SA, Soto J (2009) MR imaging in gastrointestinal emergencies. Radiographics 29:1767–1780

Ueberrueck T, Koch A, Meyer L et al (2004) Ninety-four appendectomies for suspected acute appendicitis during pregnancy. World J Surg 28:508–511

van Breda Vriesman AC, de Mol van Otterloo AJ, Puylaert JB (2001) Epiploic appendagitis and omental infarction. Eur J Surg 167:723–727

van Breda Vriesman AC, Kole BJ, Puylaert JB (2003) Effect of ultrasonography and optional computed tomography on the outcome of appendectomy. Eur Radiol 13:2278–2282

Wada M, Kikuchi Y, Doy M (1990) Uncomplicated acute diverticulitis of the cecum and ascending colon. Sonographic findings in 18 patients. AJR Am J Roentgenol 155:283–287

Mesenteric Lymphadenopathy

Giovanni Maconi

Contents

Abstract

Enlargement of mesenteric lymph nodes is a common sonographic finding, in particular in children and young adults. It may be the manifestation of various clinical disorders, mainly malignant, immunological or infectious diseases. However, normal mesenteric lymph nodes are often incidentally detected by ultrasound and should not be misdiagnosed as an early manifestation of pathological conditions. The distinction between normal and abnormal mesenteric lymph nodes, and the differential diagnosis among various neoplastic, inflammatory and infectious causes of mesenteric lymphadenitis are shown in the present chapter.

1 Introduction

With the increasing use of abdominal and bowel ultrasound in the screening and follow-up of bowel diseases, enlarged regional mesenteric lymph nodes have become a fairly common clinical finding, particularly in children and young adults. Therefore, since lymphadenopathy may often be an incidental finding in patients being examined for various reasons, the sonographer (and the physician) must decide whether it is a normal finding or a sign of a patient's condition requiring further study. Indeed, mesenteric lymphadenopathy may be a manifestation of various disorders (Table 1).

2 Normal Mesenteric Lymph Nodes

Regional mesenteric lymph nodes are usually detected as the result of a symptom-directed diagnostic work-up, by a variety of imaging techniques, including ultrasound and colour-Doppler ultrasonography, computed tomography (CT) and magnetic resonance imaging (MRI). When they are found, the main goal of the diagnostic technique is to suggest whether it is a normal finding or the sign of a past or

G. Maconi (✉)
Department of Clinical Sciences, L. Sacco University Hospital, Via G.B. Grassi, 74, 20157, Milan, Italy
e-mail: giovanni.maconi@unimi.it

G. Maconi and G. Bianchi Porro (eds.), *Ultrasound of the Gastrointestinal Tract*, Medical Radiology. Diagnostic Imaging,
DOI: 10.1007/174_2012_719, © Springer-Verlag Berlin Heidelberg 2012
Published Online: 28 September 2012

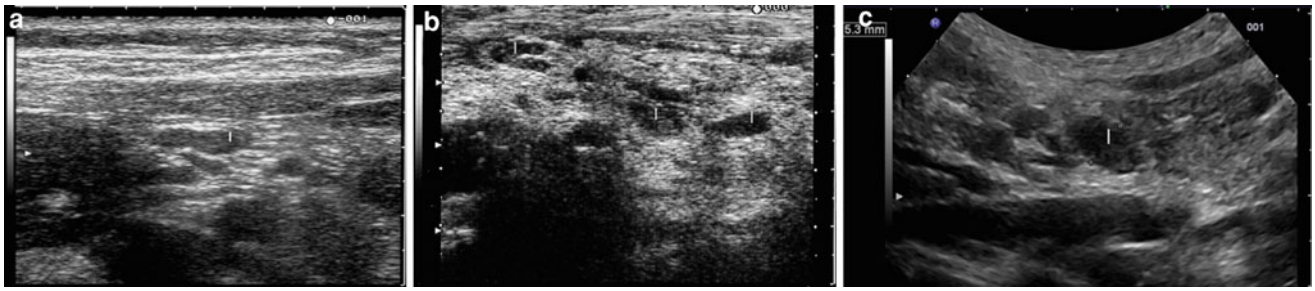

Fig. 1 Ultrasonographic appearance of normal lymph nodes (*l*) as incidental findings in adult patients (**a, b**) and in a child with constipation (**c**)

ongoing abdominal disease, and in this context, to differentiate its benign from malignant nature.

The ultrasonographic criteria of the enlargement of mesenteric lymph nodes have been variably defined as the detection of nodes larger than 4 mm in the short axis (Sivit et al. 1993) and larger than 10 mm in the long axis (Watanabe et al. 1997). This sonographic definition is in agreement with that of a study based on CT studies in an adult population where mesenteric lymphadenitis has been defined as three or more lymph nodes, each 5 mm or greater than 5 mm in the short axis (Macari et al. 2002). However, this size might not be a reliable normal cut-off value in children where it is much more controversial. Karmazyn et al. (2005) showed that mesenteric lymph nodes with a short axis of greater than 5–10 mm are commonly found in children and should be considered a non-specific finding. In this population, a threshold of short axis at least 5 mm for enlarged mesenteric lymph nodes might yield a high percentage (54 %) of false-positive results. In contrast, if a short axis greater than 8 mm was used as a cutoff value, this would yield only a 5 % false-positive rate.

Therefore, the sonographic detection of oval, elongated, U-shaped lymph nodes with a short-axis diameter up to 4 mm in adults and 8 mm in children should be considered a normal finding and should not be misdiagnosed as an early manifestation of a lympho-proliferative disorder.

Normal mesenteric lymph nodes may be routinely identified at the mesenteric root and throughout the mesentery, in particular in right iliaca fossa in children (Karmazyn et al. 2005) and at the mesenteric root in adults (Lucey et al. 2005) (Fig. 1).

Size, site and number of lymphadenopathy detected by abdominal ultrasound may help in suggesting their nature, or atleast in differentiating among their main causes that may be neoplastic, infectious or inflammatory.

3 Neoplastic Conditions

Mesenteric lymphadenopathy may result from metastatic malignancy. The ultrasonographic criteria used to differentiate between benign and malignant cervical nodes, may also be adopted to differentiate benign from malignant enlarged mesenteric lymph nodes. Shape, size and echogenicity can been considered for this purpose. Sonography can determine the long (L) axis, short (S) axis and a ratio of long to short axis. An L/S ratio of <2.0 (namely a round shape of the node) has a sensitivity and a specificity of 95 % for distinguishing benign and malignant nodes. This ratio has greater specificity and sensitivity than measurement of either the long or the short axis alone.

The most common malignancy resulting in mesenteric lymphadenopathy is lymphoma. While lymphoma usually presents as lymphadenopathy of the chest, retroperitoneum or superficial lymph node chains, it is not uncommon to also find mesenteric lymphadenopathy. Enlarged nodes may be seen at the mesenteric root and/or scattered throughout the peripheral mesentery. Early in the course of the disease, the lymph nodes may be small, soft and discrete (Fig. 2).

Table 1 Main diseases associated with mesenteric lymphadenopathy

1. Malignant diseases a. Haematologic (Hodgkin's disease, non-Hodgkin's lymphomas, amyloidosis) b. Metastatic (from numerous primary sites)
2. Immunological diseases a. Crohn's disease b. Ulcerative colitis d. Systemic lupus erythematosus e. Primary sclerosing cholangitis f. Sjögren's syndrome g. Primary biliary cirrhosis
3. Infectious diseases a. Viral (EBV, CMV, viral hepatitis, herpes simplex, adenovirus, HIV) b. Bacterial (*Yersina paratuberculosis,* Salmonella, Shigella, Campylobacter, brucellosis, tuberculosis, atypical mycobacterial infection) c. Parasitic (toxoplasmosis, leishmaniasis, trypanosomiasis, filariasis) d. Chlamydial (lymphogranuloma venereum, trachoma) e. Fungal (histoplasmosis, coccidioidomycosis)
4. Other disorders a. Lipid storage diseases (Gaucher's, Niemann-Pick, Castleman's disease) b. Sarcoidosis c. Familial Mediterranean fever

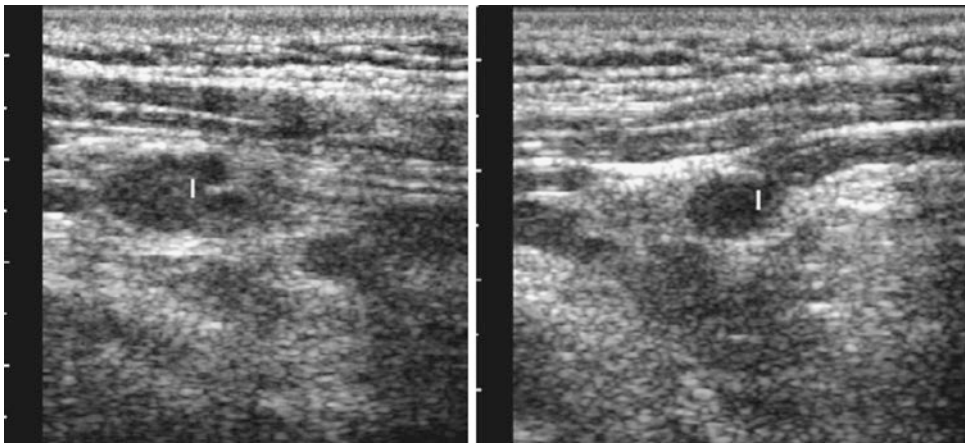

Fig. 2 Enlarged lymph nodes at mesenteric root, in a 52-year-old patient with early intestinal non-Hodgkin lymphoma

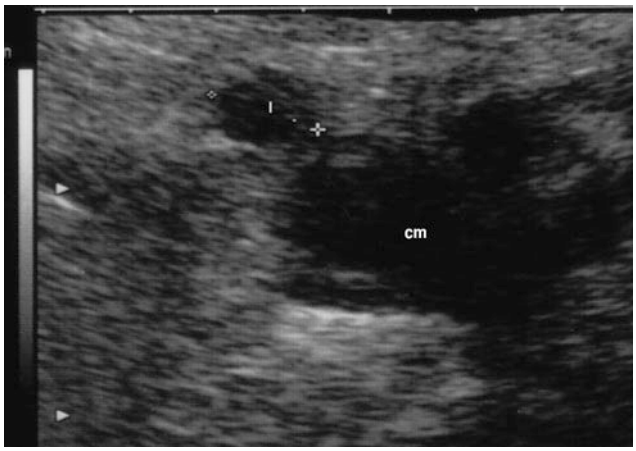

Fig. 3 Conglomerate abdominal mass formed by multiple coalescent lymph nodes (cm) (*l: lymph node*)

As the disease progresses, the enlarged nodes, often coalesce and tend to form a single mass (Fig. 3).

Extensive mesenteric lymphadenopathy due to lymphoma has a characteristic appearance. Mesenteric lymph nodes involved are usually hypoechoic, round and surrounded by hyperechoic mesenteric tissue (Fig. 4). The lymph nodes may also display a cystic appearance (Gorg et al. 1995, 1996a, b; Hollerweger et al. 2008).

Use of power Doppler sonography or contrast-enhanced ultrasound (Sonovue 2.4 ml) to visualise the nodal vascularity can help in differentiating malignant from benign lymph nodes. Malignant nodes show more frequently avascular foci and aberrant and subcapsular vessels compared to benign lymph nodes which show a uniform vascular pattern confined to the hilar vessel only (Neumann-Silkow and Görg 2010; Fig. 5). However, power Doppler sonography or contrast-enhanced ultrasound are not able to correctly identify the specific malignancy and cannot replace US-guided fine needle aspiration, when feasible, or lymph node dissection (Hocke et al. 2008).

Mesenteric lymph node involvement may be also associated with immune proliferative disorders of small intestine (Hermans et al. 2001; Fig. 6).

Primary malignancies that most commonly lead to mesenteric lymphadenopathy include carcinoma of the gastrointestinal tract (in particular, carcinomas of the colon, duodenum and ileum), pancreas and less frequently of the lung, and carcinoid (Fig. 7). Most primary malignancies involve local lymph nodes before more distant metastases are detected.

4 Inflammatory Conditions

Mesenteric lymphadenopathy may be secondary to an underlying inflammatory process, either a localised inflammatory disease or a systemic inflammatory condition.

Local inflammatory causes, leading to mesenteric lymphadenopathy, are due to local mesenteric inflammation generally due to appendicitis, diverticulitis and cholecystitis.

Appendicitis is frequently associated with lymphadenopathy, most commonly in the mesentery of the right lower quadrant. Although lymph nodes may be identified in the mesentery of the right lower quadrant in the normal population, these are usually small and few in number. Multiple enlarged right lower quadrant lymph nodes, in the presence of an abnormal appendix, are useful in the diagnosis of appendicitis, although lymphadenopathy is not necessarily present to make the diagnosis.

Mesenteric lymphadenopathy may also be seen in cases of diverticulitis. The nodes are usually identified close to the area of inflamed colon, generally small but, unfortunately, not specific. In fact, diverticulitis may mimic perforated colonic carcinoma where adjacent enlarged lymph nodes may also be present.

Mesenteric lymphadenopathy is commonly found in patients with inflammatory bowel disease, both Crohn's disease and ulcerative colitis (Maconi et al. 2005), although

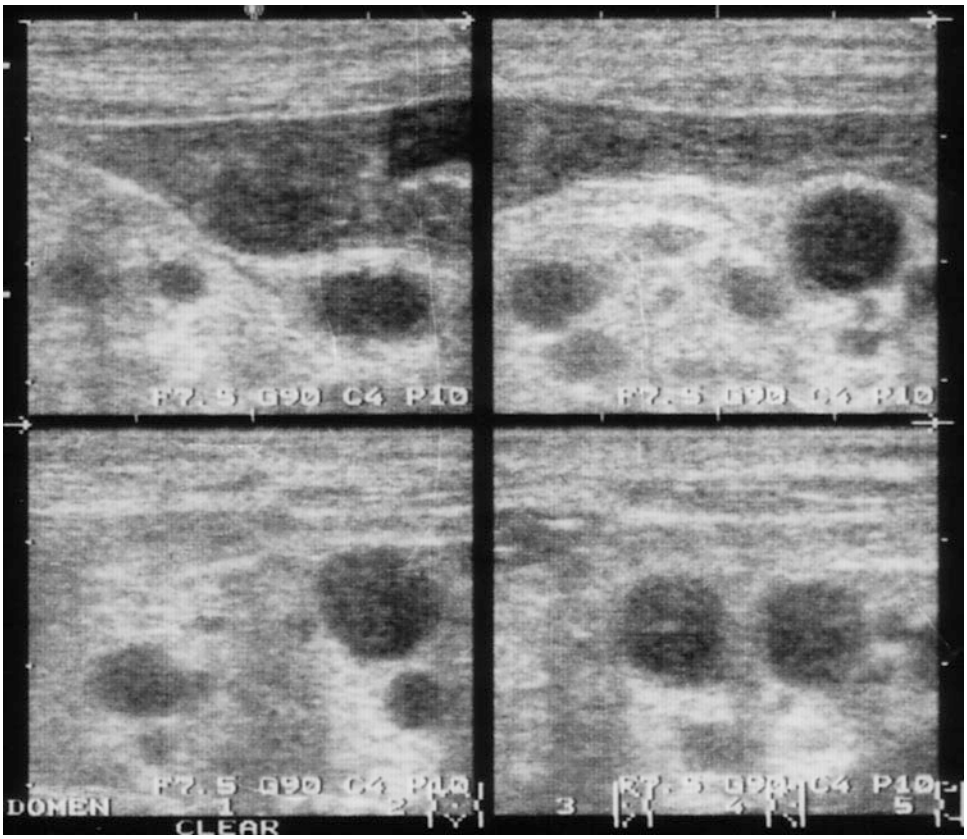

Fig. 4 Typical mesenteric lymph node involvement in lymphoma, presenting as hypoechoic, round lesions surrounded by hyperechoic mesenteric tissue

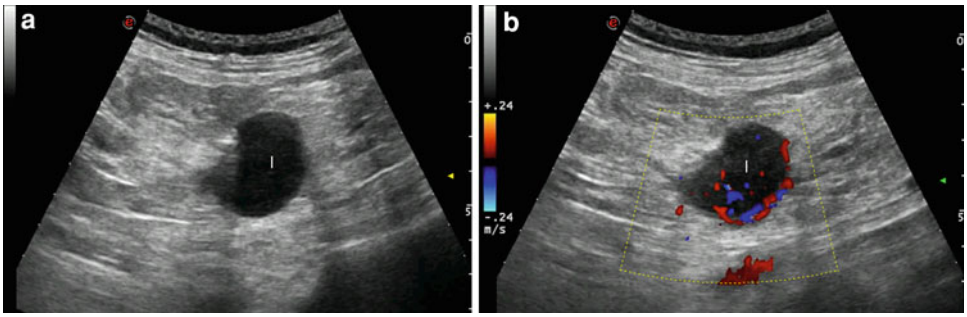

Fig. 5 **a** Ipo-anechoic round lymph node (*l*) at the mesenteric root, resembling a cyst at B-mode examination. **b** The study with colour Doppler ultrasound reveals aberrant and subcapsular vessels, suggesting the malignant nature of the node. After surgical node dissection, the final diagnosis was B-cell non Hodgkin's lymphoma

it is more common in Crohn's disease. The lymph nodes may be found at the mesenteric root, mesenteric periphery or in the right lower quadrant (Fig. 8).

In Crohn's disease, mesenteric lymph nodes are usually described as single or multiple large, hypoechoic oval nodules with homogeneous echogenicity and regular margins, or more rarely as part of a conglomerate mass (Maconi et al. 2005). Therefore, sometimes it may be difficult to distinguish between neoplastic and inflammatory conditions of enlarged abdominal lymph nodes.

The prevalence of mesenteric lymphadenopathy in Crohn's disease may vary, mainly in relation to the age of patients and to the duration of disease, lymph nodes being more frequent in young patients and in those with early disease. In particular, enlarged mesenteric lymph nodes can be detected in more than 50 % of CD patients under 30 years of age (Maconi et al. 2005; Tarjan et al. 2000) and are also a frequent finding in the presence of septic complications such as fistulas and abscesses. On the contrary, the importance of US assessment of lymph nodes, as a marker of Crohn's disease activity, is still controversial so far.

Connective tissue diseases such as systemic lupus erythematosus, systemic sclerosis or rheumatoid arthritis, may also be related to mesenteric lymphadenopathy (Calguneri et al. 2003). In these patients, mesenteric lymphadenopathy

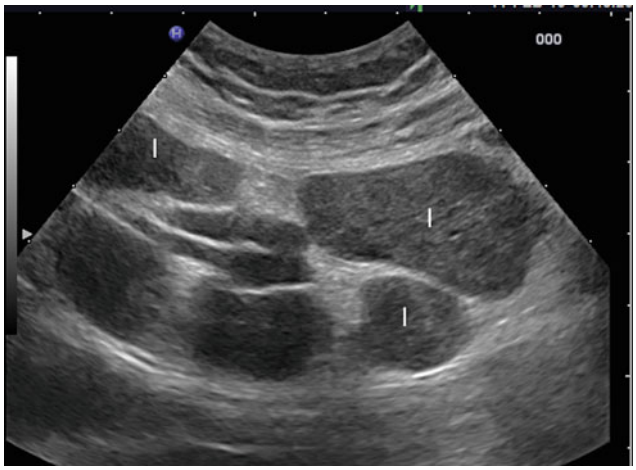

Fig. 6 Large hypoechoic lymph nodes (*l*) at the mesenteric root in a 43-year-old patient with immunoproliferative small intestinal disease (IPSID)

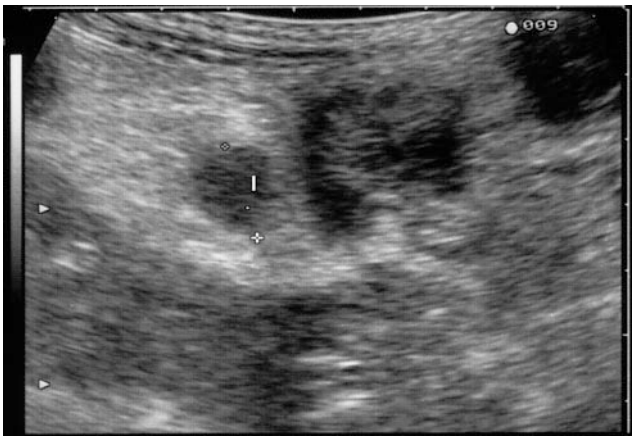

Fig. 7 Regional metastatic lymph node (*l*) involvement in patients with gastro-intestinal cancer presenting as slight hypoechoic, soft and round lesion

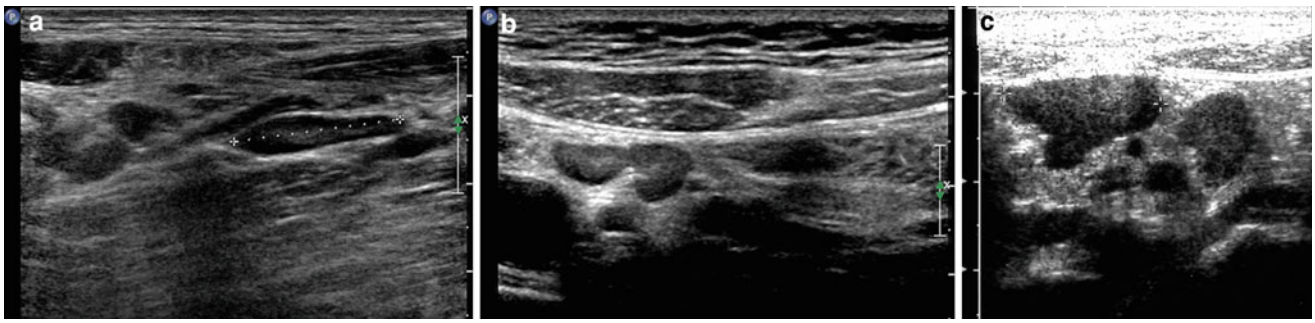

Fig. 8 Mesenteric lymphadenopathy in a 40-year-old female with Crohn's disease (**a, b**) and in a 28-year-old male with early ileal and jejunal Crohn's disease (**c**). US images show multiple peri-intestinal lymphadenopathy in mesentery of right lower quadrant

Fig. 9 Mesenteric lymphadenopathies in a 38-year-old female patient with primary sclerosing cholangitis

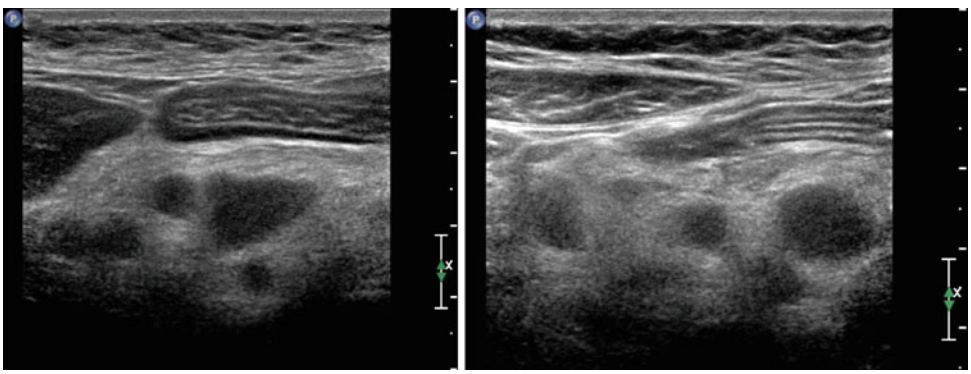

is more frequently an occasional US finding and seldom the only manifestation of lymph node involvement.

In many other inflammatory conditions, mesenteric lymphadenopathy is present, and is seldom the only manifestation of the disease such as: coeliac disease (Fraquelli et al. 2004), primary sclerosing cholangitis (Fig. 9), primary biliary cirrhosis, sarcoidosis and amyloidosis.

In coeliac disease, enlarged lymph nodes are frequently found in the mesenteric root or less commonly at the mesenteric periphery. The lymph nodes are usually oval or elongated (Fig. 10).

Cavitation of mesenteric lymph nodes is rarely seen in coeliac disease or in sprue-like intestinal diseases that fails to respond to a gluten-free diet. It is characterised by central

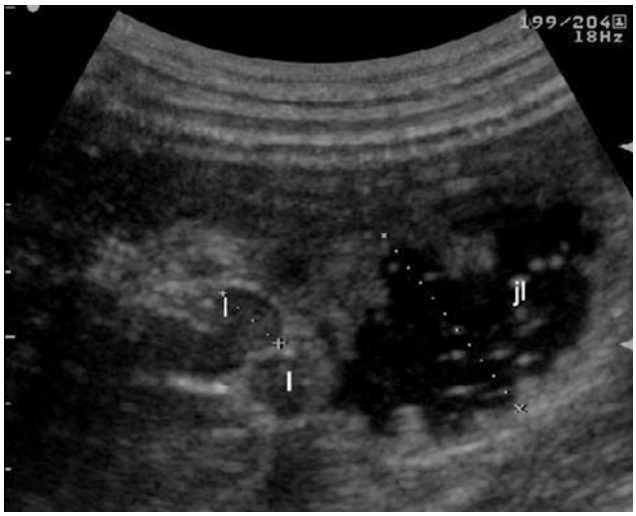

Fig. 10 Ovoidal and elongated lymphadenopathy (*l*) in a 19-year-old male patient with coeliac disease. (*jl*: dilated jejunal loop with liquid content)

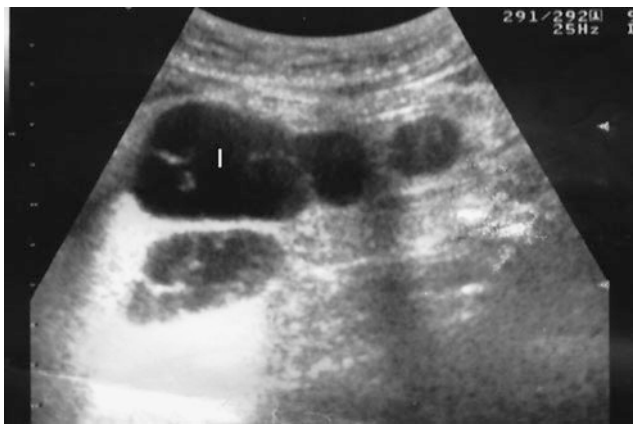

Fig. 11 Cavitated lymph nodes (*l*) in a 48-year-old male patient with refractory coeliac disease

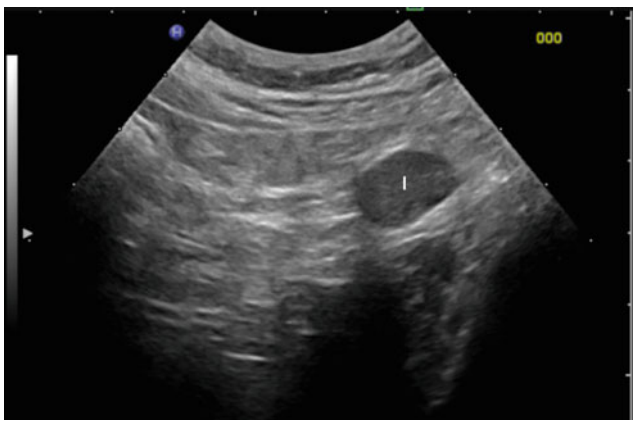

Fig. 12 Large mesenteric lymph node (*l*), in a 52-year-old male patient presenting with diarrhoea and abdominal pain and stool cultures positive for *Yersinia enterocolitica* infection

necrosis of mesenteric lymph nodes. Its cause is not known but its development during the course of the disease is usually indicative of poor prognosis and a potential for significant complications including sepsis and malignancy, particularly T cell lymphoma (Schmitz et al. 2002; Keer et al. 2010; Freeman 2010; Fig. 11).

5 Infectious Conditions

Intestinal infections, either local or systemic, may result in mesenteric lymphadenopathy.

Enlarged mesenteric lymph nodes are frequently detected in various acute infectious conditions, such as *Yersinia ileitis* and other viral or bacterial infectious forms of enterocolitis and pelvic inflammatory diseases, more commonly in the paediatric population (Puylaert 1986; Macari et al. 2002; Rao et al. 1997). Infection with *Yersinia enterocolitica* is characterised by small bowel wall thickening in the right lower quadrant in the region of the terminal ileum, and peri-intestinal regional mesenteric lymphadenopathy (Fig. 12). The clinical features (diarrhoea, fever and abdominal pain), radiological and ultrasonographic findings are similar to those of Crohn's disease (Trommer et al. 1998; Puylaert et al. 1997). Also in other forms of infectious ileocecitis, caused by *Campylobacter jejuni* or *Salmonella enteritidis,* enlarged regional mesenteric lymph nodes together with thickening of the mucosa and (less frequently) submucosa of the ileum, caecum and ascending colon along can be found. Infection with the human immunodeficiency virus (HIV) may produce isolated lymphadenopathy resulting from direct infection by the virus or from secondary infection (Radin 1995; Tarantino et al. 2003). Mesenteric lymphadenopathy in patients with HIV is far more likely to result from an opportunistic infection or even an underlying malignancy than to be caused by direct HIV infection. In this case, the lymph nodes may be enlarged but rarely massive. On the contrary, in HIV positive patients with a CD4 cell count of 50/ml or less, *Mycobacterium avium* complex (MAC) is the main cause of massive mesenteric lymphadenopathy. In HIV patients with mesenteric lymph nodes, in particular if forming a conglomerate mass, MAC infection should always be considered Koh et al. 2003; Tarantino et al. 2003; (Fig. 13).

Enlarged mesenteric lymph nodes in patients with tuberculosis are generally hypoechoic, round to ovoid and variable in size. Sometimes, the nodes may be calcified (Kedar et al. 1994; Malik and Saxena 2003; Tinsa et al. 2010). They are frequently found in the right lower quadrant, around the terminal ileum and caecum (see Chap. 17; Intestinal Tuberculosis).

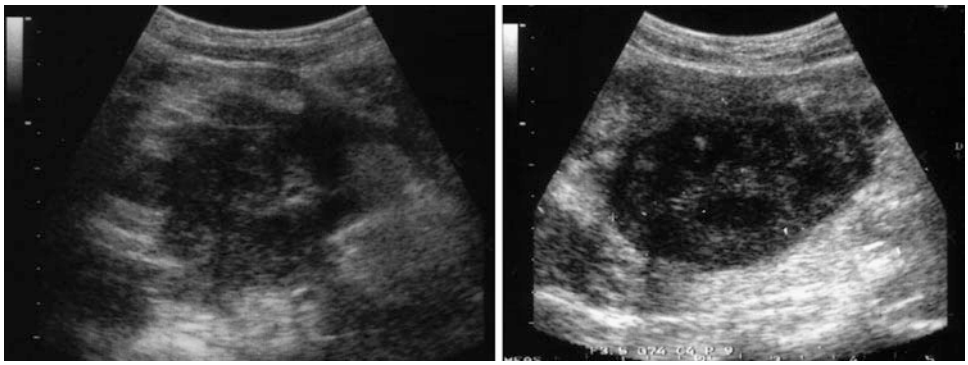

Fig. 13 Mesenteric lymph nodes, forming a conglomerate mass, in a HIV patient with MAC infection

Other causes of mesenteric lymphadenopathy are Whipple disease (see Chap. 14; Lymphangiectasia, Whipple's Disease, Eosinophilic Enteritis) and familial Mediterranean fever. In particular, mesenteric lymphadenopathy has been reported in up to one-third of patients with familial Mediterranean fever during an acute abdominal attack (Zissin et al. 2003).

6 Primary Mesenteric Lymphadenitis

Primary mesenteric lymphadenitis has been defined as right-sided mesenteric lymphadenopathy without an identifiable acute inflammatory process or with a mild (<5 mm) wall thickening of the terminal ileum (Sivit et al. 1993; Vayner et al. 2003, Macari et al. 2002). In most of these cases, an underlying infectious terminal ileitis is thought to be the cause. Mesenteric lymphadenitis is a relatively uncommon cause of acute right lower quadrant pain in adults with a reported variable prevalence between 2 and 14 % (Puylaert 1986; Rao et al. 1997). Its clinical presentation is nonspecific (abdominal pain, fever, leukocytosis) leading to a clinical and imaging differential diagnosis with appendicitis, infectious ileocecitis, diverticulitis, pelvic inflammatory conditions (Lee et al. 2009; Toorenvliet et al. 2011).

References

Calguneri M, Ozturk MA, Ozbalkan Z et al (2003) Frequency of lymphadenopathy in rheumatoid arthritis and systemic lupus erythematosus. J Int Med Res 31:345–349

Fraquelli M, Colli A, Colucci A et al (2004) Accuracy of ultrasonography in predicting celiac disease. Arch Intern Med 64:169–174

Freeman HJ (2010) Mesenteric lymph node cavitation syndrome. World J Gastroenterol 16:2991–2993

Görg C, Weide R, Schwerk WB (1995) Ultrasound assessment of extranodal abdominal lymphoma involvement: an overview. Bildgebung 62:102–108

Gorg C, Weide R, Gorg K, Restrepo I (1996a) Ultrasound manifestations of abdominal lymphomas. An overview. Ultraschall Med 17:179–184

Gorg C, Weide R, Schwerk WB (1996b) Sonographic patterns in extranodal abdominal lymphomas. Eur Radiol 6:855–864

Hermans MM, Klinkhamer P, Stronkhorst A, Creemers GJ (2001) Malabsorption syndrome in a patient of Mediterranean origin; immunoproliferative small intestinal disease. Neth J Med 58:208–213

Hocke M, Menges M, Topalidis T, Dietrich CF, Stallmach A (2008) Contrast-enhancedendoscopic ultrasound in discrimination between benign and malignant mediastinal and abdominal lymph nodes. J Cancer Res Clin Oncol 134:473–480

Hollerweger A, Macheiner P, Neureiter D, Dietze O (2008) Uncommon cystic appearance of lymph nodes in malignant lymphoma. Ultraschall Med 29:308–310

Karmazyn B, Werner EA, Rejaie B, Applegate KE (2005) Mesenteric lymph nodes in children: what is normal? Pediatr Radiol 35:774–777

Kedar RP, Shah PP, Shivde RS, Malde HM (1994) Sonographic findings in gastrointestinal and peritoneal tuberculosis. Clin Radiol 49:24–29

Keer D, Jeon P, Borganonkar M, Potoczny S (2010) Calcified cavitating mesenteric lymph node syndrome: case presentation and literature review. Can J Gastroenterol 24:355–358

Koh DM, Burn PR, Mathews G, Nelson M, Healy JC (2003) Abdominal computed tomographic findings of Mycobacterium tuberculosis and Mycobacterium avium intracellulare infection in HIV seropositive patients. Can Assoc Radiol J 54:45–50

Lee MW, Kim YJ, Jeon HJ et al (2009) Sonography of acute right lower quadrant pain: importance of increased intraabdominal fat echo. AJR Am J Roentgenol 192:174–179

Lucey BC, Stuhlfaut JW, Soto JA (2005) Mesenteric lymph nodes: detection and significance on MDCT. AJR Am J Roentgenol 184:41–44

Macari M, Hines J, Balthazar E et al (2002) Mesenteric adenitis: CT diagnosis of primary versus secondary causes, incidence, and clinical significance in pediatric and adult patients. AJR Am J Roentgenol 178:853–858

Maconi G, Di Sabatino A, Ardizzone S et al (2005) Prevalence and clinical significance of sonographic detection of enlarged regional lymph nodes in Crohn's disease. Scand J Gastroenterol 40:1328–1333

Malik A, Saxena NC (2003) Ultrasound in abdominal tuberculosis. Abdom Imaging 28:574–579

Neumann-Silkow H, Görg C (2010) Differentiation of abdominal lymphadenoptahy with power Doppler sonography. Rofo 182:229–234

Puylaert JB (1986) Mesenteric adenitis and acute terminal ileitis: US evaluation using graded compression. Radiology 161:691–695

Puylaert JB, Van der Zant FM, Mutsaers JA (1997) Infectious ileocecitis caused by Yersinia, Campylobacter, and Salmonella: clinical, radiological and US findings. Eur Radiol 7:3–9

Radin R (1995) HIV infection: analysis in 259 consecutive patients with abnormal abdominal CT findings. Radiology 197:712–722

Rao PM, Rhea JT, Novelline RA (1997) CT diagnosis of mesenteric adenitis. Radiology 202:145–149

Schmitz F, Herzig KH, Stuber E et al (2002) On the pathogenesis and clinical course of mesenteric lymph node cavitation and hyposplenism in coeliac disease. Int J Colorectal Dis 17:192–198

Sivit CJ, Newman KD, Chandra RS (1993) Visualization of enlarged mesenteric lymph nodes at US examination. Pediatr Radiol 23:471–475

Tarantino L, Giorgio A, de Stefano Farella N, Perrotta A, Esposito F (2003) Disseminated mycobacterial infection in AIDS patients: abdominal US features and value of fine-needle aspiration biopsy of lymph nodes and spleen. Abdom Imaging 28:602–608

Tarjan Z, Toth G, Gyorke T, Mester A, Karlinger K, Mako EK (2000) Ultrasound in Crohn's disease of the small bowel. Eur J Radiol 35:176–182

Tinsa F, Essaddam L, Fitouri Z et al (2010) Abdominal tuberculosis in children. J Pediatr Gastroenterol Nutr 50:634–638

Toorenvliet B, Vellekoop A, Bakker R et al (2011) Clinical differentiation between acute appendicitis and acute mesenteric lymphadenitis in children. Eur J Pediatr Surg 21:120–123

Trommer G, Bewer A, Kosling S (1998) Mesenteric lymphadenopathy in *Yersinia enterocolitica* infection. Radiologe 38:37–40

Vayner N, Coret A, Polliack G et al (2003) Mesenteric lymphadenopathy in children examined by US for chronic and/or recurrent abdominal pain. Pediatr Radiol 33:864–867

Watanabe M, Ishii E, Hirowatari Y et al (1997) Evaluation of abdominal lymphadenopathy in children by ultrasonography. Pediatr Radiol 27:860–864

Zissin R, Rathaus V, Gayer G, Shapiro-Feinberg M, Hertz M (2003) CT findings in patients with familial Mediterranean fever during an acute abdominal attack. Br J Radiol 76:22–25

Acute Colonic Diverticulitis and Diverticulosis

Norbert Gritzmann

Contents

Abstract

Sonography can be used as primary diagnostic method in the painful left lower quadrant. Experienced investigators can diagnose acute diverticulitis in more than 90 %. In unclear cases or when complications are suspected, CT should be performed. Sonography can diagnose most differential diagnosis of the painful left lower quadrant as colitis, appenagitis, or hematomas.

1 Introduction

The prevalence of colonic diverticulosis is common in developed countries and has been increasing in the past centuries. In autopsy studies from 1910, diverticulosis was found in about 5 %, in the early 1980s diverticula was seen in about 50 % of autopsy studies (Farag Soliman et al. 2004).

Prevalence clearly increases with age, varying from <10 % in those younger than 40 years, to an estimated 50–66 % of patients older than 80 (Almy and Howell 1980).

There is no apparent sex predilection.

Diverticulosis usual is clinical asymptomatic. About 80–85 % of patients with diverticulosis have no symptoms (Cheskin et al. 1990), but it is predisposing for complications such as diverticulitis, perforation, peritonitis, fistulas and even bleeding. For a clear overview presentation of diverticulosis contrast enema has been the diagnostic gold standard for many years. Diverticulosis can be also diagnosed by colonoscopy. Not only the detection of inflammatory complications but also a clinical asymptomatic diverticulosis can be seen with sonography. In case of inflammation, a cross-sectional imaging like sonography or computed tomography (CT) should be performed to evaluate complications.

N. Gritzmann (✉)
Gruppenpraxis für Radiologie,
Esslinger Hauptstr. 89,
1220 Vienna, Austria
e-mail: norbert.gritzmann@gmail.com

G. Maconi and G. Bianchi Porro (eds.), *Ultrasound of the Gastrointestinal Tract*, Medical Radiology. Diagnostic Imaging,
DOI: 10.1007/174_2012_718, © Springer-Verlag Berlin Heidelberg 2012
Published Online: 17 August 2012

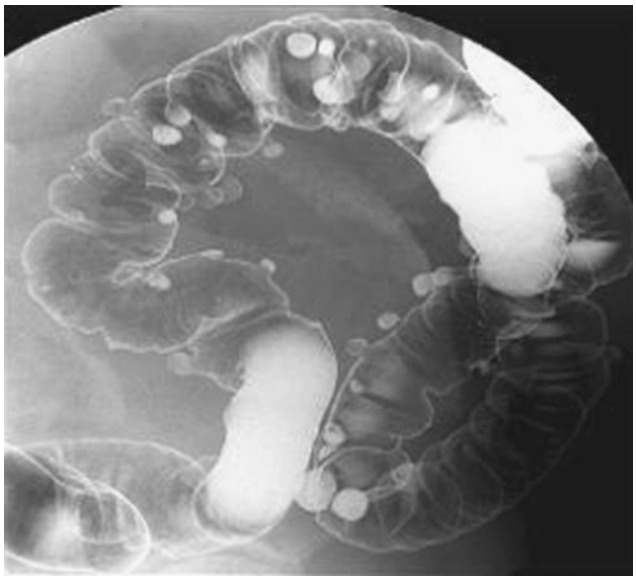

Fig. 1 Barium enema showing diverticulosis of the sigmoid colon

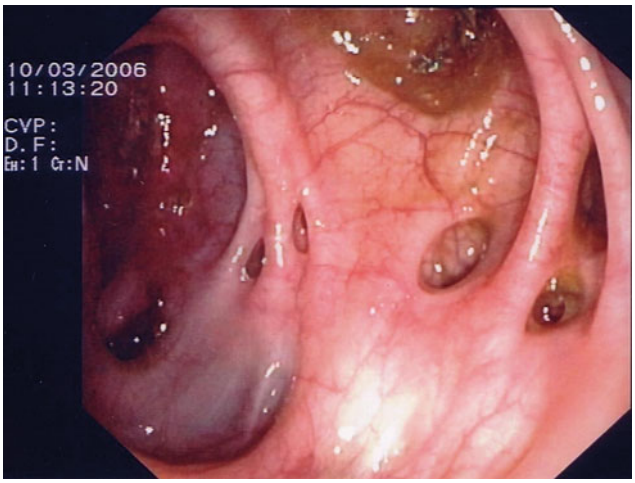

Fig. 2 Endoscopy shows diverticula

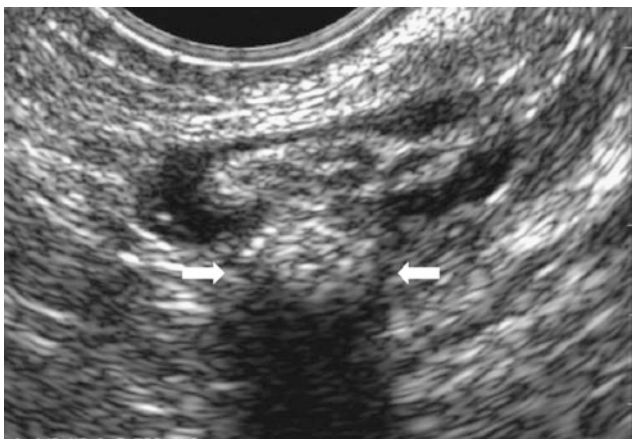

Fig. 3 Transvaginal sonography shows a large echogenic diverticulum (*arrows*) with a posterior acoustic shadow due to air

2 Diverticulosis

Particular left-sided colonic diverticula are pseudodiverticula. They are herniations of the mucosa and submucosa through a weakness in the muscle lining, but do not themselves include the muscle layers surrounding the colon. They herniate adjacent to the points of penetration of the vasa recta through the bowel wall. Diverticula, therefore, tend to be arranged in rows, situated between the mesenteric and lateral taeniae coli (Burkitt et al. 1974).

Diverticula occur mainly in the distal colon, with as many as 90 % of patients having involvement of the sigmoid colon and only 15 % having right-side involvement (Roberts and Veidernheimer 1994).

There are a lot of predisposing factors for getting diverticula. Undoubtedly these mechanisms act synergistically. The cause of colonic diverticula is related primarily to two main factors: increased intraluminal pressure and weakening of the bowel wall (Truelove 1966). Diminished stool bulk, from insufficient dietary fibre, leads to alterations in gastrointestinal transit time and to elevated colonic pressure.

Diverticula can vary in number from solitary findings to literally hundreds. In size, they are typically 5–10 mm in diameter, but can exceed 2 cm. An entity of giant colonic diverticula has been described, with sizes up to 25 cm (Levi et al. 1993).

The frequent appearance of diverticula in cases of Ehlers-Dahnlos syndrome, Marfan syndrome and polycystic kidney disease may cause a congenital weakness of the colonic wall.

In Asia, diverticula can often be found in the right-sided colon. These rare dysontogenetic diverticula are true diverticula, in which all layers of the colon wall are herniated. These patients are often younger than patients with left-sided diverticulosis.

2.1 Diagnostic Methods

Traditionally, contrast enema has been the mainstay in the evaluation of patients suspected of having diverticulosis or acute colonic diverticulitis (Fig. 1).

Barium provides better mucosal detail than water-soluble contrast media. The possibility of perforation is a contraindication to its use, for fear of barium peritonitis. In these situations, water-soluble contrast should be used. Diverticulosis can be also diagnosed by endoscopy (Fig. 2); however,

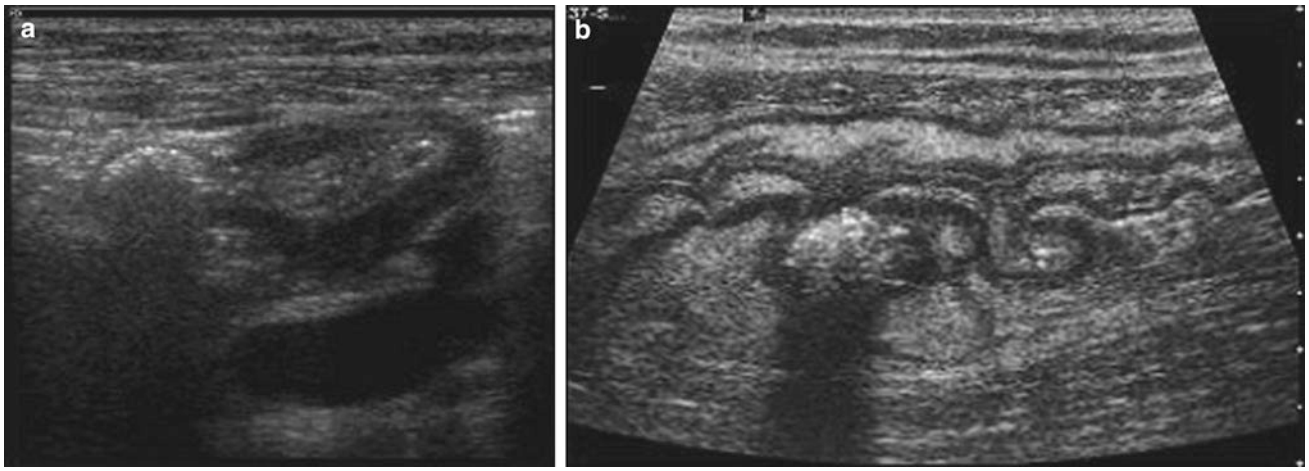

Fig. 4 Sigmoid colon with echogenic diverticulum. **a** Tansverse section with a large echogenic diverticulum. Note the muscular layer of the sigmoid colon (*hypoechogenic rim*) showing hypertrophy. **b** Longitudinal section showing a diverticulum with an echogenic faecolith inside

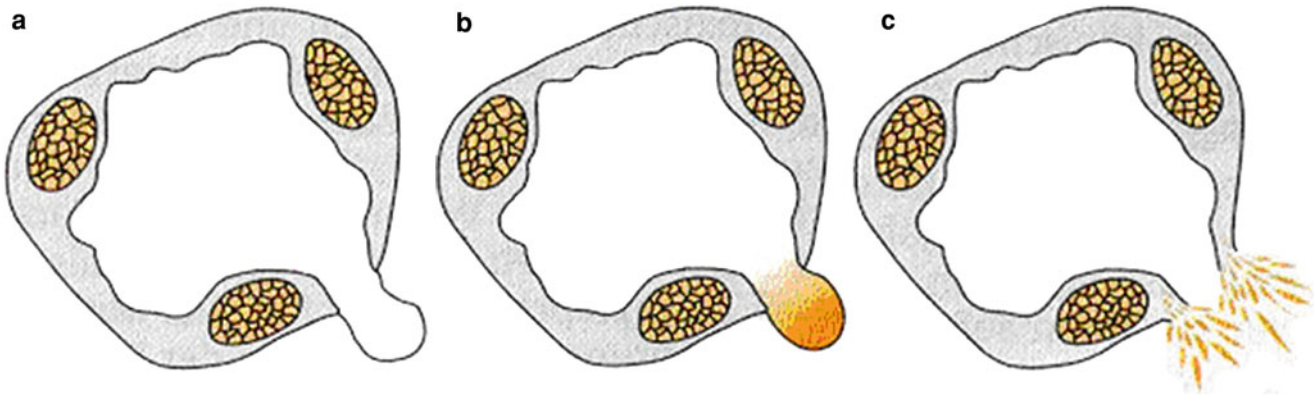

Fig. 5 Diverticulum (**a**) with inflammation (**b**) and perforation with peridiverticulitis (**c**ischaemia). In case of inflammation the diverticulum becomes obstructed by impacted stool in its neck. This faecolith abrades the mucosa and causes low-grade inflammation, blocking drainage even further. The obstruction may then cause an expansion of the normal bacterial flora, diminished venous outflow with localised and altered mucosal defence mechanisms, allowing bacteria to breach the mucosa and extend the process through the full wall, ultimately leading to perforation. The term "perforated" diverticulitis should be reserved for cases in which a peridiverticular abscess has ruptured into the peritoneal cavity and caused a purulent peritonitis

when diverticulitis is suspected clinically, endoscopy is contraindicated. After the acute phase of inflammation the colon should be examined to exclude a colon tumour. So a complete endoscopic colonic evaluation should generally be performed 6–8 weeks after the resolution of a diverticulitis. In case of inflammation, colonoscopy is often incomplete and painful for the patient. The risk for perforation is also higher because of the air insufflation.

Sonography can also diagnose diverticulosis of the left hemicolon in many cases too (Hollerweger et al. 2002; Laméris et al. 2008; Valentino et al. 2009).

Normal diverticula present as hyperechoic protuberances of colonic wall with acoustic shadowing of variable intensity (Fig. 3).

The sonographic appearance depends on the content of the diverticula. In most cases, the diverticula appear hyperechoic because of the air inside. Such echoic diverticula show typical air artefacts up to complete acoustic shadowing. Hyperechoic diverticula with clear acoustic shadowing are typical for a faecolith inside of the diverticulum (Fig. 4).

The diverticular wall is thin and often not demonstrable at sonography. Large diverticula may be misdiagnosed as haustrations.

In multi-detector computed tomography (MDCT) the air-filled protuberances are usually easier to diagnose than with sonography. Often it is difficult sonographically to differentiate small faecoliths from air within diverticula.

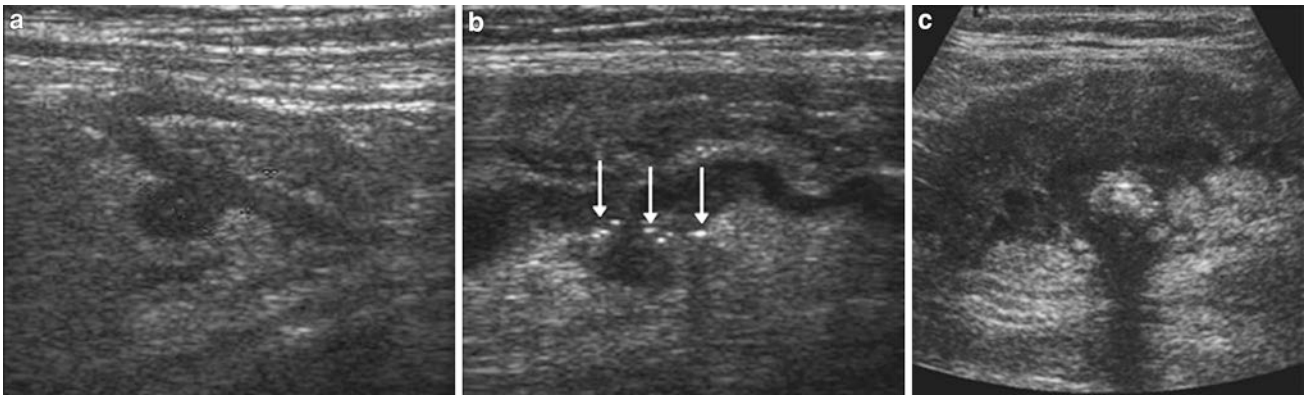

Fig. 6 Acute colonic diverticulitis. **a** Hypoechoic diverticulum with a surrounding moderate echogenic inflammation. **b** Longitudinal section of the sigmoid colon shows an echo-poor diverticulum with surrounding little air spots (*arrows*) as sign for microperforation. **c** Extensive inflammatory thickening of the sigmoid colon with an echogenic faecolith in the diverticulum

In a study, the accuracy of sonography in diagnosing diverticulosis was approximately 60 % (Hollerweger et al. 2002).

3 Diverticulitis

Acute colonic diverticulitis is a common cause of acute abdominal symptoms, especially in elderly patients. In turn, diverticulitis develops in 10–25 % of the population with diverticulosis (Roberts et al. 1995).

It is, in virtually all cases, the result of a microperforation of a single diverticulum (Fig. 5).

The clinical diagnosis and assessment of acute colonic diverticulitis can be difficult (Chappuis and Cohn 1988). The classic pattern of left lower quadrant pain, tenderness, fever and leukocytosis is suggestive of acute colonic diverticulitis but can be mimicked by numerous acute abdominal conditions. Symptoms such as nausea, vomiting, constipation or diarrhoea lead to a high rate of wrong diagnosis up to 34 % of cases.

Dysuria and urinary frequency and urgency may occur if the affected colonic segment lies close to the urinary bladder, and afferent visceral nerves from the inflamed colon, by way of the sacral plexus, may carry referred pain to the scrotum or suprapubic region.

If nearby organs become involved, or if an abscess ruptures into a nearby organ, a fistula may result. Colovesical fistulae are the most frequent type, followed by colovaginal and, less commonly, by colocutaneous fistulae.

Although 85 % of cases of diverticulitis occur in the sigmoid and descending colon, diverticula may be found throughout the colon. Right-sided diverticulitis occurs with greater frequency in Asians and tends to follow a more benign course than that which occurs on the left side (Wada et al. 1990).

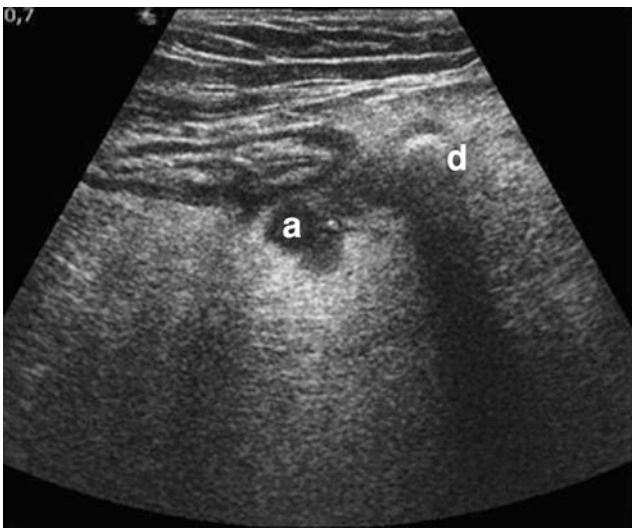

Fig. 7 Echoic diverticulum (*d*) with a nearby small peridiverticular hypoechogenic abscess (*a*)

In acute colonic diverticulitis, ultrasound can evaluate the disease with the same four criteria used with CT (Wilson and Toi 1990): (a) thickening of the bowel wall, (b) diverticula, (c) the echogenicity of these foci varying from hypoechoic (Fig. 6a to predominantly hyperechoic with a surrounding hypoechoic rim (Fig. 6b and hyperechoic with or without internal acoustic shadowing (Hollerweger et al. 2001); and (d) inflammatory pericolonic fat frequently recognised as an adjacent hyperechoic halo. Small air bubbles can be visualised as a sign for microperforation (Fig. 6c; therefore sonographic demonstration of extraluminal hyperechoic foci indicates mesenteric gas.

Longitudinal, linear echogenic tracts are suggestive of fistulous tracts. Thickening of the sigmoid colon along with the roof of the bladder and air within the bladder are signs

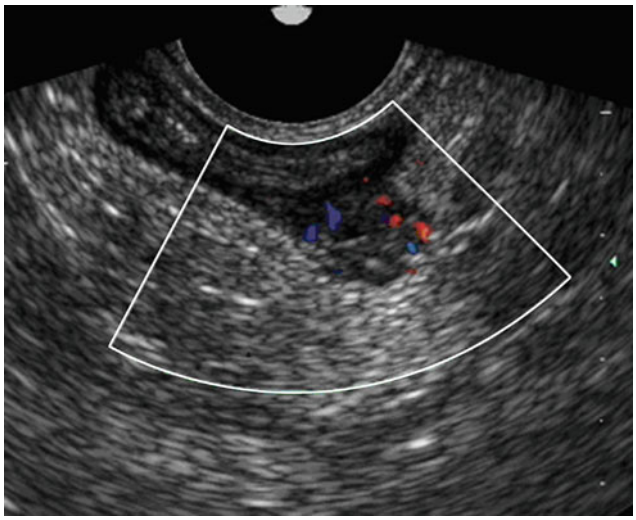

Fig. 8 Transrectal scan with 7.5 MHz probe showing an hypoechogneic diverticulum with moderate hypervascularisation and hyperechogenicity of the fat due to moderate inflammation

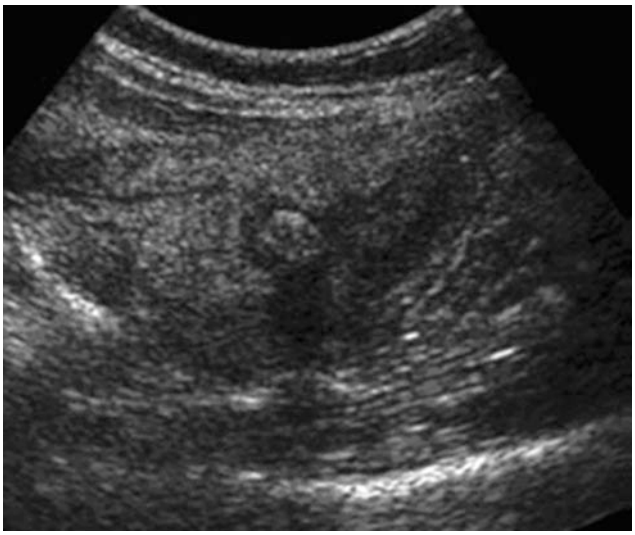

Fig. 9 Right-sided diverticulitis. An echogenic diverticulum with surrounding hyperechogenic fat is visualised

highly suggestive for a fistula into the bladder. Sonography can be limited for assessing large and complex abscesses (Fig. 7). Overall the accuracy of sonography in diagnosing diverticulitis is more than 90 % (Hollerweger et al. 2001; Gritzmann and Hübner 2006; Laméris et al. 2008).

Transrectal (Fig. 8) or endovaginal (Fig. 3) sonography can increase the sensitivity of ultrasound when the distal sigmoid or the small pelvis is affected (Hollerweger et al. 2000; Hollerweger 2007). This localisation is frequently obscured by overlaying bowel-loops gas in transabdominal sonography.

Right-sided diverticulitis may be diagnosed sonographically (Fig. 9; Wada et al. 1990). Usually large diverticula are present. In such instances, the main differential diagnosis is appendicitis. The prognosis of right-sided diverticulitis is usually good using conservative treatment. In this context, imaging procedures are important in the differential diagnosis.

In rare cases the appendix vermiformis may show diverticulitis (Macheiner et al. 1999).

At most hospitals, CT has replaced barium enema examination of the colon for diagnosis of suspected diverticulitis. Compared with sonography the operator dependency is less (Ambrosetti et al. 1997).

One of the reasons is that diverticulitis is primarily an extramural process, and barium enema diagnosis depends on the secondary effects on the barium column caused by the extramucosal manifestations of acute inflammation.

The signs of a moderate diverticulitis in CT are colonic wall thickness >5 mm associated with inflammation of the pericolonic fat (fat stranding).

In cases of a pericolonic abscess or other complications CT should be performed to evaluate the correct extensions of the inflammatory variances such as wall thickening with pericolic fat involvement (Ambrosetti et al. 1997).

Intravenous contrast should be given especially when an associated abscess was suspected (Fig. 10; Brengman and Otchy 1998).

Care must be taken with interpretation of the results. The patients with colonic carcinoma often have findings similar to that of diverticulitis with conventional CT criteria such as wall thickening with pericolonic fat involvement (Ambrosetti et al. 1997). Also, with CT the specificity increases when a diverticulum can be found in the inflammatory process. In chronic diverticulitis the degree of stenosis of the colonic lumen can be visualised better with CT. Bleeding of diverticula is usually difficult to localise by imaging. Angiography may be indicated. Nuclear medicine studies may be performed to localise unclear intestinal bleeding.

3.1 Differential Diagnosis

The differential diagnosis of acute diverticulitis is wide (Table 1; Gritzmann et al. 2002). One important reason for left lower quadrant pain can be a torsion or necrosis of appendices epiploicae of the left colon. A well-defined point of pain is typical, and is the effect of a local peritonitis.

At sonography, the torsion appears as hyperechoic fatty ovoid appendices beside the colon wall. Often these lesions are adherent to the peritoneum.

Table 1 Differential diagnosis of left-lower quadrant pain

Differential diagnosis of left-lower quadrant pain
Diverticulitis
Appenangitis
ischaemic colitis
Bowel obstruction
Adnexitis/torsion
Ectopic pregnancy
Left ureter stone
Psoas/rectus haematoma

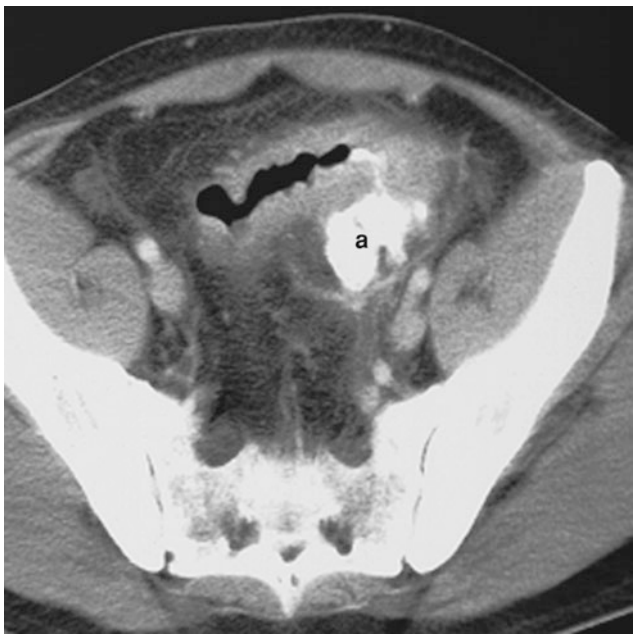

Fig. 10 CT scan of a large perisigmoid abscess that is filled with contrast media (*a*)

Any forms of colitis, such as pseudomembranous colitis, acute ulcerative colitis or Crohn's colitis can also mimic diverticulitis. Usually pseudomebranous colitis is associated with antibiotic therapy. In most cases a significant thickening of the colonic walls are found.

Crohn's disease may present with abdominal pain, fever and leucocytosis. Fistulas can complicate both diseases. Apthous ulcers, anorectal involvement and chronic diarrhoea should alert the clinician to this possible diagnosis.

Usually segmental transmural thickening of the colon and/or the small bowel is seen sonographically. A sub-ileus may be seen.

Colon carcinoma and diverticulosis both affect mainly the distal colons of ageing patients in western countries; both can present with perforation, obstruction or fistula formation. Differentiation obviously has critical prognostic importance. Chronic symptoms of weight loss or bleeding should raise suspicion for carcinoma. In carcinomas usually a circumscribed thickening of the colon is seen. In some cases it is not possible to differentiate diverticulitis from a perforated tumour by imaging methods.

Elderly people with diverticulosis may also have diffuse atherosclerotic vascular disease and thus are also at risk for ischaemic colitis. Ischaemic colitis is found frequently on the left side. Often the thickening is sharp bordered to the normal colon. A thickening with diminished vascularisation is highly suspicious for ischaemic colitis. However, colour signals in a thickened bowel loop do not exclude ischaemia, since non occlusive ischaemia may be present. Gynaecologic disorders such as ruptured ovarian cysts, ovarian torsion, ectopic pregnancy or pelvic inflammatory disease, can resemble acute diverticulitis in female patients but often these patients are younger. Transvaginal sonography may be helpful in obtaining an accurate diagnosis. Stone of the ureter on the left side may simulate diverticulitis.

4 Conclusions

Sonography can diagnose diverticulosis with an accuracy of approximately 60 %. Most diverticula present as echogenic protrusions in some cases they are hypoechogenic. In most cases, diverticulitis sonographically presents as peridiverticular inflammation. Often microperforations are present. The peridiverticular inflammation of the fat is primarily hyperechogenic, and in advanced cases hypoechogenic.

Performed by an experienced investigator, sonography shows results comparable to those of CT in diagnosing acute diverticulitis, and an accuracy of >90 % can be reached. If complications, such as abscess formation or fistulas, are suspected, CT should be performed. In distal sigmoid localisation transrectal examination provide high resolution images with a high specificity.

References

Almy TP, Howell DA (1980) Diverticular disease of the colon. N Engl J Med 302:324–331

Ambrosetti P, Grossholz M, Becker C et al (1997) Computed tomography in acute left colonic diverticulitis. Br J Surg 84:532–534

Brengman ML, Otchy DP (1998) Timing of computed tomography in acute diverticulitis. Dis Colon Rectum 41:1023–1028

Burkitt DP, Walker ARP, Painter NS (1974) Dietary fiber and disease. JAMA 229:1068–1074

Chappuis CW, Cohn I (1988) Acute colonic diverticulitis. Surg Clin North Am 68:301–313

Cheskin LJ, Bohlman M, Schuster MM (1990) Diverticular disease in the elderly. Gastroenterol Clin North Am 19:391–403

Farag Soliman M, Wustner M, Sturm J et al (2004) Primary diagnostics of acute diverticulitis of the sigmoid. Ultraschall Med 25:342–347

Gritzmann N, Hübner E (2006) Sonography in acute diverticulitis of the sigmoid colon. Praxis (Bern 1994) 95:625–629

Gritzmann N, Hollerweger A, Macheiner P, Rettenbacher T (2002) Transabdominal sonography of the gastrointestinal tract. Eur Radiol 12:1748–1761

Hollerweger A (2007) Colonic diseases: the value of US examination. Eur J Radiol 64:239–249

Hollerweger A, Rettenbacher T, Macheiner P et al (2000) Sigmoid diverticulitis: value of transrectal sonography in addition to transabdominal sonography. AJR Am J Roentgenol 175:1155–1160

Hollerweger A, Macheiner P, Rettenbacher T et al (2001) Colonic dicerticulitis: diagnostic value and appearance of inflamed diverticula—sonographic evaluation. Eur Radiol 11:1956–1963

Hollerweger A, Macheiner P, Hubner E et al (2002) Colonic diverticulosis: a comparison between sonography and endoscopy. Ultraschall Med 23:41–46

Laméris W, van Randen A, Bipat S et al (2008) Graded compression ultrasonography and computed tomography in acute colonic diverticulitis: meta-analysis of test accuracy. Eur Radiol 18:2498–2511

Levi DM, Levi JU, Roger AL et al (1993) Giant colonic diverticulum: an unusual manifestation of a common disease. Am J Gastroenterol 88:139–142

Macheiner P, Rettenbacher T, Hollerweger A et al (1999) Diverticulitis of the appendix vermiformis: ultrasonographic appearance. Ultraschall Med 20:115–117

Roberts PL, Veidernheimer MC (1994) Current management of diverticulitis. Adv Surg 27:189–208

Roberts PL, Abel M, Rosen L et al (1995) Practice parameters for sigmoid diverticulitis—supporting documentation. Dis Colon Rectum 38:126–132

Truelove SC (1966) Movements of the large intestine. Physiol Rev 46:457–512

Valentino M, Serra C, Ansaloni L et al (2009) Sonographic features of acute colonic diverticulitis. J Clin Ultrasound 37:457–463

Wada M, Kikuchi Y, Doy M (1990) Uncomplicated acute diverticulitis of the cecum and ascending colon. Sonographic findings in 18 patients. AJR Am J Roentgenol 155:283–287

Wilson SR, Toi A (1990) The value of sonography in the diagnosis of acute diverticulitis of the colon. AJR Am J Roentgenol 154:1199–1202

Intestinal Obstruction

Jae Hoon Lim

Contents

Abstract

The diagnosis of bowel obstruction used to be made by means of clinical history, physical examination, plain abdominal radiography, and in particular multidetector CT scanning that is very useful in revealing the level and cause of obstruction. Sonography is less helpful than CT in patients with intestinal obstruction due to the presence of abundant gas in the intestinal tract, which prevents the satisfactory examination of the abdomen and the detection of adhesions, the most common cause of intestinal obstruction. However, when the obstructed bowel segments are dilated and filled with fluid, the dilated segments of the bowel loops are well demonstrated and the cause of obstruction can be demonstrated by sonography using fluid-filled bowel as a sonic window. Judicious use of sonography in evaluating patients with bowel obstruction may be helpful in confirmation of the presence of obstruction, in determination of the level of obstruction, and in identification of the cause of obstruction.

1 Introduction

The diagnosis of bowel obstruction used to be made by means of clinical history, physical examination, and plain abdominal radiography. However, the abdominal radiographs are not confirmatory or are even confusing, and the cause of obstruction is rarely detected. For the management issue to initiate immediate surgical intervention or to recommend a trial of conservative management, it is mandatory to identify the cause of bowel obstruction. Barium studies are not always satisfactory (Herlinger and Maglinte 1989; Mucha 1987; Dunn et al. 1984). CT has been shown to be useful in revealing the level and cause of obstruction (Megibow 1991; Taourel et al. 1995), and recently, multidetector CT scanning was proven to be very useful (Sinha and Verma 2005a, b). Furthermore, multiplanar reformatted

J. H. Lim (✉)
Department of Radiology and Center for Imaging Science, Samsung Medical Center, Sungkyunkwan University School of Medicine, 50 Ilwon-dong, Kangnam-ku, Seoul 135-710, Korea
e-mail: jhlim@smc.samsung.co.kr

G. Maconi and G. Bianchi Porro (eds.), *Ultrasound of the Gastrointestinal Tract*, Medical Radiology. Diagnostic Imaging,
DOI: 10.1007/174_2013_798, © Springer-Verlag Berlin Heidelberg 2013
Published Online: 17 February 2013

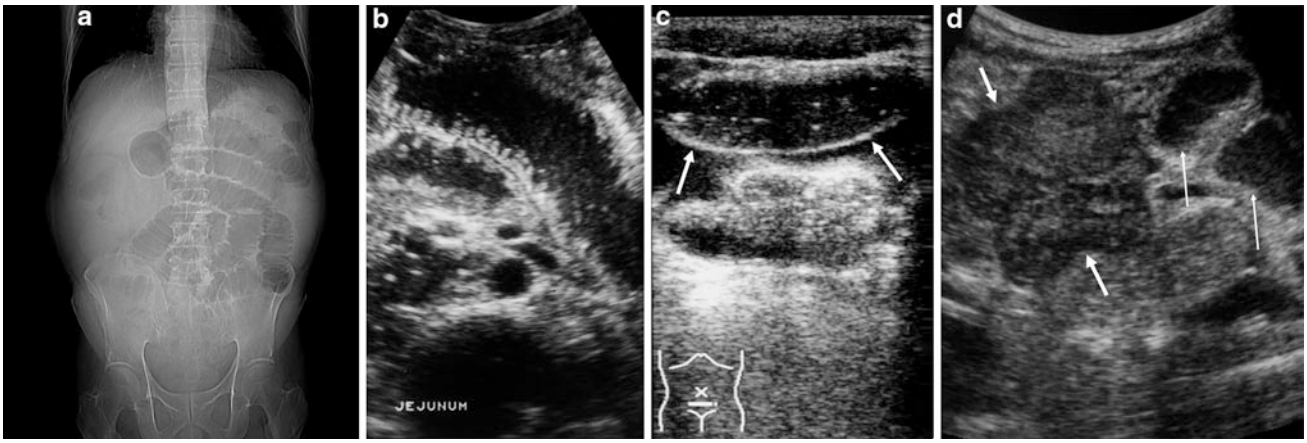

Fig. 1 Ileal obstruction due to stromal tumor. **a** Abdominal radiograph in supine position shows multiple dilated jejunal loops filled with gas. Dilated ileal loops are not visible because they are filled with fluid. These fluid-filled bowel loops are good acoustic window through which the dilated bowel loops and the cause of obstruction can be visualized. **b** Sonogram of the jejunum shows dilatation with markedly increased peristalsis, the fluid and tiny gas bubbles moving actively in the dilated bowel lumen. Note thick and compact valvulae conniventes. **c** Sonogram of the ileum shows dilatation with increased peristalsis. Note virtually absent valvulae conniventes (*arrows*). **d** Sonogram of the lower abdomen discloses a lobulated tumor (*short arrows*) arising from the ileum. Note dilated ileal loops (*long arrows*)

imaging may help to identify the site, level, and cause of obstruction and increase diagnostic confidence (Furukawa et al. 2001) when axial CT findings are indeterminate, and therefore, multidetector CT is becoming the first-line diagnostic method in the diagnosis of bowel obstruction (Patak et al. 2005).

Sonography is not considered helpful in most patients with intestinal obstruction. This is easily appreciated if one remembers that the presence of abundant gas in the intestinal tract prevents satisfactory examination of the abdomen and that adhesions, the most common cause of intestinal obstruction, are not visible on a sonogram (Wilson 1991). However, when the obstructed bowel segments are dilated and filled with fluid, the dilated segments of the bowel loops are well demonstrated and the cause of obstruction can be demonstrated by sonography using fluid-filled bowel as a sonic window (Fig. 1). Judicious use of sonography in evaluating patients with bowel obstruction may be helpful in confirmation of the presence of obstruction, in determination of the level of obstruction, and in identification of the cause of obstruction (Ko et al. 1993a).

The use of sonography in the era of multidetector CT scanning is controversial. CT diagnosis of intestinal obstruction has decided advantage in terms of accuracy in diagnosis of bowel obstruction and in demonstration of the cause. Furthermore, interpretation of multidetector CT images is not so operator dependant as sonography. However, sonography is much more widely available than multidetector CT scanner, much cheap, and there is no radiation hazard. Therefore, sonographic examination may be tried in patients with normal plain radiographs or gasless abdomen, suspected obstruction in proximal bowel loops, in children, or in pregnant women (Ko et al. 1993b).

2 Pathology of Bowel Obstruction

Bowel obstruction is characterized by dilatation of the intestinal segments proximal to the site of obstruction and collapse of the segment distal to the obstruction. The dilated bowel contains a large amount of fluid, food stuff, or gas. There is increased peristalsis to attempt to pass the luminal content beyond the obstruction site. Bowel obstruction can be due to obturation by blockage of the lumen by bowel content, such as food stuff, bezoar, or gallstone, due to bowel wall abnormality, such as neoplasm or stenosis, and due to extrinsic causes, such as adhesion and hernia. In paralytic ileus, bowel is dilated and filled with fluid and gas, but there is no peristaltic movement.

3 Small Bowel Obstruction

Characteristic sonographic findings of small bowel obstruction are demonstration of dilated bowel loops with active peristalsis (Ko et al. 1993a). Multiple segments of dilated bowel loops can be readily demonstrated when the lumen is filled with fluid. The fluid may be clear or there may be air bubbles or debris. The dilated loops are continuous, the diameter of bowel lumen being over 2.0 cm and the segments being longer than 10 cm. Valvulae conniventes or intestinal folds are prominent and compact along the jejunum and thin and sparse along the ileum (Fig. 1). Sometimes, there is no valvular conniventes in the distal ileum and the bowel wall is flat. Increased peristalsis of the proximal segment of the bowel can be directly observed. The dilated bowel loop changes in caliber as well as in

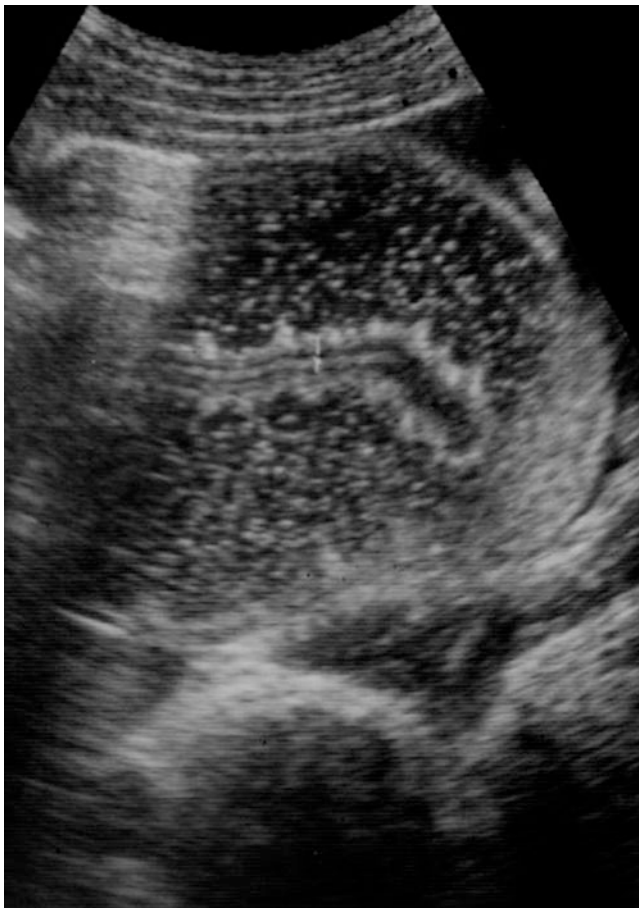

Fig. 2 Increased peristalsis. Sonogram of the jejunum shows dilated loop with increased peristalsis. The dilated loop shows vigorous change in caliber and in position. Tiny gas bubbles in the lumen show to-and-fro and whirling motion

position, very vigorously, sometimes with some pauses. The fluid and tiny gas bubbles in the involved bowel show to-and-fro or whirling motion (Fig. 2). When the lumen is filled with gas, bowel dilatation is not easily recognized and it is difficult to make a diagnosis of bowel obstruction with sonography (Fig. 3). Usually, bowel contains both fluid and gas. Sonographer should try to avoid gas filled lumen by pressing the abdomen with transducer or change the position of the patient.

The causes of bowel obstruction can be demonstrated (Ko et al. 1993a). Small bowel bezoar is usually caused by persimmons and orange, sometimes by cabbage, sauerkraut, potato peel or grapefruit. Patients who had subtotal gastrectomy or gastrojejunostomy are prone to develop bezoars.

Sonographically, bezoars are seen as an intraluminal mass with hyperechoic arclike surface casting clear posterior acoustic shadow (Fig. 4) (Ko et al. 1993b; Tennenhouse and Wilson 1990). Phytobezoar or trichbezoar are same in sonographic appearances. The obstructed small bowel loops usually contain a large amount of air and bezoars can be overlooked if sonographic examination is not done meticulously. Sonographic findings of gallstone ileus are identical to those of bezoars (Fig. 5) (Ko et al. 1993a, b; Davir 1991). Air in the biliary tree or nonvisualization of the gallbladder lumen may be a clue for gallstone ileus.

Small bowel tumor, either primary or metastatic, can be identified as a cause of bowel obstruction (Ko et al. 1993a). At the end of dilated small bowel or between the dilated bowel loops, a tumor can be identified when the tumor is sizable (Fig. 1). Fluid within the bowel may comes in direct contact with the mass indicating the mass arises from the bowel. There may be vascular structure in the mass visualized by applying Doppler study. Small bowel intussusception can be diagnosed by demonstration of bowel-within-bowel by recognizing characteristic multiple concentric rings, caused by invaginating layers of telescoped bowel, seen in cross section of the bowel loop.

Intestinal adhesion, the most frequent cause of bowel obstruction, cannot be demonstrated on sonography. Similarly, internal hernia and congenital fibrotic band can be rarely identified on sonography. Previous history of abdominal operation in patients without sonographically visible cause of obstruction can lead to a diagnosis of adhesive ileus.

By virtue of demonstrating the vascular flow signal from the vessels of the dilated bowel wall, sonography may aid in demonstrating the bowel segment at risk of strangulation. The sonographic finding of a thickened bowel wall, valvulae conniventes, and localized ascites within the leaves of the small bowel mesentery, is suggestive of complicated obstruction such as infarction or gangrene, and these cases require rapid surgical decompression (Ko et al. 1993a).

It has been reported that the accuracy of preoperative sonography in establishing the diagnosis of small bowel obstruction was 89 % (Ko et al. 1993a). The cause of obstruction, such as tumor, bezoar, gallstone, or recurrent cancer in afferent loop syndrome may be predicted (Ko et al. 1993a, b; Meiser and Meissner 1985). Sonography has decided advantages in the diagnosis of proximal obstruction, such as duodenal or proximal jejunal obstruction (Ko et al. 1993a, b): In these cases, simple abdominal radiographs are often normal or do not show gas because frequent vomiting results in lack of air in the obstructed segment (Fig. 6). Afferent loop syndrome can be reliably diagnosed with sonography (Lee et al. 1991). The superior mesenteric artery and vein are useful landmarks in the diagnosis of duodenal obstruction such as afferent loop or proximal jejunal obstruction, since the dilated lumen of the third portion of the duodenum crosses the midline anterior to the aorta and behind the superior mesenteric artery and vein (Fig. 7). By careful examination, recurrent tumor at the gastric stump as a cause of afferent loop can be diagnosed sonographically (Lee et al. 1991).

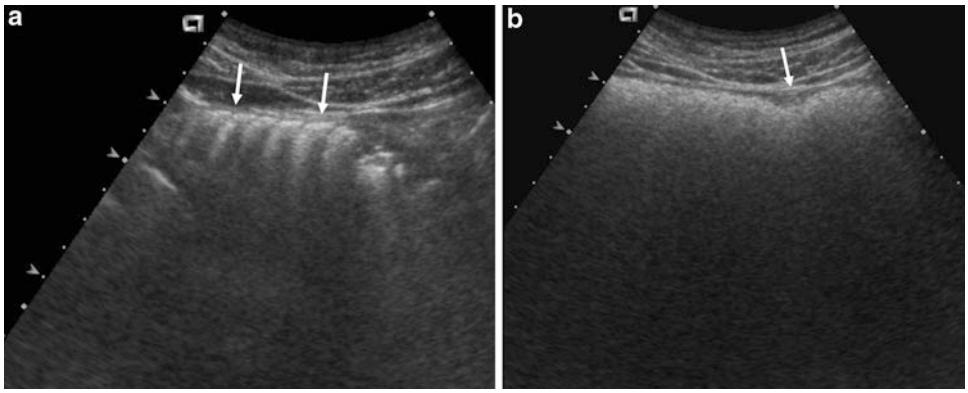

Fig. 3 Gas filled distended bowel loops. **a** Sonogram of the gas filled jejunum shows air-trapping in the valvulae conniventes (*arrows*). **b** Sagittal sonogram along the right side abdomen shows gas filled, distended ascending colon. Note a haustral indentation (*arrow*)

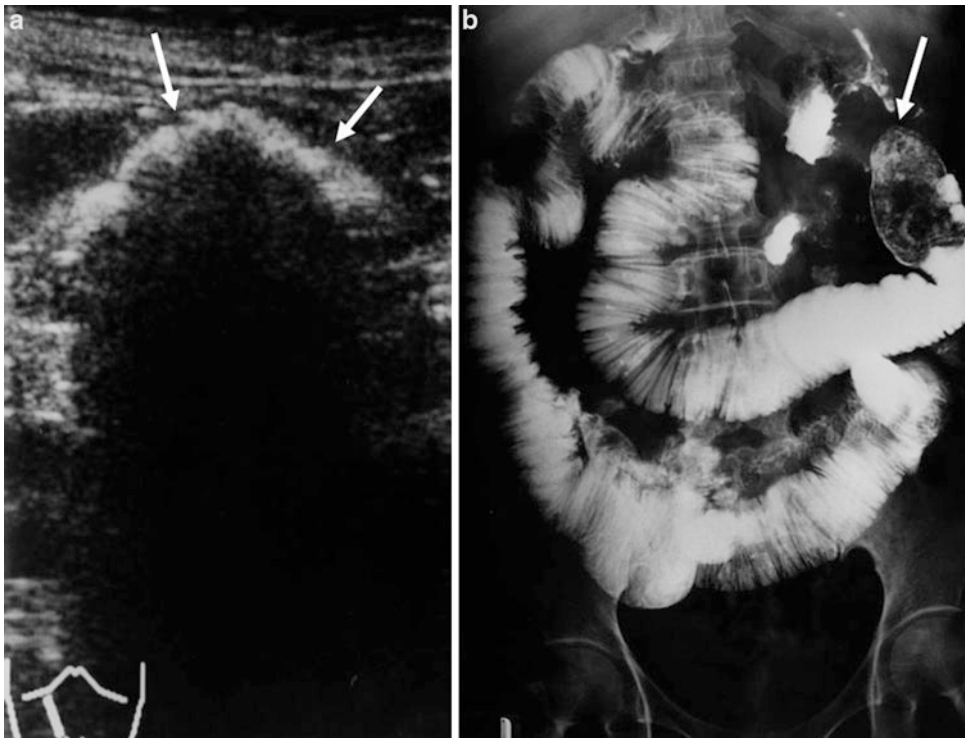

Fig. 4 Phytobezoar in the jejunum. **a** Sonogram of upper abdomen shows hyperechoic, arclike echo with clear acoustic shadow within a loop of the jejunum (*arrows*). Bowel loops proximal to the bezoar is dilated and filled with fluid. **b**. Small bowel follow-through examination shows a large intraluminal filling defect at the end of the dilated jejunum, representing bezoar (*arrow*)

4 Colon Obstruction

The most common cause of colonic obstruction is carcinoma, either primary or metastatic, whereas the most common cause of small bowel obstruction is adhesions. Therefore, it is necessary to differentiate colonic obstruction from small bowel obstruction. Radiographs of the abdomen may be useful for the diagnosis of colonic obstruction in 60–70 % of cases (Gore and Eisenberg 1994). Once colonic obstruction is suspected, contrast enema, is indicated to confirm the obstruction and to determine its level, severity, and cause (Amberg 1994). In the CT era, multidetector row CT examination is the best method for the evaluation of the patients with acute abdomen including colon obstruction (Sinha and Verma 2005b; Patak et al. 2005).

Identification of the colon with sonography is relatively difficult because the colon is filled with gas and feces, rather than fluid. As gas and feces are present in various amounts in the normal colon, the diagnosis of obstruction can be made only when the colon is found to be dilated continuously to the level of the lesion (Fig. 3), where abnormal distension ends abruptly, with the colon distal to it free of gas (Wilson 1994). Because the colon is fixed in position, each segment of colon is identified by position.

The causes of colon obstruction can be identified (Kojima et al. 1992). It was reported that sonography predicted the cause of colon obstruction in 81 % (Lim et al.

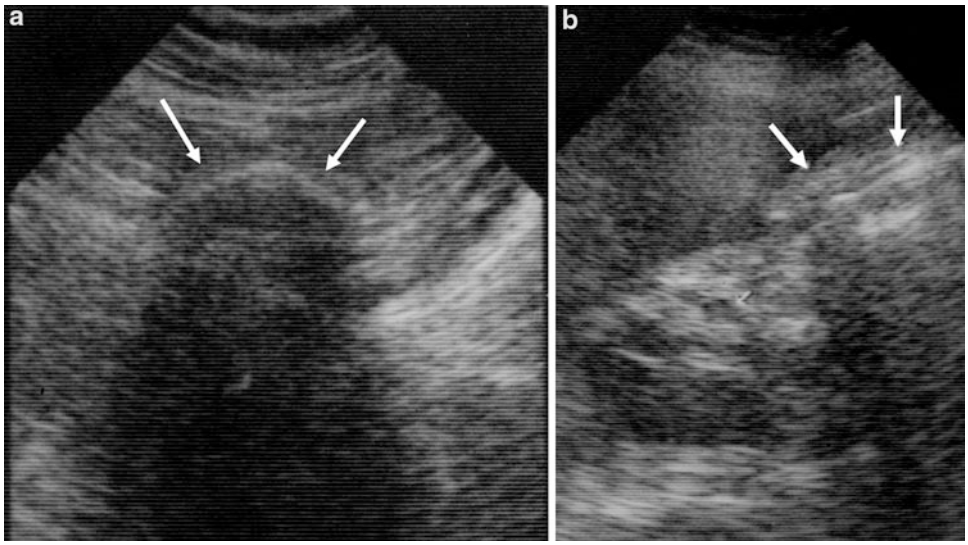

Fig. 5 Gallstone ileus. **a** Sonogram shows hyperechoic arclike echo with posterior acoustic shadow within a dilated loop of ileum, representing a large gallstone (*arrows*). **b** Sonogram of the right upper abdomen discloses the gallbladder which is empty (*arrows*)

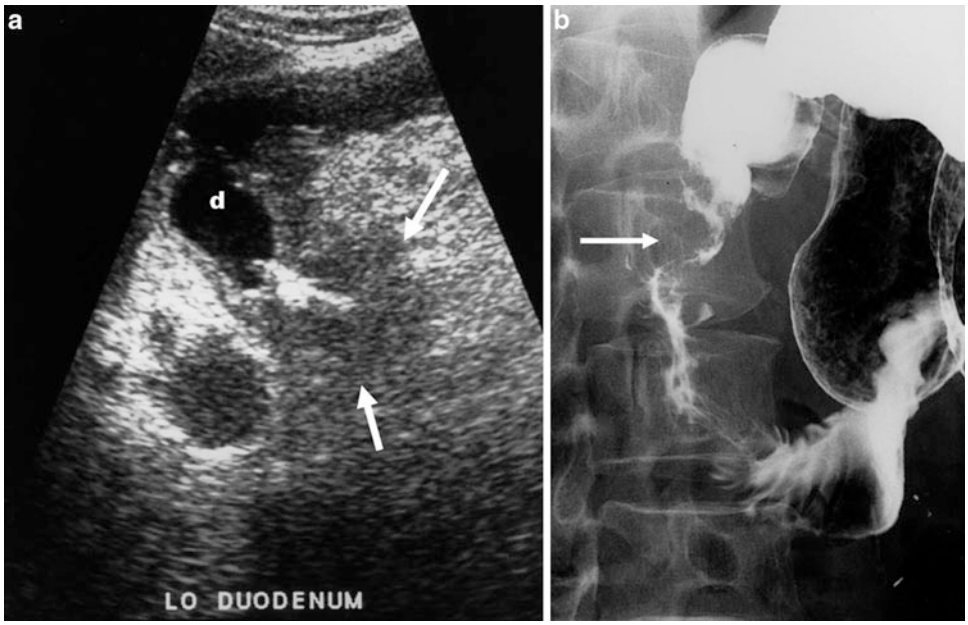

Fig. 6 Duodenal obstruction by adenocarcinoma. **a** Sagittal sonogram of the right upper abdomen discloses a mass (*arrows*) with dilated first part of the duodenum (d). **b** Upper gastrointestinal series shows near-complete obstruction by adenocarcinoma (*arrows*)

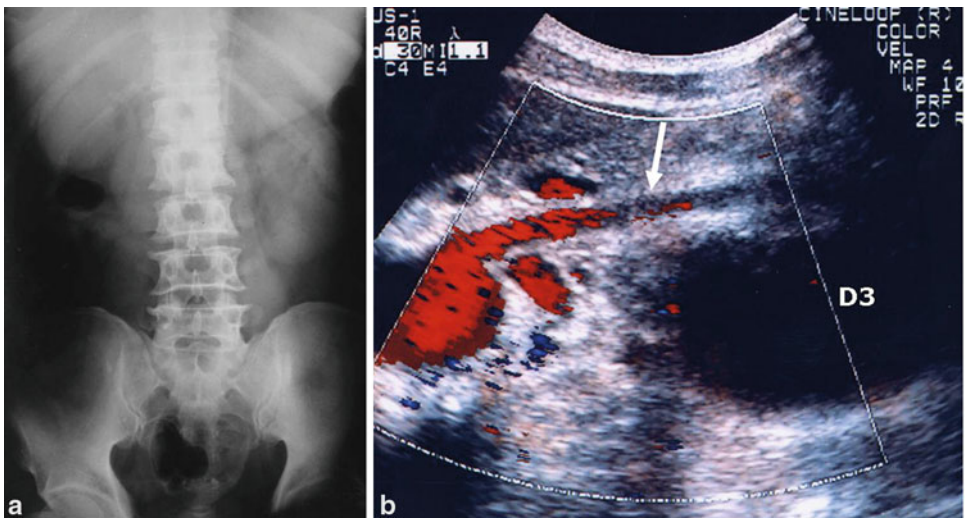

Fig. 7 Afferent loop syndrome. **a** Supine abdominal radiograph shows virtually absent bowel gas because of frequent vomiting. **b** Sagittal color Doppler sonogram of the upper abdomen shows the dilated third part of the duodenum (D3) anterior to the abdominal aorta and posterior to the superior mesenteric artery (*arrows*)

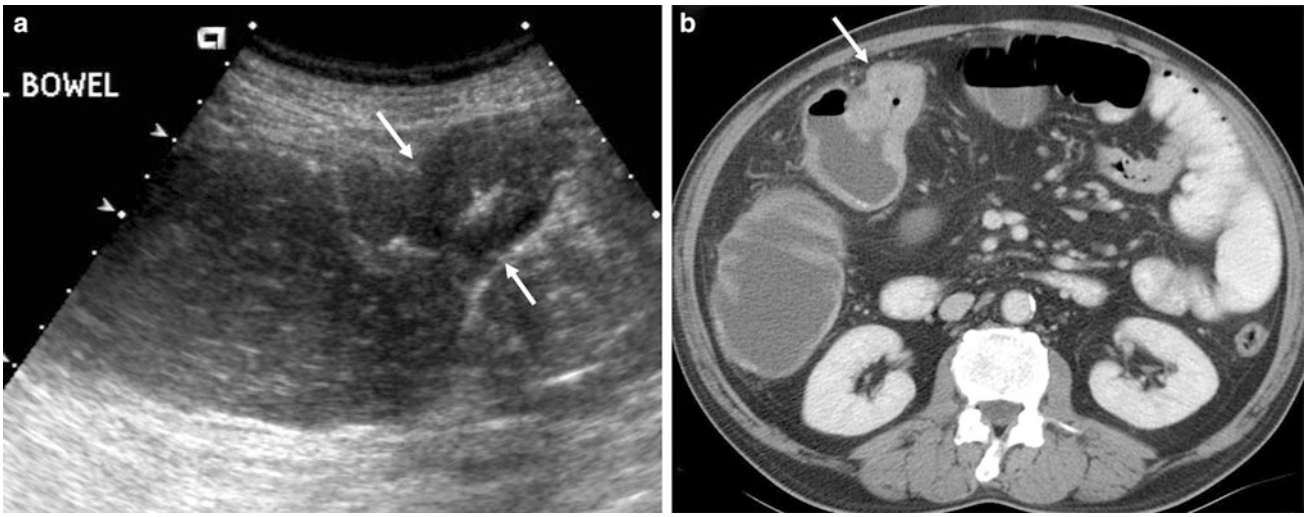

Fig. 8 Transverse colon obstruction by adenocarcinoma. **a** Transverse sonogram of the right upper abdomen discloses circumferential thickening of the wall of the transverse colon (*arrows*) and fluid filled dilated proximal colon. **b** CT image shows encircling thickening of the wall of the transverse colon (*arrow*) due to adenocarcinoma and dilated ascending and transverse colon

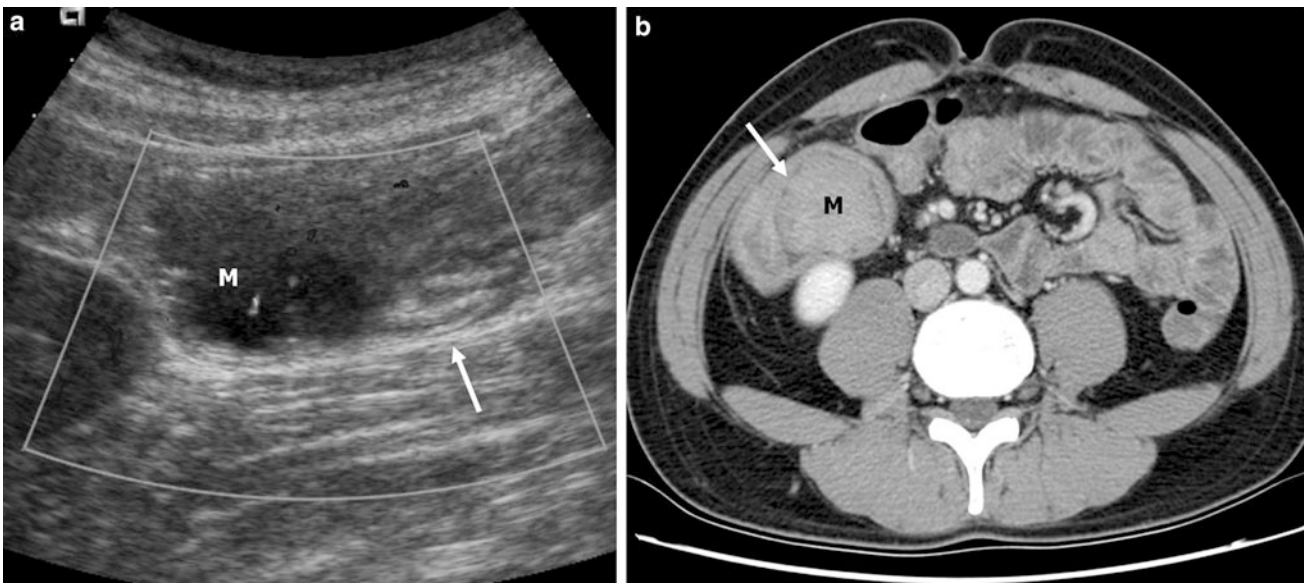

Fig. 9 Ileocolic intussusception due to lymphoma. **a** Sagittal sonogram of the right abdomen shows an oval mass (M) in intussusception. Note folded bowel wall at the orifice of intussuscepted bowel (*arrow*). **b** CT image shows a round mass (M) surrounded by a thin line of fat which is invaginated into the ascending colon (*arrow*). Note slightly dilated jejunum and ileum

1994). As majority of colon obstruction is due to colon cancer or ileocecal intussusception, sonography may reveal obstructing mass or segmental thickening of the colon wall at the end of the dilated colon (Fig. 8) (Ko et al. 1993a, b), or characteristic concentric rings along the sausage like, invaginated bowel loops in intussusception (Weissberg et al. 1977). Sometimes, a soft tissue mass as a leading point of intussusception can be demonstrated (Fig. 9). Sonography is particularly useful in child intussusception (Woo et al. 1992; Verschelden et al. 1992).

5 Paralytic Ileus

Paralytic ileus can be reliably diagnosed by sonography by demonstrating very quilt or aperistaltic dilated bowel loops (Fig. 10). When the bowel loops are filled with more gas

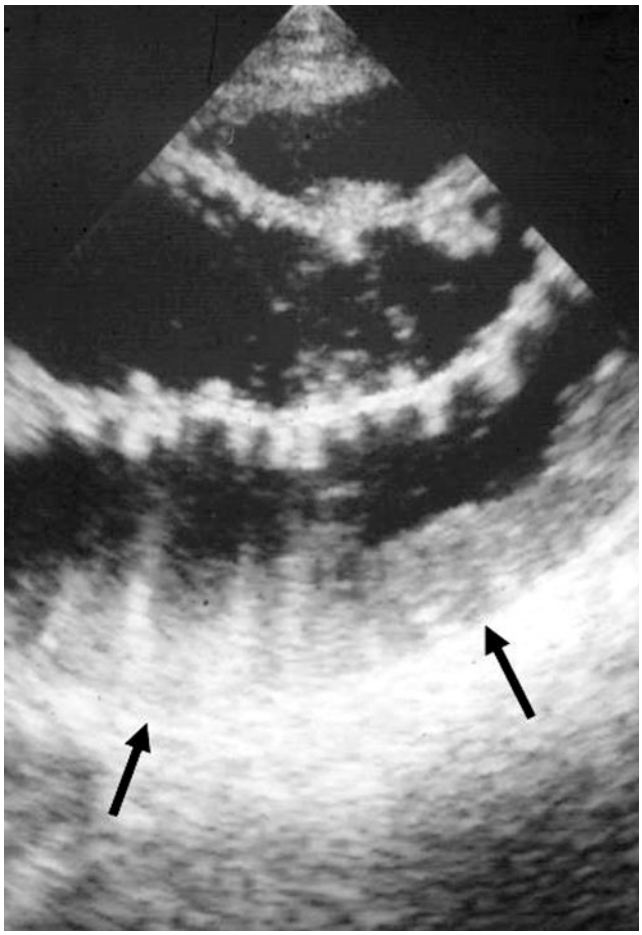

Fig. 10 Paralytic ileus. Sonogram of the lower abdomen shows dilated jejunum filled with fluid and debris. The dilated loops are essentially static and the bowel contents do not move. Note debris in the dependent part of the dilated loop (*arrows*) indicating no peristaltic movement

than fluid, sonography may be of little value. Some difficulty may arise when the obstruction becomes prolonged and the obstructed segment becomes paralytic, thus may be mistaken for paralytic ileus.

References

Amberg JR (1994) Overview: the acute abdomen. In: Margulis AR, Burhenne HJ (eds) Alimentary tract radiology, 5th edn. Mosby, St. Louis, pp 2118–2119

Davir RJ, Sandrasagra FA, Joseph AEA (1991) Ultrasound diagnosis of gallstone ileus. Clin Radiol 43:282–284

Dunn JT, Halls JM, Berne TV (1984) Roentgenographic contrast studies in acute small bowel obstruction. Arch Surg 119:1305–1308

Furukawa A, Yamasaki M, Furuichi K et al (2001) Helical CT in the diagnosis of small bowel obstruction. RadioGraphics 21:341–355

Gore RM, Eisenberg RL (1994) Large bowel obstruction. In: Gore RM, Levine MS, Laufer I (eds) Textbook of gastrointestinal radiology. Saunders, Philadelphia, pp 1247–1258

Herlinger H, Maglinte DDT (1989) Small bowel obstruction. In: Herlinger H, Maglinte DDT (eds) Clinical radiology of the small intestine. Saunders, Philadelphia, pp 479–509

Ko YT, Lim JH, Lee DH, Lee HW, Lim JW (1993a) Small bowel obstruction: sonographic evaluation. Radiology 188:649–653

Ko YT, Lim JH, Lee DH, Yoon Y (1993b) Small bowel phytobezoars: sonographic detection. Abdom Imaging 18:271–273

Kojima Y, Tsuchiyama T, Niimoto S, Nakagawara G (1992) Adult intussception caused by cecal cancer and diagnosed preoperatively by ultrasonography. J Clin Ultrasound 20:360–363

Lee DH, Lim JH, Ko YT (1991) Afferent loop syndrome: sonographic findings in seven cases. AJR Am J Rogentgenol 157:41–43

Lim JH, Ko YT, Lee DH et al (1994) Determining the site and causes of colonic obstruction with sonography. AJR Am J Rogentgenol 163:1113–1117

Megibow AJ, Balthazer EJ, Cho KC, Medwid SW, Birnbaum BA, Noz ME (1991) Bowel obstruction: evaluation with CT. Radiology 180:313–318

Meiser G, Meissner K (1985) Sonographic differential diagnosis of intestinal obstruction: results of a prospective study of 48 patients. Ultraschall Med 6:39–45

Mucha P (1987) Small intestinal obstruction. Surg Clin North Am 67:597–620

Patak MA, Mortele KJ, Ros PR (2005) Multidetector row CT of the small bowel. Radiol Clin North Am 43:1063–1077

Sinha R, Verma R (2005a) Multidetector row computed tomography in bowel obstruction. Part 1 small bowel obstruction. Clin Radiol 60:1058–1067

Sinha R, Verma R (2005b) Multidetector row computed tomography in bowel obstruction. Part 2 large bowel obstruction. Clin Radiol 60:1068–1075

Taourel PG, Fabre JM, Pradel JA, Seneterre EJ, Megibow AJ, Bruel JM (1995) Value of CT in the diagnosis and management of patients with suspected acute small bowel obstruction. AJR Am J Roentgenol 165:1187–1192

Tennenhouse JE, Wilson SR (1990) Sonographic detection of a small bowel bezoar. J Ultrasound Med 9:603–605

Verschelden P, Filiatrault D, Garel L et al (1992) Intussusception in children: reliability of US in diagnosis: a preoperative study. Radiology 184:741–744

Weissberg Dl, Scheible W, Leopold GR (1977) Ultrasonographic appearance of adult intussusception. Radiology 124:791–792

Wilson SR (1991) The gastrointestinal tract. In: Rumack CM, Wilson SR, Charboneau JW (eds) Diagnostic ultrasound. Mosby, St Louis, pp 181–206

Wilson SR (1994) The acute abdomen of gastrointestinal tract origin: sonographic evaluation. In: Margulis AR, Burhenne HJ (eds) Alimentary tract radiology, 5th edn. Mosby, St. Louis, pp 2099–2117

Woo SK, Kim JS, Suh SJ, Paik TW, Choi SO (1992) Childhood intussusception: US-guided hydrostatic reduction. Radiology 182:77–80

Abdominal Hernias, Volvulus, and Intussusception

S. Boopathy Vijayaraghavan

Contents

Abstract

Abdominal hernias are a common clinical problem. Most of them are diagnosed clinically while some are not. If clinical examination is equivocal and in the types that are not clinically made out, imaging is requested. Volvulus of bowel and intussusception are acute emergency which if not diagnosed may lead to a lot of morbidity. Sonography is very useful in the diagnosis of these conditions. This chapter arises to describe the sonographic features of these conditions

1 Abdominal Hernias

A hernia is the protrusion of an organ or tissue out of the body cavity in which it normally lies. Abdominal wall hernias are the most common type. They can be congenital or acquired. The etiological factor may be increased intraabdominal pressure or abdominal weakness. Approximately 75 % of all hernias occur in the inguinal region. Approximately 50 % of hernias are indirect inguinal hernias, and 24 % are direct inguinal hernias. Incisional and ventral hernias account for approximately 10 % of all hernias, and femoral hernias for 3 %; unusual hernias account for the remaining 5–10 %. The symptoms vary from a visible lump, local pain due to stretching, pain due to pull of the content, and that of complications. The hernia may not be seen when the patient is at rest and may require a maneuver to make it visible. It can be Valsalva maneuver (Video 1), cough, or erect position. The role of sonography consists in the confirmation of the hernia, identification of contents, differentiation of the type, diagnosis of associated conditions and complications, and postoperative follow-up.

1.1 Inguinal Hernia

Inguinal hernia is the most common abdominal hernia. There is bulging of abdominal contents into a defect in the inguinal canal in the lower abdomen. It is more common in males,

S. Boopathy Vijayaraghavan (✉)
SONOSCAN Ultrasonic Scan Centre,
15B,Venkatachalam Road, Coimbatore, 641 002,
Tamil Nadu, INDIA
e-mail: sonoscan@vsnl.com

G. Maconi and G. Bianchi Porro (eds.), *Ultrasound of the Gastrointestinal Tract*, Medical Radiology. Diagnostic Imaging,
DOI: 10.1007/174_2012_659, © Springer-Verlag Berlin Heidelberg 2012
Published Online: 17 July 2012

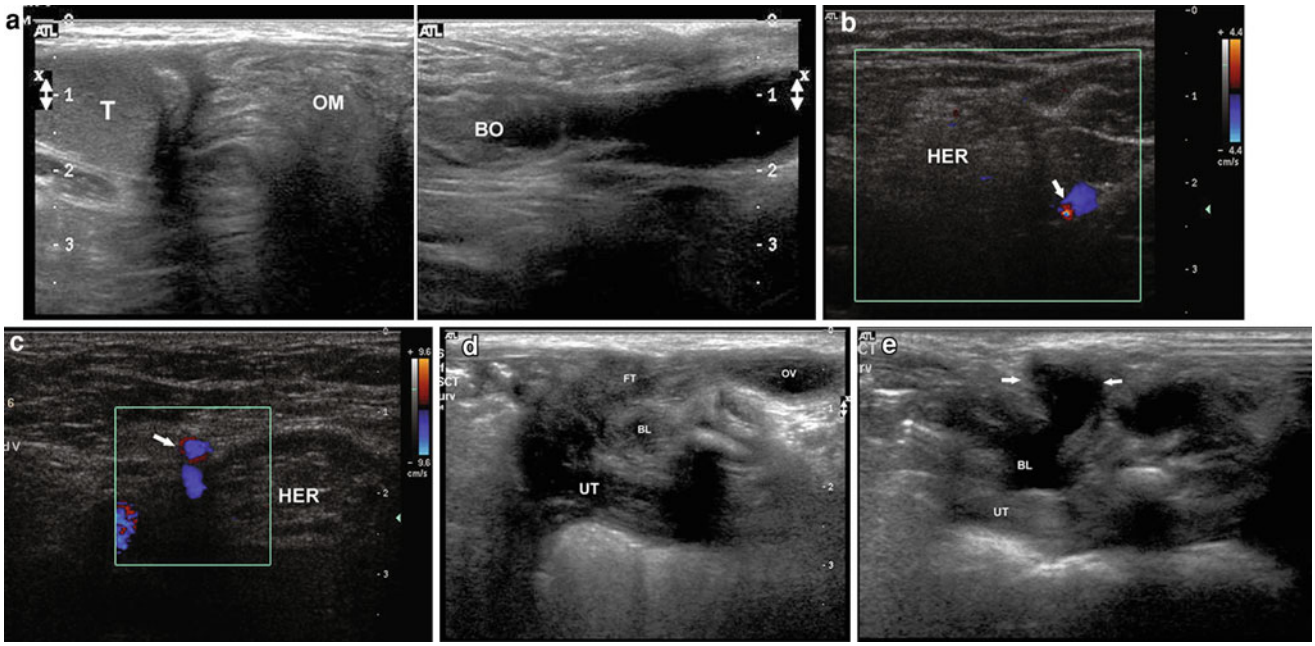

Fig. 1 Inguinal hernia. **a** Oblique scan of inguinoscrotal region showing the inguinal hernia containing omentum (OM) and bowel (BO). The testis (T) is undescended and located in the inguinal canal. **b** Transverse scan of left inguinal region showing the hernial sac (HER) located medial to the inferior epigastric vessels (*arrow*) in direct inguinal hernia. **c** Indirect inguinal hernia on *left* side with the neck of sac located lateral to inferior epigastric vessels (*arrow*). **d** Oblique scan in a premature infant showing the inguinal hernia containing the fallopian tube (FT) and ovary (OV). **e** Oblique scan of an infant showing inguinal hernia containing part of the urinary bladder (*arrows*). *BL* urinary bladder, *UT* uterus

in whom it can reach up to the scrotum. There are two types of inguinal hernia. In the more common indirect inguinal hernia, the protrusion is through a congenital weakness at the internal ring. In children, it is due to persistence of a patent peritoneal pocket: the persistent processus vaginalis in males and diverticulum of Nuck in females (Scherer and Grosfeld 1993). In the direct type of inguinal hernia, the contents push through a weak spot in the posterior wall of the inguinal canal. The inguinal canal lies between the superficial (external) and deep (internal) inguinal rings. The deep ring lies deep to the mid inguinal point, which is halfway between the symphysis pubis and the anterior superior iliac spine. In males, the inguinal canal contains the spermatic cord with vas deferens and testicular vessels. In females it contains the suspensory ligament of the ovary (Ando et al. 1997). Indirect hernia is lateral to the inferior epigastric vessels, whereas the direct one is medial to them.

Sonography of the inguinal region is done at rest and during Valsalva maneuver, cough, and erect position. Inguinal hernia is diagnosed by the presence of bowel, omentum, or other abdominal organs in the inguinal anal, with continuity within the abdomen (Dattola et al. 2002) (Fig. 1a). The contents become prominent when the patient strains, coughs, or are in erect position. This feature differentiates the hernia from mimicking conditions such as hydrocele, varicocele, and mass. The content of the hernia can be omentum and/or bowel. The omentum is recognized by its characteristic echogenic nature. The bowel is identified by the pattern produced by the contents and air. The small bowel shows peristalsis, whereas the colon lacks it. The bowel is also recognized by tracing it into the abdomen and the type of the bowel can be ascertained by continuity. Color Doppler study helps to differentiate the direct from the indirect type of inguinal hernia. The neck of the direct inguinal hernia is medial to the inferior epigastric artery, whereas it is lateral to it in indirect inguinal hernia. Firstly, the external iliac artery is sought, and then by tilting the transducer upward slightly, the inferior epigastric artery is identified. Using another Valsalva maneuver, the relation between the hernial sac and the inferior epigastric artery is analyzed. If the hernial sac appears medial to the inferior epigastric artery, a direct inguinal hernia is diagnosed (Fig. 1b). If it appears to be located laterally, an indirect hernia is assumed (Fig. 1c) (Korenkov et al. 1999; Zhang et al. 2001).

The inguinal hernia can be associated with conditions like hydrocele, varicocele, or mass of the cord, like an encysted hydrocele or lipoma, which are readily diagnosed by sonography. In male children, an indirect inguinal hernia may be associated with undescended testis. The testis may be lying by the side of the sac in the inguinal canal (Fig. 1a), or it may be intraabdominal. This information helps to avoid causing injury to the testis during surgery and

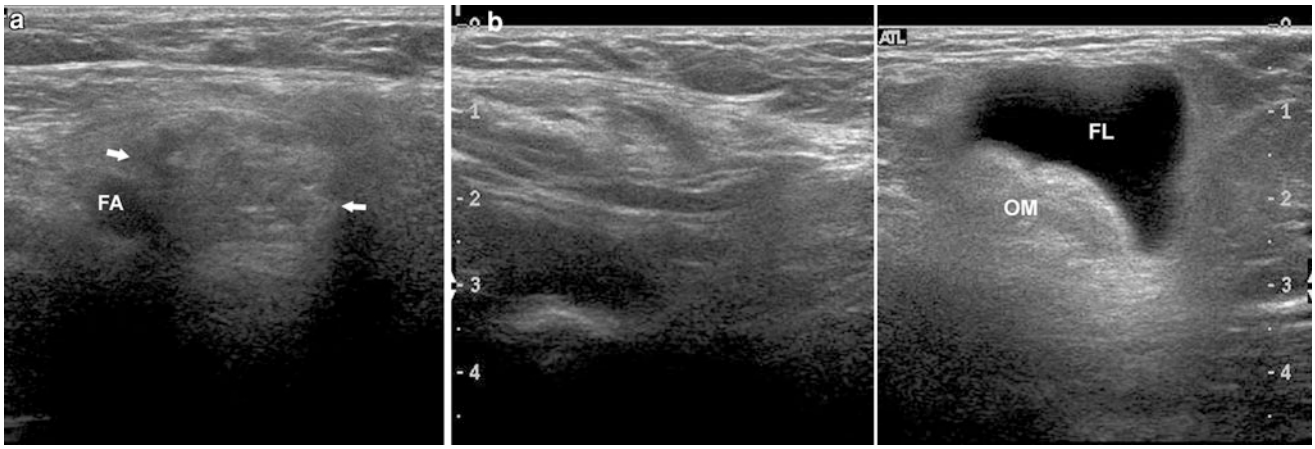

Fig. 2 Transverse scan at the level of the femoral vessels of right side showing the neck of the sac containing omentum (*arrows*) medial to the femoral artery (FA). The femoral vein is not visualized as it is compressed. **b** Longitudinal scan showing the echogenic omentum (OM) in the sac with fluid (FL) due to incarceration

to combine orchidopexy during repair. In females the inguinal hernia may contain ovary, fallopian tube, or rarely, the uterus, which are easily identified on sonography (Fig. 1d, Huang et al. 2003). The hernia containing these organs is common in premature infants (George et al. 2000). Very rarely, the urinary bladder may form the content of a sliding type of inguinal hernia (Fig. 1e, Catalano 1997).

1.2 Femoral Hernia

Femoral hernia occurs through a space bounded superiorly by the iliopubic tract, inferiorly by the Cooper's ligament, laterally by the femoral vein and medially by the insertion of the iliopubic tract into Cooper's ligament. It is more common in females than in males. On examination it reveals a mass below the inguinal ligament. On sonography, the femoral hernia is seen posterior to the inguinal ligament and medial to the femoral vein, in contrast to the inguinal hernia, which is anterior to the inguinal ligament. (Fig. 2, Deitch and Soncrant 1981; Dattola et al. 2002).

1.3 Ventral Hernia

Ventral hernia covers all protrusions through anterior and anterolateral abdominal wall, excluding groin hernias. It is suggested by the patient's clinical history and is well seen on physical examination; however, the patient's history may be atypical and physical examination may be limited in obese patients, in patients with severe abdominal pain or distension, in small hernias or with hernias located in uncommon sites (Spangen 1975; Mufid et al. 1997). In certain clinical situations, it may be necessary to relate the symptoms to the ventral hernia or, it may be necessary to know whether the ventral hernia is complicated or not. In these situations an imaging investigation becomes necessary. Sonography is a dynamic, noninvasive, easily available, and low cost modality useful in studying the ventral hernia. It is performed at rest and during a maneuver such as Valsalva, cough, or erect position. Sonographic diagnosis of ventral hernia is made when bowel or other abdominal organs or fatty tissue of the abdominal wall is seen protruding out of the abdomen with continuity within the abdomen. (Rettenbacher et al. 2001). The hernial orifice is seen as a defect in the fascia, which is seen as an echogenic line deep to the muscle layer and its location and width can be noted. Sonography reveals the contents, which can be omentum, bowel (Fig. 3a), or properitoneal fat (Fig. 3b). Some ventral hernias are not seen at rest and are brought into view with only one of the maneuvers. When the hernia is seen at rest, an attempt is made to slide the contents into the abdomen to know if the hernia is reducible (Video 2). Sonography readily differentiates other conditions that mimic ventral hernia such as lipoma, metastasis, suture granuloma, abscess, or endometriosis. Umbilical hernia is a type of ventral hernia that occurs through the weak umbilicus. Fatty epigastric hernia is protrusion of the properitoneal fat through a defect in the linea alba.

1.4 Spigelian Hernia

Spigelian hernia is a rare type of ventral hernia in which the abdominal contents protrude through an area of weakness at the junction of linea semilunaris and linea semicircularis (Sutphen et al. 1980). The linea semilunaris is a vertical band-like groove that is formed by the union of the medial edges of the aponeuroses of the external oblique, internal oblique, and transverse abdominal muscles. In its upper 75 %, the fused

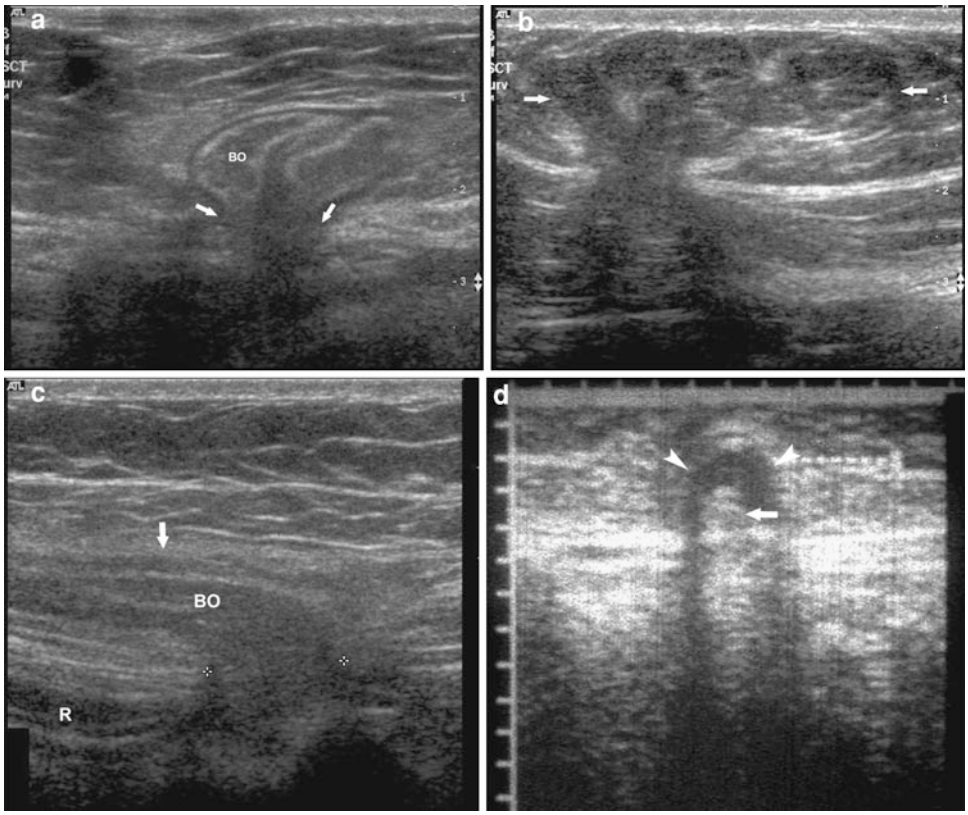

Fig. 3 Scan of the anterior abdominal wall with Valsalva maneuver showing the ventral hernia containing the bowel loops (BO) and the defect in the fascia (*arrows*). **b** Fatty epigastric hernia with herniation of the properitoneal fat (*arrows*). **c** Spigelian hernia showing the defect marked by calipers lateral to the rectus muscle (R) and the contents (BO) limited anteriorly by the Spigelian fascia (*arrow*). **d** Richter's type umbilical hernia showing fluid filled hernial sac (*arrowheads*) and irreducible herniation of only a part of the circumference of the bowel (*arrow*) which showed wriggling peristaltic movement on real time

aponeurosis of these three muscles splits medially to form the anterior and posterior rectus sheaths. Midway between the umbilicus and symphysis pubis, the aponeurosis of the three lateral abdominal muscles passes medially to cover only the anterior surface of the rectus muscle, leaving the posterior surface of the lower fourth covered only by the transversalis fascia and peritoneum. The line forming the inferior margin of the rectus sheath is called the linea semicircularis. Also, at this level, the fiber bundles of the transverse abdominal and internal oblique muscles are much thinner and more widely spaced, causing further weakening through which omentum and small intestine could potentially protrude. Spigelian hernias occur with equal frequency in men and women and in every age group (Mufid et al. 1997). Spigelian hernias may not appear as distinct masses, making them difficult to diagnose clinically. This is because these hernias always dissect between the layers of the anterior abdominal wall, rather than in the subcutaneous tissues, as other ventral hernias do. Spigelian hernias have been mistaken for abdominal abscesses, seromas, hematomas, ovarian masses, pseudocysts, and malignant omental or peritoneal implants (Wechsler et al. 1989).

On sonographic examination during the Valsalva maneuver or erect position, intraabdominal contents, including bowel, mesentery, and omentum, is seen to herniate through a defect in the left lower quadrant abdominal wall in the space between the rectus muscle medially and the external and internal oblique muscles laterally. The hernia extends medially anterior to the rectus muscle (Fig. 3c). The Spigelian fascia, which prevents its extension into the subcutaneous tissue, limits it anteriorly (Mufid et al. 1997). These hernias are also associated with a higher risk of bowel incarceration and strangulation than other abdominal wall hernias.

1.5 Richter's Hernia

In Richter's hernia, only part of the circumference of the bowel on the ante mesenteric border protrudes into a hernia. It can occur with any type of abdominal wall hernia but is more common in femoral hernia. The symptoms and clinical course vary widely, depending on the degree of obstruction, or if strangulation is present. In strangulation, the patient presents with a painful mass, nausea, and vomiting. In contrast to other types, there is no abdominal distention as there is no bowel obstruction. On sonography, complicated Richter's hernia is seen as a small segment of bowel showing wriggling movement in the neck of the hernial sac, which contains fluid (Fig. 3d). There are no dilated bowel loops in the abdomen (Middlebrook and Eftekhari 1992; Hiller et al. 1994).

If strangulated Richter's hernia is not relieved there may be perforation of the small part of the circumference of the small bowel which may present as abscess in the abdominal wall (Fig. 4).

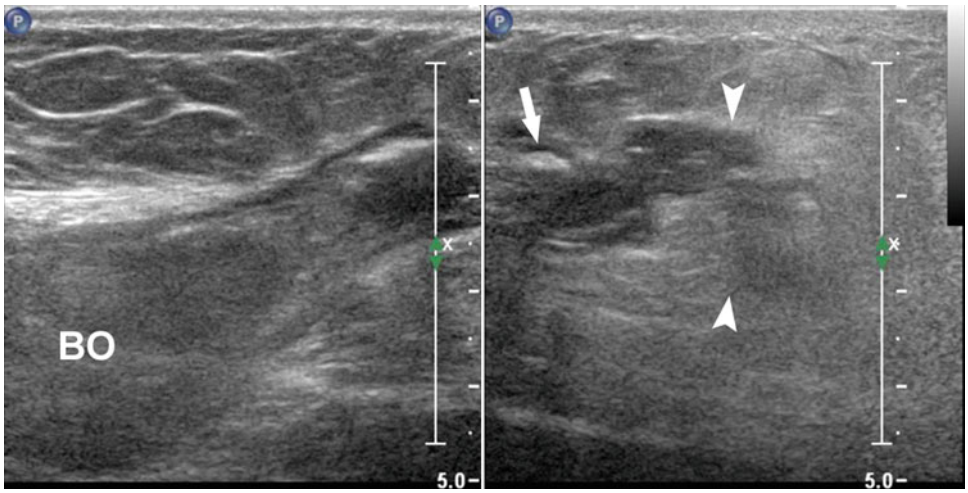

Fig. 4 Complicated Richter Hernia. Oblique scan of the periumbilical region of the abdominal wall showing herniation of a part of the circumference (*arrow*) of the intraabdominal bowel loop (BO) into the umbilical hernia. There is an abscess (*arrow heads*) close to the breach in the wall of the bowel

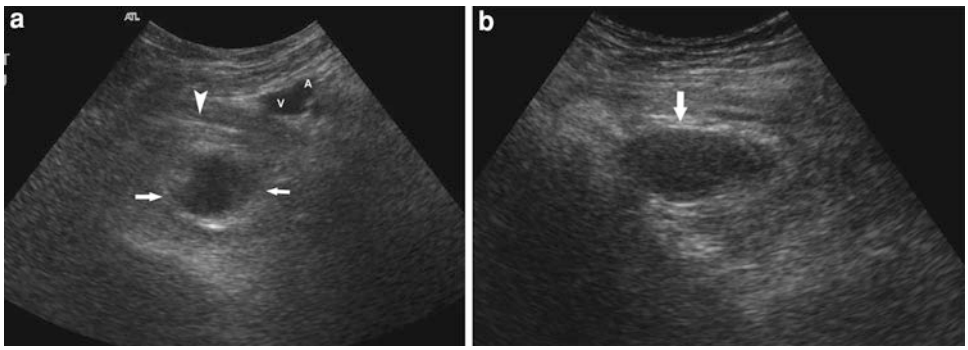

Fig. 5 Obturator Hernia. **a** Transverse scan of the *left* inguinal region showing the loop of bowel (*arrows*) deep to the pectineus muscle (*arrow head*) and far deep to the common femoral artery (A) and Vein (V). **b** Longitudinal scan showing the herniated loop (*arrow*), the upper limit of which is not well defined

1.6 Obturator Hernia

Obturator hernia occurs through the obturator foramen in pelvis which contains the obturator nerve and vessels. It is bounded superiorly and laterally by the pubic bone and inferiorly by the obturator membrane. Obturator hernia is nine times more common in females. It occurs most frequently in emaciated patients aged >70 years. It is rarely diagnosed clinically as there is no external hernia.

It is usually diagnosed at laparotomy done for small bowel obstruction. It can be diagnosed on sonography, when there is small bowel obstruction.

On axial scan of the inguinal region, it is seen as an echo poor mass deep to the pectineus muscle. It is much deeper in relation to the common femoral vessels.

On longitudinal scan the upper limit will not be seen (Fig. 5).

1.7 Complications of Hernia

The pattern of complications is common for all types of hernia. The complications are irreducibility, obstruction, and strangulation. Irreducible (incarcerated) hernia may be due to a narrow neck or adhesion of contents to the sac wall. In obstruction, the intestine in the hernia gets obstructed due to a narrow neck, adhesion or volvulus, but it is viable. Strangulation results when there is compromise to venous drainage and later arterial supply of the contents. In obstructed hernia there is colicky pain, abdominal distension, and vomiting. Incarcerated hernia is present at rest; it is irreducible and usually contains some fluid in the sac that can be seen on sonography (Fig. 2b, Rettenbacher et al. 2001). In obstructed inguinal hernia the patient has symptoms of intestinal obstruction. There are dilated bowel loops in the abdomen which show active peristalsis. The appearance of the bowel in the hernial sac depends on whether the obstruction is to afferent or efferent loop in the sac. In the more common afferent loop obstruction, the bowel loops in hernial sac remain collapsed and there is transition between the dilated intraabdominal bowel loop and collapsed bowel loop in the hernia (Fig. 6a). In efferent loop obstruction, the bowel loop in the hernial sac is dilated. The transition is between dilated loop in hernial sac and collapsed loop in abdomen (Fig. 6b). The obstruction may be of closed loop type due to block of both the afferent and efferent loops at the neck of the hernia, or due to volvulus of the loop in the hernial sac. Here, the loop of bowel in hernial sac is disproportionately more dilated than proximal intraabdominal loops, it is tensely distended and may lack air in its lumen (Fig. 6c). The peristalsis is usually absent in this loop as it is tensely distended. In strangulation

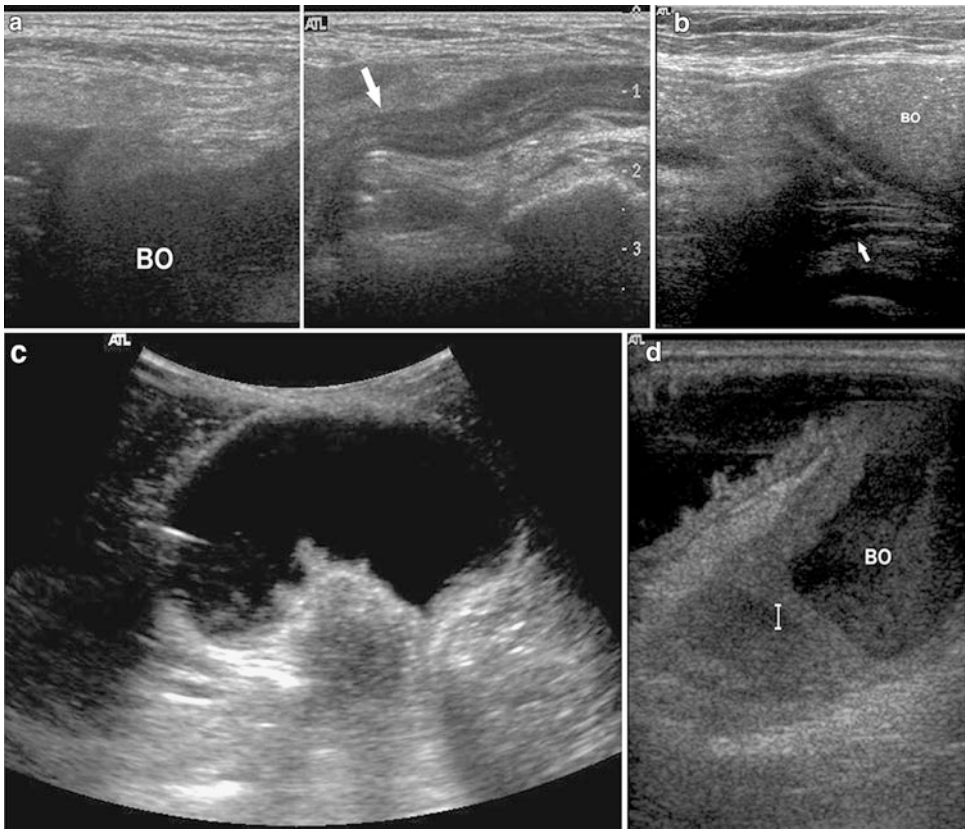

Fig. 6 Complicated hernia. **a** Afferent loop obstruction showing the transition between the dilated intraabdominal loop (BO) and collapsed loop in inguinal hernia (*arrow*). **b** Efferent loop obstruction showing dilated bowels in ventral hernia (BO) with transition between the dilated loop in hernia and collapsed intraabdominal loop at the neck of the sac (*arrow*). **c** Tensely distended loop devoid of air in a ventral hernia due to closed loop obstruction. **d** Strangulated loop of bowel (BO) in a ventral hernia showing thick walls

there is ischemia of the contents of the hernia. The hernia is tender, with free fluid in the sac. The wall of the aperistaltic bowel is thickened (Fig. 6d). On color Doppler study, no flow is seen in the omentum or bowel, which is strangulated (Liang et al. 2001). In the case of the bowel, dilated loops of bowel are seen in the abdomen.

1.8 Postoperative Sonography

Sonography is useful in postoperative follow-up of the patients with hernia. The prosthetic mesh can be seen as a brightly echogenic reticular line and curled prosthesis (Fig. 7a) or a displaced prosthesis can be recognized (Parra et al. 2004; Dattola et al. 2002). Fluid collection (seroma or abscess) is well seen and its relation to prosthesis can be assessed (Fig. 7a). If necessary, the fluid can be aspirated under sonographic guidance (Parra et al. 2004). Adhesion of bowel to the prosthesitic mesh is one of the complications that can lead to bowel obstruction. Sonography can reveal dilated loops and the bowel loop adherent to the mesh (Fig 7b, Furtschegger et al. 1995). Recurrence of hernia can be confirmed and the location of defect in relation to the mesh can be known. In the case of inguinal hernia, the vascular supply to the testis can be assessed by color Doppler study, and testicular ischemia or infarction may be recognized (Holloway et al. 1998).

1.9 Internal Hernia

Internal hernia involves protrusion of a viscus, usually the small bowel, through a normal or abnormal aperture within the peritoneal cavity. Internal hernias are rare, with reported incidence of 0.2–0.9 % of autopsies (Ghahremani 1984). A substantial proportion of these remains asymptomatic. It is an uncommon cause of small bowel obstruction. About 4 % of bowel obstruction is due to internal hernia (Feldman et al. 2002). Owing to the risk of strangulation of the contents of the hernia, even small internal hernias are dangerous and may be lethal. This hernia may be either congenital or acquired. Congenital internal hernias include paraduodenal, foramen of Winslow, mesenteric, and supravesical hernias. During fetal development, the mesentery of the duodenum, ascending colon, and descending colon becomes fixed to the posterior peritoneum. These segments of the bowel became retroperitoneal. Anomalies of mesenteric fixation may lead to abnormal openings through which internal hernias may occur. This is the likely mechanism of paraduodenal and supravesical hernias. Abnormal mesenteric fixation may lead to abnormal mobility of the small bowel and right colon, which facilitates herniation. During fetal development, abnormal openings may occur in the pericecal, small bowel, transverse colon, or sigmoid mesentery, as well as in the omentum, leading to mesenteric hernias. In the case of left paraduodenal hernia, an abnormal

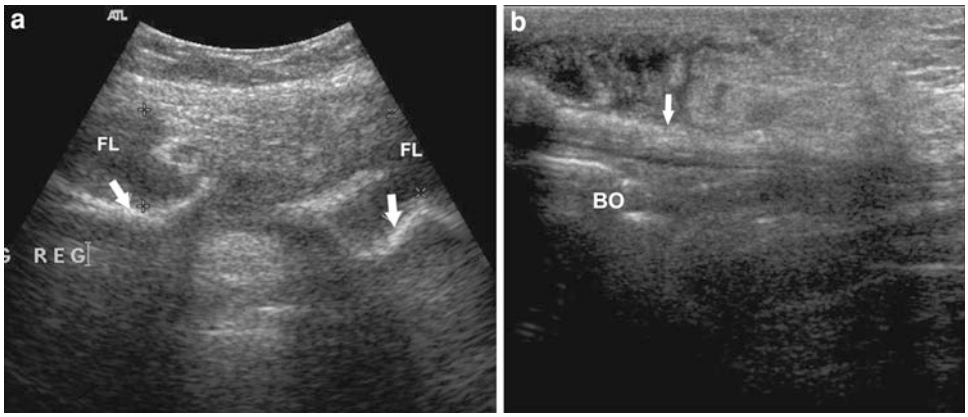

Fig. 7 Scan of the abdominal wall after hernial repair showing the curled echogenic mesh (*arrows*) with collection of fluid (FL) anterior to it in **a** and bowel (BO) adherent to the straight mesh (*arrow*) in **b**

foramen (fossa of Landzert) occurs through the mesentery close to the ligament of Treitz, leading under the distal transverse and descending colon and posterior to the superior mesenteric artery. The small bowel may protrude through this fossa. The mesentery of the colon thus forms the anterior wall of a sac enclosing a portion of the small intestine. Mesenteric hernias occur when a loop of intestine protrudes through an abnormal opening in the mesentery of the small bowel or the colon. The most common area for such an opening is in the mesentery of the small intestine, most often, near the ileocolic junction. Various lengths of intestine may herniate, posterior to the right colon, into the right paracolic gutter. Acquired internal hernias may occur as a complication of surgery, or trauma, if abnormal spaces or mesenteric defects are created. Compression of the loops in the internal hernia may lead to obstruction of the herniated intestine. Obstruction may be acute, chronic, or intermittent. Strangulation may occur by compression of vessels at the neck of the sac, or by torsion of the herniated segment. The herniated bowel may also compress arteries in the margins of the mesenteric defect, causing ischemia of non herniated intestine.

Any of the various forms of internal hernias may present with symptoms of acute or chronic intermittent intestinal obstruction. The diagnosis is difficult among patients with chronic symptoms and is rarely made preoperatively among patients who present with acute obstruction (Ghahremani 1984). About 50 % of patients with paraduodenal hernias develop intestinal obstruction, which may be of low grade, chronic, and recurrent, or may be of high grade and acute (Zimmerman and Laufman 1953; Nyhus and Condon 1989; Pershad et al. 1998). In acute bowel obstruction, the patients present with colicky abdominal pain with vomiting. The features seen on sonography are: (a) small bowel obstruction, as evidenced by dilated hyperperistaltic loops (b) zone of transition between dilated and nondilated bowel and, (c) cluster of collapsed, crowded, and compressed small bowel loops, as if enclosed in a bag (Fig. 8). This cluster of loops is seen away from the zone of transition: to the left in paraduodenal hernia and to the right in paracecal hernia. These are the features seen when the afferent loop entering the sac is obstructed because of crowding and compression of bowel loops in the sac. When there is obstruction to the efferent loop at the neck, the sac contains dilated loops of small bowel with the zone of transition at the neck of the sac (Vijayaraghavan 2005). The differential diagnosis for sonographic appearance of internal hernia is abdominal cocoon. In abdominal cocoon there is no evidence of small bowel obstruction or zone of transition. The loops do not appear to be compressed and show normal peristalsis (Vijayaraghavan et al. 2003).

1.10 Diaphragmatic Hernia

The diaphragmatic hernia is an abnormal protrusion of abdominal organs into the chest through an abnormal opening in the diaphragm or through the esophageal hiatus. The abnormal opening may be congenital, caused by improper fusion of the various parts of diaphragm during fetal development, or acquired, due to traumatic rupture of the diaphragm. The four basic types of congenital diaphragmatic hernia are the posterolateral Bochdalek hernia, the anterior Morgagni hernia, the hiatus hernia, and the rare form of herniation through the central tendon or septum transversum, otherwise called the peritoneopericardial hernia. The left-sided Bochdalek hernia is the commonest of these occurring in approximately 90 % of the cases. The congenital diaphragmatic hernia occurs in one of every 2,000–4,000 live births. While congenital diaphragmatic hernia is most commonly a disorder of the newborn period, as many as 10 % of patients may present with the condition after the newborn period and even during adulthood. The outcome in patients with late presentation of congenital diaphragmatic hernia is extremely good. During newborn period, the infants exhibit respiratory distress and cyanosis. In later age groups the condition is asymptomatic, or presents with nonspecific symptoms.

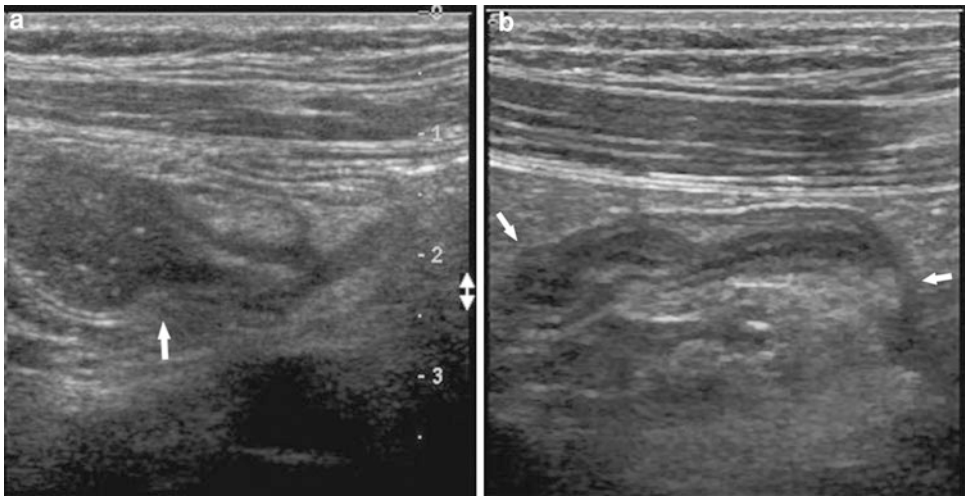

Fig. 8 Paraduodenal internal hernia. **a** Oblique scan above the umbilicus showing the zone of transition (*arrow*) between dilated and non dilated bowel. **b** Transverse scan to the *left* of zone of transition shows the cluster of crowded and compressed loops of bowel as if they are tightly packed within a sac (*arrows*)

The diagnosis of left-sided congenital diaphragmatic hernia in the newborn is revealed on a chest X-ray, as it contains air-filled bowels. The right-sided hernia containing solid liver or right kidney may be difficult to diagnose on a chest X-ray. Sonography reveals the defect in the right dome of the diaphragm and the herniated liver or right kidney. In the rare type of peritoneopericardial hernia, there is herniation of the left lobe of the liver with, or without colon, into the pericardial sac through a defect of the central tendon of the diaphragm. This hernia also presents in the newborn period as respiratory distress or cyanosis. In such a case, an X-ray of the chest will reveal an enlarged cardiac silhouette. Sonography reveals the herniation of left lobe of liver into the pericardial sac containing some pericardial fluid (Fig. 9a, Vijayaraghavan 1988). The herniated liver pushes the heart above and laterally. The diaphragmatic hernia of Bochdalek type, presenting in later ages, may be seen on sonography as a defect in the diaphragm with intrathoracic visualization of viscera such as stomach, spleen, and bowels, on the left side (Fig. 9b), and liver or right kidney on the right side.

In the hiatus hernia, the stomach herniates up through the esophageal hiatus of the diaphragm. There are two types of hiatus hernia. In the sliding type, the gastroesophageal junction and fundus of stomach slide through the hiatus and are situated above the diaphragm. It is associated with gastroesophageal reflux. In the rolling or para esophageal type, the gastroesophageal junction is in the abdomen, and the fundus of stomach herniates by the side of the esophagus. Many authors have described the sonographic findings associated with the gastroesophageal reflux caused by the hiatus hernia in children (Naik and Moore 1984; Westra et al. 1990; Le Dosseur et al. 1992). Sonography is performed after the usual feed of formula, milk, water, or juce. The transducer is placed in the midline under the xiphisternum and the distal esophagus is visualized, as it comes out of the diaphragm. The transducer is slightly rotated to obtain the longitudinal section of the intraabdominal portion of the esophagus and observed for 10 min. The length of the esophagus is measured from the diaphragm to the cardia and the thickness is measured between the serous layers. The number of episodes of gastroesophageal reflux is also noted. Normal values for these observations have been described for the different age groups of children (Westra et al. 1990; Le Dosseur et al. 1992). Aliotta et al. (1994) have described the thickness of the hiatal portion of the esophagus in adults indicative of hiatus hernia as 16 mm or more (Fig. 9c).

2 Small Bowel Volvulus

Small bowel volvulus refers to rotation of the bowel around the mesenteric axis, which often results in a closed loop obstruction, lymphatic, venous, or arterial occlusion (Fig. 10a). It is one of the conditions causing small bowel obstruction, which requires prompt diagnosis and treatment to avoid poor outcome, as it can progress rapidly to gangrene of bowel. It is a rare but a life-threatening emergency. It is more common in Africa (24–60/100,000) and Asia, compared with Western countries (1.7–5.7/100,000; Gulati et al. 1973; Cathcart et al. 1981; Schwartz and Ellis 1989; Parkes 1997). The small bowel volvulus can be primary or secondary depending on whether a predisposing factor is present or not. Predisposing condition may be congenital or acquired. Malrotation of midgut, a persistent omphalalomesenteric duct and mesenteric cyst are some of the congenital conditions. Some of the acquired conditions are adhesion, ascariasis and a mesenteric cyst, or tumor. In malrotation of midgut, there is arrest of the rotation and fixation phase of embryonic development, which results in developmental failure of peritoneal fixation and a narrow mesenteric pedicle. The narrow mesenteric pedicle predisposes to volvulus because of increased mobility. Increase in

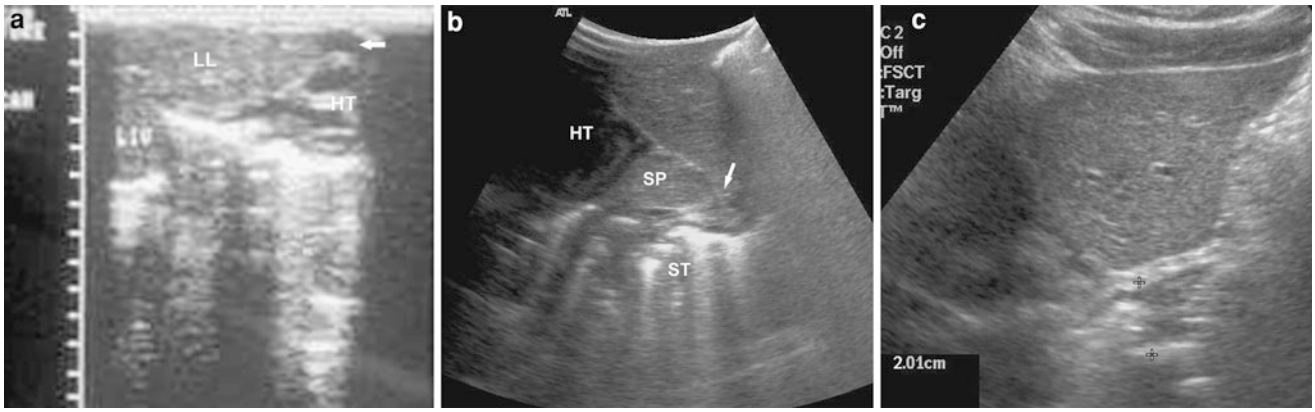

Fig. 9 Oblique scan of epigastrium and precordium showing the *left* lobe of the liver (LL) herniated into the pericardium pushing the heart (HT) better outlined by the minimal pericardial fluid (*arrow*). *LIV* intraabdominal liver. **b** Longitudinal scan of *left* hypochondrium revealing the defect (*arrow*) in the posterior part of *left* dome of diaphragm with spleen (SP) and air filled stomach (ST) lying in the chest posterior to the heart (HT) suggestive of *left* diaphragmatic hernia of Bochdalek type. **c** Longitudinal scan of *left* hypochondrium showing the shortened and thickened intraabdominal esophagus in gastro esophageal reflux of hiatus hernia

the weight of the distal aspect of mesentery due to a mesenteric cyst or tumor, a mass of ascaris worms and dilated loop of bowel in a closed loop obstruction can predispose to volvulus,. The third factor, which predisposes volvulus, is restriction of the bowel at a fixed point, which acts as a fulcrum for rotation. The point of fixation may be at the apex of the volvulus, as seen in persistent omphalalomesenteric duct and adhesion of bowel to abdominal wall or it may be at the base, as seen in adhesions between two loops of bowel with volvulus occurring at this site. Volvulus in malrotation of midgut typically presents in the neonatal period, but can also occur at a later age and even in adults. The volvulus due to other causes may occur at any age. The clinical presentation of volvulus of small bowel can be nonspecific and includes bilious vomiting, abdominal pain, and distension. Some patients may have chronic or intermittent symptoms.

Early diagnosis of small bowel volvulus is crucial for better outcome of management as it can prevent complications. The vascular occlusion can lead to ischemia and gangrene of the bowel. The closed loop obstruction may lead to tense distension of the bowel with secondary perforation and resulting peritonitis. Sonography has the advantages of easy availability, relative lack of need for patient preparation, and absence of ionizing radiation. The sonographic findings described previously such as dilated thick-walled bowel loops to the right of spine with increased peritoneal fluid (Leonidas et al. 1991) and dilated duodenum (Hayden et al. 1984), are nonspecific. The "whirlpool" sign, proposed by Pracros et al. (1992), is specific for midgut volvulus, as it directly indicates the anatomic alteration caused by the volvulus and is not seen in other conditions. Fisher (1981) was the first to describe the whirlpool sign as a CT finding of midgut volvulus. The twisted loops of bowel and branching mesenteric vessels create surrounding strands of soft tissue attenuation within the background of mesenteric fat attenuation, giving the appearance of whirlpool, or hurricane on a weather map. On gray-scale sonography, the whirlpool sign, as it is classically described for volvulus in malrotation, is seen as a round mass of incomplete concentric rings of alternative echogenic and hypoechoic bands in the transverse scan of the epigastrium below the pancreas (Fig. 10b, Pracros et al. 1992). On real-time scanning, when the transducer is moved down, the characteristic whirlpool appearance is seen where the echopoor band of superior mesenteric vessels is seen to wrap in the clockwise direction, around the central axis (Video 3). The same findings are more definitively seen on color Doppler study (Fig. 10c; Video 3). The size of the mass, the number of concentric rings, and number of turns on downward movement of the transducer will depend on the number of turns present in the volvulus. The appearance of the central axis of the mass varies. In the upper part of the mass, the central axis is formed by the superior mesenteric artery, which appears as a hypoechoic dot (Fig. 10b). In the lower part of the mass, the axis appears as a brightly echogenic dot, sometimes with a shadow (Fig. 10c). This is produced by the wrapped up mesentery. The superior mesenteric artery is not seen in the lower part as it deviates in its course, to wrap around the central axis. The same feature is seen on longitudinal scan of superior mesenteric artery as a truncated superior mesenteric artery sign (Sze et al. 2002), with only the proximal part of the superior mesenteric artery being visible (Fig. 10d, e). This is because of the fact that in volvulus, the superior mesenteric artery deviates laterally after a varying length of straight course proximally. This is in accordance with the corkscrew appearance of the superior mesenteric artery on

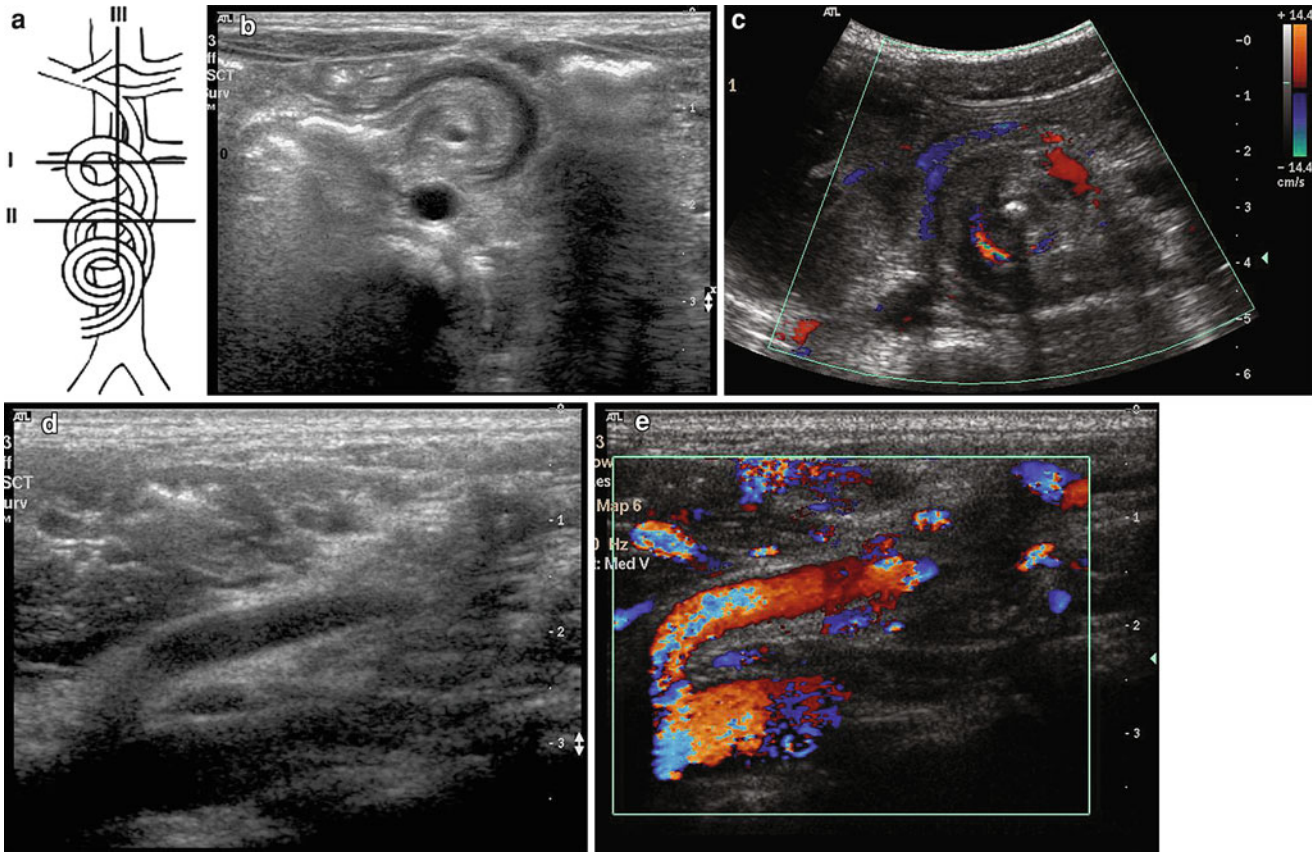

Fig. 10 Small bowel volvulus in malrotation of midgut. **a** Line diagram showing the rotation of vessels and planes of section. **b** Transverse section through plane I showing the mass of whirlpool with its axis formed by superior mesenteric artery seen as a hypoechoic dot. **c** Similar section through II with color Doppler showing the mass of whirlpool with the superior mesenteric vessels going around the central echogenic axis formed by wrapped up omentum. **d** Longitudinal section through superior mesenteric artery (plane III) shows the truncated superior mesenteric artery sign. **e** The same appearance on color Doppler study

angiography, which has been described as the "barber pole" sign (Buranasiri et al. 1973; Griska and Popky 1980). In volvulus of malrotation, in addition to the whirlpool sign, there is alteration of the relationship between the superior mesenteric artery and the vein. The vein is normally to the right of the artery. In malrotation the vein is seen either anterior to, or to the left, of the artery.

In volvulus, due to other causes, the location and axis of the mass with whirlpool appearance can vary. In a mesenteric cyst with volvulus of most of the small bowel, the mass is seen below the pancreas, as seen in volvulus of malrotation (Vijayaraghavan et al. 2004). Alternatively, when the volvulus involves only a segment of small bowel, the mass is located close to the umbilicus, just above or to the right of it. The best image of the mass is seen in slightly oblique scans and not on true transverse scans, as the axis of volvulus may be oblique. In a newborn, who had an atresia of small bowel secondary to intrauterine volvulus due to persistent omphalomesenteric duct, the mass of whirlpool was seen to right of umbilicus. Rarely, the mass may be very small and the concentric rings are not well appreciated, if the segment of bowel involved is very small. In such a situation, the movement of the transducer along the axis brings about the typical whirlpool sign (Videos 4 and 5). On CT scan, the mass of whirlpool sign has to be in the axial plane to be seen. Since oblique scans are possible with ultrasound, even obliquely placed masses of whirlpool are well seen on sonography. This fact, along with the dynamic study of movement of transducer to elicit the whirlpool sign, increases the sensitivity of ultrasound. The causative lesions of the volvulus-like mesenteric cyst, or ball of worms, will be seen. The complications of volvulus such as closed-loop obstruction, gangrene of bowel, or pneumoperitoneum (Vijayaraghavan et al. 2004) are seen, if present. In some patients, the closed loop obstruction may be the only feature seen on sonography to suggest a segmental volvulus. In the closed loop obstruction, a loop of dilated small bowel is seen filled with only fluid devoid of air (Cho et al. 1989) (Fig. 11), whereas the proximal dilated loops contain fluid and air.

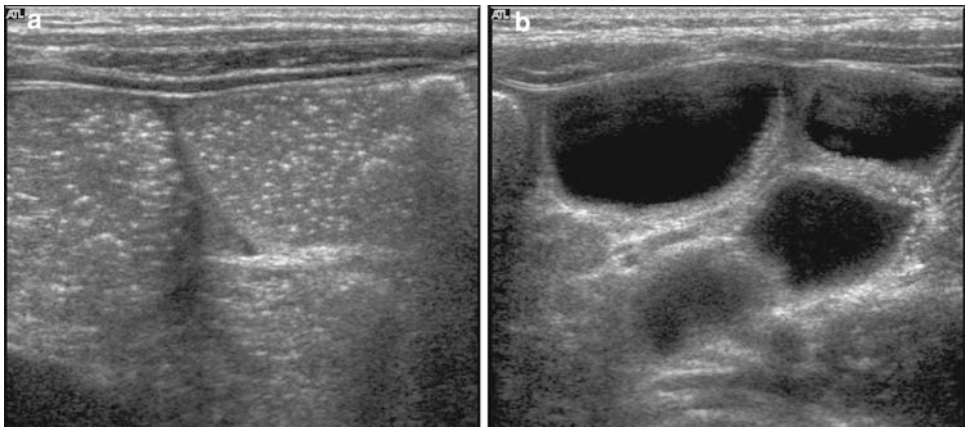

Fig. 11 Closed loop obstruction in segmental small bowel volvulus. **a** The proximal dilated loops of bowel showing intraluminal fluid with micro bubbles of air seen as echogenic dots. **b** Section through the loops of closed loop showing the lumen filled with clear fluid devoid of air

3 Gastric Volvulus

Gastric volvulus is an abnormal degree of rotation of one part of the stomach around another varying from 180–360°, leading to a closed loop obstruction and possible strangulation (Cameron and Howard 1987). It is a rare surgical emergency. It can be primary or secondary, depending upon the absence or presence of predisposing conditions, such as congenital or traumatic diaphragmatic hernia (Kohli et al. 1997; Pelizzo et al. 2001), diaphragmatic eventration (Oh et al. 2000), wandering spleen (Pelizzo et al. 2001), or asplenia—polysplenia syndromes (Aoyama and Tateishi 1986). Four types of gastric volvulus have been reported based on the axis of rotation of the stomach:

1. In the more common organoaxial volvulus (59 %), the stomach rotates on its longitudinal axis connecting the cardia and the pylorus. There is reversal of greater and lesser curvatures with two fluid filled closed compartments. This type is more commonly associated with strangulation.
2. The second type is mesenteroaxial volvulus (29 %), where the stomach rotates about a vertical axis perpendicular to the cardiopyloric line passing through the middle of lesser and greater curvatures.
3. The third type shows features of both organoaxial and mesenteroaxial volvulus (2 %).
4. The last type is unclassified (10 %; Shivanand et al. 2003).

The etiology is unclear. It is believed that, the major factor leading to gastric volvulus is the laxity of the four gastric ligaments: gastrophrenic, gastrohepatic, gastrosplenic, and gastrocolic, which anchor the stomach (Wastell and Ellis 1971; Deitel 1973; Carter et al. 1980; Llaneza and Salt 1986). The gastric volvulus may be acute or chronic. Acute volvulus is often a surgical emergency. It presents a clinical triad of violent retching with inability to vomit, acute severe epigastric pain with upper abdominal distension, and inability to pass a nasogastric tube, as described by Borchardt in 1904 (Borchardt 1904). On plain X-ray and barium meal study, the stomach is seen as two fluid-filled compartments. The stomach is thoracoabdominal in position when the gastric volvulus is associated with diaphragmatic hernia or eventration.

On sonography, there are two dilated fluid-filled compartments of stomach which is thoracoabdominal in position, with a constriction between the upper and lower parts resembling a "peanut", hence called the "peanut sign" (Fig. 12a, Matsuzaki et al. 2001). The continuity of esophagus with stomach and stomach with duodenum cannot be demonstrated (Fig. 12b, c). The spleen is seen in the epigastrium between the left lobe of liver and stomach (Fig. 12d), because it is carried with the rotating stomach. Chronic gastric volvulus is usually asymptomatic or produces non-specific abdominal symptoms. Most often it is discovered as an incidental finding on barium study or CT scan (Chiechi et al. 1992).

4 Cecal Volvulus

Volvulus of the cecum is torsion of the cecum around its own mesentery, which often results in a closed-loop obstruction. It can occur only in the small percentage (11–25 %) of the population who have a developmental failure of peritoneal fixation with resultant increased mobility of the cecum (Montes and Wolf 1999). It accounts for 11 % of all intestinal volvulus. It usually occurs in patients who are 30–60 years old. There may be history of previous abdominal surgery, violent cough, atony of the colon, extreme exertion, unpressurized air travel or third trimester pregnancy. Patients usually present with nausea, vomiting, obstipation, and acute abdominal pain. In caecal volvulus, the cecum turns in clockwise direction and also inverts, occupying the left upper quadrant of the abdomen (Field 1994; Perret and Kunberger 1998). The terminal

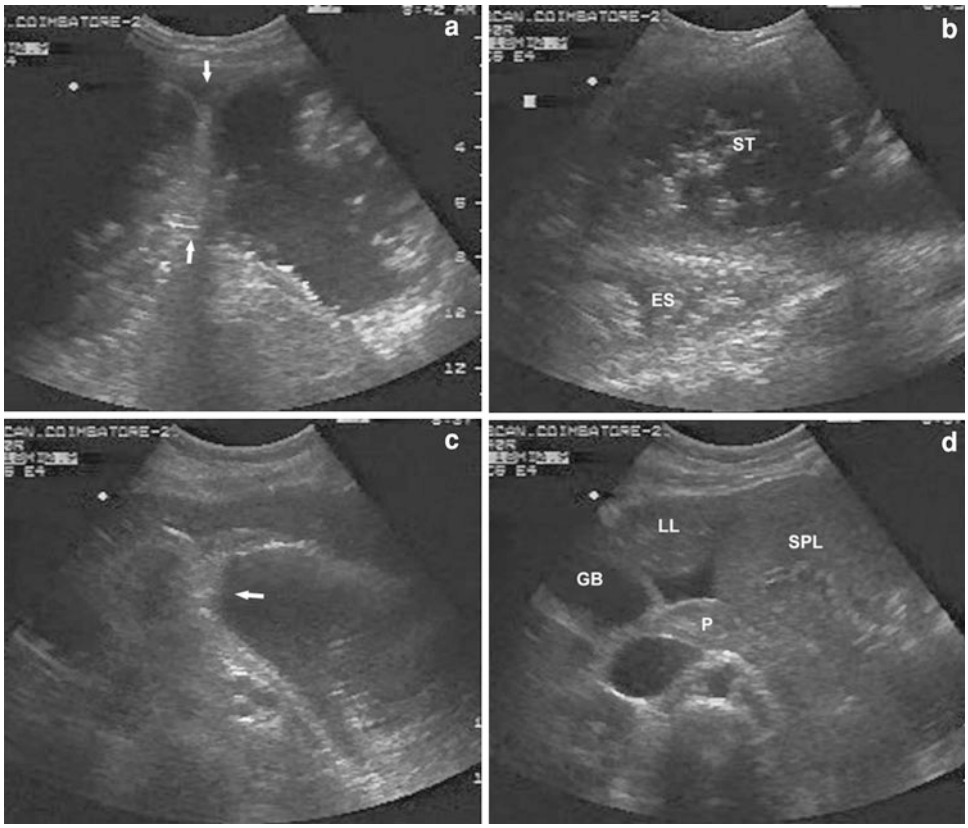

Fig. 12 Gastric volvulus. **a** Oblique scan through the *left* lower intercostal space showing the peanut sign with the stomach seen as two fluid-filled compartments with a constriction between them (*arrows*). **b** Longitudinal scan showing lack of continuity between fluid filled lower esophagus (ES) and stomach (ST). **c** Oblique scan of epigastrium showing the blind ending lower compartment of stomach with lack of continuity with duodenum (*arrow*). **d** Transverse scan of epigastrium showing the spleen (SPL) located between *left* lobe of liver (LL) and body of pancreas (P) with some free fluid in between. *GB* gall bladder

ileum is usually twisted along with the cecum. This results in closed loop of obstruction, causing massive dilatation of cecum and a small part of terminal ileum, which lies in the left upper quadrant. There is also small bowel obstruction. The CT signs of caecal volvulus are well described (Moore et al. 2001). Similar features are seen on sonography. The small bowel loops are dilated and show peristalsis indicating obstruction. The cecum, identified by its relation to the appendix, is seen as a grossly dilated bowel in left upper quadrant medial to the spleen (Fig. 13). The dilatation is disproportionately large compared with the dilated small bowels. The ascending colon is seen to be collapsed and normal.

5 Intussusception

Intussusception is defined as the invagination of a proximal segment of bowel (intussusceptum) into an adjacent distal segment (intussuscipiens). It is common in children and rare in adults. While there is no cause or lead point in children, there is an identifiable lesion as the lead point in 75–85 % of adults with intussusception (Yeh and Rabinowitz 1982; Swischuk et al. 1985). The causative lesion of small bowel is usually benign (52–61 %) and 50 % of those of colon prove to be malignant (Weilbaecher et al. 1971; Weissberg et al. 1977). Intussusception is the most common cause of bowel obstruction in children. The clinical presentation is usually acute in children. They present with abdominal pain or incessant cry in very young, vomiting, and passage of blood and mucus (red currant jelly) in stools (Bowerman et al. 1982). On clinical examination, a mass is usually located. Although no identifiable causative lesion is seen in most of the children, hypertrophied lymph follicles in distal ileum are thought to initiate the intussusception; hence, ileocolic intussusception is the common type. In adults, the presentation is usually chronic and intermittent with abdominal pain and vomiting. There are three types of intussusception depending on the segment of bowel involved: (a) enteroenteric or small bowel intussusception (small bowel into small bowel) (b) ileocolic (ileum into stationary ileocecal valve); and (c) colocolic (the colon into colon). As the intussusception progresses, the mesentery is caught between the entering and returning bowels. This leads to a cycle of venous obstruction, oedema, and eventually ischemic necrosis of the bowel.

On sonography, intussusception is seen as a mass showing the multiple concentric rings sign or doughnut sign on short axis. The multiple concentric rings sign is specific for this condition (Skaane and Skjennald 1989), with a reported accuracy of up to 100 % (Wang and Liu 1988) and is not seen in any other pathology (Fig. 14a). The various layers of the bowels forming the intussusception are seen well-differentiated when the oedema is less pronounced,

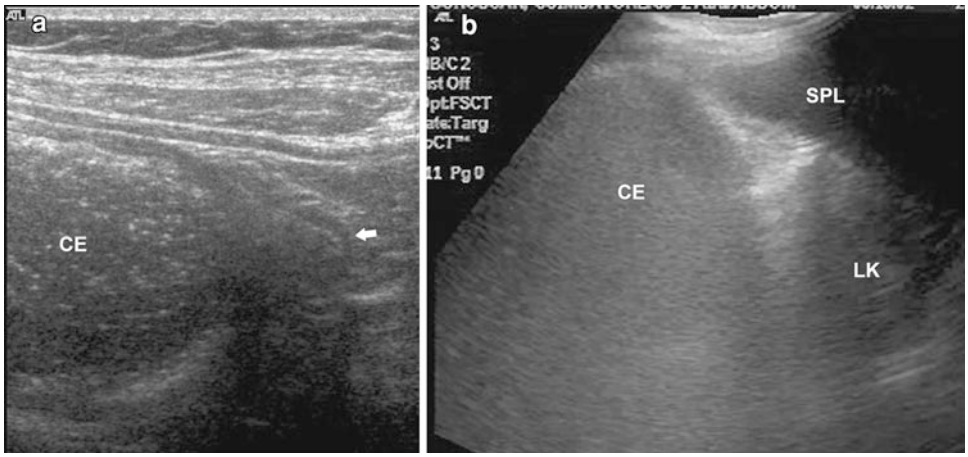

Fig. 13 Cecal volvulus. **a** Oblique scan of *left* hypochondrium showing a huge dilated cecum (CE) with cross section of appendix close to it (*arrow*). **b** Transverse scan of *left* flank showing the location of dilated cecum (CE) medial to spleen (SPL). *LK left* kidney

which results in the formation of this multiple concentric rings sign on transverse scan. In longitudinal scan, these layers are seen as multiple parallel hypoechoic and hyperechoic stripes resembling a sandwich (Fig. 14b). When the oedema of the bowel becomes marked the differentiation of layers is lost resulting in a doughnut sign (Fig. 14c). But, careful scan of the segment slightly proximal to the oedematous portion may reveal the characteristic concentric rings sign on transverse scan and multiple stripes sign in longitudinal scan in most patients (Montali et al. 1983). This maneuver is significant since the doughnut sign is a nonspecific one, seen in most of the pathological conditions of the bowel. With improved resolution of the scanners most of the intussusceptions show the characteristic multiple concentric rings sign. Although there is no differential diagnosis when the multiple concentric rings sign and multiple stripes sign are seen, care must be taken to exclude transient intussusception of small bowel. This is more so when the patient is asymptomatic and the lesion is seen centrally as in small bowel intussusception. The transient intussusception is usually (a) of short segment, (b) of small size, (c) lacking wall swelling, (d) located in central abdomen, (e) nonobstructive, (f) with persistent wall motion, and (g) without a lead-point lesion (Fig. 14d, e; Video 6; Kim 2004). Classically, the lesion is seen to move along the length of the bowel with peristalsis. The most important feature is that it is transient and a repeat scan after an interval of time fails to show the lesion. However, it is known that spontaneous reduction of an intussusception with all classical features, including oedematous walls, can happen (Kornecki et al. 2000). Rarely, small bowel intussusception can be asymptomatic and the author has seen two masses of small bowel intussusception in an asymptomatic patient with Peutz Jeghers syndrome. Even rarer is the double intussusception (Kazez et al. 2004). On sonography, the double intussusception shows three circles, called the "triple circle sign". (Fig. 14f).

Ileocolic intussusception, seen in children, is the commonest type. It is idiopathic and seen in children up to about four years. Enteroenteric or small bowel intussusception is the next common type. Here the mass of intussusception is seen in the center of the abdomen, whereas in the ileocolic and colocolic types, it is along the periphery, where the colon is located. If the small bowel intussusception starts in distal ileum, it can become ileocolic. There is a lead-point lesion in most of the small bowel intussusceptions. This can be a polyp, lipoma, lymphoma, Meckel's diverticulum, and hematoma of Henoch-Schonlein purpura. In some patients, the lead-point lesion can be seen on sonography. One study has reported identification of a lead-point lesion in two-thirds and a specific diagnosis in nearly one-third of the patients (Navarro et al. 2000). The appearance of the lead-point lesion varies from a pedunculated hypoechoic mass in adenomatous polyp (Fig. 15a), echogenic mass in inflammatory polyp (Fig. 15b), sessile echogenic mass in lipoma, and a sessile echo-poor wall thickening in lymphoma. Color Doppler study is useful in delineating the mass lesion at the tip of the intussusception (Fig. 15b). A cystic mass is seen as the lead point in an inverted Meckel's diverticulum (Daneman et al. 1997) or appendix (Koumanidou et al. 2001) (Fig. 15c). A similar cystic mass may be seen as a false cystic lead-point produced by fluid trapped within the intussuscepted mesentery (Kenney 1990). A lead-point lesion is always seen in colocolic intussusception and most of them are malignant.

Sonography is also useful in the treatment of childhood intussusception, the majority of which are idiopathic. Although barium enema and air enema were used in the past to reduce intussusception, hydrostatic reduction under sonographic control has evolved as the method of choice in the recent years. Very high success rates, up to 95.5 %, have been reported without any complications, in a large series of 337 patients (Wang and Liu 1988). It has an added advantage of lack of radiation exposure. In this technique

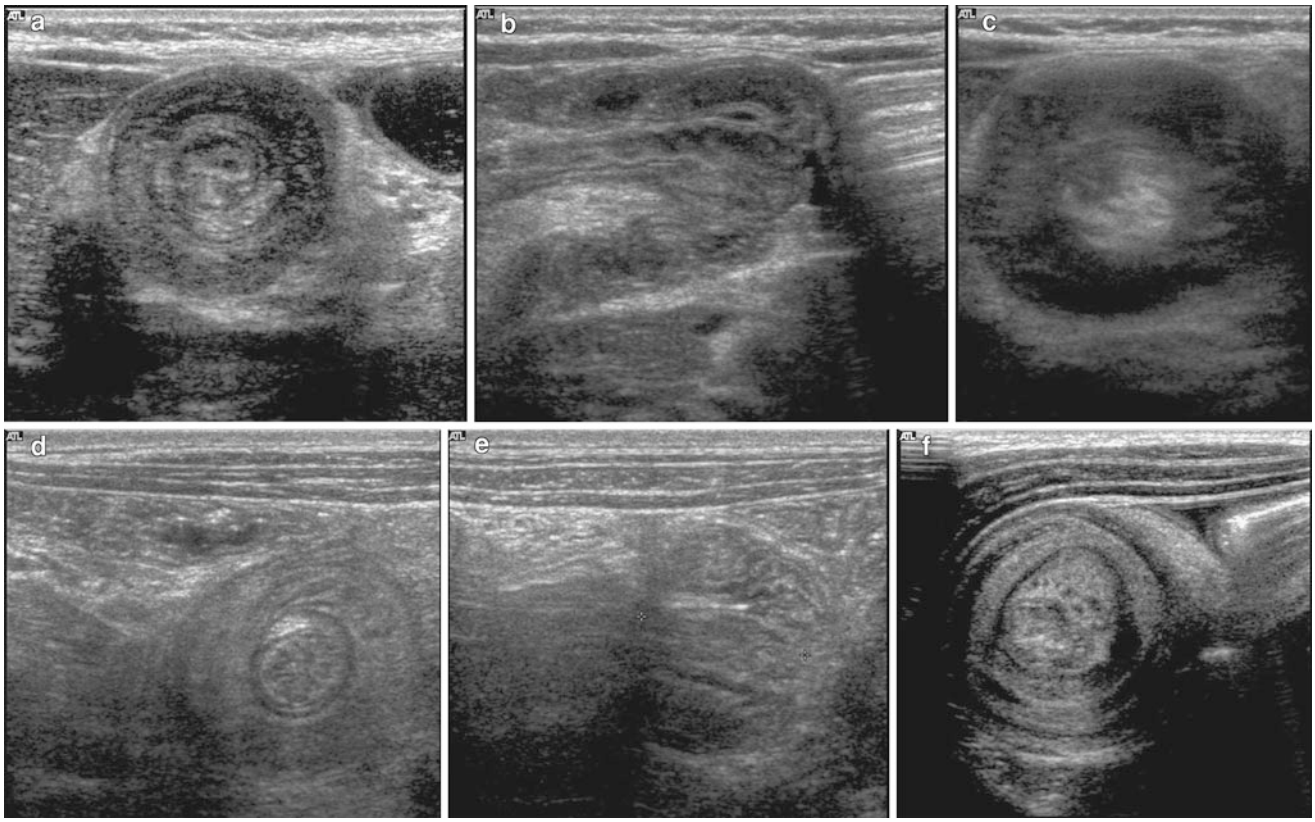

Fig. 14 Intussusception. **a** Short axis scan of the transverse colon showing the intussusception with the concentric rings sign. **b** Long axis scan showing the multiple stripes sign. **c** Doughnut sign of intussusception in short axis scan of transverse e colon. **d** Transverse and **e** Longitudinal scan of a transient intussusception. **f** Triple ring sign of a double intussusception

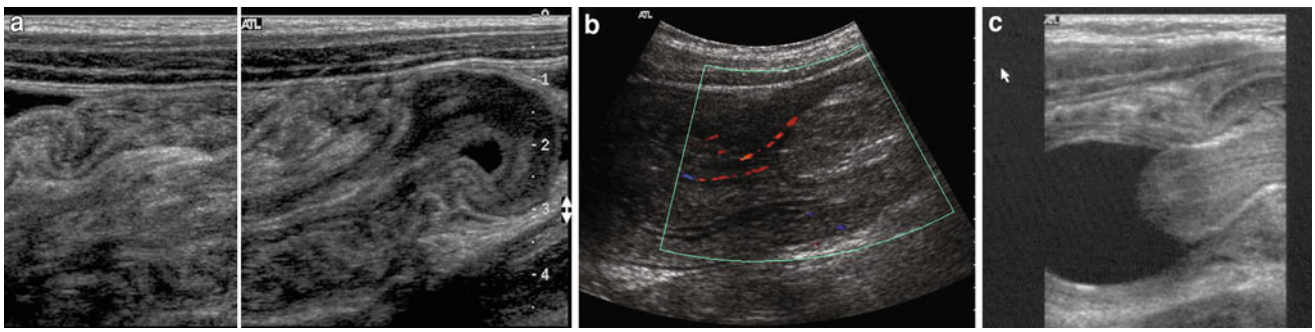

Fig. 15 Lead-point lesion in intussusception. **a** Adenomatous polyp **b** Inflammatory polyp **c** Inverted Meckel's diverticulum seen as cystic mass

after confirmation of presence of intussusception, hydrostatic reduction is attempted with introduction of an enema of tap water (Wood et al. 1992), saline (Wang and Liu 1988; Kim 2004), or Hartmann's solution (Riebel et al. 1993). The height of the enema bag is raised gradually from 80 cm (60 mm Hg) to a maximum of 155 cm (120 mm Hg). The progress of reduction of intussusception is followed by sonography. Complete reduction is confirmed by disappearance of the mass, reflux of fluid into terminal ileum and visualization of fluid-filled ileal loops (Video 7). If complete reduction is not achieved by maintaining the pressure for 5 min, the colon is drained and the same procedure is repeated after a rest of 3–5 min. When complete reduction has been achieved, sonography is repeated after an interval to rule out recurrence. The hydrostatic reduction is not attempted if certain risk factors are seen on initial sonography. These are patients older than 12 months, patients in shock, in presence of peritonitis, bowel perforation, gross abdominal distension, and sonographic features of small bowel intussusception and in recurrent intussusception of more than two episodes. Color Doppler signs predicting the ischemia of the intussusceptum have been reported with

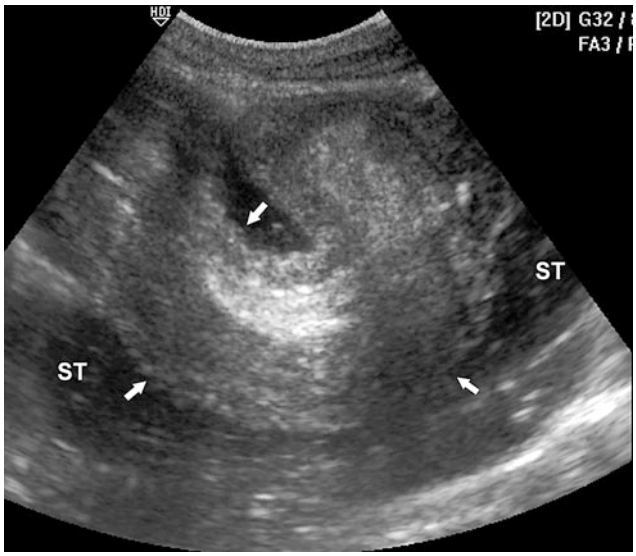

Fig. 16 Oblique scan of left hypochondrium showing the fluid distended stomach (ST) with a banana shaped mass of jejunogastric intussusception (*arrows*)

contradictory results (Lagalla et al. 1994; Kong et al. 1997; Hanquinet et al. 1998), but absence of flow on color Doppler study is not a contraindication for hydrostatic reduction (Lagalla et al. 1994). The success rate of reduction is affected by left-sided location of intussusception, presence of entrapped fluid in the intussusception and level of experience of the sonologist (Crystal et al. 2002).

5.1 Jejunogastric intussusception

Jejunogastric intussusception is invagination of the jejunum into stomach after a gastrojejunostomy. It is usually seen 10–30 years after the initial surgery (Wheatley 1989; Su et al. 2001). It results in efferent loop obstruction producing epigastric pain and vomiting. If treatment is delayed, it can produce hematemesis and necrosis of the invaginated loop (Brynitz and Rubinstein 1986; Hammond et al. 2001). Sonography is the investigation of choice, as it reveals with ease a dilated fluid-filled stomach and the intussuscepted oedematous, typically sausage, or banana-shaped mass of invaginated jejunum in the lumen of stomach (Fig. 16).

References

Aliotta A, Rapaccini GL, Pompili M et al (1994) Ultrasonographic signs of sliding, gastric, and hiatal hernia: their prospective evaluation. J Ultrasound Med 13:665–669

Ando H, Kaneko K, Ito F, Seo T, Ito T (1997) Anatomy of the round ligament in female infants and children with an inguinal hernia. Br J Surg 84:404–405

Aoyama K, Tateishi K (1986) Gastric volvulus in three children with asplenic syndrome. J Pediatr Surg 21:307–310

Borchardt M (1904) Zur pathologic and therapie des magenvolvulus. Arch Klin Chir 74:243

Bowerman RA, Silver TM, Jaffe MH (1982) Real-time ultrasound diagnosis of intussusception in children. Radiology 143:527–529

Brynitz S, Rubinstein E (1986) Hematemesis caused by jejunogastric intussusception. Endoscopy 18:162–164

Buranasiri SI, Baum S, Nusbaum M, Tumen H (1973) The angiographic diagnosis of midgut malrotation with volvulus in adults. Radiology 109:555–556

Cameron AE, Howard ER (1987) Gastric volvulus in childhood. J Pediatr Surg 22:944–947

Carter R, Brewer LA 3rd, Hinshaw DB (1980) Acute gastric volvulus. A study of 25 cases. Am J Surg 140:99–106

Catalano O (1997) US evaluation of inguinoscrotal bladder hernias: report of three cases. Clin Imaging 21:126–128

Cathcart RS 3rd, Williamson B, Gregorie HB Jr, Glasow PF (1981) Surgical treatment of midgut nonrotation in the adult patient. Surg Gynecol Obstet 152:207–210

Chiechi MV, Hamrick-Turner J, Abbitt PL (1992) Gastric herniation and volvulus: CT and MR appearance. Gastointest Radiol 17:99–101

Cho KC, Hoffman-Tretin JC, Alterman DD (1989) Closed-loop obstruction of the small bowel: CT and sonographic appearance. J Comput Assist Tomogr 13:256–258

Crystal P, Hertzanu Y, Farber B, Shabshin N, Barki Y (2002) Sonographically guided hydrostatic reduction of intussusception in children. J Clin Ultrasound 30:343–348

Daneman A, Myers M, Shuckett B, Alton DJ (1997) Sonographic appearances of inverted Meckel diverticulum with intussusception. Pediatr Radiol 27:295–298

Dattola P, Alberti A, Dattola A, Giannetto G, Basile G, Basile M (2002) Inguino-crural hernias: preoperative diagnosis and post-operative follow-up by high-resolution ultrasonography. A personal experience. Ann Ital Chir 73:65–68

Deitch EA, Soncrant MC (1981) The value of ultrasound in the diagnosis of nonpalpable femoral hernias. Arch Surg 116:185–187

Deitel M (1973) Chronic or recurring organoaxial rotation of the stomach. Can J Surg 16:195–205

Feldman M, Friedman LS, Sleisenger MH (2002) Sleisenger and Fordtran's Gastrointestinal and liver disease 7th edn, vol 2. Saunders, Phialdelphia

Field S (1994) Alimentary tract radiology, vol 1, 5th edn. Mosby, St. Louis

Fisher JK (1981) Computed tomographic diagnosis of volvulus in intestinal malrotation. Radiology 140:145–146

Furtschegger A, Sandbichler P, Judmaier W, Gstir H, Steiner E, Egender G (1995) Sonography in the postoperative evaluation of laparoscopic inguinal hernia repair. J Ultrasound Med 14:679–684

George EK, Oudesluys-Murphy AM, Madern GC, Cleyndert P, Blomjous JG (2000) Inguinal hernias containing the uterus, fallopian tube, and ovary in premature female infants. J Pediatr 136:696–698

Ghahremani GG (1984) Internal abdominal hernias. Surg Clin North Am 64:393–406

Griska LB, Popky GL (1980) Angiography in mid-gut malrotation with volvulus. AJR Am J Roentgenol 134:1055–1056

Gulati SM, Grover NK, Tagore NK, Taneja OP (1973) Volvulus of the small intestine in India. Am J Surg 126:661–664

Hammond N, Miller FH, Dynes M (2001) Intussusception into the enteroanastomosis after Billroth II gastrectomy and Roux-en-Y jejunostomy: sonographic and CT findings. AJR Am J Roentgenol 177:624–626

Hanquinet S, Anooshiravani M, Vunda A, Le Coultre C, Bugmann P (1998) Reliability of color doppler and power doppler sonography

in the evaluation of intussuscepted bowel viability. Pediatr Surg Int 13:360–362
Hayden CK Jr, Boulden TF, Swischuk LE, Lobe TE (1984) Sonographic demonstration of duodenal obstruction with midgut volvulus. AJR Am J Roentgenol 143:9–10
Hiller N, Alberton Y, Shapira Y, Hadas-Halpern I (1994) Richter's hernia strangulated in a spigelian hernia: ultrasonic diagnosis. J Clin Ultrasound 22:503–505
Holloway BJ, Belcher HE, Letourneau JG, Kunberger LE (1998) Scrotal sonography: a valuable tool in the evaluation of complications following inguinal hernia repair. J Clin Ultrasound 26:341–344
Huang CS, Luo CC, Chao HC, Chu SM, Yu YJ, Yen JB (2003) The presentation of asymptomatic palpable movable mass in female inguinal hernia. Eur J Pediatr 162:493–495
Kazez A, Ozel SK, Kocakoc E, Kiris A (2004) Double intussusception in a child: the triple-circle sign. J Ultrasound Med 23:1659–1661
Kenney IJ (1990) Ultrasound in intussusception: a false cystic lead point. Pediatr Radiol 20:348
Kim JH (2004) US features of transient small bowel intussusception in pediatric patients. Korean J Radiol 5:178–184
Kohli A, Vig A, Azad T (1997) Intrathoracic gastric volvulus—acute and chronic presentation. J Indian Med Assoc 95:522–523
Kong MS, Wong HF, Lin SL, Chung JL, Lin JN (1997) Factors related to detection of blood flow by color doppler ultrasonography in intussusception. J Ultrasound Med 16:141–144
Korenkov M, Paul A, Troidl H (1999) Color duplex sonography: diagnostic tool in the differentiation of inguinal hernias. J Ultrasound Med 18:565–568
Kornecki A, Daneman A, Navarro O, Connolly B, Manson D, Alton DJ (2000) Spontaneous reduction of intussusception: clinical spectrum, management and outcome. Pediatr Radiol 30:58–63
Koumanidou C, Vakaki M, Theofanopoulou M, Nikas J, Pitsoulakis G, Kakavakis K (2001) Appendiceal and appendiceal-ileocolic intussusception: sonographic and radiographic evaluation. Pediatr Radiol 31:180–183
Lagalla R, Caruso G, Novara V, Derchi LE, Cardinale AE (1994) Color doppler ultrasonography in pediatric intussusception. J Ultrasound Med 13:171–174
Le Dosseur P, Beaudet S, Dacher J, Al E (1992) Etude du reflux gastro-oesophagien chez l'enfant. Rev Im Med 4:153
Leonidas JC, Magid N, Soberman N, Glass TS (1991) Midgut volvulus in infants: diagnosis with US work in progress. Radiology 179:491–493
Liang RJ, Wang HP, Huang SP, Wu MS, Lin JT (2001) Color doppler sonography for ventral hernias in patients with acute abdomen: preliminary findings. J Clin Ultrasound 29:435–440
Llaneza PP, Salt WB 2nd (1986) Gastric volvulus. More common than previously thought? Postgrad Med 80(279–283):278–287
Matsuzaki Y, Asai M, Okura T, Tamura R (2001) Ultrasonography of gastric volvulus: "peanut sign". Intern Med 40:23–27
Middlebrook MR, Eftekhari F (1992) Sonographic findings in Richter's hernia. Gastointest Radiol 17:229–230
Montali G, Croce F, De Pra L, Solbiati L (1983) Intussusception of the bowel: a new sonographic pattern. Br J Radiol 56:621–623
Montes H, Wolf J (1999) Cecal volvulus in pregnancy. Am J Gastroenterol 94:2554–2556
Moore CJ, Corl FM, Fishman EK (2001) CT of cecal volvulus: unraveling the image. AJR Am J Roentgenol 177:95–98
Mufid MM, Abu-Yousef MM, Kakish ME, Urdaneta LF, Al-Jurf AS (1997) Spigelian hernia: diagnosis by high-resolution real-time sonography. J Ultrasound Med 16:183–187
Naik DR, Moore DJ (1984) Ultrasound diagnosis of gastro-oesophageal reflux. Arch Dis Child 59:366–367
Navarro O, Dugougeat F, Kornecki A, Shuckett B, Alton DJ, Daneman A (2000) The impact of imaging in the management of intussusception owing to pathologic lead points in children. A review of 43 cases. Pediatr Radiol 30:594–603
Nyhus LM, Condon RE (1989) Hernia, 3rd edn. JB Lippincott, Philadelphia
Oh A, Gulati G, Sherman ML, Golub R, Kutin N (2000) Bilateral eventration of the diaphragm with perforated gastric volvulus in an adolescent. J Pediatr Surg 35:1824–1826
Parkes G (1997) Primary small bowel volvulus in rural Nepal. Trop Doct 27:156–158
Parra JA, Revuelta S, Gallego T, Bueno J, Berrio JI, Farinas MC (2004) Prosthetic mesh used for inguinal and ventral hernia repair: normal appearance and complications in ultrasound and CT. Br J Radiol 77:261–265
Pelizzo G, Lembo MA, Franchella A, Giombi A, D'Agostino F, Sala S (2001) Gastric volvulus associated with congenital diaphragmatic hernia, wandering spleen, and intrathoracic left kidney: CT findings. Abdom Imaging 26:306–308
Perret RS, Kunberger LE (1998) Case 4: Cecal volvulus. AJR Am J Roentgenol 171:855, 859, 860
Pershad J, Simmons GT, Chung D, Frye T, Marques MB (1998) Two acute pediatric abdominal catastrophes from strangulated left paraduodenal hernias. Pediatr Emerg Care 14:347–349
Pracros JP, Sann L, Genin G, Tran-Minh VA, Morin de Finfe CH, Foray P, Louis D (1992) Ultrasound diagnosis of midgut volvulus: the "whirlpool" sign. Pediatr Radiol 22:18–20
Rettenbacher T, Hollerweger A, Macheiner P, Gritzmann N, Gotwald T, Frass R, Schneider B (2001) Abdominal wall hernias: cross-sectional imaging signs of incarceration determined with sonography. AJR Am J Roentgenol 177:1061–1066
Riebel TW, Nasir R, Weber K (1993) US-guided hydrostatic reduction of intussusception in children. Radiology 188:513–516
Scherer LR 3rd, Grosfeld JL (1993) Inguinal hernia and umbilical anomalies. Pediatr Clin North Am 40:1121–1131
Schwartz SI, Ellis H (1989) Maringot's Abdominal Operations, vol 1, 9th edn. Aleton and Large, Norwalk
Shivanand G, Seema S, Srivastava DN, Pande GK, Sahni P, Prasad R, Ramachandra N (2003) Gastric volvulus: acute and chronic presentation. Clin Imaging 27:265–268
Skaane P, Skjennald A (1989) Ultrasonic features of ileocecal intussusception. J Clin Ultrasound 17:590–593
Spangen L (1975) Ultrasound as a diagnostic aid in ventral abdominal hernia. J Clin Ultrasound 3:211–213
Su MY, Lien JM, Lee CS, Lin DY, Tsai MH (2001) Acute jejunogastric intussusception: report of five cases. Chang Gung Med J 24:50–56
Sutphen JH, Hitchcock DA, King DC (1980) Ultrasonic demonstration of spigelian hernia. AJR Am J Roentgenol 134:174–175
Swischuk LE, Hayden CK, Boulden T (1985) Intussusception: indications for ultrasonography and an explanation of the doughnut and pseudokidney signs. Pediatr Radiol 15:388–391
Sze RW, Guillerman RP, Krauter D, Evans AS (2002) A possible new ancillary sign for diagnosing midgut volvulus: the truncated superior mesenteric artery. J Ultrasound Med 21:477–480
Vijayaraghavan SB (1988) Diaphragmatic eventration into the pericardial sac: sonographic diagnosis. J Clin Ultrasound 16:510–512
Vijayaraghavan SB (2005) Sonographic features of Internal hernia. J Ultrasound Med (In press)
Vijayaraghavan SB, Palanivelu C, Sendhilkumar K, Parthasarathi R (2003) Abdominal cocoon: sonographic features. J Ultrasound Med 22:719–721

Vijayaraghavan SB, Ravikumar VR, Srimathy G (2004) Whirlpool sign in small-bowel volvulus due to a mesenteric cyst. J Ultrasound Med 23:1375–1377

Wang GD, Liu SJ (1988) Enema reduction of intussusception by hydrostatic pressure under ultrasound guidance: a report of 377 cases. J Pediatr Surg 23:814–818

Wastell C, Ellis H (1971) Volvulus of the stomach. A review with a report of 8 cases. Br J Surg 58:557–562

Wechsler RJ, Kurtz AB, Needleman L, Dick BW, Feld RI, Hilpert PL, Blum L (1989) Cross-sectional imaging of abdominal wall hernias. AJR Am J Roentgenol 153:517–521

Weilbaecher D, Bolin JA, Hearn D, Ogden W 2nd (1971) Intussusception in adults. Review of 160 cases. Am J Surg 121:531–535

Weissberg DL, Scheible W, Leopold GR (1977) Ultrasonographic appearance of adult intussusception. Radiology 124:791–792

Westra SJ, Wolf BH, Staalman CR (1990) Ultrasound diagnosis of gastroesophageal reflux and hiatal hernia in infants and young children. J Clin Ultrasound 18:477–485

Wheatley MJ (1989) Jejunogastric intussusception diagnosis and management. J Clin Gastroenterol 11:452–454

Wood SK, Kim JS, Suh SJ, Paik TW, Choi SO (1992) Childhood intussusception: US-guided hydrostatic reduction. Radiology 182:77–80

Yeh H, Rabinowitz J (1982) Ultrasonography of gastrointestinal tract. Semin Ultrasound CT MR 3:331

Zhang GQ, Sugiyama M, Hagi H, Urata T, Shimamori N, Atomi Y (2001) Groin hernias in adults: value of color doppler sonography in their classification. J Clin Ultrasound 29:429–434

Zimmerman LM, Laufman H (1953) Intraabdominal hernias due to developmental and rotational anomalies. Ann Surg 138:82–91

Ischemic Colitis

Etienne Danse

Contents

Abstract

Ischemic colitis is the most usual form of acute intestinal ischemia. It includes mainly two forms: the transient form with spontaneous resolution and the severe form. Two types of severe forms of ischemic colitis are to be considered: (a) ischemic colitis associated with a delayed stenosis caused by colic wall fibrosis, (b) ischemic colitis complicated by an early perforation caused by gangrenous evolution. Its diagnosis is based on the association of clinical data, endoscopic findings, radiological data and histology. Sonography can detect colic wall changes in cases of ischemic colitis such as increased colic wall thickening (8–9 mm), disappearance of the wall stratification (not systematic but more frequently noted than in other acute colic diseases), absence or reduced mural flow with color Doppler (in 20–50 % of patients with final diagnosis of ischemic colitis). Sonography can also detect hyperechogenicity of the pericolic fatty tissue and may be useful to delimitate the disease extension along the colic wall and its localization.

1 Introduction

Ischemic colitis is the most usual form of acute intestinal ischemia and is most commonly associated to a low mortality level, under 10 % (Martson et al. 1966; Boley 1990; Robert et al. 1993; Toursarkissian and Thompson 1997; Danse 2004; Balthazar et al. 1999). Its diagnosis is based on the association of clinical data, endoscopic findings, radiological data and histology (Martson et al. 1966; Boley 1990; Robert et al. 1993; Toursarkissian and Thompson 1997). There are mainly two forms of ischemic colitis: the transient form with spontaneous resolution and the severe form. Two types of severe forms of ischemic colitis are to be considered: (a) ischemic colitis associated with a delayed stenosis caused by colic wall fibrosis, (b) ischemic colitis complicated by an early perforation caused by gangrenous

E. Danse (✉)
Department of Radiology, St-Luc University Hospital, Université Catholique de Louvain, 10, Av Hippocrate, B-1200, Brussels, Belgium
e-mail: danse@rdgn.ucl.ac.be

G. Maconi and G. Bianchi Porro (eds.), *Ultrasound of the Gastrointestinal Tract*, Medical Radiology. Diagnostic Imaging,
DOI: 10.1007/174_2013_797, © Springer-Verlag Berlin Heidelberg 2013
Published Online: 10 February 2013

evolution (Martson et al. 1966; Boley 1990; Robert et al. 1993; Longo et al. 1997). Ischemic colitis is usually related to a good prognosis in the transient form and when there is a delayed stenosis. The gangrenous form, which is unusual, is frequently associated with a fatal outcome. Any segment of the colon can be affected, from the ileocecal valve to the rectum, but there is a predisposition for the left colon, due to its reduced vascular network.

Early identification of prognostic factors is helpful for an optimal therapy (Martson et al. 1966; Longo et al. 1992, 1997; Toursarkissian and Thompson 1997). These factors are present in 50 % of the patients and include age, duration of the symptoms, underlying disease (cardiovascular diseases and diabetes mellitus), abdominal aorta surgery and hypovolemic shock. These factors are frequently related to the severe forms of ischemic colitis (Longo et al. 1992, 1997; Danse et al. 2000a, b). It was also demonstrated that lactate dehydrogenase (LDH) levels and leucocyte counts are significantly higher in severe forms of ischemic colitis (Danse et al. 2000a).

Endoscopy is helpful for the recognition of suggestive findings for ischemic colitis. However, endoscopy is not demonstrative for the identification of the severity of the ischemic colitis if we consider its limitation for the correct delineation of the disease extension along the colon. Indeed, endoscopy is classically limited to a recto-sigmoidoscopy in the emergency context, in order to avoid perforation during the procedure. Additionally, biopsy samples are limited to the superficial layers of the colic wall (the mucosa and a part of the submucosa). For these reasons, sonography and computed tomography (CT) can contribute to the diagnosis of ischemic colitis. These techniques are also helpful for the delineation of the disease extension along the colon, and for recognition of severity factors (Balthazar et al. 1999; Federle et al. 1984; Jeffrey et al. 1994; Bozkurt et al. 1994; Philpotts et al. 1994; Ranschaert et al. 1994; Chou 2002).

2 Imaging Findings

Radiological findings suggestive of ischemic colitis were initially described on contrast enema (Boley 1990; Danse et al. 1997, 2000a, 2001). The role of conventional radiology for the recognition of severity factors is limited to its ability to show the extension in length of the colic wall changes (Martson et al. 1966; Robert et al. 1993; Toursarkissian 1997). Sonography and CT can be useful for the recognition of intestinal wall changes and insufficiency of the splanchnic arterial network. Sonography is combined with a color flow imaging of the colic wall and the main splanchnic vessels (Danse et al. 1997, 2001). CT is usually performed with intravenous contrast iodine injection. This approach allows identification of the wall vascularization and its alteration. Sonographic and CT findings include evaluation of the wall thickening, presence or absence of the wall stratification, detection of gas into the colic wall (colic pneumatosis) and the pericolic changes (Balthazar et al. 1999; Danse et al. 2000a, 2004; Federle et al. 1984; Bozkurt et al. 1994; Philpotts et al. 1994; Ranschaert et al. 1994; Teefey et al. 1996). Sonography and CT can also show signs for a prediction of the severity of ischemic colitis (Danse et al. 2000a; Chou 2002; Wiesner et al. 2001; Ripolles et al. 2005).

3 Sonographic Findings

Sonography can contribute to the visualization of colic wall changes in cases of ischemic colitis. We have to look for colic wall thickening (>5 mm), presence of the stratification, identification of the mural flow, delimitation of the disease extension along the colic wall and its localization (most frequently on the left colon) (Danse et al. 2004). The wall thickening is easy to detect. In ischemic colitis, it is usually slightly more pronounced than in inflammatory bowel disease but it is in the same range than in infectious colitis (from 8 to 9 mm) (Danse et al. 2000a; Jeffrey et al. 1994; Bozkurt et al. 1994; Teefey et al. 1996). It can mimic the nodular thickening observed in pseudomembranous colitis (Danse et al. 2004; Ranschaert et al. 1994). The increased mural thickness is caused by submucosal hematoma due to reperfusion injuries. Disappearance of the wall stratification is not systematic but more frequently noted than in other acute colic disease (Fig. 1). If absence of mural flow is noted with color Doppler, this is a clearly suggestive sign of ischemia (Danse et al. 2004; Teefey et al. 1996; Quillin and Siegel 1994; Hata et al. 1992; Siegel et al. 1997; Shirahama et al. 1999). Nevertheless, absence or reduced mural flow is reported only in 20–50 of the patients with a final diagnosis of ischemic colitis (Fig. 2) (Danse et al. 2000a; Ripolles et al. 2005).

When sonography is considered as the initial diagnostic method for ischemic colitis, it is associated with a sensitivity of 93 % for the adequate recognition of suggestive sonographic signs (Ripolles et al. 2005). Additionally, disappearance of the wall stratification and absence of mural flow are indicators of the severity of ischemic colitis with a sensitivity of 82 % and a specificity of 92 % (Danse et al. 2000a, 2004; Jeffrey et al. 1994; Cheung et al. 1992). Hyperechogenicity of the pericolic fatty tissue can be detected with sonography in patients with ischemic colitis. This sign has to be considered as a severity factor of

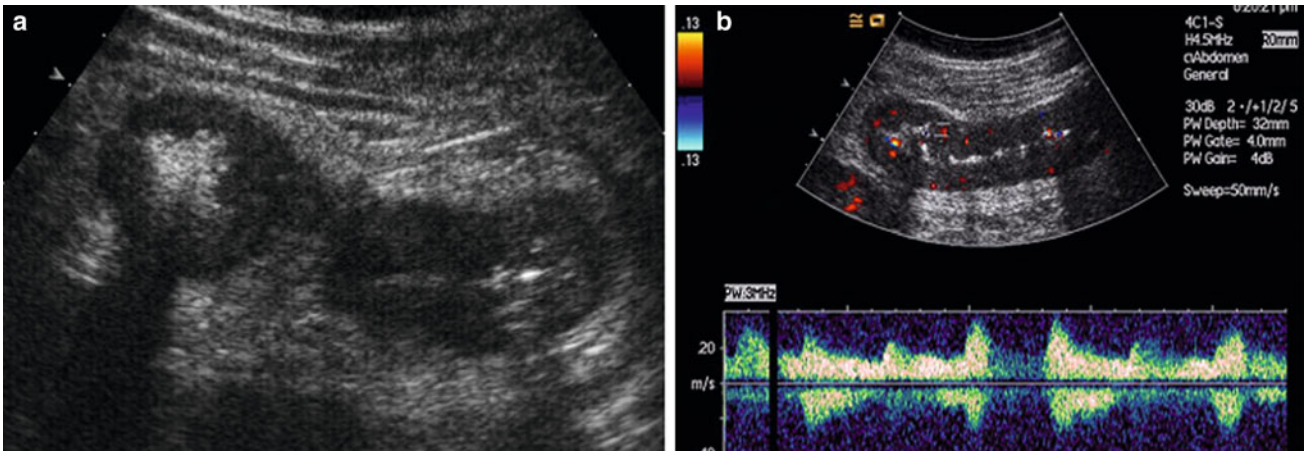

Fig. 1 Ischemic colitis in a young woman (drug addict). **a** Sonogram of the left colon showing a diffuse hypoechoic thickening of the colic wall, without stratification. **b** Preserved mural flow is demonstrated with color Doppler sonography

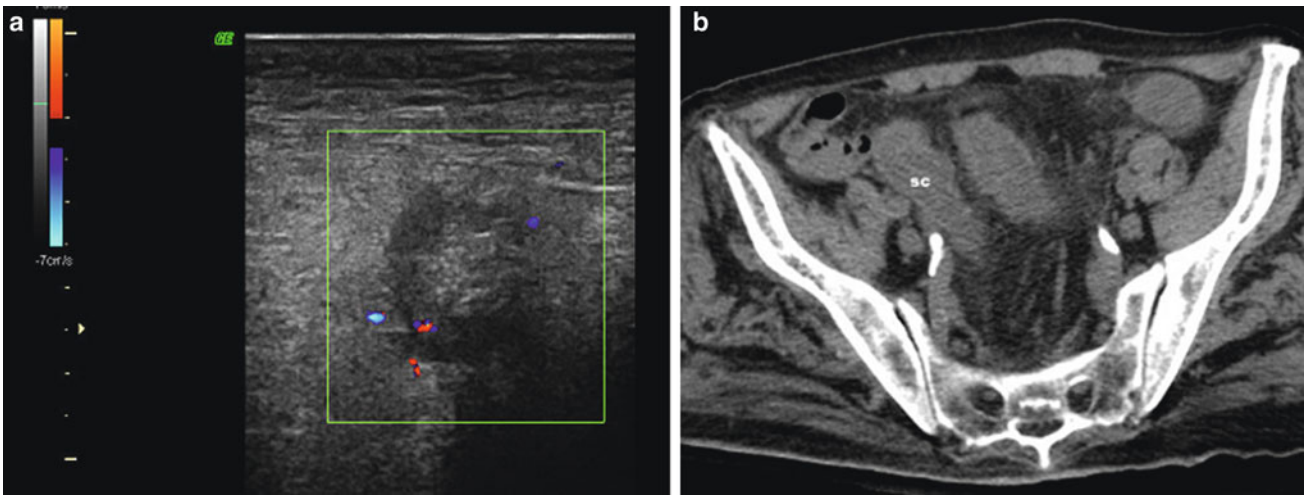

Fig. 2 Ischemic colitis in a 82-year-old patient. **a** Transverse view of the sigmoid colon showing thickening of the colon, with wall stratification and discrete mural flow detected with color Doppler sonography. The pericolic fat tissue is slightly infiltrated. **b** CT scan of the pelvis of the same patient showing diffuse thickening of the sigmoid colon

ischemia as well as the absence of mural flow (Fig. 3) (Ripolles et al. 2005). Predisposing factors can be detected with sonography when stenoses and/or occlusion of the main splanchnic arteries are visualized (celiac trunk, superior and inferior mesenteric arteries) (Danse et al. 2001). Splanchnic vascular insufficiency requires stenosis or occlusion of at least two of the three splanchnic arteries. Significant stenosis of the celiac trunk is present when the maximal systolic velocity is higher than 1.5 m/s. Superior and inferior mesenteric arteries are considered as significantly stenosed if the maximal systolic velocity is higher than 2.75–3 m/s (Bowersox et al. 1991). Sonography has been recently reported as useful for the follow-up of the patients, by showing disappearance of the colic wall changes (Ripolles et al. 2005).

4 Computed Tomography Findings

Thickening of the colic wall related to ischemic colitis is visible with CT, within the same values than sonography (8–9 mm) (Horton et al. 2000; Philpotts et al. 1994). CT findings observed in ischemic colitis are of three types: (a) heterogeneous thickening with hypoperfused areas combined with pericolic fat stranding (40–60 % of the patients), (b) homogeneous thickening without any change

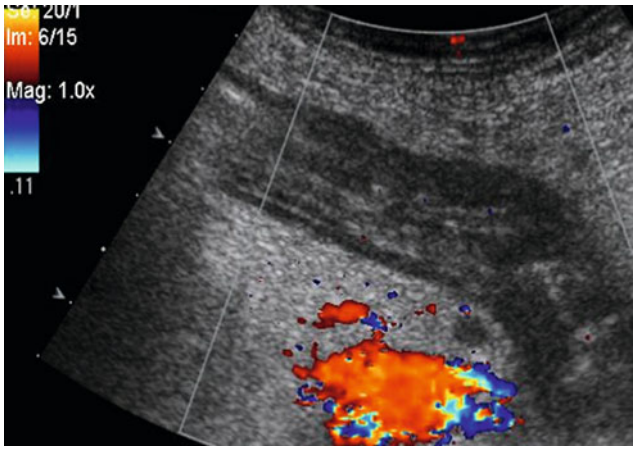

Fig. 3 Ischemic colitis with preserved wall stratification but without any mural flow. Infiltration of the pericolic fat tissue. Resection was performed in emergency, revealing extended necrosis of the *left* colon

of the pericolic fat tissue (33–37 % of the cases), (c) colic pneumatosis within a thin colic wall (6–21 % of the cases) (Balthazar et al. 1999). Ascites is present in less than 30 % of the patients (Balthazar et al. 1999; Philpotts et al. 1994). Severity factors of ischemic colitis at CT are the presence of a thin colic wall, with pneumatosis and reduced or absent colic wall enhancement when iodine contrast injection is performed (Balthazar et al. 1999).

5 Proposed Strategy

When there is a strong suspicion of ischemic colitis, rectosigmoïdoscopy is performed and can be completed with an abdominal color Doppler study. The role of sonography is to detect the extension of the colitis, and to detect suggestive signs of ischemic colitis (colic wall thickening of the left colon without identifiable mural flow). Prognosis factors are also to look for with sonography, including wall stratification, pericolic fatty tissue hyperechogenicity and ascites. Suggestive predisposing factors like stenoses and/or occlusion of the main splanchnic arteries can also be detected with color Doppler sonography. When sonography is normal or inconclusive, CT is then performed, with intravenous contrast injection if possible.

However, ischemic colitis is a frequent initially unsuspected condition. The radiologist is often the first physician to suggest intestinal ischemia when he identifies a segmental or diffuse colic wall thickening with sonography or CT, in patients for whom cross-sectional imaging studies are required for acute nonspecific abdominal pain. In these cases, when a colic wall change is noted with sonography or CT, the radiologist can suggest ischemic colitis on the basis of the localization of the affected segment, the absence of mural flow or enhancement, visualization of an infiltration of the pericolic fat tissue, pneumatosis, and stenoses or occlusions of the splanchnic arteries. In these initially unsuspected cases, endoscopy is then needed to confirm the ischemic changes of the colic wall (Danse et al. 2005).

References

Balthazar EJ, Yen BC, Gordon RB (1999) Ischemic colitis: CT evaluation of 54 cases. Radiology 211:381–388

Boley JS (1990) Colonic ischemia-25 years later. Am J Gastroenterol 85:931–934

Bowersox JC, Zwolak RM, Walsh DB et al (1991) Duplex ultrasonography in the diagnosis of celiac and mesenteric artery occlusive disease. J Vasc Surg 14:780–788

Bozkurt T, Richter F, Lux G (1994) Ultrasonography as a primary diagnostic tool in patients with inflammatory disease and tumors of the small intestine and the large bowel. J Clin Ultrasound 22:85–91

Cheung AH, Wang KY, Jiranek GC et al (1992) Evaluation of a 20 MHz ultrasound transducer used in diagnosing porcine small bowel ischemia. Invest Radiol 27:217–223

Chou CK (2002) CT manifestations of bowel ischemia. AJR Am J Roentgenol 178:87–91

Danse E (2004) Imagerie des urgences abdominales non traumatiques de l'adulte. Encyclopédie Médico-Chirurgicale 33:705

Danse EM, Laterre PF, Van Beers BE et al (1997) Early diagnosis of acute intestinal ischemia: contribution of color Doppler sonography. Acta Chir Belg 97:173–176

Danse EM, Van Beers BE, Jamart J et al (2000a) Prognosis of ischemic colitis: comparison of color Doppler sonography with early clinical and laboratory findings. AJR Am J Roentgenol 175:1151–1154

Danse EM, Van Beers BE, Materne R (2000b) Small bowel wall changes in acute mesenteric ischemia: sonographic findings. Ultrasound Med Biol 26:A128

Danse EM, Hammer F, Matondo H et al (2001) Ischémie mésentérique chronique d'origine artérielle: mise en évidence de réseaux de vicariance par échographie Doppler couleur. J Radiol 82:1645–1649

Danse E, Jamart J, Hoang P et al (2004) Focal bowel wall changes detected with colour Doppler ultrasound: diagnostic value in acute non-diverticular diseases of the colon. Br J Radiol 77:917–921

Danse E, Dewit O, Goncette L et al (2005) Que faire en cas d'affection aiguë du colon? Une échographie, un scanner, des clichés conventionnels ou une endoscopie? SFR Paris octobre 2005. Formation Médicale Continue 23:241–253

Federle MP, Chun G, Jeffrey RB, Rayor R (1984) Computed tomographic findings in bowel infarction. AJR Am J Roentgenol 142:91–95

Hata J, Haruma K, Suenaga K et al (1992) Ultrasonographic assessment of inflammatory bowel disease. Am J Gastroenterol 87:443–447

Horton KM, Corl FM, Fishman EK (2000) CT evaluation of the colon: inflammatory disease. Radiographics 20:399–418

Jeffrey RB, Sommer G, Debatin JF (1994) Color Doppler sonography of focal gastrointestinal lesions: initial clinical experience. J Ultrasound Med 13:473–478

Longo WE, Ballantyne GH, Gusberg RJ (1992) Ischemic colitis: patterns and prognosis. Dis Colon Rectum 35:726–730

Longo WE, Ward D, Vernava AM, Kaminski DL (1997) Outcome of patients with total colonic ischemia. Dis Colon Rectum 40:1448–1454

Marston A, Pheils MT, Thomas ML, Morson BC (1966) Ischaemic colitis. Gut 7:1–15

Philpotts LE, Heiken JP, Westcott MA, Gore RM (1994) Colitis: use of CT findings in differential diagnosis. Radiology 190:445–449

Quillin SP, Siegel MJ (1994) Gastrointestinal inflammation in children: color Doppler ultrasonography. J Ultrasound Med 13:751–756

Ranschaert E, Verhille R, Marchal G, Rigauts H, Ponette E (1994) Sonographic diagnosis of ischemic colitis. J Belge Radiol 77:166–168

Ripolles T, Simo L, Martinez-Perez MJ et al (2005) Sonographic findings in ischemic colitis in 58 patients. AJR Am J Roentgenol 184:777–785

Robert JH, Mentha G, Rohner A (1993) Ischaemic colitis: two distinct patterns of severity. Gut 34:4–6

Shirahama M, Ishibashi H, Onohara S, Dohmen K, Miyamoto Y (1999) Color Doppler ultrasound for the evaluation of bowel wall thickening. Br J Radiol 72:1164–1169

Siegel MJ, Friedland JA, Hildebolt CF (1997) Bowel wall thickening in children: differentiation with US. Radiology 203:631–635

Teefey SA, Roarke MC, Brink JA et al (1996) Bowel wall thickening; differentiation of inflammation from ischemia with color Doppler and duplex US. Radiology 198:547–551

Toursarkissian B, Thompson RW (1997) Ischemic colitis. Surg Clin North Am 77:461–470

Wiesner W, Mortelé KJ, Glickman JN, Ji H, Ros P (2001) Pneumatosis intestinal and portomesenteric venous gas in intestinal ischemia: correlation of CT findings with severity of ischemia and clinical outcome. AJR Am J Roentgenol 177:1319–1323

Epiploic Appendagitis

Giovanni Maconi and Federica Furfaro

Contents

Abstract

Epiploic appendagitis is an uncommon, benign inflammatory process of epiploic appendages which are adipose structures protruding from the colon. Epiploic appendagitis is an infrequent, often misdiagnosed cause of abdominal pain. Its diagnosis can be suspected in adult patients with well-localised acute abdominal pain with no or only mild systemic inflammation. Fever is usually absent or mild, and leukocytes and C reactive protein are usually normal or slightly elevated. The diagnosis can be made with ultrasonography which shows a hyperechoic, ovoid, non-compressible, solid mass at the site of maximum abdominal tenderness, often surrounded by a hypoechoic rim. Sonologists should be aware of this self-limiting and benign disease, which mimics other abdominal acute conditions, such as diverticulitis, cholecystitis and appendicitis, so that unnecessary intervention can be avoided.

1 Introduction

Epiploic appendagitis is an uncommon, benign and self-limiting inflammatory process of epiploic appendages which are pedunculated and mobile structures constituted by adipose tissue and blood vessels, protruding from the serosal surface of the colon into the peritoneal cavity. Epiploic appendagitis is an uncommon cause of acute and subacute abdominal pain.

Interest in primary epiploic appendagitis has grown because it frequently mimics acute abdominal diseases such as diverticulitis and appendicitis (Kim et al. 2001).

In fact, epiploic appendagitis is the correct diagnosis in 2–7 % of presumed diverticulitis cases and 1 % of presumed appendicitis cases (Rao et al. 1997; Molla et al. 1998).

Before the widespread use of cross-sectional imaging techniques, its diagnosis was usually made at surgery (Horton et al. 2000). Nowadays, although epiploic

G. Maconi (✉) · F. Furfaro
Gastroenterology Unit, Department of Biomedical and Clinical Sciences, "L. Sacco" University Hospital, Via G.B. Grassi, 74, 20157, Milan, Italy
e-mail: giovanni.maconi@unimi.it

G. Maconi and G. Bianchi Porro (eds.), *Ultrasound of the Gastrointestinal Tract*, Medical Radiology. Diagnostic Imaging,
DOI: 10.1007/174_2013_796, © Springer-Verlag Berlin Heidelberg 2013
Published Online: 15 February 2013

appendages are generally radiologically invisible, they become evident in inflammatory conditions and can be easily diagnosed by non-invasive imaging methods such as abdominal ultrasonography and/or computed tomography (Singh et al. 2005; Ozdemir et al. 2010).

Due to its benign, self-limited course, the appropriate radiological diagnosis allows the clinician to pursue conservative management, avoiding unnecessary intervention in particular when a right-sided appendage is affected. In these cases, the accurate diagnosis of right-sided appendagitis, bypasses unnecessary surgical treatment (Van breda vriesman et al. 1999; Hasbahceci et al. 2012). However, since most cases of epiploic appendagitis are located on the left side (Ghahremani et al. 1992; Carmichael and Organ 1985), patients with left lower quadrant pain suggestive of diverticulitis are treated medically (unless complications are present) and therefore, epiploic appendagitis is diagnosed more rarely, and its frequency remains underestimated.

2 Anatomy and Pathology

Epiploic appendages are adipose structures protruding from the colon and covered by the peritoneum. Approximately 50–100 appendages are distributed from the caecum to the rectosigmoid junction, in particular in distal sigma and sigmoid colon (80 %) and in descending colon (12 %) (Fig. 1). They are arranged in two rows along the taenia libera and the taenia omentalis except for the transverse colon, where only one row is present. This explains why most cases of epiploic appendagitis occur in the sigmoid colon.

Normal appendages can be seen on sonography or CT only if surrounded by free intraperitoneal fluid (Fig. 2). Most of them are 2–5 cm in length and 1–2 cm thick, with vessels passing through their narrow pedicle. The pedunculated nature and the great mobility of the appendages are factors that increase the possibility of torsion and infarction.

The nature of epiploic appendagitis may be primary or secondary. Primary epiploic appendagitis is attributed to either torsion or spontaneous venous thrombosis with subsequent ischemic or haemorrhagic infarction and inflammation of the epiploic appendages (Rao et al. 1997; Rioux and Langis 1994). Secondary epiploic appendagitis is caused by adjacent inflammatory processes such as diverticulitis, appendicitis or cholecystitis (Molla et al. 1998).

Epiploic appendagitis is primarily an adult disease. Epiploic appendages are rudimentary in children, reach an appreciable size in adulthood and are largest in obese patients. Obesity is a possible predisposing factor for epiploic appendagitis, and heavy exercise and excessive stretching have been reported to precede the onset of clinical symptoms (Hollerweger et al. 2002).

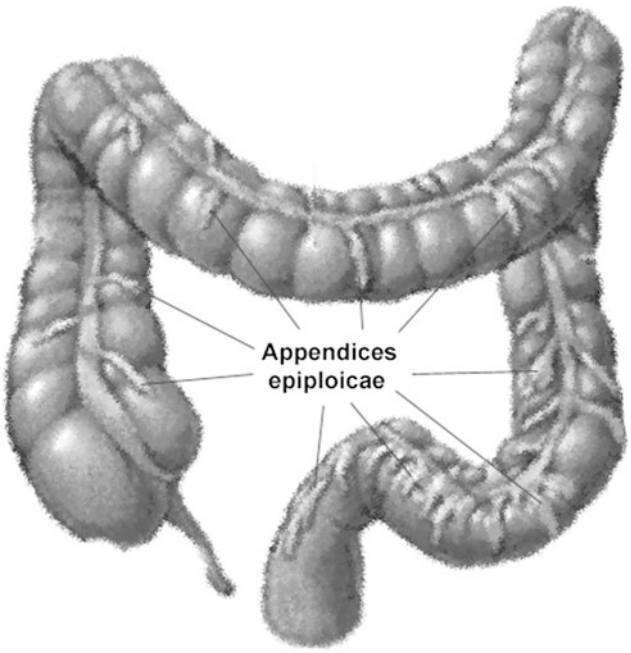

Fig. 1 Schematic view of the sigmoid colon with several epiploic appendages

3 Clinical Manifestations

Epipolic appendagitis is characterised by acute or subacute abdominal pain, mostly at the left lower quadrant, suggestive of acute diverticulitis. Pain could be localised or show signs of peritonitis. Epiploic appendagitis of the caecum or ascending colon usually presents with right lower or right upper quadrant pain that mimics appendicitis or cholecystitis (Van breda vriesman et al. 1999).

Most patients report an acute onset of abdominal pain and well-localised tenderness. Pain may intensify on coughing, deep breathing or stretching or when a skin fold is pulled upward; this is due to the adherence of the inflamed appendages to the parietal peritoneum. A few patients may experience initially mild symptoms that increase during the first days. Symptoms improve gradually within 5–7 days after their onset, but, in some cases, they may last up to 2–3 weeks.

Other notable complaints or clinical findings, such as fever >38 °C, nausea, vomiting or diarrhoea are usually absent.

Although epiploic appendagitis has some specific clinical features, this is often misdiagnosed and it is rarely considered in the differential diagnosis with other acute conditions. In this regard, the degree of inflammatory response may help in the differential diagnosis because epiploic appendagitis is associated with no or only mild systemic inflammation (Legome et al. 2002). The leukocytes count is normal or slightly superior to normal values;

Table 1 Main biochemical features of patients with epiploic appendagitis reported by the largest series of patients published in the literature

Author, year	No. of pts	C reactive protein		White blood cells	
		Increased values n, (%)	Median (range) of increased values	Increased values n, (%)	Median (range) of increased values
Sand et al. (2007)	10	5 (50)	9 (5–15)	1 (10)	11,400
Görg et al. (2009)	20	6 (30)	14 (7–23)	n.a.	n.a.
Ozdemir et al. (2010)	12	n.a.	n.a.	4 (33.3)	14,600 (12,800–20,500)
Chen et al. (2011)	21	n.a.	n.a.	6 (28.6)	11,450 (10,500–11,800)
Choi et al. (2011)	27	n.a.	n.a.	4 (12.9)	n.a.

n.a. not available

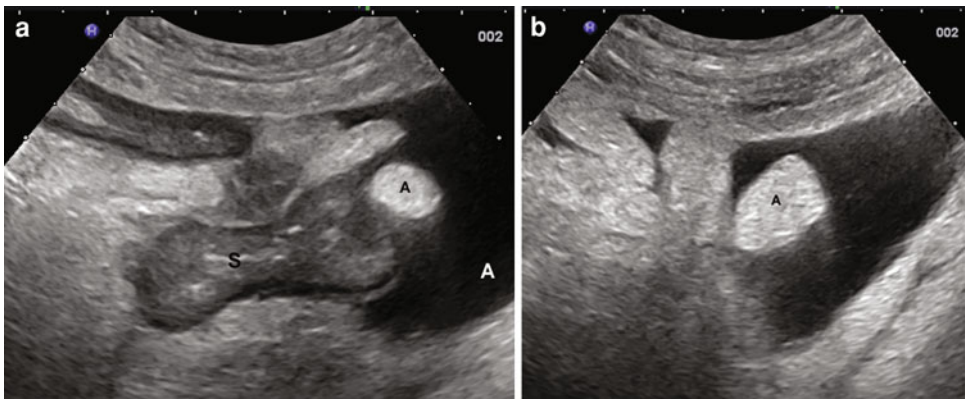

Fig. 2 **a**, **b** Ultrasonographic aspect of normal appendages (*arrows*) observed in patients with ulcerative colitis and ascites (*A*). *S* sigmoid colon

erythrocyte sedimentation rate and C reactive protein are usually normal or slightly elevated (Table 1).

Epiploic appendagitis is generally a self-limiting disease and conservative treatment is recommended unless imaging methods indicate a complicated disease. When patients are treated with mild analgesics, symptoms mostly resolve over the course of 1 week. Laparoscopic resection may be useful in selected cases, especially when abdominal pain persists (Schnedl et al. 2011).

4 Ultrasound

The first ultrasonographic description of epiploic appendagitis was reported in 1987 (Jennings and Collins 1987).

The characteristic finding on sonography is a moderately hyperechoic, ovoid, non-compressible, solid mass with a greater diameter usually ranging from 25 to 30 mm. The lesion is found at the site of maximum tenderness, usually under the abdominal wall, attached to the colon (Fig. 3).

The lesion may be surrounded by a hypoechoic rim due to thickening of the serosal surface of appendages and of the parietal peritoneum and sometimes encloses necrotic tissue or reactive inflammatory tissue which is covered with fibrinoleukocytic exudate and could give a mass effect on the adjacent bowel wall or on the abdominal wall. Occasionally, we can see a hypoechoic area in the mass, probably representing a thrombosed vessel or a haemorrhage (Fig. 4). Rarely, fascial thickening can be observed sonographically. These latter findings (the thrombosed vessel, hyperdense areas caused by haemorrhaging, and fascial thickening) can be shown more clearly on computed tomography scans.

The adjacent colon is usually normal with regular bowel-wall layers, but thickening of the bowel wall is visible in about 10 % of patients, sometimes due to hyperptrophy of muscularis propria in patients with diverticular disease. In many cases, sonography reveals more detailed information than computed tomography, for instance concerning the different layers of the colonic wall and inflamed colonic diverticula, and could show the adherence of the altered appendage to the peritoneum during deep inspiration and expiration by the patient.

If bowel-wall thickening or an inflamed diverticulum is absent in patients suspected of having acute diverticulitis, the investigator should look for a hyperechoic mass at the anterior or lateral aspect of the colon, suggesting epiploic appendagitis, in particular in a specific clinical context (see above).

In addition, a high-frequency transducer must be used in many cases for improving delineation of the altered pericolic fat. If the mass has only slightly different echogenicity

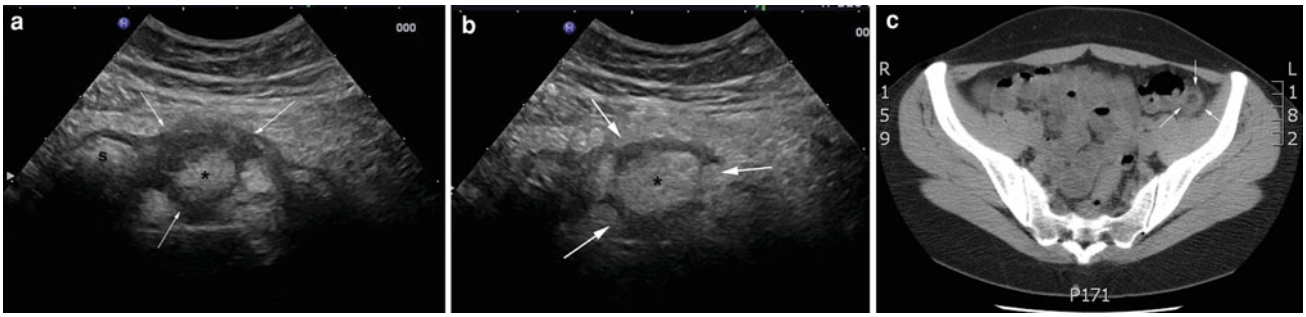

Fig. 3 **a**, **b** Ultrasonographic features of epiploic appendagitis detected in a 35-year-old woman, as a homogeneous hyperchoic mass (*asterisks*) with thin hypoechic border (*arrows*), near the sigmoid colon (*S*). **c** The same lesion detected with computed tomography, characterised by fat attenuation and a hyperdense rim (*arrows*)

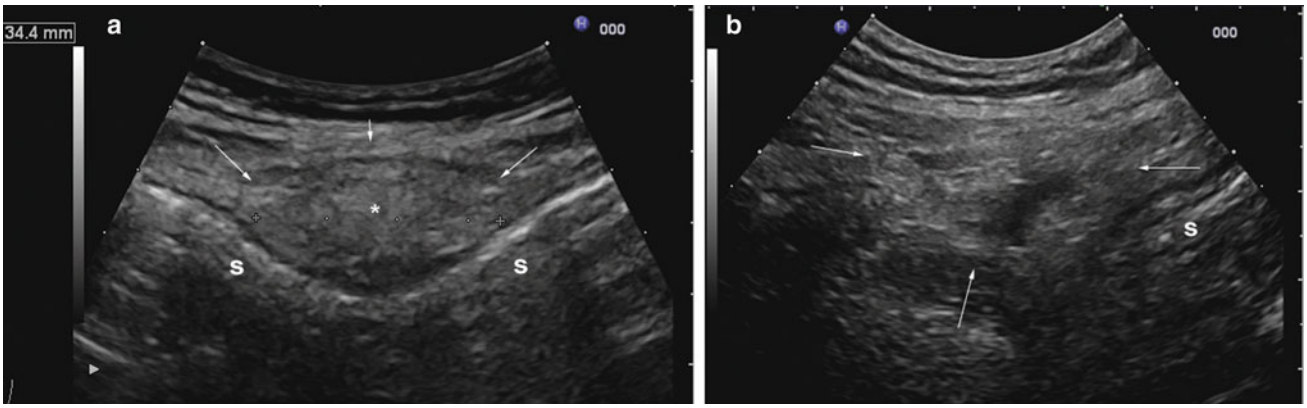

Fig. 4 Longitudinal (**a**) and transverse (**b**) ultrasonographic section of an epiploic appedagitis in a 42-year-old man with acute abdominal pain. **a** Ultrasound showed in left iliaca fossa, at the site of maximum tenderness, a hyperchoic mass (*asterisks*) with a diameter of 3 cm, with thin hypoechic border (*arrows*), adjacent to the sigmoid colon (*s*). **b** the same lesion (*arrows*) in a transverse scan showed a hypoechoic area within the mass, probably representing a thrombosed vessel or a haemorrhage

from that of normal intra-abdominal fat, testing the adherence to the anterior abdominal wall is a further useful tool.

Ultrasonographic Doppler shows absent or weak internal blood flow, unlike that of appendicitis or diverticulitis which are usually well vascularised. The use of contrast-enhanced ultrasound (for this exam a volume of 2.4 ml of contrast medium of Sonovue ® is adequate) may be helpful to confirm the diagnosis of epiploic appedagitis in equivocal cases. At contrast-enhanced ultrasound, all these lesions show a central area of no enhancement with broad perilesional enhancement (>1 cm) in most cases, or only a marginal hyperechoic rim (<1 cm) (Görg et al. 2009).

Ultrasonographic follow-up imaging can be used to show the spontaneous resolution of epiploic appendagitis. Following the initial phase, where the necrotic appendage is clearly demarcated by a hypoechoic rim, the lesion slowly decreases in size and the appendage may become detached from its peritoneal fixation. After 1–2 months, sonography generally shows complete disappearance of the lesion (Hollerweger et al. 2002).

Given the high accuracy in detecting this lesion, ultrasound has been recommended as a first line procedure in the diagnostic algorithm of patients with non-specific abdominal pain and suspected epiploic appendagitis (Fig. 5). The same study also recommends that patients with diagnostic ultrasonographic features do not need further investigation, while those with inconclusive results should undergo computed tomography (Ozdemir et al. 2010).

5 Computed Tomography

At computed tomography epiploic appendagitis appears as an oval pericolic lesion with fat attenuation slightly superior to normal fat and with a hyperdense rim (Fig. 3c). Parietal peritoneal thickening, fascial thickening and perilesional fat stranding are frequently seen. A central dot or line of high attenuation is thought to represent the thrombosed vessel and fibrous tissue or haemorrhage. If follow-up is performed, decrease of lesion size, clearing of periappendageal

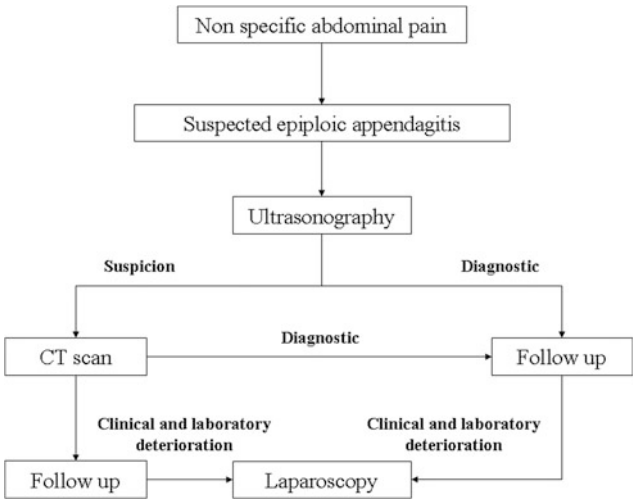

Fig. 5 Proposed algorithm for patients with suspected epiploic appendagitis (modified from Ozdemir et al. 2010)

fat stranding and loss of the smooth outline of the lesion can be observed. Occasionally, a fibrous band or calcified appendage may remain. If sonography is the first imaging method used in diagnosing epiploic appendagitis, computed tomography is often used to confirm the sonographic diagnosis and to exclude other inflammatory processes in the abdomen. Measurements of the mass can differ from sonography to computed tomography. Sonography may not differentiate between the necrotic area and adjacent inflammation unless the infarcted appendage is surrounded by a hypoechoic rim. However, if perilesional fat stranding is included in computed tomography measurements, the size of the lesion may appear greater than on sonography, because computed tomography is more sensitive in depicting slight inflammation of fat tissue (Hollerweger et al. 2002).

References

Carmichael DH, Organ CH Jr (1985) Epiploic disorders. Conditions of the epiploic appendages. Arch Surg 120:1167–1172

Chen JH, Wu CC, Wu PH (2011) Epiploic appendagitis: an uncommon and easily misdiagnosed disease. J Dig Dis 12:448–452

Choi YU, Choi PW, Park YH et al (2011) Clinical characteristics of primary epiploic appendagitis. J Korean Soc Coloproctol 27:114–121

Ghahremani GG, White EM, Hoff FL et al (1992) Appendices epiploicae of the colon: radiologic and pathologic features. Radiographics 12:59–77

Görg C, Egbring J, Bert T (2009) Contrast-enhanced ultrasound of epiploic appendagitis. Ultrashall Med 30:163–167

Hasbahceci M, Erol C, Seker M (2012) Epiploic appendagitis: is there need for surgery to confirm diagnosis in spite of clinical and radiological findings? World J Surg 36:441–446

Hollerweger A, Macheiner P, Rettenbacher T, Gritzmann N (2002) Primary epiploic appendagitis: sonographic findings with CT correlation. J Clin Ultrasound 30:481–495

Horton KM, Corl FM, Fishman EK (2000) CT evaluation of the colon: inflammatory disease. Radiographics 20:399–418

Jennings CM, Collins MC (1987) The radiological findings in torsion of an appendix epiploica. Br J Radiol 60:508–509

Kim YS, Kim Y, Cho OK et al (2001) Sonography for right lower quadrant pain. J Clin Ultrasound 29:157–185

Legome EL, Belton AL, Murray RE et al (2002) Epiploic appendagitis: the emergency department presentation. J Emerg Med 22:9–13

Molla E, Rippoles T, Martinez MJ et al (1998) Primary epiploic appendagitis: US and CT findings. Eur Radiol 8:435–438

Ozdemir S, Gulpinar K, Leventoglu S et al (2010) Torsion of the primary epiploic appendagitis: a case series and review of the literature. Am J Surg 199:453–458

Rao PM, Wittenberg J, Lawrason JN (1997) Primary epiploic appendagitis: evolutionary changes in CT appearance. Radiology 204:713–717

Rioux M, Langis P (1994) Primary epiploic appendagitis: clinical, US, and CT findings in 14 cases. Radiology 191:523–526

Sand M, Gelos M, Bechara FG et al (2007) Epiploic appendagitis–clinical characteristics of an uncommon surgical diagnosis. BMC Surg 7:11

Schnedl WJ, Krause R, Tafeit E et al (2011) Insights into epiploic appendagitis. Nat Rev Gastroenterol Hepatol 8:45–49

Singh AK, Gervais DA, Hahn PF, Sagar P, Mueller PR, Novelline RA (2005) Acute epiploic appendagitis and its mimics. Radiographics 25:1521–1534

van Breda Vriesman AC, Lohle PNM, Coercamp EG et al (1999) Infarction of omentum and epiploic appendage: diagnosis, epidemiology and natural history. Eur Radiol 9:1886

Neutropenic Enterocolitis and Graft Versus Host Disease

Christoph Dietrich and Stefan Klein

Contents

Abstract

High-end sonography of the bowel is a helpful tool for diagnosis, assessment of prognosis and follow-up of patients with neutropenic colitis (NPC) and acute graft versus host disease (aGvHD). In NPC ultrasonography revealed bowel thickness reflecting the severity and the course of the disease, and seems to be predictive for the clinical outcome. In aGvHD abdominal ultrasound has been introduced as a useful imaging method including functional assessment applying colour Doppler imaging (CDI) for diagnosis of patients with intestinal GvHD. Typical sonographic findings have been identified. Thus, high resolution ultrasonography and CDI can be used to differentiate between sGvHD and major differential diagnosis.

1 Neutropenic Enterocolitis

1.1 Introduction

Neutropenic enterocolitis (NPC) was first described by Cooke in 1930 and the first reports were published in children treated with induction therapy for acute leukemia (Sloas et al. 1993).

Neutropenic enterocolitis is also known as typhlitis (*greek: typhlon = cecum*), neutropenic colitis, necrotizing enterocolitis, cecitis, ileocecal syndrome (Alt et al. 1985; Williams and Scott 1997). It is a necrotizing inflammatory disease of the ileocecal region, although other parts of the bowel can be affected as well (Katz et al. 1990).

The finding of a thickened bowel wall, in association with a clinical syndrome characterized by fever, diarrhoea, and abdominal pain, confirms the clinical diagnosis of NPC in neutropenic patients who have completed intensive chemotherapy (Dietrich et al. 2006). Neutropenic enterocolitis has a wide spectrum of severity ranging from mild gastrointestinal symptoms to peritonism and sepsis with lethal

C. Dietrich (✉)
Caritas Krankenhaus Uhlandstr. 7, 97980 Bad Mergentheim, Germany
e-mail: Christoph.dietrich@ckbm.de

S. Klein
III. Medizinischen Klinik, Universitätsmedizin Mannheim, Theodor-Kutzer-Ufer 1–3, 68167 Mannheim, Germany

G. Maconi and G. Bianchi Porro (eds.), *Ultrasound of the Gastrointestinal Tract*, Medical Radiology. Diagnostic Imaging,
DOI: 10.1007/174_2012_720, © Springer-Verlag Berlin Heidelberg 2012
Published Online: 11 August 2012

outcome. As abdominal discomfort and diarrhea are common in patients receiving chemotherapy, the prevalence of this condition is not known.

Ultrasound is the first imaging method to evaluate the gastrointestinal tract in particular for acute abdomen (Dietrich et al. 2007a; Nuernberg et al. 2007; Nuernberg et al. 2008). New methods have been introduced to evaluate gastrointestinal vascularity and enhancement patterns for differential diagnosis and estimation of the severity of the disease (Piscaglia et al. 2012).

1.2 Epidemiology and Pathogenesis

In recent years, the knowledge of NPC has increased (Dietrich et al. 2006; Gorschluter et al. 2006; Fike et al. 2011; Yazdi et al. 2011). The incidence of NPC in cytopenic patients ranges from 2.6 to 33 % (Mower et al. 1986; Shamberger et al. 1986) with a 5.3 % pooled incidence rate in adult patients hospitalized for the treatment of hematological malignancies, high-dose chemotherapy in solid tumors, or aplastic anemia (Gorschluter et al. 2005). With the use of more intensive chemotherapy regimens, especially after autologous and allogeneic stem-cell transplantations, a higher incidence of NPC should be expected (Davila 2007; Avigan et al. 1998; Boggio et al. 2000).

The pathogenesis of NPC is not completely understood, although cytotoxic drugs and an impaired host defense, in combination with bacterial infection of damaged mucosa are the key players. Bacterial superinfection, e.g., clostridia and other bacteria, seems to play an important role. Neutropenic enterocolitis is a typical complication of severe neutropenia, often in patients after (high-dose) chemotherapy or other cytotoxic drugs. Although most cases are in patients who received chemotherapy, it has been also seen in other conditions, e.g., aplastic anemia, benign cyclic neutropenia, AIDS, and allergic or toxic agranulocytosis (Davila and Bresalier 2008).

Various factors play a role in the pathogenesis of NPC. Apart from direct damage to the mucosa by rarely recognized leukemic or lymphatic infiltrates, toxic effects of chemotherapy agents contribute to the pathogenesis (Gorschluter et al. 2006). The first step is the severe initial damage to the mucosa, caused by release of pro-inflammatory cytokines from macrophages and monocytes, followed by a near complete arrest of the cell cycle, inhibition of mechanisms of repair, and finally apoptosis. The high concentration of lymphatic tissue in the ileocecal region, the special anatomy of the terminal branches of the superior mesenteric artery with consecutively decreasing vascular perfusion, and the distensibility of the cecal region may contribute to ischemia. The role of bacteria and viruses in the pathogenesis of NPC is controversial. Abnormal bacterial colonization in connection with cytotoxic effects or the neurotoxic effects of, e.g., vincristine are thought to contribute to the pathogenesis. Clostridia may play a relevant role. *Clostridium septicum* is found in stool cultures of healthy persons only in 2 %, but is detectable in a higher percentage in the ileocecal region and up to 63 % in the healthy appendix (Rexroth et al. 1998). Clostridia produce a number of tissue degrading enzymes that may play a significant role in the development of mucosal injury. In the absence of neutrophil granulocytes, which produce toxin degrading proteases, an important defence mechanism is missing. Similar pathogenic mechanisms have been described for other Clostridial species (e.g., *C. perfringens*, *paraperfringens* and *C. tertium*) (Dietrich et al. 2006).

1.3 Symptoms

Symptoms most often occur 10–14 days after initiation of cytotoxic chemotherapy (Wade et al. 1992). The symptoms consist of a combination of abdominal pain, often in right lower quadrant (98 % of patients), fever (87 %), diarrhea occasionally with blood (61 %) and a palpable mass and tenderness in the right lower quadrant, with rebound as sign of peritonism (30 %) (Dietrich et al. 2006). Sepsis and signs of perforation with peritonism, as well as profuse bleeding, are life-threatening complications and the most common causes of death. A localized tenderness and rebound tenderness above the affected area is very often the only clinical sign in these severely ill patients (Dietrich et al. 2006). Recurrent abdominal pain, caused by mechanical obstruction of the ileocecal area, indicates symptoms of ileus with dilatation of the bowel loops of the small intestine. Other more non-specific symptoms such as abdominal distension, nausea, vomiting, and meteorism have also been described in the literature.

1.4 Diagnosis

Routine laboratory and microbiological tests for bacteria (e.g., *C. difficile* and toxin), parasites, and viruses including CMV PCR- and the CMV early (pp65) antigen test should be performed. Endoscopy during pancytopenia is relatively contraindicated, although the definitive diagnosis of CMV colitis, leukemic, or neoplastic infiltrates can be made only by histological examination. Ultrasound is the imaging modality of choice (Dietrich et al. 2006).

The characteristic sonographic features of NPC are an echogenic, asymmetric thickening of the mucosal wall (Dietrich et al. 1998a; Dietrich et al. 2006) with transmural

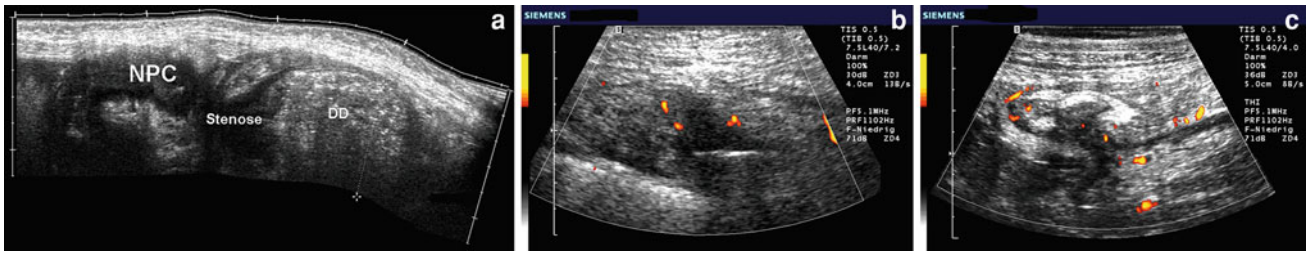

Fig. 1 Neutropenic entercolitis**. a** Asymmetric hypoechoic non-homogenous tumour-like bowel wall thickening in the ileocecal region are the characteristic sonographic findings in NPC. The stenosis (Stenose) and dilatation of the small bowel (DD) is also indicated. **b** Asymmetric and non-homogenous wall thickening in the ileocecal region with transmural inflammatory reaction in a patient with NPC. CDI is helpful for characterization. **c** Asymmetric and inhomogenous and in this case hyperechoic wall thickening of the ileo-cecal valve in a patient with NPC. CDI is helpful for characterization

inflammatory reaction and areas of different echogenicity, caused by edema, necrosis, and/or circumscript hemorrhages (Fig. 1).

Intramural air suggests an infection with anaerobic bacteria. Pericolic fluid is a sign of a (possible) perforation. Sonography may demonstrate free abdominal air, which is usually detected on the right side, e.g., perihepatic. In advanced disease with catastrophic prognosis, air bubbles in the portal vein may be demonstrated, resembling late phases after application of contrast enhancing agents. Another feature may be pneumatosis cystoides intestinalis, as seen in premature infants with necrotizing enterocolitis. It is noteworthy that the hydrogen content of the expired air in these patients is massively increased (Dietrich et al. 2006).

A few prospective studies used ultrasound to evaluate patients after chemotherapy. Bowel wall thickness (>4 mm) was seen only in those patients who fulfilled symptom criteria for NPC, and not in those patients with mucositis alone or in those who remained asymptomatic (Gorschluter et al. 2002). Besides the wall thickness, its overall echotexture and appearance of surrounding structures should be considered (Nuernberg et al. 2008; Dietrich et al. 1998b).

Bowel wall thickness has also been shown to be an important prognostic factor. Cartoni et al. (2001) evaluated neutropenic patients with fever and abdominal pain. A bowel wall thickness of >5 mm was considered as diagnostic of NPC. The mean duration of symptoms was significantly longer among patients with (7.9 days) than among patients without (3.8 days) bowel wall thickening and the related mortality was also higher (29.5 versus. 0 %). The degree of bowel wall thickness correlated with the outcome of patients: 60 % of patients with bowel wall thickness >10 mm died from this complication, compared with only 4.2 % of those with mural thickness ≤10 mm (Cartoni et al. 2001). These results are similar to those of our (not yet published) prospective study. Recently, 14 neutropenic patients (absolute neutrophil count <500/mm^3) with sonographic features of NPC were evaluated regarding clinical findings, sonographic features, and outcome (8 male, mean age 48 years). Bowel wall thickness was measured at terminal ileum, cecum, sigmoid colon, and small intestine by high resolution sonography with moderate pressure. A thickness <2 mm was considered normal, a thickness >2 and <5 mm was considered as non-specific bowel wall thickening, and a thickness >5 mm was considered abnormal confirming the diagnosis of NPC (Dietrich et al. 2006). The morphology and the five layers of ileum and colon were evaluated assessing a mucosal or transmural pattern of inflammation. Bowel wall vascularity was examined by color Doppler imaging (CDI) and graded as ischemic (no flow pattern), normal, or hypervascular as per standard GvHD criteria (Klein et al. 2001).

In all 14 patients treatment consisted of bowel rest and total parenteral nutrition and multiple antibiotics. G-CSF was given in eight patients to shorten the time of neutropenia. Three patients died due to sepsis with multiorgan failure. High C-reactive protein ($P < 0.001$) and the sonographically demonstrated bowel wall thickness ($P < 0.03$) were associated with lethal outcome. The surviving 11 patients recovered from NPC and the reduction of abdominal symptoms was accompanied by progressive reduction of intestinal mural thickening in follow-up ultrasound examinations. Nearly, all patients with NPC (13 of 14) presented a transmural inflammatory pattern of thickened bowel wall. In all patients, the ileocecal region was involved. The thickness of the inflamed bowel wall was at least 10 mm. Hypervascularity on CDI and the detection of small amounts of free fluid in the abdomen were documented in the majority of patients with NPC. Typical sonographic characteristics in NPC are depicted in Fig. 1a.

Other imaging methods include computed tomography (CT) and abdominal X-ray whereas barium enema and enteroclysis are relatively contraindicated as they increase the luminal pressure and the risk of perforation. Although most authors favor CT as the most sensitive diagnostic tool for NPC, sonography has the advantage of being easily performed with repeated examinations (e.g., at the bedside) even in severely ill patients in intensive care or transplantation

units. The findings on abdominal X-ray are often nonspecific and may show small bowel ileus, an ill-defined soft tissue density in the region of the cecum, thickened air-filled loops of bowel or signs of pneumatosis intestinalis. Other methods such as scintigraphy are not routinely used in clinical practice.

Several conditions should be taken into account in the differential diagnosis. Appendicitis is very often the main diagnosis. Because of the high perioperative mortality in these patients [most often from 50 to 100 % (Wade et al. 1992)] the operative approach should be avoided. Other acute or chronic inflammatory diseases of the ileocecal area are viral (e.g., CMV colitis) and bacterial ileocecitis, Crohn′s disease, pseudomembranous and ischemic colitis, and colonic pseudo-obstruction (Nuernberg et al. 2008). In post allogeneic stem-cell transplantation patients, one has to think of graft versus host disease (GvHD), although this usually occurs after engraftment (Klein et al. 2001). A neoplastic (leukemic of lymphocytic) infiltration of the ileocecal region must be excluded especially in case of a palpable mass in this area. In pancytopenic patients one also has to think of an acute hemorrhage into the mucosal wall (Dietrich et al. 2006).

Penicillin-induced segmental hemorrhagic colitis shows characteristic sonographic features with asymmetric wall thickening of the colon (typically in the right colon) with loss of intestinal wall layers due to edema and bleeding. Relative hypovascularization can be detected with CDI. The surrounding colon may appear normal. The past medical history is decisive. Intestinal tuberculosis has become increasingly observed since the occurrence of the AIDS pandemic. As with NPC, many regions of the intestine may be involved, although the ileocecal region is affected in up to 90 % of patients. The ultrasound image displays a hyperechoic (sometimes asymmetrically thickened) mucosa with loss of folds and unclear demarcation from (sometimes asymmetrically) thickened submucosa, so that a pseudopolypoid image prevails. Short stenoses, mesenteric hyperechoic inflammatory signs, development of fistula, and abscesses can also be seen. Other characteristic signs include severe mesenteric lymphadenopathy (sometimes more than 10 hyperechoic round- to oval-shaped lymph nodes are detected) and a distended ileocecal valve, with asymmetrical (sometimes tumorous) thickening, especially affecting the medial cecal wall. Patients with peritoneal tuberculosis may also have ascites and thickening of the peritoneum (Barreiros et al. 2008).

1.5 Management and Prognosis

The conservative approach, total parenteral nutrition, nasogastric suction, broad spectrum antibiotics, and antifungal treatment should be placed at the forefront. As neutropenia represents the "sine qua non" of NPC, time of neutropenia should be shortened, e.g., with granulocyte colony-stimulating factors or granulocyte transfusions (Dietrich et al. 2006; Wade et al. 1992). Antibiotic coverage for *C. difficile* infection should be added (Davila 2007), but no prospective randomized trials or high-quality retrospective studies on the treatment of NPC have been published so far. As the perioperative mortality in these patients is very high, early surgical intervention is not recommended. On the other hand, the right time for surgery should not be missed. Therefore, a close clinical evaluation of the patient by physicians and surgeons is mandatory. The indications for surgery are the same as in persistent gastrointestinal bleeding, free perforation, and clinical deterioration suggesting uncontrolled sepsis (Wade et al. 1992).

The mortality rate in patients with signs of perforation, sepsis, and multi-organ failure is higher than 50 % (Abbasoglu and Cakmakci 1993). The main prognostic factor is neutrophil recovery and overall time of neutropenia, as neutropenia allows for continuous bacterial invasion of the bowel wall, perpetuating the lesion, with possible necrosis and perforation (Wade et al. 1992).

The sonographically demonstrated thickened bowel wall is associated with poor prognosis and is also a useful tool for monitoring disease progression by showing the decreasing bowel wall thickening in responding patients. In addition, sonography might indicate complications of the disease by detecting free abdominal air or intramural hemorrhage.

2 Acute Graft versus Host Disease

2.1 Introduction

Graft versus host disease (GvHD) is a major complication after allogeneic stem cell transplantation (HCT). It has been classically divided into acute and chronic disease based upon the time of onset. As per definition, classic acute GvHD (aGvHD) occurs within the first 100 days after hematopoietic cell transplantation (HCT). Chronic GvHD (cGvHD) has a later onset. However, new criteria were developed in 2005 (Filipovich et al. 2005; Table 1).

2.2 Epidemiology and Pathogenesis

Graft versus host disease is a donor T cell-mediated reaction against tissue of the recipient. It occurs predominantly in skin, liver, and gastrointestinal (GI) tract. Frequency and severity of aGvHD are mainly dependent on the grade of

Table 1 Categories of acute and cGvHD according to NIH consensus

Category	Time point of onset of symptoms after HCT or donor lymphocyte infusion (DLI)	Signs of aGvHD	Signs of cGvHD
Acute GvHD			
Classic aGvHD	≤ day 100	Yes	No
Persisting, relapsed or late onset aGvHD	> day 100	Yes	No
Chronic GvHD			
Classic cGvHD	No time limit	No	Yes
Overlap syndrome	No time limit	Yes	Yes

Table 2 Modified Glucksberg criteria for staging and grading of aGvHD (Przepiorka et al. 1995)

Clinical staging of aGvHD according to Organ Involvement				
Organ stage	Skin	Liver		GI-tract
1	Maculopapular rash < 25 % of body surface	Serum bilirubin 2–3 mg/dl		Diarrhoea 500–1000 ml/day or nausea
2	Maculopapular rash 25–50 % of body surface	Serum bilirubin 3–6 mg/dl		Diarrhoea 1000–1500 ml/day
3	Maculopapular rash > 50 % of body surface	Serum bilirubin 6–15 mg/dl		Diarrhoea 1500–2000 ml/day
4	Generalized erythroderma with bullous formation and desquamation	Serum bilirubin > 15 mg/dl		Diarrhoea > 2000 ml/day Severe abdominal pain with or without ileus
Overall grading of aGvHD				
	Stage per organ			ECOG
Overall grade	Skin	Liver	GI-Tract	Performance
I	1–2	0	0	0
II	1–3 or	1 or	1 or	1
III	–	2–3 or	2–3 or	2–3
IV	4 or	4 or	4 or	3–4

HLA match between donor and recipient, the intensity of conditioning, donor type (sibling vs. unrelated), and the stem cell source (bone marrow vs. peripheral blood). After HCT 10–80 % of patients develop aGvHD and 30–75 % of patients suffer from clinically relevant grade II-IV aGvHD of the GI tract (Mielcarek et al. 2003).

The pathogenesis of acute intestinal GvHD has been described by Ferrara et al. (1999) in a three-phase model. The first phase involves damage of host tissues by inflammation from the conditioning prior to transplantation. As a second phase, recipient and donor antigen-presenting cells as well as proinflammatory cytokines led to an activation of donor T cells. In the third phase, called the effector phase, activated donor T-cells confer cytotoxicity against target host cells through Fas–Fas ligand interactions, perforin-granzyme B, and the additional production of cytokines, such as TNF-α (Jacobsohn and Vogelsang 2007).

2.3 Symptoms

The main target organs of aGvHD are skin, liver, and GI tract. A maculopapular rash is the most common and earliest manifestation of aGvHD. The rash is often confluent and can occur simultaneously with hematologic engraftment. Typical areas for skin aGvHD are palm and sole. Hyperbilirubinemia or elevated liver enzymes can be signs of aGvHD with liver involvement (McDonald 2006). Involvement of the GI tract with aGvHD is often severe and difficult to treat. It is characterized by diarrhea, abdominal cramping, nausea, or vomiting. The severity of GI involvement is determined by the volume of diarrhoea, which can occasionally exceed 10 l per day. Diarrhea may be watery or bloody. Additionally, severe ileus may develop (Cox and McDonald 1990). The severity of aGvHD is determined by assessing the degree of skin, liver, and GI

Table 3 Sonographic features of aGvHD. Number of patients with the specific sonographic finding/all patients described in the cited paper

	Haber et al. 2000	Klein et al. 2001	Görg et al. 2005	Schreyer et al. 2011
Bowel wall thickening (colon)	1/1	12/12	6/7	
Bowel wall thickening (small bowel)	1/1	6/12	5/7	
Dilatation of the colon			7/7	
Hyperperistalsis		6/12	6/7	
Wall stratification of the colon	1/1		3/7	
Signs of secretory diarrhoea[a]		6/12		
Penetration of microbubbles through the bowel wall into the bowel lumen				9/9

[a] Signs of secretory diarrhea: hyperdynamic bowel motility and reduction in Kerckring's plicae circulars with a loss of their uniformity

tract involvement. This is subsequently combined with the results on performance scales to produce an overall grade (Przepiorka et al. 1995; Table 2).

2.4 Diagnosis

The diagnosis of aGvHD can be made clinically in the patient presenting with a classic rash, abdominal cramps with diarrhoea, and a rising serum bilirubin concentration, within the first 100 days following transplantation. After allogeneic HCT the key symptoms of intestinal aGvHD such as diarrhea, nausea, or vomiting are frequent and nonspecific. Differential diagnoses include side effects of pre-transplant conditioning, neutropenic colitis, *C. difficile* colitis, side effects of immunosuppressants (e.g., MTX or mycofenolate mofetil), or antibiotics and viral infections (Norovirus, Rotavirus, Adenovirus, Herpes Simplex Virus, Varicella Zoster Virus and Cytomegalovirus).

A clinical impression of intestinal aGvHD has to be corroborated by endoscopy (esophago-gastroduodenoscopy and ileocoloscopy) with biopsies. Endoscopic features of aGvHD described as 'Freiburg Criteria' are spotted erythema, aphthous lesions, confluent defects, ulcerations, and complete denudation of the mucosa (Kreisel et al. 2012). For the diagnosis of intestinal aGvHD histologic confirmation is mandatory and since viral infections often occur simultaneously with aGvHD, biopsies have to be investigated by immune staining and by virological methods, respectively.

2.5 High Resolution Sonography

The first article on sonographic findings in intestinal aGvHD was published in 2000 (Haber et al. 2000) and identified the key finding of bowel wall thickening, particularly in the ileocoecal region.

Thereafter, high resolution ultrasound and CDI were demonstrated to be helpful for diagnosis and differential diagnosis of aGvHD identifying several songraphic features of gastrointestinal aGvHD, which are summarized in Table 3 (Gorg et al. 2005; Klein et al. 2001; Dietrich 2010).

Our own group published data on 12 patients with intestinal aGvHD describing sonographic findings and applying high resolution ultrasound and color Doppler imaging to define extent, severity, and prognosis of aGvHD. The typical finding was ileocecal involvement and, according to our experience, sloughing (Klein et al. 2001; Fig. 2).

In all patients, thickened submucosal bowel wall ($\geq$2 mm) segments were detected sonographically. Only in the ileocecal region (ascending colon and terminal ileum) thickened bowel wall segments were observed in all patients. In six patients the small bowel demonstrated wall thickening, increased motility, and reduction of Kerckring's plicae with a loss of their uniformity as a sign of secretory diarrhea. All patients with a thickened small bowel wall and evidence of secretory diarrhoea on ultrasound had a high grade aGvHD with a stool volume >1500 ml. In contrast, those patients with a low grade intestinal aGvHD had no sonographic signs of secretory diarrhoea. Three patients had no clinical evidence for intestinal aGvHD, but thickening of the bowel wall could be detected. Endoscopic examinations with biopsies subsequently confirmed an asymptomatic GI aGvHD, thus indicating that it might be detected by ultrasound prior to clinical symptoms.

Bowel wall vascularity was examined by CDI and graded as ischemic (no flow pattern) or non-ischemic (i.e. normal or hypervascular). Systolic and diastolic blood flow of superior mesenteric artery (SMA) was also determined to differentiate between reduced (high resistance flow pattern with systolic velocity $\leq$110 cm/sec, small band systolic flow, no diastolic flow), normal (systolic velocity >110 cm/sec, significant diastolic flow, resistance index up to 1) and increased (systolic velocity >225 cm/sec, significant diastolic flow resulting in a resistance index significant below <1) perfusion (Fig. 3).

An increased arterial perfusion of the bowel wall and/or SMA was detectable in most GvHD patients as a typical but

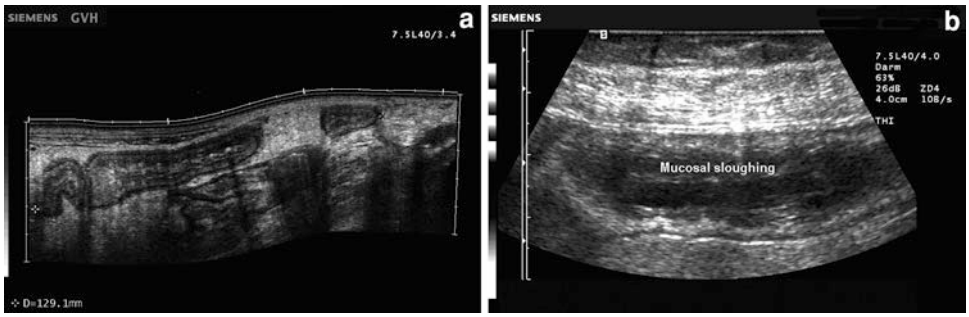

Fig. 2 **a** Bowel wall thickening with predilection for ileocecal region. **b** Sloughing of the mucosa. This sign, not reported by Gorg et al. 2005, was a typical B-mode sign of GvHD

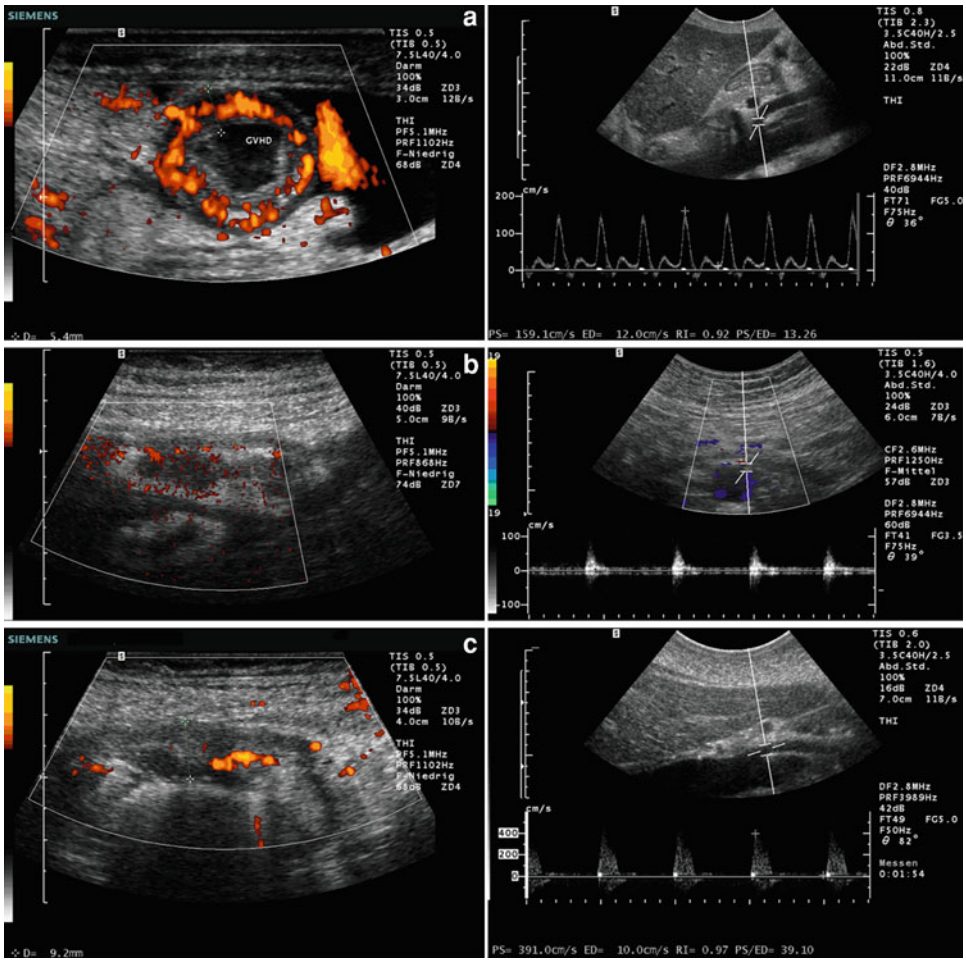

Fig. 3 **a** Increased vascularity and perfusion within the ileocecal bowel wall (*left* panel) and in the SMA (*right* panel). **b** Decreased vascularity and perfusion within the ileocecal bowel wall (*left* panel) and in the superior mesenteric artery (*right* panel). **c** Intermediate pictures of vascularity and perfusion can be observed

non-specific sign of an inflammatory intestinal process. An increased or normal perfusion of SMA blood flow and the ileocecal wall was detectable in 8 of 12 patients by CDI. In contrast, 4 patients demonstrated a reduced blood flow in the SMA and an ischemic bowel wall. In these patients the systolic velocity in the SMA was always <110 cm/sec. Only a low amplitude band of systolic flow without any diastolic flow was detected. Although the ileocecal bowel wall was thickened, no blood vessels could be observed, even with a maximal sensitivity of gain. All patients with an ischemic bowel wall and a reduced SMA blood flow did not, or only initially, respond to immunosuppressive therapy. Despite escalation of GvHD therapy, all 4 patients died within 2–5 weeks due to intestinal aGvHD. However, all patients with a normal or increased blood flow responded at least to the second- or third-line immunosuppressive

Table 4 Findings in color doppler imaging (modified from Klein et al. 2001)

Patient	SMA blood flow		Bowel wall perfusion	Response to immunosuppression	Clinical outcome
	Systolic (cm/sec)	Diastolic (cm/sec)			
1	100	0	Ischemic	No	+ at day + 75 due to GvHD
2	187	32	Nonischemic	Yes	day + 460, alive and well
3	313	101	Nonischemic	Yes	day + 424, alive and well
4	269	63	Nonischemic	Yes	+ at day + 275 after relapse of leukemia
5	92	0	Ischemic	No	+ at day + 80 due to GvHD
6	280	25	Nonischemic	Yes	day + 228, alive and well
7	109	0	Ischemic	No	+ at day + 140 due to GvHD
8	N.a.[a]	N.a.[a]	Ischemic	No	+ at day + 115 due to GvHD
9	150	32	Nonischemic	Yes	+ at day + 175 after relapse of leukemia
10	123	28	Nonischemic	Yes	+ at day + 175 due to respiratory failure
11	122	15	Nonischemic	Yes	day + 400, alive and well
12	371	10	Nonischemic	Yes	day + 220, alive and well
Controls (n = 12)	110–225	> 0	Nonischemic		

SMA: superior mesenteric artery; [a] Determination of the blood flow in the SMA not applicable due to a common celiac-mesenteric trunk

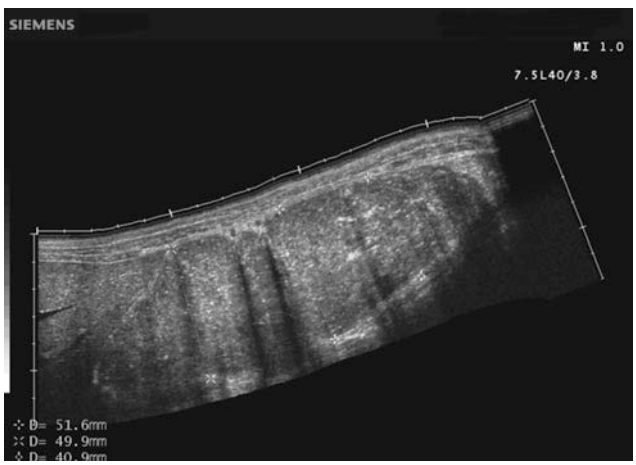

Fig. 4 Dilatation of the ascending colon using panoramic imaging (SieScape)

treatment. Thus, the assessment of SMA blood flow and bowel wall perfusion can be used as a prognostic marker in aGvHD (Table 4; Fig. 3).

The study by Gorg et al. (2005) on the use of ultrasound in intestinal aGvHD included 24 consecutive patients who had received allogeneic HCT. A total of 7 out of these 24 patients developed clinical signs of intestinal aGvHD at a median of 36 days (range: 14–159 days) after transplantation. The clinical severity of GvHD was grade II in two patients, grade III in three patients, and grade IV in a further two patients. In all patients GvHD was confirmed histologically. Seven consecutive patients who had undergone bone marrow transplantation without developing gastrointestinal GvHD served as a control group. Ultrasound was performed within the first 7 days of onset of symptoms and every 7–14 days during follow-up mainly under fasting conditions. The GI tract was assessed with respect to the thickness of the wall, stratification of wall layers, dilatation, and motility. The gastrointestinal wall was classified as pathologically thickened if it was greater than 4 mm and considered dilated if the widest part exceeded 35 mm in the small bowel and 40 mm in the colon. Motility was assessed semiquantitatively and classified as hypoperistaltic, normoperistaltic, or hyperperistaltic based on the overall impression of the investigator. Ultrasound revealed in all 7 patients dilatation of the colon. Figure 4 shows an example of dilatation of the colon of approximately 6 cm.

The same patient had small bowel dilatation. Thickening of colon wall was found in six of seven patients and thickening of small bowel wall in five patients. No definite bowel wall layer stratification of the colon was seen in four patients while three patients had wall stratification of the colon. Hyperperistalsis was present in six patients. Only one patient had hypoperistaltic bowel motility during sonographic examination. In a single patient who was clinically classified as having grade II GvHD, a dilated ascending colon and hyperperistaltic small bowel without any bowel wall thickening was observed. Five patients had involvement of two or more GI sites. No echogenic thickening

around bowel segments suggested that there was no relevant mesenteric inflammation. Free abdominal fluid was found in 5 patients (Gorg et al. 2005). The most frequent finding was dilatation of the colon, which was apparent early, together with the clinical manifestation of GvHD, but vanished within days in some patients irrespective of the clinical course of the disease. Bowel wall thickening with predilection of ileocecal region was the next frequent finding. Bowel wall thickening seemed to correlate with the severity of GvHD as it was absent in one patient with grade II clinical GI GvHD, but massive in three patients with grade III and IV GvHD. The authors emphasized that all sonographic GI findings such as loss of wall stratification, bowel wall thickening, and dilated bowel are non-specific signs that are found in various bowel diseases such as ischemic and radiation-induced colitis, inflammatory bowel disease, intussusception, colonic carcinoma, and others. However, they found that in contrast to other diseases, GvHD bowel wall thickening was often visible in multiple sites of the GI tract, involving small as well as large bowel.

In a recent article, Schreyer et al. (2011) presented their data on contrast enhanced ultrasound (CEUS) in nine patients with histologically proven GvHD (5 classic aGvHD, 3 delayed onset aGvHD, 1 acute worsening of severe cGvHD). The control group consisted of four healthy volunteers and six patients with Crohn's disease (CD). In six of nine patients the predominant bowel wall thickening was identified in the terminal ileum and caecum. In three patients the preterminal ileum was the affected part of the bowel. After the injection of 2.4 ml SonoVue® intravenously patients with CD and GvHD showed significant contrast uptake in the bowel wall. In contrast to CD patients and healthy volunteers, patients with GvHD showed transmural penetration of microbubbles into the bowel lumen. The authors concluded that the damaged gut mucosa is more permeable in patients with GvHD and therefore responsible for the permeation of microbubbles through the mucosa into the bowel lumen. The authors suggest using the penetration of microbubbles into the bowel lumen as a novel diagnostic feature for GvHD if confirmed in controlled clinical trials.

2.6 Alternative Imaging Methods

Computed tomography (CT) has been used as a diagnostic tool in GI aGvHD (Kalantari et al. 2003; Brodoefel et al. 2010). Frequent CT findings are bowel wall thickening, mucosal enhancement, bowel dilatation, and engorgement of the vasa recta. None of the CT findings are specific for GI aGvHD. However, they may corroborate the suspected diagnosis and exclude some differential diagnoses. In the literature there is less evidence for the use of MRI in GI aGvHD.

3 Conclusion

Since an early treatment of aGvHD with immunosuppressive agents is essential, a reliable differentiation between aGvHD and infections is desirable. If aGvHD with intestinal involvement is suspected, endoscopy with multiple biopsies is needed to confirm the diagnosis, to determine the extent of the disease, and to exclude other important differential diagnoses. In addition to the clinical grading no objective clinical prognostic factors for the outcome have been described so far.

Efficiency and success of immunosuppressive therapy for aGvHD are usually monitored by quantifying the stool volume, assessment of the clinical performance status, and by repeating endoscopic examinations.

Abdominal ultrasonography has been used as non-invasive procedure for diagnosis and monitoring of aGvHD of the bowel. It is sensitive in evaluating bowel wall thickness and architecture and CDI can be used to differentiate between inflammatory and ischemic bowel segments (Gorg et al. 2005; Dietrich et al. 2007b). In almost all patients with aGvHD thickened bowel wall segments can be observed and the bowel wall thickening is mainly due to a thickened submucosa. The ileocecal region is the most common site of intestinal aGvHD.

Abdominal ultrasonography may also detect aGvHD already in early stages prior to the development of clinical symptoms. By CDI, an increased arterial perfusion of the bowel wall and SMA was detectable in the majority of GvHD patients as a typical but non-specific sign of an inflammatory process.

In contrast, some patients showed the unique combination of a thickened bowel wall in conjunction with high resistance flow pattern in the SMA and an ischemic ileocecal bowel wall. These sonographic signs suggest a poor prognosis. Another finding of advanced disease with poor prognosis is mucosal sloughing on CEUS, indicating a denuded mucosa. The unique finding of microbubbles penetrating the bowel wall in patients with intestinal GvHD might also help to differentiate between GvHD and the major differential diagnoses.

Therefore, we suggest adding the non-invasive methods of high resolution ultrasound, CEUS, and CDI into the diagnostic repertoire for aGvHD. They can also be used to monitor allografted patients prior to the development of clinical symptoms. Moreover, the described tools should be applied to define success or failure of treatment.

References

Abbasoglu O, Cakmakci M (1993) Neutropenic enterocolitis in patients without leukemia. Surgery 113:113–116

Alt B, Glass NR, Sollinger H (1985) Neutropenic enterocolitis in adults. Review of the literature and assessment of surgical intervention. Am J Surg 149:405–408

Avigan D, Richardson P, Elias A et al (1998) Neutropenic enterocolitis as a complication of high dose chemotherapy with stem cell rescue in patients with solid tumors: a case series with a review of the literature. Cancer 83:409–414

Barreiros AP, Braden B, Schieferstein-Knauer C, Ignee A, Dietrich CF (2008) Characteristics of intestinal tuberculosis in ultrasonographic techniques. Scand J Gastroenterol 43:1224–1231

Boggio L, Pooley R, Roth SI, Winter JN (2000) Typhlitis complicating autologous blood stem cell transplantation for breast cancer. Bone Marrow Transplant 25:321–326

Brodoefel H, Bethge W, Vogel M et al (2010) Early and late-onset acute GvHD following hematopoietic cell transplantation: CT features of gastrointestinal involvement with clinical and pathological correlation. Eur J Radiol 73:594–600

Cartoni C, Dragoni F, Micozzi A et al (2001) Neutropenic enterocolitis in patients with acute leukemia: prognostic significance of bowel wall thickening detected by ultrasonography. J Clin Oncol 19:756–761

Cox GJ Jr, McDonald GB (1990) Graft-versus-host disease of the intestine. Springer Semin Immunopathol 12:283–299

Davila ML (2007) Neutropenic enterocolitis: current issues in diagnosis and management. Curr Infect Dis Rep 9:116–120

Davila M, Bresalier RS (2008) Gastrointestinal complications of oncologic therapy. Nat Clin Pract Gastroenterol Hepatol 5:682–696

Dietrich CF, Brunner V, Lembcke B (1998a) Intestinal ultrasound in rare small and large intestinal diseases. Z Gastroenterol 36:955–970

Dietrich CF, Zeuzem S, Caspary WF, Wehrmann T (1998b) Ultrasound lymph node imaging in the abdomen and retro peritoneum of healthy probands. Ultraschall Med 19:265–269

Dietrich CF, Hermann S, Klein S, Braden B (2006) Sonographic signs of neutropenic enterocolitis. World J Gastroenterol 12:1397–1402

Dietrich CF, Muller G, Ignee A (2007a) Acute abdomen, gastroenterologists view. Praxis (Bern 1994) 96:645–659

Dietrich CF, Jedrzejczyk M, Ignee A (2007b) Sonographic assessment of splanchnic arteries and the bowel wall. Eur J Radiol 64:202–212

Dietrich CF (2010) Ultrasonography of the small and large intestine. In: Rose BD (ed) Up to date. Wellesley, Massachusetts

Ferrara JL, Levy R, Chao NJ (1999) Pathophysiologic mechanisms of acute graft-versus-host disease. Biol Blood Marrow Transplant 5:347–356

Filipovich AH, Weisdorf D, Pavletic S et al (2005) National Institutes of Health consensus development project on criteria for clinical trials in chronic graft-versus-host disease: I. Diagnosis and staging working group report. Biol Blood Marrow Transplant 11:945–956

Fike FB, Mortellaro V, Juang D, St Peter SD, Andrews WS, Snyder CL (2011) Neutropenic colitis in children. J Surg Res 170:73–76

Gorg C, Wollenberg B, Beyer J, Stolte MS, Neubauer A (2005) High-resolution ultrasonography in gastrointestinal graft-versus-host disease. Ann Hematol 84:33–39

Gorschluter M, Marklein G, Hofling K et al (2002) Abdominal infections in patients with acute leukaemia: a prospective study applying ultrasonography and microbiology. Br J Haematol 117:351–358

Gorschluter M, Mey U, Strehl J et al (2005) Neutropenic enterocolitis in adults: systematic analysis of evidence quality. Eur J Haematol 75:1–13

Gorschluter M, Mey U, Strehl J et al (2006) Invasive fungal infections in neutropenic enterocolitis: a systematic analysis of pathogens, incidence, treatment and mortality in adult patients. BMC Infect Dis 6:35

Haber HP, Schlegel PG, Dette S, Ruck P, Klingebiel T, Niethammer D (2000) Intestinal acute graft-versus-host disease: findings on sonography. AJR Am J Roentgenol 174:118–120

Jacobsohn DA, Vogelsang GB (2007) Acute graft versus host disease. Orphanet J Rare Dis 2:35

Kalantari BN, Mortele KJ, Cantisani V et al (2003) CT features with pathologic correlation of acute gastrointestinal graft-versus-host disease after bone marrow transplantation in adults. AJR Am J Roentgenol 181:1621–1625

Katz JA, Wagner ML, Gresik MV, Mahoney DH Jr, Fernbach DJ (1990) Typhlitis. An 18-year experience and post mortem review. Cancer 65:1041–1047

Klein SA, Martin H, Schreiber-Dietrich D et al (2001) A new approach to evaluating intestinal acute graft-versus-host disease by transabdominal sonography and colour doppler imaging. Br J Haematol 115:929–934

Kreisel W, Dahlberg M, Bertz H et al (2012) Endoscopic diagnosis of acute intestinal GVHD following allogeneic hematopoietic SCT: a retrospective analysis in 175 patients. Bone Marrow Transplant 47:430–438

McDonald GB (2006) Review article: management of hepatic disease following haematopoietic cell transplant. Aliment Pharmacol Ther 24:441–452

Mielcarek M, Martin PJ, Leisenring W et al (2003) Graft-versus-host disease after nonmyeloablative versus conventional hematopoietic stem cell transplantation. Blood 102:756–762

Mower WJ, Hawkins JA, Nelson EW (1986) Neutropenic enterocolitis in adults with acute leukemia. Arch Surg 121:571–574

Nuernberg D, Ignee A, Dietrich CF (2007) Current status of ultrasound in gastroenterology–bowel and upper gastrointestinal tract–part 1. Z Gastroenterol 45:629–640

Nuernberg D, Ignee A, Dietrich CF (2008) Current status of ultrasound in gastroenterology–bowel and upper gastrointestinal tract–part 2. Z Gastroenterol 46:355–366

Piscaglia F, Nolsoe C, Dietrich CF et al (2012) The EFSUMB guidelines and recommendations on the clinical practice of contrast enhanced ultrasound (CEUS): update 2011 on non-hepatic applications. Ultraschall Med 33:33–59

Przepiorka D, Weisdorf D, Martin P et al (1995) 1994 consensus conference on acute GVHD grading. Bone Marrow Transplant 15:825–828

Rexroth G, Altmannsberger HM, Hassenstein EO, Rosch W (1998) Neutropenic enterocolitis. Z Gastroenterol 36:27–33

Schreyer AG, Landfried K, Zorger N et al (2011) Transmural penetration of intravenously applied microbubbles during contrast-enhanced ultrasound as a new diagnostic feature in patients with GVHD of the bowel. Bone Marrow Transplant 46:1006–1011

Shamberger RC, Weinstein HJ, Delorey MJ, Levey RH (1986) The medical and surgical management of typhlitis in children with acute nonlymphocytic (myelogenous) leukemia. Cancer 57:603–609

Sloas MM, Flynn PM, Kaste SC, Patrick CC (1993) Typhlitis in children with cancer: a 30-year experience. Clin Infect Dis 17:484–490

Talebian Yazdi A, De Smet K, Verdries E et al (2011) Neutropenic colitis JBR-BTR 94:138–139

Wade DS, Nava HR, Douglass HO Jr (1992) Neutropenic enterocolitis. Clinical diagnosis and treatment Cancer 69:17–23

Williams N, Scott AD (1997) Neutropenic colitis: a continuing surgical challenge. Br J Surg 84:1200–1205

Part II

Chronic Inflammatory Bowel Diseases

Crohn's Disease

Giovanni Maconi

Contents

Abstract

Intestinal ultrasound has been proven to be a useful as a screening tool in patients with clinically suspected Crohn's disease as well as in the follow-up of patients already diagnosed with Crohn's disease. In these patients, it is possible to assess the site and extent of the lesions and ensure early detection of intra-abdominal complications, in particular abscesses and strictures. Intestinal ultrasound may be also used for monitoring Crohn's disease following surgery, revealing early recurrence of the disease and suggesting the clinical and endoscopic outcome. Despite several attempts to correlate the ultrasonographic findings with Crohn's disease activity, to date, only ultrasonographic assessment of endoscopic activity is convincing.

1 Introduction

Abdominal ultrasound (US) thanks to its accuracy, good repeatability and noninvasiveness is currently employed in many chronic inflammatory conditions, not only for purely diagnostic purposes, but also for management of the disease. In Crohn's disease (CD) patients, US has become the first-line imaging procedure for early diagnosis of the disease (Parente et al. 2004a), and more frequently for the follow-up, to detect intra-abdominal complications (strictures, fistulae and abscesses), to assess activity and monitor the course of disease, as a prognostic index of recurrence (Table 1).

2 Pathological Features

Crohn's disease is a chronic granulomatous inflammatory condition of the alimentary tract of unknown origin. Although there are no pathognomonic features of the disease, it is characterised by a segmental and transmural

G. Maconi (✉)
Chair of Gastroenterology, Department of Clinical Sciences, "L. Sacco" University Hospital, Via G. B. Grassi, 74, 20157 Milan, Italy
e-mail: giovanni.maconi@unimi.it

G. Maconi and G. Bianchi Porro (eds.), *Ultrasound of the Gastrointestinal Tract*, Medical Radiology. Diagnostic Imaging,
DOI: 10.1007/174_2013_805, © Springer-Verlag Berlin Heidelberg 2013
Published Online: 16 March 2013

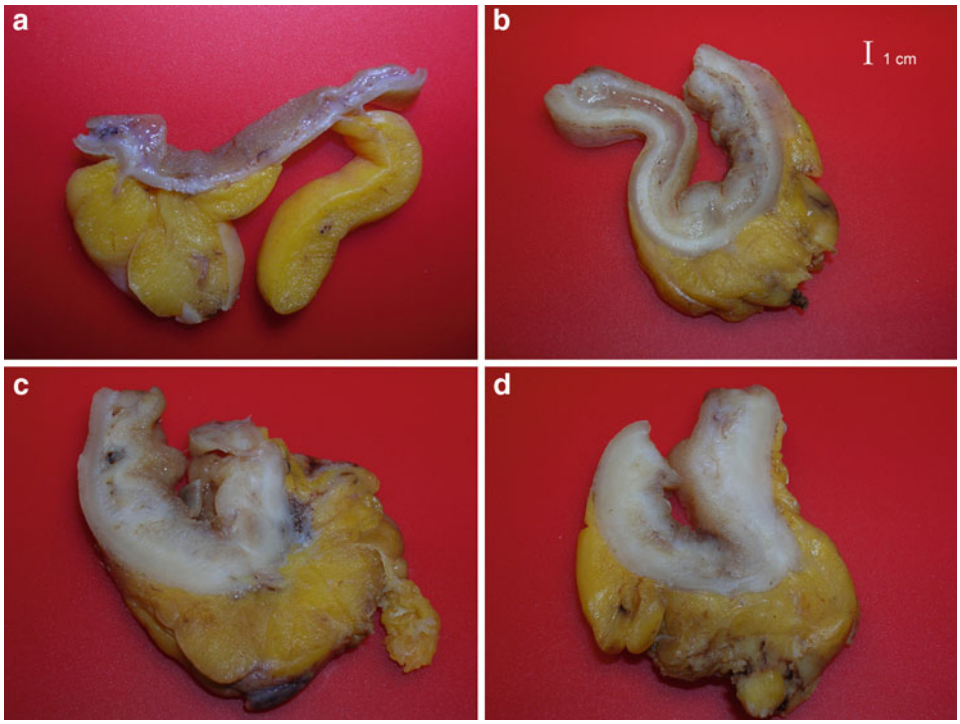

Fig. 1 Opened transverse sections of a normal ileal wall (**a**); thickened bowel wall in a CD patient with loose (*left side*) and markedly inflamed (*right side*) submucosa (**b**); markedly thickened bowel wall with fibrosis and loss of stratification (**c**,**d**). (Courtesy by dr. Paolo Fociani, Department of Pathology, 'L. Sacco' University Hospital, Milan)

Table 1 Indications for bowel US in CD

Early evaluation of patients with suspected CD
Evaluation of site and extension of CD
Differential diagnosis between chronic inflammatory colitis
Diagnosis of CD abdominal complications
Stenosis and intestinal occlusion
Internal and external fistulae
Intra-abdominal abscesses
Perforation and toxic megacolon
Assessment of CD activity
Post-operative follow-up and prediction of CD recurrence

inflammation of the intestinal wall, particularly ileum (30 %), colon (20 %) or both the large and small bowel (50 %). Macroscopically, the bowel wall often appears greatly thickened, and hypo-elastic or stiff with luminal narrowing (Fig. 1).

Mucosal abnormalities consist of longitudinal and aphtous ulcerations, which, in advanced disease, may penetrate into the submucosa and muscularis leading the serosa and outside, creating fissures and fistulas. These may invade the adjacent loops, organs, skin or end blindly in the mesentery, sometimes resulting in intra-abdominal or retroperitoneal abscesses. The mesentery is often thickened and fatty, surrounding the thickened walls and containing enlarged lymph nodes.

3 Ultrasonographic Features of Bowel Walls

The abnormalities of bowel wall include bowel wall thickening, alterations of bowel wall echopattern, hyperemia, loss of elasticity and peristalsis, creeping fat and mesenteric lymph nodes. Intra-abdominal complications of CD typically include stenoses and obstruction, fissures and fistulae, inflammatory masses (phlegmon or abscesses).

3.1 Bowel Wall Thickening

US examination in CD patients frequently reveals stiff and thickened bowel walls, usually >4 mm (which is considered the limit of normal bowel wall for the ileum and colon) up to 15 mm. The wall thickness of a diseased segment is measured in a transverse section from the central hyperechoic line of the lumen (representing interface between content of the lumen and the mucosa) to the outer hyperechoic margin of the wall (representing the serosa) (Fig. 2). Literature usually considers the maximum bowel wall thickness, that can be reproduced along the bowel wall for at least 2–4 cm.

The abnormal thickening of bowel walls is the most widely and commonly US finding reported in the literature

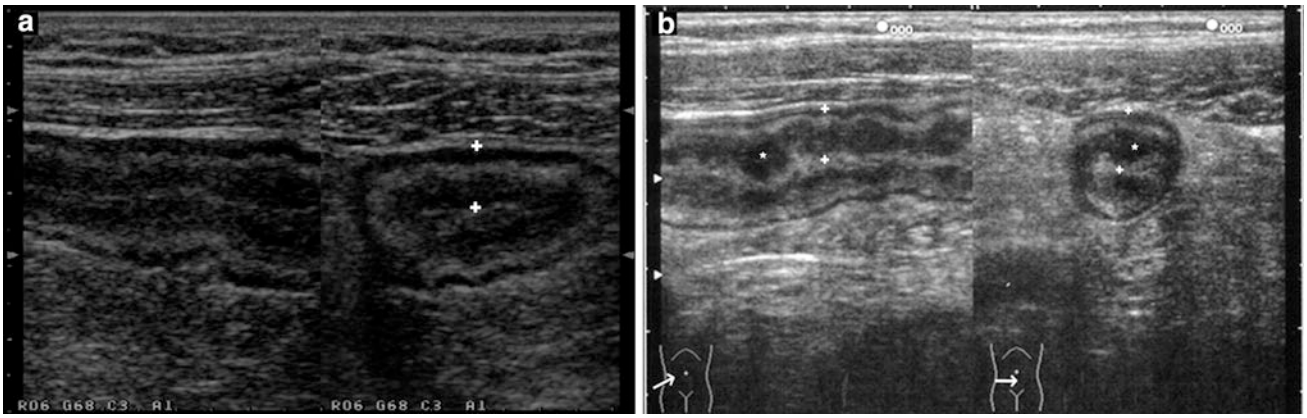

Fig. 2 **a**, **b** Longitudinal (*left*) and transverse (*right*) sections of a thickened bowel wall characterised by stratified echopattern showing the markers (+) on the inner hyperechoic line (lumen) and outer hyperechoic margin (serosa) of the thickened wall. (* = gross nodularity of the mucosa)

to diagnose CD. In a meta analysis aiming at evaluating the impact of different cut-off values of bowel wall thickening (3 vs 4 mm) in determining the presence of CD, it has been shown that when a >3-mm cut-off level was observed for abnormality, sensitivity and specificity were 88 and 93 %, respectively, whilst when a cut-off level of >4 mm was used sensitivity was 75 % and specificity 97 % (Fraquelli et al. 2005). The accuracy of US in detecting CD has been also compared with that of other cross-sectional imaging techniques, in a systematic review. This study showed that US has high accuracy for evaluation of suspected CD (overall per-patient sensitivity and specificity: 85 and 98 %, respectively), comparable to that of magnetic resonance imaging (MRI) (overall per-patient sensitivity and specificity: 78 and 85 %, respectively) (Panes et al. 2011).

However, these remarkable data also show that intestinal US, even in expert hands, may result in false-negative and false-positive findings. False-negative findings may be in obese patients or when CD is characterised by only superficial lesions, such as rare aphtous ulcers or mucosal erosions (Maconi et al. 1996a). False-positive findings rely on the fact that thickening of the bowel walls is not specific for CD, being present also in infectious, neoplastic and other inflammatory diseases (Truong et al. 1998). Therefore, when US is used as a first imaging diagnostic procedure, the diagnosis of CD is suggested when wall thickening involves the terminal ileum, is circumferential and segmental. However, the definitive diagnosis—when possible, and always for colonic lesions—should rely on endoscopic and histological examinations of pathological tissues. US may represent a useful tool, prior to other invasive or expensive diagnostic investigations, which can be postponed in the case of negative US findings.

In CD patients, US can be usefully employed in localising CD lesions within the bowel (particularly ileal lesions, which can be detected in more than 90 %) and in assessing the length of small bowel involvement (Brignola et al. 1993; Maconi et al. 1996a; Parente et al. 2003, 2004a, 2011).

The clinical significance of the degree of thickening of diseased bowel wall in CD is controversial. Several studies attempted to establish a relationship between maximum bowel wall thickness and clinical severity (Crohn's disease activity index, CDAI) and biochemical activity (Erythrocyte Sedimentation Rate, C Reactive Protein) of CD. However, almost all the results of these studies produced weak correlations, although somewhat significant (Maconi et al. 1996a; Futagami et al. 1999; Mayer et al. 2000; Bru et al. 2001; Haber et al. 2000, 2002; Parente et al. 2003). On the contrary, the thickening of bowel wall significantly correlates with endoscopic activity of CD. It has been shown that US thickening of bowel wall has an overall high sensitivity and specificity (85 and 91 %, respectively) for the detection of endoscopic active CD (Panes et al. 2011).

Likewise, the US assessment of bowel wall thickening is useful to identify postoperative recurrences following resection, to assess the efficacy of conservative surgical treatment, and to obtain predictive data on the risk of recurrences in these patients. Postoperative endoscopic recurrences of CD may be correctly identified using bowel US in more than 80 % of patients (Di Candio et al. 1986; Andreoli et al. 1998). Moreover, US offers the possibility to assess the behaviour of diseased bowel walls following conservative surgery (namely strictureplasty and minire-section), in CD patients. In fact, in patients showing an improvement or return to normality of the bowel wall thickening 6 months after conservative surgery, the clinical and surgical recurrence rate have being significantly lower than in those maintaining the same level of bowel wall thickening (Maconi et al. 2001). Likewise, it has been shown that a high bowel wall thickness (>7 mm) at US is a major risk factor for intestinal resection (Rigazio et al. 2009; Castiglione et al. 2004).

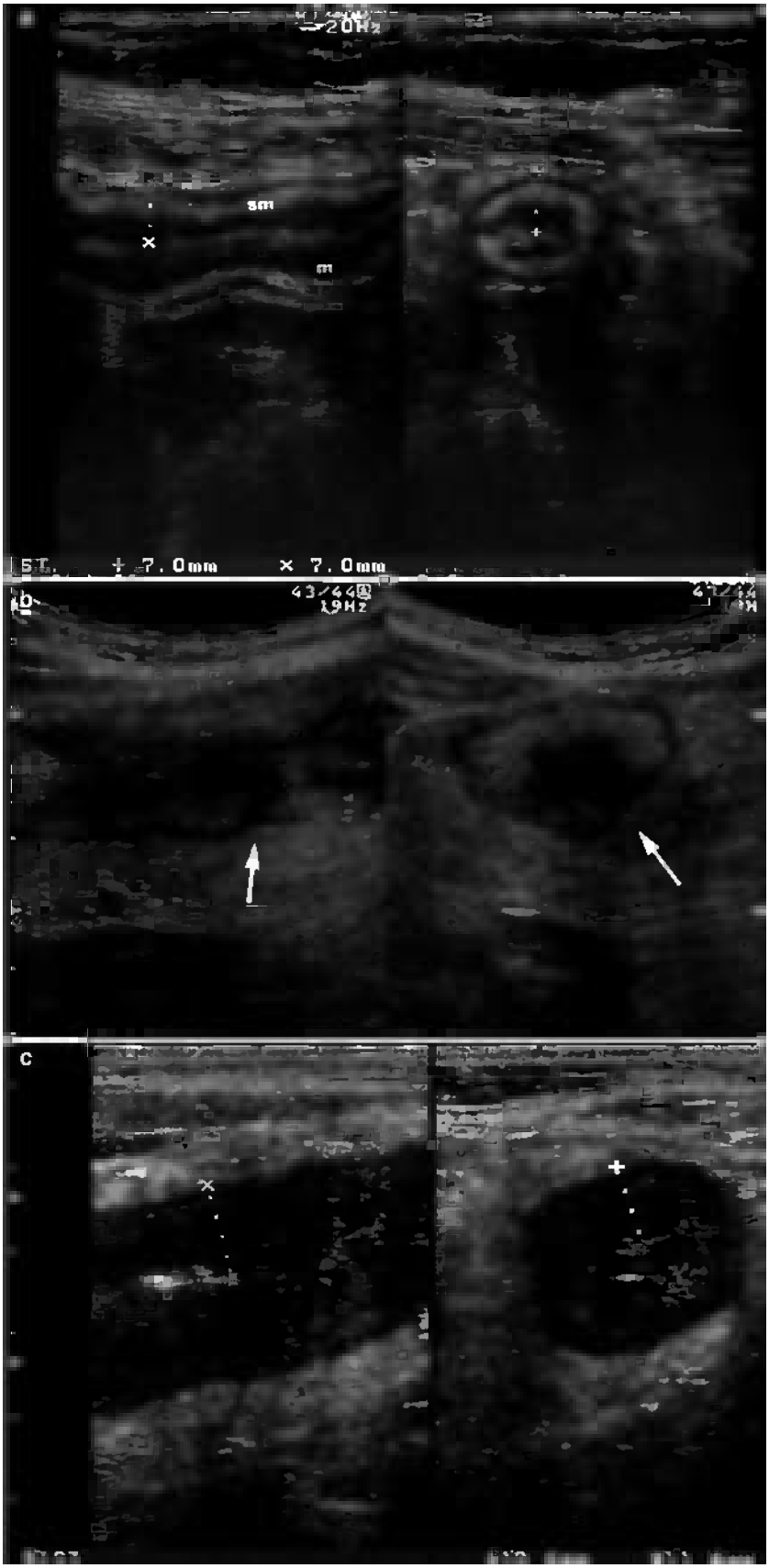

Fig. 3 Echopattern of thickened bowel walls. **a** Longitudinal (*left*) and transverse (*right*) sections of thickened bowel walls characterised by stratified echopattern with thickening of mucosal (*m*) and submucosal (*sm*) layers. **b** Longitudinal (*left*) and transverse (*right*) sections of thickened bowel walls characterised by stratified echopattern interrupted at the mesenteric side by hypoechoic areas (*arrows*), suggesting the presence of deep ulcers. **c** Longitudinal (*left*) and transverse (*right*) sections of thickened bowel walls characterised by hypoechoic echopattern with disappearance of wall stratification

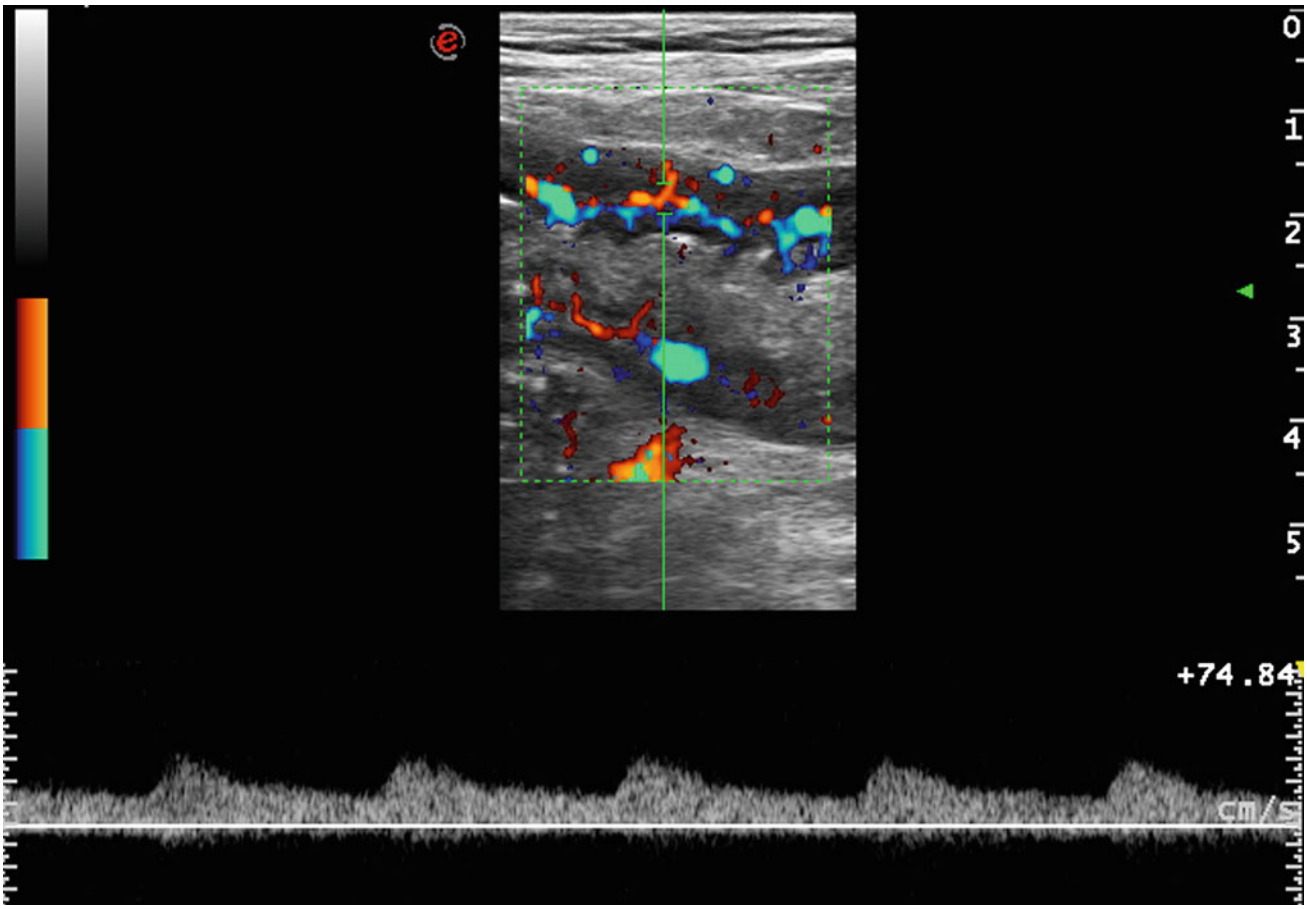

Fig. 4 Increased vascularity within the bowel wall showed by color Doppler ultrasound. Pulsed Doppler at this level detects the presence of low resistance arterial blood flow (*bottom side*)

Therefore, bowel US offers a useful alternative to invasive procedures in the postsurgical follow-up of CD patients, in particular for those CD patients who have undergone conservative surgery in whom endoscopy is not suitable to identify CD patients at high risk of clinical and surgical relapse, thus offering the opportunity to tailor the appropriate postoperative medical treatment.

3.2 Bowel Wall Echopattern

The thickened bowel wall in CD may show different echopattern. It may maintain the regular stratification (Fig. 2) or may be characterised by a partial or complete loss of layering. Sometimes, bowel segments with alternate persistence and loss of stratification, may be observed.

In stratified echopattern, the thickened walls display a variable enlargement of the mucosal, submucosal or muscular layers. Often the layer corresponding to the submucosa is thicker than others (Fig. 3a). The echo-stratification may be interrupted by hypoechoic areas (some with hyperechoic spots) corresponding to deep ulcers (Fig. 3b), or may completely disappear (Fig. 3c). The disappearance of echo-stratification indicates the presence of large, deep longitudinal ulcers associated with intense inflammation and neovascularisation (Kunihiro et al. 2004).

The clinical and pathological significance of bowel echopattern and, in particular, its importance in defining CD activity has been investigated in two studies, one of which in patients with stenosis. In vitro studies, that compared US images with the in vitro histopathological findings of related resected specimens, showed that the loss of stratification (hypoechoic echopattern) correlated with the severity of inflammation and that persistence of stratification in bowel wall of strictures suggested a high degree of fibrosis within the submucosa and *muscularis mucosae* (Hata et al. 1994; Maconi et al. 2003a). A recent study showed that fibrosis is correlated with an increase of echogenicity in the muscularis propria and a decrease of echogenicity in the submucosa (Nylund et al. 2008).

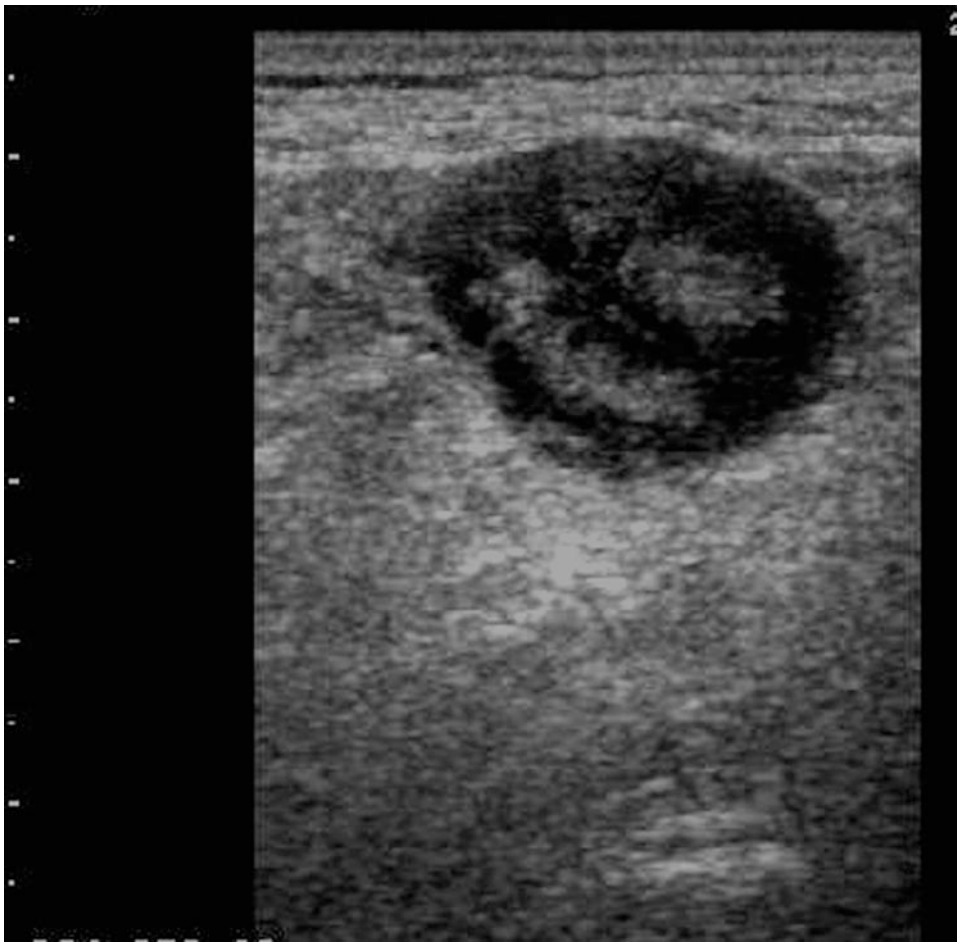

Fig. 5 Mesenteric hypertrophy, appearing at US as hyperechoic, sometimes inhomogeneous area surrounding thickened bowel walls

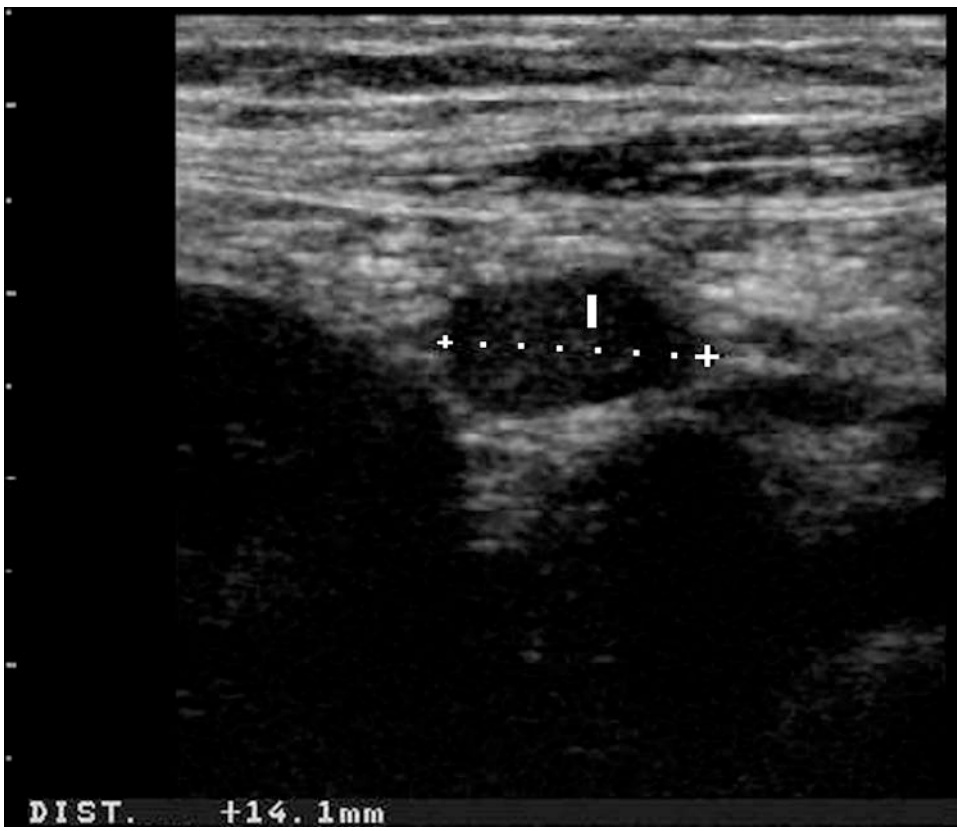

Fig. 6 Enlarged mesenteric lymph node (*l*) appearing at US as oval, homogeneous hypoechoic nodules with regular margins

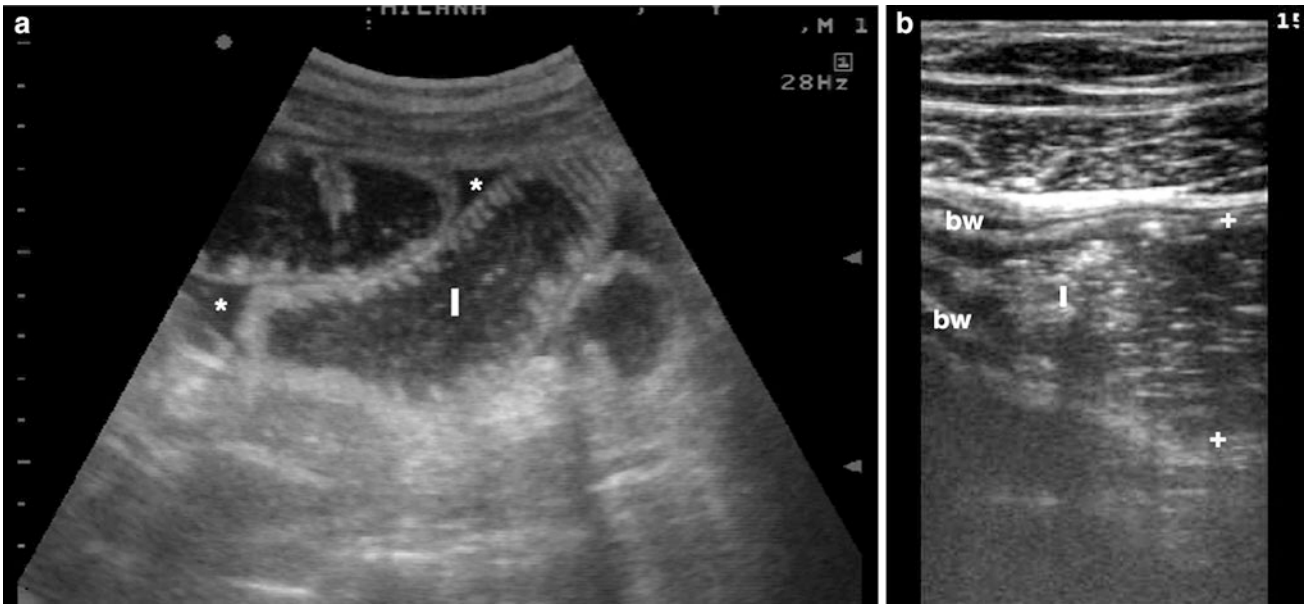

Fig. 7 Stenosis at US presented as thickened bowel wall, with narrowing of lumen associated with pre-stenotic dilatation >3 cm in diameter, and often associated with liquid content and air in the lumen. **a** Acute obstruction associated with a variable amount of liquid within the lumen (*l*) of the proximal loop, increased peristalsis and small amount of free peritoneal fluid (*asterisks*). **b** Chronic stenosis characterised by stratified bowel wall echopattern, showing an amount of gas within the proximal loop and weak peristalsis (*bw*, bowel wall; *l*, lumen)

Table 2 Sensitivity and specificity of Ultrasound, Magnetic Resonance Imaging (MRI) and Computed Tomography (CT) in detecting stenosis, fistulae and abscesses complicating CD (modified form Panes et al. 2011)

	Ultrasound % (IC95 %)	MRI % (IC95 %)	CT % (IC95 %)
Stenosis			
Sensitivity	79 (71–84)	89 (84–92)	89 (83–94)
Specificity	92 (87–96)	94 (90–96)	99 (95–100)
Fistulae			
Sensitivity	74 (67–79)	76 (71–82)	70 (64–76)
Specificity	95 (91–97)	96 (92–98)	97 (94–99)
Abscesses			
Sensitivity	84 (79–88)	86 (79–91)	84 (78–90)
Specificity	93 (89–95)	93 (88–79)	97 (94–99)

3.3 Bowel Wall Vascularity

The increased vascularity is often observed in bowel wall with decreased echogenicity. This is likely due to hyperaemia and neovascularisation related to the increased inflammatory response (Maconi et al. 2003a; Di Sabatino et al. 2004). Therefore, vascularity within the thickened bowel walls, assessed by power-color Doppler US, has been used as an index of CD activity (Fig. 4).

Vascularity has been evaluated using a simple scoring system according to the semi-quantitative (and subjective) intensity of colour signals and/or by analysis of Doppler curves (measurement of resistive index) obtained from vessels detected within the bowel walls. However, neither of these parameters correlated well with clinical or biochemical activity in most studies, whereas often a significant correlation was often found between vascularity and endoscopical/radiological activity (Spalinger et al. 2000; Esteban et al. 2001; Haber et al. 2002; Heyne et al. 2002; Scholbach et al. 2004; Neye et al. 2004; Yekeler et al. 2005).

The vascularity of diseased bowel walls in CD has been recently assessed by US i.v. contrast agents. This issue will be widely discussed elsewhere (see "Intravenous contrast-enhanced bowel ultrasound").

3.4 Elasticity and Peristalsis

Thickened bowel walls in CD may be associated with reduction or absence of peristalsis in the small bowel and loss of haustra coli in the colon (Sarrazin and Wilson 1996; Di Mizio et al. 2004). Although this manifestation is quite subjective and difficult to quantitatively assess, it has been regarded as relevant sign in most US studies, probably because associated with intestinal stenosis. Waiting for the

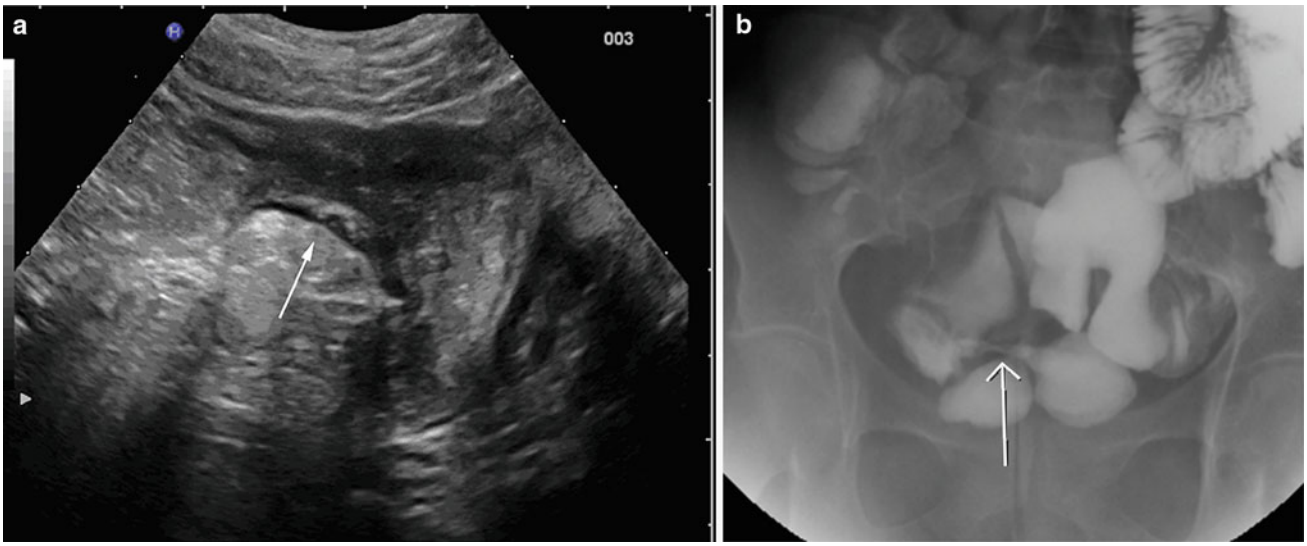

Fig. 8 **a** Longitudinal section of the bowel wall showing mixed (hypoechoic and stratified) echopattern at level of a short stenosis (*arrow*). **b** Correspondent radiographic imaging of the same stricture (*arrow*) given small bowel enteroclysis

results of US elastography (see "Imaging of Tissue Elasticity in Gastrointestinal Disorders"), oral contrast agents may be used for a more accurate US assessment of this feature (Parente et al. 2004b).

3.5 Mesenteric Hypertrophy and Mesenteric Lymph Nodes

Mesenteric hypertrophy (also named mesenteric fibrofatty proliferation or creeping fat) appears at US as hyperechoic, sometimes inhomogeneous area surrounding thickened bowel walls (Fig. 5). It is found in up to 50 % of CD patients (Goldberg et al. 1983; Maconi et al. 2008) and is correlated with biochemical and clinical activity of CD and with internal fistulas and increase bowel wall thickness (Maconi et al. 2008).

Enlarged mesenteric lymph nodes appear at US as oval, homogeneous hypoechoic nodules with regular margins (Fig. 6). This is a frequent finding in CD patients, in particular in young CD patients, in an earlier phase of CD and in patients with septic complications such as internal fistulas and abscesses. Its prevalence and clinical significance is discussed elsewhere in this book (see "Mesenteric Lymphadenopathy").

4 Crohn's Disease Abdominal Complications

The clinical course of CD is often characterised by abdominal complications such as stenosis, fistulae or abscesses and rarely by free perforation.

4.1 Stenosis and Intestinal Occlusion

Stenosis develops in 21 % of patients with ileal CD and in 8 % of those with ileocolic disease (Fenoglio-Preiser et al. 1989; Simpkins and Gore 1994). It is the most frequent cause of surgery. The diagnostic gold standard of this complication is contrast radiography that reveals all the occluded sites, the degree of intestinal narrowing and the length of the stenotic segments.

Bowel stenosis can be revealed by US as thickened bowel walls, associated with narrowed lumen and increased diameter of the proximal loop >2.5–3 cm. Acute stenoses are often associated with a variable amount of liquid and gas within the lumen of the proximal loop and with increased peristalsis (Fig. 7a) (Ko et al. 1993). In chronic, non-occlusive, stenoses the amount of air within the proximal loop prevails, and peristalsis is usually weak (Fig. 7b).

Using this definition, US correctly diagnoses stenosis in 70–79 % of unselected CD patients and in >90 % of patients with severe intestinal stenoses needing surgery, with false-positive diagnoses limited to 7 % (Maconi et al. 1996b; Gasche et al. 1999; Parente et al. 2002, 2004b). Results may be even better using an oral contrast agent (see "Intravenous Contrast-Enhanced Bowel Ultrasound") and are comparable to those of MRI and computed tomography (Table 2; Panes et al. 2011).

US assessment of the echopattern of the bowel wall of the strictures may also offer an insight into the histological features, discriminating between fibrotic and inflammatory strictures (Maconi et al. 2003a). Loss of stratification of the bowel wall at the level of the stricture suggests its inflammatory nature with a low degree of fibrosis, whilst the

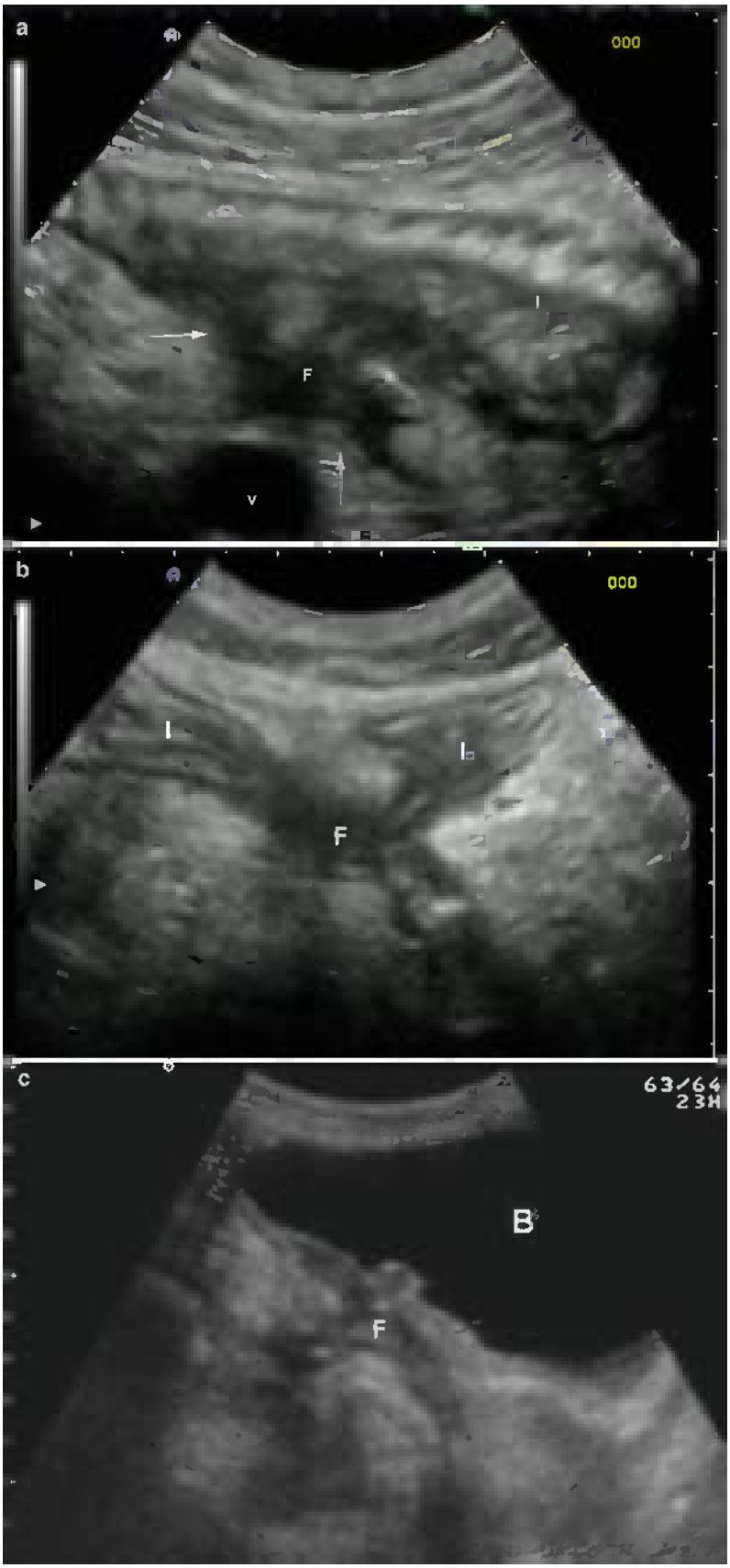

Fig. 9 Ultrasonographic appearance of internal fistulae. Entero-mesenteric (**a**), entero-enteric (**b**) and entero-vescical (**c**) fistulae (*F*) revealed at US as hypoechoic area deforming the margins of bowel wall (*arrows*), as hypoechoic ducts between the intestinal loops (*l*) and as hypoechoic areas between intestinal loops and bladder (*B*), respectively. *v*: iliac vein

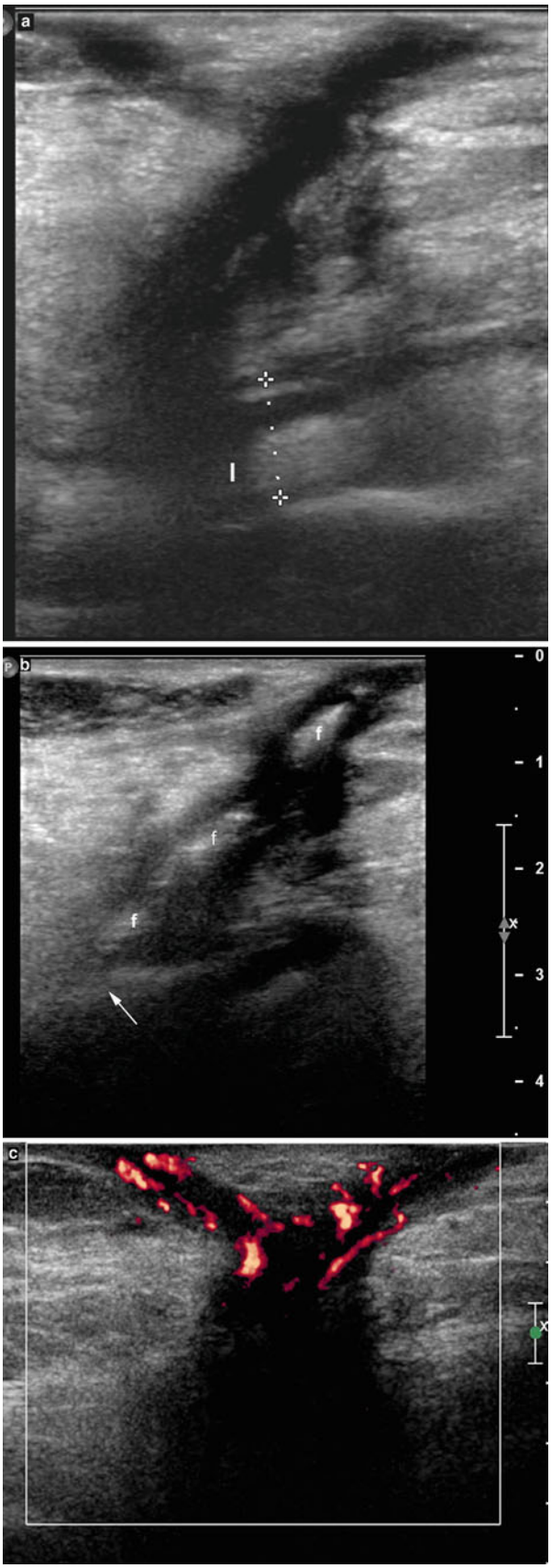

◀ **Fig. 10** Assessment of enterocutaneous fistula by US fistulography. **a** US assessment of the enetrocutaneous fistula and **b** evaluation of the same lesion by the injection of contrast agent within the fistula (*f*) that reveals its openness (*arrow*) previously not clear and defines the extension and the configuration of the lesion. **c** The presence of blood flow detected within the fistula wall can also suggest the activity of the fistula, despite the absence of conspicuous drainage. (*f*, Fistula; *l*, Intestinal loop)

presence of stratification suggests a higher degree of fibrosis of the stenosis (Fig. 8a, b).

4.2 Sinus Tracks and Fistulae

Fistulae occur in 17–82 % of CD patients. They are a transmural extension of the disease, often resulting from intestinal stenosis (Oberhuber et al. 2000), which ends blindly in the surrounding mesentery or connects intestinal loops or adjacent organs. Depending on their site and extension, abdominal fistulae are commonly subdivided into external or internal (enteroenteric, enteromesenteric).

Fistulae may appear on US as hypoechoic ducts or hypoechoic areas between intestinal loops or between loops and other structures such as the bladder (enterovescical fistula) or the skin (enterocutaneous fistulae) (Fig. 9a, b, c). Sometimes, fistulae display internal echoic spots due to the presence of air, debris or intestinal material (Maconi et al. 1996b; Gasche et al. 1999).

At present, there is no reliable technique for the diagnosis of this complication. Using surgical findings as reference standard, we showed that the accuracy of US and X-ray studies in detecting internal fistulae was comparable, with a sensitivity of 71.4 % for US and 69.6 % for X-ray studies, and a specificity of 95.8 % for both. We also showed that the combination of these two techniques significantly improved preoperative diagnostic performance (sensitivity 97.4 % and specificity 90 %) and that in selected severe cases of CD, with clinical suspicion of septic complications (i.e. abdominal mass or fever), sensitivity of US is even higher (88.5 %), thus confirming the high sensitivity of a previous US study (Gasche et al. 1999; Maconi et al. 2003b).

Noteworthy, US, MRI and CT have comparable sensitivity and specificity in detecting internal fistulae in CD (Panes et al. 2011). Since fistula wall is characterised by granulation tissue and neoangiogenesis, it may be easily recognised at US by detecting intra-mural blood flow using power-Doppler or i.v. contrast-enhanced US (Maconi et al. 2002).

US may also be usefully employed to define the features of external fistulae, particularly if US is combined with the injection of echoic contrast medium composed of hydrogen

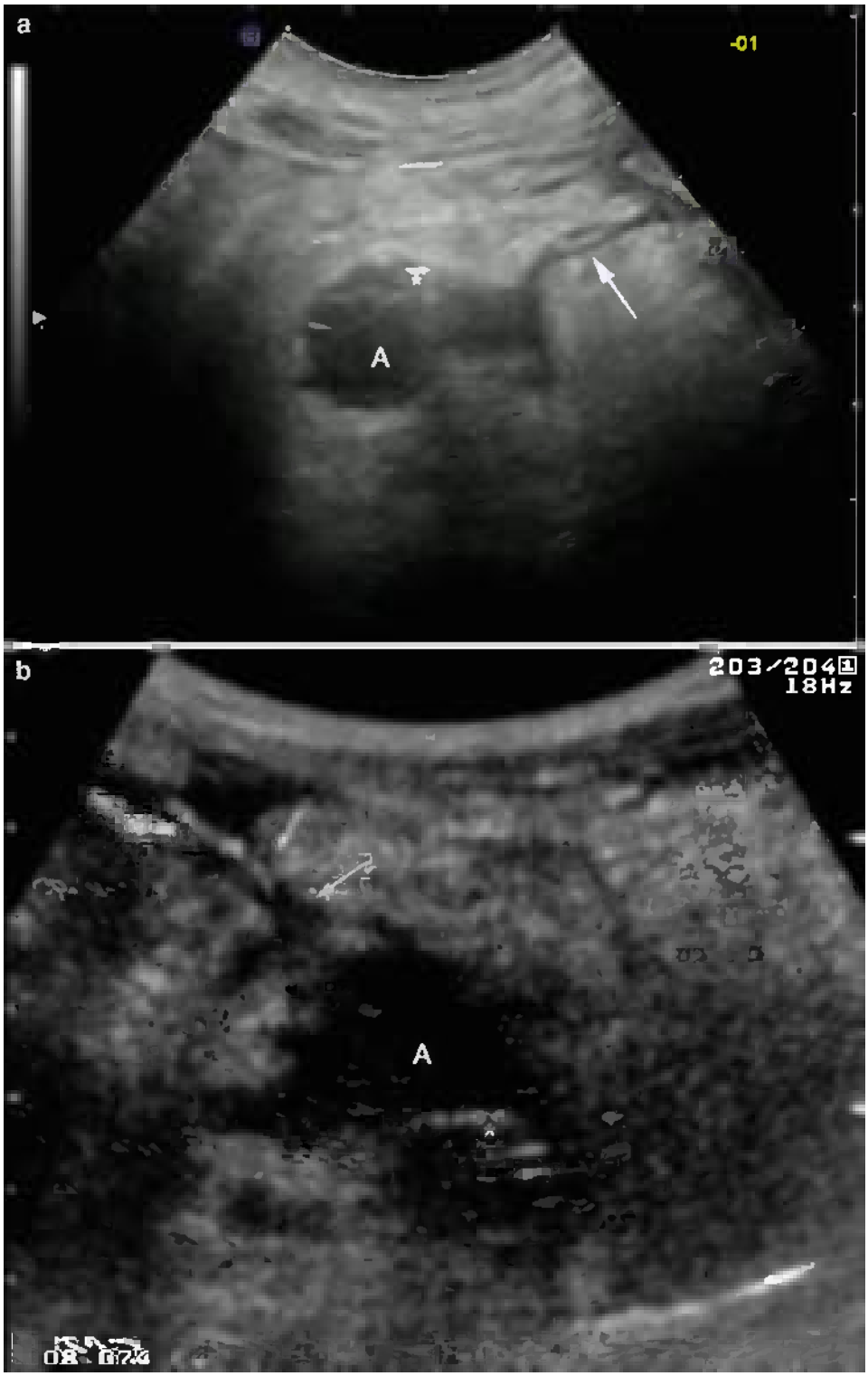

Fig. 11 **a**, **b** Intra-abdominal abscesses (*A*) appearing as hypo-anechoic lesions, often originating form a fistula (*arrow*), with irregular wall, with internal echoes due to presence of debris or air (*asterisk*), and characterised by posterior echo-enhancement

peroxide and povidone iodine into the fistula. This sort of US fistulography defines the extension and the configuration (linear or with ramifications) of the enterocutaneous fistulae (Fig. 10) is well tolerated and does not expose the patient to the risk of septic dissemination during the injection of the contrast medium (Maconi et al. 1999).

4.3 Intra-Abdominal Abscesses and Inflammatory Masses

Intra-abdominal abscesses occur in 12–30 % of CD patients, usually as a consequence of fistulising disease or as a postoperative complication (Steinberg et al. 1973;

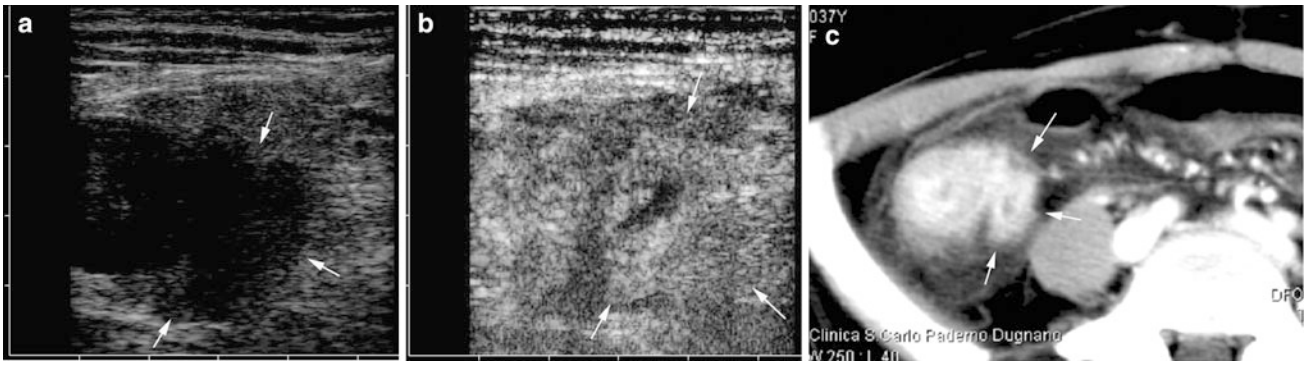

Fig. 12 Inflammatory mass detected by US (**a**) and characterised by i.v. contrast agent (**b**) that shows the absence of fluid within the mass. **c** Correspondent i.v. contrast CT imaging of the same lesion

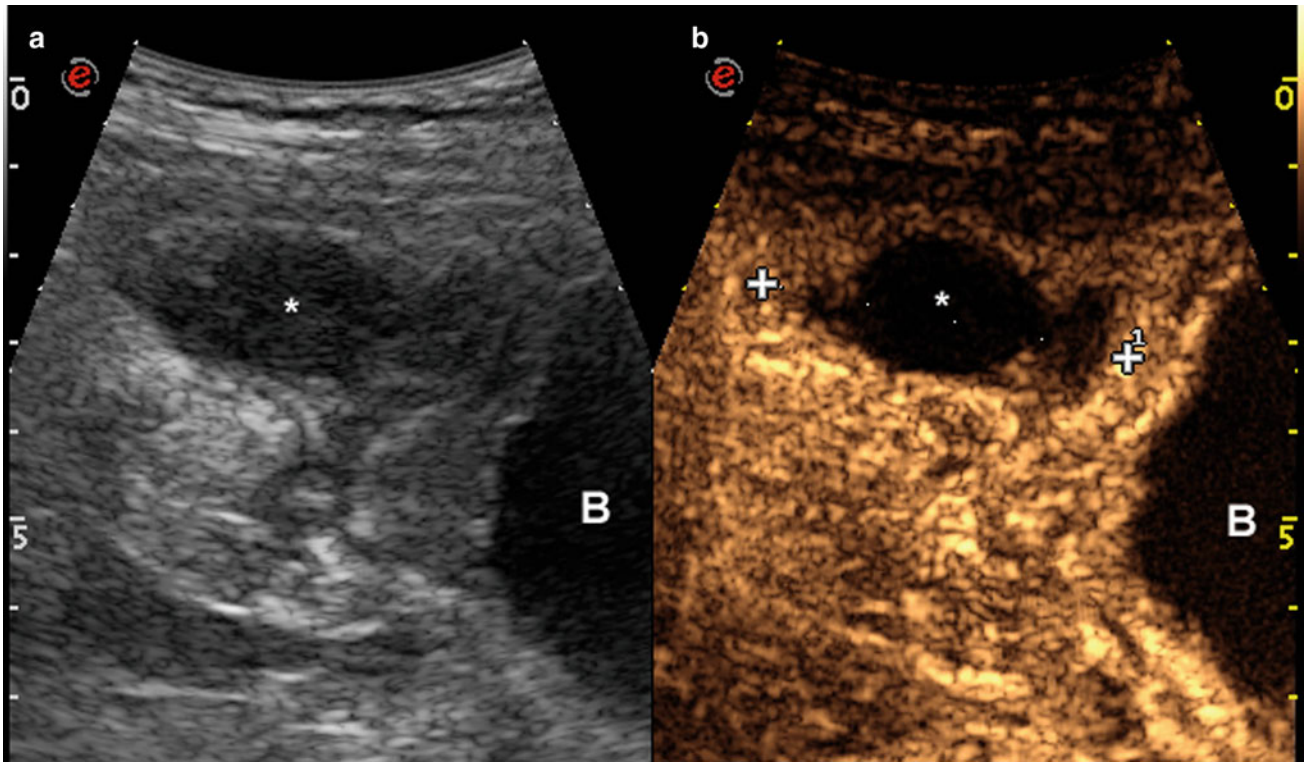

Fig. 13 Intra-abdominal abscess (*asterisks*) detected by b-mode US (**a**) and characterised by i.v. contrast agent (**b**) that shows the absence of vascularity within the mass. *B* bladder

Nagler et al. 1979). At US, abscesses appear as hypoanechoic lesions with fluid collection and irregular thickened walls, sometimes containing internal echoes due to the presence of debris or air, and characterised by a posterior echo enhancement (Fig. 11). Hypoechoic masses, especially those of small size and located close to the intestine, may be missed or mistaken for large sinus track, hypoechoic lymph nodes or phlegmon. Conventionally, these lesions are diagnosed when characterised by irregular borders, no identifiable wall or liquefaction. Inflammatory masses, phlegmons and intra-abdominal abscesses, identified or suspected at US, may be confirmed and distinguished detecting vascular signals by color-power Doppler US or, better, by i.v. contrast-enhanced US, around and/or within the lesions. Phlegmon and inflammatory masses, in fact, show increased colour signals within (Fig. 12), whilst abscesses present fluid collections with a peripheral flow (Fig. 13) (Tarjan et al. 2000; Maconi et al. 2002).

US detection of intra-abdominal abscesses shows a mean sensitivity and specificity of 84 and 93 %, respectively, quite similar to those of MRI and CT (Table 2; Panes et al. 2011). In particular, US shows a higher sensitivity in the detection of superficial intra-peritoneal abscesses, while the diagnosis of deep pelvic or retroperitoneal abscesses is more difficult due to the presence of overlying bowel gas and the difficulty in differentiating an abscess from an intestinal loop with stagnating fluid.

4.4 Perforation

Perforation is a potentially lethal complication of CD. It occurs in 1–2 % of the patients as a consequence of deep fissures in the intestinal wall. Free perforation should be suspected when US shows the presence of intra-peritoneal liquid and air, indicative of purulent peritonitis or the presence of free air under the diaphragm.

Focal perforations are more frequent than free perforations and may be diagnosed by US as areas of asymmetric and focal thickening of the wall associated with small peripariental collections of liquid and air.

References

Andreoli A, Cerro P, Falasco G et al (1998) Role of ultrasonography in the diagnosis of postsurgical recurrence of Crohn's disease. Am J Gastroenterol 93:1117–1121

Brignola C, Belloli C, Iannone P et al (1993) Comparison of scintigraphy with indium-111 leukocyte scan and ultrasonography in assessment of X-ray-demonstrated lesions of Crohn's disease. Dig Dis Sci 38:433–437

Bru C, Sans M, Defelitto MM et al (2001) Hydrocolonic sonography for evaluating inflammatory bowel disease. AJR Am J Roentgenol 177:99–105

Castiglione F, de Sio I, Cozzolino A et al (2004) Bowel wall thickness at abdominal ultrasound and the one-year-risk of surgery in patients with Crohn's disease. Am J Gastroenterol 99:1977–1983

Di Candio G, Mosca F, Campatelli A et al (1986) Sonographic detection of postsurgical recurrence of Crohn disease. AJR Am J Roentgenol 146:523–526

Di Mizio R, Maconi G, Romano S et al (2004) Small bowel Crohn disease: sonographic features. Abdom Imaging 29:23–35

Di Sabatino A, Ciccocioppo R, Armellini E et al (2004) Serum bFGF and VEGF correlate respectively with bowel wall thickness and intramural blood flow in Crohn's disease. Inflamm Bowel Dis 10:573–577

Esteban JM, Maldonado L, Sanchiz V et al (2001) Activity of Crohn's disease assessed by colour Doppler ultrasound analysis of the affected loops. Eur Radiol 11:1423–1428

Fenoglio-Preiser CM, Lantz PE, Listrom MB et al (1989) Gastrointestinal pathology; an atlas and text. Raven Press, New York, pp 427–484

Fraquelli M, Colli A, Casazza G et al (2005) Role of US in detection of Crohn's disease: meta-analysis. Radiology 236:95–101

Futagami Y, Haruma K, Hata J et al (1999) Development and validation of an US activity index of Crohn's disease. Eur J Gastroenterol Hepatol 11:1007–1012

Gasche C, Moser G, Turetschek K et al (1999) Transabdominal bowel sonography for detection of intestinal complication in Crohn's disease. Gut 44:112–117

Goldberg HI, Gore RM, Margulis AR et al (1983) Computed tomography in the evaluation of Crohn's disease. AJR Am J Roengtenol 140:277–282

Haber HP, Busch A, Ziebach R, Stern M (2000) Bowel wall thickness measured by ultrasound as a marker of Crohn's disease activity in children. Lancet 355:1239–1240

Haber HP, Busch A, Ziebach R et al (2002) US findings correspond to clinical, endoscopic, and histologic findings in inflammatory bowel disease and other enterocolitides. J Ultrasound Med 21:375–382

Hata J, Haruma K, Yamanaka H et al (1994) US evaluation of the bowel wall in inflammatory bowel disease: comparison of in vivo and in vitro studies. Abdom Imaging 19:395–399

Heyne R, Rickes S, Bock P et al (2002) Non-invasive evaluation of activity in inflammatory bowel disease by power Doppler sonography. Z Gastroenterol 40:171–175

Ko YT, Lim JH, Lee DH et al (1993) Small bowel obstruction: sonographic evaluation. Radiology 188:649–653

Kunihiro K, Hata J, Haruma K et al (2004) Sonographic detection of longitudinal ulcers in Crohn disease. Scand J Gastroenterol 39:322–326

Maconi G, Parente F, Bollani S et al (1996a) Abdominal ultrasound in the assessment of extent and activity of Crohn's disease: clinical significance and implication of bowel wall thickening. Am J Gastroenterol 91:1604–1609

Maconi G, Bollani S, Bianchi Porro G (1996b) Ultrasonographic detection of intestinal complications in Crohn's disease. Dig Dis Sci 41:1643–1648

Maconi G, Parente F, Bianchi Porro G (1999) Hydrogen peroxide enhanced ultrasound-fistulography in the assessment of enterocutaneous fistulas complicating Crohn's disease. Gut 45:874–878

Maconi G, Sampietro GM, Cristaldi M et al (2001) Preoperative characteristics and postoperative behaviour of bowel wall on risk of recurrence after conservative surgery in Crohn's disease a prospective study. Ann Surg 233:345–352

Maconi G, Sampietro GM, Russo A et al (2002) The vascularity of internal fistulae in Crohn's disease: an in vivo power Doppler ultrasonography assessment. Gut 50:496–500

Maconi G, Carsana L, Fociani P et al (2003a) Small bowel stenosis in Crohn's disease: clinical, biochemical and US evaluation of histological features. Aliment Pharmacol Ther 18:749–756

Maconi G, Sampietro GM, Parente F et al (2003b) Contrast radiology, computed tomography and ultrasonography in detecting internal fistulas and intra-abdominal abscesses in Crohn's disease: a prospective comparative study. Am J Gastroenterol 98:1545–1555

Maconi G, Greco S, Duca P et al (2008) Prevalence and clinical significance of sonographic evidence of mesenteric fat alterations in Crohn's disease. Inflamm Bowel Dis 14:1555–1561

Mayer D, Reinshagen M, Mason RA et al (2000) Sonographic measurement of thickened bowel wall segments as a quantitative parameter for activity in inflammatory bowel disease. Z Gastroenterol 38:295–300

Nagler SM, Poticha SM (1979) Intra-abdominal abscesses in regional enteritis. Am J Surg 173:350–354

Neye H, Voderholzer W, Rickes S et al (2004) Evaluation of criteria for the activity of Crohn's disease by power Doppler sonography. Dig Dis 22:67–72

Nylund K, Leh S, Immervoll H et al (2008) Crohn's disease: comparison of in vitro ultrasonographic images and histology. Scand J Gastroenterol 43:719–726

Oberhuber G, Stangl PC, Vogelsang H et al (2000) Significant association of strictures and internal fistula formation in Crohn's disease. Virchows Arch 437:293–297

Panes J, Bouzas R, Chaparro M et al (2011) Systematic review: the use of ultrasonography, computed tomography and magnetic resonance imaging fro the diagnosis, assessment of activity and abdominal complications of Crohn's disease. Aliment Pharmacol Ther 34:125–145

Parente F, Maconi G, Bollani S et al (2002) Bowel ultrasound in assessment of Crohn's disease and detection of related small bowel strictures. a prospective comparative study versus X-ray and intraoperative findings. Gut 50:490–495

Parente F, Greco S, Molteni M et al (2003) Role of early ultrasound in detecting inflammatory intestinal disorders and identifying their anatomical location within the bowel. Aliment Pharmacol Ther 18:1009–1016

Parente F, Greco S, Molteni M et al (2004a) Modern imaging of Crohn's disease using bowel ultrasound. Inflamm Bowel Dis 10:452–461

Parente F, Greco S, Molteni M et al (2004b) Oral contrast enhanced bowel ultrasonography in the assessment of small intestine Crohn's disease. a prospective comparison with conventional ultrasound, x ray studies, and ileocolonoscopy. Gut 53:1652–1657

Rigazio C, Ercole E, Laudi C et al (2009) Abdominal bowel ultrasound can predict the risk of surgery in Crohn's disease: proposal of an ultrasonographic score. Scand J Gastroenterol 44:585–593

Sarrazin J, Wilson SR (1996) Manifestation of Crohn disease at US. Radiographics 16:499–520

Scholbach T, Herrero I, Scholbach J (2004) Dynamic color Doppler sonography of intestinal wall in patients with Crohn disease compared with healthy subjects. J Pediatr Gastroenterol Nutr 39:524–528

Simpkins KC, Gore RM (1994) Crohn's disease. In: Gore RM, Levine MS, Laufer I (eds) Textbook of gastrointestinal radiology. Saunders, Philadelphia, pp 2660–2681

Spalinger J, Patriquin H, Miron MC et al (2000) Doppler US in patients with Crohn disease: vessel density in the diseased bowel reflects disease activity. Radiology 217:787–791

Steinberg DM, Cooke WT, Alexander Williams J (1973) Abscesses and fistulae in Crohn's disease. Gut 14:865–869

Tarjan Z, Toth G, Gyorke T et al (2000) Ultrasound in Crohn's disease of the small bowel. Eur J Radiol 35:176–182

Truong M, Atri M, Bret PM et al (1998) Sonographic appearance of benign and malignant conditions of the colon. Am J Roentgenol 170:1451–1455

Yekeler E, Danalioglu A, Movasseghi B et al (2005) Crohn disease activity evaluated by Doppler ultrasonography of the superior mesenteric artery and the affected small-bowel segments. J Ultrasound Med 24:59–65

Ulcerative Colitis

Giovanni Maconi

Contents

Abstract

Endoscopy is the method of choice in the diagnosis and in assessing the extent and severity of ulcerative colitis (UC). However, if endoscopy is incomplete or contraindicated, transabdominal ultrasound (US) may be a valid alternative to detect disease extension and activity in UC. The main ultrasonographic features of UC include bowel wall thickening, alterations of the bowel wall echopattern, hyperaemia and loss of haustra coli. The degree of thickness of colonic walls depends on disease activity, being greater in active disease, and normal in the quiescent phases. Recent data also show that bowel US may evaluate the response to medical treatment in active UC and predict future relapses of the disease after therapy.

1 Introduction

The role of abdominal ultrasound (US) has been less extensively investigated in ulcerative colitis (UC) than in Crohn's disease (CD). This is due to the different peculiar features between these two intestinal diseases. In fact in UC, unlike in CD, inflammatory lesions are confined to the colon, have a predictable spreading involving mainly the rectum that is considered difficult to image by transabdominal US and affect only the inner wall layer of the colon. Therefore, endoscopy is considered the method of choice in the diagnosis and in assessing the extent and severity of the disease.

However, transabdominal US has been demonstrated to be a reliable diagnostic tool for diagnostic purposes, to detect disease extension and activity in UC, thus providing important information if endoscopy is incomplete or contraindicated and, more recently, for prognostic purposes to predict the outcome of disease after therapy (Table 1).

G. Maconi (✉)
Gastroenterology Unit—Department of Biomedical and Clinical Sciences, "L. Sacco" University Hospital, Via G. B. Grassi, 74, 20157 Milan, Italy
e-mail: giovanni.maconi@unimi.it

G. Maconi and G. Bianchi Porro (eds.), *Ultrasound of the Gastrointestinal Tract*, Medical Radiology. Diagnostic Imaging,
DOI: 10.1007/174_2013_806,
Published Online: 14 February 2013

Table 1 Indications and potential usefulness of bowel ultrasound in UC

Early evaluation of patients with suspected UC
Evaluation of extension
Assessment of activity
Assessment of short-term response to therapy
Long-term prediction of UC outcome (relapse/remission)
Diagnosis of abdominal complications
Toxic megacolon
Massive pseudopolyposis
Differential diagnosis in chronic inflammatory colitis

2 Clinical and Pathological Features

Ulcerative colitis is a chronic idiopathic inflammatory disease of unknown origin. Depending on the extension and activity, the presence and severity of leading symptoms of the disease such as diarrhoea, rectal blood loss, abdominal pain and fever, can vary and laboratory parameters of the acute phase response (e.g. C-reactive protein, erythrocyte sedimentation rate, faecal calprotectin) may be normal or abnormal. These findings usually depend on the severity and extent of colonic involvement.

Ulcerative colitis involves the rectum and extends proximally to all or different portions of the colon (ulcerative proctitis, sigmoiditis, left-sided colitis or pancolitis). Rectosigmoid involvement is present in almost all patients at endoscopy, with approximately 40–50 % of patients having disease limited to the rectum and rectosigmoid, 30–40 % disease extending beyond the sigmoid colon but not involving the entire colon and 20 % total colitis. Mucosal inflammation of the terminal ileum, the so-called backwash ileitis, is observed in up to 20 % of patients with pancolitis, but rarely in patients without caecal involvement. However, involvement of the appendix as a skip lesion is reported in up to 75 % of patients with UC, and the patchy inflammation in the caecum (the so-called "caecal patch") may also be observed in patients with left-sided colitis, but both these conditions do not seem to be associated with a worse disease outcome.

Proximal spread of the disease, from the rectum to the caecum, occurs in continuity without areas of uninvolved mucosa. However, macroscopical sparing of the rectum has been described in children presenting with UC prior to treatment. In adults, normal or patchy inflammation of the rectum is likely to be due to topical therapy and although macroscopic activity may suggest skip areas, endoscopic biopsies from mucosa with a normal appearance are usually abnormal.

Indeed, the mucosa may appear normal when disease is in remission, whereas with mild and moderate inflammation it is erythematous and of granular appearance. In more severe cases, the mucosa is ulcerated and haemorrhagic (Fig. 1). In long-standing disease, the mucosa may appear atrophic and inflammatory polyps or pseudopolyps may be present as a result of epithelial regeneration.

In UC, histological changes are limited to the mucosa and superficial submucosa with deeper layers being unaffected, except in fulminant colitis. The major changes are distortion of crypt architecture and basal plasma cells and basal lymphoid cell infiltrate. Mucosal vascular congestion with oedema, focal haemorrhage and inflammatory cell infiltration may also be present (Fig. 2).

These histological changes, as well as endoscopic features, correlate well with sonographic images. However, since the disease is confined to the inner layers of the colon, endoscopy alone may be sufficient to detect and assess the extent and activity of the disease in UC, unlike CD. In this context, the role of cross sectional imaging, US included, may be marginal although useful, in some instances, since it can be repeated and is non-invasive.

3 Ultrasonographic Features of Bowel Walls

The US features of UC include bowel wall thickening, alterations of the bowel wall echopattern, hyperaemia and loss of haustra coli. Occasionally mesenteric hypertrophy and mesenteric lymph nodes, or complications such as stenosis or toxic megacolon, can be found.

Ultrasonographic features of bowel wall, and particularly bowel wall thickening, largely depend on the activity of the disease. In active UC patients, US frequently reveals thickened bowel walls, usually >4 mm, frequently ranging from 5 to 7 mm, rarely >10 mm (Worlicek et al. 1987; Valette et al. 2001; Fig. 3).

However the abnormal thickening of bowel walls at US (bowel wall thickness >4 mm) is not specific, since several intestinal disorders, including UC, are characterised by US thickening of bowel walls. The degree of thickness in UC depends on disease activity, being greater in active disease and normal in the quiescent phases (Fig. 4).

Sonographic diagnosis of UC relies on different features of the bowel wall. In UC, the thickness of the bowel wall is usually homogeneous and continuous, predominates in the left colon and is, therefore, usually found in the left iliaca fossa and in the hypogastric region and extends throughout the entire colon in pancolitis (Fig. 5). Loss of haustration is a frequent finding in active and extensive disease. The thickness of the bowel wall is circumferential and symmetrical.

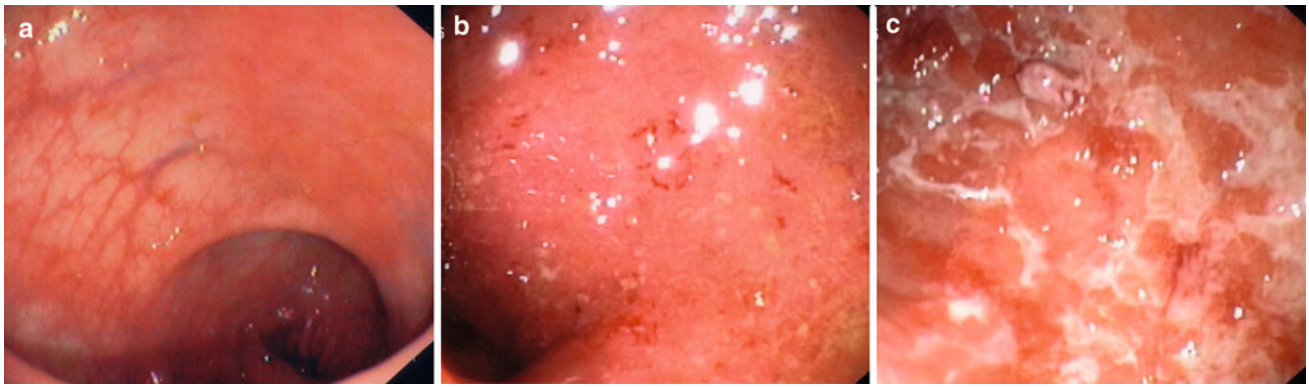

Fig. 1 Different endoscopic aspects of colon in ulcerative colitis. **a** Inactive disease: presence of distorted mucosal vascular pattern without ulcerations, friability or spontaneous bleeding. **b** Moderate disease: marked erythema, absent vascular pattern, friability, coarse granularity with small erosions. **c** Severe disease: gross ulceration and spontaneous bleeding

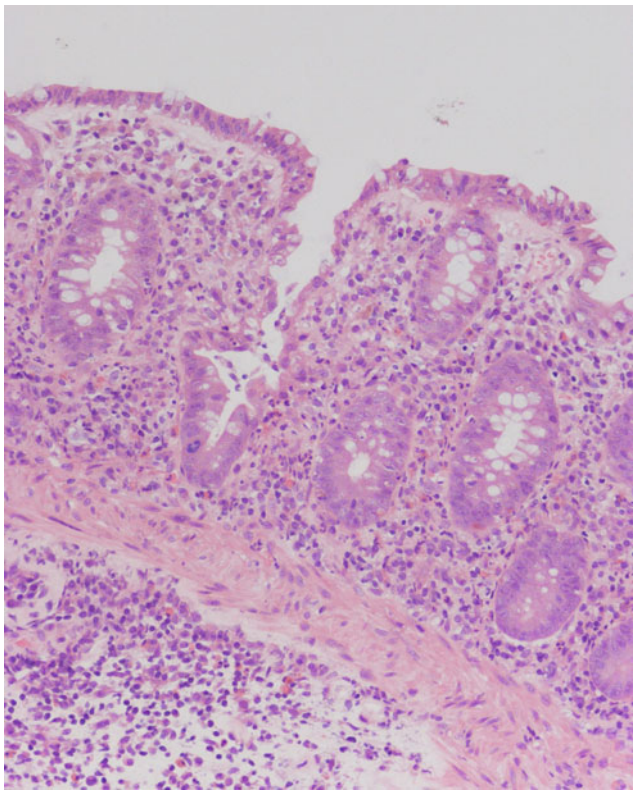

Fig. 2 Histological feature of ulcerative colitis. Changes are limited to mucosa (*muscularis mucosae* is normal) and consist in distortion of crypt architecture, vascular congestion of mucosa, oedema and basal inflammatory cell infiltrate

Since inflammation involves the mucosa and the superficial submucosa, the stratified echopattern of the bowel wall is usually preserved (Fig. 5). However, in cases of acute inflammation, the thickening involves the submucosa which may appear slightly hypoechoic and dishomogeneous, sometimes giving the bowel wall the US appearance of pathological wall thickening with loss of stratification, with increased bowel wall vascularity (Fig. 6).

The muscularis propria, which is imaged at US as an external hypoechoic line is preserved, therefore external profiles of the bowel walls in UC are usually linear and regular (Fig. 5).

Unlike CD, ulcerations are superficial and, therefore, not usually revealed by US. No deep or penetrating ulcers are present, except in severe UC in which a pre-perforative laceration of the submucosa is found. Therefore, in mild to moderate active UC, the inner layers of the colonic wall are usually regular. On the contrary, in severe active disease, the inner layer may be regular or even irregular with fine multiple hyperechoic spots, representing deep penetrating ulcers, but within a severely thickened and hypoechoic bowel wall (Fig. 7).

Since the colon returns, at endoscopy, to a normal appearance after resolution of inflammation, US also reveals a normal colonic wall. Indeed, after several recurrences, in quiescent disease, as well as in some cases with mild inflammation, the colonic wall shows normal or only slight thickening with a predominant echogenic submucosa contrasting with the hypoechoic inner mucosa and outer muscularis (Fig. 8).

Particular US findings may be observed in UC patients with extensive pseudopolyposis. Pseudopolyps may be observed as small echogenic nodules visible at the surface of the mucosa or echogenic indentations into the fluid-filled intestinal lumen. However, while isolated inflammatory polyps can be detected (Fig. 9), better imaged by hydrocolonic sonography, extensive pseudopolyposis appears as an increased and inhomogeneous thickness of the bowel wall (up to 15 mm) without the typical wall stratification (at least in inactive UC), markedly irregular internal margins and/or as a dilated incompressible bowel with echogenic inhomogeneous content (Fig. 10). To obtain confirmation of the pseudopolypoid nature of the intestinal content, colour-power Doppler can be used to assess the blood flow within the echogenic material.

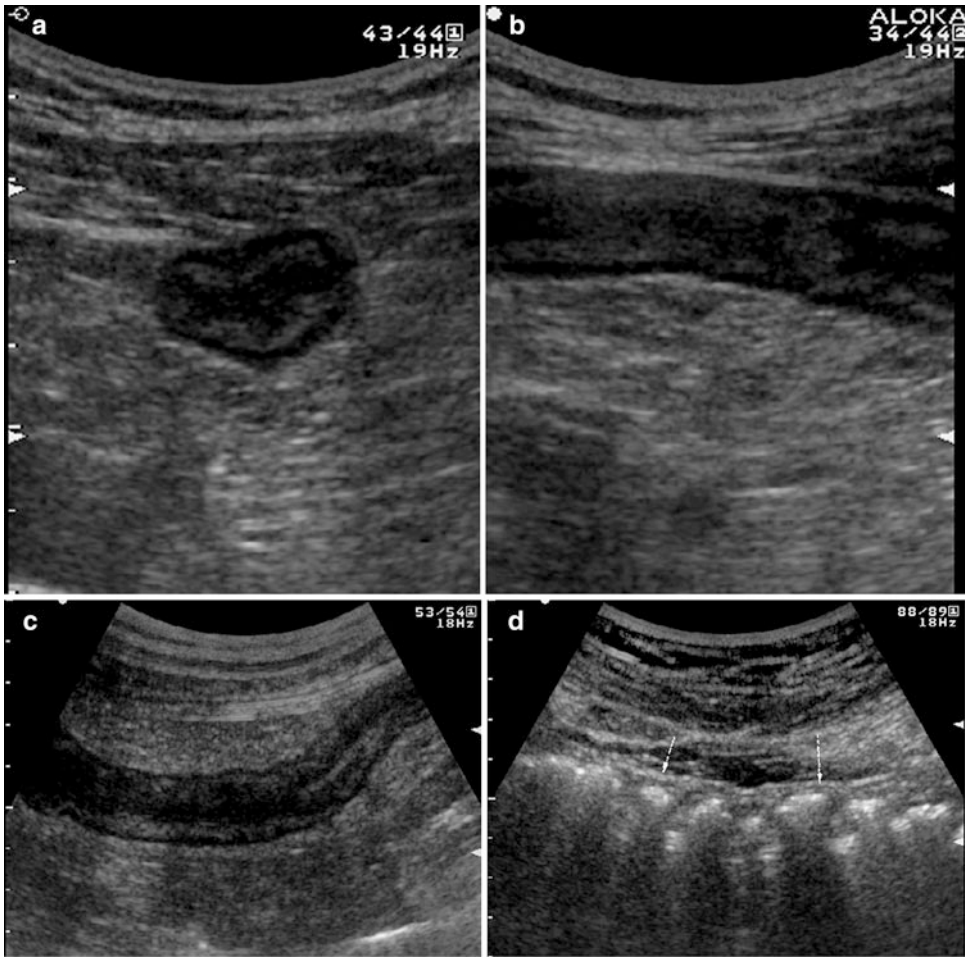

Fig. 3 Ultrasonographic features of bowel wall in patient with ulcerative colitis. Transverse (**a**) and longitudinal (**b**) sections of descending colon in patient with left-sided active ulcerative colitis. Thickened bowel walls characterised by stratified echopattern and absence of haustra coli (**c**) in the left colon. The presence of haustra coli (*arrows*) in the transverse colon (**d**) defines the extension of the disease

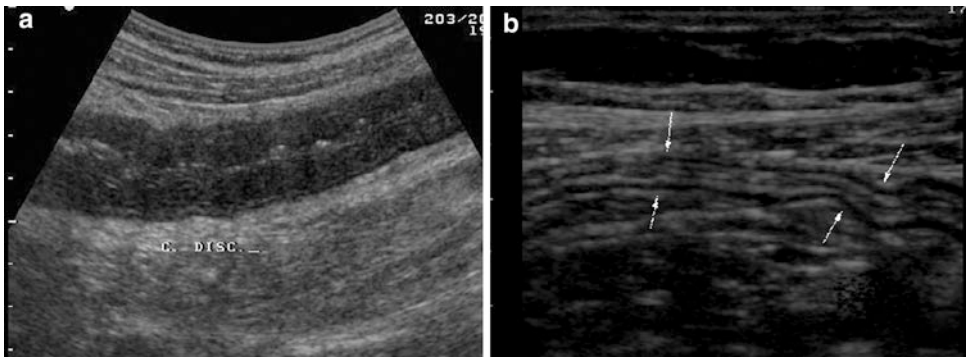

Fig. 4 Longitudinal ultrasonographic sections of descending colon in patients with **a** active and **b** non-active UC. Note the increased thickness and hypoechoic echopattern in patient with active disease and normal-appearing aspect of bowel wall (*arrows*) in patient with quiescent disease

4 Detection and Assessment of Extension

The US diagnosis of UC relies upon the above-mentioned findings, mainly upon visualisation of bowel wall thickening greater than 4 mm.

So far, few studies have focused on the accuracy of bowel US in diagnosing UC and in assessing the extent of inflammation (Arienti et al. 1996; Maconi et al. 1999). When bowel wall thickness >4 mm was used for abnormality in adults, the sensitivity of conventional transabdominal US in detecting bowel inflammation in UC showed

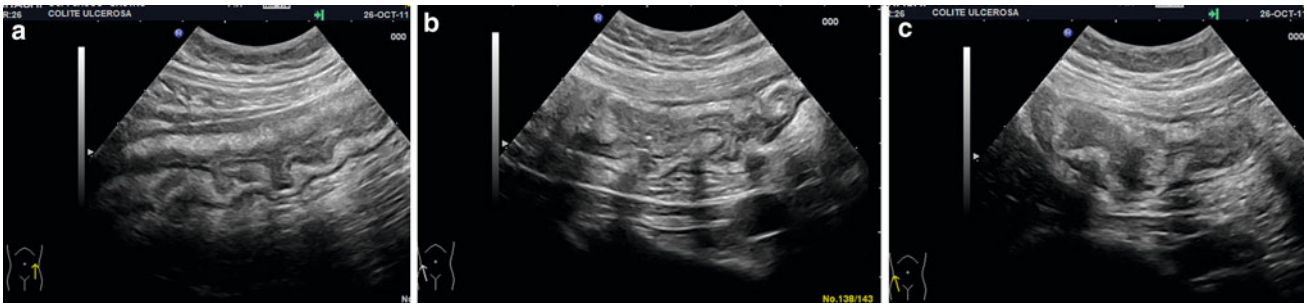

Fig. 5 Ultrasonographic features of pancolitis. Homogeneous and continuous thickening of the colonic walls with preserved stratified echopattern in **a** hypogastric region and left iliaca fossa, which extends throughout the entire colon up to **b** ascending colon and **c** caecum

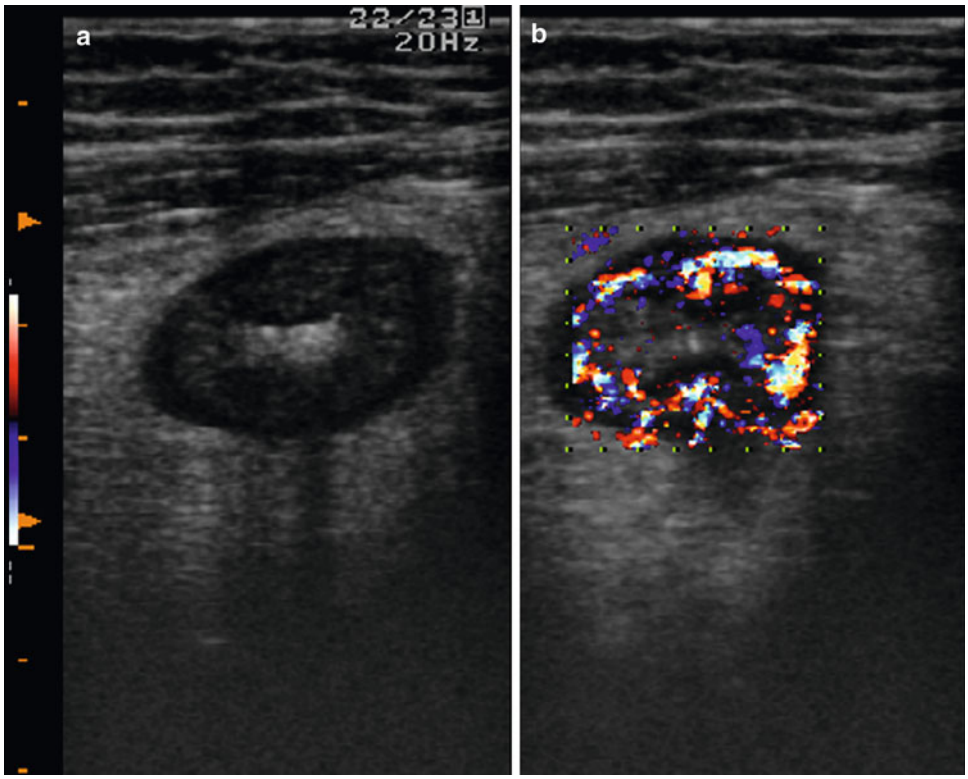

Fig. 6 Ultrasonographic aspect of bowel wall in patient with active ulcerative colitis. The thickening involves the submucosa which may appear slightly hypoechoic (**a**), with increased bowel wall vascularity (**b**)

a mean of 74 % and a median of 76 % (range: 53–89 %) (Limberg 1989; Pascu et al. 2004; Hollerbach et al. 1998; Schwerk et al. 1992; Worlicek et al. 1987; Hata et al. 1994; Parente et al. 2003; Astegiano et al. 2001; Sonnenberg et al. 1982). As demonstrated by these authors, these results are inferior to those observed in CD. The lower accuracy of US in detecting UC may be explained by the superficial mucosal involvement of the disease, the less marked bowel wall thickening in UC and, in particular, by the distal localisation of the disease. In fact, inactive disease or UC characterised by mild inflammation may have normal bowel wall thickening (<4 mm) and, therefore, can be missed by US. However, the main problem in detecting UC is that distal localisation of the disease is difficult to reveal by US and, therefore, proctitis or diseases confined to the rectum and distal part of the sigmoid colon can be missed with this technique.

In fact, studies assessing the accuracy of bowel US in evaluating the anatomical extension of the inflammatory process, during disease flare-up, have shown that the technique has a very high sensitivity in detecting left-sided colitis and a very low sensitivity in identifying proctitis. In particular, despite the fact that the rectum is not difficult to assess by US (it is detectable behind appropriately distended urinary bladder, in transverse and longitudinal sections), the sensitivity in detecting the rectal involvement in UC is poor (Parente et al. 2003). On the contrary, UC involvement of other colonic diseased segments can be correctly detected in more than 70 % of patients (Fig. 11).

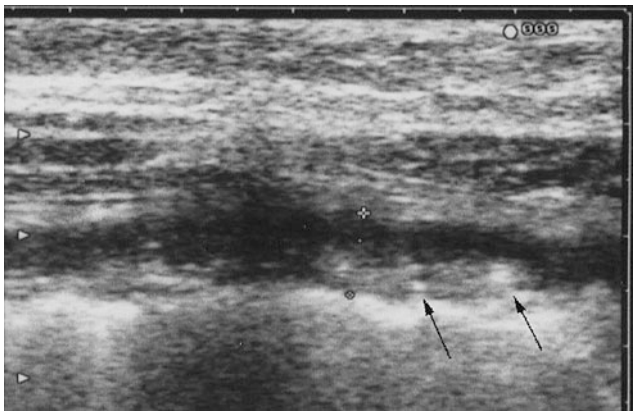

Fig. 7 Severe active UC showing severely thickened and hypoechoic bowel walls, with irregular inner layer due to fine multiple hyperechoic spots, representing deep penetrating ulcers (*arrows*)

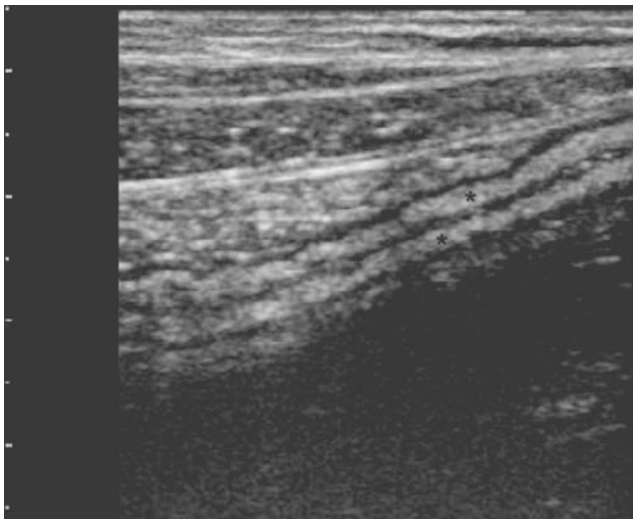

Fig. 8 Quiescent UC, showing colonic wall presenting normal or slight thickening, with a predominant echogenic submucosa (*asterisks*) contrasting with the hypoechoic inner mucosa and outer muscularis propria

These findings suggest that bowel US may be a valid alternative to invasive procedures in assessing the extension of UC, provided that the disease is active (e.g. bowel examination should be performed only during flare-up of the disease) and not limited to the rectum (e.g. bowel examination may be negative in patients presenting without diarrhoea and only with rectal bleeding).

5 Assessment of Disease Activity

Assessment of bowel wall features, namely the degree of wall thickening in diseased segments and their echopattern, together with bowel wall and mesenteric vascularity, can

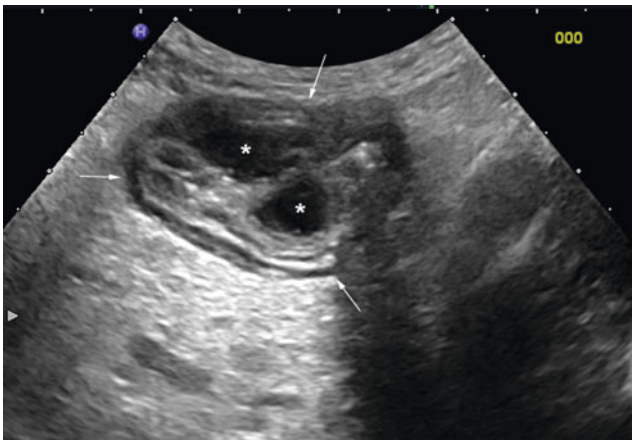

Fig. 9 Ultrasonographic findings in UC patient with pseudopolyposis. Note the slight thickness of sigmoid colonic wall (*arrows*), with irregular internal margins due to presence of two hypoechoic lesions corresponding to inflammatory peudopolyps (*asterisks*)

provide useful information to evaluate the activity in UC. Unlike CD, where the role of these US features in assessing disease activity is still controversial, in UC, most studies have demonstrated a significant correlation between the degree of bowel wall thickening, hypoechoic echopattern of bowel walls and increased mesenteric and bowel wall vascularity and active disease.

Indeed, several studies have shown that the degree of bowel wall thickening correlates well with clinical activity (Worlicek et al. 1987; Schwerk et al. 1992; Arienti et al. 1996; Maconi et al. 1999; Ruess et al. 2000; Bru et al. 2001; Haber et al. 2002), biochemical (namely C-reactive protein and erythrocyte sedimentation rate values) (Maconi et al. 1999; Ruess et al. 2000; Antonelli et al. 2011), endoscopic (Maconi et al. 1999; Bru et al. 2001; Parente et al. 2010; Antonelli et al. 2011) and scintigraphic (Arienti et al. 1996) activity of UC. Indeed, other studies have shown that the loss of bowel wall stratification (hypoechoic echopattern) (Hata et al. 1994) and increased bowel wall vascularity (Heyne et al. 2002) strongly suggest the presence of active UC. On the contrary, very few studies fail to show any correlation between US features of bowel wall (e.g. bowel wall thickening) and disease activity in UC (Mayer et al. 2000).

6 Assessment of Response to Therapy and Outcome

Bowel US may evaluate the response to medical treatment in active UC and predict future relapses of the disease (Maconi et al. 1999; Arienti et al. 1996). In particular, it has been used as a surrogate of colonoscopy to assess the short-

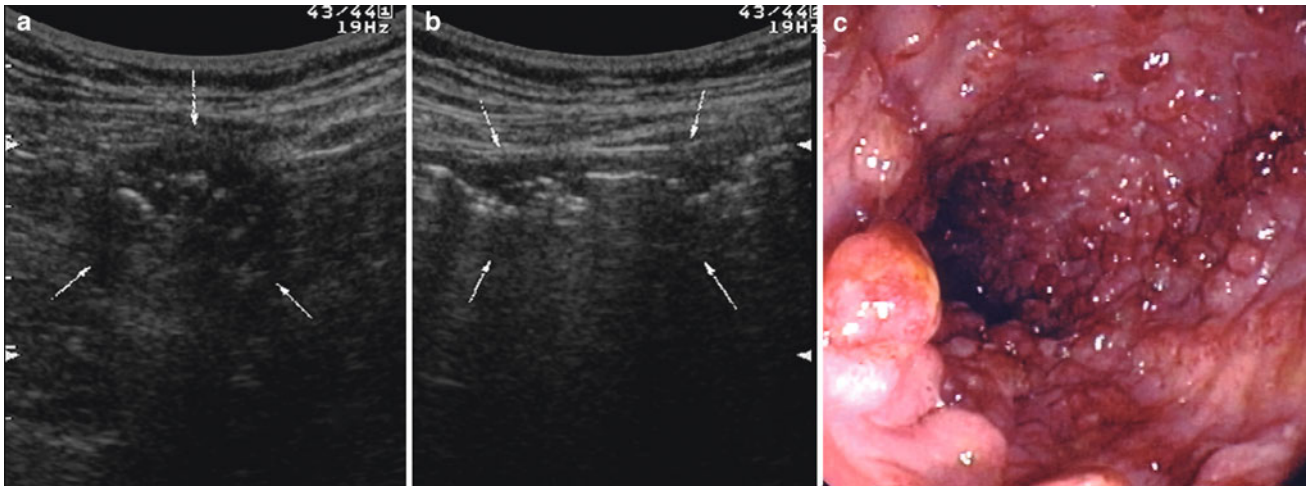

Fig. 10 Ultrasonographic (**a**, **b**) and endoscopic (**c**) findings in UC patient with extensive pseudopolyposis. Note inhomogeneous thickness of distal descending colon at US without typical wall stratification. **a** Bowel was also incompressible with echogenic inhomogeneous content

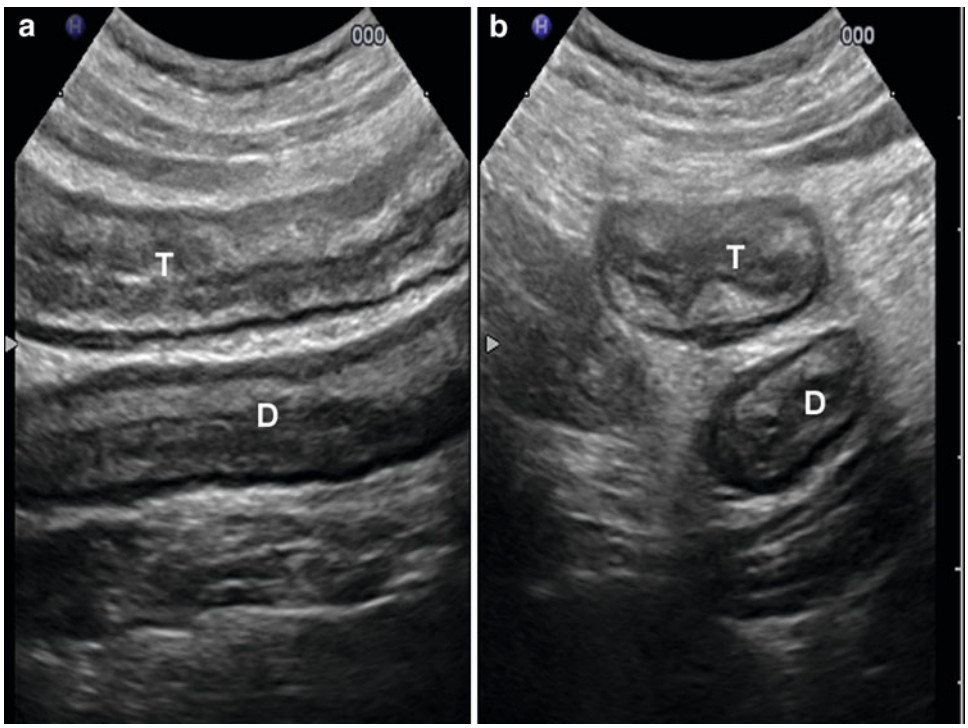

Fig. 11 Thickened walls of proximal descending colon (*D*) and distal transverse colon (*T*) simultaneously imaged by longitudinal (**a**) and transverse (**b**) ultrasonographic sections, with the probe placed in left flank, in a patient with active UC Along with thickened walls, note the regular external margins, the stratified echopattern and the absence of haustra coli

term response to high-dose steroid therapy or cytapheresis in severe UC, thus predicting the long-term outcome of disease (Parente et al. 2010; Yoshida et al. 2011). In this regard, it has been shown that the absence of significant decrement in wall thickness from baseline shortly after a course of therapy is associated with a high risk of severe endoscopic activity or relapse at 1 year (Parente et al. 2010; Yoshida et al. 2011).

The vascularity of the inferior mesenteric artery and superior mesenteric artery has been also shown to be well correlated with clinical and endoscopic activity in patients with UC. Indeed, several studies have shown that at Doppler sonography, mean velocity is significantly reduced, and pulsatility and resistance indexes of these arteries are increased compared to those in control subjects (Pascu et al. 2004; Kalantzis et al. 2002; Sigirci et al. 2001; Ludwig et al.

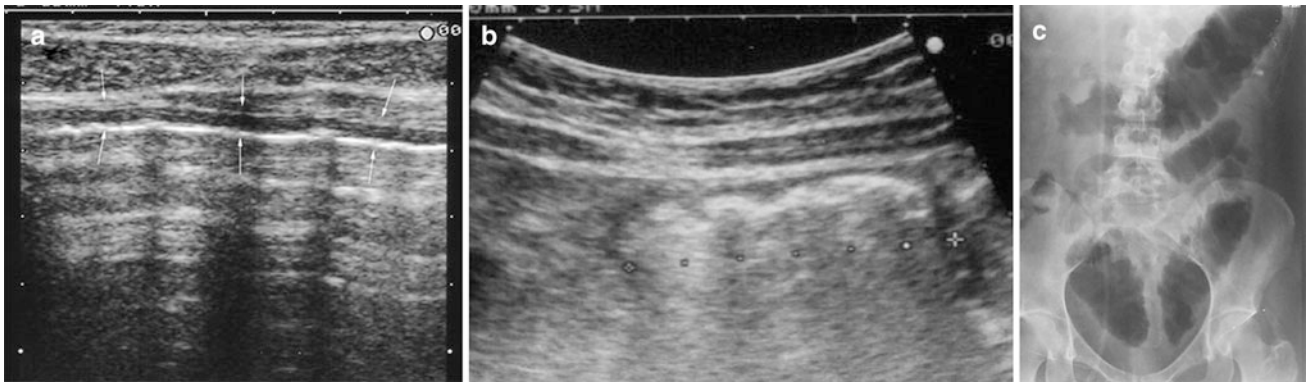

Fig. 12 Ultrasonographic (**a**, **b**) and radiographic (**c**) findings in UC patient with toxic megacolon. Note the thin bowel wall (*arrow*) without haustration (**a**) and dilated transverse colon (**b**). Plan X-ray of the abdomen shows the typical dilated transverse colon (**c**)

Table 2 Main ultrasonographic features in differential diagnosis between ulcerative colitis and Crohn's disease

	Ulcerative colitis	Crohn's disease
Bowel wall		
Thickness	5–7 mm	5–14 mm
Echopattern	Variable	Variable
Vascularity	Variable	Variable
Contour	Well defined	Variable
Stiffness	Absent	Often present
Austra coli	Absent	Absent
Persistalsis		Often weak or absent
Location and extention		
Site	Recto-sigmoid and colon	Ileum (70 %), Colon (60 %)
Bowel involvement	Continuous	Often divided in segments
Extra-intestinal alterations		
Mesenteric hypertrophy	Uncommon	Common
Enlarged lymph nodes	Uncommon	Common
Fistulae and abscesses	Rare	Common

1999; Mirk et al. 1999; Maconi et al. 1996; Bolondi et al. 1992), thus suggesting their potential usefulness in the evaluation of inflammation of the colon and to document their response to therapy.

7 Toxic Megacolon

The presence of toxic megacolon should be suspected when, at US, marked decrease in thickness (<2 mm) of the colonic wall is found associated with dilatation (>6 cm) of the colon and the presence of increased fluid and dilation of the ileal loops (Fig. 12) (Maconi et al. 2004). US plays a supportive role in the event of clinical suspicion of this type of complication. Despite the advantage of rapid diagnostic and therapeutic interventions, its role is still marginal in comparison to the reference investigation of plain abdominal radiography.

8 Differential Diagnosis Between UC, Crohn's Disease and Other Inflammatory Diseases

Unfortunately, there are no specific US features of the intestinal walls that can be employed usefully in the differential diagnosis between UC and CD or other inflammatory bowel diseases. However, the site and degree of bowel wall thickness and other features of the bowel wall may be helpful in differentiating between UC and CD (Table 2). Indeed, the diagnosis of CD seems to be easier than that of UC due to specific features that are not usually

present in this disease: namely abdominal complications (e.g. strictures and fistulae), skip areas, ileal localisation and deep ulcerations with transmural involvement. The assessment of these signs may be useful to differentiate chronic inflammatory bowel diseases, in particular in patients who, for various reasons (e.g. colonic stricture, lack of tolerance to radiographic examinations, pregnancy) are not amenable to adequate endoscopic or radiological evaluation of the bowel. The US features of the colonic wall may discriminate between UC and CD in approximately 80 % of cases, relying only on features of the bowel walls (Pera et al. 1988; Limberg 1989; Limberg and Osswald 1994).

The differential diagnosis is more difficult between UC and acute inflammatory conditions such as infectious colitis, diverticular sigmoiditis and ischaemic lesions. Infectious colitis shows a similar echopattern to that of UC, although the more frequent right localisation of infectious colitis may help in differentiating these entities.

Diverticular sigmoiditis is different from UC since the thickening is classically segmental and eccentric, with diverticula on the outer border of the colon. The differential diagnosis between UC and ischaemic colitis may be very difficult. Bowel wall thickening and echopattern may vary depending on the extent of devascularisation and type of vascular obstruction and, in this context, study of mesenteric circulation may be significant.

References

Antonelli E, Giuliano V, Casella G et al (2011) Ultrasonographic assessment of colonic wall in moderate-severe ulcerative colitis: comparison with endoscopic findings. Dig Liver Dis 43:703–706

Arienti V, Campieri M, Boriani L et al (1996) Management of severe ulcerative colitis with the help of high resolution ultrasonography. Am J Gastroenterol 91:2163–2169

Astegiano M, Bresso F, Cammarota T et al (2001) Abdominal pain and bowel dysfunction: diagnostic role of intestinal ultrasound. Eur J Gastroenterol Hepatol 13:927–931

Bolondi L, Gaiani S, Brignola C et al (1992) Changes in splanchnic hemodynamics in inflammatory bowel disease. Non-invasive assessment by Doppler ultrasound flowmetry. Scand J Gastroenterol 27:501–507

Bru C, Sans M, Defelitto MM et al (2001) Hydrocolonic sonography for evaluating inflammatory bowel disease. AJR Am J Roentgenol 177:99–105

Haber HP, Busch A, Ziebach R, Dette S, Ruck P, Stern M (2002) Ultrasonographic findings correspond to clinical, endoscopic, and histologic findings in inflammatory bowel disease and other enterocolitides. J Ultrasound Med 21:375–382

Hata J, Haruma K, Yamanaka H et al (1994) US evaluation of the bowel wall in inflammatory bowel disease: comparison of in vivo and in vitro studies. Abdom Imaging 19:395–399

Heyne R, Rickes S, Bock P, Schreiber S, Wermke W, Lochs H (2002) Non-invasive evaluation of activity in inflammatory bowel disease by power Doppler sonography. Z Gastroenterol 40:171–175

Hollerbach S, Geissler A, Schiegl H et al (1998) The accuracy of abdominal ultrasound in the assessment of bowel disorders. Scand J Gastroenterol 33:1201–1208

Kalantzis N, Rouvella P, Tarazis S et al (2002) Doppler US of superior mesenteric artery in the assessment of ulcerative colitis. A prospective study. Hepatogastroenterology 49:168–171

Limberg B (1989) Diagnosis of acute ulcerative colitis and colonic Crohn's disease by colonic sonography. J Clin Ultrasound 17:25–31

Limberg B, Osswald B (1994) Diagnosis and differential diagnosis of ulcerative colitis and Crohn's disease by hydrocolonic sonography. Am J Gastroenterol 89:1051–1057

Ludwig D, Wiener S, Bruning A et al (1999) Mesenteric blood flow is related to disease activity and risk of relapse in ulcerative colitis: a prospective follow up study. Gut 45:546–552

Maconi G, Imbesi V, Porro GB (1996) Doppler ultrasound measurement of intestinal blood flow in inflammatory bowel disease. Scand J Gastroenterol 31:590–593

Maconi G, Ardizzone S, Parente F, Porro GB (1999) Ultrasonography in the evaluation of extension, activity, and follow-up of ulcerative colitis. Scand J Gastroenterol 34:1103–1107

Maconi G, Sampietro GM, Ardizzone S et al (2004) US detection of toxic megacolon in inflammatory bowel diseases. Dig Dis Sci 49:138–142

Mayer D, Reinshagen M, Mason RA et al (2000) Sonographic measurement of thickened bowel wall segments as a quantitative parameter for activity in inflammatory bowel disease. Z Gastroenterol 38:295–300

Mirk P, Palazzoni G, Gimondo P (1999) Doppler sonography of hemodynamic changes of the inferior mesenteric artery in inflammatory bowel disease: preliminary data. AJR Am J Roentgenol 173:381–387

Parente F, Greco S, Molteni M et al (2003) Role of early ultrasound in detecting inflammatory intestinal disorders and identifying their anatomical location within the bowel. Aliment Pharmacol Ther 18:1009–1016

Parente F, Molteni M, Marino B et al (2010) Are colonoscopy and bowel ultrasound useful for assessing response to short-term therapy and predicting disease outcome of moderate-to-severe forms of ulcerative colitis? A prospective study. Am J Gastroenterol 105:1150–1157

Pascu M, Roznowski AB, Muller HP, Adler A, Wiedenmann B, Dignass AU (2004) Clinical relevance of transabdominal ultrasonography and magnetic resonance imaging in patients with inflammatory bowel disease of the terminal ileum and large bowel. Inflamm Bowel Dis 10:373–382

Pera A, Cammarota T, Comino E et al (1988) Ultrasonography in the detection of Crohn's disease and in the differential diagnosis of inflammatory bowel disease. Digestion 41:180–184

Ruess L, Blask AR, Bulas DI (2000) Inflammatory bowel disease in children and young adults: correlation of sonographic and clinical parameters during treatment. AJR Am J Roentgenol 175:79–84

Schwerk WB, Beckh K, Raith M (1992) A prospective evaluation of high resolution sonography in the diagnosis of inflammatory bowel disease. Eur J Gastroenterol Hepatol 4:173–182

Sigirci A, Baysal T, Kutlu R, Aladag M, Sarac K, Harputluoglu H (2001) Doppler sonography of the inferior and superior mesenteric arteries in ulcerative colitis. J Clin Ultrasound 29:130–139

Sonnenberg A, Erckenbrecht J, Peter P, Niederau C (1982) Detection of Crohn's disease by ultrasound. Gastroenterology 83:430–434

Valette PJ, Rioux M, Pilleul F, Saurin JC, Fouque P, Henry L (2001) Ultrasonography of chronic inflammatory bowel diseases. Eur Radiol 11:1859–1866

Worlicek H, Lutz H, Heyder N, Matek W (1987) Ultrasound findings in Crohn's disease and ulcerative colitis: a prospective study. J Clin Ultrasound 15:153–163

Yoshida A, Kobayashi K, Ueno F et al (2011) Possible role of early transabdominal ultrasound in patients undergoing cytapheresis for active ulcerative colitis. Intern Med 50:11–15

Coeliac Disease

Mirella Fraquelli

Contents

M. Fraquelli (✉)
Seconda Divisione Gastroenterologia,
IRCCS Fondazione Cà Granda Ospedale Maggiore,
Policlinico di Milano, Università degli Studi di Milano,
Pad. Granelli. Piano 3 Via F Sforza 35, 20122 Milano, Italy
e-mail: mfraquelli@yahoo.it

Abstract

Celiac disease is a common immune-mediated enteropathy that occurs in genetically predisposed individuals following the ingestion of gluten, a protein found in foods processed from wheat and related grain species. In this chapter an overview is provided regarding the most frequent ultrasonographic findings observed in association with the disease.

1 Introduction

Celiac disease (CD) is an autoimmune chronic enteropathy triggered by the ingestion of gluten that is a protein contained in grains such as wheat, rye and barley. It occurs in susceptible individuals and it is the result of the interplay between environmental and genetic factors (Lionetti and Catassi 2010).

Its prevalence is now known to be far greater than previously reported, with an increasing number of silent cases being diagnosed. According to some population-based studies of Caucasians using serological screening, such a number ranges from 0.2 to about 1 %.

Furthermore, some recent epidemiological studies performed in the developing world show prevalence rates overlapping European figures, especially in North Africa (i.e., 0.53 % in Egypt, 0.79 % in Libya, and 0.6 % in Tunisia), Middle East (i.e., 0.88 % in Iran and 0.6 % in Turkey) and India (i.e., 0.7 %) (Lionetti and Catassi 2010). The incidence pattern of the disease is also changing, and a larger number of cases are now diagnosed during adulthood (Farrell and Kelly 2002; Rewers 2005; Freeman et al. 2011; Armstrong et al. 2012).

The clinical spectrum is wide, including cases with typical intestinal or atypical extra-intestinal features, and silent forms. Absorption is impaired to a varying degree; and patients can experience gastrointestinal symptoms and malabsorption leading to the development of diarrhoea,

G. Maconi and G. Bianchi Porro (eds.), *Ultrasound of the Gastrointestinal Tract*, Medical Radiology. Diagnostic Imaging,
DOI: 10.1007/174_2012_660,
Published Online: 21 July 2012

anaemia, osteoporosis or other complications. However, the clinical picture is extremely variable, as it can range from pauci-symptomatic to severe forms.

The diagnosis is supported by the determination of serological markers and confirmed by consistent histological duodenal findings (Rostom et al. 2005).

Serological markers of significance include anti-endomysial (EMA) and anti-transglutaminase (tTG) antibodies. The sensitivity of tTG is 98 % and its specificity 96 %, whereas the EMA is 100 % specific and its sensitivity is greater than 90 %. The overt disease is pathologically characterised by a flattened small intestine mucosa, with lymphocytic infiltrate, crypt hyperplasia and villous atrophy (Farrell and Kelly 2002).

Untreated CD is associated with significant morbidity and increased mortality, largely related to the development of enteropathy-associated T cell lymphomas (EATL). Other less common complications include: refractory sprue, carcinomas of the oropharynx, oesophagus and small bowel and ulcerative jejunoileitis and its collagenous variant (Logan et al. 1989; Holmes et al. 1976; Catassi et al. 2005).

Patients with gastrointestinal symptoms normally first undergo abdominal ultrasonography (US), the accuracy of which has been markedly improved by the widespread availability of high-resolution transducers. A number of US signs have proved to be valuable in supporting or ruling out a diagnosis of CD. In addition, several US studies have reported impaired gallbladder and gastric motility in association with GI hormone abnormalities in patients with untreated CD.

2 Abdominal Ultrasound in the Diagnosis of Coeliac Disease

In the past barium examination of the small bowel demonstrated a pattern of abnormal findings caused by the pathophysiological changes induced by malabsorption, which suggested the possible presence of coeliac disease or other diseases characterised by malabsorption. Although not specific, such a pattern prompted further patient evaluation. Nowadays, the number of barium examinations performed and the skills required to interpret their results are both in decline. Abdominal bowel US is a technique that has improved a lot in the last decades as it is cheap, rapid, non invasive and easily repeatable. Its accuracy has recently markedly improved thanks to the widespread availability of high-resolution equipment.

Different US signs have been reported in association with CD in both paediatric and adult populations (Peck et al. 1997; Riccabona and Rossipal 1993; Rettenbacher et al. 1999; Fraquelli et al. 2004).

In a case series of 39 children with overt malabsorption and a definite histology-based CD diagnosis (Table 1), Riccabona and Rossipal (1993) found that 36 children (92 %) had an "abnormal-looking" small intestine, 32 (82 %) showed increased peristalsis and 30 (76 %) the presence of free abdominal fluid. Interestingly, half of the cases also presented pericardial effusion. On the basis of such findings, the authors concluded that, although intestinal biopsy remains the reference standard for diagnosing CD, an awareness of CD-associated US abnormalities can accelerate the diagnostic work-up and allow for the earlier introduction of a gluten-free diet (GFD).

In a case–control study of 11 adults with histologically proven CD and 20 healthy subjects (Table 2) Rettenbacher et al. (1999) found that the controls were negative whereas the cases showed: an increase of intraluminal fluid content, the presence of moderate small bowel dilatation, increased peristalsis and moderate bowel wall thickness. Further extra-intestinal signs, such as the mesenteric lymph node enlargement, free abdominal fluid, a dilated superior mesenteric artery or portal vein and hepatic steatosis were also identified with overall frequencies of 52–84 %.

A prospective study on an adult population by Fraquelli et al. (2004) evaluated the diagnostic accuracy of several US signs in predicting CD in a cohort of 162 patients consecutively examined, who presented with chronic diarrhoea or iron-deficiency anaemia or dyspepsia. These conditions are all frequent manifestations of CD. This population had a pretest CD probability of about 10 %, as estimated from a previous series (Hin et al. 1999). All the patients underwent anti-endomysial IgA antibody determination and a duodenal biopsy. Two operators, blind to the clinical, serological and histological findings, evaluated the presence of six US signs: the increased transverse diameter of small bowel loops contained increased fluid (Fig. 1a, b), the increased small bowel wall thickness (Fig. 1c) with hypertrophic valvulae conniventes (Fig. 1d, e), the pattern of peristalsis, the presence of free abdominal fluid within the abdominal cavity (Fig. 2a, b), the presence of enlarged mesenteric lymph nodes (Fig. 3) and the presence of enlarged fasting gallbladder volume (Fig. 4).

A total of 12 patients (7 %) were diagnosed as having CD on the basis of EMA positivity and histological duodenal findings consistent with Marsh grade III (11 cases) or IV (1 case). Out of the 150 EMA-negative cases, all having normal duodenal histology, 72 (48 %) were eventually diagnosed as having functional disease, and 78 (52 %) as having organic disease, including nine showing ileal involvement (six with Crohn's disease and three with the final diagnosis of giardiasis and common variable immunodeficiency, primary lymphangiectasia, and ileal carcinoid). Interestingly, the US pattern in the patients with ileal

Table 1 US findings in a series of 39 paediatric patients with histologically proven CD (from Riccabona and Rossipal 1993)

Ultrasonographic findings	Patients witha positive sign (#)
Abnormal aspect of the small intestine	36
Increased peristalsis	32
Abdominal fluid	30
Pericardial effusion	18

Table 2 US findings in a series of 11 adult patients with histologically proven CD (from Rettenbacher et al. 1999)

Ultrasonographic findings	Patients with a positive sign (#)
Moderate small bowel dilatation	8
Increased intraluminal fluid content	11
Small bowel wall thickness	7
Increased peristalsis	8
Mesenteric lymph node hypertrophy	9
Free abdominal fluid	5
Dilated superior mesenteric artery or portal vein	7
Hepatic steatosis	6

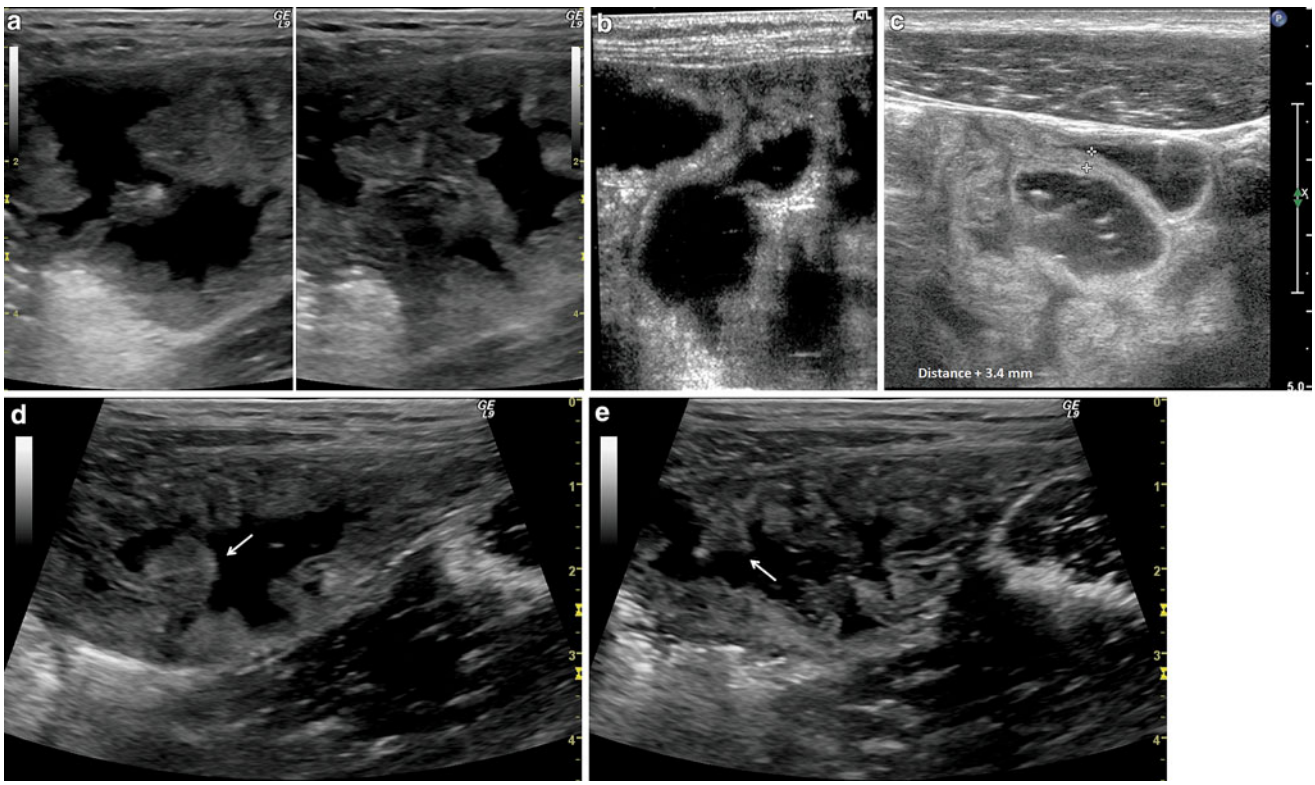

Fig. 1 **a, b** Dilated small bowel loops with anechoic liquid content in coeliac disease. **c** US image showing small bowel loops with increased small bowel wall thickness. **d, e** Dilated small bowel loops with hypertrophic valvulae conniventes (*arrows*) in coeliac disease

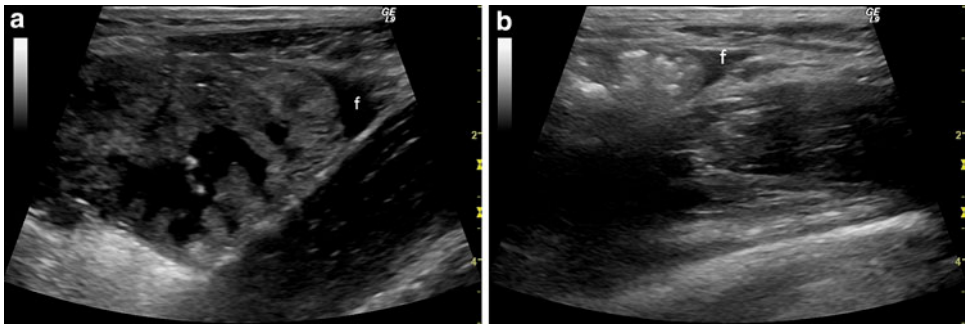

Fig. 2 **a, b** US images showing a small amount of anechoic free fluid (*f*) within the abdominal cavity in coeliac disease

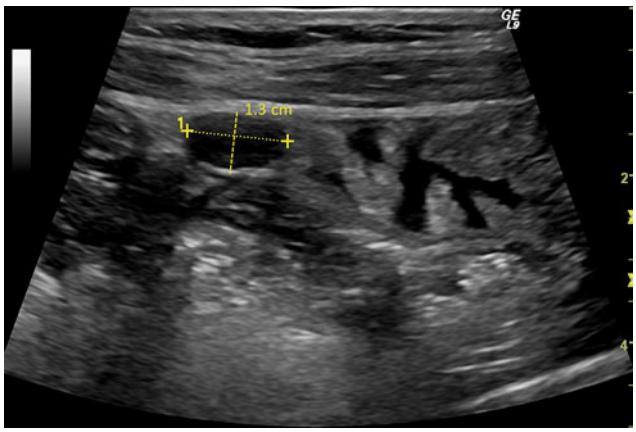

Fig. 3 Enlarged mesenteric lymph node in coeliac disease

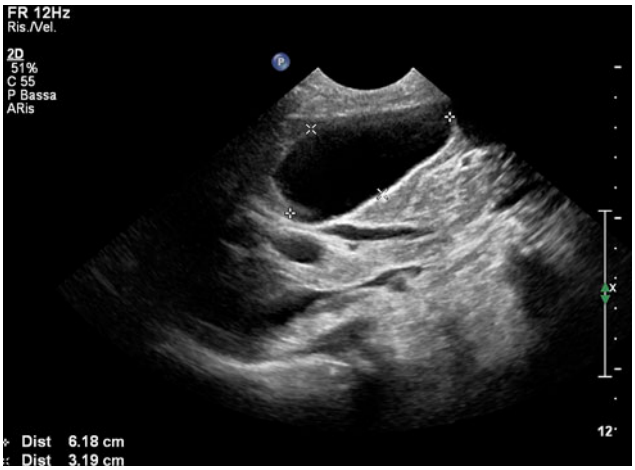

Fig. 4 Enlarged gallbladder in coeliac disease

Crohn's disease, showing a localised and marked bowel wall thickening, was completely different from that observed in CD patients. The details concerning the diagnostic accuracy of the six US signs are shown in Table 3.

Furthermore, the positive likelihood ratios (LR+) of >10 observed for increased gallbladder volume, free abdominal fluid and enlarged mesenteric lymph nodes allowed for a confirmatory strategy, whereas the negative likelihood ratios (LR−) of 0.1 observed for dilated small bowel loops and increased peristalsis supported an exclusion strategy (Sackett and Haynes 2002).

The *k* values (i.e. the statistical measure of inter-rate agreement between US sing and duodenal histologic findings) ranged from 0.76 for increased peristalsis to 0.95 for dilated small bowel loops, and were consistent with the good interobserver agreement in evaluating the US signs. It is interesting to note that a strict GFD led to EMA negativity and the complete reversal of the US abnormalities after 1 year.

Overall, increased gallbladder volume, abdominal free fluid and mesenteric lymph node enlargement reliably and accurately predict CD, whereas the lack of intestinal dilatation and increased peristalsis makes it possible to rule out the diagnosis. The specificity of US was 99 % in the presence of all six signs, with an obvious decrease in sensitivity (33 %). Moreover, an LR+ value of 50 allowed for a confirmatory strategy and a PPV of 80 %. Conversely, in the presence of at least one US sign, sensitivity was 92 % with an LR− value of 0.10 and an NPV of 99 %, a diagnostic performance that was comparable to that of dilated small bowel loops.

The above findings support the role of US in predicting CD; however, its role in a diagnostic algorithm should be varied on the basis of the probability of the disease in a given population.

A 2007 retrospective study focused on 250 adult patients with suspected or proved CD: among them 59 had histologically proven CD. The US of the small intestine revealed irregular peristalsis of the small intestine in 79 % cases and intermittent invaginations in 30 %. The thickening, shortening and decrease in number of the jejunum folds (ileum like transformation) at US was observed in 90 % patients. An increase in the number of ileal folds (jejunum like transformation) was evident in 75 % patients. Mesenterial lymphadenopathy was observed in 95 % patients. (Bartusek et al. 2007).

In the case–control study by Castiglione et al. (2007), 50 CD patients and 50 dyspeptic subjects (control group) underwent abdominal US. The presence of fluid-distended small bowel loops with thickened *valvulae conniventes* and

Table 3 Sensitivity, specificity, positive and negative likelihood ratio (LR+ and LR−), and positive and negative predictive value (PPV and NPV) of six US signs in predicting CD

US parameters	Sensitivity %	Specificity %	LR+	LR−	PPV %	NPV %
Increased GB volume Increased gallbladder volume (reference value: ≤20 mL)	73 (46–99)	96 (92–99)	17.0 (7.3–41.0)	0.28 (0.1–0.7)	57 (31–83)	98 (95–100)
Dilated small bowel loops + increased fluid content (reference value: ≤2.5 cm)	92 (76–100)	77 (70–84)	4.0 (2.8–5.5)	0.10 (0.1–0.7)	24 (11–36)	99 (97–100)
Thickened small bowel wall (reference value: ≤3 mm)	75 (50–99)	91 (86–95)	8.0 (4.4–14.5)	0.27 (0.1–0.7)	39 (19–59)	98 (95–100)
Increased peristalsis	83 (62–100)	87 (82–92)	6.6 (4.0–10.7)	0.10 (0.05–0.7)	34 (17–51)	98 (96–100)
Free abdominal fluid	50 (22–78)	96 (93–99)	12.5 (4.7–33)	0.52 (0.3–0.9)	50 (22–78)	96 (92–99)
Enlarged mesenteric lymph nodes (reference value: ≤5 mm)	42 (14–69)	97 (95–99)	15.6 (6.8–50.6)	0.59 (0.4–0.9)	55 (23–88)	95 (92–99)

The corresponding 95 % confidence intervals are given in parentheses

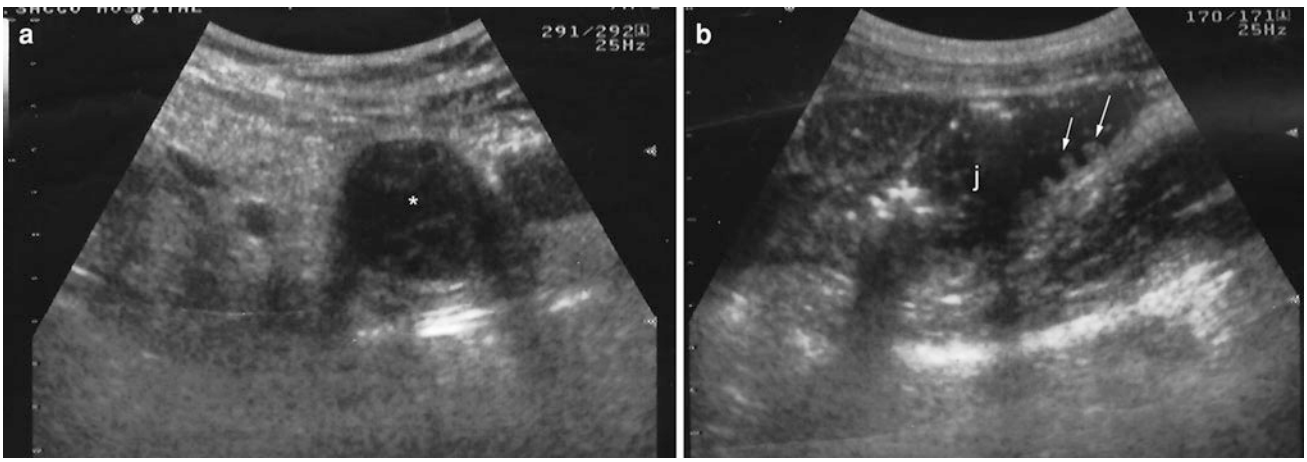

Fig. 5 61-year-old man with 4–5 month history of diarrhoea, fatigue, and weight loss showing at ultrasound **a** cavitation of mesenteric lymph nodes (*asterisk*) and **b** dilated jejunal loops (*j*) with liquid and gaseous content and hypertrophic valvulae conniventes (*arrows*). Small bowel endoscopy and jejunal biopsies revealed a malabsorption pattern and a clinical diagnosis of coeliac diasease was made

increased peristalsis was considered a US sign of coeliac disease. All clinical, biochemical and all US signs were assessed at the diagnosis and re-evaluated after 1 year of gluten-free diet: signs were present in 66 % of CD patients. Sensitivity, specificity, positive and negative predictive values resulted: 66, 96, 94 and 74 %, respectively. Abnormal US findings were recorded in 82 % of the patients with endoscopical markers of CD, in 87.5 % of the symptomatic patients, and in 61 % of the patients without symptoms. After 1 year of gluten-free diet US was still abnormal in 20 % patients, with no correlation with laboratory tests e/o symptoms.

A very recent study on a paediatric population aimed at assessing the usefulness of abdominal US for the diagnostic work up of those cases suspected of having CD involving negative serum antibodies and difficult cases. A diagnosis of CD with negative serum antibodies was probable in 71 patients who underwent US and duodenal biopsy for histologic examination. Intestinal histology and subsequent clinical and histologic follow-up confirmed the diagnosis in 11 patients and excluded it in 59. Abdominal US showed that the presence of dilated bowel loops and thickened bowel wall had a sensitivity of 83 % and a negative predictive value of 93 % in CD diagnosis. The concomitant presence of the two signs increased the sensitivity to 92 % and the NPV to 98 % (Soresi et al. 2011), once again confirming that the absence of dilated bowel loops is the indicator with the highest probability of excluding the diagnosis of CD.

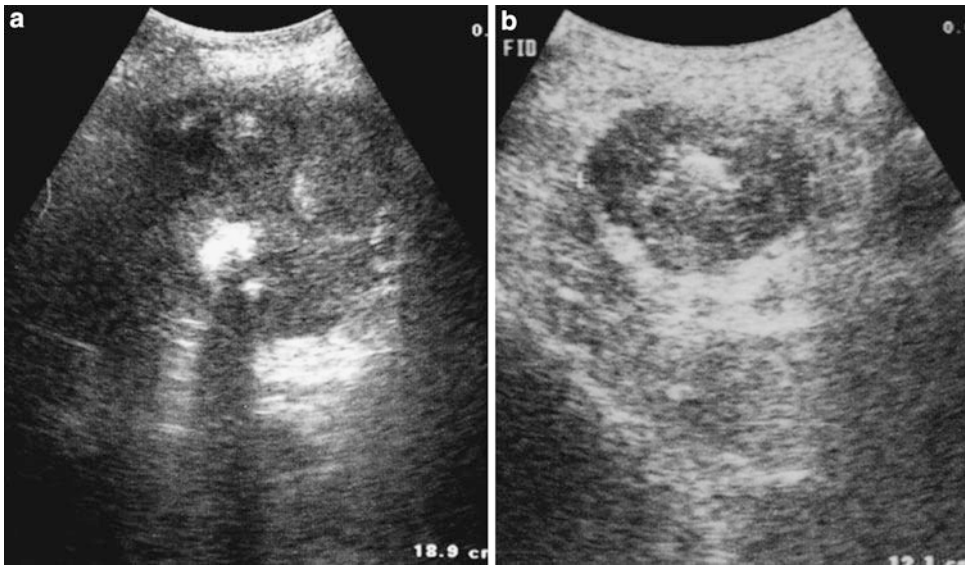

Fig. 6 **a, b** US images showing a target lesion in the small bowel due to the presence of a T cell non-Hodgkin lymphoma (EATL-NHL)

The combination of small intestine US and an anechoic contrast agent (SICUS) have been assessed in a case–control study which involved 33 patients with histologically proven CD and 30 healthy volunteers matched for sex and age. Loop diameter, Kerckring's folds number, peristaltic waves, and Doppler resistance index [RI; i.e. (peak systolic velocity—end diastolic velocity)/peak systolic velocity] appeared to be significantly different between CD patients and controls. In addition, liquid content, ileal jejunalization and mesenteric lymphoadenomegaly were only present in CD patients (52, 48 and 96 %, respectively), but in none of the controls. Only the Doppler RI values significantly correlated with the histologic degree of damage (Dell'Aquila et al. 2005).

2.1 Rare Manifestations of Coeliac Disease

Other less common manifestations of CD that can be discovered with abdominal US examination are the presence of mesenteric lymph node cavitation and the presence of transient small bowel intussusceptions (Hec et al. 2012).

The cavitation of mesenteric lymph nodes is a rare complication of CD but its pathogenesis remains to be clarified (Fig. 5). It has been described as being revealed by US or computed tomography in a few cases, and was sometimes associated with hyposplenism (Burrell et al. 1994; Bahlouli et al. 1998; Bardella et al. 1999; Reddy et al. 2002; McBride et al. 2010).

Transient small bowel intussusception is a rare event that has been described in case reports of both paediatric and adult patients: in some it was demonstrated by US (Cohen and Lintott 1978; Gonzalez et al. 1998; Mushraq et al. 1999; Maconi et al. 2007).

3 Splanchnic Circulation in Coeliac Disease

Basal and post-prandial splanchnic blood flow (i.e. in the superior mesenteric artery and portal vein) has been evaluated in CD patients by means of Doppler-US. Under fasting conditions, increased superior mesenteric artery velocity and flow with a lower RI, and greater portal vein velocity and flow, have been uniformly observed in comparison with controls (Arienti et al. 1996; Aliotta et al. 1997; Giovagnorio et al. 1998; Magalotti et al. 2003). Furthermore, in the post-prandial phase all of these parameters vary interestingly significantly less than in healthy subjects.

Once again, the use of a long-term GFD reverses all these abnormalities.

4 Role of Ultrasonography in Diagnosing the Complications of Coeliac Disease (Intestinal Lymphoma and Small Bowel Adenocarcinoma)

Enteropathy-associated T cell non-Hodgkin lymphoma (EATL-NHL), the annual incidence of which is 0.5–1 per million people, is confined to patients with previously or concomitantly diagnosed CD and also complicates the refractory form of the enteropathy. An increased risk of small bowel adenocarcinoma (an exceedingly rare malignancy with an annual incidence of 0.6–0.7 per 100,000 individuals in a general population) has also been reported (Swinson et al. 1983).

Table 4 Main data from studies evaluating gallbladder motility in CD patients

Study	Pts (#)	Technique	Type of stimulus	Post-prandial GB motility
Low-Beer et al. (1975)	18	Scintigraphy	CCK analogue	↓
Brown et al. (1987)	8	Scintigraphy	CCK analogue	↓
Fraquelli et al. (1999)	10	US	Liquid	↓
Maton et al. (1985)	8	US	Liquid	↓
Delamarre et al. (1984)	4	US	Solid	↓
Benini et al. (2011)	19	US	Solid	↓

The typical US pattern is similar in the presence of both these neoplasms, with evidence of the so called "bull's eye", "target" or "pseudo-kidney" signs related to the eccentric and localised bowel wall thickening (Fig. 6).

Under the above conditions, US is useful in locating and staging the disease and also allows for the detailed characterisation of adjacent and distant lymph nodes and, when indicated, their sampling for histological purposes. However, US should not generally be considered the reference technique for diagnosing an intestinal lymphoma superimposed on CD because of its poor sensitivity, even when performed by well-trained operators. It should therefore be considered ancillary to endoscopy and others more sensitive imaging techniques in identifying and staging EATL in CD patients.

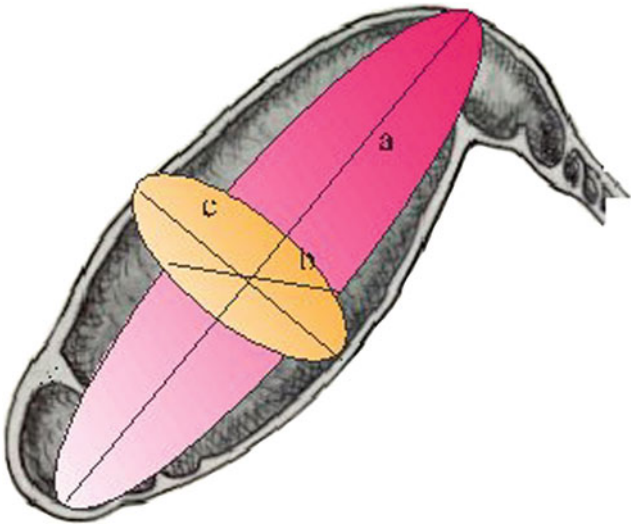

Fig. 7 Schematic drawing of the gallbladder (GB). The *dotted lines* represent the longitudinal, transversal and antero-posterior GB diameters which are used to calculate GB volume using the ellipsoid formula

5 Gallbladder Motility and Gastric Emptying in Coeliac Disease: Ultrasonographic Studies

Impaired gallbladder (GB), stomach and small bowel motility have been reported in patients with untreated CD, and attributed to the impaired secretion of enteric hormones or decreased sensitivity to them (Brown et al. 1987; Bardella et al. 2000; Fraquelli et al. 1999; Tursi 2004).

As shown in Table 4, a number of studies of untreated CD patients have reported a reduction in absolute and net GB emptying in response to various stimuli: this could be mainly attributed to reduced cholecystokinin (CCK) secretion by the specialised cells located in the upper tract of the duodenum (Low-beer et al. 1975; Delamarre et al. 1984; Maton et al. 1985; Masclee et al. 1991; Brown et al. 1987; Fraquelli et al. 1999).

Some authors have reported about decreased post-prandial CCK levels in untreated CD patients despite a concomitant increase in the number of CCK-secreting duodenal cells, which are not adequately stimulated to release the hormone because of the impaired lipolysis of exogenous fat (Low-beer et al. 1975; Maton et al. 1985; Masclee et al. 1991; Hopman et al. 1995; Fraquelli et al. 2003). The resulting gallbladder inertia also contributes to impairing small bowel transit time and the enterohepatic circulation of bile salts.

In addition, the somatostatin (SS) secretion is also altered in CD patients at diagnosis, and fasting SS levels are significantly higher than in controls. This could be due to an increased number of SS-secreting cells accounting for the increased basal GB volume: a correlation between SS levels and gallbladder size under fasting conditions has been clearly confirmed in patients with somatostatinomas and those treated with SS or SS analogues.

Gallbladder ultrasonography is reliable to estimate GB volume in fasting state and in response to test meal or exogenous stimulus. Figure 7 shows a simple and reliable method, the ellipsoid one (Dodds et al. 1985), to determine GB volume by measuring the longitudinal (a), transversal (b) and antero-posterior (c) GB diameters, applying the formula: $1/6\ \pi\ (a \times b \times c)$.

Untreated CD patients also show increased serum levels of neurotensin (NT): the physiological post-prandial increase of this hormone is a reliable index of nutrient delivery to the ileum. NT may impair GB motility both directly and indirectly by delaying gastric emptying. Interestingly, the abnormalities in GI hormone release and their effects on gallbladder, gastric and small bowel motility completely revert after successful treatment with a GFD.

Various scintigraphic and US studies have assessed gastric emptying in patients with untreated CD, and the results of most of them are consistent with a marked delay in gastric emptying that normalised after gluten withdrawal (Benini et al. 2001; Bardella et al. 2000).

A very recent study has assessed in 19 untreated CD patients and in 14 during GFD both the mouth-to-cecum transit time using breath test and GB motility using US after a solid meal. Their results have then been compared with those of 20 healthy volunteers. The mouth-to-cecum transit time was prolonged in celiacs as compared to controls and GB fasting volume and GB emptying were both significantly reduced. During GFD, GB emptying reverted to normal whereas the intestinal transit time remained abnormal and more prolonged in CD patients (Benini et al. 2011).

References

Aliotta A, Pompili M, Rapaccini GL et al (1997) Doppler ultrasonographic evaluation of blood flow in the superior mesenteric artery in celiac patients and in healthy controls in fasting conditions and after saccharose. J Ultrasound Med 16:85–91

Arienti V, Califano C, Brusco G et al (1996) Doppler ultrasonographic evaluation of splanchnic blood flow in coeliac disease. Gut 39:369–373

Armstrong MJ, Hegade VS, Robins G (2012) Advances in celiac disease. Curr Opin Gastroenterol 28:104–112

Bahlouli F, Seror O, Mathieu E et al (1998) Mesenteric lymph node cavitation disclosing celiac disease in adults. J Radiol 79:431–433

Bardella MT, Trovato C, Quatrini M, Conte D (1999) Mesenteric lymph node cavitation: a rare hallmark of celiac disease. Scand J Gastroenterol 34:1257–1259

Bardella MT, Fraquelli M, Peracchi M et al (2000) Gastric emptying and plasma neurotensin levels in untreated celiac patients. Scand J Gastroenterol 35:269–273

Bartusek D, Valek V, Husty J, Uteseny J (2007) Small bowel ultrasound in patients with celiac disease. Retrospective study. Eur J Radiol 63:302–306

Benini L, Sembenini C, Salandini L et al (2001) Gastric emptying of realistic meals with and without gluten in patients with coeliac disease. Effect of jejunal mucosal recovery. Scand J Gastroenterol 36:1044–1048

Benini F, Morea A, Turini D et al (2011) Slow gallbladder emptying reverts to normal but small intestine transit of a physiological meal remains slow in celiac patients during gluten-free diet. Neurogastroenterol Motil 20 (in press)

Brown AM, Bradshaw MJ, Richardson R et al (1987) Pathogenesis of the impaired gall bladder contraction of coeliac disease. Gut 28:1426–1432

Burrell HC, Trescoli C, Chow K, Ward MJ (1994) Case report: mesenteric lymph node cavitation, an unusual complication of coeliac disease. Br J Radiol 67:1139–1140

Castiglione F, Rispo A, Cozzolino A et al (2007) Bowel sonography in adult celiac disease:diagnostic accuracy and ultrasonographic features. Abdom Imaging 32:73–77

Catassi C, Bearzi I, Holmes GK (2005) Association of celiac disease and intestinal lymphomas and other cancers. Gastroenterology 128:S79–S86

Cohen MD, Lintott DJ (1978) Transient small bowel intussusception in adult coeliac disease. Clin Radiol 29:529–534

Delamarre J, Capron JP, Joly JP et al (1984) Gallbladder inertia in celiac disease: ultrasonographic demonstration. Dig Dis Sci 29:876–877

Dell'Aquila P, Petrini L, Barone M et al (2005) Small intestine contrast ultrasonography-based scoring system: a promising approach for the diagnosis and follow-up of celiac disease. J Clin Gastroenterol 39:591–595

Dodds WJ, Groh WJ, Darweesh RMA et al (1985) Sonographic measurement of gallbladder volume. Am J Roentgenol 145:1009–1011

Farrell LJ, Kelly CP (2002) Celiac sprue. N Engl J Med 346:180–188

Fraquelli M, Colli A, Colucci A et al (2004) Accuracy of ultrasonography in predicting celiac disease. Arch Intern Med 164:169–174

Fraquelli M, Bardella MT, Peracchi M et al (1999) Gallbladder emptying and somatostatin and cholecystokinin plasma levels in celiac disease. Am J Gastroenterol 94:1866–1870

Fraquelli M, Pagliarulo M, Colucci A et al (2003) Gallbladder motility in obesity, diabetes mellitus and coeliac disease. Digest Liver Dis 35:S12–S16

Freeman HJ, Chopra A, Clandinin MT et al (2011) Recent advances in celiac disease. World J Gastroenterol 17:2259–2272

Giovagnorio F, Picarelli A, Di Giovambattista F, Mastracchio A (1998) Evaluation with Doppler sonography of mesenteric blood flow in celiac disease. Am J Roentgenol 171:629–632

Gonzalez JA, Gonzalez JB, Crespo MJ, Sancho CI (1998) Acute gallbladder distension and recurrent small bowel intussusception in a child with celiac disease. J Pediatr Gastroenterol Nutr 27:444–445

Hec F, Vernier-Massouille G, Mariette C (2012) Recurrent small bowel intussusceptions in coeliac disease (in press)

Hin H, Bird G, Fisher P et al (1999) Coeliac disease in primary care: case finding study. BMJ 318:164–167

Holmes GK, Stokes PL, Sorahan TM et al (1976) Coeliac disease, gluten-free diet and malignancy. Gut 17:612–619

Hopman WP, Rosenbusch G, Hectors MP, Jansen JB (1995) Effect of pre-digested fat on intestinal stimulation of plasma cholecystokinin and gallbladder motility in coeliac disease. Gut 36:17–21

Lionetti E, Catassi C (2010) New clues in celiac disease epidemiology, pathogenesis, clinical manifestations, and treatment. Int Rev Immunol 30:219–231

Logan RF, Rifkind EA, Turner ID, Ferguson A (1989) Mortality in celiac disease. Gastroenterology 97:265–271

Low-Beer TS, Harvey RF, Davies ER, Read AF (1975) Abnormalities of serum cholecystokinin and gallbladder emptying in celiac disease. N Engl J Med 292:961–963

Maconi G, Radice E, Greco S et al (2007) Transient small-bowel intussusceptions in adults: significance of ultrasonographic detection. Clin Radiol 62:792–797

Magalotti D, Volta U, Bonfiglioli A et al (2003) Splanchnic haemodynamics in patients with coeliac disease: effects of a gluten-free diet. Digest Liver Dis 35:262–268

Masclee AA, Jansen JB, Driessen WM et al (1991) Gallbladder sensitivity to cholecystokinin in coeliac disease. Correlation of gallbladder contraction with plasma cholecystokinin-like

immunoreactivity during infusion of cerulein. Scand J Gastroenterol 26:1279–1284
Maton PN, Selden AC, Fitzpatrick ML, Chadwick VS (1985) Defective gallbladder emptying and cholecystokinin release in celiac disease. Reversal by gluten-free diet. Gastroenterology 88:391–396
McBride OM, Skipworth RJ, Leitch D, Yalamarthi S (2010) Cavitating mesenteric lymph node syndrome in association with coeliac disease and enteropathy associated T-cell lymphoma: a case report and review of the literature. Case Report Med 2010:478269
Mushraq N, Marven S, Walker J et al (1999) Small bowel intussusception in celiac disease. J Pediatr Surg 3:1833–1835
Peck RJ, Jackson A, Gleeson D (1997) Case report: ultrasound of coeliac disease with demonstration of response to treatment. Clin Radiol 52:244–245
Reddy D, Salomon C, Demos TC (2002) Mesenteric lymph node cavitation in celiac disease. Am J Roentgenol 178:247
Rettenbacher T, Hollerweger A, Macheiner P et al (1999) Adult celiac disease: US signs. Radiology 211:389–394
Rewers M (2005) Epidemiology of celiac disease: what are the prevalence, incidence, and progression of celiac disease? Gastroenterology 128:S47–S51
Riccabona M, Rossipal E (1993) Sonographic findings in celiac disease. J Pediatr Gastroenterol Nutr 17:198–200
Rostom A, Dube C, Cranney A et al (2005) The diagnostic accuracy of serologic tests for celiac disease: a systematic review. Gastroenterology 128:S38–S46
Sackett DL, Haynes RB (2002) The architecture of diagnostic research. BMJ 324:539–541
Swinson CM, Slavin G, Coles EC, Booth CC (1983) Coeliac disease and malignancy. Lancet 8316:111–115
Soresi M, Pirrone G, Giannitrapani I et al (2011) A key role for abdominal ultrasound examination in "difficult" diagnoses of celiac disease. Ultraschall Med 32:S53–S61
Tursi A (2004) Gastrointestinal motility disturbances in celiac disease. J Clin Gastroenterol 38:642–645

Lymphangiectasia, Whipple's Disease, Eosinophilic Enteritis

Mirella Fraquelli

Contents

Abstract

Primary intestinal lymphangiectasia, Whipple's disease and eosinophilic enteritis are rare chronic conditions mainly involving the small bowel tract. In this chapter are presented the most frequent ultrasonographic findings observed in association with these diseases.

1 Primary Intestinal Lymphangiectasia

Primary intestinal lymphangiectasia (PIL) is a rare disorder characterized by a protein-losing gastroenteropathy leading to secondary hypoproteinemia due to lymphatic vessel obstruction and the loss of lymphatic fluid in the gastrointestinal tract. It is believed to be a congenital disorder, although the time of its clinical onset can widely vary. Etiology remains unknown even if very rare family cases have been reported.

Clinically, the most relevant symptoms are: bilateral lower limbs edema, diarrhea, and lymphocytopenia due to both lymphatic leakage and rupture. Edema may be moderate to severe with anasarca and includes pleural effusion, pericarditis, and chylous ascites. The finding by small bowel biopsy of numerous dilated lymphatic vessels consistent with diffuse or focal lymphangiectasia, definitely supports the diagnosis (Vignes and Nellanger 2008; Wen et al. 2010).

A strict dietary regimen including low fat diet associated with medium-chain triglycerides (MCT) supplementation is recommended: it is the cornerstone of PIL treatment. Increase in tissue fibrinolytic activity in the mucosa of intestinal lymphangiectasia has been reported. There are also some reports indicating that antiplasmin therapy can dramatically reduce protein loss by inhibiting lymphatic permeability. It has recently been observed that octreotide, which is somatostatin analog, may play a therapeutic role.

There are only a few published case reports concerning the ultrasonography (US) findings observed in association with primary intestinal lymphangiectasia. Although diagnosis still relies on intestinal histology, the US picture is fairly

M. Fraquelli (✉)
Seconda Divisione,
Gastroenterologia IRCCS Fondazione Cà
Granda Ospedale Maggiore Policlinico di Milano,
Università degli Studi di Milano,
Pad. Granelli. Piano 3, Via F Sforza 35,
20122 Milan, Italy
e-mail: mfraquelli@yahoo.it

G. Maconi and G. Bianchi Porro (eds.), *Ultrasound of the Gastrointestinal Tract*, Medical Radiology. Diagnostic Imaging,
DOI: 10.1007/174_2012_658, © Springer-Verlag Berlin Heidelberg 2012
Published Online: 14 July 2012

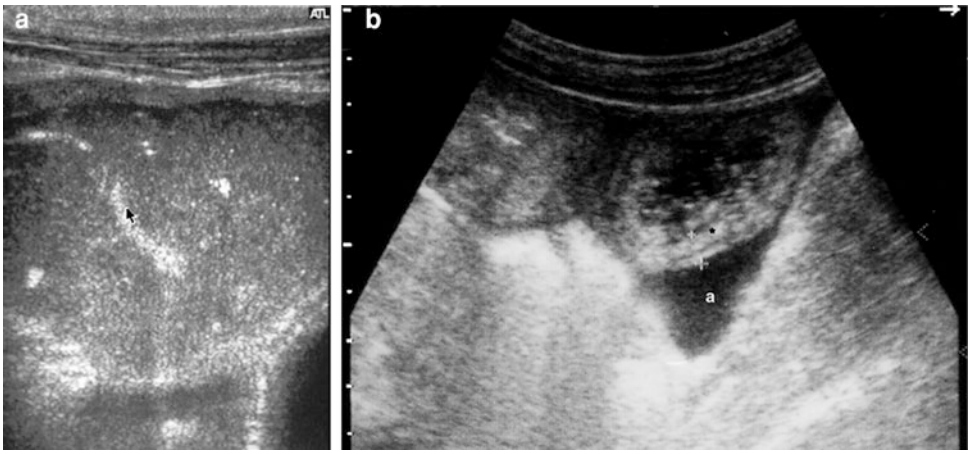

Fig. 1 **a** US images showing a dilated small bowel loop with increased mixed, mainly echogenic intraluminal fluid content and **b** diffuse bowel wall thickening with ascites **a**

indicative of the disease, especially in patients with protein-losing enteropathy. In the first study of three pediatric patients, Dorne and Jequier (1986) most frequently observed ascites, diffuse bowel wall thickening, mesenteric edema, dilated mesenteric lymphatic vessels, and thickening of the gallbladder and urine bladder wall.

In 1998, Maconi et al. described the case of a 20-year-old woman with histologically proven primary intestinal lymphangiectasia, presenting a protein-losing enteropathy and right leg lymphedema. The US findings showed the dilatation of the intestinal loops with regular and diffuse thickening of the bowel wall, plical hypertrophy, and considerable mesenteric edema. Similar findings were also reported by Loreti et al. (2003) in a 26-year-old woman presenting with protein-losing enteropathy, lymphedema, severe steatorrhea, and malabsorption.

Frequent US findings of primary intestinal lymphangiectasia are: a markedly dilated small intestinal loop with increased (mixed but mainly echogenic) fluid content (Fig. 1), and a small bowel tract with regular and diffuse bowel wall thickening and mesenteric edema (Fig. 2).

2 Whipple's Disease

Whipple's disease is a rare, multisystemic chronic infectious disease (approximate annual incidence less than 1 per 1,000,000 population) that preferentially affects middle-aged white men (Schneider et al. 2008).

Whipple's disease is a chronic disorder characterized by diarrhea, weight loss, arthralgias and cardiac, and neurological involvement. It is caused by a small gram-positive bacillus, *Tropheryma whippelii*, a low-virulence but highly infectious action bacterium. The onset can be very insidious and is characterized by gastrointestinal symptoms such as diarrhea, steatorrhea, and abdominal pain, associated with migratory large joint arthropathy, fever, and ophthalmological and neurological manifestations (Bai et al. 2004).

Whipple's disease most frequently occurs in middle-aged Caucasian men. Its diagnosis is suggested by the clinical findings, and confirmed by tissue sampling from the small intestine and/or other involved organs (lymph nodes, liver, central nervous system, etc.). The presence of PAS-positive (periodic acid Schiff stain) macrophages containing small bacilli, definitely supports the diagnosis. The treatment is based on a prolonged antibiotic course, with the first-choice regimen being the use of trymethoprim/sulphamethoxazole for 1 year, and the second choice chloramphenicol. PAS-positive bacilli can persist after successful treatment, and their presence outside macrophages is indicative of persistent infection. The recurrence of the disease, especially with dementia, carries an extremely poor prognosis and, in this case, the use of antibiotics crossing the blood–brain barrier can be very useful.

A number of reports on individual cases and a few case series have described the US abdominal findings, which can suggest the presence of the disease even if they are not very specific (Albano et al. 1984; Bruggemann et al. 1992; Carroccio et al. 1996; Castagnone et al. 1991). In particular, most of these studies have identified a moderately dilated and thickened small bowel wall, with the disappearance of normal bowel wall stratification and brilliant hyperechoic luminal contents mixed with a few hypoechogenic parts (Fig. 3), as well as an unusual, distinctive, and diffusely echogenic retroperitoneal lympadenopathy (Davis and Patel 1990), sometimes with concomitant free abdominal fluid or lymph node cavitation (Waziéres et al. 1993). It is interesting to note that the US abnormalities revert with an appropriate long-term antibiotic therapy.

3 Eosinophilic Gastroenteritis

Eosinophilic gastroenteritis is an uncommon condition of unknown etiology, although it is generally believed to be due to intestinal allergy and affects both children and adults.

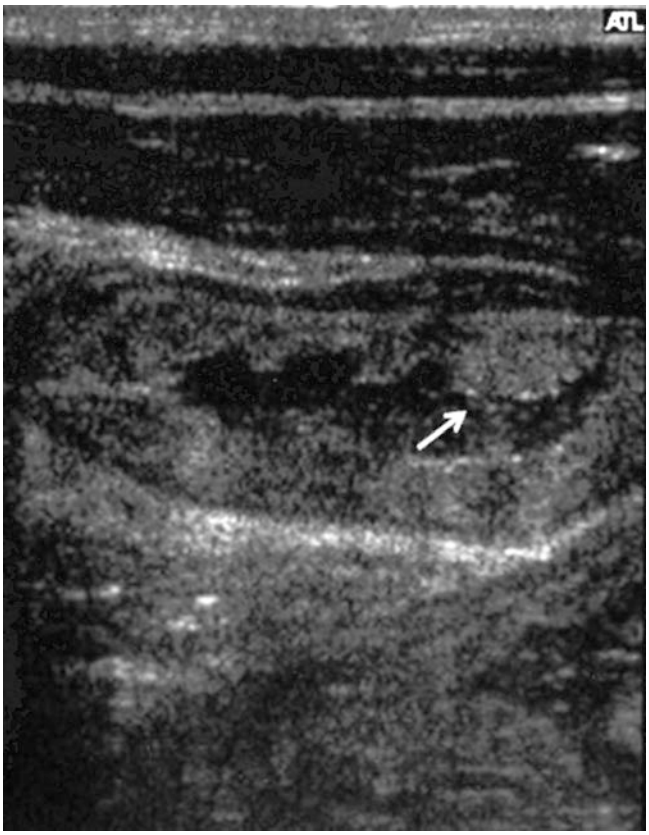

Fig. 2 US image showing a dilated small bowel loop with a thickened bowel wall with plical hypertrophy (*arrow*), and mesenteric edema

Its clinical manifestations can be very heterogeneous and the disease may mimic peptic ulcer, subacute (or chronic) intestinal obstruction, gastroenteritis, irritable bowel syndrome, or inflammatory bowel disease.

It is characterized by a selective eosinophilic infiltration of the stomach and/or small intestine. The eosinophil eotaxin and Th-2 cytokines are important in the pathogenesis of the disease. It may be confused with parasitic and bacterial infections, inflammatory bowel disease, hypereosinophil syndrome, myeloprolipherative disorders, periarteritis, vasculitis, scleroderma, drug hypersentitivity, or injury (Oh and Chetty 2008).

Primary eosinophilic gastroenteritis include multiple disease entities depending on the level of histological involvement, and may be mucosal, muscular, or serosal (Lee et al. 1993).

The *mucosal* form (i.e. the most common variant) is characterized by vomiting, abdominal pain, diarrhea, blood loss, iron deficiency anaemia, malabsorption, and protein-losing enteropathy. The *muscular* form is characterized by eosinophilic infiltration in the muscular layer leading to the thickening of the bowel wall which may cause bowel obstruction. The *serological* form occurs in only a minority of cases, and is characterized by exudative ascites and a higher peripheral eosinophil count than that associated with the other forms (Talley et al. 1990; Lee et al. 1993; Rothenberg 2004).

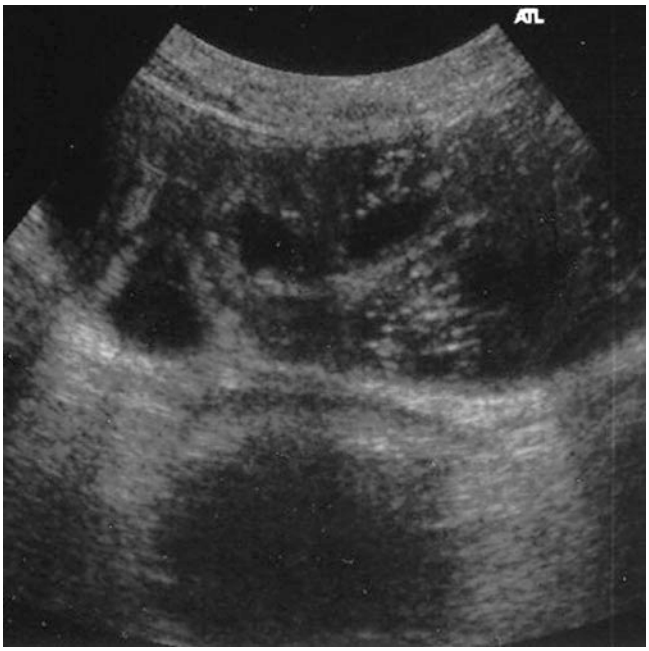

Fig. 3 US image showing dilated and thickened small bowel loops with the disappearance of normal bowel wall stratification and brilliant, hyperechoic luminal contents

Diagnosis is often difficult, and most cases are only diagnosed after a surgical procedure and histological sampling. The withdrawal of the types of food being supposedly involved by means of skin prick testing (or RASTs Radio-Allergo-Sorbent Test) has variable effects. The treatment of choice is the administration of anti-inflammatory drugs, such as systemic or topical steroids. In those severe cases, when the dietary restriction fails, intravenous feeding or immunosuppressive antimetabolite therapy (azathioprine or 6-mercaptopurine) should be considered (Talley et al. 1990).

The most frequently reported US finding is a moderate thickening of the part of the gastrointestinal wall running from the stomach to the terminal ileum. Normal bowel wall stratification is lost, and the wall is hyperechoic with hypertrophic *valvulae conniventes*; the contents of the lumen may be anechoic (completely liquid) (Fig. 4a) or slightly brilliant (in the case of a corpusculate content) (Fig. 4b) (Buljevac et al. 2005). Abundant ascitic fluid is sometimes present, and should be sampled since it may reveal a diagnostic increase in the proportion of eosinophilic cells.

A very recent report (Savino et al. 2011) highlighted the utility of sonography in pediatric patients who present with gastrointestinal symptoms, since this rapid, inexpensive and noninvasive technique may provide useful diagnostic information. In fact, the ultrasonographic detection of features such as bowel wall thickness, ascites, and peritoneal

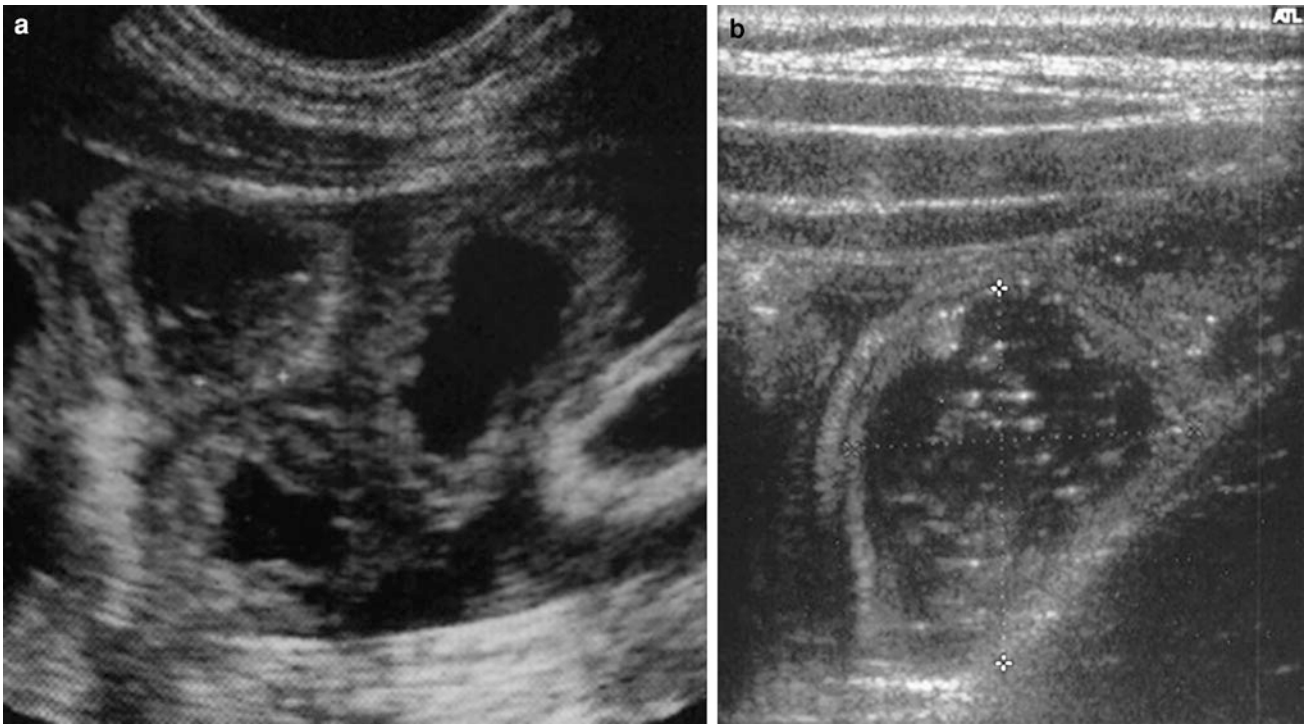

Fig. 4 **a** US images showing moderately dilated small bowel loops with a slightly thickened bowel wall and increased, prevalently anechoic intraluminal contents. **b** US images showing moderately dilated small bowel loops with a slightly thickened bowel wall and increased, slightly brilliant corpusculate content

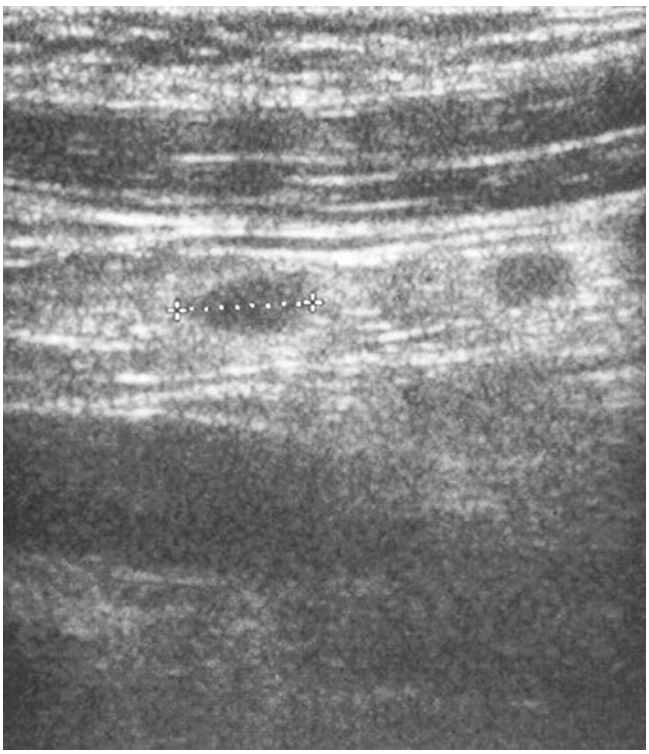

Fig. 5 US images showing some mesenteric lymph nodes slightly enlarged

nodules may be largely suggestive of eosinophilic gastroenteritis and may prevent other invasive exams and abdominal surgery.

In a case report, eosinophilic enteritis was diagnosed by US as presenting bowel intussusception in an adult (Shin et al. 2007). US can also be easily used in the follow-up of patients, and may obviate the frequent and potentially dangerous exposure to radiation.

The pancreas is sometimes swollen, and the mesenteric lymph nodes (Fig. 5) may be enlarged. Similar US findings have been reported also in a case of eosinophilic enteritis presenting as acute abdomen (Seelen et al. 1992).

Bulijevac et al. (2005) have recently published a case report about an 18-year-old patient with the serosal form of the disease. Basal US visualized nodular peritoneal deposits associated with ascites, the cytological sampling of which revealed the presence of numerous eosinophils. After 2 weeks of corticosterid treatment, the clinical, laboratory, and US findings normalized.

References

Albano O, Carrieri V, Vinciguerra V et al (1984) Ultrasonic findings in Whipple's disease. J Clin Ultrasound 12:286–288

Bai JC, Mazure RM, Vazquez H et al (2004) Whipple's disease. Clin Gastroenterol Hepatol 2:849–860

Bruggemann A, Burchardt H, Lepsien G (1992) Sonographical findings in Whipple's disease. A case report with regard to the literature. Surg Endosc 6:138–140

Buljevac M, Urek MC, Stoos-Veic T (2005) Sonography in the diagnosis and follow-up of serosal gastroenteritis treated with corticosteroid. J Clin Ultrasound 33:43–46

Carroccio A, Soresi M, Montalto G et al (1996) Whipple's disease: a non-invasive approach for suspected diagnosis. Case Rep Ital J Gastroenterol 28:229–231

Castagnone D, Mandelli C, Rivolta R et al (1991) Echography and computerized tomography of the abdomen in Whipple's disease. Radiol Med 82:540–542

Davis SJ, Patel A (1990) Distinctive echogenic lymphadenopathy in Whipple's disease. Clin Radiol 42:60–62

Dorne HL, Jequier S (1986) Sonography of intestinal lymphangiectasia. J Ultrasound Med 5:13–16

Lee CM, Changchien CS, Chen PC et al (1993) Eosinophilic gastroenteritis: 10 years experience. Am J Gastroenterol 88:70–74

Loreti L, Masselli G, Melisi MT et al (2003) Intestinal lymphangiectasia. Rays 28:409–416

Maconi G, Molteni P, Manzionna G et al (1998) Ultrasonographic features of long-standing primary intestinal lymphangiectasia. Eur J Ultrasound 7:195–198

Rothenberg ME (2004) Eosinophilic gastrointestinal disorders (EGID). J Allergy Clin Immunol 113:11–28

Oh HE, Chetty R (2008) Eosinophilic gastroenteritis: a review. J Gastroenterol 43:741–750

Savino A, Salvatore R, Cafarotti A (2011) Role of ultrasonography in the diagnosis and follow-up of pediatric eosinophilic gastroenteritis: a case report and review of the literature. Ultrashall Med 32:57–62

Schneider T, Moos V, Loddenkemper C, Marth T, Fenollar F, Raoult D (2008) Whipple's disease: new aspects of pathogenesis and treatment. Lancet Infect Dis 8:179–190

Seelen JL, You PH, de Vries AC, Puylaert JB (1992) Eosinophilic enteritis presenting as acute abdomen: US features of two cases. Gastointest Radiol 17:19–20

Shin WG, Park CH, Lee YS et al (2007) Eosinophilic enteritis presenting as intussusception in adult. Korean J Intern Med 22:13–7

Talley NJ, Shorter RG, Phillips SF, Zinsmeister AR (1990) Eosinophilic gastroenteritis: a clinicopathological study of patients with disease of the mucosa, muscle layer, and subserosal tissue. Gut 31:54–58

Vignes S, Nellanger J (2008) Primary intestinal lymphangiectasia (Waldmann's disease). Orphanet J Rare Dis 22(3):5

Waziéres De, Fest T, Litzler JF, Simon G, Rohmer P, Dupond JL (1993) Mesenteric lymph node cavitation in Whipple's disease. Apropos Case J Radiol 74:661–663

Wen J, Tang Q, Wu J, Wang Y, Cai W (2010) Primary intestinal lymphangiectasia: four case reports and a review of the literature. Dig Dis Sci 55:3466–7342

Cystic Fibrosis, Amyloidosis, Vasculitis and other Rare Disorders

Michela Monteleone, Francesco Esposito, Gabriella Carnevale, and Giovanni Maconi

Contents

Abstract

Intestinal ultrasonography has been proved as valid tool in inflammatory conditions of the gastrointestinal tract. However, little is known about the ultrasonographic features of rarer intestinal diseases, like cystic fibrosis, amyloidosis, vasculitis, HIV-related enteropathy. In these conditions, ultrasound may show changes of the intestinal wall, which together with clinical features, may speed up the diagnostic work up, and reduce the need of invasive and expensive procedures. Intestinal ultrasound may also be useful in the follow-up of these diseases.

1 Cystic Fibrosis

Cystic fibrosis (CF) (also known as mucoviscidosis) is an autosomal recessive genetic disorder that affects most critically the lungs, and also the pancreas, liver and intestine. It is characterised by abnormal epithelial transport of chloride and sodium that leads to thick and viscous secretions (Yankaskas et al. 2004). The disease, which is characterised by chronic pulmonary obstruction and infections, and by digestive disorders such as pancreatic insufficiency, is caused by mutations in a gene which encodes a protein called CFTR (cystic fibrosis transmembrane conductance regulator).

Prior to prenatal and newborn screening, cystic fibrosis was often diagnosed when a newborn infant failed to pass feces (meconium). Meconium may completely block the intestines, causing a mechanical obstruction of the ileum. This condition, called meconium ileus, occurs in 5–10 % of newborns with CF. In addition, protrusion of internal rectal membranes (rectal prolapse) is common, occurring in as many as 10 % of children with CF, and it is caused by increased fecal volume, malnutrition, and increased intra–abdominal pressure due to coughing (Eggermont and De Boeck 1991). Other intestinal symptoms are bowel

M. Monteleone · G. Maconi (✉)
Gastroenterology Unit, Department of Biomedical and Clinical Sciences, "L. Sacco" University Hospital, Milan, Italy
e-mail: giovanni.maconi@unimi.it

F. Esposito
Radiology Unit, Azienda Ospedaliera, Santobono—Pausilipon, Naples, Italy

G. Carnevale
First Department of Medicine, Fondazione IRCCS Policlinico San Matteo, University of Pavia, Pavia, Italy

G. Maconi and G. Bianchi Porro (eds.), *Ultrasound of the Gastrointestinal Tract*, Medical Radiology. Diagnostic Imaging,
DOI: 10.1007/174_2013_825, © Springer-Verlag Berlin Heidelberg 2013
Published Online: 15 March 2013

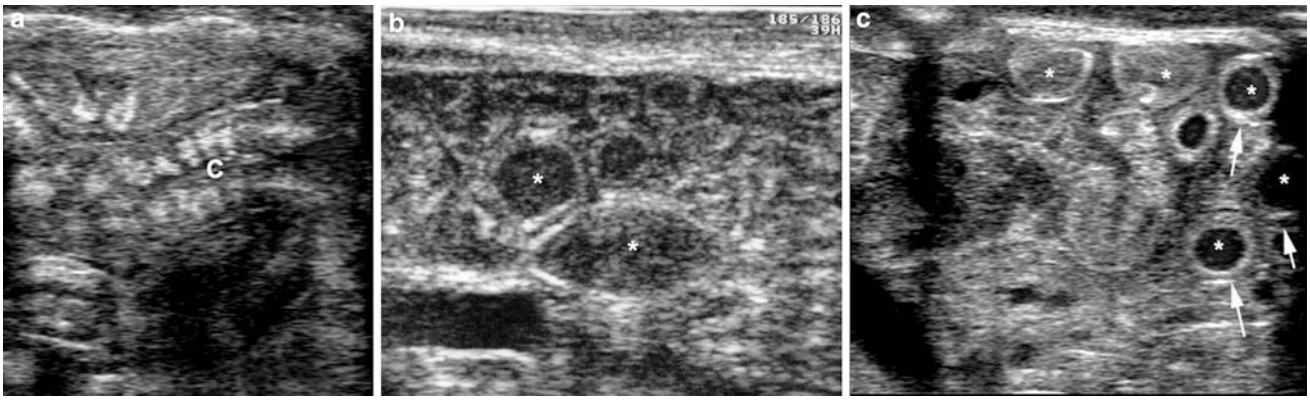

Fig. 1 Newborn infant with cystic fibrosis, presenting with intestinal occlusion due to meconium ileus. Small empty colon (C) (**a**) is associated with distension of the small-bowel (*asterisks*) with liquid (*arrows*) and inspissated faecal content (**b**, **c**)

occlusion by intussusception and constipation (Khoshoo and Udall 1994). Older individuals with CF may develop distal intestinal obstruction syndrome when thickened faeces cause intestinal blockage and fibrosing colonopathy, which is a complication with unknown aetiology characterised by increased bowel wall thickness (Irmela et al. 2003).

1.1 Ultrasonographic Features

Patients with CF may have a variety of gastrointestinal manifestations such as meconium ileus, intestinal obstruction, intussusception, mucoid appendix and fibrosing colopathy (Haber 2007; Liong et al. 2011). These abnormalities can be imaged by intestinal ultrasound that represents a useful tool for a prompt and effective management of the CF patients with abdominal complaints, in various age periods.

Meconium ileus is caused by impaction of inspissated meconium in the terminal ileum. At sonography, this condition may be shown as a small empty colon, associated with marked distension of small-bowel (Fig. 1). Unfortunately, a number of these patients may also present with volvulus, bowel atresia or meconium peritonitis, and require further examinations, such as standard radiology and barium enema. Intestinal impaction with partial or complete bowel obstruction may be also observed in children and older patients as the life expectancy of CF patients continues to increase. In older patients, bowel obstruction may be due to a lot of faecal material in ileocecal region. This may be detected by ultrasound as a mass of solid faecal content with shadowing in cecum or terminal ileum, and leads to conservative management, avoiding unnecessary surgery. Likewise, intestinal intussusception may be transient and asymptomatic, or may involve ileo-cecal region and requires hydrostatic enema under US guidance to reduce intussusception. It can be

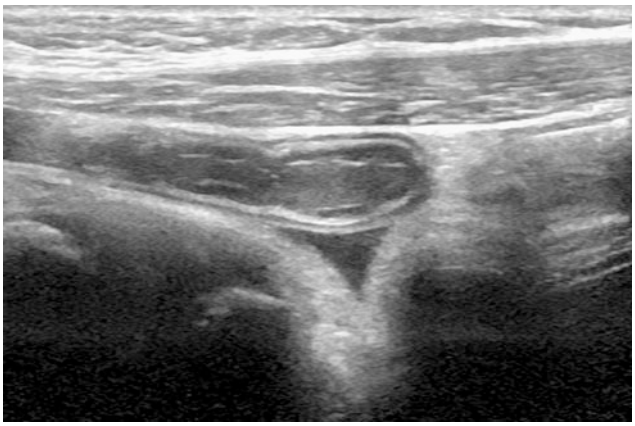

Fig. 2 Ultrasonographic features of appendiceal involvement in CF. The diameter is enlarged due to mucoid content and the typical inflammatory findings such as wall thickening, changes of the wall echopattern, hypertrophy of periappendiceal fat and pain under compression are absent

due to inspissated intestinal content and loss of elasticity and fibrosis of intestinal wall. These complications have typical US features, and are well described in the "Abdominal Hernias, Volvulus, and Intussusception".

Involvement of the appendix may be found in 16 % of patients with CF, but acute appendicitis is uncommon, affecting 1–2 % of CF patients compared with an overall 7 % of general population (Coughlin et al. 1990). Abnormalities of appendix in CF include enlargement of outer diameter (>6 mm) in > 80 % of patients due to accumulation of inspissated mucoid content. It is important noting that these patients are asymptomatic, that no wall thickening or changes in appendiceal wall echopattern occur, and that involvement of periappendiceal and omental fat, and pain under gentle compression are absent (Lardenoye et al. 2004; Menten et al. 2005) (Fig. 2).

Another complication of CF is fibrosing colonopathy, a condition characterised by fibrosis of submucosa,

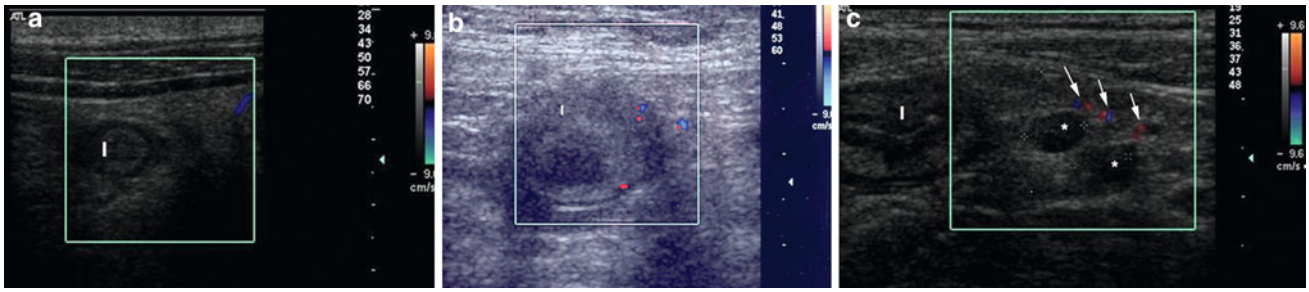

Fig. 3 Ultrasonographic features of small bowel amyloidosis, characterised by wall thickening (*arrows*) associated with decreased vascularity at color Doppler (**a**, **b**) and (**c**) enlarged mesenteric lymph nodes (*asterisks*) and mesenteric hypertrophy with dilated vascular structures (*arrows*). *I*, Ileum

predominantly involving the proximal portion of the colon, leading to the formation of local or pancolonic stenosis. Sonographic appearance of this abnormality is a diffuse thickened colon wall (up to 6.5 mm) with the maintenance of echo-stratification (Haber et al. 1997). The aetiology of this condition is uncertain. It does not seem to be correlated with intestinal inflammation (Pohl et al. 1997), previous meconium ileus, intestinal resection, distal intestinal obstruction syndrome, abdominal pain, or with high-dose pancreatic enzyme treatment (Haber et al. 1997), but it has been rather interpreted as an expression of glandular dysfunction in the CF intestine (Dialer et al. 2003). Another aspect of colonic wall in CF is colonic wall redundancy, also called jejunalisation of the colon. This condition, described for the first time in 2008, is more frequently seen in adult CF patients (it is described in up to 39 % of adult CF patients) and is usually asymptomatic or associated with non specific gastrointestinal symptoms (Webb et al. 2008; Caruso et al. 2012). Colonic wall redundancy is characterised at US by a hypertrophic colonic wall that appears wrinkled, doubled or tripled. Sometimes it is associated with pericolonic edema and mimics an intussusception.

2 Amyloidosis

Amyloidosis is a rare disease, characterised by forming pathological protein deposits—amyloid—in many organs and tissues. The deposition of amyloid is usually systemic, only 20 % of patients shows a localised, organ-specific, disease. Up to 15 % of the patients with myeloma are forming the deposits of amyloid. The primary amyloidosis affects both parenchymatous organs and the digestive tube. Mean age of the patients varies around 55–60 years. Renal insufficiency is a common sign. Heart, tongue, skin, kidney, nerves and the digestive tract are usually affected.

Amyloidosis may be inherited or acquired and can be also classified as primary or secondary. The primary amyloidoses have a familiar predisposition very often accompanied by the monoclonal gammopathy. The secondary or reactive amyloidoses occur as a complication of some long-lasting chronic inflammatory or tissue destructive diseases. The amyloid tends to form deposits in parenchymatous organs of the abdominal cavity and in lymph nodes.

Amyloidosis of the gastrointestinal tract is rare, occurring in 3.2 % of patients with all types of amyloidosis. It may be a dominant gastrointestinal involvement of a systemic amyloidosis (80 % of patients) or localised to the gastrointestinal tract without evidence of an associated plasma cell dyscrasia or other organ involvement (approximately 20 % of patients) (Cowan et al. 2012). Clinical symptoms depend on the actual location of the deposits. Weight loss, gastrointestinal bleeding, diarrhoea as well as intestinal obstruction, malabsorption, infarction and perforation may occur.

2.1 Ultrasonographic Features

The involvement of the small bowel in systemic forms of amyloidosis may be diffuse or very rarely focal. Rare cases of focal amyloidosis of the duodenum, jejunum and sigmoid colon have been described (Hirata et al. 1997; Matsui et al. 1996; Mainenti et al. 2010). These forms are characterised by amyloid infiltration of the entire intestinal wall thickness.

The sonographic features of intestinal amyloidosis may be non-specific, characterised by thickening of the bowel wall, mainly of the mucosa with hypoechoic and nodular plicae, decreasing of peristalsis, intestinal dilatation and mesenteric lymph nodes with diameter ranging between 10 and 20 mm (Mainenti et al. 2010). Thickened bowel walls did not show significant increase in vascularisation. In particular, the thickened intestinal walls are more frequently remarkably hypovascularised, and dilated vascular structures can be visible within the mesentery (Fig. 3).

Focal dilatation of the small bowel or gastric lumen associated to wall thickening may represent a radiological sign for suggesting intestinal amyloidosis in the differential diagnosis (Fig. 4; Kala et al. 2007). In fact, amyloid may

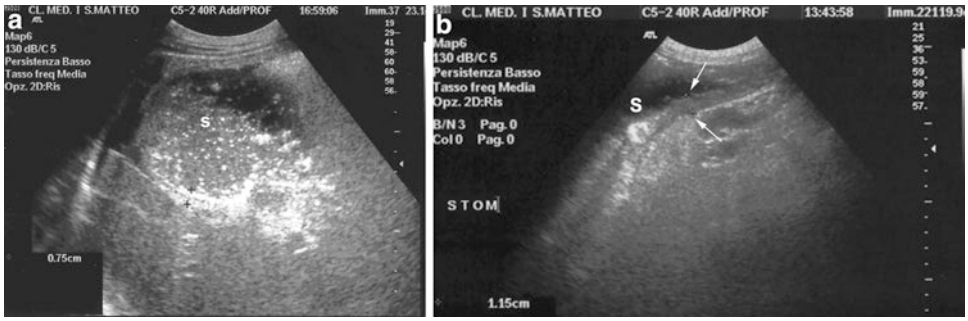

Fig. 4 **a** Dilatation of the stomach (*S*) associated to wall thickening (*arrows*) with absence of peristalsis **b** in a patient with gastric amyloidosis

form deposits within the neural myenteric plexus, which determine the hypotonia of the gastrointestinal wall and promote the pseudoaneurysmal dilatation (Araoz et al. 2000).

3 Vasculitis

Vasculitis includes a group of inflammatory disorders that affect both arteries (arteritis) and veins (phlebitis). It is primarily due to the leukocyte migration and to the resultant damage of blood vessels, and can be classified according to the cause, location, type and the size of the vessels (Gardner-Medwin et al. 2002).

Vasculitis may present with systemic symptoms such as fever and weight loss, skin alterations such as palpable purpura and livedo reticularis and gastrointestinal manifestations such as abdominal pain, diarrhea, bloody stool and perforation.

Vasculitides that most commonly affect the gastrointestinal system are Bechet's disease, Henoch Shoenlein purpura and polyarteritis nodosa.

Bechet's disease usually presents with abdominal pain, flatulence, diarrhea, constipation, mucus or blood in the stool, and intestinal ulcers.

Henoch Shoenlein purpura is characterised by abdominal pain, nausea, vomiting, diarrhea or constipation and in one third of patients by gastrointestinal bleeding and intestinal intussusception.

Polyarteritis nodosa shows abdominal pain due to the damage to the medium- and small-sized arteries of the bowel.

3.1 Ultrasonographic Features

Various ultrasonographic features have been described in the vasculitides, depending on the specific disease. However, vasculitides share common ultrasonographic features such as bowel wall thickening, loss of bowel stratification and focal dilatation of the bowel, due to their vascular and inflammatory pathogenesis.

These features are present in Henoch-Shoenlein purpura, where sometime can be also observed an extra-echoic layer internal to the submucosa that may be due to the bleeding within the deep mucosa and submucosa. These changes may be also the result of bowel wall oedema due to vasculitis of the supplying vessels (Fig. 5; Couture et al. 1992; Nchimi et al. 2008).

In Kawasaki disease, intestinal ultrasound can show a segmental thickening of the small-bowel wall, with loss or poor differentiation of the wall stratification, and focal intestinal dilatation. Along with these findings, hydrops of the gallbladder, due to the vasogenic oedema, may be observed (Maurer et al. 2008; Akikusa et al. 2004). Therefore US finding of segmental bowel wall thickening, in particular if associated with gallbladder hydrops, in an acutely ill, febrile child should raise the suspicion of Kawasaky disease.

Hereditary angioedema can also lead to segmental bowel wall thickening, with uniform prominent hypoechoic folds, easily observed by intestinal ultrasound. Hereditary angioedema is the autosomal dominant deficiency of C1-esterase inhibitor. Symptoms of this disease include cutaneous angioedema, laryngeal oedema, acute abdominal pain, and ascites. Acute abdominal attacks of the disease can mimic surgical emergencies. Therefore a prompt and accurate diagnosis is essential.

Ultrasonographic features of this condition include intestinal swelling on the initial day of the episode of abdominal pain and ascites. Oedema regresses rapidly, whereas free peritoneal fluid may persist for at least 3 days. It is therefore important to perform the intestinal ultrasound in the acute phase to demonstrate the intestinal oedema, and its regression after symptomatic relief (Dinkel et al. 2001; Farkas et al. 2001; Pedrosa et al. 2009).

4 Rare Disorders

HIV enteropathy. HIV-associated enteropathy is a syndrome characterised by chronic diarrhoea without an identified infectious cause, in an HIV-positive individual. It is thought

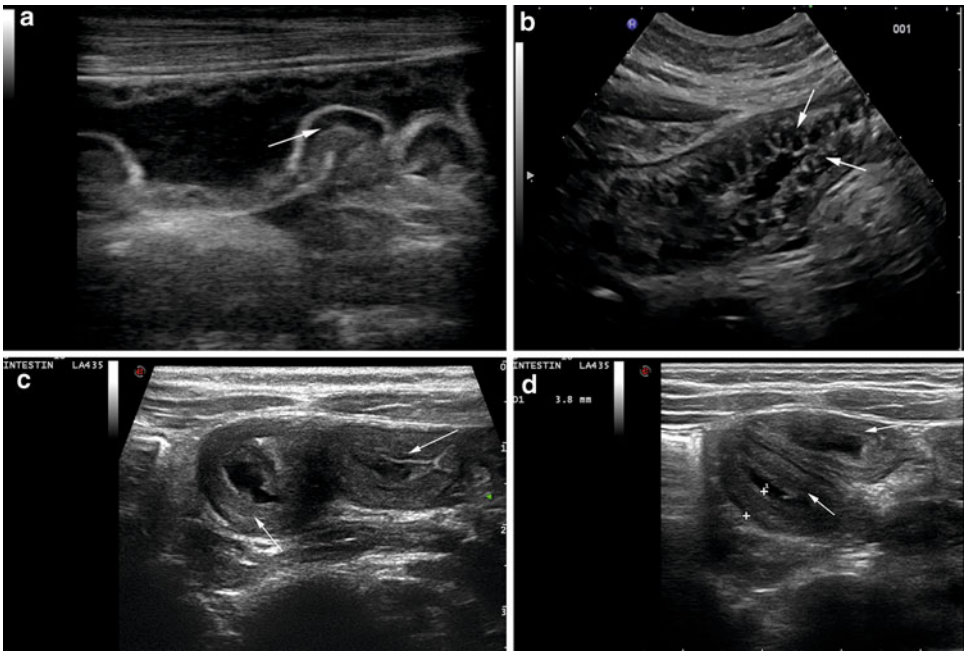

Fig. 5 Ultrasonographic features of bowel wall in Henoch-Shoenlein purpura. Longitudinal views of the bowel in a 10-year-old male patients (**a, b**) showing a slight thickening of the bowel wall, with an extra-echoic layer, internal to the submucosa (*arrows*). Transversal views of the bowel in 4-year-old female patient (**c, d**) showing the wall thickening with loss of stratification (*arrows*)

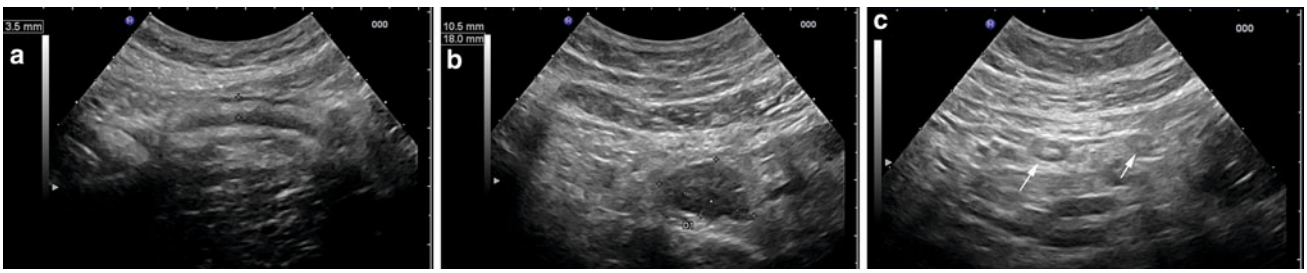

Fig. 6 34-year-old patient with HIV enteropathy. **a**, Slight thickening of the wall of the small bowel, with enlargement of the hyperechoic submucosal layer, enlarged mesenteric lymph nodes with hypoechoic (**b**) and hyperechoic (*arrows*) (**c**) echopattern

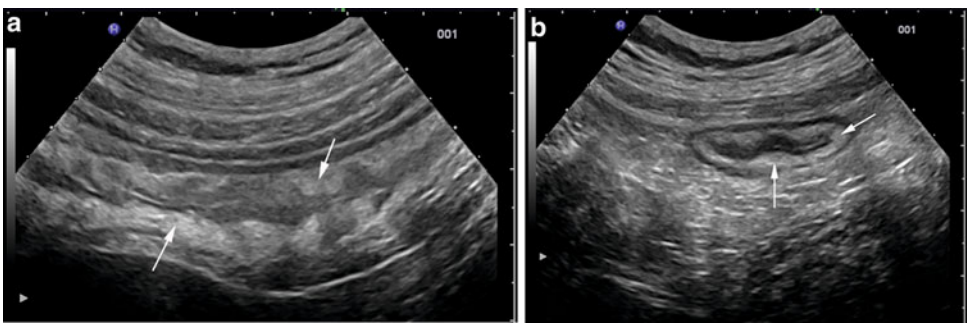

Fig. 7 Longitudinal scan of the right colon (**a**) and transversal scan of the descending colon (**b**) of a patients with microscopic colitis showing the slight thickening of the wall with moderate thickening of the hyperechoic submucosal layer (*arrows*)

to be due to direct or indirect effects of HIV on the enteric mucosa. It is essentially a diagnosis of exclusion, and can be made only after other forms of diarrheal illness have been ruled out.

In this condition, sonography can show an echogenic thickening of the wall of the small intestine, mainly of the mucosal layer, sometimes the so called aspect of "white bowel", which described the hyperechoic appearance of the

bowel wall. Enlarged mesenteric lymph nodes (with both hypoechoic and occasionally hyperechoic appearance) are present in the majority of cases (Fig. 6; Hollerweger and Dietrich 2005).

Microscopic colitis. Microscopic colitis includes two medical conditions: collagenous colitis and lymphocytic colitis. These diseases are characterised chronic watery diarrhoea, normal colonoscopy and specific histopathology findings. The pathological hallmark of this condition is an increase of inflammatory cells in the surface epithelium and lamina propria in lymphocytic colitis, which is associated with subepithelial collagen deposition in collagenous colitis. Sonography may reveal the following nonspecific findings: watery stool in the entire colon, slight thickening of the hypoechoic mucosal layer, and moderate thickening of the hyperechoic submucosal layer of the colon, and the absence of pathologic findings in the small intestine (Fig. 7). Follow up sonography performed at recovery of the patient, may reveal the normalisation of the bowel and disappearance of the thickened submucosal layer of the colon (Hollerweger et al. 2003).

References

Akikusa JD, Laxer RM, Friedman JN (2004) Intestinal pseudoobstruction in Kawasaki disease. Pediatrics 113:e504–e506

Araoz PA, Batts KP, MacCarty RL (2000) Amyloidosis of the alimentary canal: radiologic-pathologic correlation of CT findings. Abdom Imaging 25:38–44

Caruso S, Crinó F, Maruzzelli L et al (2012) Imaging findings of colonic wall redundancy in cystic fibrosis patients: two case reports. Abdom Imaging 37:566–569

Couture A, Veyrac C, Baud C et al (1992) Evaluation of abdominal pain in Henoch-Schönlein syndrome by high frequency ultrasound. Pediatr Radiol 22:12–17

Coughlin JP, Gauderer MW, Stern RC et al (1990) The spectrum of appendiceal disease in cystic fibrosis. J Pediatr Surg 25:835–839

Cowan AJ, Skinner M, Seldin DC et al (2012) Amyloidosis of the gastrointestinal tract: a 13-year single center referral experience. Haematologica (Jun 24) In press

Dialer I, Hundt C, Bertele-Harms RM, Harms HK (2003) Sonographic evaluation of bowel wall thickness in patients with cystic fibrosis. J Clin Gastroenterol 37:55–60

Dinkel HP, Maroske J, Schrod L (2001) Sonographic appearances of the abdominal manifestations of hereditary angioedema. Pediatr Radiol 31:296–298

Eggermont E, De Boeck K (1991) Small-intestinal abnormalities in cystic fibrosis patients. Eur J Pediatr 150:824–828

Farkas H, Harmat G, Kaposi PN et al (2001) Ultrasonography in the diagnosis and monitoring of ascites in acute abdominal attacks of hereditary angioneurotic oedema. Eur J Gastroenterol Hepatol 13:1225–1230

Gardner-Medwin JM, Dolezalova P, Cummins C et al (2002) Incidence of Henoch-Schönlein purpura, Kawasaki disease, and rare vasculitides in children of different ethnic origins. Lancet 360:1197–1202

Haber HP, Benda N, Fitzke G et al (1997) Colonic wall thickness measured by ultrasound: striking differences in patients with cystic fibrosis versus healthy controls. Gut 40:406–411

Haber HP (2007) Cystic fibrosis in children and young adults: findings on routine abdominal sonography. AJR Am J Roentgenol 189:89–99

Hirata K, Sasaguri T, Kunoh M et al (1997) Solitary "amyloid ulcer" localized in the sigmoid colon without evidence of systemic amyloidosis. Am J Gastroenterol 92:356–357

Hollerweger A, Dietrich CF (2005) "White bowel". A sonographic sign of intestinal lymph edema? Ultraschall Med 26:127–133

Hollerweger A, Macheiner P, Brunner W (2003) Suspicion of microscopic colitis raised by sonographic examination. J Clin Ultrasound 31:207–210

Kala Z, V′alek V, Kysela P (2007) Amyloidosis of the small intestine. Eur J Radiol 63:105–109

Khoshoo V, Udall JN (1994) Meconium ileus equivalent in children and adults. Am J Gastroenterol 89:153–157

Irmela D, Cornelia H, Rose-Marie B et al (2003) Sonographic Evaluation of Bowel Wall Thickness in Patients With Cystic Fibrosis. J Clin Gastroenterol 37:55–60

Lardenoye SW, Puylaert JB, Smit MJ, Holscher HC (2004) Appendix in children with cystic fibrosis: US features. Radiology 232:187–189

Liong SY, Awad D, Jones AM, Sukumar SA (2011) The adult cystic fibrosis patient with abdominal pain: what the radiologist needs to know. Clin Radiol 66:132–139

Matsui H, Kato T, Inoue G, Onji M (1996) Amyloidosis localized in the sigmoid colon. J Gastroenterol 31:607–611

Maurer K, Unsinn KM, Waltner-Romen M et al (2008) Segmental bowel-wall thickening on abdominal ultrasonography: an additional diagnostic sign in Kawasaki Disease. Pediatr Radiol 38:1013–1016

Mainenti P, Segreto S, Mancini M et al (2010) Intestinal amyloidosis: Two cases with different patterns of clinical and imaging presentation. World J Gastroenterol 16:2566–2570

Menten R, Lebecque P, Saint-Martin C, Clapuyt P (2005) Outer diameter of the vermiform appendix: not a valid sonographic criterion for acute appendicitis in patients with cystic fibrosis. AJR Am J Roentgenol 184:1901–1903

Nchimi A, Khamis J, Paquot I et al (2008) Significance of bowel wall abnormalities at ultrasound in Henoch-Schönlein purpura. J Ped Gastroent Nutr 46:48–53

Pedrosa M, Caballero T, Gómez-Traseira C et al (2009) Usefulness of abdominal ultrasonography in the follow-up of patients with hereditary C1-inhibitor deficiency. Ann Allergy Asthma Immunol 102:483–486

Pohl M, Krackhardt B, Posselt HG, Lembcke B (1997) Ultrasound studies of the intestinal wall in patients with cystic fibrosis. J Pediatr Gastroenterol Nutr 25:317–320

Yankaskas JR, Marshall BC, Sufian B et al (2004) Cystic fibrosis adult care: consensus conference report. Chest 125:1S–39S

Webb EM, Kleinhenz ME, Coakley FV et al (2008) Colonic wall redundancy at CT in patients with cystic fibrosis. Radiology 248(3):869–875

Part III

Infections

Infectious Enteritis

Giovanni Maconi and Luciano Tarantino

Contents

Abstract

Bacterial infectious enteritis is one of the most frequent causes of morbidity worldwide. In otherwise healthy adults it is usually of short course and self-limiting. The most common symptoms are diarrhoea, fever, nausea, vomiting and abdominal pain, which may be generalised or localised and cause a syndrome that mimics appendicitis or inflammatory bowel disease. Symptoms are not specific and cannot distinguish the bacterial cause. The sonographic signs of salmonellosis, yersiniosis and infectious enterocolitis, are usually characterised by symmetric and homogeneous wall thickening of terminal ileum and proximal colon, associated with enlarged regional mesenteric lymph nodes. However, even these sonographic signs are not specific. However, since sonography is a rapid, non-invasive and simple diagnostic tool, it may be used in specific clinical contexts, to discriminate between self-limiting infectious conditions and inflammatory bowel diseases or appendicitis, and to appropriately plan the treatment and follow-up of the patients.

1 Clinical Features

Bacterial infectious enteritis is one of the most frequent causes of morbidity worldwide. Major causes are Salmonellosis, Shigellosis and infections due to *Yersina enterocolitis* and *Yersinia paratuberculosis* and *Campylobacter jejuni*. In otherwise healthy adults, infections due to these agents are frequently of short course and self-limiting. However, due to these infections, morbidity and mortality are highest among the elderly, infants and children, as well as immuno-compromised individuals.

Enteric infections result in gastroenteritis occurring 6–48 h after ingestion of contaminated food or water. The most common symptoms are diarrhoea, fever, nausea and vomiting as well as abdominal pain. Abdominal pain

G. Maconi (✉)
Gastroenterology Unit,
Department of Biomedical and Clinical Sciences,
"L. Sacco" University Hospital,
Via G.B. Grassi, 74, 20157 Milan, Italy
e-mail: giovanni.maconi@unimi.it

L. Tarantino
Interventional Ultrasound Unit,
Department of Medicine, S. Giovanni di Dio Hospital, Via Mario Vergara Padre, 187, 80027 Frattamaggiore, Naples, Italy

G. Maconi and G. Bianchi Porro (eds.), *Ultrasound of the Gastrointestinal Tract*, Medical Radiology. Diagnostic Imaging,
DOI: 10.1007/174_2013_804,
Published Online: 20 February 2013

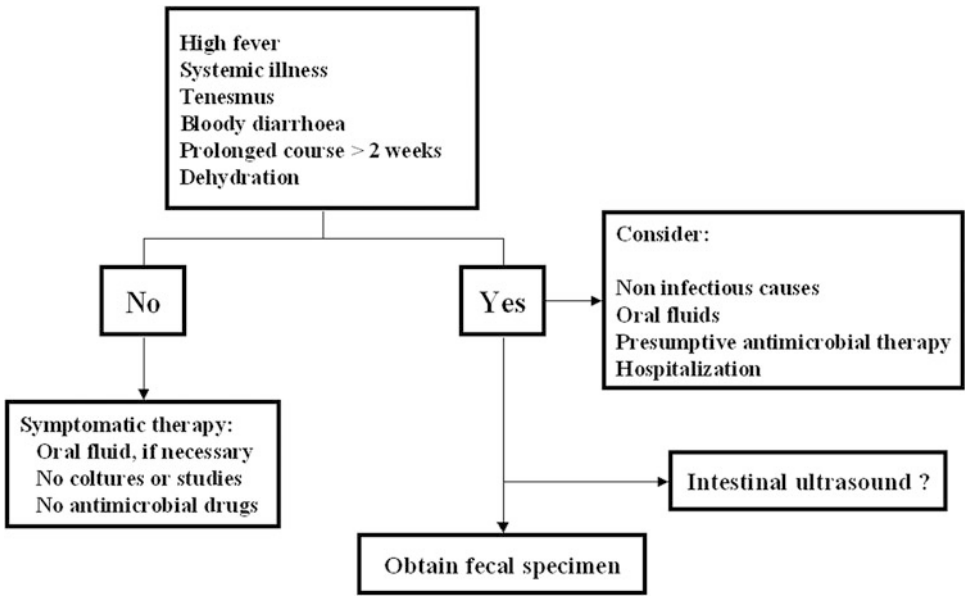

Fig. 1 Algorithm in patients presenting with suspicious infectious gastroenteritis

usually consists of cramping and, in most cases, may be the most prominent symptom. It may be generalised but, in some instances, may be localised and cause a syndrome or disorder that mimics appendicitis or inflammatory bowel disease.

Indeed, symptoms of pathogen-specific enteritis are not sufficiently unusual to distinguish a separate illness among those due to Salmonella, Shigella, Campylobacter or Yersinia or other pathogens. The combination of fever and faecal markers of intestinal inflammation, such as faecal lactoferrin or faecal calprotectin, is indicative of inflammatory diarrhoea, but the definite etiologic diagnosis is based on culture or demonstration of specific organisms on stained faecal smears.

For this reason, the importance of radiographic and sonographic imaging in the diagnosis of infectious enteritis is limited. However, since ultrasound is a rapid, simple, cheap and non-invasive diagnostic tool, in some instances, it may be usefully employed to discriminate between self-limiting infectious conditions and severe enterocolitic syndromes, such as inflammatory bowel diseases or appendicitis and their complications, or other conditions requiring surgery or specific medical treatment. Therefore, in individuals presenting with abdominal pain, diarrhoea and fever, or patients with acute or atypical symptoms and infants, as well as immunocompromised and elderly patients where a differential diagnosis between bacterial infectious enteritis and other acute abdominal conditions is mandatory, ultrasound can be employed to avoid unnecessary laparotomies and to avoid delay of surgery or specific therapy (Fig. 1) (Puylaert 1994; Tarantino et al. 2003).

2 Infectious Enteritis and Colitis

2.1 Salmonellosis

Gastroenteritis infection with non-typhoidal salmonella often results in gastroenteritis which is indistinguishable from that caused by other bacterial or viral pathogens. It is usually self-limited, and fever and diarrhoea resolve within 3 and 7 days, respectively. In a minority of patients (< 5 %), particularly neonates, infants, elderly and immunocompromised patients, carriage of the pathogen and/or a bacteraemia is prolonged with endovascular or localised (intra-abdominal, central nervous system, pulmonary) infections.

Sonographic features of Salmonella enterocolitis have been described both in children and adults. The first report described ileocaecal wall thickening and lymph node enlargement in a patient with typhoid fever (Puylaert 1989). Further series confirmed that Salmonella enteritis is usually seen as symmetric and homogeneous thickening (up to 7 mm; range 5–11 mm) of the wall of the terminal ileum and proximal colon (Fig. 2), sometimes with a small amount of free peritoneal fluid and more often associated with enlarged mesenteric lymph nodes (Hennedige et al. 2012; Mathis and Metzler 1992). However, sometimes colonic involvement may be seen in the absence of ileal involvement mimicking a pseudomembranous colitis (Adeniran et al. 2005).

In children, increased colonic wall thickening has been observed in up to 40 % of cases. The mean thickness was 6.2 mm, resulting predominantly from a gross submucosa

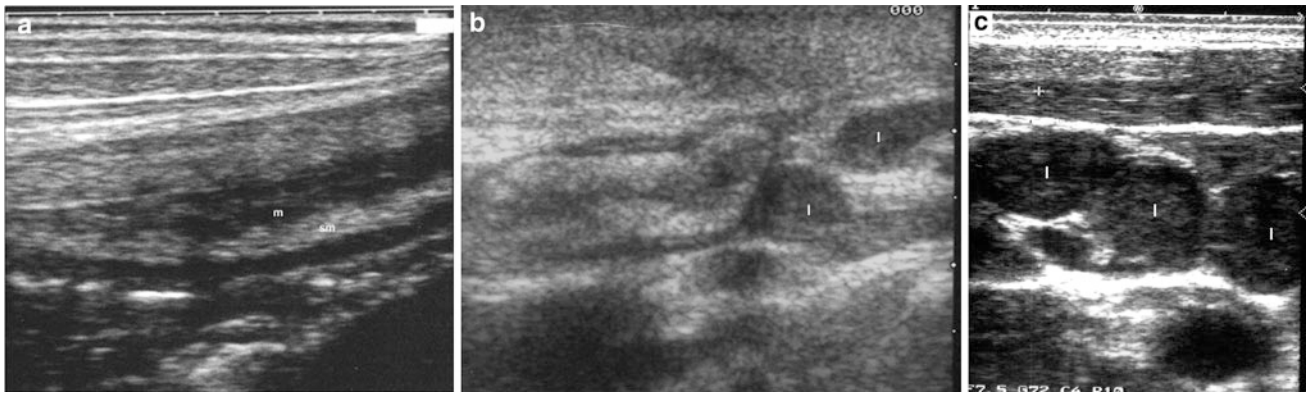

Fig. 2 Sonographic features of gastroenteritis infection with non-typhoidal salmonella in a 16-year-old female. Ultrasound showed marked wall thickening of ileum **a, b** and caecum, confined to mucosa (m) and submucosa (sm) and multiple enlarged mesenteric lymph nodes (l) distributed in "rosary-like" appearance **c**

oedema. Peristalsis has been described to be either increased or attenuated. Ascites has been observed in 60 % of patients and enlarged mesenteric lymph nodes in less than 10 % of patients (Ueda et al. 1999). In children, the sonographic detection of ascites and the increased colonic wall thickening correlated well with serum levels of C reactive protein and stool occult blood and, therefore, these may be useful signs by which to determine the severity of salmonella enterocolitis. However, whether they have also a prognostic factor is still unknown. In this regard, the persistence of positive stool culture 3 months after infection may result in the persistence of slight bowel wall thickening and in enlarged intra-abdominal lymph nodes (Fig. 3). Sonographic detection of ascites or intra-abdominal fluid in children with infectious enteritis, can distinguish Salmonella enteritis from colitis due to Rotavirus where ascites is usually absent (Ueda et al. 1999; Bass et al. 2004).

Typhoid fever is a systemic infectious disease caused by *Salmonella typhi*, characterised by fever, paradoxical bradycardia, abdominal pain and a rose coloured rash. Sonographic findings of typhoid fever in children and young patients (4–20 years) have been assessed in an endemic area in India. In a series of consecutive patients suspected to be having typhoid fever, the most frequent findings at abdominal ultrasound performed within three days of the onset of fever were splenomegaly (100 %), ileal and caecal thickening (85 %), mesenteric lymphadenopathy (77 %) and thickened gallbladder walls (62 %) (Mateen et al. 2006). A high rate of mesenteric lymphadenopathy (70 %) in typhoid fever has been also reported in another study form Pakistan (Nakachi et al. 2003) and in adult patients in an Italian area with high incidence of *Salmonella typhi* infection. In this study, the wall thickening of the ileum and/or ascending colon was reported in 36 % of patients and mesenteric lymph node enlargement in 56 % of patients (Tarantino et al. 1997).

2.2 Shigellosis

Shigellosis is the main bacterial cause of dysentery and should be taken into consideration in patients presenting with bloody diarrhoea. It is an acute bacterial infection caused by Shigella species (*S. dysenterie, S. flexneri, S. sonnei*) usually involving the distal colon and progressively decreasing in the more proximal segments of the large bowel. Sporadic case reports have depicted the sonographic features of shigelliosis. A diffuse wall thickening (8 mm) with distinct layer stratification in the descending and sigmoid colon in an 81-year-old woman was observed, ruling out the presence of an ischaemic colitis on the basis of clinical history and sonographic findings (Fujii et al. 2001).

2.3 Yersiniosis

Yersiniosis is bacterial zoonosis caused by infection with one or other of two enteropathogenic Yersinia species: *Y. enterocolitica* or *Y. pseudotuberculosis*, which are transmitted to humans predominantly via the oral route. The most frequent clinical manifestations of *Y. enterocolitica* are enteritis or enterocolitis and mesenteric adenitis presenting with fever, abdominal pain and diarrhoea, which is often bloody and persists for an average of 2 weeks, but may last up to many months during which symptoms diminish. In older children and adults right-sided abdominal pain and fever may be the predominant symptoms and may be confused with appendicitis. This presentation is much more common with *Y. pseudotuberculosis*, which is characterised by mesenteric adenitis and terminal ileitis. In a small proportion of cases, skin rash, joint pains, bacteriaemia can occur. The results of routine laboratory tests are often nonspecific and isolation of these micro-organisms from faeces is difficult, being impaired by their slow growth

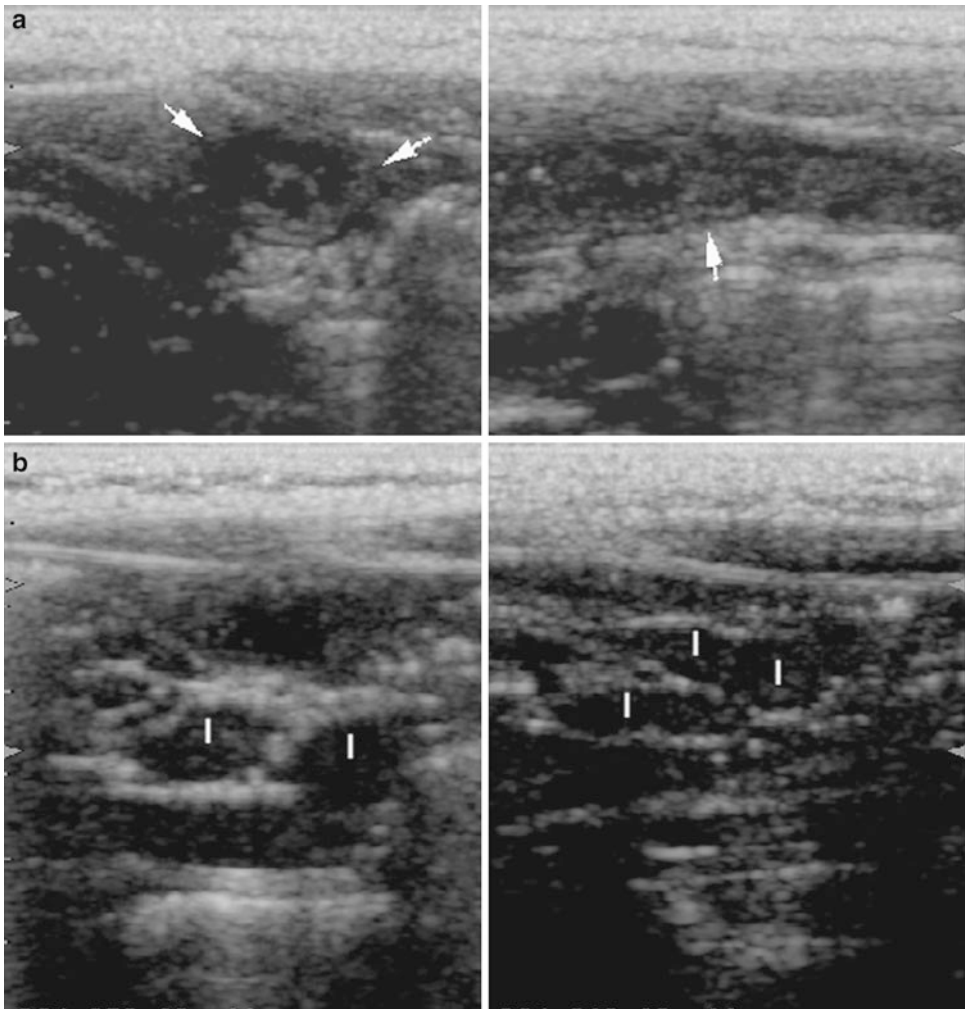

Fig. 3 Presence of **a** slight bowel wall thickening (*arrows*) and **b** enlarged intra-abdominal lymph nodes (*l*) in a 10-year-old patient with persistence of positive stool culture 3 months after infection with Salmonella

and overgrowth of other bacteria. Serologic tests, namely specific IgA and IgG antibodies to Yersinia or antigen detection in biopsies may be used, but are not widely available (Stolk-engelaar et al. 1996). Therefore, in patients with yersiniosis, abdominal ultrasound can be of assistance by excluding acute appendicitis and showing inflammatory changes in the terminal ileum and proximal colon. In the acute phase of the disease, sonography reveals thickening of the bowel wall (usually ranging from 7 to 10 mm), which is characterised by regular contours and hypoechoic echopattern (Fig. 4). Enlarged lymph nodes are always present, in numbers of 2–6 per patient, and detectable in the right iliaca fossa and along the iliac vessels (Matsumoto et al. 1991). The lymph nodes are usually sharply demarcated, oval or roundish, hypoechoic, with a variable diameter usually not exceeding 25 mm, sometimes presenting as an abdominal mesenteric mass with coalescent lymph nodes containing areas of necrosis or as an abscess (Jelloul et al. 1997; Pallister and Rotstein 2001; Perdikogianni et al. 2006) (Video). In patients with Yersinia sepsis, particularly if affected also by alcoholism, malnutrition or iron overload, ultrasound may reveal liver abscesses (Strungs et al. 1995; Leyman et al. 1989).

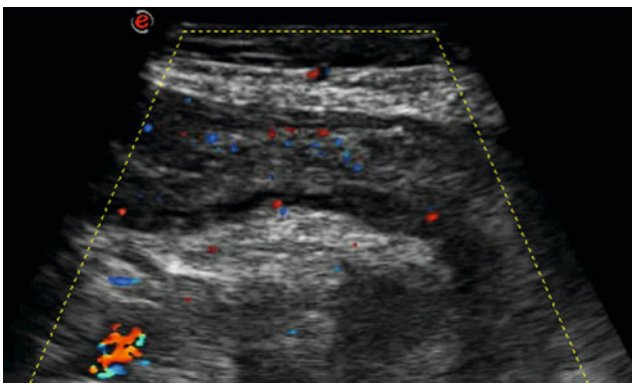

Fig. 4 Infectious ileocecitis due to Yersina enterocolitica in a 21-year-old male with clinical signs of appendicitis. Ultrasound showed wall thickening of ileum with hypoechoic echopattern and increased vascularization, a complex mesenteric mass with a small fluid area (Video) within, and enlarged mesenteric nodes

Table 1 Main differences in sonographic features of infectious ileocecitis caused by Yersinia, Campylobacter or Salmonella, Crohn's disease and appendicitis

	Infectious ileocecitis	Crohn's disease	Appendicitis
Bowel wall thickening	Mild and confined to superficial layers	Moderate and involving all layers	Present or mild (ileum)
Echo-pattern	Preserved	Preserved, altered or loss	Preserved (ileum)
Compressibility of ileum	Preserved	Usually not preserved	Preserved
Mesenteric hypertrophy	Sometimes present	Often present	Often present
Haustration of right colon	Preserved	Often lost (in diseased tract)	Preserved
Appendix	Normal	Normal or enlarged	Enlarged
Regional lymph nodes	Moderately to grossly enlarged	Often present	Often present
Abscess	Absent or Rarely present	Often present	Sometimes present
Fistula	Absent	Often present	Absent
Pre-stenotic dilatation	Absent	Often present	Absent

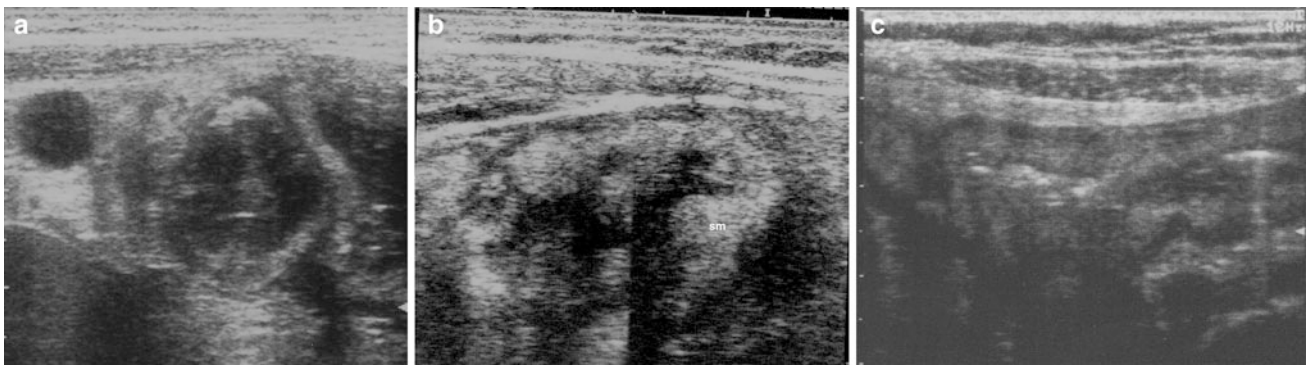

Fig. 5 Infectious ileocecitis in a 20-year-old male with clinical signs of appendicitis. **a** Ultrasound showed marked wall thickening of ileum confined to mucosa and submucosa. **b** Marked thickening of the caecal wall mainly confined to submucosa (*sm*). **c** Wall thickening of the ascending colon

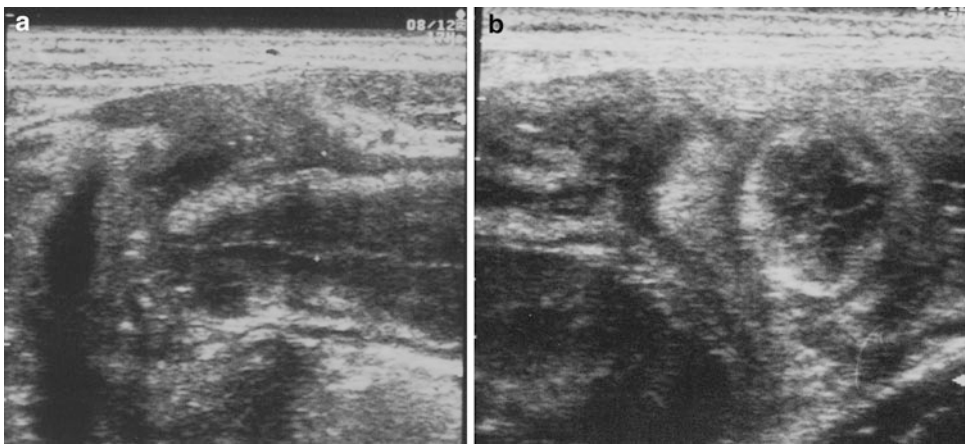

Fig. 6 Sagittal view of caecum, ileocaecal valve and ascending colon **a**, and axial view of the ileum ileocaecal valve and caecum **b** are the most typical US features of infectious ileocecitis

3 Infectious Ileocecitis

Infectious ileocecitis is an infection of the terminal ileum and caecum that is caused by *Yersinia enterocolitica*, *Campylobacter jejuni* or *Salmonella enteritidis*. The clinical features of infectious ileocecitis are very similar to those commonly found in acute appendicitis, with localised pain in the right lower quadrant being the main symptom, whereas diarrhoea is absent or mild. Local tenderness may be less prominent and acute phase reactants more elevated than in appendicitis. Due to these symptoms, infectious ileocecitis may lead to unnecessary laparotomy for suspected appendicitis.

At laparotomy, the appendix is normal, whereas the wall of the ileum and caecum is thickened and surrounded by enlarged mesenteric lymph nodes. However, these findings may be subtle and underestimated at laparotomy. Stool cultures are rarely requested since diarrhoea is absent and, therefore, the diagnosis is rarely made.

It has been widely shown that ultrasound may reveal a high incidence of infectious ileocecitis in patients with acute right lower quadrant pain where appendicitis is suspected (Puylaert et al. 1988, 1989, 1997; Tarantino et al. 2003). Sonography may also reveal the features of the bowel wall useful in the differential diagnosis between infectious ileocolitis, Crohn's disease and appendicitis (Table 1).

According to Puylaert et al. (1997), the sonographic involvement of the terminal ileum, caecum and proximal ascending colon and mesenteric lymph nodes in infectious ileocecitis caused by different micro-organisms may be different, thus suggesting a possible aetiological diagnosis.

The sonographic features of infectious enterocolitis are characteristic, consisting of thickening of the mucosa and (less frequently) submucosa of the ileum, caecum and ascending colon together with enlarged regional mesenteric lymph nodes (Fig. 5). Usually, the thickened ileo-caecal valve can be seen in these cases (Fig. 6). The appendix is normal.

In the differential diagnosis between infectious ileocecitis and Crohn's disease, the latter is characterised by transmural inflammation and intestinal complications. Therefore, the bowel wall is usually thicker than in infectious ileocecitis, and may be non-compressible with transmural inflammation involving the muscularis layer and resulting in disappearance of the normal stratified echopattern. The thickened bowel wall may be surrounded by mesenteric hypertrophy and complications, such as abscess or fistula and prestenotic dilatation can be found. None of these features are present in infectious ileocecitis. Nevertheless, when sonographic features suggest the presence of an inflammatory/infectious ileocecitis, bacteriological tests are mandatory to differentiate between Crohn's disease and infectious ileocecitis.

References

Adeniran JO, Taiwo JO, Abdur-Rahman LO (2005) *Salmonella* intestinal perforation (27 perforations in one patient, 14 perforations in another): are the goal posts changing? J Indian Assoc Pediatr Surg 10:248–251

Bass D, Cordoba E, Dekker C, Schuind A, Cassady C (2004) Intestinal imaging of children with acute rotavirus gastroenteritis. J Pediatr Gastroenterol Nutr 39:270–274

Fujii Y, Taniguchi N, Itoh K (2001) Sonographic findings in shigella colitis. J Clin Ultrasound 29:48–55

Hennedige T, Bindl DS, Bhasin A, Venkatesh SK (2012) Spectrum of imaging findings in Salmonella infections. AJR Am J Roentgenol 198:W534–W539

Jelloul L, Frémond B, Dyon JF, Orme RL, Babut JM (1997) Mesenteric adenitis caused by Yersinia pseudotuberculosis presenting as an abdominal mass. Eur J Pediatr Surg 7:180–183

Leyman P, Baert AL, Marchal G, Fevery J (1989) Ultrasound and CT of multifocal liver abscesses caused by *Yersinia enterocolitica*. J Comput Assist Tomogr 13:913–915

Mateen MA, Saleem S, Rao PC, Reddy PS, Reddy DN (2006) Ultrasound in the diagnosis of typhoid fever. Indian J Pediatr 73:681–685

Mathis G, Metzler J (1992) Sonography in salmonella enterocolitis. Ultraschall Med 13:106–109

Matsumoto T, Iida M, Sakai T, Kimura Y, Fujishima M (1991) Yersinia terminal ileitis: sonographic findings in eight patients. AJR Am J Roentgenol 156:965–967

Nakachi S, Nakamura T, Agha N et al (2003) Clinical features and early diagnosis of typhoid fever emphasizing usefulness of detecting mesenteric lymphadenopathy with ultrasound as diagnostic method. Southeast Asian. J Trop Med Public Health 34 Suppl 2:153–157

Pallister C, Rotstein OD (2001) Yersinia enterocolitica as a cause of intra-abdominal abscess: the role of iron. Can J Surg 44:135–136

Perdikogianni C, Galanakis E, Michalakis M et al (2006) Yersinia enterocolitica infection mimicking surgical conditions. Pediatr Surg Int 22:589–592

Puylaert JMBC (1989) Typhoid fever: diagnosi by ultrasonography. Am J Roentgenol 153:745–746

Puylaert JBCM (1994) When in doubt, sound it out. Radiology 191:320–321

Puylaert JB, Lalisang RI, van der Werf SD, Doornbos L (1988) Campylobacter ileocolitis mimicking acute appendicitis: differentiation with graded-compression US. Radiology 166:737–740

Puylaert JB, Vermeijden RJ, van der Werf SD, Doornbos L, Koumans RK (1989) Incidence and sonographic diagnosis of bacterial ileocaecitis masquerading as appendicitis. Lancet 2:84–86

Puylaert JB, Van der Zant FM, Mutsaers JA (1997) Infectious ileocecitis caused by *Yersinia, Campylobacter*, and *Salmonella*: clinical, radiological and US findings. Eur Radiol 7:3–9

Stolk-Engelaar VM, Hoogkamp-Korstanje JA (1996) Clinical presentation and diagnosis of gastrointestinal infections by Yersinia enterocolitica in 261 Dutch patients. Scand J Infect Dis 28:571–575

Strungs I, Farrell DJ, Matar LD, Dekker L, Franz RJ (1995) Multiple hepatic abscesses due to *Yersinia enterocolitica*. Pathology 27:374–377

Tarantino L, Giorgio A (1997) Value of bowel ultrasonography in the diagnosis of typhoid fever. Eur J Ultrasound 5:77–83

Tarantino L, Giorgio A, de Stefano G et al (2003) Acute appendicitis mimicking infectious enteritis: diagnostic value of sonography. J Ultrasound Med 22:945–950

Ueda D, Sato T, Yoshida M (1999) Ultrasonographic assessment of *Salmonella enterocolitis* in children. Pediatr Radiol 29:469–471

Intestinal Tuberculosis

Dong Ho Lee and Jae Hoon Lim

Contents

Abstract

Intestinal tuberculosis is a chronic inflammation of the bowel caused by Mycobacterium tuberculosis. The ileocecal area is the most common site. In patients with intestinal tuberculosis sonography may detect bowel wall thickening and hyperemia, usually associated with luminal narrowing and mesenteric lymphadenopathy. When tuberculous peritonitis coexists, sonography shows ascites, omental cake, and thickened mesentery with an adherent small bowel loop. Ultrasonography may be used as a primary investigative tool in patients with suspected or recurrent tuberculosis.

1 Introduction

Sonography may be used in patients with intestinal tuberculosis to document its classic features, i.e., bowel wall thickening, hyperemia, stricture, and mesenteric lymphadenopathy. When tuberculous peritonitis coexists, sonography shows ascites, omental cake, and thickened mesentery with an adherent small bowel loop. Thus, ultrasonography may be used as a primary investigative tool in patients with suspected or recurrent tuberculosis.

2 Pathology

Intestinal tuberculosis is a chronic inflammation of the bowel caused by Mycobacterium tuberculosis. The ileocecal area is the most common site. The classic radiographic appearance of ileocecal tuberculosis on barium enema has been described as a conical, shrunken, retracted cecum associated with a narrow ulcerated terminal ileum (Reeder and Palmer 1989). This cecal deformity is the result of spasm early in the disease and transmural infiltration with fibrosis in advanced phases. Narrowing of the terminal ileum may be caused by persistent irritability with rapid

D. H. Lee
Department of Radiology, Kyung Hee University Hospital, 1, Hoeki-dong, Dongdaemun-gu, Seoul, Korea

J. H. Lim (✉)
Department of Radiology, Samsung Medical Center, Sungkyunkwan University School of Medicine 50, Ilwon-dong, Kangnam-ku, Seoul, Korea
e-mail: jhlim@smc.samsung.co.kr

G. Maconi and G. Bianchi Porro (eds.), *Ultrasound of the Gastrointestinal Tract*, Medical Radiology. Diagnostic Imaging,
DOI: 10.1007/174_2013_803, © Springer-Verlag Berlin Heidelberg 2013
Published Online: 16 February 2013

emptying of the narrowed segment, corresponding to the acute inflammatory phase, or it may be the result of stricture with thickening and ulceration.

Grossly, there is ulceration with diffuse fibrosis extending through the bowel wall, causing stenosis and obstruction (Rosai 2004). Coexistent tuberculous peritonitis is observed in relatively few cases. Microscopically, typical granulomas are usually present accompanied by ulceration and extensive desmoplasia. These granulomas can be caseating or noncaseating, suppurative or fibrous. Features favoring tuberculosis are caseation and granuloma coalescence.

3 Sonographic Findings of Intestinal Tuberculosis

3.1 Bowel Wall Thickening

The normal bowel wall is visualized as a single, circular, hypoechoic layer surrounding hyperechoic bowel contents, such as gas, foodstuffs, or feces. The hypoechoic layer is considered to be the muscle layer (Lim 2000). The normal bowel wall is uniform with an average thickness of 2–3 mm if distended and 3–5 mm if not (Wilson 1998). When the wall thickness in transverse section is more than 5 mm, the bowel wall is regarded as being pathologically thickened (Malik and Saxena 2003).

The ileocecal region is most commonly involved in tuberculosis. The principal sonographic features of intestinal tuberculosis are diffuse, uniform, concentric, and circumferential wall thickenings of the terminal ileum, cecum, and ascending colon (Figs. 1, 2 and 3) (Lee et al. 1993; Kedar et al. 1994). These wall thickenings are continuous without skip lesions. Concentric involvement is more common than eccentric involvement (Fig. 4) (Lee et al. 1993). The detection of bowel wall thickening is important when making a diagnosis of intestinal tuberculosis and the detection rates range from 86 to 96 % (Malik and Saxena 2003; Lee et al. 1993; Lim et al. 1994). Mild wall thickening of small bowel may be overlooked (Fig. 5), and it is difficult to distinguish individual loops when they adhere to each other (Lee et al. 1991).

Ultrasonography detects ulceration within the thickened wall in only a few cases, whereas it is seen frequently during small bowel follow through examination or barium enema studies. This low sensitivity for the detection of ulcers on sonography may be due to the associated spasm (Kedar et al. 1994). Lymphoid tissue involvement in the ileal wall with ulceration, necrosis, fibrosis and often with extensive granulomatous infiltrate can be observed (Khaw et al. 1991). In a few cases of intestinal tuberculosis, a spasm of the cecum is identified by a collapsed lumen and irritability of the thickened wall (Lee et al. 1993).

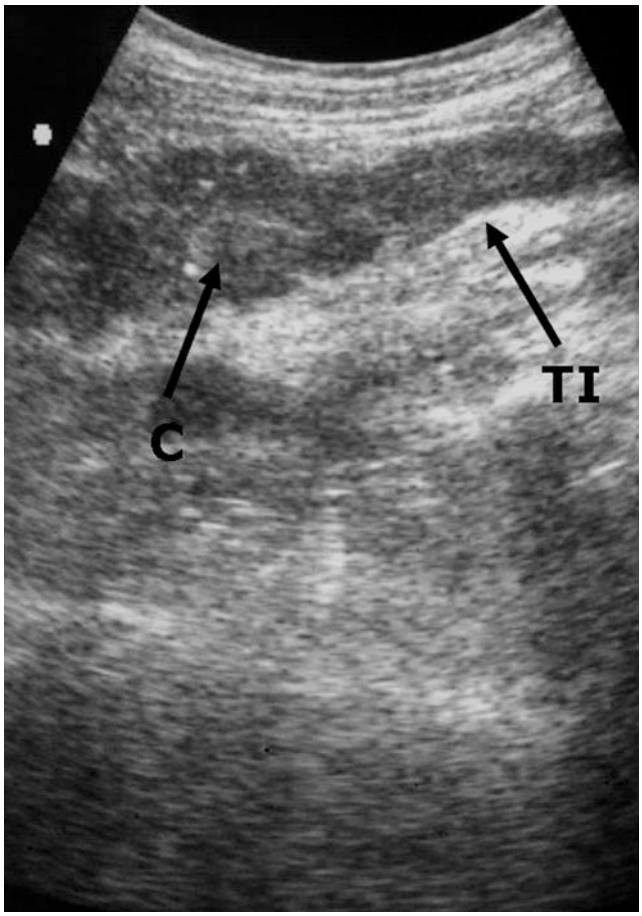

Fig. 1 Ileocecal tuberculosis. Transverse sonogram of the right lower abdomen shows diffuse thickening of the terminal ileum (*TI*) and cecum (*C*)

3.2 Hyperemia

Although subjective, color Doppler imaging is helpful for distinguishing active inflammatory changes in the thickened bowel wall from other pathologies (Fig. 3) (Wilson 1998; Teefey et al. 1996). Power Doppler imaging may improve the visualization of intramural gastrointestinal vascularity (Clautice-Engle et al. 1996). Thus, recent advances in color Doppler and power Doppler imaging improve the accuracy of sonography by allowing the detection of hyperemia of the inflamed bowel wall and of adjacent inflamed fat.

3.3 Stricture

In the active stage of intestinal tuberculosis, bowel wall thickening is usually accompanied by luminal narrowing, which results from spasm and edema. Later, fibrosis and scarring lead to permanent stricture (Fig. 5). However, it is difficult to detect stricture during sonographic examinations (Kedar et al. 1994).

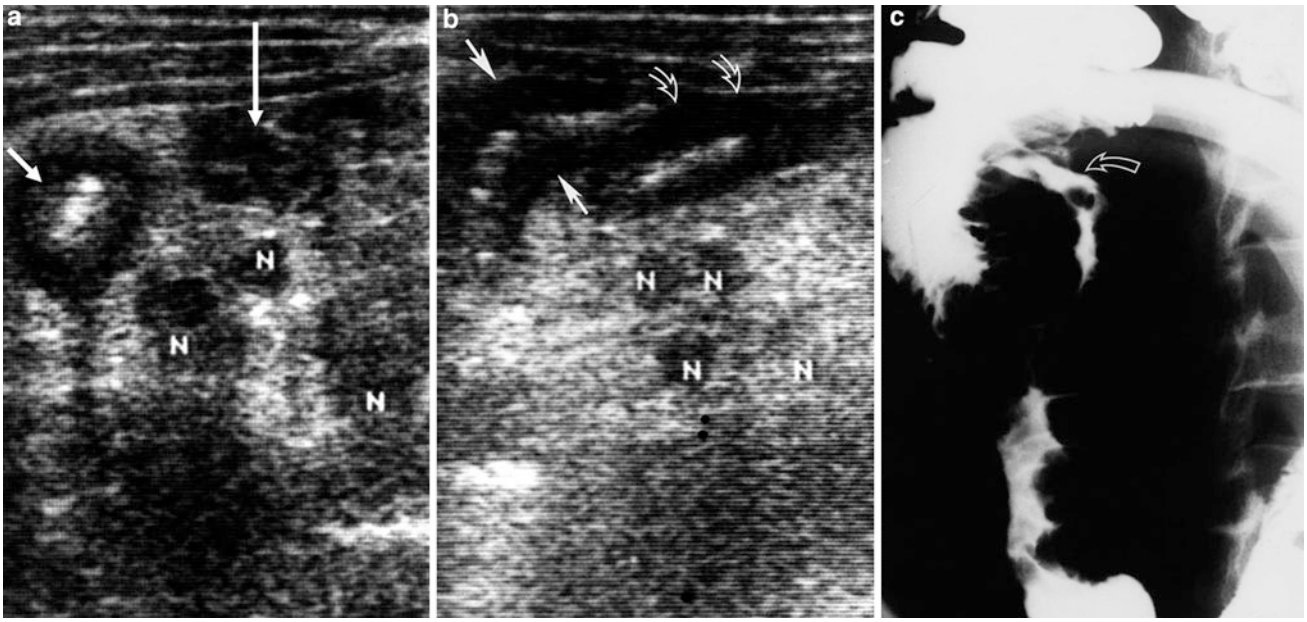

Fig. 2 Ileocecal tuberculosis and associated mesenteric lymphadenitis (reproduced with permission, Lim et al. 1994). **a** Transverse sonogram of ileocecal region shows thickening of the wall of the cecum (*short arrow*) and terminal part of the ileum (*long arrow*). Note enlarged mesenteric lymph nodes (*N*) and thickened mesentery around lymph nodes. **b** Longitudinal sonogram shows thickening of the cecum (*solid arrows*) and terminal part of the ileum (*open arrows*) and enlarged lymph nodes (*N*). **c** Barium examination shows irregular narrowing of the terminal part of the ileum and cecum. Note longitudinal ulcer (*curved arrow*) at the terminal part of the ileum. Mucosal folds are markedly thickened and irregular

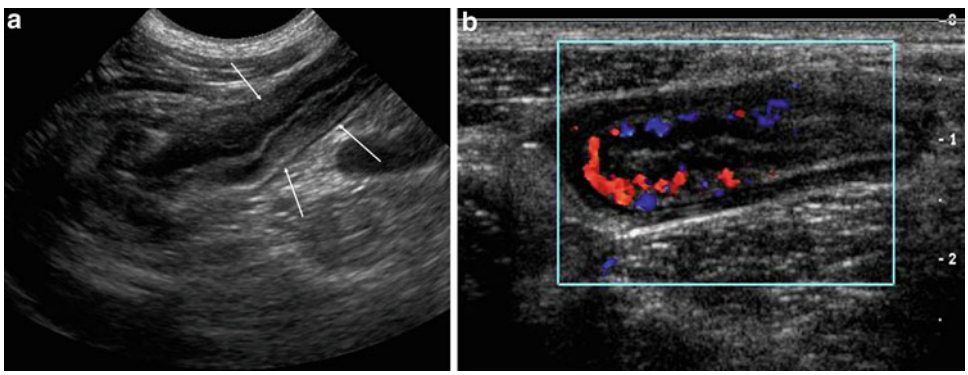

Fig. 3 Ileal tuberculosis. **a** Transverse sonogram of right low quadrant abdomen shows diffuse mural thickening of the terminal ileum. The terminal ileum shows concentric thickening (*arrows*). The thickness of the anterior and posterior walls is the same. **b** Transverse color Doppler sonogram of the terminal ileum shows numerous color signals

3.4 Mesenteric Lymphadenitis

In active tuberculosis, enlarged mesenteric nodes are frequent. Lymphadenopathy is mainly located at the mesentery around the ileum (Fig. 2) (Lee et al. 1993), but sometimes found at the periportal (Fig. 6), peripancreatic, mesenteric, and upper periaortic regions (Malik and Saxena 2003). However, the retroperitoneal lymph node is rarely involved, which can be explained by the fact that mesenteric lymph nodes drain directly into the thoracic duct via the cisterna chyli (Jain et al. 1995). Enlarged lymph nodes are hypoechoic, round to ovoid, and variable in size. Sometimes the

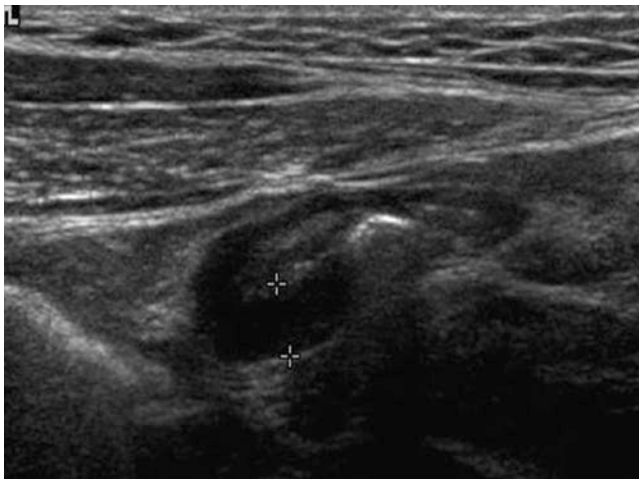

Fig. 4 Ileal tuberculosis. Transverse sonogram of the right lower quadrant abdomen discloses eccentric thickening of the posterior wall of the terminal ileum

4 Sonographic Findings of Tuberculous Peritonitis

4.1 Ascites

Three types of tuberculous peritonitis are generally recognized: the wet-ascitic type, the dry-plastic type, and the fibrotic-fixed type (Malik and Saxena 2003; Lee et al. 1991). The wet-ascitic type is characterized by ascites that may be free or loculated, whereas the dry-plastic type presents with enlarged lymph nodes with central caseation necrosis and adhesion, and the fibrotic-fixed type is observed as an omental mass and matted loops of bowel and mesentery. Combinations of these three forms are also found (Kedar et al. 1994). The characteristic sonographic finding of tuberculous peritonitis of the wet-ascitic type is

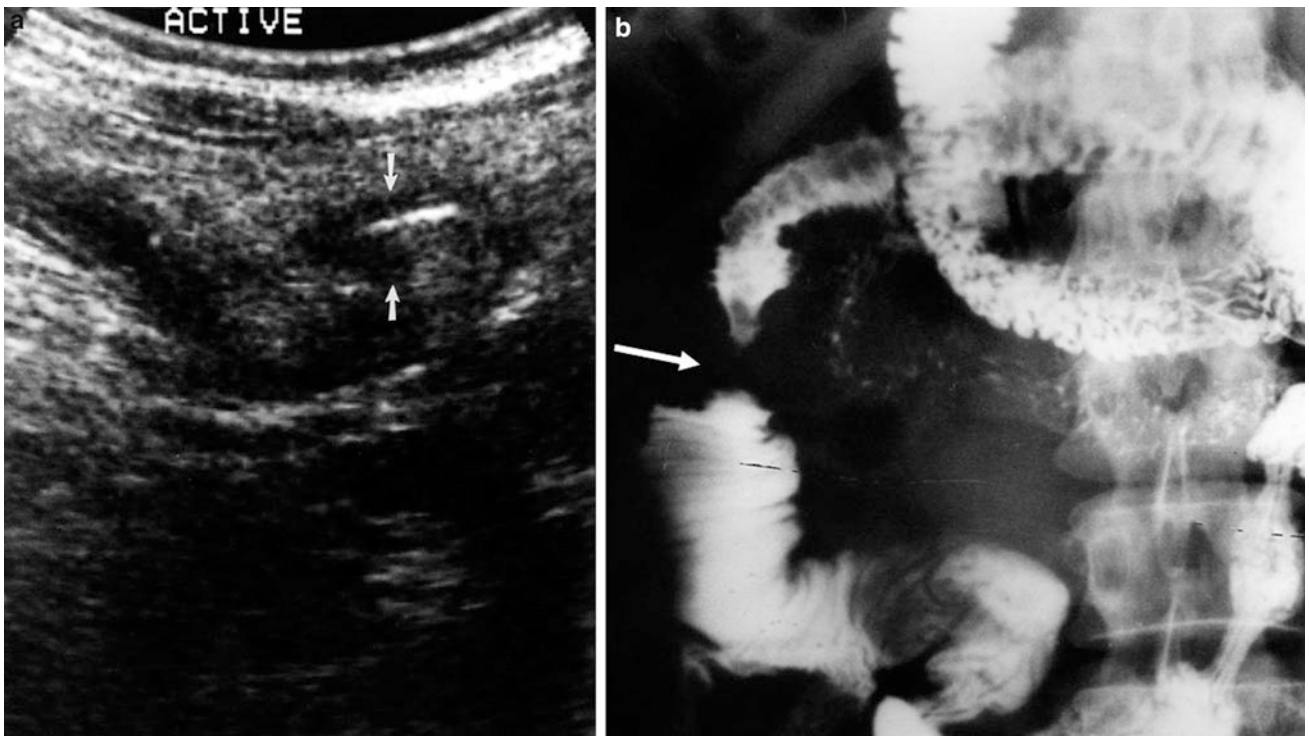

Fig. 5 Jejunal tuberculosis. **a** Transverse sonogram of the right upper abdomen shows a short segmental wall thickening of the jejunum (*arrows*). **b** Small bowel follow-through examination shows a segmental stricture of the jejunum (*arrow*). Note thickening of the mucosal folds at the proximal loop

nodes may be calcified (Malik and Saxena 2003; Kedar et al. 1994); calcification in healing tuberculosis is seen as a discrete reflective arc with posterior shadowing.

ascites. The most common pattern of ascites is clear fluid, though sometimes ascites is associated with membranes, septa, fine mobile strands, or floating debris (Fig. 7).

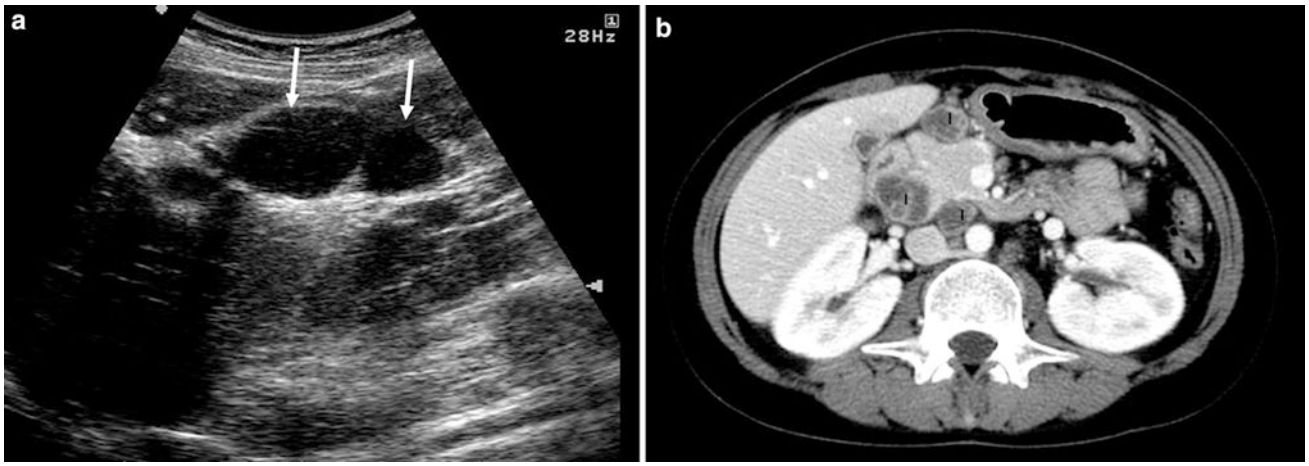

Fig. 6 Tuberculous lymphadenitis. **a** Transverse sonogram of the right upper quadrant abdomen shows hypoechoic lymph node enlargement at porta hepatic (*arrows*). **b** Abdominal CT shows multiple peripancreatic lymph node (*l*) enlargement. The enlarged lymph nodes show central low attenuation with marginal rim enhancement due to central caseous necrosis

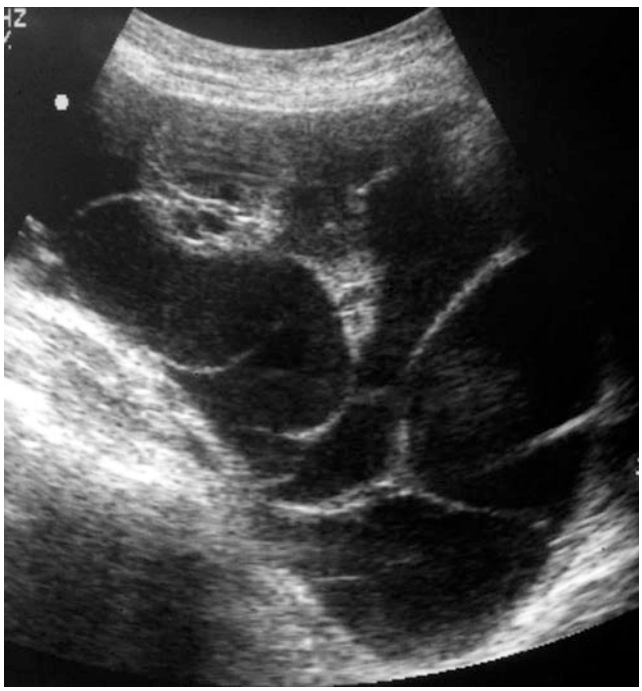

Fig. 7 Tuberculous peritonitis. Longitudinal sonogram of low abdomen shows a large amount of ascites with multiple, interlacing, thin septae

4.2 Omental Cake

About 20–30 % of patients with tuberculous peritonitis have omental cake (Lee et al. 1991). Omental cake is defined as a pancake-like diffuse thickening of the greater omentum, stretching from the greater curvature of the stomach down to the lower abdomen. Omental cakes are depicted as diffuse, hyperechoic, or heterogeneously echogenic thickening on sonographic examination (Lee et al. 1991). They may be seen in cancer peritonitis, and thus, it is impossible to differentiate by sonography.

4.3 Thickened Mesentery with a Matted Small Bowel Loops

The important sonographic features of early abdominal tuberculosis are a mesenteric thickness of 15 mm or more, and an increase in mesenteric echogenicity (Jain et al. 1995), which increases markedly, presumably because of fat deposition due to lymphatic obstruction. Pathologically, this mesenteric thickening results from edema, lymphadenopathy, and fat deposition. Another sonographic finding is matted, fixed small bowel loops and mesenteric strands, resembling spokes radiating from the mesenteric root, i.e., the sonographic 'stellate' sign (Kedar et al. 1994).

5 Differential Diagnosis

The principal sonographic features of intestinal tuberculosis are diffuse wall thickening of the terminal ileum and ascending colon with mesenteric lymphadenopathy. Other diseases that show wall thickening of the terminal ileum and colon are Crohn's disease, bacterial ileocolitis, and lymphoma (Lee et al. 1993). In Crohn's disease, bowel wall thickening is more severe and lymphadenopathy is rare (Limberg 1990; Worlicek et al. 1987). Frequently, the normal stratification of the bowel wall is no longer evident in involved areas owing to transmural inflammation (Limberg 1990). Abscess, fistula, and skip lesions are often

seen in Crohn's disease, but they are rare in tuberculosis (Sarrazin and Wilson 1996). In Yersinia ileitis, thickening of the ileal wall and mesenteric lymphadenopathy are the main findings, but the cecum and the ascending colon are usually spared (Matsumoto et al. 1991). In neutropenic typhlitis, wall thickening is confined to the right colonic wall and patients are usually in an immunosuppressed state (Teefey et al. 1987). In typhoid fever, there may be mural thickening of the terminal ileum and cecum and enlarged mesenteric lymph nodes (Puylaert et al. 1989). Clinical symptoms and course are usually different in Campylobacter ileocolitis from those in tuberculosis (Puylaert et al. 1988). In lymphoma, bowel wall thickening is severe. However, the sonographic findings of all these diseases are sometimes similar. Therefore, it is necessary to confirm the nature of bowel pathology by barium studies, CT, or colonoscopic biopsy.

References

Clautice-Engle T, Jeffrey RB Jr, Li KC, Barth RA (1996) Power Doppler imaging of focal lesions of the gastrointestinal tract: comparison with conventional color Doppler imaging. J Ultrasound Med 15:63–66

Jain R, Sawhney S, Bhargava DK, Berry M (1995) Diagnosis of abdominal tuberculosis: sonographic findings in patients with early disease. AJR Am J Roentgenol 165:1391–1395

Kedar RP, Shah PP, Shivde RS, Malde HM (1994) Sonographic findings in gastrointestinal and peritoneal tuberculosis. Clin Radiol 49:24–29

Khaw KT, Yeoman LJ, Saverymuttu SH, Cook MG, Joseph AEA (1991) Ultrasonic patterns in inflammatory bowel disease. Clin Radiol 43:171–175

Lee DH, Lim JH, Ko YT, Yoon Y (1991) Sonographic findings in tuberculous peritonitis of wet-ascitic type. Clin Radiol 44:306–310

Lee DH, Ko YT, Yoon Y, Lim JH (1993) Sonographic findings of intestinal tuberculosis. J Ultrasound Med 12:537–540

Lim JH (2000) Ultrasound examination of gastrointestinal tract diseases. J Korean Med Sci 15:371–379

Lim JH, Ko YT, Lee DH, Lim JW, Kim TH (1994) Sonography of inflammatory bowel disease: findings and value in differential diagnosis. AJR Am J Roentgenol 163:343–347

Limberg B (1990) Sonographic features of colonic Crohn's disease: comparison of in vivo and in vitro studies. J Clin Ultrasound 18:161–166

Malik A, Saxena NC (2003) Ultrasound in abdominal tuberculosis. Abdom Imaging 28:574–579

Matsumoto T, Iida M, Sakai T, Kimura Y, Fujishima M (1991) Yersinia terminal ileitis: sonographic findings in eight patients. AJR Am J Roentgenol 156:965–967

Puylaert JBCM, Lalisang RI, van der Werf SDJ, Doornbos L (1988) Campylobacter ileocolitis mimicking acute appendicitis: differentiation with graded-compression US. Radiology 166:737–740

Puylaert JBCM, Kristjansdottir S, Golterman KL, de Jong GM, Knecht NM (1989) Typhoid fever: diagnosis by using sonography. AJR Am J Roentgenol 153:745–746

Reeder MM, Palmer PES (1989) Infections and infestations. In: Freeny PC, Stevenson GW (eds) Margulis, burhenne's alimentary tract radiology, 4th edn. Mosby, St. Louis, pp 1479–1481

Rosai J (2004) Rosai and Ackerman's surgical pathology, 9th edn. Mosby, Edinburgh, pp 793–794

Sarrazin J, Wilson SR (1996) Manifestations of Crohn disease at US. RadioGraphics 16:499–520

Teefey SA, Montana MA, Goldfogel GA, Shuman WP (1987) Sonographic diagnosis of neutropenic typhlitis. Am J Roentgenol 149:731–733

Teefey SA, Roarke MC, Brink JA et al (1996) Bowel wall thickening: differentiation of inflammation from ischemia with color Doppler and duplex US. Radiology 198:547–551

Wilson SR (1998) The gastrointestinal tract. In: Rumack CM, Wilson SR, Charboneau JW (eds) Diagnostic ultrasound, 2nd edn. Mosby, St. Louis, pp 279–327

Worlicek H, Lutz H, Heyer N, Matek W (1987) Ultrasound findings in Crohn's disease and ulcerative colitis: a prospective study. J Clin Ultrasound 15:153–163

Pseudomembranous Colitis

Etienne Danse and Daphne Geukens

Contents

Abstract

Pseudomembranous colitis (PMC) is a severe form of colitis frequently due to the toxins produced by *Clostridium difficile*, mainly due to antibiotic therapy. It is characterized by a wide spectrum of clinical manifestations: diarrhea, abdominal pain, fever, and leucocytosis. In patients with PMC, sonography may be required as first examination to rule out acute abdominal diseases. Specific sonographic findings related to PMC include pronounced colic wall thickening related to edema of the haustral folds and giving the "accordion sign" or a "gyral" pattern. The wall thickness ranges from 10 to 30 mm but the colic wall stratification is usually preserved. Reduced or absent mural flow is noted and ascites is present in 30–77 % of the cases. These signs allow the sonographic detection of the disease with a sensitivity of 78 % and a specificity of 94 %.

1 Introduction

Pseudomembranous colitis (PMC) is a severe form of colitis characterized by a wide spectrum of clinical manifestations, observed in poorly symptomatic or critically ill patients. PMC is included in the group of pseudomembranous enterocolitis (PMEC). This condition is defined as an affection of the intestine related to the presence of pseudomembranous covering the colic or the small bowel mucosal surface. The colon is the most frequently affected site but small bowel involvement is described alone or in association with the colon (Ros et al. 1996). PMC is most frequently due to the mucosal effect of the toxins produced by *Clostridium difficile*. Other unusual infectious agents have been considered as cause for a similar condition (*staphylococcus aureus*). The proliferation of Clostridium is due to antibiotic therapy, most frequently ampicillin, clindamycin, and cephalosporin. Erythromycin and tetracyclines have also been reported as causes of PMC. Diarrhea

E. Danse (✉)
Department of Radiology, Université Catholique de Louvain, St-Luc University Hospital, 10, Av Hippocrate, B-1200 Brussels, Belgium
e-mail: danse@rdgn.ucl.ac.be

D. Geukens
University Hospital Center, Charleroi, Belgium

G. Maconi and G. Bianchi Porro (eds.), *Ultrasound of the Gastrointestinal Tract*, Medical Radiology. Diagnostic Imaging,
DOI: 10.1007/174_2013_802, © Springer-Verlag Berlin Heidelberg 2013
Published Online: 14 February 2013

appears between 2 and 10 weeks after the beginning of the antibiotic treatment (Megibow et al. 1984). PMC is the so-called "antibiotic-associated diarrhea". PMC can also develop without *C. difficile* infection. In this setting, similar macroscopic colic wall changes are due to mucosal ischemia related to ischemic colitis, mechanical bowel obstruction, intestinal surgery, or chemotherapy (Ros et al. 1996).

Risk factors contributing to the development of PMC are: age (>60 years), previous surgical intervention, non-surgical gastrointestinal procedures, presence of a naso-gastric tube and enteral feeding, anti-ulcer medication, hospitalization in an intensive care unit, malignancies (lymphoma, leukemia), immunosuppression, transplantation, irradiation, pulmonary disease, severe cardiac disease, and heavy metal exposure (Ros et al. 1996; Cleary 1998; Dallal et al. 2002).

The mortality rate in patients having a *difficile* colitis is reported to be of 1.6–3.2 %, but these percentages can rise to 13.5 % when we take into account all causes of death for patients with the diagnosis of *C. difficile* colitis (Dallal et al. 2002).

The role of radiology in the management of PMC has to be considered in two fields. First, acute abdominal pain, fever, and leucocytosis are initial symptoms in patients with PMC. These clinical data can necessitate imaging studies, including usually sonography and/or computed tomography (CT). These imaging procedures are required to rule out acute abdominal diseases necessitating prompt therapy. Acute intestinal disorders are in the list of the diagnostic conditions that the radiologist has to look for during these imaging procedures performed in emergency situations (Ros et al. 1996). Therefore, the radiologist has to be prepared to detect suggestive radiological signs of PMC. Second, in patients with a confirmed diagnosis of PMC, cross-sectional imaging studies can contribute to the evaluation of the extension of the disease initially demonstrated with rectosigmoidoscopy. Sonography and/or CT can also be helpful for the recognition of complications including toxic megacolon, ischemia, abscesses, and perforation (Merine et al. 1987; Ros et al. 1996).

2 Microbiology

C. difficile is a Gram-positive bacteria, spore-forming, responsible for 15–20 % of the antibiotic-associated diarrheas (Hamrick et al. 1989; Eckel et al. 2002). The gold standard technique for the detection of *C. difficile* is the stool cytotoxin assay. The microbiological mechanism is related to the production of two toxins (toxins A and B) by *C. difficile* (Kyne et al. 2000). Disturbance of the normal bacterial flora in the colonic lumen is an important factor for the development of PMC (Ros et al. 1996). Children younger than 1 year develop symptomatic disease probably because of immature enterocyte membrane receptors for the toxin (Ros et al. 1996).

3 Clinical Manifestations

Clinical manifestations of PMC classically include watery or bloody diarrhea (Ros et al. 1996). The patients have moderate fever, abdominal cramps, leukocytosis, and hypoalbuminemia. Severe forms can cause electrolyte disturbances, dehydration, hypoalbuminemia (with anasarca), and even life-threatening conditions like toxic megacolon and perforation of the colon. Hypoalbuminemia is due to the rapid loss of protein in the gastrointestinal tract (Merine et al. 1987).

The diagnosis of PMC is based on endoscopy and stool assays. When the endoscopic findings are nonspecific, sonography or CT can show suggestive signs of PMC.

4 Endoscopy

Endoscopy is helpful for the diagnosis of PMC by showing typical raised yellowish-white plaques separated by areas of normal mucosa, edema, or erythema (Megibow et al. 1984). The plaques usually have a thickness of 2–10 mm. These plaques can be larger, extended, and are adherent to the mucosa (Ros et al. 1996). Epithelial necrosis, infiltration of the lamina propria with polymorphonuclear cells and eosinophilic exudates are histologically demonstrated. The "pseudomembrane" is composed of cellular debris, fibrin, mucous, and polymorphonuclear cells (Hamrick et al. 1989).

5 Imaging Study

5.1 Plain Films

Nonspecific abnormalities can be seen on plain films in patients having PMC. These findings include bowel dilatation, haustral fold thickening, thumbprinting, small bowel, and colonic ileus. Rare complications of the disease can be seen and include toxic megacolon and perforation (Merine et al. 1987; Ros et al. 1996).

5.2 Sonography

Suggestive findings of acute colitis can be detected during this examination by showing modification of colic wall thickness, which is considered thickened when the colic

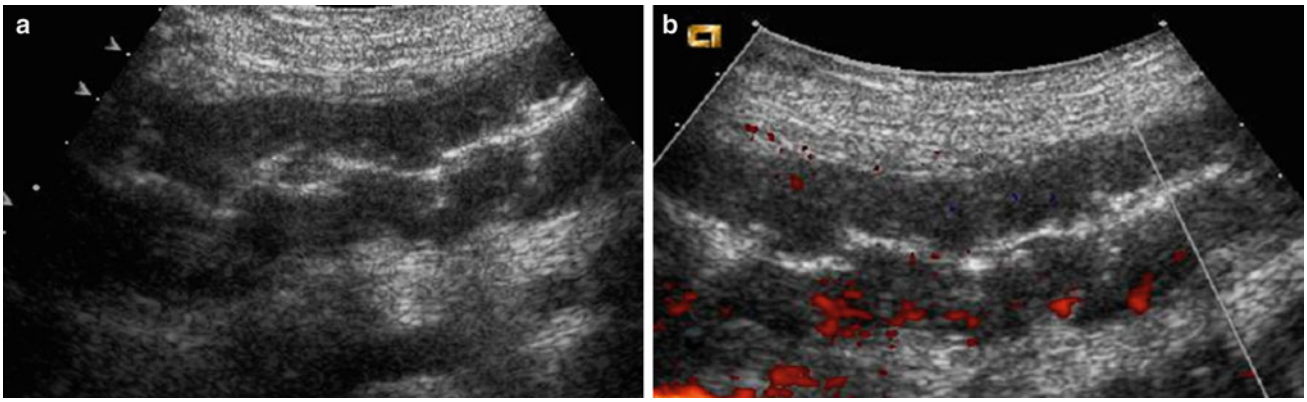

Fig. 1 Sagittal views of the *left colon* in a severe form of PMC. **a** B-mode sonogram showing hypoechoic, nodular and diffuse thickening of the haustral relief of the colic wall; **b** Discrete mural flow of the thickened colic wall is observed in the same patient when color Doppler evaluation is performed. On both images, there is a mild hyperechogenicity of the pericolic fat tissue

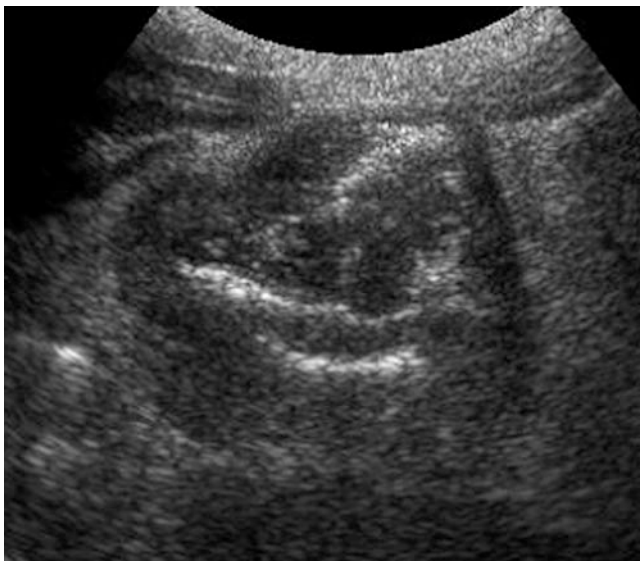

Fig. 2 PMC affecting the *right colon*. Transverse view on B-mode imaging showing the "accordion sign" related to edema of the haustral folds

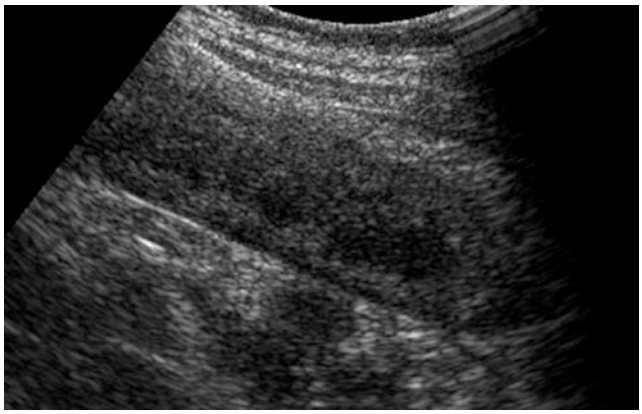

Fig. 3 PMC of the *right colon*. Thickening of the colic wall with preserved wall stratification

wall is thicker than 5 mm. Other colic wall changes due to acute colitis and detected with sonography include disappearance of the wall stratification (related to the severity of the disease whatever the type of colitis, infectious, ischemic or inflammatory colitis), increasing or absence of mural flow (in relation to the colic wall vascularization and its edema), and mural gas indicating pneumatosis (Danse et al. 2004, 2005) (Fig. 1). Ascites is also visible with sonography.

Specific sonographic findings related to PMC include pronounced colic wall thickening related to edema of the haustral folds and giving the "accordion sign" or a "gyral" pattern (Fig. 2) (O'Malley and Wilson 2003). The lumen of the colon is narrowed and the submucosa appears as congestive due to the acute inflammation of the colic wall (Frisoli et al. 2000; O'Malley and Wilson 2003). The wall thickness is ranging from 10 to 30 mm (mean 11 mm) (Downey and Wilson 1991; Truong et al. 1998). Despite the increased wall thickness, the colic wall stratification is usually preserved (Fig. 3) (Truong et al. 1998). Reduced or absent mural flow is noted and ascites is present in 30–77 % of the cases (Downey and Wilson 1991; Truong et al. 1998; Ledermann et al. 2000). Infiltration of the pericolic fatty tissue is noted in 50 % of the cases (Truong et al. 1998).

A prospective study evaluating sonography as a first line method for the detection of PMC has shown a sensitivity of this technique of 78 % for the diagnosis of PMC and a specificity of 94 % (Gallix et al. 1997). In this setting, relevant sonographic signs were the increased wall thickness, the hyperechoic thickening of the submucosa, and the presence of the "accordion sign". At the opposite, mural vascularization, pericolic wall changes, and presence of ascites were not demonstrated to significantly contribute for the positive sonographic diagnosis of PMC.

Table 1 Synoptic view of the main sonographic findings used for the differential diagnosis of acute diseases of the colon

	Localization	Thickness (mm)	Stratification	Mural flow (%)
Crohn colitis	Right colon	<13	Preserved	100
Ulcerative colitis	Left colon	<9	Preserved	100
PMC	Left colon	11	Absent / Preserved	–
Infection	Right colon	9	Preserved (apart neutropenic colitis)	90
Ischemic colitis	Left colon > Right colon	9	50 %	60
Malignancy	Anywhere	>12	20 %	80

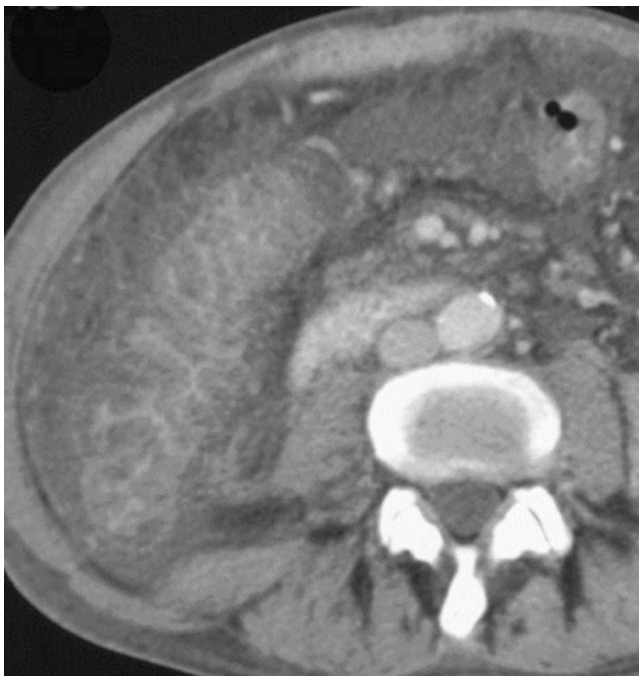

Fig. 4 CT of the abdomen in a case of PMC showing the "accordion sign", due to contrast trapping between thickened haustral folds. In this case, pericolic fat stranding and ascites are also visible

PMC can be differentiated from other colitides (ischemic colitis and inflammatory colitis) when colic wall changes are evaluated. These sonographic colic wall changes include the wall thickness, the presence of wall stratification, detection of mural flow, the visualization of the haustration, and the localization of the disease along the colon (Table 1) (Truong et al. 1998; Danse et al. 2004, 2005).

In comparison with PMC, which is more frequently seen on the left colon, acute forms of Crohn's disease have a predisposition for the right colon, are associated to a wall thickness lower than 13 mm, have a preserved stratification, with visualization of the haustral folds and an increased mural flow when color Doppler study of the colic wall is performed.

Acute forms of ulcerative colitis are more frequently observed on the left side of the colon, with a mild wall thickness (<9 mm), a preserved stratification, and an increased mural flow. Infectious colitis is more frequently detected on the right colon together with limited or extended involvement of the distal small bowel. The colic thickness is usually lower than 9 mm. Preserved stratification is noted as well as the persistence of the haustral relief. Mural flow is present in 90 % of the cases. Ischemic colitis is most frequently detected on the left colon but can affect any part of the colon. Wall thickness of ischemic colitis is in the same range as that in PMC (11–12 mm) (Truong et al. 1998; Danse et al. 2000, 2004). Stratification is present in 50 % of the patients; disappearance of haustral folds is the rule. Absence of mural flow is noted in 60 % of the cases. Disappearance of the stratification and absence of flow in the colic wall are related to the severity of the disease (Danse et al. 2000, 2004). Malignancy of the colon is related to pronounced colic wall thickening (higher than 12 mm) (Truong et al. 1998, 2004). The wall thickening has a limited extension (on a length lower than 10 cm). Preservation of the stratification is noted in only 20 % of the cases and mural flow is visible in 80 % of the cases (Danse et al. 2004).

5.3 Computed Tomography

The diagnosis of PMC can be suggested with CT. As with sonography, there is a need for further examinations to confirm the diagnosis (Megibow et al. 1984; Merine et al. 1987; Hamrick et al. 1989; Blickman et al. 1995; Wilcox et al. 1995). CT signs of PMC include pronounced hypodense or heterogeneous colic wall thickening (ranging from 3 to 32 mm) (Ros et al. 1996). Wall nodularity combined with the entrapment of contrast medium within the thickened haustra is leading to the "accordion sign" (Ros et al. 1996) (Fig. 4). This latter CT sign was presented as specific for PMC but it has been described as a nonspecific colic wall edema, observed in severe Crohn's disease, infectious or ischemic colitis, or in colic wall congestion related to cirrhosis (Macari et al. 1999; Mountanos and Manolakakis 2001). Ascites is noted in 20–57 % of the patients, as well as pericolic stranding.

References

Blickman JG, Boland GWL, Cleveland RH, Bramson RT, Lee MJ (1995) Pseudomembranous colitis: CT findings in children. Pediatr Radiol 25:S157–S159

Cleary RK (1998) Clostridium difficile-associated diarrhea and colitis. Dis Colon Rectum 41:1435–1449

Dallal RM, Harbrecht BG, Boujoukas AJ et al (2002) Fulminant clostridium difficile: an underappreciated and increasing cause of death and complications. Ann Surg 235:363–372

Danse E, Van Beers BE, Jamart J et al (2000) Prognosis of ischemic colitis: comparison of color Doppler sonography with early clinical and laboratory findings. AJR Am J Roentgenol 175:1151–1154

Danse E, Jamart J, Hoang P, Laterre PF, Kartheuser A, Van Beers BE (2004) Focal bowel wall changes detected with colour Doppler ultrasound: diagnostic value in acute non-diverticular diseases of the colon. Br J Radiol 77:917–921

Danse E, Dewit O, Goncette L, Sempoux C, Kartheuser A, Van Beers B (2005) Que faire en cas d'affection aiguë du colon? Une échographie, un scanner, des clichés conventionnels ou une endoscopie? SFR Paris Octobre Formation Médicale Continue 23:241–253

Downey DB, Wilson SR (1991) Pseudomembranous colitis: sonographic features. Radiology 180:61–64

Eckel F, Huber W, Weiss W, Lersch C (2002) Recurrent pseudomembranous colitis as a course of recurrent severe sepsis. Z Gastroenterol 40:255–258

Frisoli JK, Desser TS, Jeffrey RB (2000) A sonographic sign of acute gastrointestinal abnormality representing submucosal oedema or haemorrhage. AJR Am J Roentgenol 175:1595–1599

Gallix B, Atri M, Bret P (1997) Evaluation prospective de l'échographie haute résolution pour le diagnostic des colites pseudomembraneuses (CPM). J Radiol 78:S877

Hamrick KM, Tishler JM, Schwartz ML, Koslin DB, Han SY (1989) The CT findings in pseudomembranous colitis. Comput Med Imaging Graph 13:343–346

Kyne L, Warny M, Qamar A, Kelly CP (2000) Asymptomatic carriage of Clostridium difficile and serum levels of IgG antibody against toxin. N Eng J Med 342:390–397

Ledermann HP, Börner N, Strunk H et al (2000) Bowel wall thickening on transabdominal sonography. AJR Am J Roentgenol 174:107–117

Macari M, Balthazar EJ, Megibow AJ (1999) The accordion sign at CT: non specific finding in patients with colonic edema. Radiology 211:743–746

Megibow AJ, Streiter ML, Balthazar EJ, Bosniak MA (1984) Pseudomembranous colitis: diagnosis by computed tomography. J Computed Assist Tomogr 8:281–283

Merine D, Fishman EK, Jones B (1987) Pseudomembranous colitis: CT evaluation. J Comput Assist Tomogr 11:1017–1020

Mountanos GI, Manolakakis IS (2001) The accordion sign at CT: report of a case of Crohn' disease with diffuse colonic involvement. Eur Radiol 11:1433–1434

O'Malley ME, Wilson SR (2003) US of gastrointestinal tract abnormalities with CT correlation. Radiographics 23:59–72

Ros PR, Buetow PC, Pantograg-Brown L, Forsmark CE, Sobin LH (1996) Pseudomembranous colitis. Radiology 198:1–9

Truong M, Atri P, Bret P et al (1998) Sonographic appearance of benign and malignant conditions of the colon. AJR Am J Roentgenol 170:1451–1455

Wilcox MC, Gryboski D, Fernandez M, Stahl W (1995) Computed tomographic findings in pseudomembranous colitis: an important clue to the diagnosis. South Med J 88:929–933

Amoebic, Ascariasis and Other Parasitic Enteritis

S. Boopathy Vijayaraghavan

Contents

Abstract

Parasitic infections of the GastroIntestinal tract and infectious enteritis are common clinical conditions. Most of them present with abdominal pain and hence sonography is requested. In this chapter sonographic features of these conditions are described.

1 Amoebiasis

Amoebiasis is a disease caused by infection with a unicellular parasite *Entamoeba histolytica*. It is most common in people living in developing counties of tropical and subtropical regions in areas with poor sanitary conditions. The main source of infection is the cyst-passing chronic patient or asymptomatic carrier. The cyst reaches humans through contaminated water and vegetables. The cyst, which is resistant to the acidic digestive juices of the stomach, passes to the lower part of the small intestine. There, under the influence of the neutral or alkaline juices, the cyst wall disintegrates, liberating a metacystic amoeba. They move downward to the large intestine. The lesions produced are primary intestinal and secondary extra intestinal. The most frequent primary sites are the caecal and sigmoidorectal regions (Neva and Brown 1994). As the infection progresses, additional colonic sites of invasion develop. The severity of the disease depends on (a) the resistance of the host, (b) the virulence and invasiveness of the amoebic strain and (c) the condition in the intestinal tract. The early lesion is a tiny area of necrosis in the superficial mucosa or a small nodular elevation with a minute opening that leads to a flask-shaped cavity containing cytolysed cells, mucus and amoebas. There is rapid lateral and downward extension of the ulcerative process to both superficial and deep layers of the intestine. Eventually, the mucosa may slough off, exposing large necrotic areas (Neva and Brown 1994). The complications of intestinal amoebiasis include granuloma, appendicitis, perforation, haemorrhage and stricture. Amoebic granulomas

S. Boopathy Vijayaraghavan (✉)
SONOSCAN: Ultrasonic Scan Centre,
15B Venkatachalam Road, Coimbatore,
Tamilnadu 641002, India
e-mail: sonoscan@vsnl.com

G. Maconi and G. Bianchi Porro (eds.), *Ultrasound of the Gastrointestinal Tract*, Medical Radiology. Diagnostic Imaging,
DOI: 10.1007/174_2012_662,
Published Online: 14 July 2012

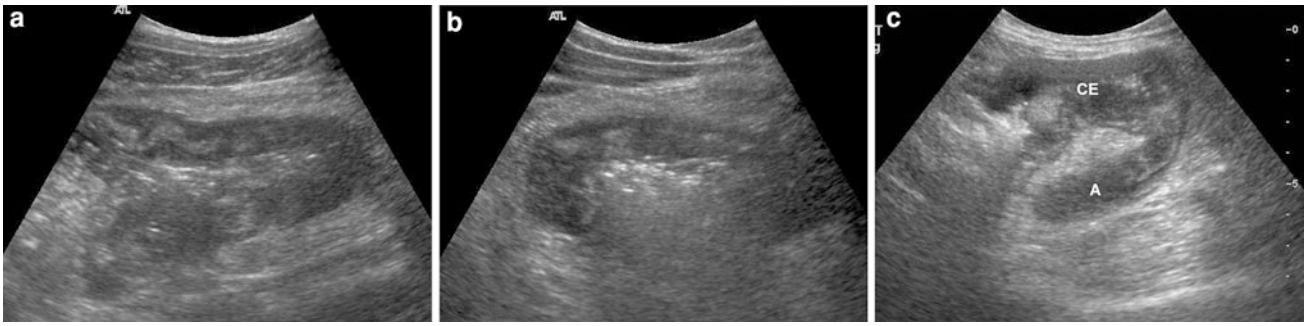

Fig. 1 **a** Longitudinal and **b** transverse scans of *right* iliac fossa showing asymmetric thickening of walls of the caecum, suggestive of amoeboma in a patient with amoebic liver abscess. **c** Non-tender thickening of appendix (*A*) in amoebiasis. Cecal walls are also slightly thickened (*CE*)

(amoeboma) are firm, painful, nodular, inflammatory thickening of the intestinal wall around ulcers. It occurs most commonly in caecum and rarely in the sigmoid colon. Perforation occurs most frequently in the caecum. Erosion of a large blood vessel may produce a massive haemorrhage. Very occasionally, rectal amoebiasis can lead to anorectal abscesses or perianal fistulas. In acute intestinal amoebiasis, there is severe dysentery with numerous small stools containing blood, mucus and necrotic mucosa, accompanied by acute abdominal pain, tenderness and fever. Chronic amoebiasis is characterised by recurrent attacks of dysentery.

The diagnosis of amoebiasis rests upon the identification of the parasite in the faeces or tissues and upon serological studies. On sonography, acute amoebic dysentery is seen as a tender asymmetrically thick-walled caecum. Nonvisualisation of a thickened appendix differentiates it from acute appendicitis. Amoebic granuloma (amoeboma) of caecum or colon is seen as an asymmetrically thick-walled segment of bowel measuring about 8–17 mm in thickness (Hussain and Dinshaw 1990). On transverse scan, there is target, doughnut or pseudo kidney appearance (Fig. 1a, b). This appearance is nonspecific. There are no distinctive sonographic features to differentiate amoeboma from Crohn's disease or ulcerative colitis. A concomitant liver abscess strongly suggests an amoebic aetiology. Rarely, amoebiasis of appendix is seen as an enlarged non-tender appendix, either as an isolated finding, or along with amoeboma of the caecum (Fig. 1c; Oran 2000). Perforation of bowel, essentially the caecum, occurs occasionally in virulent amoebiasis. This results in a retroperitoneal abscess containing air in relation to caecum and ascending colon that is similar to an appendicular abscess in the same location.

2 Ascariasis

Ascariasis is the infestation of the humans with the round worm, *Ascaris Lumbricoides*. The adult worms normally live in the lumen of the small bowel of an infected individual. The eggs of the worm are passed in the faeces of these individuals and can contaminate water or food. Humans become infected when they ingest contaminated water or food. Gastric juices cause the eggs to hatch in the small bowel. The larvae penetrate the intestinal wall to enter the blood stream and reach the lungs. They migrate, or are carried by the bronchioles to bronchi, ascend the trachea to the glottis and pass down the oesophagus to the small intestine (Neva and Brown 1994). Ascariasis is worldwide in distribution and is more common in warm countries and is most prevalent where sanitation is poor. It occurs at all ages, but it is most prevalent in children aged 5–9 years. The incidence is approximately the same in both sexes. The usual infection consists of 5–10 worms and often goes unnoticed by the host. The most frequent complaint of patients with ascariasis is vague abdominal pain. When the infestation is heavy, a bolus of worms may cause serious complications such as intestinal obstruction (Malde and Chadha 1993; Wasadikar and Kulkarni 1997; Mahmood et al. 2001), perforation (Hangloo et al. 1990; Chawla et al. 2003), intussusception (Villamizar et al. 1996) or volvulus (Rodriguez et al. 2003). The prognosis of these complications depends on prompt diagnosis and treatment. Delay in diagnosis may give rise to small bowel gangrene. Clinical findings in such cases are those of the complications, which are acute pain in the abdomen, vomiting or signs of peritonitis.

On sonography, the appearance of the round worms varies with the frequency of transducer used. When the recent high-resolution probes are used, the ascaris worm is seen as a chord of four echogenic lines in longitudinal scans (Fig. 2a, b). These lines represent the reflections from the external walls of the worm and the walls of alimentary tract of the worm (Mahmood et al. 2001). Sometimes the alimentary canal appears echogenic when it is filled with air (Fig. 2c). In cross-section it appears like a small doughnut (Fig. 2d). It is clearly visible if there is fluid around the worm. On low-frequency scans, it is seen as two parallel lines on longitudinal scan (Fig. 2e) and a circle on transverse scan. On real-time scan, the worm shows non-directed curling movement.

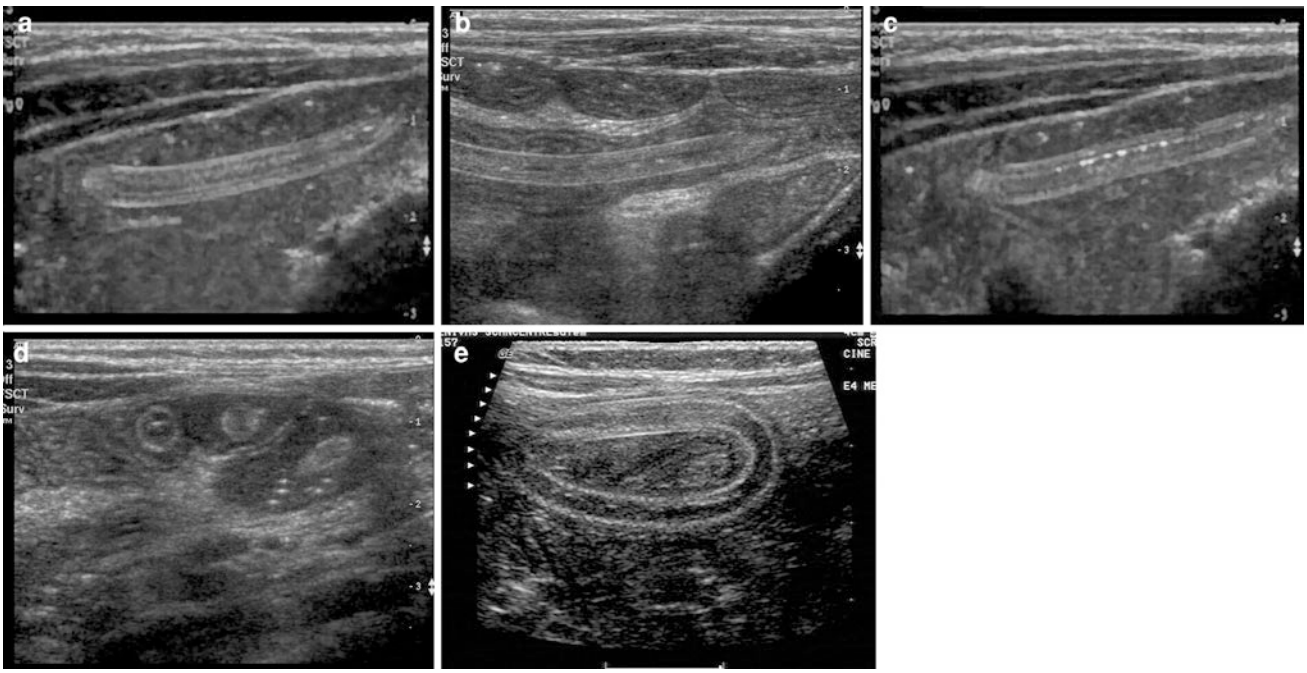

Fig. 2 Sonographic appearance of the ascaris worm. Longitudinal scan of the worm showing the 4-line appearance in (**a**), hypoechoic fluid-filled alimentary tract of the worm in (**b**) and air-filled echogenic alimentary tract in (**c**). **d** Transverse scan of multiple worms showing the small doughnut appearance. **e** On low-frequency scan the worm is seen as two *parallel lines*

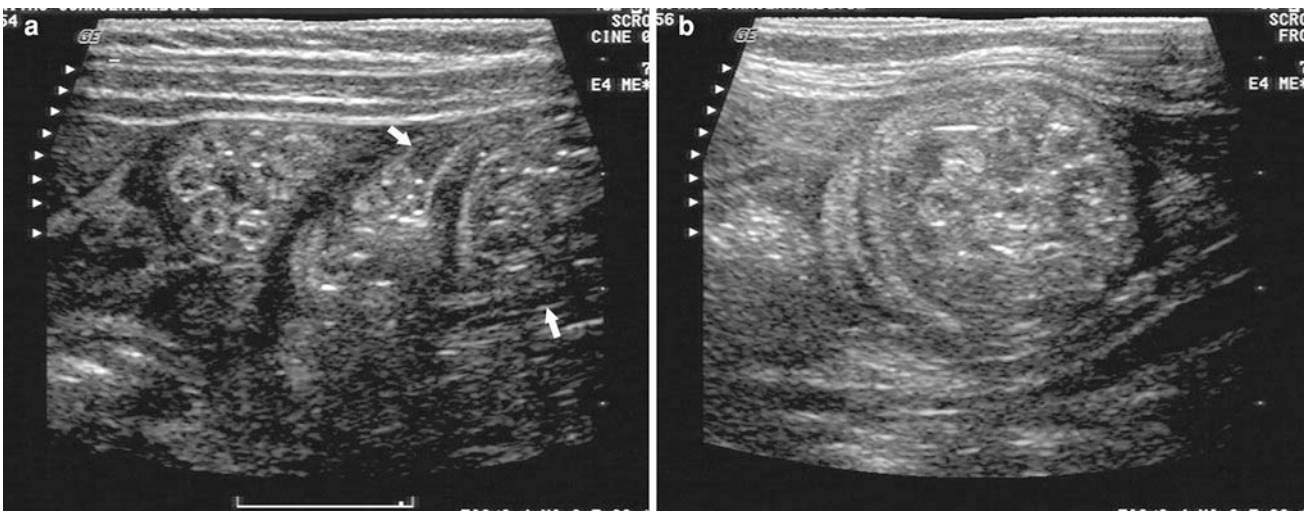

Fig. 3 **a** Longitudinal scans at the site of bowel obstruction showing the spaghetti appearance of curled up worms; **b** transverse scan of the same region shows the "shack of cigars" appearance of cross-section of multiple worms. (Courtesy of Dr. R. Subramaniam, DMRD, Sreenivas Ultrasound Scan Centre, Salem, India)

In the presence of small bowel obstruction due to a ball of worms, sonography shows signs of small bowel obstruction, namely, dilated small bowel loops with peristalsis. At the site of obstruction the ball of worms, or helminthoma, appears like spaghetti on longitudinal scan (Fig. 3a) and a "shack of cigars" on transverse scan (Fig. 3b; Malde and Chadha 1993; Wasadikar and Kulkarni 1997). Sonography is useful in the follow-up of these patients after initiating the treatment. It can reveal resolution of the obstruction or occurrence of other complications, such as volvulus or ischaemia of the bowel. In volvulus and ischaemia of the small bowel due to ascariasis, sonography shows multiple loops of unusually dilated, aperistaltic small bowel, containing the ascaris worms with the classical appearance and movement. There is free fluid in

the peritoneal cavity. The walls of the bowel are thickened (Rodriguez et al. 2003). Perforation of the bowel due to ascariasis can very occasionally occur because of direct pressure and irritation of the bowel wall by impacted ascaridial masses, leading to ulceration, necrosis and perforation. Lytic secretion from ascarides probably also plays a role (Hangloo et al. 1990). In perforation, sonography reveals live ascaris worms moving freely within the extraluminal fluid (Chawla et al. 2003). Very rarely, ascariasis worm can enter the appendix and cause appendicitis (Misra et al. 1999).

3 Trichuriasis

Trichuriasis is infestation with the whipworm *Trichuris Trichiura*. Man is the principal host. Infection results from ingestion of embryonated eggs via hands, food or drink that have been contaminated by infested soil. When humans ingest the embryonated egg, the activated larva escapes in the upper small bowel. It penetrates a villus and remains there for 3–10 days. Then it passes downward to caecum, where it usually remains. The worms are also found in terminal ileum and appendix. Patients with light infection are asymptomatic. Patients with very heavy chronic infection present a characteristic clinical picture consisting of: (a) frequent, small, blood streaked diarrhoeal stools, (b) abdominal pain, (c) nausea and vomiting, (d) anaemia and (e) weight loss. *Trichuris* worm may attach itself to the appendiceal mucosa and provide a ground for secondary bacterial infection resulting in acute and subacute appendicitis (Neva and Brown 1994). On sonography, a thick-walled fluid-distended appendix is seen with the motile worms present in the lumen (video 1).

4 Oesophagostomiasis

Oesophagostomiasis is infestation with *Oesophagostomum bifurcum*, a human parasitic intestinal helminth. It is endemic in parts of West Africa (Polderman et al. 1991, 1999). *Oesophagostomum bifurcum* juveniles develop in the colonic wall causing pus-filled granulomas (Storey et al. 2000). Many people appear to tolerate this histotropic developmental phase of the worm's life cycle; however, there are two distinct clinical presentations of the pathology. Multinodular *Oesophagostomiasis bifurcum* comprises hundreds of pea-sized nodules in the thickened oedematous submucosa and subserosa of the colonic wall. These patients present with weight loss, persistent mucosal diarrhea, diffuse abdominal pain and occasionally rectal bleeding. Urgent surgery may be required for luminal narrowing of the colon or bowel obstructions secondary to inflammatory adhesions (Anthony and Mcadam 1972).

The Dapaong tumor, the uninodular form of the disease, presents as a painful ligneous mass of 30–60 mm in the abdominal wall or within the abdominal cavity (Pages et al. 1988). It is usually associated with fever. This can lead to cutaneous abscess and fistula, peritonitis due to rupture of nodule, obstruction of bowel due to adhesion and volvulus. Clinical symptoms are often vague and indeterminate. They mimic a lot of other conditions (Storey et al. 2001).

Sonography shows a long segment of thick-walled right colon displaying target or pseudo kidney appearance. This is a non-specific appearance seen in most of the colonic pathologies. However, the presence of a distinct nodularity within the thick wall of the colon helps to differentiate it from other conditions in a patient in an endemic area. The Dapaong tumor is seen on sonography as a hypoechoic oval lesion, with a well-defined poorly reflective wall in the abdominal wall, or within the abdomen (Storey et al. 2000).

References

Anthony PP, McAdam IW (1972) Helminthic pseudotumours of the bowel: thirty-four cases of helminthoma. Gut 13:8–16

Chawla A, Patwardhan V, Maheshwari M, Wasnik A (2003) Primary ascaridial perforation of the small intestine: sonographic diagnosis. J Clin Ultrasound 31:211–213

Hangloo VK, Koul I, Safaya R et al (1990) Primary ascaridial perforations of small intestine and Meckel's diverticulum. Indian J Gastroenterol 9:287

Hussain S, Dinshaw H (1990) Ultrasonography in amebic colitis. J Ultrasound Med 9:385–388

Mahmood T, Mansoor N, Quraishy S, Ilyas M, Hussain S (2001) Ultrasonographic appearance of *Ascaris lumbricoides* in the small bowel. J Ultrasound Med 20:269–274

Malde HM, Chadha D (1993) Roundworm obstruction: sonographic diagnosis. Abdom Imaging 18:274–276

Misra SP, Dwivedi M, Misra V, Singh PA, Agarwal VK (1999) Preoperative sonographic diagnosis of acute appendicitis caused by *Ascaris lumbricoides*. J Clin Ultrasound 27:96–97

Neva FA, Brown HW (1994) Basical clinical parasitology, 6th edn. Appleton & Lange, Norwalk

Oran I (2000) Transient appendiceal enlargement in a patient with colonic amebiasis: sonographic detection and follow-up. J Clin Ultrasound 28:368–370

Pages A, Kpodzro K, Boeta S, Akpo-Allavo K (1988) Dapaong "tumor". Helminthiasis caused by Oesophagostomum. Ann Pathol 8:332–335

Polderman AM, Krepel HP, Baeta S, Blotkamp J, Gigase P (1991) Oesophagostomiasis, a common infection of man in northern Togo and Ghana. Am J Trop Med Hyg 44:336–344

Polderman AM, Anemana SD, Asigri V (1999) Human oesophagostomiasis: a regional public health problem in Africa. Parasitol Today 15:129–130

Rodriguez EJ, Gama MA, Ornstein SM, Anderson WD (2003) Ascariasis causing small bowel volvulus. Radiographics 23: 1291–1293

Storey PA, Anemana S, van Oostayen JA, Polderman AM, Magnussen P (2000) Ultrasound diagnosis of oesophagostomiasis. Br J Radiol 73:328–332

Storey PA, Faile G, Crawley D, van Oostayen JA, Anemana S, Polderman AM, Magnussen P (2001) Ultrasound appearance of

preclinical Oesophagostomum bifurcum induced colonic pathology. Gut 48:565–566

Villamizar E, Mendez M, Bonilla E, Varon H, de Onatra S (1996) *Ascaris lumbricoides* infestation as a cause of intestinal obstruction in children: experience with 87 cases. J Pediatr Surg 31:201–204; discussion 204–205

Wasadikar PP, Kulkarni AB (1997) Intestinal obstruction due to ascariasis. Br J Surg 84:410–412

Part IV

Neoplasm

Colorectal Cancer

Giovanni Maconi and Elena Bolzacchini

Contents

Abstract

Colorectal cancer is a major cause of morbidity and mortality in Western countries. Computed tomography (CT) colonography and conventional colonoscopy are the procedures of choice for the diagnosis. However, sonography, being the first imaging study in patients with aspecific abdominal symptoms, may detect unexpected abdominal tumors. The main sonographic features of colorectal cancer are a short segment with bowel wall thickening or a focal mass of the colon, usually with hypoechoic echo pattern and with irregular margins. The detection of these ultrasonographic signs can lead to prompt appropriate investigations and speedup the diagnostic process.

1 Introduction

Colorectal cancer is a major cause of morbidity and mortality in Western countries. Although screening has reduced the possibility of dying from colorectal cancer, it remains the fourth most commonly diagnosed cancer in the world.

Colonoscopy is the gold standard screening method for colorectal cancer and it is still the conventional procedure to obtain the histological diagnosis. Computed tomography (CT) colonography, given its high sensitivity and specificity in particular when cathartic and tagging agents are combined in bowel preparation, may also be a useful screening method for colorectal cancer in populations with a low prevalence of the disease.

Sonography is often the first imaging study in patients with aspecific abdominal symptoms, such as changes in bowel habit, abdominal pain or discomfort, weight loss, fever, nausea or vomiting, and those with suspected abdominal masses or alteration of liver function tests (Speets et al. 2006; Grubel 2011; Maconi et al. 2011). All these conditions may be the presenting features of colorectal cancer, depending on the location and stage of the tumor. The increasing use of sonography as an initial

G. Maconi (✉) · E. Bolzacchini
Gastroenterology Unit, Department of Biomedical and Clinical Sciences, "L. Sacco" University Hospital, Via G.B. Grassi 74, 20157, Milan, Italy
e-mail: giovanni.maconi@unimi.it

G. Maconi and G. Bianchi Porro (eds.), *Ultrasound of the Gastrointestinal Tract*, Medical Radiology. Diagnostic Imaging,
DOI: 10.1007/174_2013_801, © Springer-Verlag Berlin Heidelberg 2013
Published Online: 16 February 2013

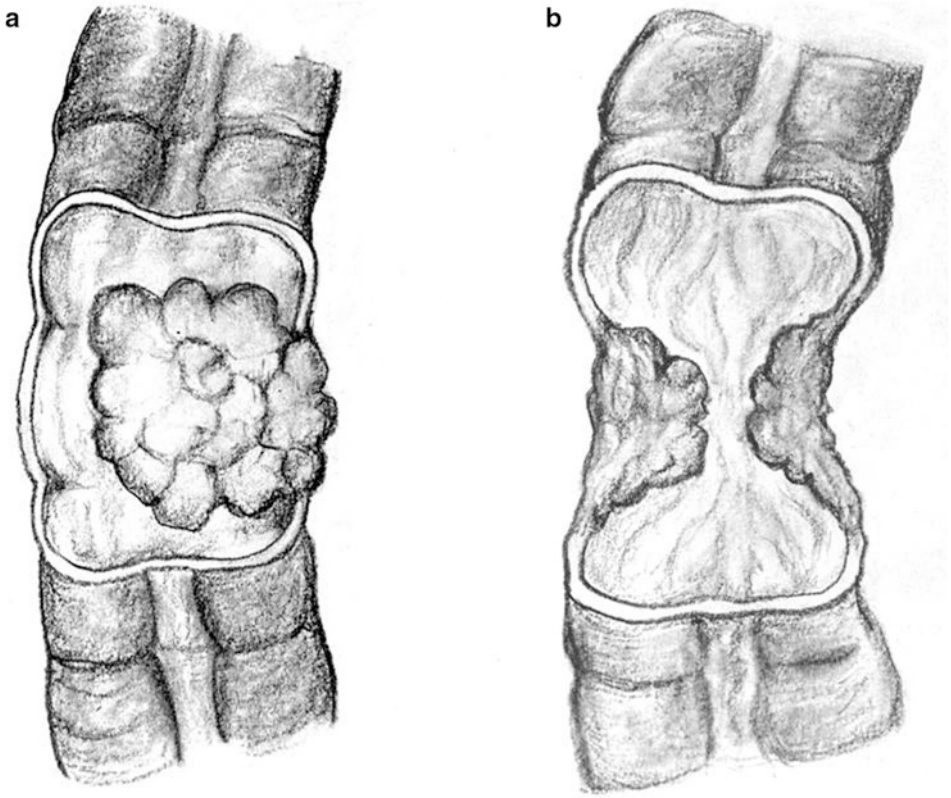

Fig. 1 Schematic drawing of two types of colorectal cancer. **a** Mass-forming colorectal cancer. **b** Short segmental wall thickening

evaluation in patients with these complaints, in particular elderly patients and in those not included in a colonoscopy screening program, may detect unexpected abdominal tumors (Schwerk et al. 1979; Price and Metreweli 1988; Rutgeerts et al. 1991). Abdominal sonography may also reveal colon cancers during the work-up of anemia and in patients with liver metastasis. In these cases sonographic examination can show a focal mass or bowel wall thickening of the colon and rectum, which can lead to prompt further investigations such as colonoscopy or CT colonography, to confirm the diagnosis.

2 Pathology

Colorectal cancer is characterized by a protruding mass or segmental thickening of the wall of the colon. Cancers on the right side (ascending colon and cecum) tend to be exophytic, so the tumor grows outwards from one location in the bowel wall and protrudes into the intestinal lumen. Cancer on this side is often ulcerated and characterized by occult bleeding and anemia. Very rarely cancer in the right colon causes obstruction, unless the mass involves the ileocecal valve. In these cases patients may present with abdominal pain because of bowel obstruction. Left-sided tumors tend to be circumferential, and can obstruct the bowel like a napkin ring (Fig. 1)

Adjacent lymph node involvement is frequent and the liver is the most frequent site of distant metastasis.

3 Sonographic Findings of Colon Cancer

Sonographic features of colorectal cancer reflect its macroscopic pathology. Colorectal carcinoma classically appears as segmental thickening or as a bulky mass of the colonic wall with heterogeneous low echogenicity (Lim 1996).

Segmental wall thickening is usually short and asymmetric, eccentric or circumferential, with irregular contours (Fig. 2). This type of cancer is more frequently found in the left colon, where it determines narrowing of the lumen up to colonic obstruction. In this context, the lumen usually does not contain feces, but a small amount of gas, which may be also observed in the proximal pre-stenotic tract of the colon. Indeed, pre-stenotic tract may contain a large amount of fecal and gaseous content that may make the evaluation of the colonic walls more difficult (Fig. 3).

The mass involving the colonic wall is more frequently found in the right colon. It may be variable in size, hypoechoic, and with irregular contours (Fig. 4). Often high echoes denoting intraluminal gas and feces may be visible within the mass, so that it appears as a "pseudokidney" (Fig. 5).

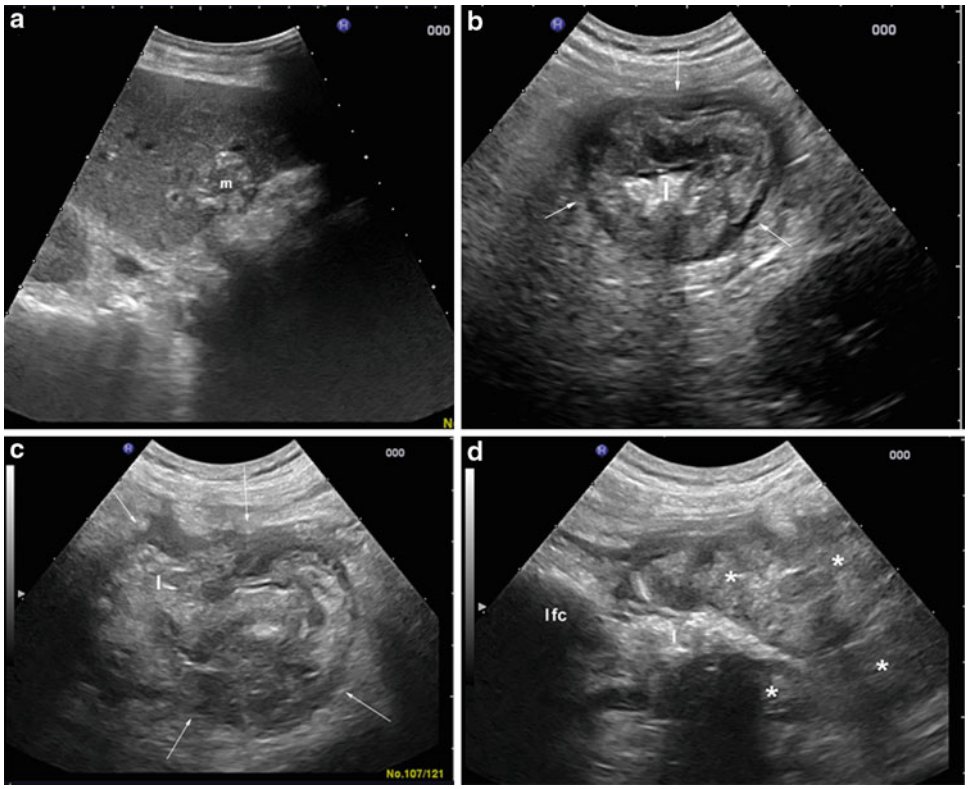

Fig. 2 Abdominal and intestinal ultrasound in a 76-year-old man presenting with alteration of liver function tests and abdominal discomfort. The abdominal ultrasound showed a solid lesion of the liver (*m*) suspected for metastasis from colorectal cancer (**a**). The following examination of the bowel, showed a lesion highly suspected for a carcinoma of sigmoid colon. In particular, transversal (**b, c**) and longitudinal (**d**) scans showed a segmental and asymmetric wall thickening (*asterisks*), with hypoechoic and dishomogeneous echo pattern. The bowel lesion showed was also characterized by irregular contours (*arrows*) with narrowing of the lumen (*l*) and prestenotic dilatation with solid fecal content (*l fc*)

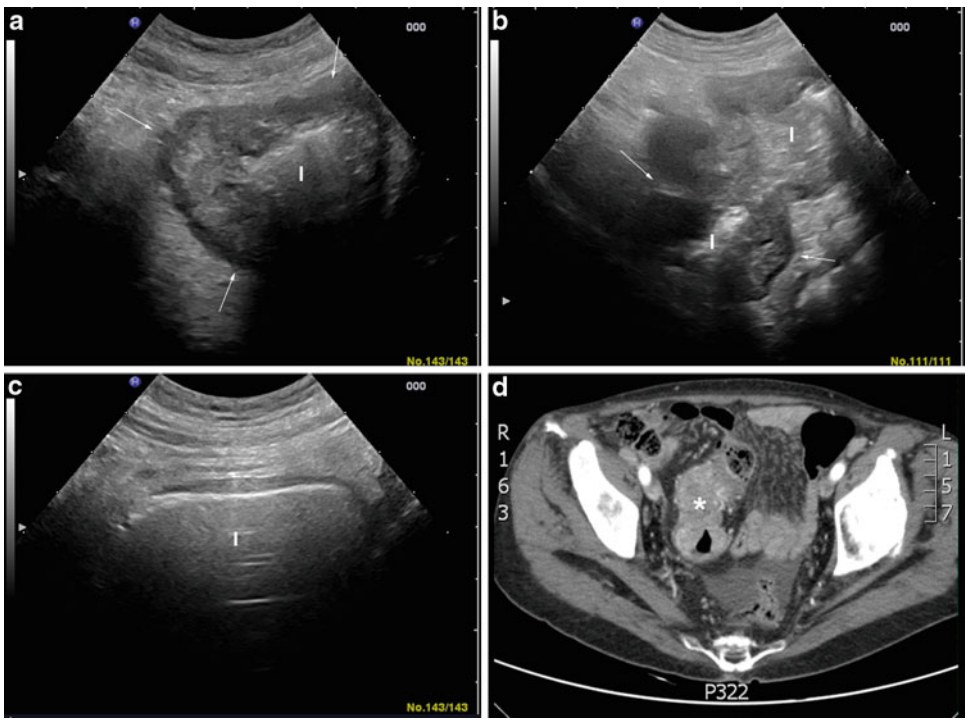

Fig. 3 Sonographic aspect of a carcinoma of sigmoid colon. **a** Transversal scan shows a short segmental and asymmetric wall thickening with hypoechoic echo pattern (*arrows*); **b** longitudinal and **c** transversal scans showing the irregularity and the length of narrowed lumen (*l*) and the dilatation of the prestenotic segment (*l*), where fecal and gaseous content makes the evaluation of the colonic walls more difficult. **d** The same lesion detected by CT scan (*asterisk*)

The wall thickening with abrupt segmental loss of wall layer stratification and disappearance of haustra coli may be features of malignancy (Kuzmich et al. 2009) (Fig. 6; Video). Colonic wall may also show increased vascularity at color Doppler (Fig. 7). However, these signs are not specific, as they can also be observed in inflammatory diseases or colonic ischaemia (Lim 1996; Shirahama et al. 1994). Adjacent regional roundish hypoechoic lymphadenopathies should also be searched for because their presence may reinforce the suspicion of malignancy.

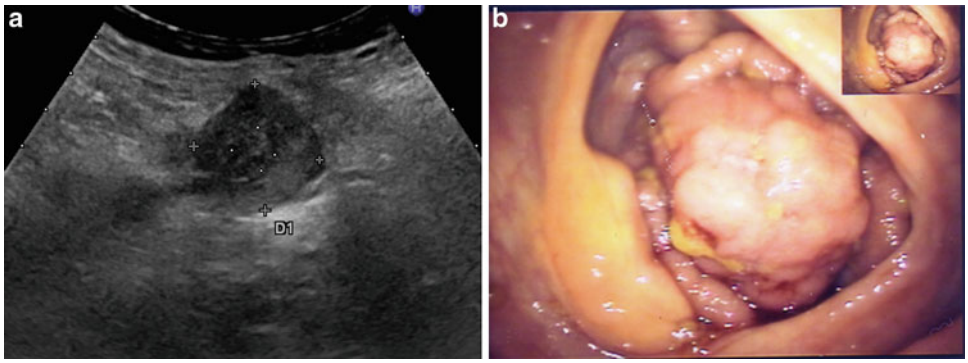

Fig. 4 Mass forming cancer of the cecum. **a** Ultrasound scan shows a well-defined, irregular mass (diameter 3 cm), representing an adenocarcinoma of the cecum. **b** The same lesion detected by colonoscopy

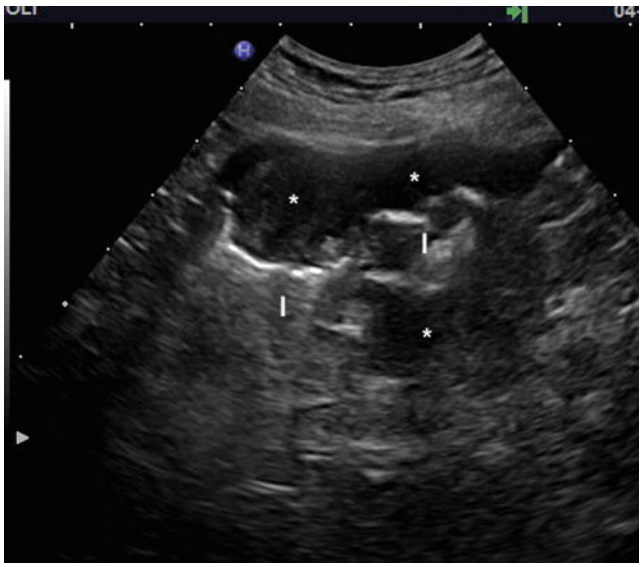

Fig. 5 Sonographic aspect of a carcinoma of ascending colon. Transversal scan shows a segmental and asymmetric wall thickening (*asterisks*) with hypoechoic echo pattern also called as "pseudokidney sign". High echoes denoting intraluminal gas and feces may be visible within the mass (*l*)

Sonography of the liver should be performed as well to assess the presence of metastasis when a colorectal cancer is detected or suspected.

However, it should be kept in mind that the absence of these findings at sonography does not exclude the diagnosis of colonic carcinoma. Small cancers and polyps can be overlooked, and the suboptimal diagnostic quality of the scan—due to bowel gas or obesity—can lead to false-negative results. On account of these limitations sonography is not an effective technique of screening for colonic cancer.

Several studies have evaluated the accuracy of transabdominal ultrasound in detecting colorectal cancer. Most of these studies showed that ultrasound detects accurately advanced colorectal tumors, included those causing colonic obstruction, but misses small cancers and polypoid lesions (Price and Metreweli 1988; Rutgeerts et al. 1991; Richardson et al. 1998; Grunshaw et al. 2000; Martínez-Ares et al. 2005; Gluvic et al. 2008). This has also been shown using transabdominal hydrocolonic sonography, namely the assessment of the colonic walls after bowel preparation with laxatives and following instillation of water into the colon (see "Oral Contrast-Enhanced Bowel Ultrasound"). Eleven studies have assessed the accuracy of hydrocolonic sonography in detecting colorectal cancer showing a mean sensitivity of 90 % (range 0–97 %). High sensitivity has also been reported in assessing the T stage of colorectal cancer (mean, 85.2 %), but more than 80 % of these lesions were in an advanced stage (T3 or T4). On the contrary, the sensitivity of this technique in assessing the N stage of the tumour and polyps was much more disappointing (Maconi et al. 2009).

4 Transrectal Sonography

Accurate staging of rectal and anal carcinoma is crucial for planning surgery and indicating adjuvant therapy. The extension of the tumor can be evaluated with transrectal sonography, CT, and magnetic resonance imaging (MRI) (Zagoria et al. 1997; Gualdi et al. 2000).

Transrectal sonography and endorectal coil MRI imaging are superior to CT in evaluating tumor depth through the wall, local extension, and lymph nodes.

Transrectal sonography can be performed with either blind and rigid probes or flexible echoendoscopes. The rigid probes have limitations in imaging tumors located 8–10 cm above the anal verge.

The procedure, with both instruments, needs rectum preparation with two Fleets enemas 2–3 h prior to the examination, and is performed with the patient in the left lateral decubitus.

After the insertion of the probe, the examination should begin using a frequency of 5–7.5 MHz. Then, the probe should be gently withdrawn and—when using the flexible echoendoscope—the lumen deflated and the degree of tip deflection of the probe and water-balloon fill should be adjusted to avoid false findings owing to tumor compression, tangential imaging, and air artifact. Filling the lumen

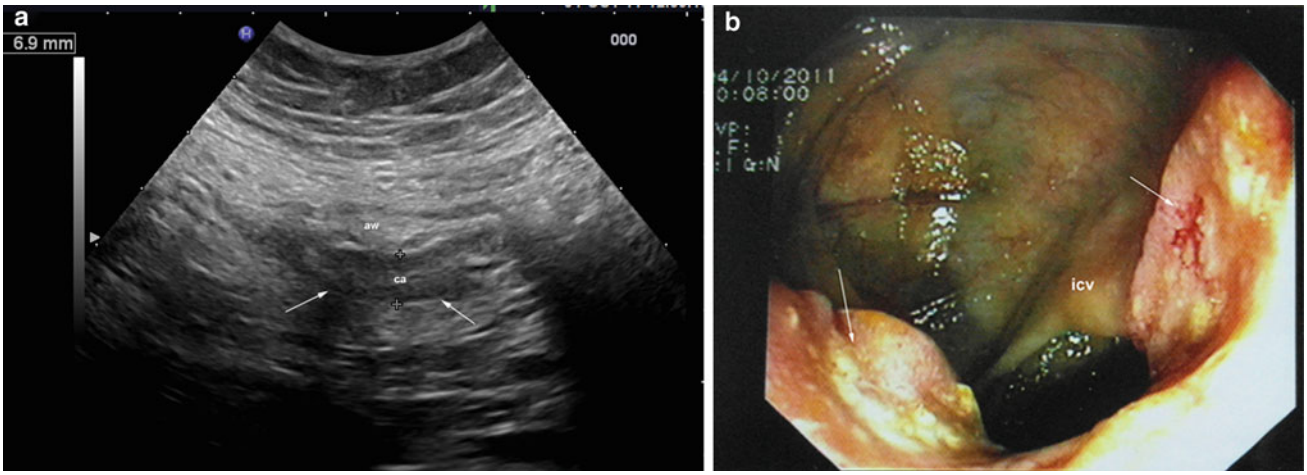

Fig. 6 56-year-old woman with abdominal discomfort and anemia. The bowel ultrasound showed a segmental thickening (*ca*) of the bowel walls (6.9 mm), with abrupt loss of stratification, in the ascending colon (*arrows*) (**a**). The following colonscopy showed an ulcerated colorectal cancer, involving half of the circumference of colon, just distal to the ileo-cecal valve (*icv*) (**b**). *aw* anterior wall of the ascending colon

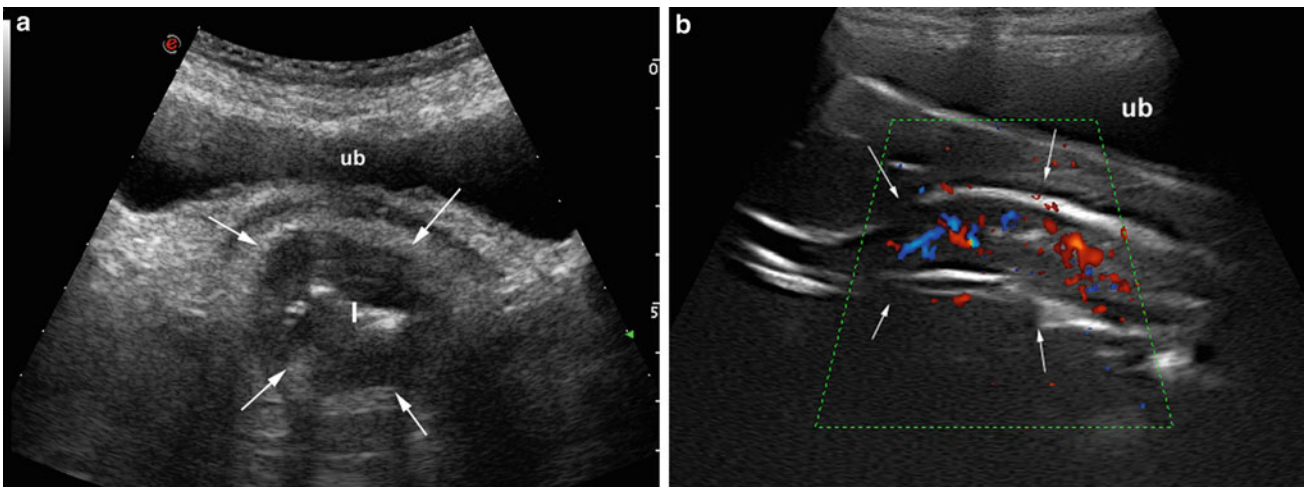

Fig. 7 Carcinoma of the rectosigmoid junction. **a** Transverse ultrasonographic scan showing thickened hypoechoic walls (*arrows*). **b** Longitudinal ultrasonographic scan showing vascular signals within the bowel wall (*arrows*) at color Doppler denoting the hypervascularity of the lesion. *Ub* urinary bladder

with water through the accessory channel is often necessary to achieve optimal imaging.

When a lesion is found, the echoendoscope is advanced and withdrawn over the lesion to achieve satisfactory imaging over its length and the tumor should be targeted to determine its depth of penetration into or through the rectal wall. Depending on the lesion size, the frequency of the probe should be adjusted. Usually it should be kept higher (7.5–12 MHz or more) for small lesions and lower (5 MHz) for imaging larger lesions. In any case, it should be the best setting used to image the contours of the lesion to assess the T-staging of the tumor.

During the examination, the operator should also look for surrounding lymph nodes that should be assessed for size, shape, and echo pattern. Finally, the scope is withdrawn to the anal verge to assess the anal sphincters for tumor invasion.

Endosonographically, the rectal wall is seen as five alternating hyperechoic and hypoechoic layers (Fig. 8), corresponding to the histology as follows: (a) the first layer (hyperechoic) is an interface between water or a water-filled balloon and the superficial mucosa, (b) the second layer (hypoechoic) represents the deep mucosa and muscularis mucosa, (c) the third layer (hyperechoic) denotes the submucosa and its interfaces, (d) the fourth layer (hypoechoic) represents the muscularis propria, and (e) the fifth layer (hyperechoic) indicates the interface between the serosa and perirectal fat. Rectal cancer appears as homogeneous hypoechoic soft tissue, and invasion appears as disruption of the normal echo-layer pattern of the wall.

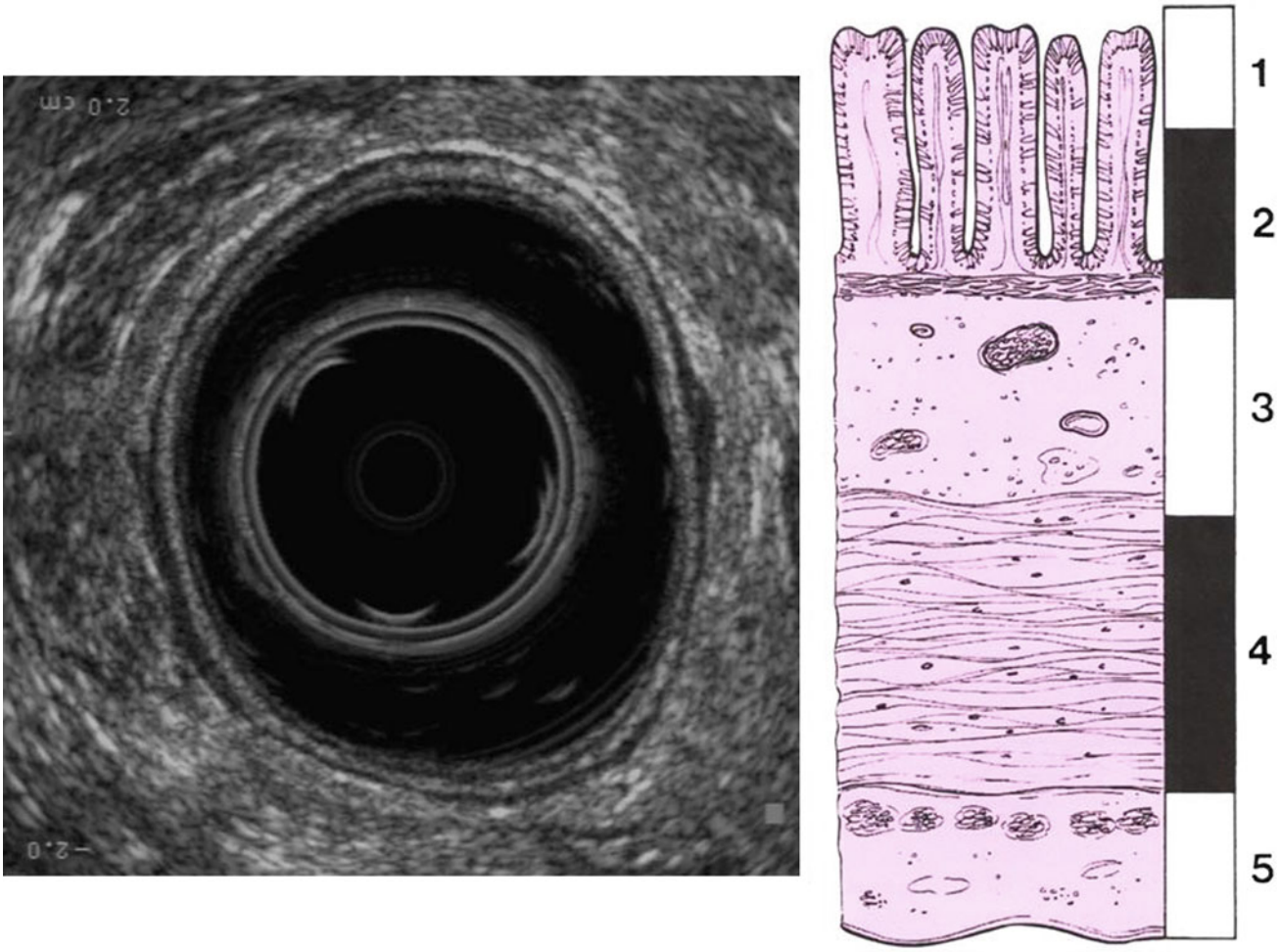

Fig. 8 Normal rectal wall. Transrectal sonographic appearances of the normal rectal wall and schematic drawing of histologic anatomy and sonographic appearances of the rectal wall. *1* Hyperechoic—lumen/mucosal interface and superficial mucosa; *2* Hypoechoic—deep mucosa including muscularis mucosa; *3* Hyperechoic—submucosa plus submucosa/muscularis propria interface; *4* Hypoechoic—muscularis propria minus interface with submucosa; *5* Hyperechoic—muscularis propria/perirectal interface and perirectal fat

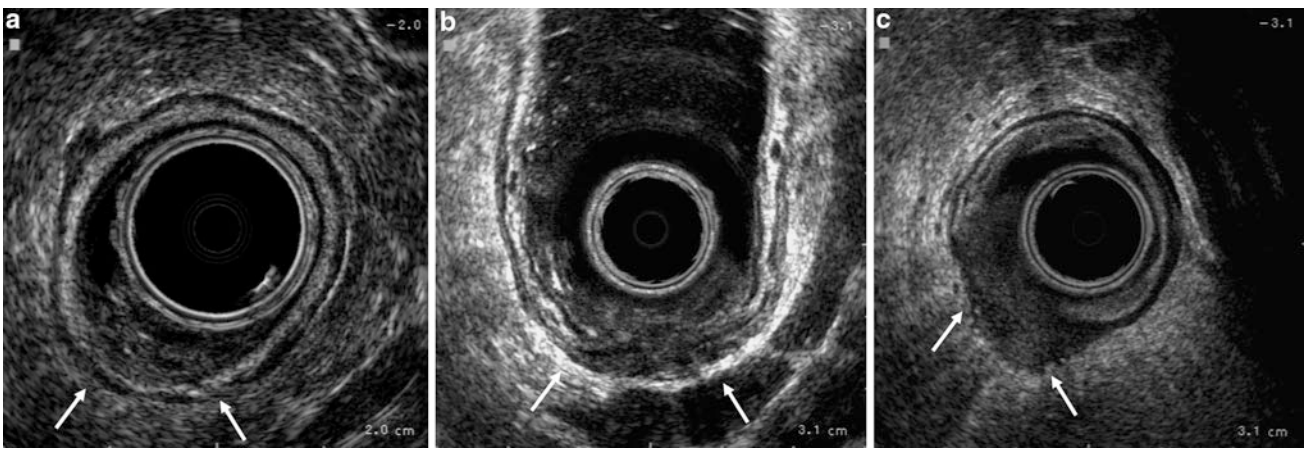

Fig. 9 **a** Rectal cancer confined to the mucosa (T1 cancer). Transrectal sonogram shows a hypoechoic mass (*arrows*) with thinning of the submucosal layer. **b** Rectal cancer extended to the submucosa (T2 cancer). Transrectal sonogram shows an irregular hypoechoic mass with interruption of the submucosal layer and thickening of the hypoechoic proper muscle layer (*arrows*). **c** Rectal cancer involving the entire wall and perirectal fat (T3 cancer). Transrectal sonogram shows an irregular hypoechoic mass with interruption of the submucosa and muscle layers and serrated hypoechoic lesion in the hyperechoic perirectal fat space (*arrows*)

A tumor that appears to be limited to the mucosa or submucosa (first three echo-layers) is classified as a T1 lesion (Fig. 9a), whereas a tumor that invades the muscularis propria (the hypoechoic fourth layer) is a T2 lesion (Fig. 9b). A T3 lesion penetrates through the rectal wall, extending beyond the five echo-layers and into the surrounding perirectal fat (Fig. 9c). A T4 lesion displays direct invasion into an adjacent organ such as the prostate gland, sacrum, vagina, or bladder. (Giovannini and Ardizzone 2006).

The accuracy of tumor and nodal staging depends on the experience and expertise of the endosonographer. The overall accuracy of T-staging for rectal cancer has been reported as being 81–91 % (Marusch et al. 2002; Stergiou et al. 2003; Kim et al. 2004; Bipat et al. 2004), while the accuracy in detecting locoregional lymph node metastasis was reported as being 64–88 % (Schaffzin and Wong 2004).

References

Bipat S, Glas A, Slors FJM, Zwinderman AH, Bossuyt PMM, Stoker J (2004) Rectal cancer: local staging and assessment of lymph node involvement with endoluminal US, CT, and MR imaging—a meta-analysis. Radiology 232:773–783

Giovannini M, Ardizzone S (2006) Anorectal ultrasound for neoplastic and inflammatory lesions. Best Pract Res Clin Gastroenterol 20:113–135

Gluvic Z, Slovic M, Dugalic P et al (2008) Is the routine abdominal ultrasound a sufficiently sensitive method for the detection of colonic malignancy? Intern Med 47:827–831

Grubel P (2011) Evaluation of abdominal ultrasound performed by the gastroenterologist in the office. J Clin Gastroenterol 45:405–409

Grunshaw ND, Renwick IG, Scarisbrick G, Nasmyth DG (2000) Prospective evaluation of ultrasound in distal ileal and colonic obstruction. Clin Radiol 55:356–362

Gualdi GF, Casciani E, Guadalaxara A, d'Orta C, Dolettini E, Peppalardo G (2000) Local staging of rectal cancer with transrectal ultrasound and endorectal magnetic resonance imaging. Dis Colon Rectum 43:338–345

Kim SA, Lim HK, Lee SJ et al (2004) Depiction and local staging of rectal tumors: comparison of transrectal US before and after water instillation. Radiology 231:117–122

Kuzmich S, Howlett DC, Andi A, Shah D, Kuzmich T (2009) Transabdominal sonography in assessment of the bowel in adults. AJR Am J Roentgenol 192:197–212

Lim JH (1996) Colorectal cancer: sonographic findings. AJR Am J Roentgenol 167:45–47

Maconi G, Radice E, Bareggi E, Bianchi Porro G (2009) Hydrosonography of the gastrointestinal tract. AJR Am J Roentgenol 193:700–708

Maconi G, Terracciano F, de Sio I et al (2011) Referrals for bowel ultrasound in clinical practice: a survey in 12 nationwide centres in Italy. Dig Liver Dis 43:165–168

Martínez-Ares D, Martín-Granizo Barrenechea I, Souto-Ruzo J, Yáñez López J, Pallarés Peral A, Vázquez-Iglesias JL (2005) The value of abdominal ultrasound in the diagnosis of colon cancer. Rev Esp Enferm Dig 97:877–886

Marusch F, Koch A, Schmidt U et al (2002) Routine use of transrectal ultrasound in rectal carcinoma: result of prospective multi-center study. Endoscopy 34:385–390

Price J, Metreweli C (1988) Sonographic diagnosis of clinically non-palpable primary colonic neoplasm. Br J Radiol 61:190–195

Richardson NG, Heriot AG, Kumar D, Joseph AE (1998) Abdominal ultrasonography in the diagnosis of colonic cancer. Br J Surg 85:530–533

Rutgeerts LJ, Verbanck JJ, Crape AW et al (1991) Detection of colorectal cancer by routine ultrasound. J Belge Radiol 74:11–13

Schaffzin DM, Wong WD (2004) Endorectal ultrasound in the preoperative evaluation of rectal cancer. Clin Colorectal Cancer 4:124–132

Schwerk W, Braun B, Dombrowski H (1979) Real-time ultrasound examination in the diagnosis of gastrointestinal tumors. J Clin Ultrasound 7:425–431

Shirahama M, Koga T, Ishibashi H, Uchida S, Ohta Y (1994) Sonographic features of colon carcinoma seen with high-frequency transabdominal ultrasound. J Clin Ultrasound 22:359–365

Speets AM, Hoes AW, van der Graaf Y et al (2006) Upper abdominal ultrasound in general practice: indications, diagnostic yield and consequences for patient management. Fam Pract 23:507–511

Stergiou N, Haji-Kermani N, Schneider C, Menke D, Köckerling F, Wehrmann T (2003) Staging of colonic neoplasms by colonoscopic miniprobe ultrasonography. Int J Colorectal Dis 18:445–449

Zagoria RJ, Schlarb CA, Ott DJ et al (1997) Assessment of rectal tumor infiltration utilizing endorectal MR imaging and comparison with endoscopic rectal sonography. J Surg Oncol 64:312–317

Gastric Cancer

Jiro Hata, Ken Haruma, Noriaki Manabe, and Hiroshi Imamura

Contents

Abstract

Thanks to the improvements in sonographic equipment, transabdominal ultrasonography has recently been reported to be useful in the assessment of gastric cancer.This chapter describes the sonographic features of early and advanced gastric cancer. In particular, alterations of the gastric wall and perigastric findings that can suggest the disease and be useful in differential diagnosis and in staging of gastric cancer, are imaged and discussed.

1 Introduction

Gastric cancer is still of major importance worldwide despite declining incidence. Endoscopy, radiologic examination, and computed tomography are the diagnostic imaging modalities employed for gastric cancer. For early gastric cancers, in particular, endoscopy is the essential diagnostic method of choice; however, with the remarkable improvements in sonographic equipment, transabdominal ultrasonography has recently been reported to be useful in the assessment of gastric cancer. Endoscopic ultrasound is another imaging modality using ultrasound which has not necessarily been as widely used as transabdominal ultrasound due to its invasiveness. In this chapter, sonographic imaging of gastric cancer, mainly transabdominal, is described.

2 Sonographic Assessment of the Gastric Wall

2.1 Preparation and Equipment

For the screening of advanced gastric cancers, special preparations, such as the ingestion of water, and the injection of anticholinergic agents, are not necessary in most cases; however, such preparations are required to visualize

J. Hata · N. Manabe · H. Imamura
Department of Clinical Pathology and Laboratory Medicine, Kawasaki Medical School, 577, Matsushima, Kurashiki-city, Okayama 701-0192, Japan
e-mail: ultrajiro@nifty.com

K. Haruma (✉)
Division of Gastroenterology, Department of Internal Medicine, Kawasaki Medical School, 577, Matsushima, Kurashiki-city, Okayama 701-0192, Japan
e-mail: kharuma@med.kawasaki-m.ac.jp

G. Maconi and G. Bianchi Porro (eds.), *Ultrasound of the Gastrointestinal Tract*, Medical Radiology. Diagnostic Imaging,
DOI: 10.1007/174_2012_664,
Published Online: 9 October 2012

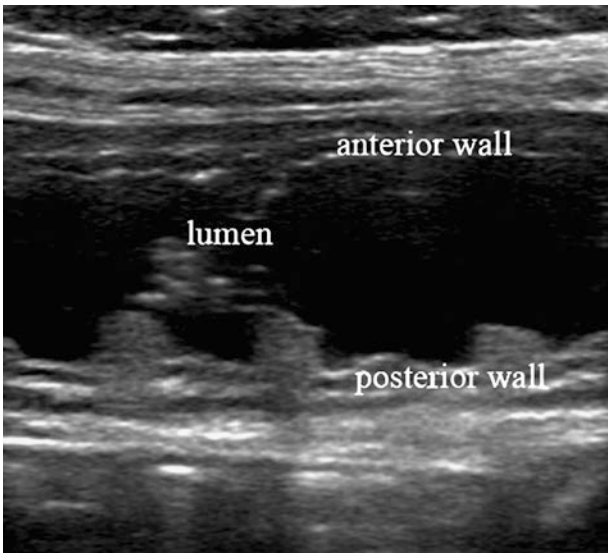

Fig. 1 Transverse scan of the gastric body. The 5-layer structure of the gastric wall and the gastric fold is demonstrated

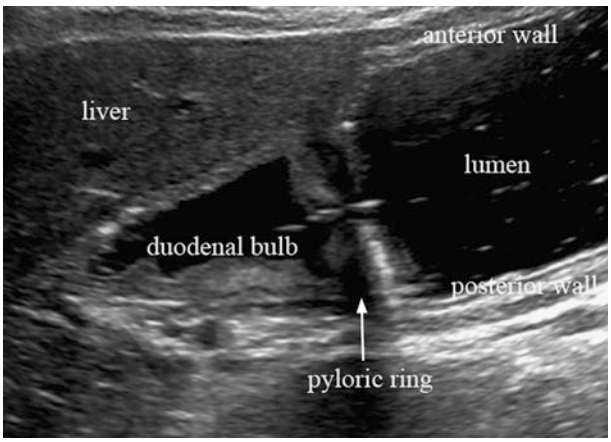

Fig. 2 Longitudinal scan of the gastric antrum, pylorus, and the duodenal bulb. Gastroduodenal lumen is filled with water

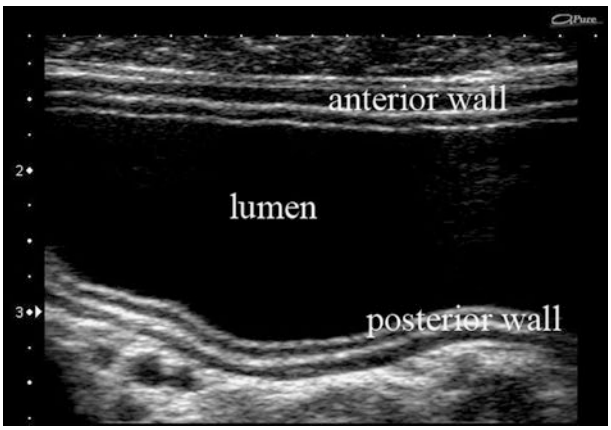

Fig. 3 The close-up view of gastric antrum. The 5-layer structure is clearly demonstrated

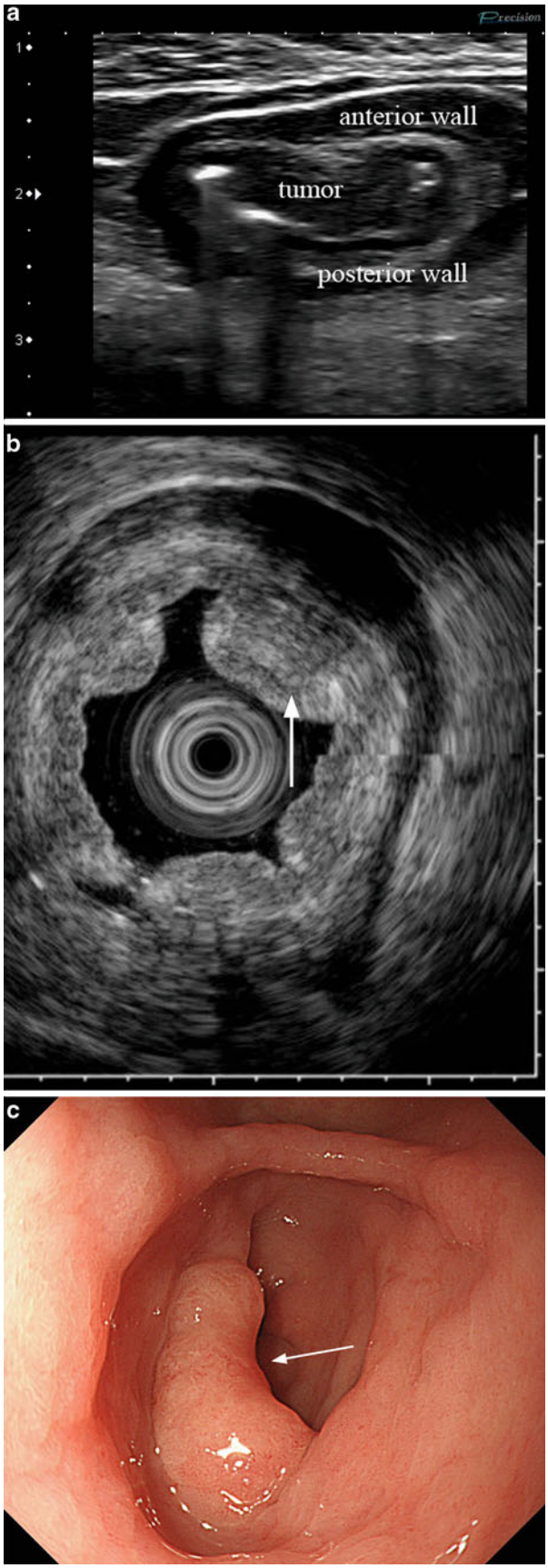

◀ **Fig. 4** Sonographic image of early (intramucosal) gastric cancer. **a** Focal wall thickening is demonstrated. The thickening is limited to the mucosal layer. **b** Echo-endoscopic feature of the same patient as shown in **a**. Focally elevated lesion is visualized (*arrow*). **c** Endoscopic image of the same. The lesion is recognized as the focal elevated area (*arrow*)

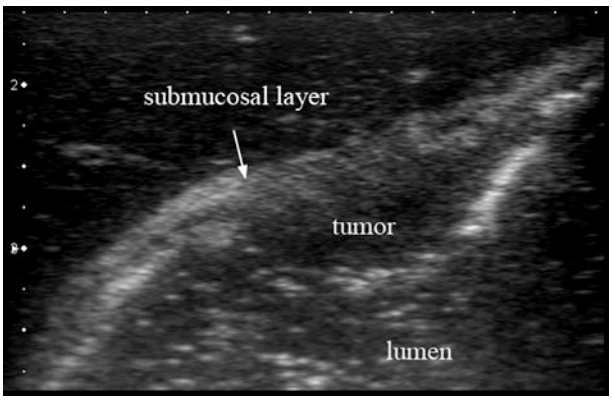

Fig. 5 Sonographic image of early (deep submucosa) gastric cancer. The blurring of submucosal layer indicates the deep submucosal invasion

smaller lesions. After an overnight fast, the ingestion of approximately 200–400 ml of water makes it easier to detect smaller lesions located in the posterior wall of the gastric circumflex. The injection of spasmolytic agents is seldom necessary.

While a 3–4 MHz curved array scanner is used for routine screening for gastric cancers, detailed examination including the evaluation of wall stratification should be performed with a high frequency (5–12 MHz) linear probe for its superior spatial resolution. Tissue harmonic imaging is also recommended to reduce noises such as side lobe artifacts.

2.2 Sonographic Image of the Normal Gastric Wall

The abdominal esophagus is visualized between the abdominal aorta and the left lobe of the liver by a left middle subcostal scan. Below the abdominal esophagus lies the gastric fundus. The gastric body is usually located in the left middle upper abdomen. The gastric fold is often observed at the greater curvature of the gastric body (Fig. 1). Gastric antrum is located in the right middle upper abdomen. The pylorus is identified as the segmental thickening of the proper muscle (Fig. 2). The thickness of the normal gastric wall is usually <5 mm and wall thickening of >6 mm is considered pathological.

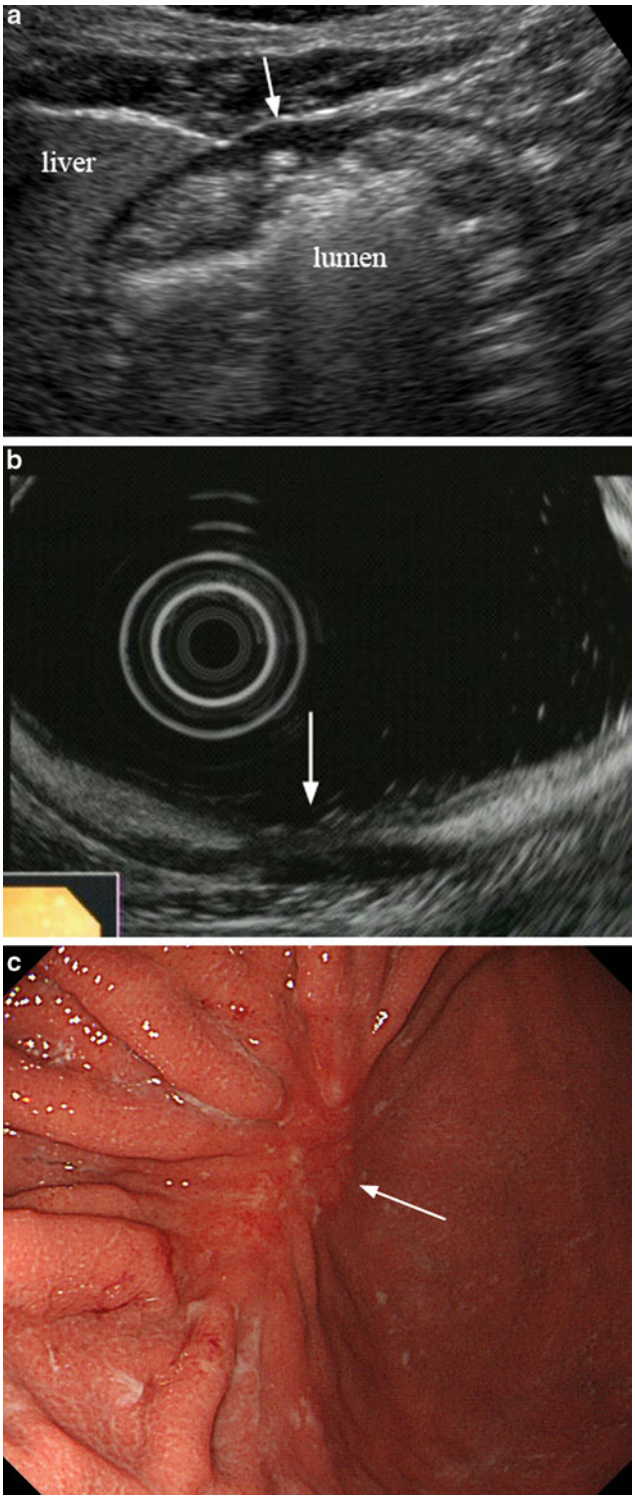

Fig. 6 Sonographic feature of advanced (mostly intramucosal with minute invasion into proper muscle) gastric cancer, complicated with ulcer scar (*arrow*). **a** Although the wall stratification has disappeared, the wall thickness is rather thinner than the normal gastric wall. **b** Endoscopic ultrasonography of the same lesion (*arrow*). **c** Endoscopic view of the same lesion. Ulcer scar is demonstrated (*arrow*)

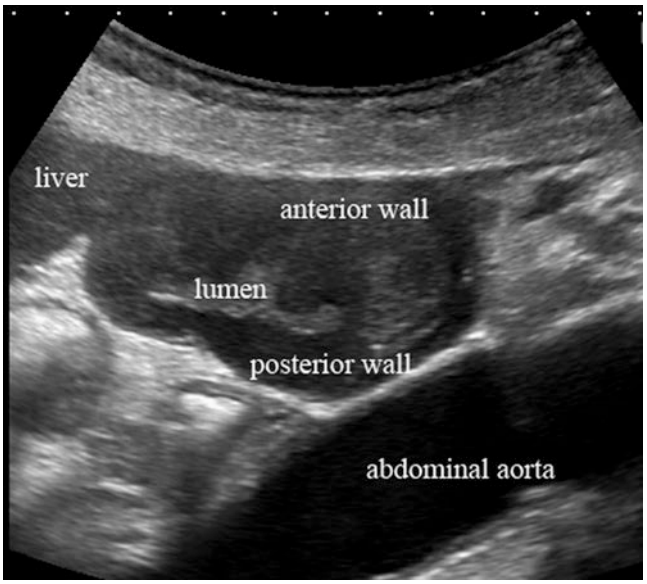

Fig. 7 Sonographic feature of an advanced gastric cancer showing the so-called "pseudokidney sign"

The normal gastric wall is demonstrated as a five-layer structure (Fig. 3). The first layer is hyperechoic, and corresponds to the luminal boundary and the part of the mucosal layer. The second layer is hypoechoic and includes the remaining part of the mucosa and mucosal muscle layer. The third layer is hyperechoic and corresponds to the submucosal layer. The fourth layer is hypoechoic and corresponds to the proper muscle layer. The fifth layer is hyperechoic and corresponds to the serosa and the extramural boundary.

3 Sonographic Features of Gastric Cancer

3.1 Early Gastric Cancer

It is not always easy, and often rather difficult to detect early gastric cancer by means of usual ultrasonographic screening because both the wall thickening and alteration of wall stratification are too subtle to be detected with transabdominal ultrasound. In this respect, ingestion of water is useful to obtain a clear image of such subtle changes.

Early gastric cancer is usually expressed as focal wall thickening originating in the second layer. No changes of the submucosal layer are shown with intramucosal cancer (Fig. 4). When the tumor invades the submucosal layer, the shape and the width of that layer changes (Fig. 5) and it finally disappears as the tumor invades proper muscle.

However, the evaluation of cancer invasion becomes difficult when it is complicated by an ulcer because the fibrosis accompanying ulcer healing is expressed as a hypoechoic area which resembles cancer (Fig. 6).

The diagnostic accuracy of determination of cancer depth with transabdominal ultrasound is generally thought to be inferior to that with endoscopic ultrasound, which provides a clear image with fewer artifacts and high resolution, although there are several contradictive reports (Ishigami et al. 2004; Meining et al. 2002). Even with endoscopic ultrasound, however, it is difficult to differentiate fibrotic tissue from cancer.

3.2 Advanced Gastric Cancer

Advanced gastric cancer is demonstrated as focal wall thickening without wall stratification. The typical sonographic figure is a "pseudokidney sign"; i.e., an echogenic area surrounded by a hypoechoic rim that resembles the image of kidney (Fig. 7).

In most cases, although, the advanced cancer only shows eccentric or segmental wall thickening without wall stratification, which does not actually mimic the shape of kidney (Fig. 8a). In addition, sonographic evaluation of tissue elasticity has become possible recently to help us distinguish cancer from other disorders showing gastric wall thickening (Fig. 8b).

Furthermore, 3D ultrasound imaging to demonstrate "virtual endoscopic image" is also now available by extracorporeal ultrasound equipment (Fig. 9).

In scirrhous cancers, wall stratification is demonstrated although it is somewhat blurred (Fig. 10a, b). The lesions of advanced gastric cancer show poor compliance and compressibility, as well as reduced peristalsis or even loss of it. The vascularity on color/power Doppler depends on the nature of cancer and may not necessarily be useful for differentiation between benign and malignant conditions, although the irregularity of vascular structure is often appreciated in cancer lesions (Fig. 10c).

Differential diagnoses should be decided among the following: benign gastric ulcer, malignant lymphoma, acute gastric mucosal lesion, and anisakiasis. Ultrasound is useful for this purpose (Okanobu et al. 2003). Benign gastric ulcers show focal wall thickening with a wall defect at the center. Since the wall thickening around the ulcer is due to submucosal edema, wall stratification is basically preserved (Fig. 11).

Malignant lymphoma also shows focal wall thickening without stratification which resembles advanced gastric cancer, but the thickened wall is characterized by very low echogenicity, often lower than that of gastric carcinoma (Fig. 12).

Acute gastric mucosal lesions and gastric anisakiasis are characterized by diffuse wall thickening with wall stratification, brought on mainly by submucosal edema, which occasionally resembles scirrhous cancer (Fig. 13).

In scirrhous cancers, the width of every layer is irregular, and the boundary of each layer is often blurred.

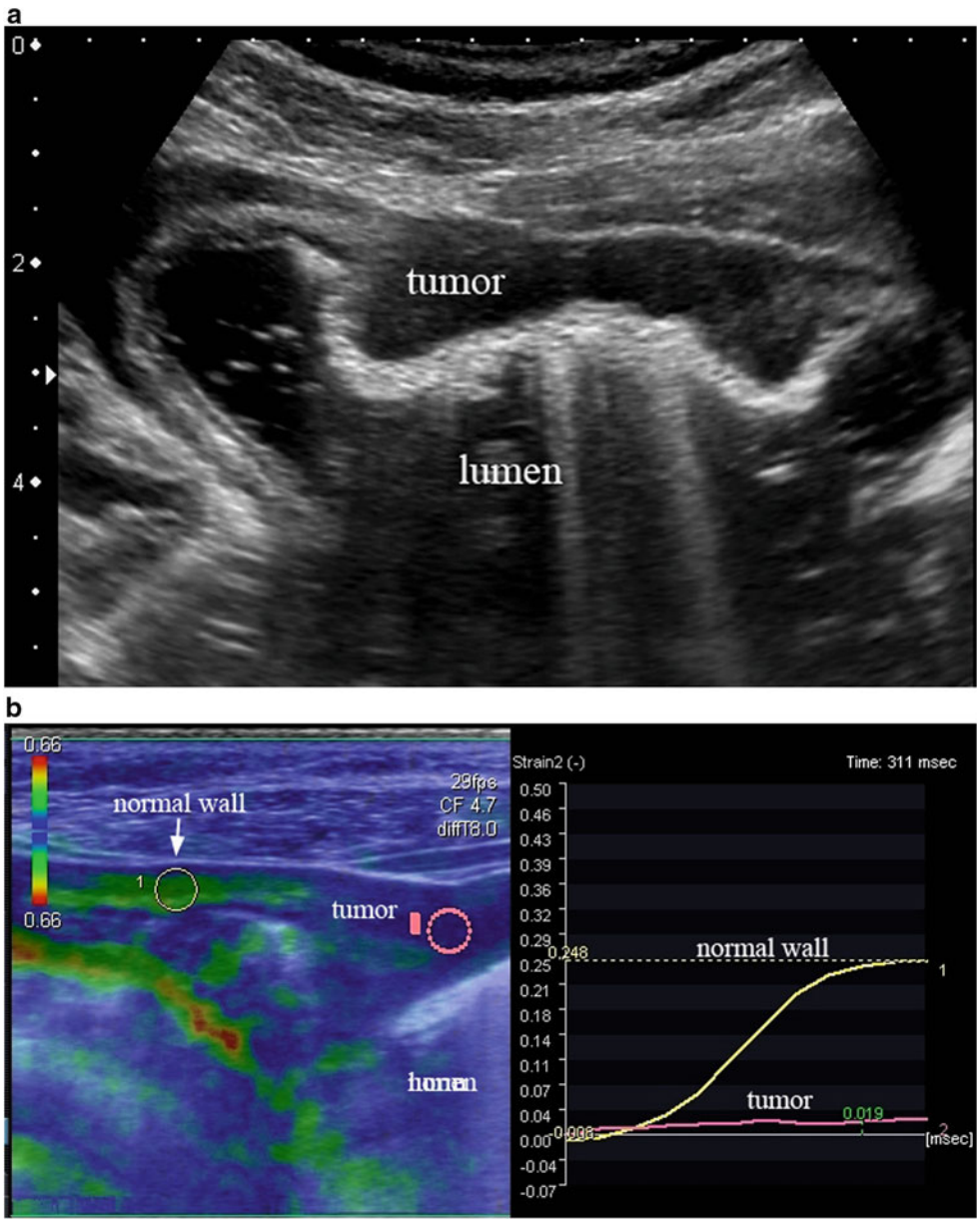

Fig. 8 Typical sonographic figure of an advanced gastric cancer. **a** Focal wall thickening without wall stratification is demonstrated. **b** The sonographic elasticity-image of the same lesion. The lesion is demonstrated as bluish area which indicates the lesion is relatively hard, showing much less strain compared with the adjacent normal gastric wall

Furthermore, the compressibility/compliance is poor and the peristalsis is remarkably reduced.

4 Staging of Gastric Cancer

For the staging of gastric cancer, cancer depth and metastases (to remote organs, lymph nodes, and peritoneum) must be assessed. There have been a few reports on the cancer staging with ultrasound showing high diagnostic ability (Liao et al. 2004; Lim et al. 1994).

The depth of cancer for an early gastric cancer is decided by assessment of alteration of wall stratification. The extension of an advanced gastric cancer is decided by careful evaluation of the tumor margin. When the outer margin of the tumor is smooth and a fat pad or boundary echo is observed between every other contiguous organ and the tumor, the cancer is considered to be within serosa. Irregularity of the outer margin suggests high risk of the tumor exceeding serosa. Loss of the boundary echo accompanied by loss of sliding movement between other organs is an important finding suspicious of minimal invasion into an adjacent organ. The invasion is obvious when the tumor boundary lies in the contiguous organ and deforms the contour of the organ (Fig. 14).

One should be careful in the assessment of extramural invasion of scirrhous cancer into mesenteric fat, which often shows mere thickening of adjacent fat tissue (Fig. 15).

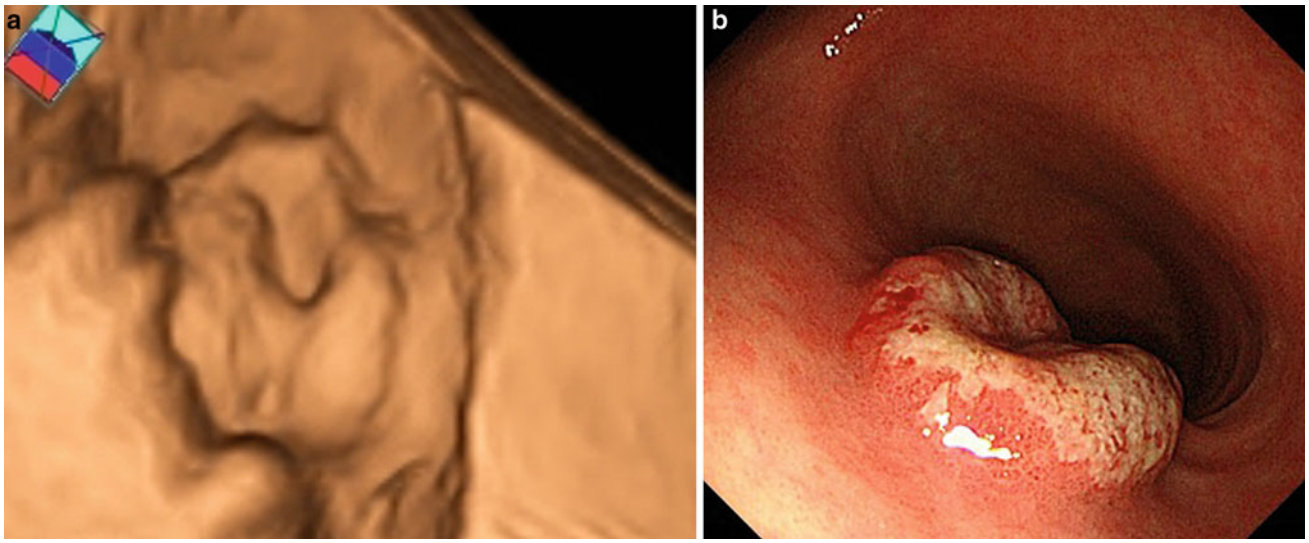

Fig. 9 The sonographic 3D image of an advanced gastric cancer. **a** The lesion is demonstrated as a focally elevated area with depression at the center. **b** The endoscopic image of the same lesion

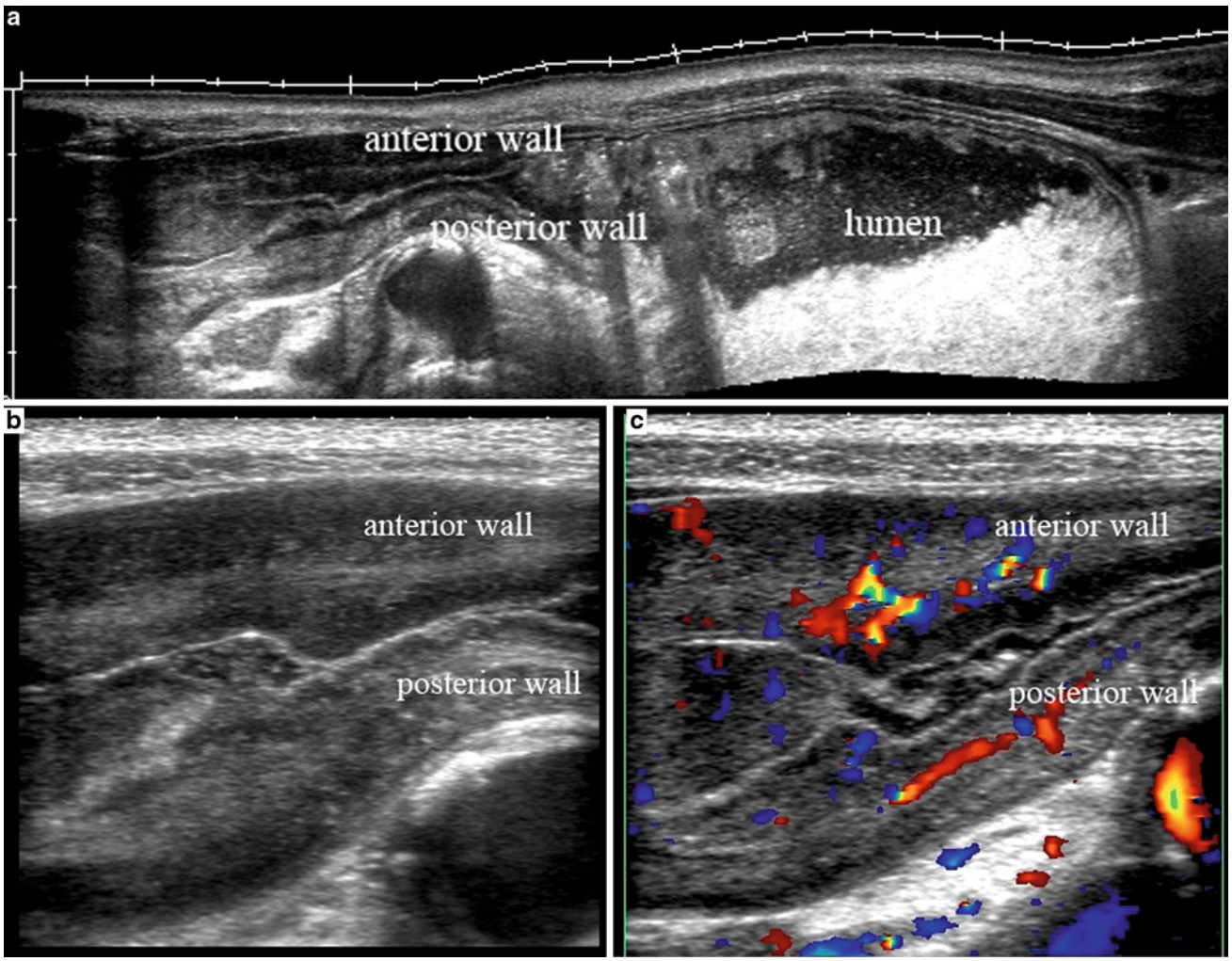

Fig. 10 Longitudinal scan of the pylorus stenosis due to advanced gastric cancer. **a** Diffuse wall thickening of the antrum is demonstrated. **b** Close-up view of the lesion with 7 MHz linear probe. Wall stratification is blurred to some extent although not disappeared. **c** Color Doppler image of the same lesion. Irregular vascular structure is appreciated (*arrow*)

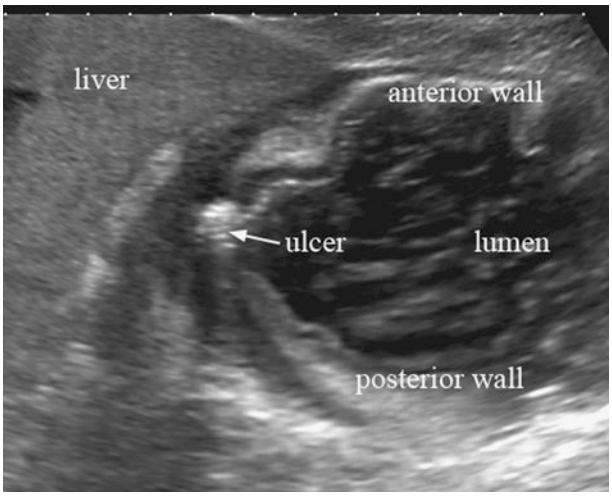

Fig. 11 Benign gastric ulcer . The wall defect and the edematous thickening of the surrounding wall with stratification is demonstrated

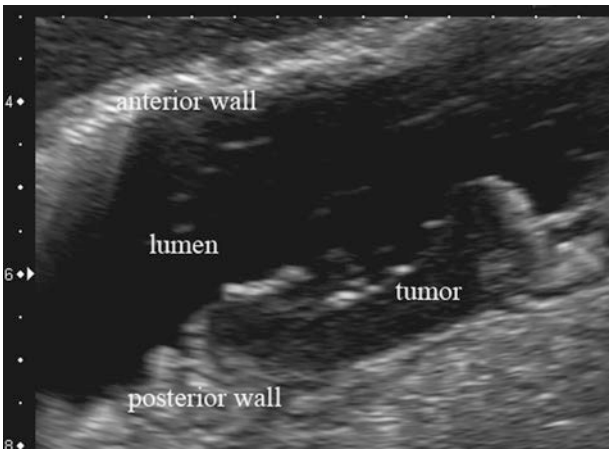

Fig. 12 Malignant lymphoma. The focal wall thickening without stratification is demonstrated. Note that the echogenicity of the lesion is extremely low, which is one of the characteristic feature of malignant lymphoma

Fig. 13 Gastric anisakiasis. **a** Diffuse wall thickening with preserved wall stratification due to marked submucosal edema is demonstrated. **b** Endoscopic image of the same lesion. The anisakis larva is clearly identified (*arrow*)

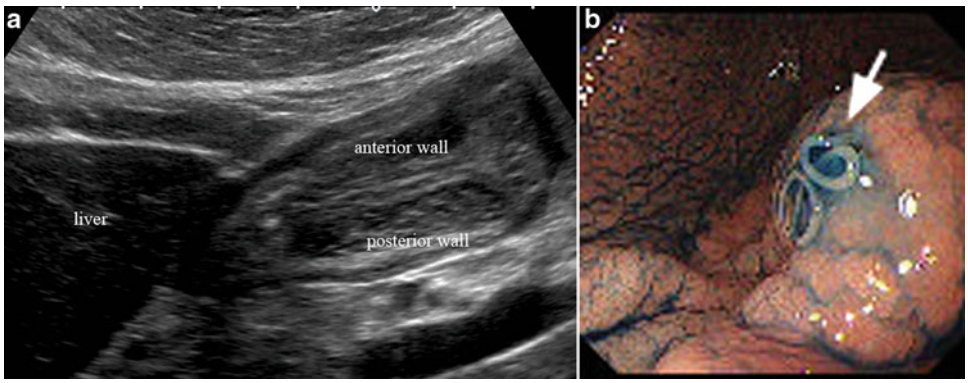

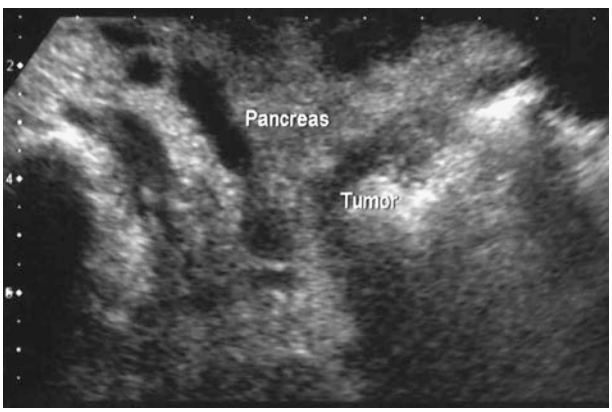

Fig. 14 Gastric cancer invasion into the tail of pancreas is demonstrated. The hypoechoic tumor has deformed the contour of the pancreas tail

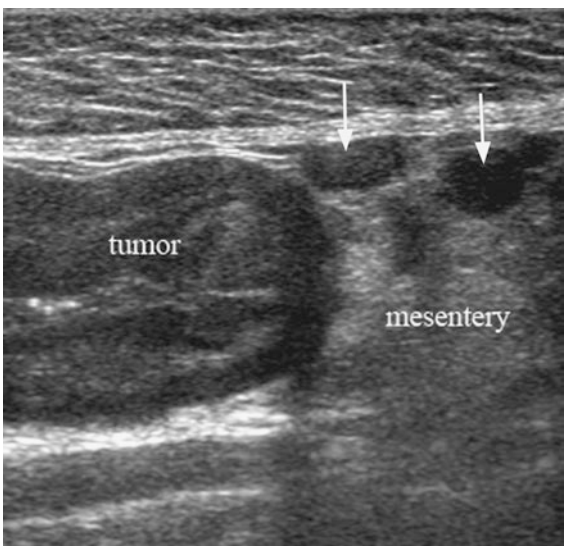

Fig. 15 Tumor invasion of a Scirrhous type gastric cancer into greater omentum. The thickening of mesenteric fat as well as lymph node swellings (*arrows*) are appreciated

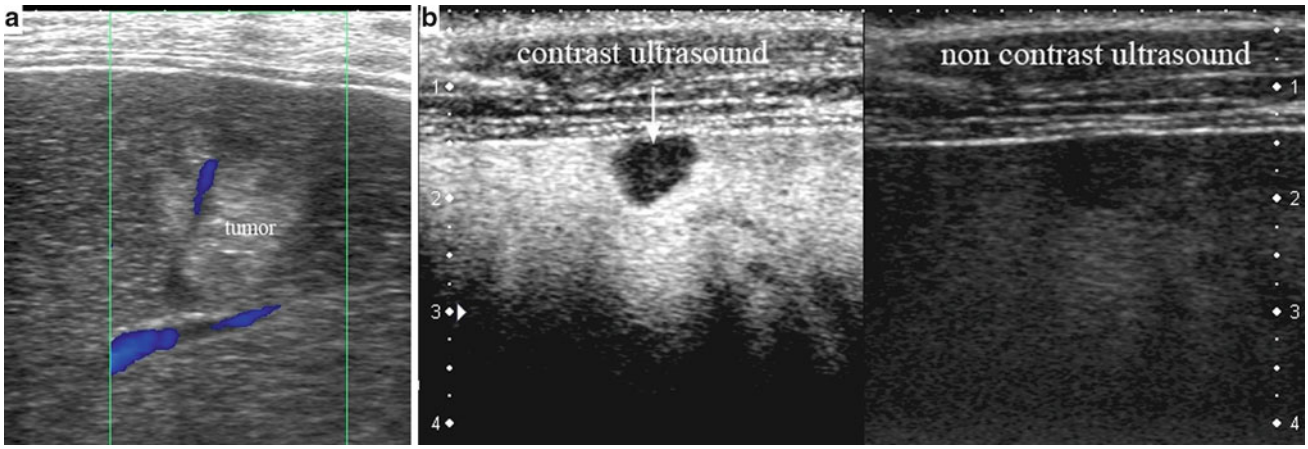

Fig. 16 Metastatic liver tumor. **a** Color Doppler image. Penetration of the normal vascular structure through the tumor is demonstrated. **b** Contrast ultrasound. The lesion is identified as a perfusion defect (*arrow*)

Fig. 17 Supraclavicular lymph node metastases (*arrows*)

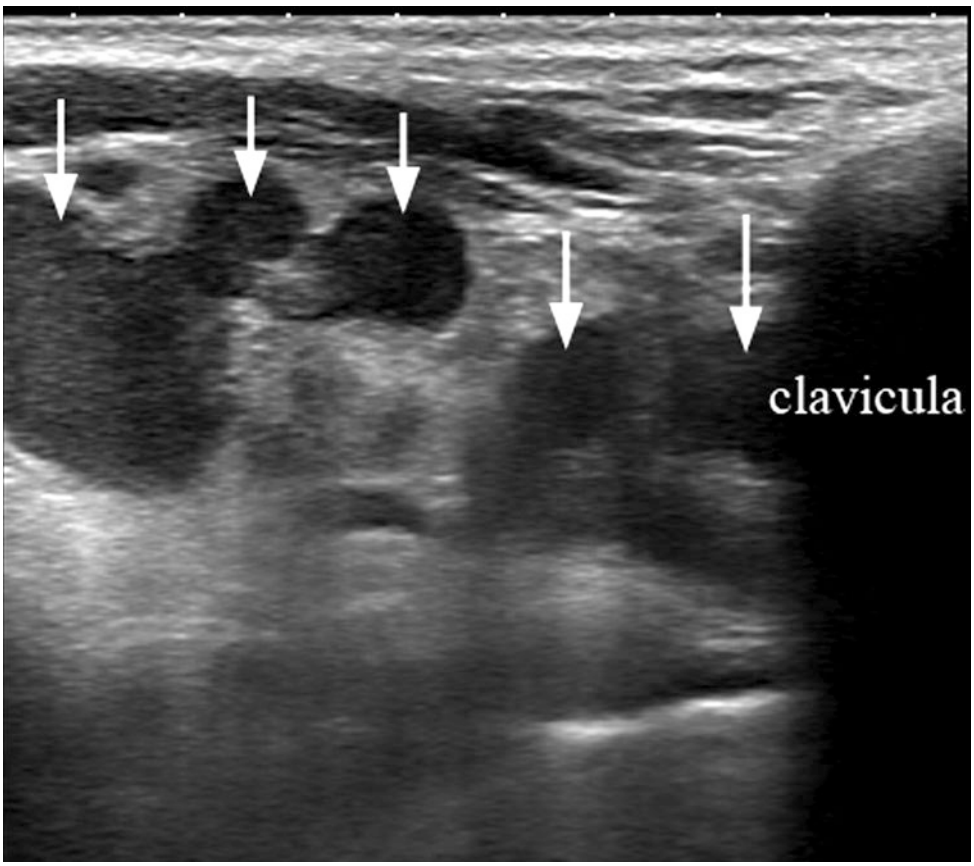

Typical metastatic liver tumors have a thick hypoechoic rim with a relatively hyperechoic center, known as the "bull's eye" sign. However, this finding cannot be applied to all metastatic liver tumors. Penetration of the normal vascular structure through the tumor proven by color/power Doppler (Fig. 16a), ring-shaped enhancement in the arterial phase and loss of enhancement in the postvascular phase as determined by contrast ultrasound using Sonazoid™ (Daiichi-Sankyo, Co., Ltd, Tokyo, Japan) which is phagocytosed by Kuppfer cells (Fig. 16b), are helpful findings for the diagnosis of metastatic liver tumors.

Lymph node metastases are characterized by the round-shaped swelling of lymph nodes (Fig. 17). One must be careful in the differentiation from inflammatory swelling of

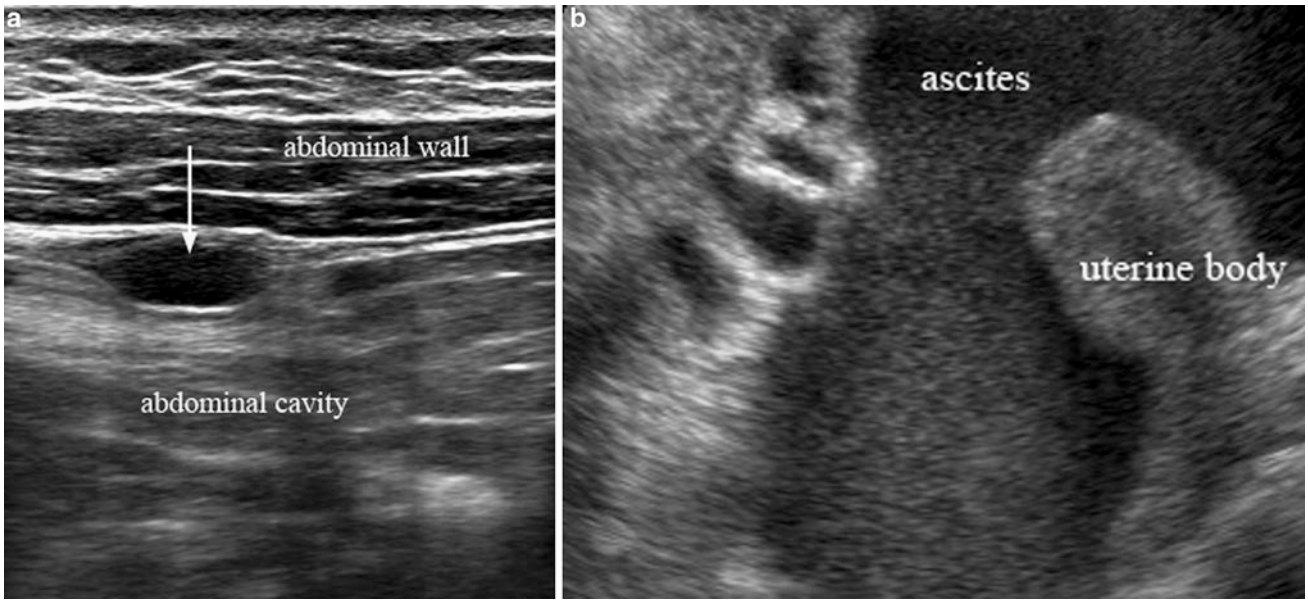

Fig. 18 Advanced gastric cancer. **a** A seeding nodule (*arrow*) and **b** ascites rich in echogenic particles seen in a patient with peritonitis carcinomatosa

lymph nodes caused by a benign gastric ulcer, which is more elliptical in shape than that of metastatic lymph nodes.

Tumor seeding is demonstrated as a hypoechoic nodule on the visceral or parietal peritoneum (Fig. 18a). Often ascites with floating echogenic particles accompanies tumor seedings, indicating peritonitis carcinomatosa (Fig. 18b).

References

Ishigami S, Yoshinaka H, Sakamoto F et al (2004) Preoperative assessment of the depth of early gastric cancer invasion by transabdominal ultrasound sonography (TUS): a comparison with endoscopic ultrasound sonography (EUS). Hepatogastroenterology 51:1202–1205

Liao SR, Dai Y, Huo L et al (2004) Transabdominal ultrasonography in preoperative staging of gastric cancer. World J Gastroenterol 23:3399–3404

Lim JH, Ko YT, Lee DH (1994) Transabdominal US staging of gastric cancer. Abdom Imaging 19:527–531

Meining A, Dittler HJ, Wolf A et al (2002) You get what you expect? A critical appraisal of imaging methodology in endosonographic cancer staging. Gut 50:599–603

Okanobu H, Hata J, Haruma K et al (2003) Giant gastric folds: differential diagnosis at US. Radiology 228:986–990

Peritoneal Metastasis

Ilario de Sio, Luigi Castellano, Fulvia Terracciano, Luigi Maria Vitale, Marco Niosi, and Carmelina Loguercio

Contents

Abstract

Peritoneal metastasis is frequently observed in patients with adenocarcinomas of ovary, stomach, intestine ,gall-bladder or biliary tree, pancreas, lung, ovary, and uterus. The most common ultrasonographic findings are represented by ascites, omental and mesenteric involvement, serosal and parietal peritoneal implants, with liver metastasis, and/or lymphadenopathies as accessory findings. Ultrasonography is a highly sensitive test in detecting ascites and ultrasound guided aspiration of ascites is frequently used in patients with small amount of ascites. Neoplastic involvement of the great omentum is visualized by ultrasound as "omental cake", a uniformly thick hyposonic band-shaped structure adjacent to the anterior and lateral walls of the abdomen. The involvement of the peritoneum is visualized as peritoneal parietal and serosal implants with evidence of soft tissue mass or nodules adhering to peritoneum or as irregularity or interruption of the peritoneal line. Anechoic area in the thickened peritoneum is a specific sign indicating the diagnosis of pseudoyixoma peritonei. Liver metastasis and lymphadenopathies are present in about 38 and 24 % of patients with peritoneal carcinomatosis but they do not represent a specific sign of peritoneal involvement. Ultrasonographic findings of peritoneal metastasis highly correlate with computed thomography signs and ultrasound-guided needle biopsy of peritoneal and/or omentum masses is a higly accurate method for differential diagnosis between peritoneal metastasis or peritoneal mesotelioma. The biopsy of peritoneal and/or omental masses has been performed by using fine needle but experience exists with the use of large cutting needle, thus avoiding the necessity of exploratory surgery.

I. de Sio (✉) · L. Castellano · L. M. Vitale · M. Niosi
Department of Internal Medicine and Gastroenterology, Ultrasonography Section II University, Via S. Pansini 5, 80131 Naples, Italy
e-mail: ilades@tiscalinet.it

F. Terracciano
Gastroenterology Unit, Ultrasonographic Section Casa Sollievo della Sofferenza, S. Giovanni Rotondo, Foggia, Italy

C. Loguercio
Department of Internal Medicine and Gastroenterology, II University, Via S. Pansini 5, 80131 Naples, Italy

G. Maconi and G. Bianchi Porro (eds.), *Ultrasound of the Gastrointestinal Tract*, Medical Radiology. Diagnostic Imaging,
DOI: 10.1007/174_2012_721,
Published Online: 11 August 2012

Table 1 Prevalence of ultrasonographic findings in peritoneal carcinomatosis (From Rioux and Michaud 1995)

Omental involvement	97 %
Ascites	49 %
Serosal implants	19 %
Mesenteric involvements	16 %
Peritoneal implants	54 %
Interruption of the anterior peritoneal line	16 %
Liver metastasis	38 %
Lymphadenopathies	24 %
Gallbladder wall thickening	32 %

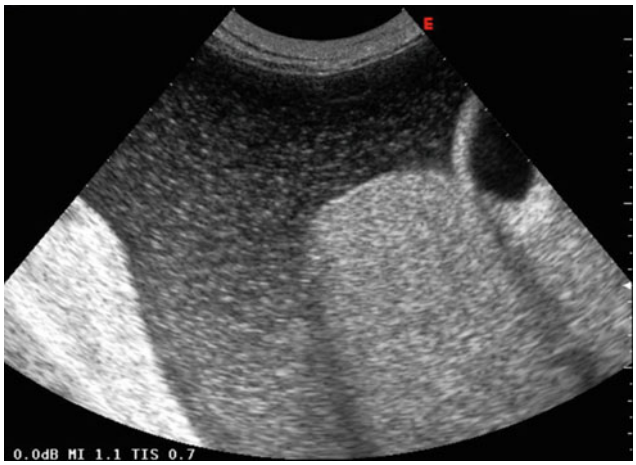

Fig. 1 Echogenic malignant ascites in a case of ovarian cancer: the fluid is echogenic with fine corpuscolated echoes and declivous sediment

1 Introduction

Metastatic involvement of peritoneum (peritoneal carcinomatosis) is by far the most common peritoneal tumor (Walsh and Williams 1971; Bell and Scully 1990). Tumors that preferentially metastasize to the peritoneum include the following adenocarcinomas: stomach, intestine (colon-rectum), gallbladder or biliary tree, pancreas, breast, lung, ovary and uterus (Runyon et al. 1988), as well as lymphoma and other tumors, such as the sarcomas (Runyon and Hoefs 1986). About two-thirds of women with ovarian cancer present abdominal dissemination of the disease (Johnson 1993; Longatto Pilho et al. 1997), while sarcomas account for only 3 % of metastatic peritoneal malignant tumors (Walsh and Williams 1971). Neoplastic diffusion of cancer to peritoneum occurs both from contiguity and lymphatic or hematic spreading. Pseudomyxoma peritonei (PMP) is a special case in metastatic peritoneal tumors: it derives from the rupture of an ovary or appendix tumor with accumulation of mucin in the peritoneal cavity (Mann et al. 1990). Its malignancy is variable and diagnosis is usually made when jelly-like material is observed during surgery, at laparoscopy or is aspired by interventional procedure such as guided ultrasound (US) and/or computed tomography (CT) (Novell and Lewis 1990). Clinical presentation of peritoneal carcinomatosis includes abdominal pain and distension, early satiety, important ascites (usually bloody), abdominal masses which determine bowel obstruction and weight loss. Prognosis is generally poor (Yamada et al. 1983). Ultrasonography is the first choice procedure in evaluation of patients with abdominal pain, distension and palpable masses. It is used as a guide for cyto-histological evaluation of ascites and abdominal masses, thus avoiding either laparoscopy or laparotomy for diagnosis.

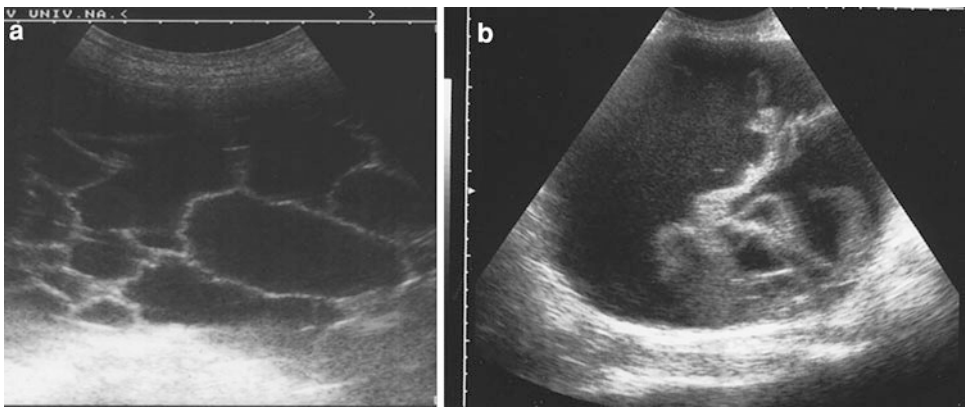

Fig. 2 **a** Ascites with fine hyperechogenic septa are clearly visible in malignant ascites due to pancreatic cancer. **b** More evident thickened hyperechogenic septa in malignant ascites due to gastric cancer

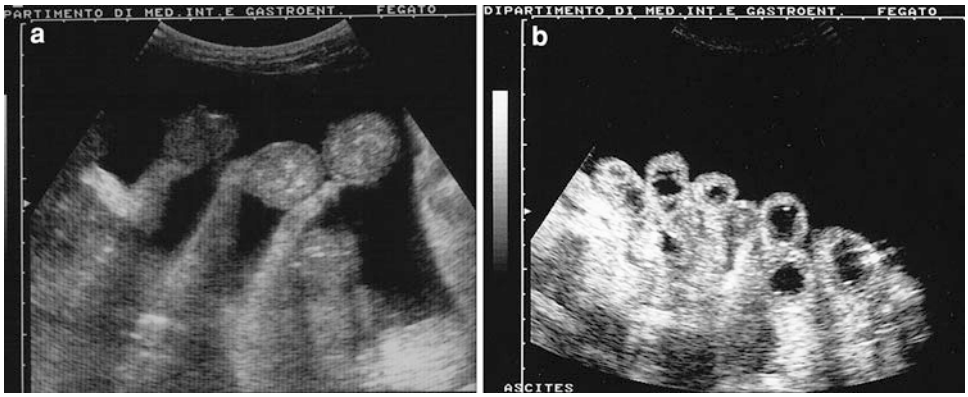

Fig. 3 **a** A case of benign ascites: note the bowel loops free in the anechoic fluid. **b** Contrary to what is seen in **a**, the intestinal loops are fixed and smashed in malignant ascites

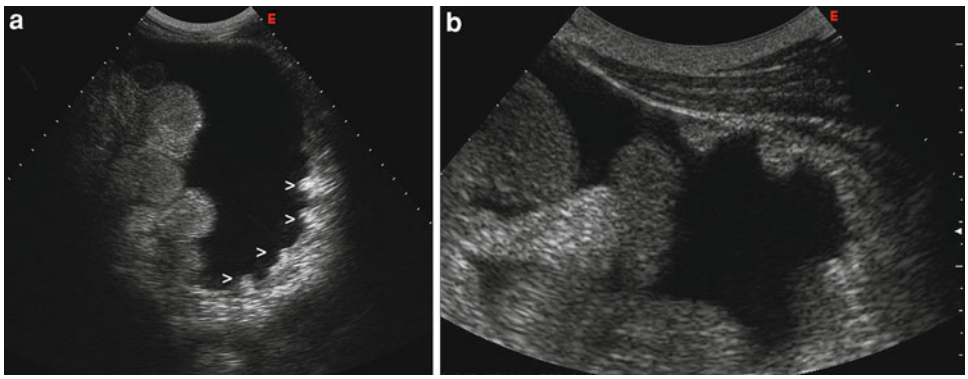

Fig. 4 **a** Very small nodules (>) are clearly visible on the posterior abdominal wall in a case of peritoneal involvement (colon cancer). **b** Small solid nodules (*arrows*) adhering to the anterior abdominal wall in a patient with ovarian cancer

Table 2 Ultrasonographic differential diagnosis between benign and malignant ascites

Ultrasonographic findings	Benign ascites	Malignant ascites
Echogenic ascites	±	+ + +
Septa	Absent	Present
Peritoneal line	Regular	Irregular, interruption, evidence of nodules
Omentum	Thin	"Omental cake"
Mesentery	Free	Fixed
Intestinal loops	Free	Fixed-smashed
Liver metastasis	Absent	Present
Lymphadenopathies	Absent	Present
Other US signs	Liver cirrhosis Pancreatitis Cardiac failure	Absent

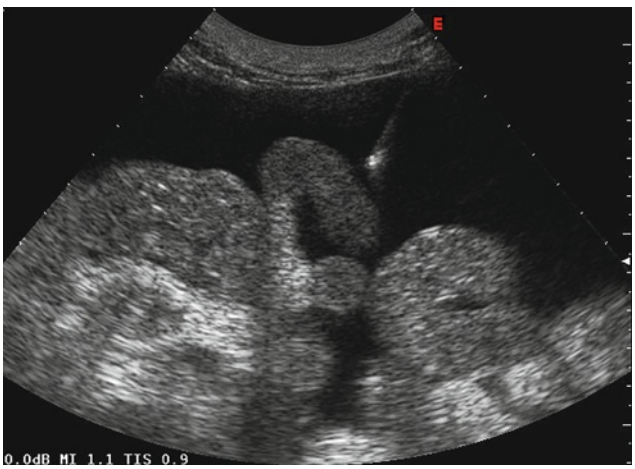

Fig. 5 Ultrasound guided percutaneous fine needle aspiration of ascitic fluid. Note the tip of the needle clearly visible in the fluid

2 Ultrasonographic Findings

Presence of ascites, omental involvement, serosal implants, mesenteric involvement, peritoneal implants, and interruption of the anterior peritoneal line are the most frequently described ultrasonographic findings in patients with peritoneal metastasis. Accessory findings are represented by liver metastasis, lymphadenopathies, and gallbladder wall thickening (Rioux and Michaud 1995). Ultrasonography is also useful in detecting primary cancer in patients without known malignancy: in fact, in a consecutive series on 37 patients, ultrasonography revealed a primary tumor in 16 (57 %) out of 28 patients with no clinical or imaging signs of primary cancer (Rioux and Michaud 1995).

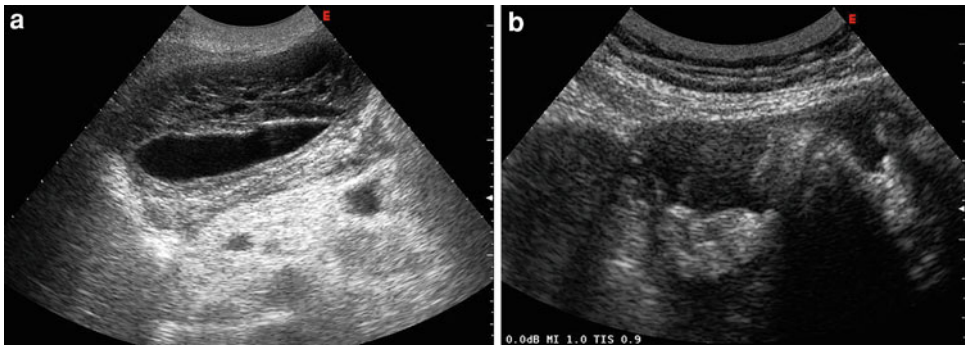

Fig. 6 (**a**, **b**) The "omental cake sign": neoplastic infiltration of the great omentum is visualized by ultrasound as uniformly thick, hyposonic band-shaped structure adjacent to the anterior and lateral walls of the abdomen, following the contour of the abdominal convexity and containing low-level non-structural internal echoes

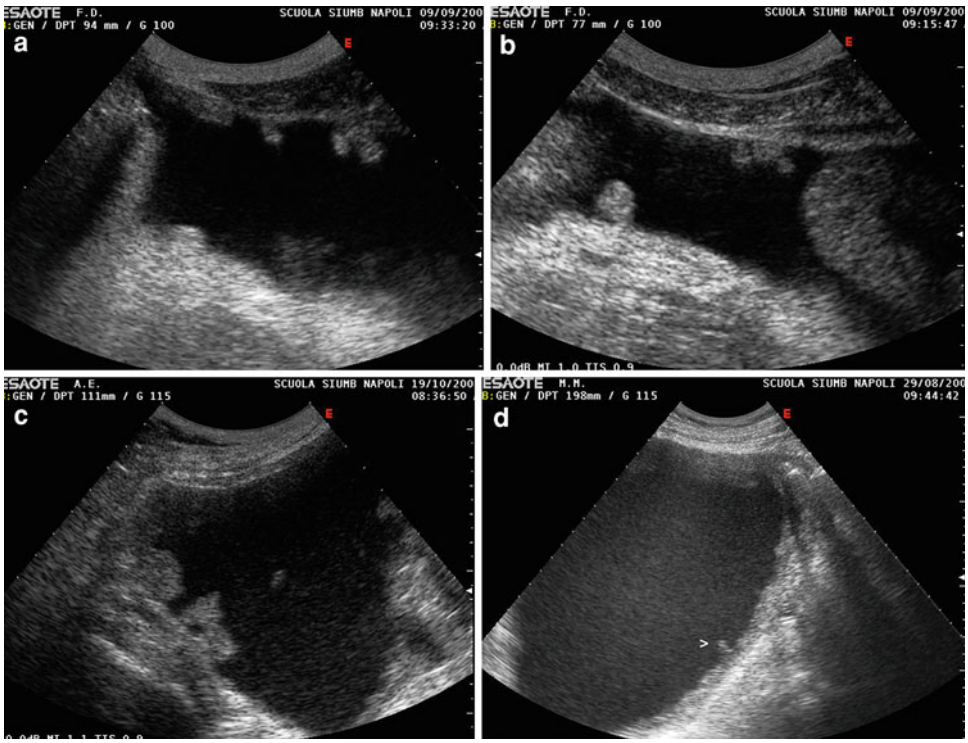

Fig. 7 Small peritoneal implants are clearly visible as hypoechoic nodules on the peritoneal line (**a–c**) or as irregularity (>) of the peritoneal line (**d**). **d** Echogenic ascites is also clearly visible

Table 1 summarizes the prevalence of ultrasonographic signs in peritoneal carcinomatosis.

2.1 Ascites

Ultrasonography is a highly sensitive test in detecting ascites of small volume; (Branney and Wolfe 1995) for example, 5–10 ml ascites are clearly detectable. However, ascites is common in many benign conditions such as liver cirrhosis, portal hypertension, nephrotic syndrome, cardiac insufficiency, etc. (Runyon et al. 1988). Even if ultrasonography is often unable to distinguish between benign and malignant ascites, its presence in patients with known neoplasia is highly suggestive for neoplastic involvement of the peritoneum, and its presence in the lesser omentum (in absence of pancreatitis) is also highly suggestive for malignancy (Dodds et al. 1985). Some ultrasonographic characteristics may be helpful to differentiate benign from malignant ascites.

Frequently, in malignant ascites the fluid is echogenic (due to the presence of blood and/or neoplastic cells) (Fig. 1), septa are often present (Fig. 2), bowel loops are fixed and smashed for mesenteric involvement (Fig. 3), serosal and parietal peritoneal implants are often visible.

Indeed, abundant ascites facilitates visualization of small nodules infiltrating parietal peritoneum, since it acts as a means of contrast (Fig. 4; Goerg and Schwerk 1991).

Table 2 summarizes differential ultrasonographic characteristics between benign and malignant ascites; however, significant ascites is present in about 50 % of patients with peritoneal metastasis (Rioux and Michaud 1995).

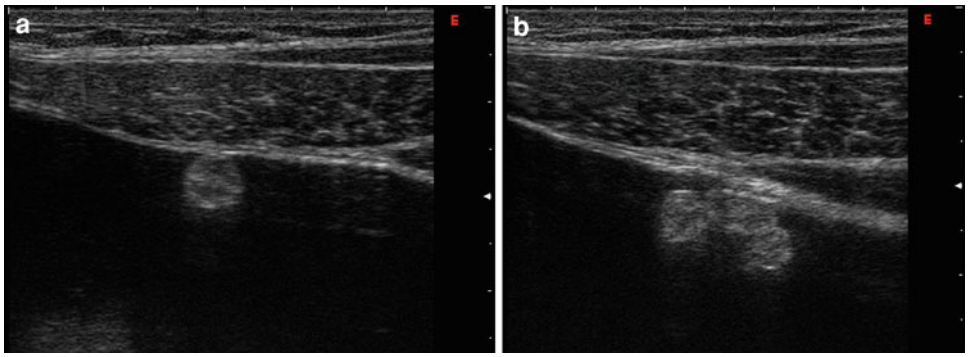

Fig. 8 **a**, **b** The ultrasonography study with high frequency probes (cases showed in Fig. 7) clearly documented the peritoneal metastatic implants

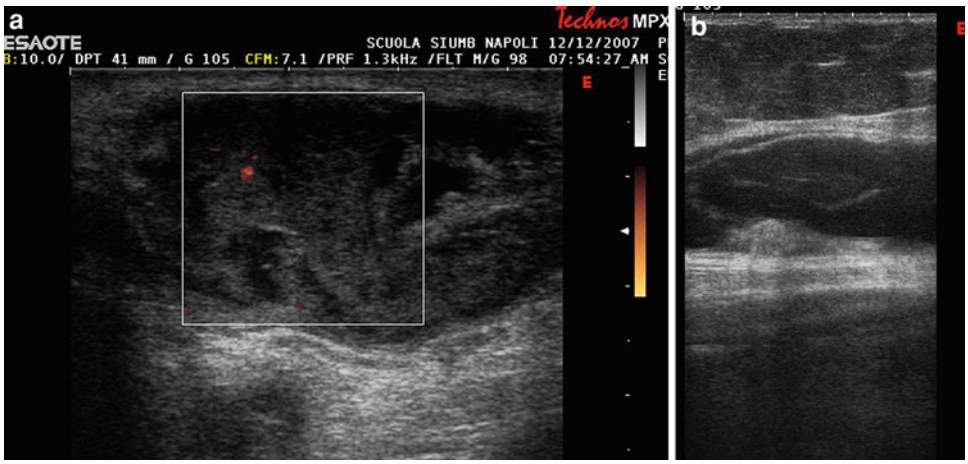

Fig. 9 **a**, **b** Pseumomyxoma peritonei: anechoic area in the thickened peritoneum was a specific sign in indicating the diagnosis of PMP and high-frequency transducer could reveal these tiny anechoic areas more explicitly

Diagnosis of peritoneal metastatic involvement is often based on fluid analysis and ultrasound-guided aspiration of ascites is frequently used in patients with small amounts of liquid (Fig. 5).

Combined with repeated cytological examination of fluid, ultrasound offers 92 % of sensitivity in the diagnosis of peritoneal carcinomatosis thus avoiding laparotomy or laparoscopy (Gerbes 1991; Runyon et al. 1988).

2.2 Omental Involvement

Stein (1977) clearly described the omental band as a new sign of peritoneal metastasis. Neoplastic infiltration of the great omentum is visualized by ultrasound as a uniformly thick, hyposonic band-shaped structure adjacent to the anterior and lateral walls of the abdomen, following the contour of the abdominal convexity and containing low-level non-structural internal echos (omental-cake) (Fig. 6). From this finding, a diffuse metastatic involvement of the omentum can probably be inferred with a high degree of reliability.

Omental involvement is present in about 97 % of patients with peritoneal metastasis (Rioux and Michaud 1995).

2.3 Peritoneal Parietal and Serosal Implants

Peritoneal parietal and serosal implants are visible on ultrasound study as soft tissue masses or nodules adhering to peritoneum, as irregularity or interruption of the anterior hyperechoic peritoneal line (Fig. 7). Visualization is facilitated by the presence of ascites. The ultrasonographic study of the peritoneal line is facilitated by the use of high frequency ultrasound probes, which allow also the visualization of very small peritoneal implants (Fig. 8; Lorenz et al. 1990).

Peritoneal implants, serosal implants, and interruption of the anterior hyperechoic peritoneal lines are present at the rates of about 54, 19, and 16 %, respectively, in patients with peritoneal carcinomatosis (Rioux and Michaud 1995).

Anechoic area in the thickened peritoneum is a specific sign indicating the diagnosis of PMP and high-frequency transducer could reveal these tiny anechoic areas more clearly. In the pelvic cavity, echogenic foci in ascites of PMP could be observed to be mobile and scalloping of the liver margin and "starburst" appearance also played a significant role in indicating PMP (Fig. 9; Que et al. 2012).

2.4 Accessory Findings

Liver metastases are found in about 38 % of patients with peritoneal carcinomatosis, but they represent a non-specific finding. In fact, liver metastases are frequently found even in the absence of peritoneal involvement. Lymphadenopathies are present in about 24 % of cases, but like liver metastases, they do not represent a specific sign of peritoneal carcinomatosis (Rioux and Michaud 1995).

3 Differential Diagnosis and Role of Ultrasound-Guided Biopsy of Peritoneal Masses

The definitive diagnosis of metastatic peritoneal carcinomatosis and its differentiation from peritoneal mesothelioma may be difficult on account of the clinical, macroscopic, and microscopic variability of the latter. Conventionally, these criteria may be established only after surgical exploration and extensive sampling. The recent imaging literature shows excellent correlation between CT or ultrasound and operative or autopsy findings. These imaging modalities have shown soft-tissue masses or nodules, thickened omentum (omental cake), peritoneum, mesentery, bowel wall thickening, pleural plaques, and usually disproportionably small, if any, ascites. The latter two observations may be useful in differentiating macroscopically mesothelioma from peritoneal carcinomatosis (Raptopoulos 1985). Furthermore, fine-needle aspiration biopsy, after performing wide sampling of the tumors in different locations under US or CT guidance (Pombo et al. 1997; Sistrom et al. 1992) produced diagnostic cytologic specimens. Thus, the need for exploratory surgery may be reduced and the differential diagnosis between peritoneal metastasis and peritoneal mesothelioma may be made prospectively and relatively non invasively at the same time using CT or US and fine-needle aspiration biopsy.

Ultrasound-guided needle biopsy in peritoneal masses has been mostly performed by using fine needle (i.e., needle with an outer diameter <1 mm or 20 gauge), but very little experience exists regarding the use of large needle with core biopsy. In the experience of Rioux and Michaud (1995), sonographic findings, confirmed by percutaneous biopsy, avoided 24 unnecessary exploratory laparotomies. Spencer et al. (2001) performed image-guided peritoneal biopsy in 35 women using a 18-gauge core biopsy in omental cake (25 cases), peritoneal (7 cases) and adnexal (3 cases) sites. A correct diagnosis was obtained in 77 % of cases with no false positives and only one false -negative result without significant complications, leading the authors to conclude that image-guided peritoneal biopsy is a simple, safe, and accurate technique for providing site-specific diagnosis in women with undiagnosed peritoneal carcinomatosis.

Gottlieb et al. (1998) determined the effectiveness of sonographically guided biopsies of extra-visceral masses in the peritoneal cavity (outside solid organs). They retrospectively reviewed the results of sonographically guided biopsies of extra-visceral masses found in the peritoneal cavity of 52 patients, 51 of whom underwent biopsy through the abdominal wall. Placement of the biopsy needle within the lesion was successful in all patients. Biopsy results were true positives for malignancy in 37 patients (no false positives), true negatives for benign masses in 10 patients, and false negatives for malignancy in 3 patients (sensitivity 93 %; specificity 100 %; accuracy 94 %). Non-diagnostic samples were obtained only in two patients (4 %). Treatment was based on diagnostic biopsy results in 43 patients (86 %). The authors concluded that sonography is an effective alternative to CT in guiding the biopsy of extra-visceral masses in the peritoneal cavity. Ho et al. (2003) performed 25 percutaneous biopsy of mesenteric masses in 23 patients with a sensitivity and specificity of 95 % and 100 %, respectively, when compared to surgical specimen. Yanhong et al. (2009) performed US-guided biopsy of greater omentum in patients with unclear ascites and thickened omentum. Sensitivity and specificity of the procedure in distinguishing benign from malignant ascites were 95.6 % and 92.9 %, respectively. In conclusion these studies show that US-guided percutaneous biopsy of peritoneal, omental, and mesenteric masses is a safe and highly accurate procedure in the evaluation of neoplastic involvement.

References

Bell DA, Scully RE (1990) Serous borderline tumors of peritoneum. Am J Surg Pathol 14:230–234

Branney SW, Wolfe RE (1995) Quantitative sensitivity of ultrasound in detecting free intraperitoneal fluid. J Trauma 39:375–380

Dodds WJ, Foley WD, Lawson TL et al (1985) Anatomy and imaging of the lesser peritoneal sac. AJR Am J Roentgenol 144:567–575

Gerbes A (1991) Ascitic fluid analysis for the differentiation of malignancy-related and non-malignant ascites. Cancer 68: 1808–1812

Goerg C, Schwerk WB (1991) Malignant ascites: sonographic signs of peritoneal carcinomatosis. Eur J Cancer 27:720–723

Gottlieb RH, Tan R, Widjaja J et al (1998) Extravisceral masses in the peritoneal cavity: sonographically guided biopsies in 52 patients. AJR Am J Roentgenol 171:697–701

Johnson RJ (1993) Radiology in the management of ovarian cancer. Clin Radiol 48:75–82

Ho L, Thomas J, Fine SA et al (2003) Usefulness of sonographic guidance during percutaneous biopsy of mesenteric masses. AJR Am J Roentgenol 180:1563–1566

Longatto Pilho A, Bisi H, Alves VA et al (1997) Adenocarcinoma in females detected in serous effusions: cytomorphologic aspects and immunocytochemical reactivity to cytokeratins 7 and 20. Acta Cytol 41:961–971

Lorenz R, Krestin GP, Neufang KF et al (1990) Diagnosis and differential diagnosis of a peritoneal carcinosis. Conventional techniques, sonography, computed tomography, magnetic resonance tomography. Radiology 30:477–480

Mann WJ, Wagner J, Chumas J et al (1990) The management of pseudomyxoma peritonei. Cancer 66:1636–1640

Novell R, Lewis A (1990) Role of surgery in the treatment of pseudomyxoma peritonei. J R Coll Surg Edinb 35:21–26

Que Y, Tao C, Wang X et al (2012) Pseudomyxoma peritonei: some different sonographic findings. Abdom Imaging 11: (Epub ahead of print)

Pombo F, Rodriguez E, Martin R et al (1997) CT guided core needle biopsy in omental pathology. Acta Radiol 38:978–981

Raptopoulos V (1985) Peritoneal mesothelioma. Crit Rev Diagn Imaging 24:293–328

Rioux M, Michaud C (1995) Sonography detection of peritoneal carcinomatosis: a prospective study of 37 cases. Abdom Imaging 20:47–51

Runyon B, Hoefs JC (1986) Peritoneal lymphomatosis with ascites: a characterization. Arch Intern Med 146:887–889

Runyon B, Hoefs JC, Morgan TR (1988) Ascitic fluid analysis in malignancy related ascites. Hepatology 8:1104–1109

Sistrom CL, Abbitt PL, Feldman PS (1992) Ultrasound guidance for biopsy of omental abnormalities. J Clin Ultrasound 20:27–31

Spencer JA, Swift SE, Wilkinson R et al (2001) Peritoneal carcinomatosis: image-guided peritoneal core biopsy for tumor type and patient care. Radiology 221:173–177

Stein MA (1977) Omental band: new sign of metastasis. J Clin Ultrasound 5:410–412

Walsh D, Williams G (1971) Surgical biopsy studies of omental and peritoneal nodules. Br J Surg 58:428–431

Yamada S, Takeda T, Matsumoto K (1983) Prognostic analysis of malignant pleural and peritoneal effusions. Cancer 51:136–139

Yanhong Q, Xuemei W, Yanjun L et al (2009) Ultrasound guided biopsy of greater omentum: an effective method to trace the origin of unclear ascites. Eur J Radiol 70:331–335

Carcinoid and Submucosal Tumors

Jiro Hata, Ken Haruma, Noriaki Manabe,
and Hiroshi Imamura

Contents

J. Hata · N. Manabe · H. Imamura
Department of Clinical Pathology and Laboratory Medicine, Kawasaki Medical School, 577 Matsushima, Kurashiki City, Okayama 701-0192, Japan

K. Haruma (✉)
Division of Gastroenterology, Department of Internal Medicine, Kawasaki Medical School, 577 Matsushima, Kurashiki City, Okayama 701-0192, Japan
e-mail: kharuma@med.kawasaki-m.ac.jp

Abstract

In this chapter, the sonographic diagnosis of carcinoid and submucosal tumors is discussed. For the sonographic diagnosis of these tumors, the assessment of wall stratification is essential. After deciding the main layer of the tumor, the shape, echogenicity, and blood vessel patterns are evaluated to diagnose each tumor. Contrast ultrasound is also useful for the evaluation of microperfusion of tumors. In most cases, the diagnostic ability of extracorporeal ultrasound, which is noninvasive and easy to execute, is almost equivalent to that of endoscopic ultrasound.

1 Introduction

The diagnosis of carcinoid and submucosal tumors by endoscopy or barium contrast studies is not easy since these tumors are usually covered with a normal mucosal layer. Determining the main portion of the wall stratification in the gastrointestinal wall in which the tumors lie is the most important part of the diagnostic imaging of submucosal tumors. For this purpose, endoscopic ultrasound (EUS), including the use of an EUS-guided fine needle aspiration biopsy (FNA), is the best choice (Arantes et al. 2004; Vander et al. 2004); however, not all institutions have the equipment or experienced staff to easily execute EUS in all cases with submucosal tumors. Transabdominal ultrasound, with the remarkable improvement of equipment, can be used as an alternative method (Polkowski et al. 2002; Futagami et al. 2001; Tsai et al. 2000). There have been several reports on transabdominal ultrasound as an acceptable alternative for the diagnosis of submucosal tumors. In this chapter, the sonographic images of carcinoid and submucosal tumors are discussed.

G. Maconi and G. Bianchi Porro (eds.), *Ultrasound of the Gastrointestinal Tract*, Medical Radiology. Diagnostic Imaging,
DOI: 10.1007/174_2012_722, © Springer-Verlag Berlin Heidelberg 2012
Published Online: 22 August 2012

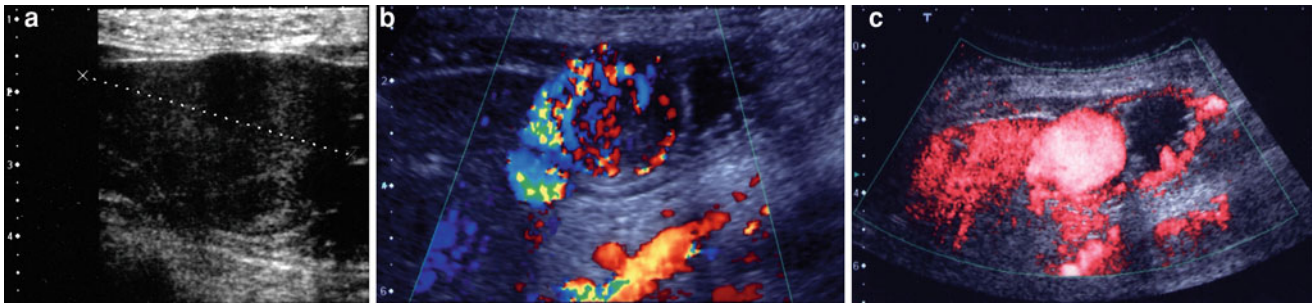

Fig. 1 **a** Sonographic feature of a gastric carcinoid. A *round-shaped* hypoechoic tumor is demonstrated. Wall stratification is not demonstrated clearly in this figure. **b** Color Doppler ultrasound shows the rich vascularity of the tumor. **c** Contrast-enhanced ultrasound of the tumor also reveals the rich blood perfusion

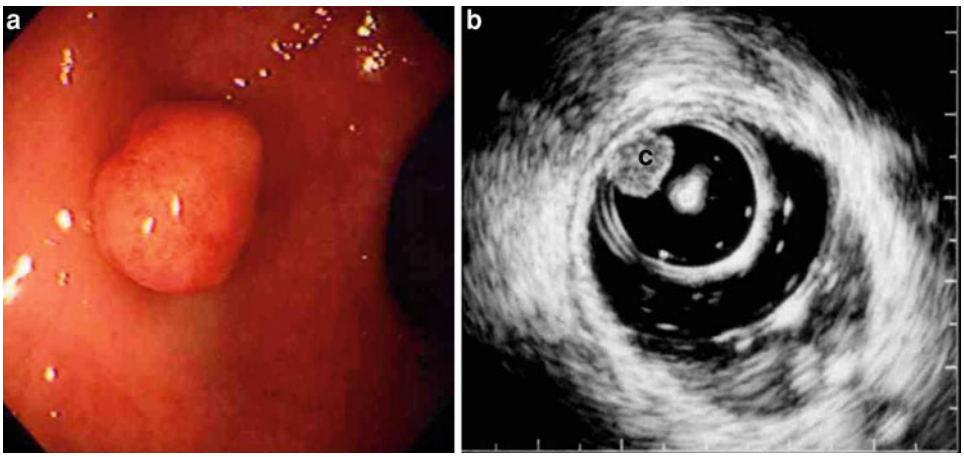

Fig. 2 **a** Endoscopic feature of rectal carcinoid. A small (5 mm in diameter) submucosal tumor is demonstrated. **b** Endosonography with a miniature ultrasound probe (12 MHz). A small *round-shaped* tumor (*C*) is demonstrated beneath the first layer and no changes in submucosal layer are seen

2 Preparations for Sonographic Assessment of Submucosal Tumors

For the evaluation of gastroduodenal lesions, an overnight fast and the ingestion of water (200–400 ml) are useful. However, for the small bowel lesions, such preparations are not so advantageous for better visualization; therefore, intestinal lesions, especially when they are small in size, are not easy to detect with transabdominal ultrasound. The retrograde water filling method is effective for the assessment of colonic lesions, but it requires total clearance of colonic contents before the examination, which makes its routine use difficult.

3 Carcinoid Tumor

Since carcinoid tumors usually originate in the deep mucosa, they appear as a focal mass with a clear margin and smooth contour located in the second layer (Figs. 1, 2). The echogenicity of the tumor is homogenous and relatively low compared with that of the surrounding mucosal layer. As the gastrointestinal wall is invaded more deeply by the tumor, the stratification of the wall is deformed, and it is finally destroyed when the tumor grows transmurally. Even with EUS, the differentiation of a carcinoid tumor from a myogenic tumor arising from the muscularis mucosae or a granular cell tumor is often difficult.

4 Submucosal Tumors

4.1 Cyst and Lymphangioma

Cysts and lymphangiomas are located in the submucosal layer (Figs. 3, 4). They are well demarcated by a thin wall and are anechoic. Posterior echo enhancement as an artifact is a characteristic figure. They show good compressibility and change their shapes with external compression. Color Doppler does not reveal any vascular structure inside. Often septal structures are seen inside the tumor.

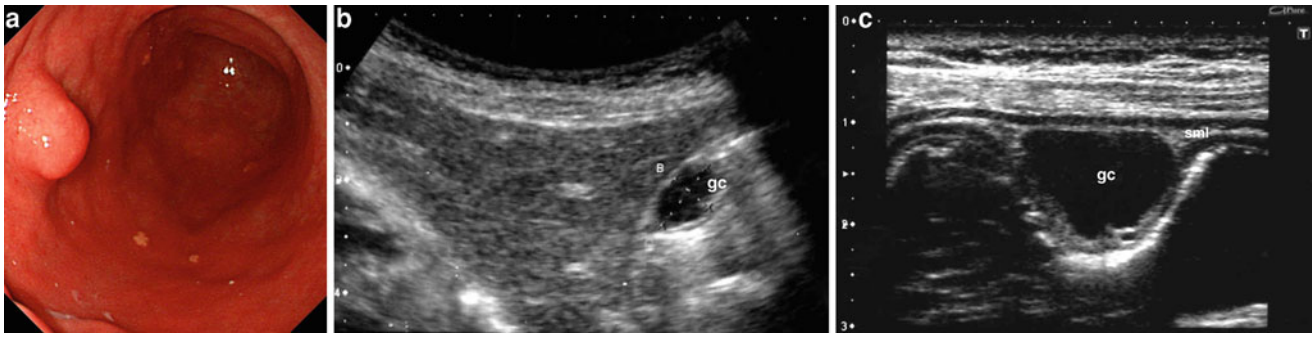

Fig. 3 **a** Endoscopy of a gastric cyst. The tumor is located in the anterior wall of the antrum and is covered with normal mucosa without indentation or erosion. **b** Sonography with a convex probe (3 MHz) of the gastric cyst (*gc*). A small anechoic tumor is demonstrated although the main layer where the tumor lies is not clear. **c** Scanning with a high-frequency linear probe (7 MHz) revealed that the lesion (*gc*) lies in the submucosal layer (*sml*). *S* stomach

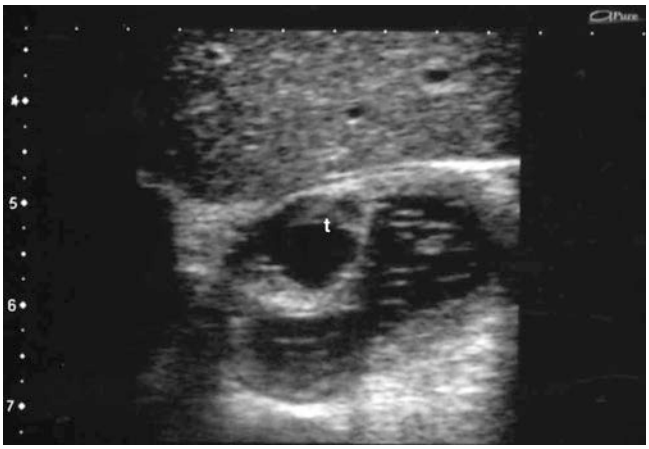

Fig. 4 Lymphangioma at the duodenal bulb. A cystic tumor (*t*) with septa is seen in the submucosal layer

4.2 Lipoma

Lipomas also lie in submucosal layer (Fig. 5). They are very soft, their shape can be changed easily by external compression or peristalsis. Their internal echoes are generally equivalent or slightly lower than that of the adjacent submucosal layer. Vascular signals are seldom detected with color Doppler. Usually no changes are seen in the mucosal and proper muscle layers.

4.3 Ectopic Pancreas

An ectopic pancreas is characterized as a hypoechoic tumor mainly located in the submucosal layer with thickening of the adjacent proper muscle layer (Fig. 6). A tiny cystic area representing the ductal structure may be demonstrated.

4.4 Hemangioma

A hemangioma is demonstrated as a hyperechoic tumor in the submucosal layer. Calcification is occasionally seen inside the tumor (Fig. 7). Since the blood flow of the capillaries making up the tumor is extremely slow, it is difficult to detect blood flow signals using the conventional color Doppler method.

Pyogenic granuloma is one form of hemangioma, often found to involve the skin and the gastrointestinal lesion is relatively rare. A pyogenic granuloma in the ileum shows rich vascularity both with color Doppler and contrast ultrasound.

4.5 Gastrointestinal Stromal Tumor

Gastrointestinal stromal tumors (GISTs) are demonstrated as focal hypoechoic nodules originating in the proper muscle layer (Figs. 8 and 9). They are usually well demarcated and round shaped. In accordance with the tumor growth, the internal echo tends to be more heterogenic with hyper/hypoechoic nodules inside representing the focal degeneration of the tumor. With color Doppler, rich vascular structures running toward the center of the tumor (centripetal) are visualized. Although there is a study showing that heterogeneous echo texture, size >3 cm, and irregular margins are the risks for presence of malignancy (Brand et al. 2002), it is not easy to decide the malignant potential of each GIST with ultrasound preoperatively (Rosch et al. 2002). GISTs exceeding 5 cm in diameter generally require surgical resection following FNA.

4.6 Schwannoma

A schwannoma usually lies in the proper muscle layer and is demonstrated as a well-demarcated round tumor with a smooth contour (Fig. 10). It is difficult to differentiate this tumor from

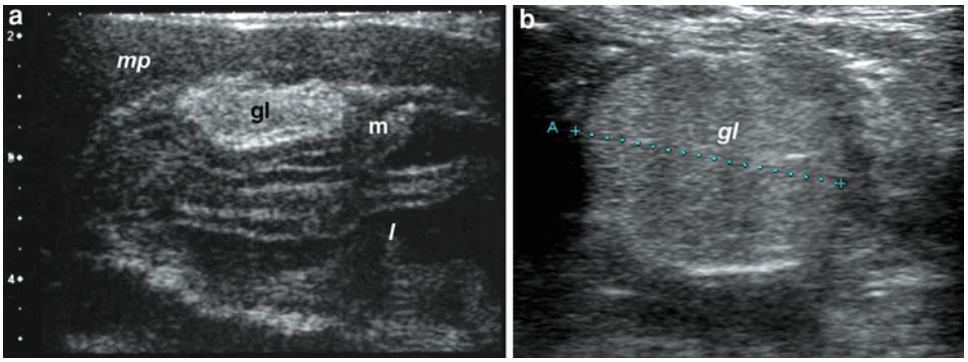

Fig. 5 **a** Sonographic features of gastric lipomas (*gl*). a Hyperechoic tumor located in the submucosal layer of the gastric wall is demonstrated. **b** Sonography of duodenal lipoma, which resembles that of gastric lipoma

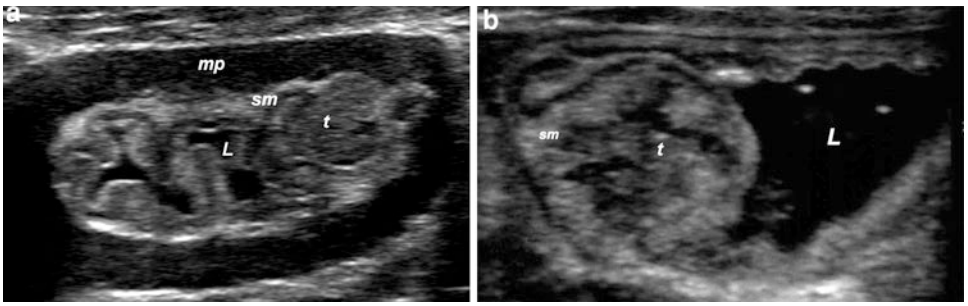

Fig. 6 **a** Aberrant pancreas at the greater curvature of the stomach. A hypoechoic tumor (*t*) with a small cystic area inside mainly located in the submucosal layer (*sm*) is observed. **b** Aberrant pancreas at the ileum. A hypoechoic tumor (*t*) involving cystic areas in the submucosal layer is demonstrated. *mp* Muscularis propria. *L* Lumen

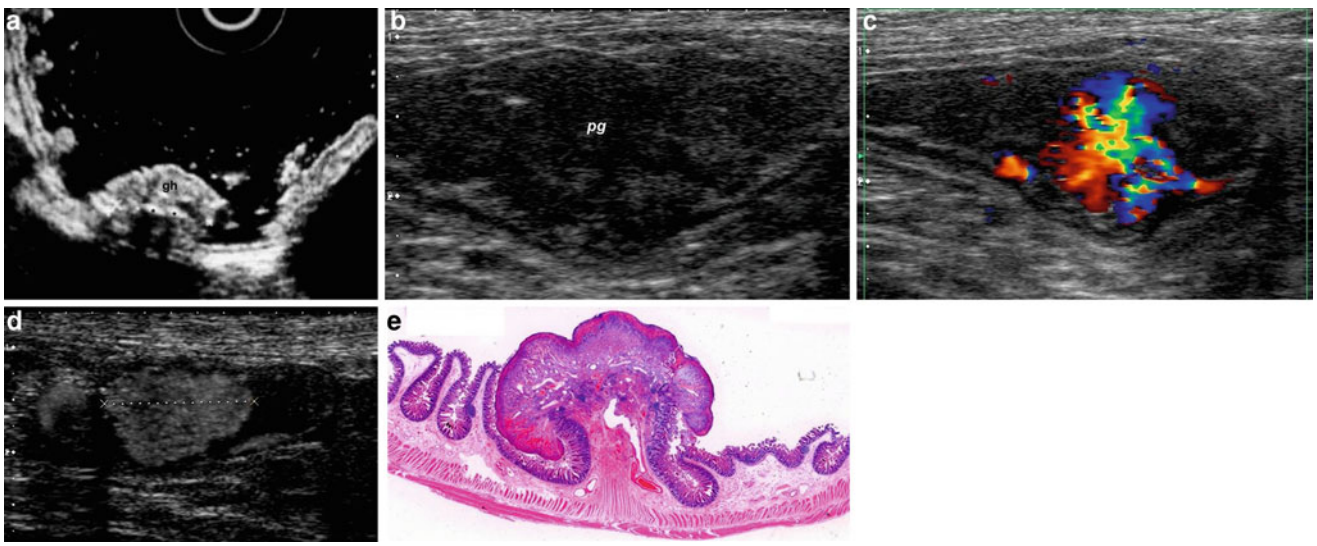

Fig. 7 **a** Endoscopic ultrasound of a gastric hemangioma (*gh*). The tumor lies in the submucosal layer and calcifications inside the tumor are seen (*asterisks*). **b** Sonography of a pyogenic granuloma (*pg*) in the ileum. Hypoechoic tumor with irregular contour is demonstrated. **c** Color Doppler image of the tumor. Extremely rich vascularity is shown. **d** Contrast ultrasound also shows rich perfusion of the tumor. **e** Hematoxylin and Eosin stain of the resected specimen

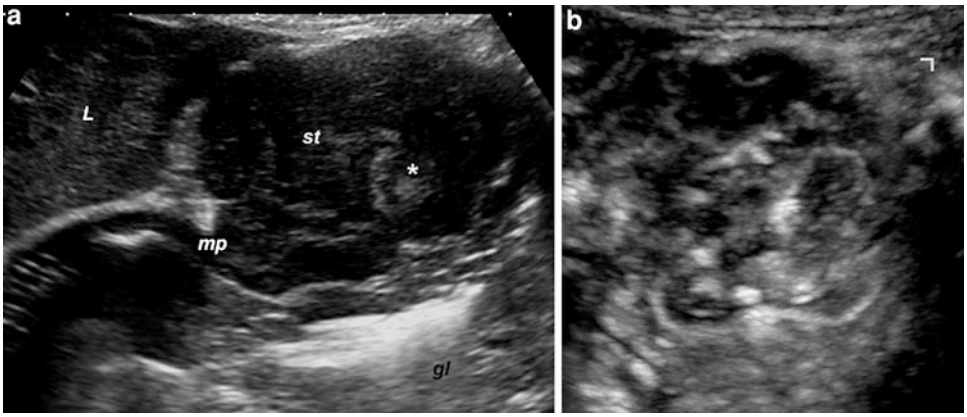

Fig. 8 Sonography of gastrointestinal stromal tumors (GISTs). **a** Well-demarcated hypoechoic tumors (*st*), strongly connected to the proper muscle layer (*mp*). **b** Contrast ultrasound shows the rich vascularity of the tumor. *gl* Gastric lumen; *L* Liver

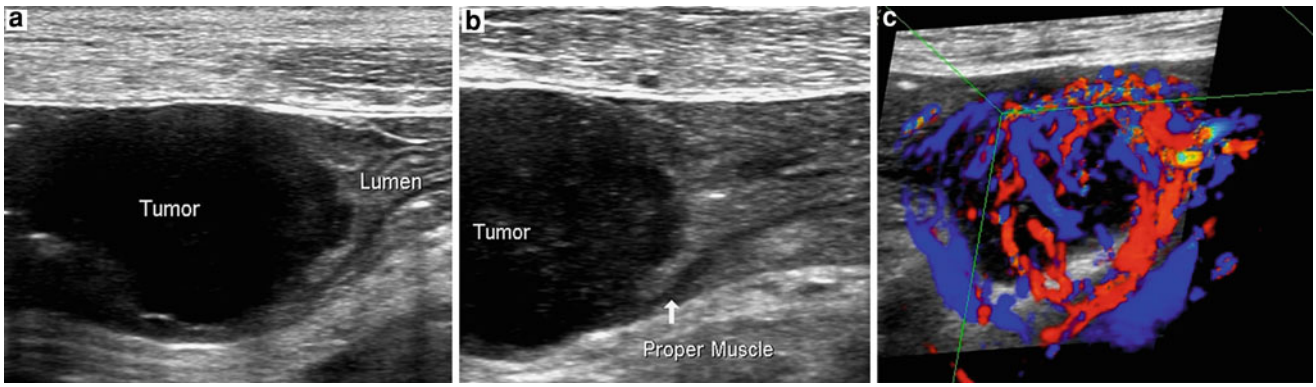

Fig. 9 Sonography of the jejunal GIST. **a**, **b** An oval-shaped hypoechoic tumor, well-demarcated and with smooth contours. The tumor is connected to the proper muscle. **c** Color Doppler image (3D) of the tumor shows the basket-like pattern of the tumor vessels

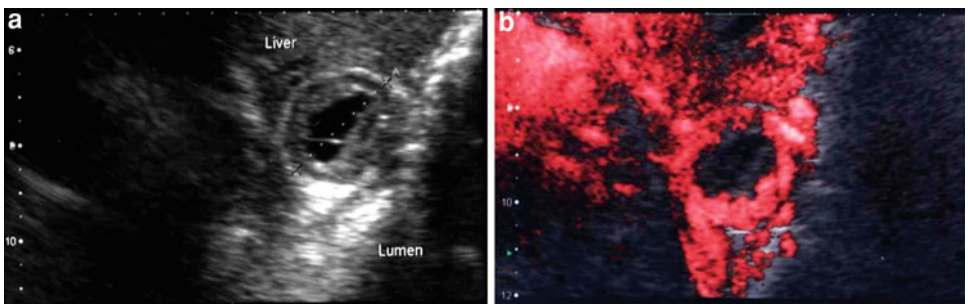

Fig. 10 **a** Sonography of a gastric schwannoma with massive central necrosis. A hypoechoic tumor with a cystic area inside is demonstrated at the anterior wall of the gastric body. **b** Contrast ultrasound reveals loss of perfusion in the cystic area

GIST, since the main layer in which the tumor lies and the shape and echogenicity of both tumors are very similar.

4.7 Inflammatory Fibroid Polyp

Since inflammatory fibroid polyps usually arise from submucosa and often project into lumen, it is not easy to decide the main layer of the tumor. Typically, a relatively small, round-shaped tumor with straight vessel structure toward the center of the tumor is demonstrated with ultrasound (Fig. 11).

4.8 Extramural Compression

The most frequently encountered condition mimicking submucosal tumors is extramural compression. Diagnosis is decided by demonstrating the normal five-layer structure in

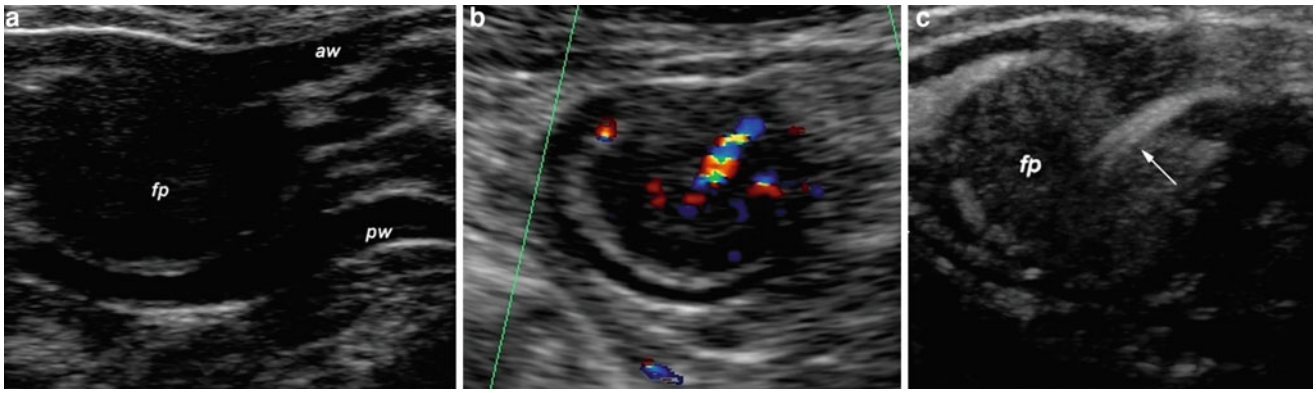

Fig. 11 Sonography of the inflammatory fibroid polyp in the ileum. **a** The polyp is well demarcated and the contour is smooth. **b** Color Doppler ultrasound of the tumor shows a straight vessel toward the center of the tumor although the vascularity evaluated with color Doppler is not as rich as that of GIST. **c** Contrast-enhanced ultrasound reveals the minute perfusion and the straight vessel structure (*arrow*)

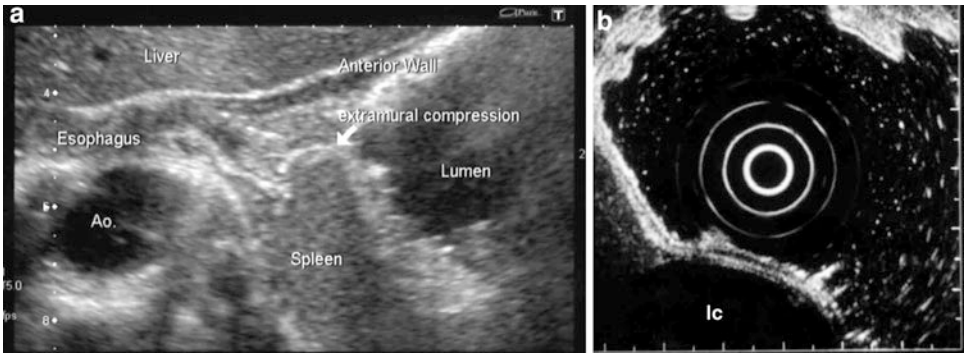

Fig. 12 **a** Extramural compression of the gastric wall by the spleen. An elevated area due to compression of spleen is shown. **b** Endosonographic feature of the extramural compression by a liver cyst (*lc*). The normal five-layer structure is observed at the elevated area

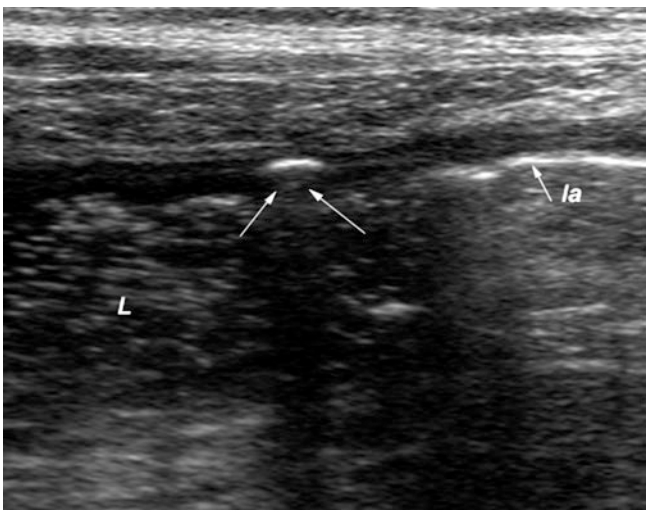

Fig. 13 Sonographic feature of the pneumatosis cystoides intestinals in the ileum. A strong echo with comet-tail echo is demonstrated at the submucosal layer of the bowel wall (*arrow*). *L* lumen; *la* luminal air

the elevated portion and the cause of compression, such as the adjacent spleen or a liver cyst (Fig. 12).

4.9 Pneumatosis Cystoides Intestinals

Pneumatosis cystodies intestinalis is not actually a submucosal tumor, but the endoscopic feature resembles that of a submucosal tumor. EUS shows an echogenic spot with a comet-tail artifact in the submucosal layer, which represents the air bubble (Fig. 13).

4.10 Enteric Duplication Cyst

Enteric duplication cyst has proper muscle layer in common with the adjacent normal ileum that may mimic submucosal tumor. Duplication cysts usually show stratification in the wall and fluid collection in the lumen, which is helpful in differentiating GIST (Fig. 14).

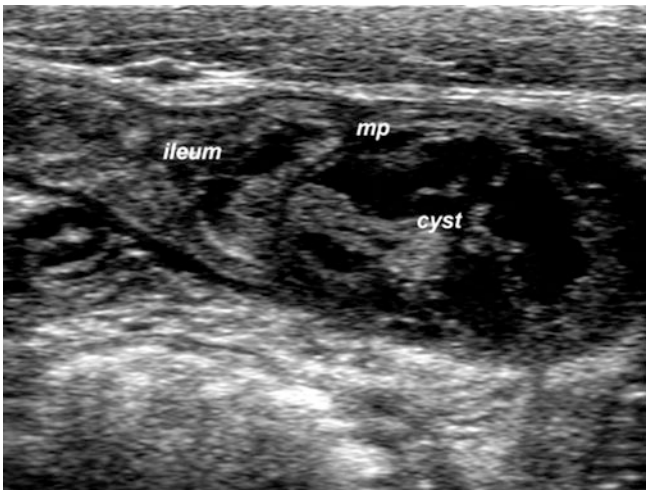

Fig. 14 Sonography of an enteric duplication cyst in the ileum. The lesion has proper muscle (*mp*) in common with the adjacent normal ileum

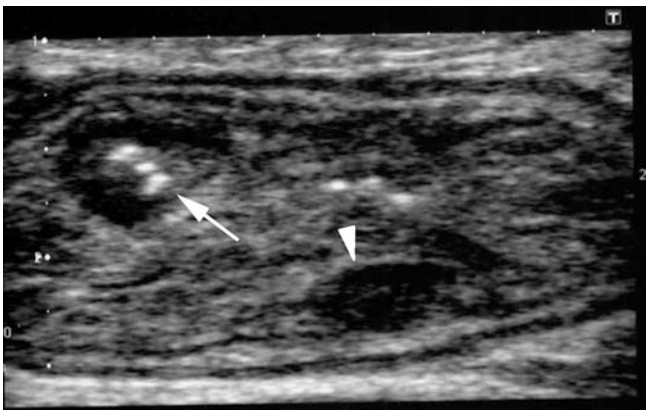

Fig. 15 Sonography of metastatic ileal tumors (lung cancer). Although one lesion has an ulceration in the center (*arrow*), the other looks like a submucosal tumor located in the submucosa (*arrowhead*)

4.11 Metastatic Gastrointestinal Tumor

Metastatic gastrointestinal tumors may mimic submucosal tumors. Since they are usually observed in the deep mucosa or submucosa, it is not easy to distinguish between metastatic tumors and carcinoid or other disorders such as lymphoma (Fig. 15).

5 Conclusion

Transabdominal ultrasonography, which is a noninvasive and easy method of approach for diagnosing gastrointestinal tract including small bowel, can be a useful alternative modality to EUS in the assessment of carcinoid or submucosal tumors.

References

Arantes V, Logrono R, Faruqi S et al (2004) Endoscopic sonographically guided fine-needle aspiration yield in submucosal tumors of the gastrointestinal tract. J Ultrasound Med 23:1141–1150

Brand B, Oesterhelweg L, Binmoeller KF et al (2002) Impact of endoscopic ultrasound for evaluation of submucosal lesions in gastrointestinal tract. Dig Liver Dis. 34:290–297

Futagami K, Hata J, Haruma K et al (2001) Extracorporeal ultrasound is an effective diagnostic alternative to endoscopic ultrasound for gastric submucosal tumours. Scand J Gastroenterol 36:1222–1226

Polkowski M, Palucki J, Butruk E (2002) Transabdominal ultrasound for visualizing gastric submucosal tumors diagnosed by endosonography: can surveillance be simplified? Endoscopy 34:979–983

Rosch T, Kapfer B, Will U et al (2002) Accuracy of endoscopic ultrasonography in upper gastrointestinal submucosal lesions: a prospective multicenter study. Scand J Gastroenterol 37:856–862

Tsai TL, Changchien CS, Hu TH et al (2000) Demonstration of gastric submucosal lesions by high-resolution transabdominal sonography. J Clin Ultrasound 28:125–132

Vander NMR III, Eloubeidi MA, Chen VK et al (2004) Diagnosis of gastrointestinal tract lesions by endoscopic ultrasound-guided fine-needle aspiration biopsy. Cancer 102:157–163

Intestinal Endometriosis

Giovanni Maconi, Michela Monteleone, Cristina Bezzio, and Francesco P. G. Leone

Contents

Abstract

Endometriosis is defined as the presence of endometrial tissue outside the uterus. Endometriosis occurs almost exclusively in women between 20 and 45 years old, in particular up to 15 % of fertile women and up to 30 % of infertile women. Most women with endometrial implants on bowel serosa are asymptomatic; those with deep infiltrating implants may complain of abdominal pain, dysmenorrhea, dyspareunia, low backache, and localized tenderness. At sonography, intestinal endometriosis can appear as hypoechoic thickening or nodules/masses with irregular contours or, less frequently, as cystic lesions with anechoic fluid content and hyperechoic blood deposits, which often deforms the profiles of the bowel, and rarely causes complications such as invagination and volvulus.

1 Introduction

Endometriosis is defined as the presence of ectopic endometrial glands and stroma outside the uterus. Endometriosis occurs in up to 15 % of fertile women and up to 30 % of infertile women (Olive and Schwarz 1993). Endometriosis usually presents with painful symptoms, such as cyclic pelvic pain (dysmenorrhea), pain on intercourse (dyspareunia), or non-menstrual pelvic pain (Moore et al. 2002).

Most often the ectopic tissue is located in the vicinity of the uterus, but also the gastrointestinal tract may be involved. In contrast to endometrial involvement of the female reproductive organs, gastrointestinal involvement is less common and usually asymptomatic (Zwas and Lyon 1991). The most frequent intestinal organs involved are rectosigmoid colon (85–96 %), appendix (6–10 %), and ileum (5–8 %) (Weed and Ray 1987; Chapron et al. 2006). Intestinal involvement is characterized by serosal

Electronic supplementary material The online version of this article (doi:10.1007/174_2013_831) contains supplementary material, which is available to authorized users.

G. Maconi (✉) · M. Monteleone · C. Bezzio
Gastroenterology Unit,
Department of Biomedical and Clinical Sciences,
"L. Sacco" University Hospital,
Via G. B. Grassi, 74, 20157 Milan, Italy
e-mail: giovanni.maconi@unimi.it

F. P. G. Leone
Gynaecology Unit,
Department of Biomedical and Clinical Sciences,
"L. Sacco" University Hospital,
Via G. B. Grassi, 74, 20157 Milan, Italy

G. Maconi and G. Bianchi Porro (eds.), *Ultrasound of the Gastrointestinal Tract*, Medical Radiology. Diagnostic Imaging,
DOI: 10.1007/174_2013_831,
Published Online: 23 March 2013

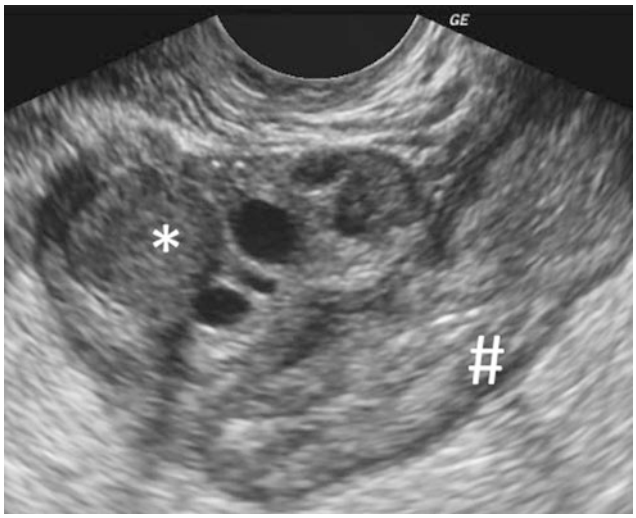

Fig. 1 Transvaginal sonography showing an ovarian endometrioma (*) along with a sigmoid colon with thickened bowel wall and hyperechoic submucosal layer (#) in a Crohn's disease patient

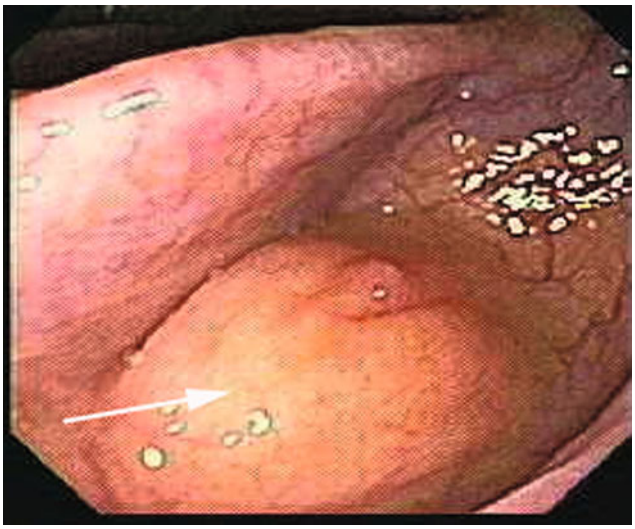

Fig. 2 Colonoscopy showing an area of extrinsic compression (*arrow*) due to intestinal endometriosis with normal appearing mucosa

implantation with a variable degree of intramural extension. Deep penetrating lesions might manifest with hematochezia and mime a wide variety of inflammatory, infectious, and neoplastic intestinal disorders (Shah et al. 1995). Recently, an association between pelvic endometriosis and Crohn's disease has been reported (Jess et al. 2012) (Fig. 1).

2 Etiology and Pathogenesis

Several hypotheses have been advanced to explain the ectopic location of endometrial tissue (Oral and Arici 1997). The most common explanation is the retrograde passage of endometrial tissue, which then implants on pelvic organs and peritoneum. From these sites, more distant localizations may arise via hematogenous or lymphatic dissemination; further dissemination may occur during surgical interventions. A less accepted hypothesis is that of endometrial metaplasia, an alteration caused by the metaplastic transformation of multipotential peritoneal mesothelial cells in endometrial tissue.

Endometrial tissue is regulated by hormonal influence: estrogen promotes and progesterone inhibits growth. These repetitive cycles of growth and sloughing of ectopic tissue can lead to serosal irritation and progressive invasion of bowel muscle with fibrosis and muscular hypertrophy. This may lead to bowel strictures or intestinal kinking with the risk of developing chronic abdominal pain (Rock and Markham 1992).

3 Clinical Features

Endometriosis is almost exclusively found in women between 20 and 45 years old. Women who experience endometriosis beyond menopause presumably have chronic fibrosis or exacerbation induced by exogenous estrogens. Although most women with endometrial implants on intestinal structures are asymptomatic, those with serosal implantation may complain of abdominal pain, dysmenorrhea, dyspareunia, low backache, and localized tenderness.

Symptoms due to the penetration of endometrial tissue into the bowel wall may depend on the location of the ectopic tissue. If the rectum or the sigmoid colon are involved (posterior pelvic compartment), the main symptoms are dyschezia, tenesmus, and rectal bleeding, primarily during the menstrual cycle (52 % of cases), or partial obstruction with intermittent abdominal pain, constipation, and diarrhea (14 % of cases), respectively (Bianchi et al. 2007; Chapron et al. 2003). The invasion of the wall of the appendix or the ileum by the endometrial tissue may generate acute appendicitis, or strictures of the small bowel, with symptoms of acute intestinal obstruction due to fibrosis, volvulus, or intussusception, respectively. Symptoms are not always cyclical and may be independent from hormonal levels, and gastrointestinal manifestations are not necessarily associated with gynecological symptoms. For example, the hematochezia may occur when endometrial implants penetrate the mucosa of the bowel wall or when severe and chronic fibrosis results in ischemia (Bontis and Vavilis 1997).

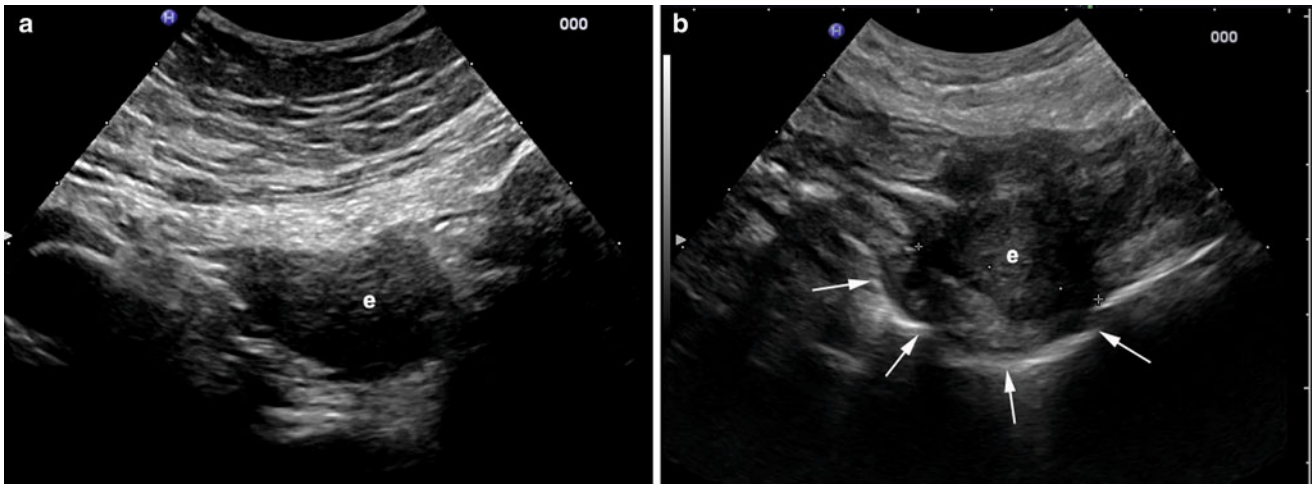

Fig. 3 Intestinal endometriosis detected by transabdominal ultrasound. **a**, **b** The lesions appear as hypoechoic nodules with irregular contours (e) involving the deep layers of the bowel wall. **b** The lesion deforms the intestinal lumen (*arrows*), easily detectable for its gaseous content

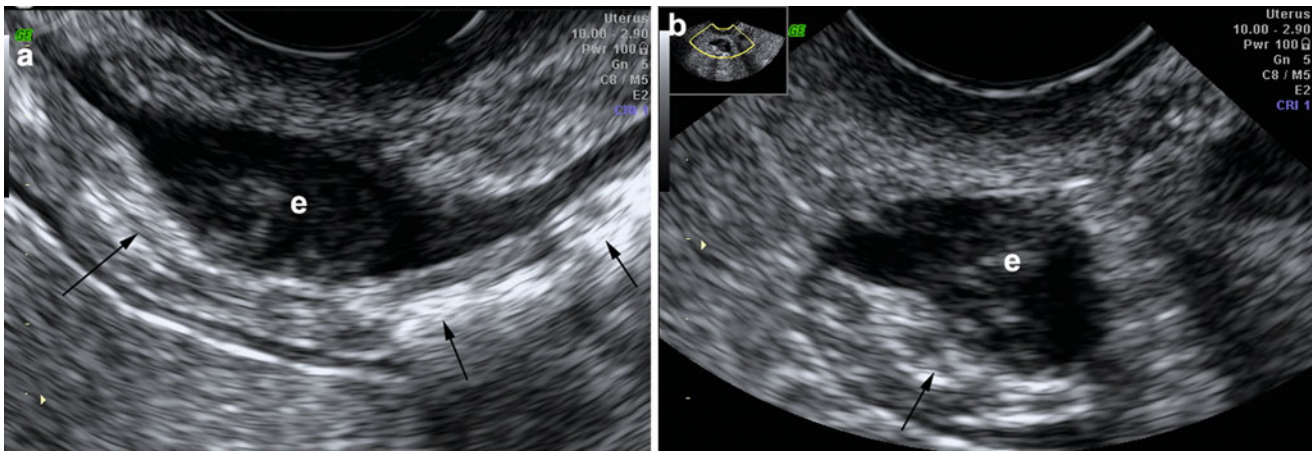

Fig. 4 Transvaginal ultrasound showing an endometriotic lesion of the sigmoid colon. Longitudinal (**a**) and transversal (**b**) scans of the lesion appearing as a hypoechoic nodule (e) that involves the deep layer of the wall, imprinting and deforming the lumen (*arrows*) detectable for its gaseous content

4 Diagnosis

The clinical diagnosis of intestinal endometriosis may be difficult because symptoms and signs often are nonspecific and not always related to the menstrual cycle. Endometriosis should always be considered in women between 20 and 45 years old with gynecologic complaints and with recurrent abdominal pain or gastrointestinal symptoms.

An important component of the evaluation in suspected endometriosis is a careful examination of the pelvis that includes combined recto-vaginal palpation. The presence of a nodule or the irregularity in the recto-uterine pouch is highly suggestive of this disease. The pelvic examination should be performed before and after the menstrual phase because the lesion may vary during the menstrual cycle.

If the predominant symptom is hematochezia, colonoscopy is recommended. In patients without hematochezia, colonoscopy may be normal except for areas of extrinsic compression or strictures (Fig. 2) (Bozdech 1992). More helpful in these patients is the double-contrast barium enema, computed tomography (CT) colonography or magnetic resonance imaging (MRI), which can demonstrate submucosal polypoid masses or lesions narrowing the lumen.

Computed tomography scans, ultrasonography, and magnetic resonance imaging all have been reported to assist the diagnosis or the assessment of the extent of endometrial involvement. High-resolution transvaginal and transrectal

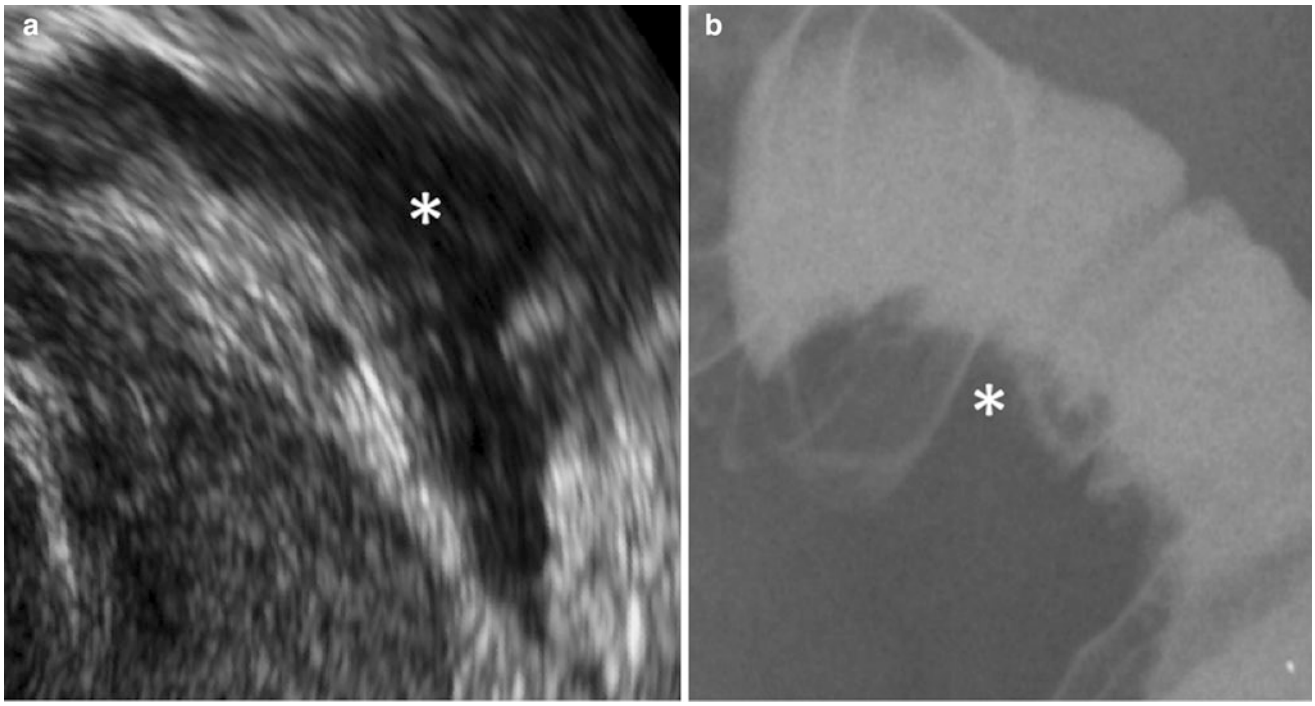

Fig. 5 "Indian hair-dress sign" at 2D-TVS compared to the tethering effect at barium enema. Pulling-out TVS (**a**) versus tethering effect barium enema (**b**)

ultrasound also may be useful in detecting endometrial implants, in particular in the retroperitoneal structures (Brosens et al. 2003).

However, definitive diagnosis of endometriosis is often made by laparoscopy or laparotomy with biopsy (Jansen and Russell 1986). The appreciation that endometrial tissue may be nonpigmented has increased the yield of these procedures considerably. Histology shows endometriotic foci characterized by variably sized glands lined by columnar epithelium embedded in endometrial stroma. Usually, fibrosis of the adjacent fat accompanies the process. Mucosal involvement can cause inflammation, polypoid lesions, ulcers, and fibrosis. The involvement of the submucosa often produces a smooth muscle reaction, featuring thick and irregularly arranged bundles of muscle. If the disease is extended to the muscularis propria it produces a disorganized hyperplasia of the adjacent smooth muscle (Kaufaman et al. 2011).

Recently, peripheral biomarkers, combined with non-invasive diagnostic procedures such as ultrasound or MRI, have been suggested as diagnostic aids in women with suspected intestinal endometriosis. However, despite Ca-125 and Ca19-9 are currently used in clinical practice, to date there are not a single biomarker or panel of biomarkers that have unequivocally been shown to be clinically useful in routine clinical care.

4.1 Ultrasonography

Ultrasound examination of the pelvis is the first diagnostic choice to identify endometriosis. The transabdominal ultrasound used to explore the pelvis, should be followed by transvaginal ultrasound (TVS) to obtain more details of the anatomical structures, such as the bladder, the ovaries, the uterus, the uterus-sacral ligaments, the recto-vaginal septum, and the recto-sigmoid (Piketty et al. 2009). Over the past decade, the use of TVS has improved the quality of non-invasive assessment of patients with suspected pelvic pathologies. Bazot et al. (2003) have suggested the potential value of TVS for the diagnosis of endometriosis and confirmed that the technique was able to accurately diagnose the endometriosis of the rectum, ovaries, uterosacral ligament, recto-vaginal space, pouch of Douglas, vagina, and urinary bladder. The sensitivities, specificities, and positive and negative likelihood ratios in six studies using gray-scale ultrasonography ranged between 64 and 89 %, 89 and 100 %, 7.6 and 29.8 %, and 0.1 and 0.4 %, respectively (Moore et al. 2002).

Improvement of the diagnostic accuracy may be obtained by performing TVS with saline solution in the vagina or with water-contrast enema in the rectum.

At sonography, both TVS and transabdominal sonography, endometriosis appears less frequently as cystic lesions

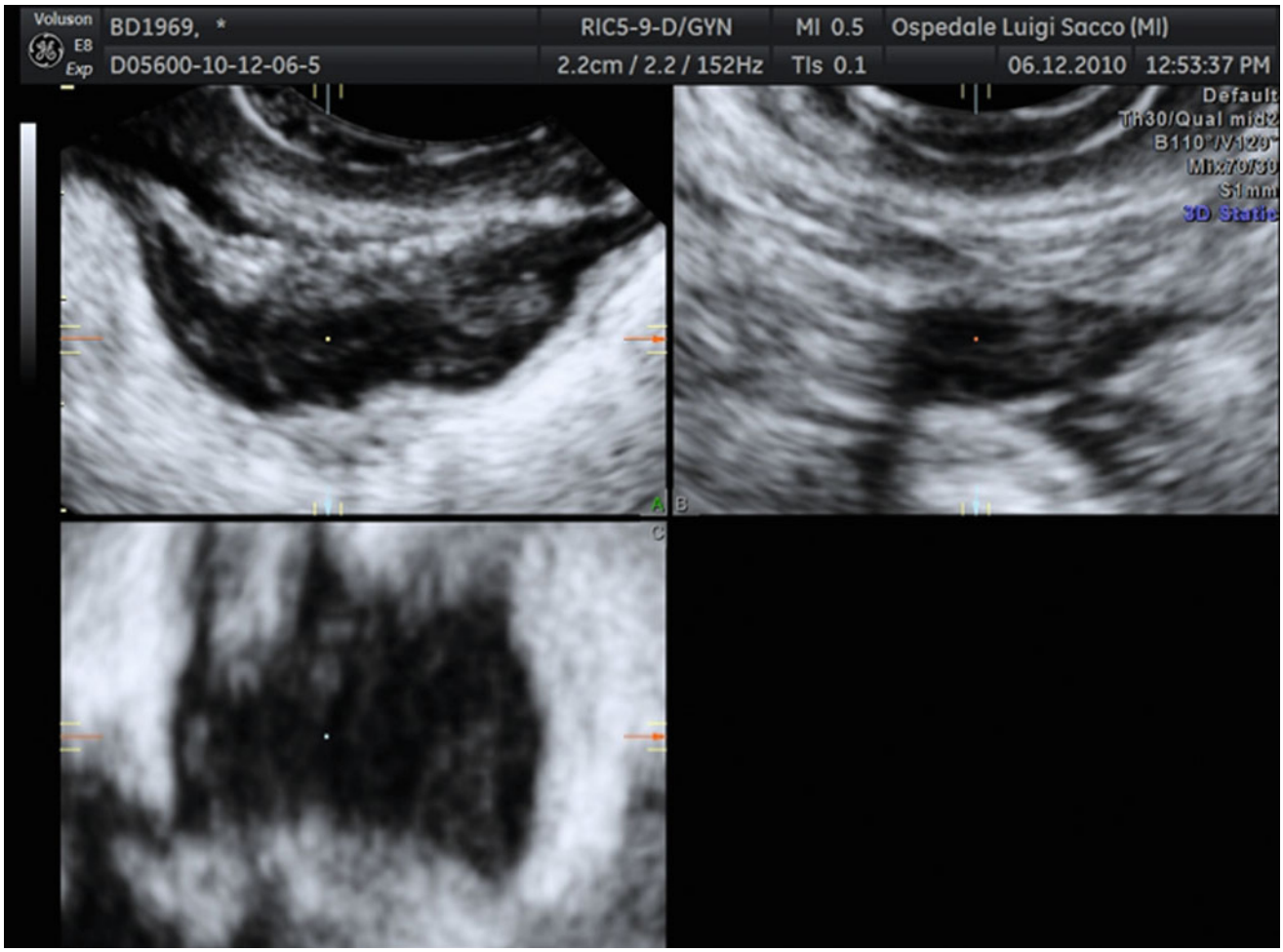

Fig. 6 "Pulling-out sign" at 3D-TVS of a muscular layer nodule without submucosal involvement

with anechoic fluid content and hyperechoic blood deposits, or, more often, as hypoechoic thickening or nodules/masses with irregular contours, usually involving the deep layers of the bowel wall (Saba et al. 2012) (Fig. 3; Fig. 4).

Hudelist et al. (2011) in a recent meta-analysis reported that TVS, with or without the use of prior bowel preparation, is an accurate diagnostic test for non-invasive detection of deep infiltrating endometriosis of the rectum and sigmoid colon, with a positive and negative likelihood ratio of 30.36 and 0.09, respectively. Furthermore, in the last decade, several authors have investigated the accuracy of TVS in predicting infiltration depth in patients with deep infiltrating endometriosis of the rectum (Hudelist et al. 2009; Koga et al. 2003). The "Indian head-dress sign" at 2D-TVS and the "pulling-out sign" at 3D-TVS were defined to describe the typical spiky and irregular outline of the hypoechoic thickened muscular nodule, which stretches the submucosal layer of the rectum and sigmoid colon (Fig. 5). Conversely, in cases of muscular layer without submucosal involvement the nodule appears as a hypoechoic nodule with smooth surface (Fig. 6) (Guerriero et al. 2008; Leone et al. 2007).

A number of studies showed that rectal endosonography or transrectal ultrasonography are useful in the diagnosis of pelvic endometriosis, especially for evaluating colorectal infiltration, for which the sensitivity ranged from 78 to 100 % and specificity from 66 to 100 % (Bazot et al. 2003).

4.2 Other Imaging Techniques

Several studies have evaluated the role of MRI in the diagnosis of deep pelvic endometriosis and rectal involvement, reporting sensitivities ranging from 77 to 100 % and specificities from 93 to 100 %. Rectal endosonography seems to be superior to MRI in the diagnosis of rectal wall infiltration, but MRI has the advantage of better demonstration of concomitant extrapelvic lesions and of ureteral obstruction. The limitations of MRI are that fibrosis in the

endometriotic foci can alter the signal intensity pattern, and bowel peristalsis can cause motion artefacts.

Computed tomography (CT) is a helpful diagnostic method in the diagnosis of endometriosis thanks to its panoramic view. A study that included 98 patients showed that CT colonography has a sensitivity of 99 % and a specificity of 100 % for diagnosing bowel endometriosis. By using CT colonography, 3D endoluminal views can be rapidly correlated with 2D multiplanar reformatted images to easily identify cases of extrinsic compression (Pickhardt et al. 2007).

Double-contrast barium enema has been long used in the investigation of intestinal endometriosis, but only few prospective studies have investigated its accuracy. In a retrospective study, 99 % accuracy for predicting the need for intestinal surgery in 108 patients with symptoms suggestive of intestinal endometriosis was reported. Other studies investigated the role of double-contrast barium enema in endometriosis and have shown rectal infiltration correctly in only 54 and 33 %, respectively. Moreover, double-contrast barium enema does not allow assessing the whole bowel wall and the depth of infiltration of intestinal endometriosis (Kruse et al. 2012).

References

Bazot M, Detchev R, Cortez A et al (2003) Transvaginal sonography and rectal endoscopic sonography for the assessment of pelvic endometriosis: a preliminary comparison. Hum Reprod 18:1686–1692

Bianchi A, Pulido L, Espin F et al (2007) Endometriosis intestinal. Estado actual. Cir Esp 81:170–176

Bontis JN, Vavilis DT (1997) Etiopathology of endometriosis. Ann N Y Acad Sci 816:305–309

Bozdech JM (1992) Endoscopic diagnosis of colonic endometriosis. Gastrointest Endosc 38:568–570

Brosens I, Puttemans P, Campo R et al (2003) Noninvasive methods of diagnosis of endometriosis. Curr Opin Obstet Gynecol 15:519–522

Chapron C, Fauconnier A, Vieira M et al (2003) Anatomic distribution of deeply infiltrating endometriosis: surgical implications and proposition for a classification. Hum Reprod 18:157–161

Chapron C, Chopin N, Borghese B et al (2006) Deeply infiltrating endometriosis: pathogenetic implications of the anatomical distribution. Hum Reprod 21:1839–1845

Guerriero S, Ajossa S, Gerada M, Virgilio B, Angioni S, Melis GB (2008) Diagnostic value of transvaginal 'tenderness-guided' ultrasonography for the prediction of location of deep endometriosis. Hum Reprod 23:2452–2457

Hudelist G, Tuttlies F, Rauter G, Pucher S, Keckstein J (2009) Can transvaginal sonography predict infiltration depth in patients with deep infiltrating endometriosis of the rectum? Hum Reprod 24:1012–1017

Hudelist G, English J, Thomas AE, Tinelli A, Singer CF, Keckstein J (2011) Diagnostic accuracy of transvaginal ultrasound for non-invasive diagnosis of bowel endometriosis: systematic review and meta-analysis. Ultrasound Obstet Gynecol 37:257–263

Jansen RP, Russel P (1986) Nonpigmented endometriosis: clinical laparoscopic, and pathological definition. Am J Obstet Gynecol 155:1154–1159

Jess T, Frisch M, Jørgensen KT, Pedersen BV, Nielsen NM (2012) Increased risk of inflammatory bowel disease in women with endometriosis: a nationwide Danish cohort study. Gut 61:1279–1283

Kaufman LC, Smyrk TC, Levy MJ et al (2011) Symptomatic intestinal endometriosis requiring surgical resection: clinical presentation and preoperative diagnosis. Am J Gastroenterol 106:1325–1332

Koga K, Osuga Y, Yano T et al (2003) Characteristic images of deeply infiltrating rectosigmoid endometriosis on transvaginal and transrectal ultrasonography. Hum Reprod 18:1328–1333

Kruse C, Seyer-Hansen M, Forman A (2012) Diagnosis and treatment of rectovaginal endometriosis: an overview. Acta Obstet Gynecol Scand 91:648–657

Leone FPG, Petullà M, Maconi G et al (2007) The 'pulling-out sign' for intestinal deep infiltrating endometriosis: prognostic role of findings at 3D transvaginal sonography. Ultrasound Obstet Gynecol 30:375

Moore J, Copley S, Morris J et al (2002) A systematic review of the accuracy of ultrasound in the diagnosis of endometriosis. Ultrasound Obstet Gynecol 20:630–634

Olive DL, Schwarz LB (1993) Endometriosis: medical progress. N Engl J Med 328:1759–1769

Oral E, Arici A (1997) Pathogenesis of endometriosis. Obstet Gynecol Clin North Am 24:219–233

Pickhardt PJ, Kim DH, Menias OC et al (2007) Evaluation of submucosal lesions of the large intestine. Radiographics 27:1693–1703

Piketty M, Chopin N, Dousset B et al (2009) Preoperative work-up for patients with deeply infiltrating endometriosis: transvaginal ultrasonography must definitely be the first-line imaging examination. Hum Reprod 24:602–607

Rock JA, Markham SM (1992) Pathogenesis of endometriosis. Lancet 240:1264–1267

Saba L, Guerriero S, Sulcis R et al (2012) MRI and ''Tenderness Guided'' transvaginal ultrasonography in the diagnosis of rectosigmoid endometriosis. J Magn Reson Imaging 35:352–356

Shah M, Tager D, Feller E (1995) Intestinal endometriosis masquerading as common digestive disorders. Arch Intern Med 155:977–980

Weed JC, Ray JE (1987) Endometriosis of the bowel. Obstet Gynecol 69:727–730

Zwas FR, Lyon DT (1991) Endometriosis: an important condition in clinical gastroenterology. Dig Dis Sci 36:353–364

Part V

Procedures and Technical Developments

Intravenous Contrast-Enhanced Bowel Ultrasound

Doris Schacherer

Contents

Abstract

In this chapter, we describe the role of ultrasound in case of gastrointestinal disorders. We try to illustrate the historical development and different types of contrast agents and their advantages, limitations, and applications with respect to bowel diseases. Brightness mode (B-Mode) represents an early diagnostic tool for almost all entities of intestinal disease and is able to investigate the localization of intestinal disease, length of the intestinal segments involved, loss of stratification, intestinal obstruction or stenoses, and mesenterial changes as well as associated. B-mode imaging is always a prerequisite for the useful application of Doppler and ultrasound contrast imaging techniques. Combining (Power) Doppler imaging and ultrasound contrast agents improves the visualization of smaller vessels and vessel continuity (i.e., length). Several studies were performed to detect bowel wall hyperemia in inflammatory bowel disease. Contrast harmonic imaging at a low mechanical index is technically feasible for the demonstration of increased intestinal perfusion in inflammatory bowel disease by using high frequency ultrasound transducers. Furthermore, contrast-enhanced power Doppler sonography may help to discriminate the origin of small bowel stenosis in Crohn‘s disease. Different studies evaluated the vascularization of the thickened terminal ileum in Crohn‘s disease patients using CEUS and compared the clinical activity measured by the Crohn‘s disease activity index (CDAI) with the sonographic findings. Using certain perfusion parameters (peak value, time-to-peak, regional blood volume), studies could show differences between inflamed and normal bowel wall vascularity in terms of significant higher peak values and significant higher regional blood volume in the bowel wall of patients with an active episode of Crohn‘s disease. Additionally, CEUS can be a useful technique to monitor the activity of Crohn‘s disease, to increase the accuracy of color Doppler ultrasound in diagnosis, and followup

D. Schacherer (✉)
Department of Internal Medicine I,
University of Regensburg, Regensburg 93042, Germany
e-mail: Doris.schacherer@klinik.uni-r.de

G. Maconi and G. Bianchi Porro (eds.), *Ultrasound of the Gastrointestinal Tract*, Medical Radiology. Diagnostic Imaging,
DOI: 10.1007/174_2012_663, © Springer-Verlag Berlin Heidelberg 2012
Published Online: 19 July 2012

of patients with Crohn‘s disease and to assess disease activity. Fewer studies exist concerning ulcerative colitis, bowel ischemia, graft-versus-host-disease, and appendicitis.

1 Introduction

To evaluate gastrointestinal tract disorders, there are several imaging methods available. With respect to sonography, important progress in equipment technology has improved its diagnostic capabilities in the last years. Compared to other imaging modalities, ultrasound has multiple advantages. These include real-time imaging, relatively low costs, portability, wide availability, non-invasiveness, and lack of ionizing radiation. For these reasons, many patients with abdominal symptoms are referred for an ultrasound study as their initial diagnostic evaluation. However, optimal imaging by sonography is often limited by artifacts arising from gas in the stomach and the adjacent bowel. The sound beam is almost totally reflected at soft tissue–gas interfaces due to the marked differences in acoustic impedance and the high compressibility and low density of gas. As a consequence, the results of this examination are often inconclusive, leading to supplementary imaging by means of more expensive imaging modalities, such as computed tomography (CT) or magnetic resonance imaging (MRI).

In this chapter, we describe the role of contrast-enhanced ultrasound (CEUS) in gastrointestinal disorders. We then illustrate the historical development and different types of contrast agents and their advantages, limitations, and applications with respect to bowel diseases.

2 Bowel Sonography (B-Mode, Doppler, and Power Doppler sonography)

Already in the 1970s, grayscale ultrasound examination was performed in patients with Crohn’s disease (CD; Holt and Samuel 1979). At present, the principle tools for the diagnosis of inflammatory bowel disease are colonoscopy with multiple biopsies and radiologic examinations. However, colonoscopy, barium enema, and enteroclysis cannot assess the transmural extent of the inflammation or extraintestinal involvement of the disease, and computed tomography is associated with a certain radiation dose. Consequently, a non-invasive test avoiding radiation such as ultrasound would be preferable. Brightness mode (B-Mode) represents an early diagnostic tool for almost all entities of intestinal disease and is able to investigate the localization of intestinal disease, length of the intestinal segments involved, loss of stratification, intestinal obstruction or stenoses, and mesenterial changes, as well as associated complications such as abscesses, fistulas, perforation, ascites, and stenoses. B-mode imaging is always a prerequisite for the useful application of Doppler and ultrasound contrast imaging techniques (Schlottmann et al. 2005b). In B-mode sonography, five layers of the normal bowel wall can be visualized by high-resolution sonography: superficial mucosa, deep mucosa, submucosa, muscularis propria, and serosa with serosal fat. If any pathology of the bowel is suspected, special attention should be paid to the distal ileum in the right iliac fossa and all areas of tenderness or localized pain. In experienced hands, B-mode sonography helps to assess bowel-wall thickening, free intraperitoneal fluid, and mesenteric masses (phlegmon, abscess, lymph nodes).

According to data in the literature, transabdominal ultrasonography has a high sensitivity (up to 85 %) and specificity (95 %) in the initial assessment of inflammatory bowel disorders and has similar diagnostic values to CT (Parente et al. 2003; Tarjan et al. 2000). B-mode together with Doppler sonography can visualize transmural bowel inflammation in Crohn’s disease, discriminate Crohn’s disease from ulcerative colitis, determine the extent and anatomic location of lesions and detect complications such as strictures/stenoses, fistulas, and abscesses (Tarjan et al. 2000). Of stenoses, 90 % documented by small-bowel enema and subsequently confirmed at surgery, are correctly diagnosed by the use of high-resolution ultrasound (Parente et al. 2002). In addition, the use of Doppler sonography has been shown to be able to discriminate between active and inactive disease by measuring the superior mesenteric artery blood flow (Ludwig et al. 1999).

In general, the greatest advantages of combining power Doppler imaging and ultrasound contrast agents are the ability to better visualize smaller vessels, and vessel continuity (i.e. length). The possibility to improve the visualization of complex neovascularity is of particular importance in tumor diagnosis. Comparing color Doppler imaging and power Doppler imaging in combination with ultrasound contrast agents, the latter improved visualization of both normal and abnormal blood flow in 70 % of all cases (Goldberg et al. 1996). Due to the fact that this mode is more susceptible to color artifacts, it is not suitable for the evaluation of flow in structures with significant motion. Motion artifacts caused by peristalsis or heartbeat often disturb the measurement of Doppler signals, but such artifacts do not impair contrast-enhanced sonography at low mechanical index (MI).

Moreover, color and power Doppler sonography have other limitations. In particular, no objective parameters exist permitting definition of the type of echostructure or flow patterns (such as the Hounsfield scale in CT). The vascular flow signal is often too weak because of beam attenuation or signal absorption or distortion and power Doppler sonography fails to assess blood flow direction (Table 1).

Table 1 Characteristics of power doppler sonography (from Forsberg and Goldberg 1997)

Advantages	Disadvantages
Increases display dynamic range (increased sensitivity)	Susceptible to tissue motion artifacts
No multiple angle artifact	No direction information
No aliasing	No velocity information
Limited angle dependence	Limited temporal resolution
Better functional lumen/vessel wall definition	

3 Intravenous Contrast Agents

3.1 History

Echocardiographers recognized by chance in the 1960s that the tiny air bubbles incidentally introduced into the circulation after intravenous injections produce transient echo enhancement in the right side of the heart. Such bubbles do not pass through the normal pulmonary circulation, but systemic enhancement effects can be used to test for a right-to-left shunt (Blomley and Cosgrove 1997).

The first microbubble agents were described by Gramiak and shah in 1968. They were discovered during the injection of indocyanine green as M-mode echocardiography was being developed. More precisely, their first encounter with the contrast phenomena came in late April 1967 in the cardiac catheterization laboratory during study of a patient with aortic regurgitation. Contrast injections were decisive in identifying the walls of the aortic root, distinguishing it from the left ventricular outflow tract and detailing normal cusp motion. The resulting publication was the first report of the use of ultrasonic contrast agents (Gramiak and Shah 1968). Serious attempts to develop intravenous contrast agents for ultrasound began in the late 1970s and early 1980s. It was subsequently surmised that bubbles were responsible for the contrast effect. In the early 1980s, clinical echocardiography was performed with a sector scanner, a stand-alone Doppler unit capable of pulsed and continuous-wave mode operation, a spectral analyzer with high temporal resolution and an in-house "black box" which allowed EKG display along with the spectra (Gramiak and Holen 1984). Due to the fact that small gas bubbles dissolve rapidly in blood, the next aim was the production of agents small enough to traverse the pulmonary capillary bed.

Smith et al. (1984, 1989) used a galactose-based contrast agent called SHU-454 (Echovist, Schering AG, Berlin, Germany), whereas successful transpulmonary delivery of microbubbles was achieved by using an agent similar to SHU-454 with the addition of palmitic acid surfactant—called SHU-508A (Levovist, Schering AG, Berlin, Germany; Smith et al. 1984, 1989).

In the late 1980s, the systematic development of contrast media started. Nearly all of them consisted of gas bubbles, since gas has, for physical reasons, the optimum prerequisites for an ultrasound contrast agent. Due to the high efficacy and low specific density of gas, only small amounts of foreign substance have to be administered (Ophir and Parker 1989). To make the contrast-giving gas bubbles suitable for transpulmonary passage after intravenous injection, the bubbles were surrounded with a thin film to prevent dissolution of the bubble in the blood stream. The material of the protective layer around the microbubble is in most cases a highly flexible structure which does not reduce the acoustic response by limiting the oscillation of the bubble. Transpulmonary passage was now possible and, therefore, the arterial part of the vascular system could be assessed. For imaging of different organs, contrast agents which are concentrated in organs were necessary. Therefore, there was a need for agents which can survive cellular uptake without losing their acoustic properties.

Although backscatter is highly dependent on bubble size, microbubbles must have a limited size range. If the bubble is too small, it will be short-lived (i.e. it will collapse under cardiac and systemic pressures). If the bubble is too large (> than 10 μm), the pulmonary capillaries will trap it or the bubbles may transiently obstruct the capillaries and act as gas emboli. Therefore, microbubble size is limited from 1 to 5 μm in diameter. At present, all microbubble contrast agents which have been developed for ultrasound are small gas filled microbubbles, about 3 μm in size and all commercial ultrasound contrast media for human applications are encapsulated microbubbles. So, microbubbles are too large to escape the capillaries and, contrary to most X-ray and MR contrast media, which are rapidly distributed to the extravascular, extracellular space, most microbubbles are confined to the vascular bed. The increase in Doppler signal intensity they produce is linearly proportional to relative microbubble concentration.

3.2 Types

Levovist ® (Schering AG, Berlin, Germany) is an agent like those described above, made of galactose microparticles and palmitic acid. The microparticles adsorb the gas

dissolved in the water, forming micrometer-sized air bubbles that remain stable for several minutes, thanks to the palmitic acid additive. After transit through the pulmonary circulation, the bubbles reach the systemic circulation where they enhance the backscattering of signals from blood vessels (Bouakaz et al. 1998).

The main mechanisms for signal enhancement are backscattering, bubble resonance and bubble rupture. These mechanisms are highly dependent on the acoustic power of the transmitted ultrasound, which is reflected by the mechanical index (MI). Backscattering means that ultrasound is reflected whenever there is a change in acoustic impedance. The larger the change, the more ultrasound is reflected. Bubble resonance means that at intermediate acoustic power (MI between 0.1 and 0.5) gas microbubbles may show strong oscillatory motion, provided the frequency of the ultrasound beam is close to the resonant frequency of the microbubbles. Small bubbles (< than 5 μm) will have resonance frequencies in the frequency range used in medical ultrasound imaging. The bubbles are more easily expanded than compressed, and this nonlinear behavior creates harmonics, which are exploited in nonlinear imaging. At a MI > 0.5, the microbubble resonance frequency will cause the bubbles to rupture.

In summary, microbubbles work by resonating in an ultrasound beam, rapidly contracting and expanding in response to the pressure changes of the sound wave. By a coincidence, they vibrate particularly strongly at the high frequencies used for diagnostic ultrasound imaging. This makes them several thousand times more reflective than normal body tissues. In this way, they enhance both gray-scale images and Doppler signals (by raising the intensity of weak signals to a detectable level; Blomley et al. 2001).

SonoVue ® (Bracco, Milan, Italy) is a second generation ultrasound contrast agent. It contains sulfur hexafluoride (SF_6), a gas with low solubility in blood for the gaseous phase of the microbubbles, and of a phospholipidic monolayer for the shell. Due to the high flexibility of the shell, the microbubbles are strongly echogenic in a wide range of frequencies and acoustic pressure. The mean microbubble diameter is 2.5 μm. The concentration of the microbubbles is between 100 and 500 million per milliliter. Contrast agents of the second generation, e.g., SonoVue®, are of diagnostic value even at very low transmission power (MI < 0.3) because of their physical behavior during insonation. The high molecular weight gas with low solubility in water was selected since laboratory tests showed that it confers to the bubbles a good resistance to pressure changes such as those that occur in the left ventricle, in the pulmonary capillaries, or in the coronary circulation (Schneider 1999), therefore, continuous real-time sonography can be performed without destruction of the microbubbles, which is a benefit for the dynamic analysis of contrast enhancement in the early phase. The microbubbles circulate in vessels, crossing the pulmonary and systemic capillary circulation. During low-MI imaging, the SonoVue® microbubbles have a much higher nonlinear behavior than native tissue, resulting in detectable echoes. Due to the long persistence of the microbubbles, SonoVue® is also potentially useful in the assessment of myocardial perfusion, as well as microcirculatory disorders. Real-time observation of microbubbles allows the detection of all parts of the vascular system. Even single microbubbles slowly traversing tissue, which is indicative of the presence of capillaries, can be shown. In comparison with Levovist®, SonoVue® has the advantage that its microbubbles are stable against the ultrasound beam, which allows continuous real-time observation of microbubble signals (Von herbay et al. 2004). In contrast, analysis of Levovist® enhancement has to be performed with the interval delay technique because the rupture of Levovist microbubbles does not allow real-time scanning.

3.3 Indications/Applications

Levovist® as an intravenous microbubble contrast agent is particularly useful in detection of small vessel flow, especially in those areas in which Doppler sensitivity limits performance, including Doppler examinations, in which the signal-to-noise ratio determines detectability. Intravenous administration of Levovist is an effective method of markedly enhancing cardiac, femoral arterial, and transcranial Doppler signal intensity (Campani et al. 1998; Meairs et al. 2000), in the evaluation of breast tumors (Duda et al. 1993), and in the detection of liver metastases (Blomley et al. 1999). Concerning the role of microbubble contrast agents in cardiology, they help in assessing the left ventricular function, and they can estimate the ejection fraction, assess the wall motion, and detect left ventricular thrombus. Emerging roles of microbubbles in cardiology include assessing myocardial perfusion (Mulvagh et al. 2000). Contrast agents represent a useful and safe method in the case of an insufficient native signal in transcranial Doppler investigation, where the scull greatly attenuates the ultrasound signal (Ries et al. 1993). Microbubbles can also be administered into body cavities, allowing simple functional tests to be performed. For example, vesicoureteric reflux in children can be revealed by injecting them into the bladder cavity and scanning the kidneys and ureters (Darge et al. 1999). Color-mode sonography can show the angioarchitecture of superficial lymph nodes to detect vessel abnormalities, a possible feature of malignancy. Although more intranodal flow patterns can be detected in such lymph nodes with contrast-enhanced sonography, the use of these agents does not improve the diagnostic accuracy in

identifying malignant lymph nodes (Schulte-Altedorneburg et al. 2003). Contrast-enhanced sonography is used in several other clinical settings, to the point of assessing ophthalmic tumor perfusion (Schlottmann et al. 2005a).

Perhaps, the most promising clinical application of contrast-enhanced sonography is the imaging of the liver. The main practical importance is that many focal liver lesions, particularly metastases and hepatocellular carcinoma, appear as defects. Scanning in pulse-inversion mode after Levovist improves the detection of liver metastases and reveals more lesions of smaller size than conventional ultrasonography and computed tomography (Harvey et al. 2000). The method seems particularly useful in detecting small lesions (<1 cm diameter), for which all imaging methods lack sensitivity. Contrast agents may also increase specificity in liver imaging since some lesions can be characterized by their enhancement patterns. Because the bubbles are destroyed by ultrasound, e.g., liver enhancement lasts for 1 or 2 frames as the transducer is swept across the bubble-filled liver. Because space-occupying lesions lack sinusoids and reticulo-endothelial cells, they appear hypoechoic relative to the enhanced background of the liver. Even biopsies of liver lesions under real-time continuous contrast harmonic imaging at low MI are feasible (Schlottmann et al. 2004); however, one limitation of this imaging modality is the difficulty in accessing the whole of the liver.

Concerning the bowel wall, contrast enhancement of defined layers of the wall can be shown even though B-mode visualization of small vessels in the bowel wall is impossible. The more or less homogenous enhancement of particular layers will increase with the level of hyperperfusion of the intestinal wall (Schlottmann et al. 2005b).

In general, the nonlinear harmonic echoes generated by the SHU 508 bubbles are visualized at high transmit power. This high MI technique is used more widely to analyze tissue perfusion and hepatic metastases rather than perfusion of visceral vessels (Schlottmann et al. 2005b).

Using the contrast agent SonoVue®, the microbubbles act as reflectors for the ultrasound beam enhancing backscatter beam. The agents remain in the circulation and, according to the perfusion phase (arterial, capillary, portal venous), lead to enhancement of different structures. This imaging modality allows an analysis of tumor perfusion under real-time conditions.

3.4 Safety

Injecting a gas into the circulation may seem potentially hazardous, but extensive clinical experience has shown that the tiny volume of the air or gas given (<200 µl) is not dangerous, and the safety of microbubbles compares well to that of conventional agents in radiography and MRI (Nanda and Carstensen 1997). Ionescu reported a clinical case of a patient who developed a rare but dramatic sequence of reversible complications (anaphylactic shock, threatened myocardial infarction, and transient renal failure) from exposure to SonoVue® (Ionescu 2009). In 2009, Geleijnse et al. (2009) described side effects (from mild allergic reactions to nonfatal shock) in 2 % of their patients (n = 352) (Geleijnse et al. 2009). At the moment, the use of SonoVue® is not permitted in mechanically ventilated intensive care unit patients and in patients with heart failure or severe hypertonus.

4 Contrast Harmonic Imaging

The observation that insonation of microbubbles induces nonlinear harmonic echoes caused by the oscillation or disruption of the microbubbles was followed by the development of imaging techniques which visualized the nonlinear harmonic signals of bubble oscillation and disruption (contrast harmonic imaging, CHI). Contrast harmonic imaging (CHI) utilizes the nonlinear properties of contrast agents by transmitting at the fundamental frequency but receiving at the second harmonic. The advantage of this processing scheme lies in the difference in backscattering for tissue and contrast agent at two frequencies. The extent of the backscattered contrast-enhanced signal at the harmonic frequency is much greater than that of the tissue. This technology works in grayscale imaging as well as in Doppler sonography. The harmonic response of the agent is strong and, in combination with the high stability of the microparticles, blood flow in small vessels can be directly visualized. This method is not influenced by attenuation.

5 Instrumentation Technology

The other area of significant expansion in this field was brought by the instrumentation technology, where specific pulsing and post-processing techniques have been developed to take advantage of the presence of microbubbles in the circulation.

Pulse-inversion sonography (also called second harmonic) is a technique that works by sending two separate pulses, 180° out of phase, and summing the reflected echoes to form the final sonographic signal.

Increasingly sophisticated, broadband or multiple focusing transducers also play an important role. Contrast-enhanced sonography can be performed not only with 3.5 MHz transducers usually used in abdominal ultrasound, but also with 5–12 MHz transducers which offer a higher spatial resolution.

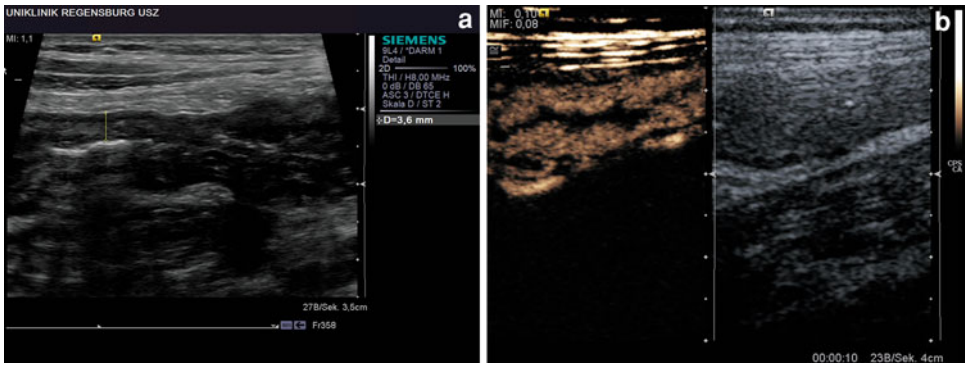

Fig. 1 25-year-old male patient with ulcerative colitis. **a** B-mode sonography shows a thickened bowel wall (about 4 mm). **b** Contrast-enhanced sonography shows a rapid and increased bowel wall perfusion—10 s after injection of 2.4 ml SonoVue®

6 Intravenous Contrast-Enhanced Bowel Sonography

6.1 Inflammatory Bowel Diseases

Crohn's disease (CD) manifests with highly variable signs and symptoms, and the assessment of the status of the disease, in the single patient, can be difficult. Being a chronic inflammatory bowel disease, it is characterized by an inflammatory process that involves the full thickness of the bowel wall, including the mesentery and the lymph nodes. Many clinical and laboratory parameters have been proposed to indicate disease activity; however, none of these indices can provide a fully reliable assessment of disease status. As mentioned above, in recent years, transabdominal bowel sonography has become increasingly important as a reliable and non-invasive tool in the diagnosis and follow-up of patients with CD disease. Ultrasonography is able to diagnose and locate transmural bowel inflammation in CD, discriminate it from ulcerative colitis (UC) and detect complications such as fistulas, strictures, and abscesses. However, small intraperitoneal abscesses may remain unidentified (Kolkman et al. 1996). Nevertheless, the early detection of intestinal complications in Crohn's disease is probably one of the most important aspects of the management of these patients. The detection of such complications in the initial stages of the disease allows effective medical therapy to control their progression, thus avoiding surgical treatment in some cases.

Intestinal hyperemia is a sign of active disease in the inflamed intestine which can be detected by Doppler sonography. Tissue motion artifacts (peristalsis) sometimes make the assessment difficult, but visualization of vessels by using contrast harmonic imaging at a low MI is not restricted by peristalsis (Fig. 1).

Esteban et al. (2003) have demonstrated for the first time the usefulness of contrast agents in the detection and follow-up of inflammatory abdominal masses associated with CD. Grayscale, Doppler, and pulse-wave ultrasound was undertaken with additional contrast-enhanced power Doppler examination. These findings were correlated with each other and with contrast-enhanced CT as the gold standard. After Levovist® injection, all the lesions showed intense vascularization in the interior and/or the peripheral soft tissue. The authors could show that contrast-enhanced power Doppler sonography demonstrated more abdominal masses than CT (Esteban et al. 2003).

Several studies were performed to detect bowel-wall hyperemia in inflammatory bowel disease (Fig. 2).

Contrast harmonic imaging at a low MI is technically feasible for the demonstration of increased intestinal perfusion in inflammatory bowel disease by using high frequency ultrasound transducers (Plikat et al. 2004; Migaleddu et al. 2009; Kumar et al. 2009). One of the drawn conclusions of a study of Rapaccini et al. (2004) was that intestinal loops with thickened walls should be subjected to color power Doppler sonography, and if intramural flow signals are absent the examination should be repeated with echo enhancement since the presence of color flow signals shows good concordance with clinical and laboratory indices of active disease. In patients with active disease, power Doppler signals emerged in the intestinal wall. In other words, the utilization of echo-enhancer media improves the diagnostic sensitivity of intestinal wall power Doppler scan (Table 2).

Robotti et al. (2004) evaluated the intestinal wall vascularization of 52 patients with Crohn's disease after intravenous injection of SonoVue® and compared their results with those from clinical and laboratory tests and follow-up. They demonstrated, that the US examination was most useful in the follow-up of the affected patients.

Kratzer et al. (2002) investigated 11 patients with confirmed CD and sonographically visualized stenoses of small bowel. Contrast-enhanced power Doppler sonography was repeated after application of SHU 508 (Levovist®). Semiquantitative evaluation based on sonography, indicated that the degree of vascularisation led to the presumptive diagnosis of either inflammatory or cicatricial intestinal obstruction. Sonographic diagnoses were compared with the

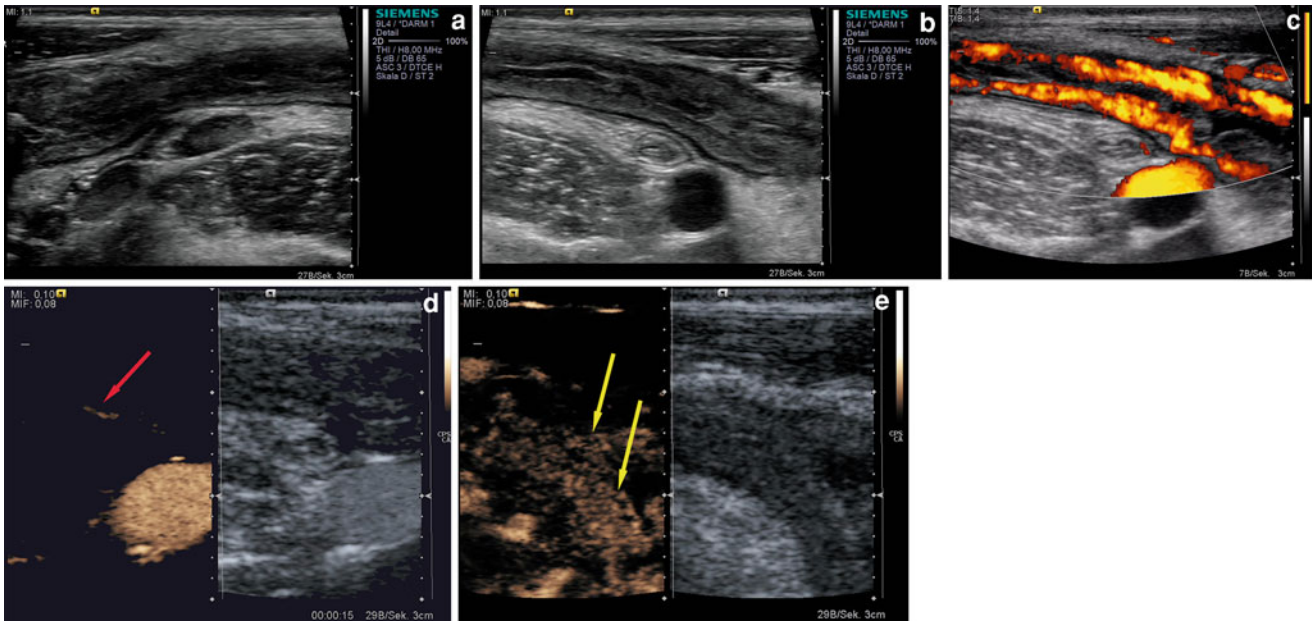

Fig. 2 24-year-old female patient with Crohn's disease. **a** B-mode sonography shows an increased bowel-wall thickness with surrounding lymph nodes in the right lower quadrant of the abdomen. **b** B-mode sonography about the same region showing a prominent appendix. **c** Power Doppler sonography shows increased vascular signals. **d** Contrast-enhanced sonography (15 s after injection of 2.4 ml SonoVue®) shows the arterial arrival of the microbubbles and the feeding vessel (*red arrow*) of the bowel wall. **e** Slightly later, the signals in the bowel wall are seen (*yellow arrows*)

Table 2 Characteristics of patient subgroups with active and quiescent crohn's disease (From Rapaccini et al. 2004)

	Quiescent disease	Active disease	*P*
No. of patients	26	22	–
Intestinal wall thickness[a]	6.8 ± 1.3 mm	7.5 ± 1.3 mm	*0.11*
SMA RI[b]	0.83 ± 0.02	0.81 ± 0.01	*0.001*
Intramural flow signals in affected intestinal loops (power Doppler sonography)	5/26 (20 %)	11/22 (50 %)	*0.052*
Intramural flow signals in affected intestinal loops (contrast-enhanced power Doppler sonography)	8/26 (31 %)	22/22 (100 %)	*<0.001*

[a] Maximal thickness measured in affected loops on B-mode sonography
[b] Resistence index of the superior mesenteric artery

findings of surgery and subsequent histologic examination or with patients' response to conservative therapy. The authors concluded that contrast-enhanced power Doppler sonography appears to be effective in the recognition of predominantly cicatricial stenoses in patients with CD (Kratzer et al. 2002). Recently, Schirin-Sokhan et al. (2011) could show that the semiquantitative analysis of bowel-wall vascularity, the length of stenosis, and the Crohn's Disease Activity Index (CDAI) may help to discriminate the origin of small-bowel stenosis in CD (Schirin-Sokhan et al. 2011).

Serra et al. (2007) prospectively evaluated the vascularization of the thickened terminal ileum in Crohn's disease patients using CEUS and compared the clinical activity measured by the Crohn's disease activity index (CDAI) with the sonographic findings. It was found that the pattern of contrast enhancement and the ratio of enhanced to entire wall thickness had a prospective value of 63.0 and 58.6 %, respectively, in distinguishing active from inactive disease (Serra et al. 2007). Therefore, Dietrich et al. (2007) proposed that CEUS may be particularly able to more precisely characterize bowel-wall thickness by differentiating fibrosis from edema and may, thereby, grade inflammation by assessing presence and distribution of vascularity within the intestinal layers, particularly the submucosa and/or the entire bowel wall (Dietrich et al. 2007). Using certain perfusion parameters (peak value, time-to-peak, regional blood volume), Girlich et al. (2009) could show differences between inflamed and normal bowel-wall vascularity in terms of significant higher peak values and significant higher regional blood volume in the bowel wall of patients

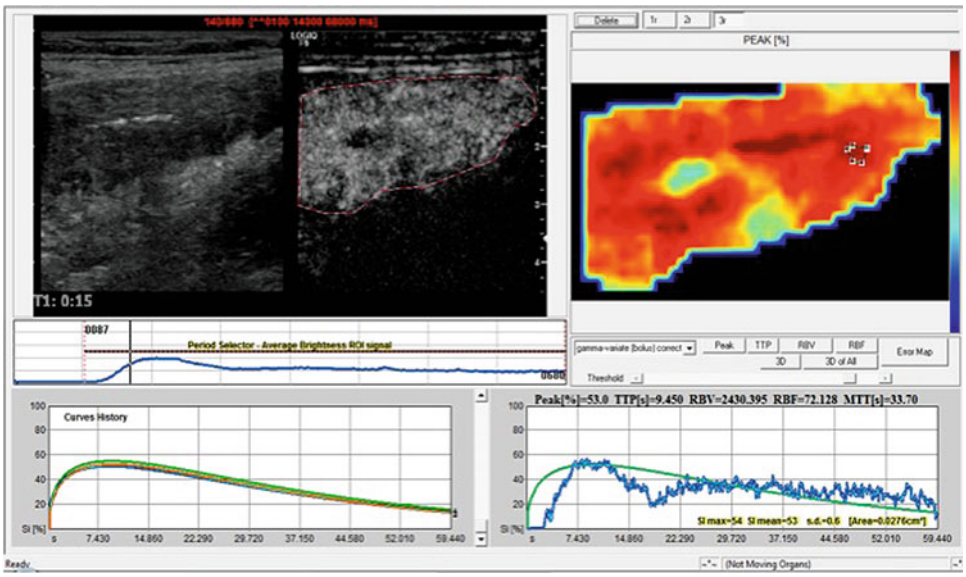

Fig. 3 21-year-old female patient with active ulcerative colitis. Quantitative analysis of bowel-wall vascularity (e.g. peak value) with the specific software Qontrast®

with an active episode of Crohn's disease (Girlich et al. 2009). Therefore, CEUS can be a useful technique to monitor the activity of Crohn's disease (Ripollés et al. 2009).

In summary, several studies could show that contrast agents further increase the accuracy of color Doppler ultrasound in diagnosis and follow-up of patients with Crohn's disease (Rapaccini et al. 2004; Schreyer et al. 2008). Furthermore, the contrast agent SonoVue® has been successfully used to assess disease activity, and also the response to infliximab therapy in a preliminary Italian study (Guidi et al. 2006). Clinical improvement after 6 months of infliximab treatment was clearly reflected by parallel alterations in the pattern of contrast-enhanced echo-signal (Quaia et al. 2009).

Furthermore, CEUS has been helpful in surgical management, e.g., in the decision of conservative versus surgical treatment (Kunihiro et al. 2007; Maconi et al. 2008).

An early sonographic sign of ulcerative colitis (UC) is a thickened hypoechoic layer representing the swollen mucosa. More severe cases show a transmural bowel-wall thickening due to transmural inflammation similar to CD. Because none of the sonographic findings in ulcerative colitis is specific, the value of sonography is less well established than in CD. Yamaguchi et al. (2009) evaluated different patterns of CEUS findings in steroid refractory dependent ulcerative colitis as predictors for response to granulocyte and monocyte adsorption apheresis and leukocytapheresis. Recently, Girlich et al. (2009) evaluated 15 patients with proven ulcerative colitis with CEUS and a special quantification software (Fig. 3). The authors found a trend to higher peak (%) values with increasing histologic inflammation (Girlich et al. 2009). In another study, the authors found a significant correlation between the quantification results and a histopathologic scoring system applied after surgery of 20 patients with proven CD (Girlich et al. 2011a).

6.2 Bowel Ischemia

To our knowledge, only few studies have described the use of contrast agents in patients with bowel ischemia. In the study by Hata et al. (2005), 51 patients with evidence of small-bowel dilatation at conventional radiography underwent contrast-enhanced ultrasound with SHU-508. The authors demonstrated that this method is able to depict microperfusion of the gastrointestinal wall as a strong signal produced by the destruction of microbubbles. By pooling diminished and absent color signals together as a diagnostic indicator of bowel ischemia against normal color signals, the sensitivity was 85 % and the specificity was 100 %. Although some limitations of this study exists (subjective assessment of color signals without evaluation of interobserver agreement, small number of patients), this method constitutes a promising tool for the assessment of bowel ischemia (Hata et al. 2005). Another study of Hamada et al. (2007) aimed to prospectively evaluate the importance of contrast-enhanced sonography with advanced dynamic flow in the diagnosis of intestinal ischemia in bowel obstruction. The two studies differ in the assessment methods used. Assuming that the absent and diminished color signals obtained by contrast-enhanced sonography indicate the presence of intestinal ischemia, the sensitivity in the study of Hamada et al. was 94 %, whereas the specificity was 100 % (Hamada et al. 2007). Both authors conclude that contrast-enhanced sonography is a highly sensitive method for the diagnosis of intestinal ischemia.

Table 3 Power doppler sonography (PD US) and contrast-enhanced power doppler sonography (CEPD US) correlation in 50 patients with suspected appendicitis (%) (From Incesu et al. 2004)

Parameter	PD US	CEPD US	*P*
Sensitivity	74	100	*<0.01*
Specificity	93	93	*>0.05*
Accuracy	80	98	*<0.05*
Positive predictive value	96	97	*>0.05*
Negative predictive value	61	100	*<0.05*

6.3 Appendicitis

In grayscale ultrasound, the normal appendix can be visualized as a blind ending, tubular, compressible intestinal loop, continuous with the cecum with a diameter <6 mm. The normal appendix seldom shows Doppler signals, because normal appendiceal vessels are small and the blood flow in the vessels is slow. In acute appendicitis, the feeding vessels and the vessels in the periappendicular soft tissues enlarge due to inflammation, and the blood flow, increases as well as the appendix diameter, increases. High-resolution real-time sonography with graded compression has shown a sensitivity up to of 89 % and a specificity of up to 95 % in the diagnosis of acute appendicitis (Jeffrey et al. 1987; Keyzer et al. 2005). Incesu et al. (2004) demonstrated that power Doppler sonography has a sensitivity of 74 % and contrast-enhanced power Doppler US a sensitivity of 100 %, respectively, in the diagnosis of acute appendicitis (Table 3). In their study, feeding vessels of all inflamed appendices were visible. They concluded that contrast-enhanced power Doppler sonography is a promising method in the diagnosis of acute appendicitis and determination of inflammation stage (Incesu et al. 2004).

6.4 Other Indications

Acute graft-versus-host disease (aGvHD) of the gastrointestinal tract is one of the major complications after allogeneic hematopoetic cell transplantation. Symptoms include watery diarrhea, intestinal bleeding, abdominal cramps, and ileus. Bowel-wall thickening in the ileocaecal region with poor wall stratification or colonic dilatation in bone marrow-transplanted patients together with the clinical symptoms (nausea, vomiting, aversion to food, weight loss, discomfort in the upper abdomen) might differentiate between infectious bowel disease and aGvHD. High-resolution sonography and color Doppler imaging proved to be useful tools for detecting acute bowel GvHD even before clinical symptoms (Klein et al. 2001; Gorg et al. 2005). Schreyer et al. (2011) tried to evaluate contrast-enhanced sonography in patients with GvHD to assess typical imaging features. Not surprisingly, significant contrast uptake in the bowel wall was seen (Fig. 4). The authors stated that the damaged gut mucosal barrier in GvHD enables the microbubbles to penetrate through the bowel wall into the bowel lumen, which could serve as a novel diagnostic feature in GvHD. However, these results have to be proven by larger studies.

In a small study including 13 patients with gastrointestinal stromal tumor (GIST), the vascular imaging pattern in contrast-enhanced sonography differed between benign and malignant stromal tumors (Fukuta et al. 2005). In another study involving 24 patients with GIST, CEUS allowed early prediction of tumor response to imatinib treatment (Lassau et al. 2006).

At present, there are no literature data available concerning contrast-enhanced sonography and infectious colitis or diverticulitis.

The small intestine is the most difficult part to examine of the gastrointestinal tract because of its length and tortuous course. There are challenges for ultrasound such as depth penetration, intestinal air precluding optimal imaging quality, and the lack of a systematic approach by the examiner. The development of improved equipment technology such as high-resolution transducers, offers new possibilities in the imaging of small intestine diseases, however, due to my knowledge, there exist no studies concerning contrast-enhanced sonography.

7 Future Prospects

In recent years, ultrasound has evolved into an easy-to-use imaging method in medicine and in the context of gastrointestinal disorders. Its record of success has grown over the years and the method became the most commonly used imaging modality at the end of the twentieth century. Bowel sonography is currently recommended as the primary imaging procedure in patients with acute and chronic bowel symptoms.

At present, contrast media is used in many applications of modern diagnostic imaging, regardless of which modality is used. Both CT and MRI have gone through the very same process and contrast agents were first needed to improve the poor quality of morphological images. Contrast-enhanced sonography has recently gained much attention in several

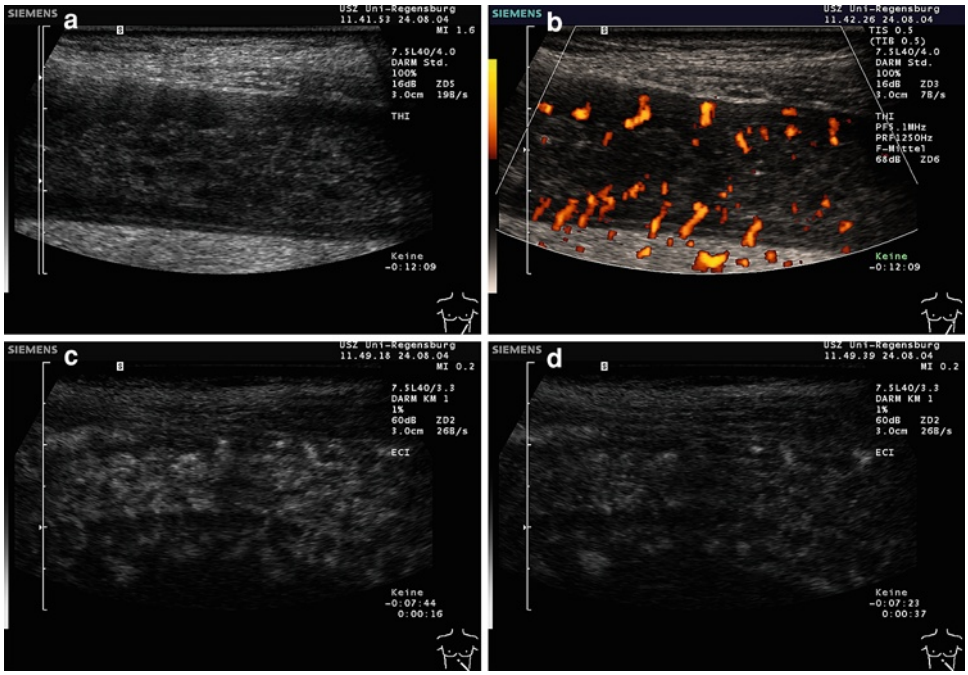

Fig. 4 Descending colon of a patient with acute GvHD. **a** B-mode sonography shows increased motility and loss of bowel-wall stratification. **b** Power Doppler sonography shows increased bowel-wall perfusion. **c** 16 s and **d** 37 s after injection of SonoVue®: contrast enhancement with microbubbles mainly in the submucosal layer, which was formerly not definable

different settings. Due to recent advantages in sonographic equipment and the application of intravenous contrast agents, contrast-enhanced ultrasonography has been established as a new diagnostic imaging method concerning bowel sonography. Its usefulness for evaluating hemodynamics in the diagnosis of gastrointestinal disorders in various organs has been reported.

It might be expected, that improved ultrasound technology and less expensive ultrasound devices will help to spread this technology and to reduce expensive and unnecessary CT and MRI examinations. The use of contrast agents opens totally new prospects within the foreseeable future, on the one hand, and represents a challenge for every sonographer on the other.

References

Blomley MJ, Albrecht T, Cosgrove DO et al (1999) Improved imaging of liver metastases with stimulated acoustic emission in the late phase of enhancement with the US contrast agent SH U 508A: early experience. Radiology 210:409–416

Blomley MJ, Cooke JC, Unger EC et al (2001) Microbubble contrast agents: a new era in ultrasound. Br Med J 322:1222–1225

Blomley M, Cosgrove D (1997) Microbubble echo-enhancers: a new direction for ultrasound? Lancet 349:1855–1856

Bouakaz A, De Jong N, Cachard C (1998) Standard properties of ultrasound contrast agents. Ultrasound Med Biol 24:469–472

Campani R, Calliada F, Bottinelli O (1998) Contrast enhancing agents in ultrasonography: clinical applications. Eur J Radiol 27(Suppl 2): 161–170

Darge K, Troeger J, Duetting T et al (1999) Reflux in young patients: comparison of voiding US of the bladder and retrovesical space with echo enhancement versus voiding cystourethrography for diagnosis. Radiology 210:201–207

Dietrich CF, Jedrzejczyk M, Ignee A (2007) Sonographic assessment of splanchnic arteries and the bowel wall. Eur J Radiol 64:202–212

Duda VF, Rode G, Schlief R (1993) Echocontrast agent enhanced color flow imaging of the breast. Ultrasound Obstet Gynecol 3:191–194

Esteban JM, Aleixandre A, Hurtado MJ et al (2003) Contrast-enhanced power doppler ultrasound in the diagnosis and follow-up of inflammatory abdominal masses in Crohn's disease. Eur J Gastroenterol Hepatol 15:253–259

Forsberg F, Goldberg BB (1997) New imaging techniques with ultrasound contrast agents. In: Goldberg BB (ed) Ultrasound contrast agents. Martin Dunitz Ltd, London, pp 177–192

Fukuta N, Kitano M, Maekawa K (2005) Estimation of the malignant potential of gastrointestinal stromal tumors: the value of contrast-enhanced coded phase-inversion harmonics US. J Gastroenterol 40:247–255

Geleijnse ML, Nemes A, Vletter WB et al (2009) Adverse reactions after the use of sulphur hexafluoride (SonoVue) echo contrast agent. J Cardiovasc 10:75–77

Girlich C, Jung EM, Huber E et al (2011a) Comparison between preoperative quantitative assessment of bowel wall vascularization by contrast-enhanced ultrasound and operative macroscopic findings and results of histopathological scoring in Crohn's disease. Ultraschall Med 32:154–159

Girlich C, Jung EM, Iesalnieks I et al (2009) Quantitative assessment of bowel wall vascularization in Crohn's disease with contrast-enhanced ultrasound and perfusion analysis. Clin Hemorheol Microcirc 43:141–148

Goldberg BB, Merton DA, Forsberg F et al (1996) Color amplitude imaging: preliminary results using vascular sonographic contrast agents. J Ultrasound Med 15:127–134

Gorg C, Wollenberg B, Beyer J et al (2005) High-resolution ultrasonography in gastrointestinal graft-versus-host disease. Ann Hematol 84:33–39

Gramiak R, Holen J (1984) CW and pulsed Doppler echocardiography utilizing a stand-alone system. Ultrasound Med Biol 10:215–224

Gramiak R, Shah PM (1968) Echocardiography of the aortic root. Invest Radiol 3:356–366

Guidi L, De Franco A, De V et al (2006) Contrast-enhanced ultrasonography with SonoVue after infliximab therapy in Crohn's disease. Eur Rev Med Pharmacol Sci 10:23–26

Hamada T, Yamauchi M, Tanaka M et al (2007) Prospective evaluation of contrast-enhanced ultrasonography with advanced dynamic flow for the diagnosis of intestinal ischaemia. Br J Radiol 80:603–608

Harvey CJ, Blomley MJ, Eckersley RJ et al (2000) Pulse-inversion mode imaging of liver specific microbubbles: improved detection of subcentimetre metastases. Lancet 355:807–808

Hata J, Kamada T, Haruma K et al (2005) Evaluation of bowel ischemia with contrast-enhanced US: initial experience. Radiology 236:712–715

Holt S, Samuel E (1979) Grey scale ultrasound in Crohn's disease. Gut 20:590–595

Incesu L, Yazicioglu AK, Selcuk MB et al (2004) Contrast-enhanced power doppler US in the diagnosis of acute appendicitis. Eur J Radiol 50:201–209

Ionescu A (2009) Bubble trouble: anaphylactic shock, threatened myocardial infarction, and transient renal failure after intravenous echo contrast for left ventricular cavity opacification preceding dobutamine stress echo. Eur J Echocardiography 10:707–710

Jeffrey RB Jr, Laing FC, Lewis FR (1987) Acute appendicitis: high-resolution real-time US findings. Radiology 163:11–14

Keyzer C, Zalcman M, De Maertelaer V et al (2005) Comparison of US and unenhanced multi-detector row CT in patients suspected of having acute appendicitis. Radiology 236:527–534

Klein SA, Martin H, Schreiber-Dietrich D et al (2001) A new approach to evaluating intestinal acute graft-versus-host disease by transabdominal sonography and colour doppler imaging. Br J Haematol 115:929–934

Kolkman JJ, Falke TH, Roos JC et al (1996) Computed tomography and granulocyte scintigraphy in active inflammatory bowel disease. Comparison with endoscopy and operative findings. Dig Dis Sci 41:641–650

Kratzer W, von Tirpitz C, Mason R et al (2002) Contrast-enhanced power doppler sonography of the intestinal wall in the differentiation of hypervascularized and hypovascularized intestinal obstructions in patients with Crohn's disease. J Ultrasound Med 21:158–159

Kumar P, Domja J, Bhandari P et al (2009) Is there an association between intestinal perfusion and Crohn's disease activity? A feasibility study using contrast-enhanced ultrasound. Br J Radiol 82:112–117

Kunihiro K, Hata J, Manabe N (2007) Predicting the need for surgery in Crohn's disease with contrast harmonic ultrasound. Scand J Gastroenterol 42:577–585

Lassau N, Lamuraglia M, Chami L et al (2006) Gastrointestinal stromal tumors treated with imatinib: monitoring response with contrast-enhanced sonography. Am J Roentgenol 187:1267–1273

Ludwig D, Wiener S, Brüning A et al (1999) Mesenteric blood flow is related to disease activity and risk of relapse in Crohn's disease: a prospective follow-up study. Am J Gastroenterol 94:2942–2950

Maconi G, Sampietro GM, Sartani A et al (2008) Bowel ultrasound in Crohn's disease: surgical perspective. Int J Colorectal Dis 23:339–347

Meairs S, Daffertshofer M, Neff W et al (2000) Pulse-inversion contrast harmonic imaging: ultrasonographic assessment of cerebral perfusion. Lancet 355:550–551

Migaleddu V, Scanu AM, Quaia E et al (2009) Contrast-enhanced ultrasonographic evaluation of inflammatory activity in Crohn's disease. Gastroenterology 137:43–61

Mulvagh SL, DeMaria AN, Feinstein SB et al (2000) Contrast echocardiography: current and future applications. J Am Soc Echocardiogr 13:331–342

Nanda NC, Carstensen C (1997) Echo-enhancing agents: safety. In: Nanda NC, Schlief R, Goldberg BB (eds) Advances in echo imaging using contrast enhancers. Kluwer Academic Publishers, Dordrecht, pp 115–131

Ophir J, Parker KJ (1989) Contrast agents in diagnostic ultrasound. Ultrasound Med Biol 15:319–333

Parente F, Greco S, Molteni M et al (2003) Role of early ultrasound in detecting inflammatory intestinal disorders and identifying their anatomical location within the bowel. Aliment Pharmacol Ther 18:1009–1016

Parente F, Maconi G, Bollani S et al (2002) Bowel ultrasound in assessment of Crohn's disease and detection of related small bowel strictures: a prospective comparative study versus x ray and intraoperative findings. Gut 50:490–495

Plikat K, Klebl F, Buchner C et al (2004) Evaluation of intestinal hypereamia in inflamed bowel by high resolution Contrast Harmonic Imaging (CHI). Ultraschall Med 25:257–262

Quaia E, Migaleddu V, Baratella E et al (2009) The diagnostic value of small bowel wall vascularity after sulfur hexafluoride-filled microbubble injection in patients with Crohn's disease. Correlation with the therapeutic effectiveness of specific anti-inflammatory treatment. Eur J Radiol 69:438–444

Rapaccini GL, Pompili M, Orefice R et al (2004) Contrast-enhanced power doppler of the intestinal wall in the evaluation of patients with crohn's disease. Scand J Gastroenterol 39:188–194

Ries F, Honisch C, Lambertz M et al (1993) A transpulmonary contrast medium enhances the transcranial doppler signal in humans. Stroke 24:1903–1909

Ripollés T, Martinez MJ, Paredes JM et al (2009) Crohn's disease: correlation of findings at contrast-enhanced US with severity at endoscopy. Radiology 253:241–248

Robotti D, Cammarota T, Debani P et al (2004) Activity of crohn disease: value of color-power-doppler and contrast-enhanced ultrasonography. Abdom Imaging 29:648–652

Schirin-Sokhan R, Winograd R, Tischendorf S et al (2011) Assessment of inflammatory and fibrotic stenoses in patients with crohn's disease using contrast-enhanced ultrasound and computerized algorithm: a pilot study. Digestion 83:263–268

Schlottmann K, Fuchs-Koewel B, Demmler-Hackenberg M et al (2005a) High-frequency contrast-harmonic imaging of ophthalmatic tumor perfusion. AJR Am J Roentgenol 184:574–578

Schlottmann K, Klebl F, Zorger N et al (2004) Contrast-enhanced ultrasound allows for interventions of hepatic lesions which are invisible on conventional B-mode. Z Gastroenterol 42:303–310

Schlottmann K, Kratzer W, Schoelmerich J (2005b) Doppler ultrasound and intravenous contrast agents in gastrointestinal tract disorders: current role and future implications. Eur J Gastroenterol Hepatol 17:263–275

Schneider M (1999) Characteristics of SonoVue (trademark). Echocardiography 16:743–746

Schreyer AG, Finkenzeller T, Gossmann H et al (2008) Microcirculation and perfusion with contrast enhanced ultrasound (CEUS) in crohn's disease: first results with linear contrast harmonic imaging (CHI). Clin Hemorhoeol Microcirc 40:143–155

Schreyer AG, Landfried K, Zorger N et al (2011) Transmural penetration of intravenously applied microbubbles during contrast-enhanced ultrasound as a new diagnostic feature in patients with GVHD of the bowel. Bone Marrow Transplant 46:1006–1011

Schulte-Altedorneburg G, Demharter J, Linné R et al (2003) Does ultrasound contrast agent improve the diagnostic value of colour and power doppler sonography in superficial lymph node enlargement? Eur J Radiol 48:252–257

Serra C, Menozzi G, Labate AM et al (2007) Ultrasound assessment of vascularization of the thickened terminal ileum wall in crohn's disease patients using a low-mechanical index real-time scanning technique with a second generation ultrasound contrast agent. Eur J Radiol 62:114–121

Smith MD, Elion JL, McClure RR et al (1984) Left heart opacification with peripheral venous injection of a new saccharide echo contrast agent in dogs. J Am Coll Cardiol 13:1622–1628

Smith MD, Kwan OL, Reiser HJ et al (1989) Superior intensity and reproducibility of SHU-454, a new right heart contrast agent. J Am Coll Cardiol 3:992–998

Tarjan Z, Toth G, Gyorke T et al (2000) Ultrasound in crohn's disease of the small bowel. Eur J Radiol 35:176–182

von Herbay A, Vogt C, Willers R et al (2004) Real-time imaging with the sonographic contrast agent SonoVue—differentiation between benign and malignant hepatic lesions. J Ultrasound Med 23:1557–1568

Yamaguchi T, Yoshida S, Tanaka S et al (2009) Predicting the clinical response to cytapheresis in steroid-refractory or—dependent ulcerative colitis using contrast-enhanced ultrasonography. Scand J Gastroenterol 44:831–837

Oral Contrast-Enhanced Bowel Ultrasound

Giovanni Maconi

Contents

Abstract

Bowel ultrasound has become accepted in clinical practice as a primary useful tool in the diagnostic workup and follow-up of several gastrointestinal disorders. The major limit of sonographic evaluation the gastrointestinal tract is the presence of air, which makes difficult in achieving a detailed evaluation of the bowel wall structure and its changes. To overcome this limitation, filling of the stomach, small bowel, and colon with luminal contrast agents such as water or another echo-poor liquid has been proposed. Several studies examined efficacy of luminal contrast bowel ultrasound, showing that it provides an accurate evaluation of bowel wall structure and detects of bowel wall changes. Luminal contrast ultrasound showed an overall benefit over conventional ultrasound in the assessment of stomach, small bowel, and colon. However, comparative studies are still scanty and biased in study design and patient selection. The benefit of luminal contrast ultrasound may vary according to site examined, sonologist's experience, and indication. The use of luminal contrast agent in bowel ultrasound may improve results, but should be adopted on case-by-case basis, according to the clinical context and the sonologist's experience

1 Introduction

In recent decades, sonography of the gastrointestinal tract has become increasingly important in the diagnostic workup for gastrointestinal disorders. For a long time, sonography was considered inappropriate for evaluation of the gastrointestinal tract, because bowel loops contain gas, which was considered a major impediment to the visualization of the gastrointestinal tract.

In fact, intestinal gas is a frequent cause of a poor and unreliable US image, sometimes preventing complete and detailed evaluation of the bowel wall structure and its changes. However, since the 1990s, hydrosonography of the stomach,

G. Maconi (✉)
Chair of Gastroenterology, Department of Clinical Sciences, L. Sacco University Hospital, Via G.B. Grassi, 74, 20157 Milan, Italy
e-mail: giovanni.maconi@unimi.it

G. Maconi and G. Bianchi Porro (eds.), *Ultrasound of the Gastrointestinal Tract*, Medical Radiology. Diagnostic Imaging,
DOI: 10.1007/174_2012_723, © Springer-Verlag Berlin Heidelberg 2012
Published Online: 14 August 2012

small bowel, and colon has been proposed to overcome this limitation. This method entails filling the intestinal tracts with fluid, either by oral administration or by direct instillation of water or a non-absorbable solution (e.g., polyethylene glycol [PEG] solution) into the intestinal lumen by a nasojejunal or rectal probe, before US examination.

2 Hydrosonography of the Stomach and Duodenum

Sonography of the stomach and duodenum is frequently impaired by artifacts due to the presence of gas. However, filling the stomach with water or liquids may reduce acoustic gaseous artifacts and improve evaluation of the gastric wall. For this purpose, water, orange juice, or specific contrast agents such as methylcellulose and simethicone have been used (Lund et al. 1992; Worlicek 1986a; Worlicek et al. 1986b, 1989). A clear advantage with the use of a specific contrast agent, in the detection of bowel wall abnormalities, has not been demonstrated. However, compared to water, the orally administered ultrasonographic contrast agents may improve visualization of the stomach and duodenum, with a decrease in the gas artifact. In particular, cellulose-based suspension may provide a better uniform low level intraluminal echogenicity and fewer gas artifacts compared to water due to the better bulk and surface tension properties, which optimize displacement of intra-luminal gas and interfere with mural gas-adherence (Harisinghani et al. 1997; Lund et al. 1992).

To achieve adequate visualization of the gastric walls, a variable amount (from 500 to 1000 ml) of the above-mentioned fluids should be given to the fasting patient. Just before the examination, 20 mg of Hyoscine-N-butylscopolamine (Buscopan® Boehringer, Germany) could be injected intravenously to ensure appropriate relaxation of the gastric wall, reducing peristalsis, and delaying gastric emptying. In head-down (angle of inclination 20°) and left lateral position, the fundus and body of the stomach can be better examined. In head-up (angle of inclination 30–40°) left-lateral and supine position, the body and proximal antrum can be displayed, while in head-up right-lateral and standing position a better visualization of the distal antrum and duodenum can be obtained.

The different parts of the stomach can be examined using a transducer operating at a frequency of 5–12 MHz, but for more distant areas of the fundus and cardia 3.5–5 MHz transducers can guarantee a greater depth of penetration and better visualization.

Hydrosonography of the stomach and duodenum has proven to be of value in the assessment of various conditions, such as peptic ulcer (Joharjy et al. 1990), gastric cancer and lymphoma (Lee et al. 2001; Düx et al. 1997; Segura et al. 1999), polypoid lesions and submucosal tumors (Futagami et al. 2001; Polkowski et al. 2002), gastric web, and duodenal duplication (Tiao et al. 2005; Guibaud et al. 1996).

As far as gastric cancer is concerned, prospective studies have shown that transcutaneous hydrosonography has a sensitivity in detecting lesions ranging from 60 to 84 %, and that may also be useful in staging the disease, with the exception of cardial gastric cancer, which may easily be missed (Lee et al. 2001; Düx et al. 1997; Segura et al. 1999; Ishigami et al. 2004).

However, even if hydrosonography of the stomach can accurately detect and stage gastric cancer, gastric submucosal tumors and gastro-duodenal ulcers, it is not an appropriate tool for routine assessment of the stomach in dyspeptic patients and for the diagnostic workup of cancer, endoscopy, EUS, and CT being much more accurate diagnostic tools (Fig. 1 and Fig. 2).

However, when these investigations, for various reasons, cannot be performed, or in the case of surveillance of benign submucosal lesions previously assessed by EUS, hydrosonography of the stomach can be taken into consideration as an inexpensive, non-invasive and simple alternative. In particular, hydrosonography of the stomach can be considered a valid alternative to EUS for: (1) diagnosis (and follow-up) of extraluminal gastric compression, and (2) detection and surveillance of gastric submucosal tumours. In this regard, it has been shown that in gastric submucosal tumors can be visualized (and measured) using trans-abdominal ultrasound in 69–93 % of patients (Tsai et al. 2000; Futagami et al. 2001; Polkowski et al. 2002). In particular, Futagami et al. (2001) showed that the overall detection of the lesions was 82.5 %, but the detection rate varied according to the lesion size, being approximately 95 % for submucosal tumors over 20 mm in diameter, and 97 % for the lesions over 30 mm in diameter.

3 Small Intestine Contrast Ultrasonography

Like the stomach and duodenum, the sonographic visualization of the small bowel can be improved by filling the bowel with water or echo-poor liquids, either directly infused into the small bowel using a nasojejunal tube and a peristaltic pump (Folvik et al. 1999) or administered orally (Pallotta et al. 1999a).

In both cases, the liquid contrast medium should be non-absorbable and non-fermentable. Isotonic anechoic electrolyte solutions containing PEG, which are used for bowel cleansing prior to colonoscopy, are now considered the contrast media of choice. PEG solutions comprise various products with similar composition (e.g., polyethylene glycol

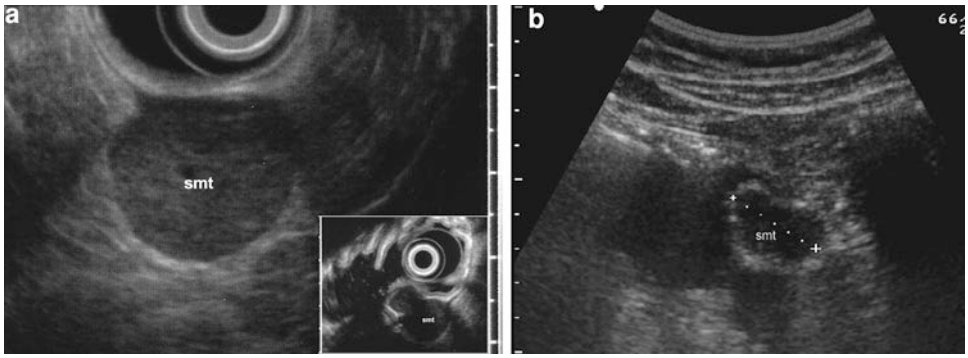

Fig. 1 Submucosal tumor (*smt*) of gastric antrum. Endosonography (**a**) and gastric hydrosonography (**b**) show a small submucosal lesion

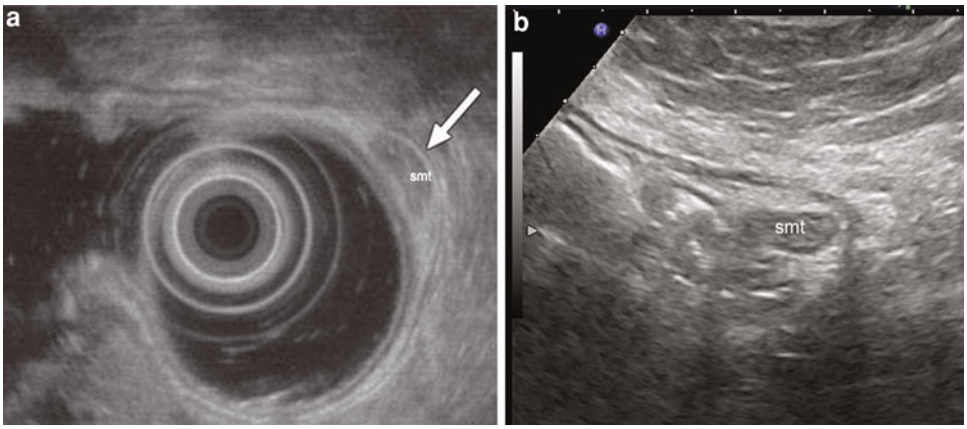

Fig. 2 Submucosal tumor (*smt*) of gastric antrum. Endosonography (**a**) and gastric hydrosonography (**b**) show a small submucosal lesion

4000 or 3350 at a dose of 58–59 g, magnesium sulphate 7 g, sodium sulphate 2.8–5.7 g, sodium bicarbonate 1.7 g, sodium chloride 0.8–1.5 g, and potassium chloride 0.74 g) and osmolarity (280–290 mOsm/kg). The difference between PEG 4000 and PEG 3350 is the molecular weight (4000 and 3350, respectively).

The ingestion of a variable amount of PEG, usually between 250 and 500 ml, provides an adequate distension of the intestinal loops, removes gas making sequential visualization of the entire small bowel, from the duodenum to terminal ileum, easier and also allowing measurement of wall thickness and luminal diameter (Pallotta et al. 1999a, 1999b, 2000) (Table 1).

Sonographic assessment of the small bowel should be performed, after overnight fasting. After ingestion, the contrast solution passes from the stomach to the duodenum, jejunum, and ileum, distending the intestinal loops and thus improving the examination of the morphological and functional aspects of the bowel wall, such as thickening, echopattern, *valvulae conniventes*, and modality of contraction and relaxation (Fig. 3).

If distension and visualization of the entire bowel up to the terminal ileum is not adequate, further aliquots of PEG can be used. The amount of ingested US contrast agent does not significantly affect the luminal diameter or the wall thickness, at any level of the small bowel, in normal controls (Pallotta et al. 1999b).

Bowel examination can be performed immediately after ingestion of PEG or performed 10 min after PEG ingestion and then repeated at 10-minute intervals until the contrast can be seen to flow through the terminal ileum into the cecum. The mean duration of the entire examination is usually 30 min (Table 1). On account of the small amount of ingested contrast and palatability, the procedure is well-accepted and safe. None of the studies have reported significant side effects or major complaints during or immediately after PEG ingestion, apart from 2 studies, where five patients complained nausea and vomiting, which precluded the examination (Parente et al. 2004; Chatu et al. 2012). One study also reported minor and uneventful adverse events, such as nausea in 6.9 % and slight abdominal distension in 3.9 % of Crohn's disease patients (Parente et al. 2004). In this regard, caution should be taken in using PEG in patients with confirmed or suspected small bowel occlusion. In these cases, as a safer oral contrast agent, variable amounts of tap water can be used.

Hydrosonographic assessment of the small bowel has been shown to be highly accurate in most studies, with sensitivity ranging between 63 and 100 % (median, 97.1 %) and specificity between 20 and 100 % (median, 97.2 %)

Table 1 Type and amount of PEG used in small bowel evaluation and duration of examination, defined as time taken to image terminal ileum, and side effects, reported by various authors in the literature

Author (ref)	Contrast medium	Amount of PEG (ml) Mean (Range)	Time to image terminal ileum (min) Mean (Range)	Inconclusive incomplete exam due to side effects (%)
Cittadini et al. 2001	PEG 4000	500	31 (10–90)	0
Pallotta et al. 2001	PEG 4000	388 (200–670)	37 (12–90)	0
Parente et al. 2004	PEG 3350	624 (500–800)	31 (20–60)	1 (1)
Calabrese et al. 2005	PEG 4000	375 (250–500)	40 (35–90)	0
Dell'Aquila et al. 2005	PEG 4000	n.r. (500–800)	n.r. (30–60)	0
Pallotta et al. 2005	PEG 4000	370 (200–500)	39 (12–90)	0
Castiglione et al. 2008	PEG 3350	750	> 30	3 (7)
Chatu et al. 2012	PEG 4000	1000	30	5 (3.5)
Folvik et al. 1999[a]	MW 3350	2000	40 (20–90)	n.r
Nagi et al. 2006[a]	n.r.	(1000–1500)	34 (n.r.)	0
Válek et al. 2007[a]	HP 7000	2000	n.r.	0

[a] Hydrosonography of small bowel by naso-jejunal tube; n.r. not reported

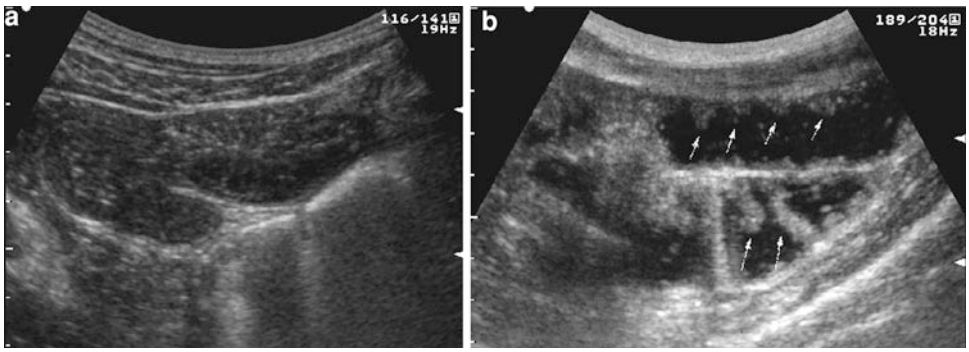

Fig. 3 Real-time ultrasonography of small bowel in basal fasting condition (**a**) and following administration of 500 ml of oral contrast agent (**b**). After contrast ingestion, entire small bowel is distended and visualized, and bowel wall and Kerckring's folds may be well delineated

depending on the underlying disease (Maconi et al. 2009). In fact, accuracy seems to be greater when patients with Crohn's disease are well represented in the case series (Table 2).

In fact, in these studies the diagnostic accuracy of small intestine contrast US was comparable to ileocolonoscopy, wireless capsule endoscopy, and small bowel X-ray in the assessment of number, site, extension, and post-operative recurrence of small bowel lesions (Pallotta et al. 2001, 2005; Parente et al. 2004; Onali et al. 2010; Calabrese et al. 2009; Fig. 4).

When compared to conventional bowel US, the use of PEG slightly improved the overall sensitivity in the detection of small bowel lesions in Crohn's disease patients (from 4 to 11 %; median, 4.85 %), also in the post-operative follow-up, but seemed to offer a greater advantage, compared to conventional bowel US, in detecting proximal small bowel lesions (sensitivity, 80 vs. 100 %, respectively) and in assessing the number and site of small bowel stenoses (Parente et al. 2004; Calabrese et al. 2005). As far as the detection of stenosis is concerned, small intestine contrast US may increase the sensitivity by 15–18 % vs transabdominal US in detecting patients with at least one stricture and by 22.2 % (sensitivity from 55.5 to 77.7 %) in detecting patients with at least two or more stenoses (Parente et al. 2004; Pallotta et al. 2012; Fig. 5). This advantage is presumably due to the fact that contrast agent, by favoring the assessment of dilatation of prestenotic jejunal/ileal loops, permits a better visualization of the narrowed segment or other causes of stenosis (Fig. 6).

It is worthwhile pointing out that oral contrast US may increase the accuracy in detecting small bowel lesions by inexpert sonologists. Two studies compared the usefulness of oral contrast US by two ultrasonologists, one fully skilled, and the other in training. In the first study, performed in a consecutive series of patients, the oral contrast agent was judged particularly useful in 32 % of studies performed by the less experienced ultrasonologist (Cittadini et al. 2001).

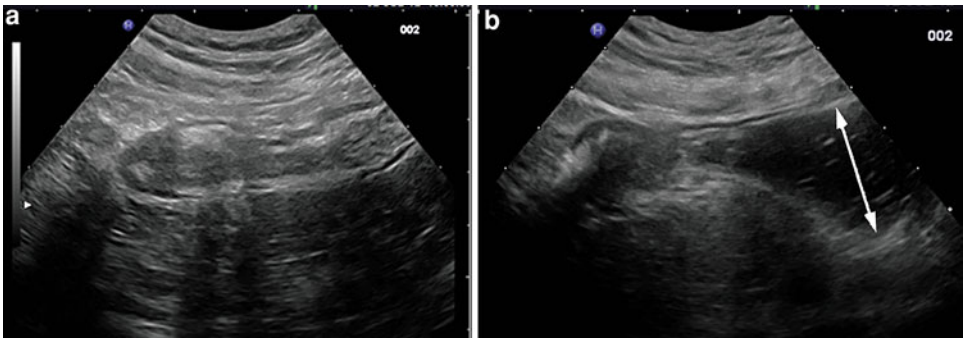

Fig. 5 Crohn's disease stricture of terminal ileum assessed by (**a**) conventional US (longitudinal section) and (**b**) US with oral contrast agent. In this patient, only the use of contrast agent (PEG 500 ml), allowed the assessment of the prestenotic dilatation (*arrow*)

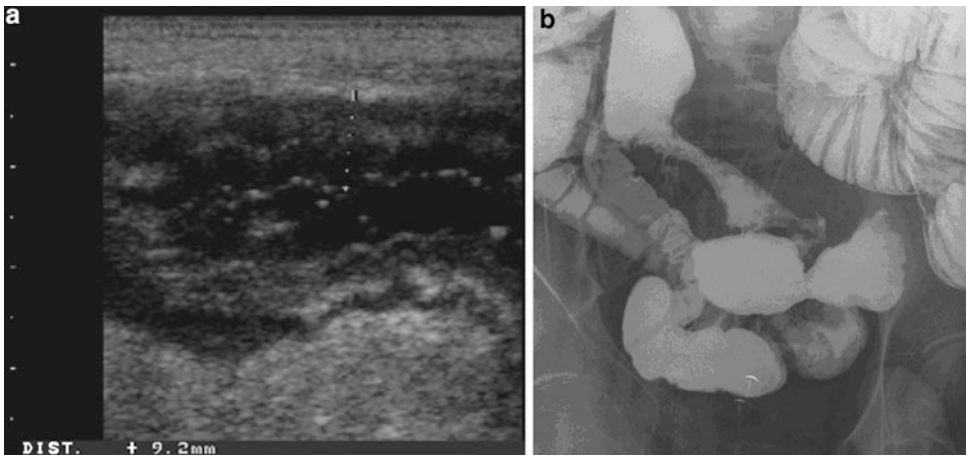

Fig. 4 Crohn's disease lesions of small intestine well delineated by means of oral contrast ultrasound. The US oral contrast agent allows a more accurate evaluation of mucosal surface showing nodular and ulcerated appearance (**a**) comparable to that at contrast barium radiology (**b**), and providing information regarding thickening and transmural changes of ileal wall

In the second study, performed in Crohn's disease patients, the oral contrast increased accuracy of small bowel detection by inexpert sonologist, which become comparable or better than that of an expert sonologist who uses transabdominal US (Calabrese et al. 2005).

The use of oral contrast US may also be used as a reliable and non-invasive technique in the detection and follow-up of coeliac disease patients. Indeed, with these techniques, a clearer visualization of ultrasonographic signs of coeliac disease can be obtained (see Chap. 13, Coeliac Disease), such as increased loop diameter and jejunal wall thickness, reduced number of Kerckring's folds (including ileal jejunalization) and increased peristaltic waves (Dell'Aquila et al. 2005) (Fig. 7).

SICUS can be considered to have some diagnostic advantages, although these are limited to expert sonologists. SICUS could be used by non-expert sonologists for examination of the bowel, in difficult patients, and when complications such as stenosis are likely, on a clinical basis, but not observed at conventional US.

Despite the advantages of small intestine contrast US to obtain a more detailed evaluation of the bowel wall in suspected Crohn's disease and in patients with suspicion of stenosis, particularly when used by a non-expert sonologist, it is a time-consuming procedure (mean duration 30–40 min), compared to conventional bowel US, a limitation that is not in keeping with the peculiar features of abdominal US, which is a simple, practical, and rapidly performed examination. Therefore, for most sonologists, particularly for those expert in bowel US, the advantages, compared to conventional US, are too modest to suggest its routine use in the diagnostic setting (Castiglione et al. 2008).

4 Hydrocolonic Sonography

Since the late 1980s, ultrasonographic evaluation of the colon following water enema, also known as hydrocolonic sonography, has been proposed as an alternative to barium enema and colonoscopy for imaging of the colon and colonic walls.

Table 2 Results of comparative studies showing sensitivity and specificity of small bowel contrast ultrasonography (SICUS) or US enteroclysis ([a]) and conventional transabdominal ultrasonography (TUS) in detecting at least one small bowel lesion assessed by contrast radiology

	Total	Patients with lesions	Patients with CD	Sensitivity		Specificity	
Author	n.	n. (%)	n. (%)	TUS	SICUS	TUS	SICUS
Folvik et al. 1999[a]	55	11 (20.0)	17 (30.9)	n.e.	7/11 (63.3)	n.e.	44/44 (100)
Pallotta et al. 1999a	31	8 (25.8)	5 (16.1)	n.e.	8/8 (100)	n.e.	22/23 (95.6)
Cittadini et al. 2001	53	25 (47.2)	16 (30.2)	n.e.	18/25 (72.0)	n.e.	28/28 (100)
Pallotta et al. 2001	53	17 (32.1)	8 (15.1)	n.e.	17/17 (100)	n.e.	35/36 (97.2)
Parente et al. 2004	102	102 (100)	102 (100)	n.r. (91.4)	n.r. (96.1)	n.e.	n.e.
Calabrese et al. 2005	28	25 (89.3)	25 (89.3)	24/25 (96.0)	25/25 (100)	n.e.	n.e.
Pallotta et al. 2005	91	35 (38.5)	16 (17.6)	20/35 (57.1)	33/35 (94.3)	56/56 (100)	55/56 (98.2)
Pallotta et al. 2005	57	55 (96.5)	55 (96.5)	48/55 (87.3)	54/55 (98.2)	n.e.	n.e.
Biancone et al. 2007	22	21 (95.4)	22 (100)	n.e.	21/21 (100)	n.e.	0/1 (0)
Castiglione et al. 2008	40	22 (55.0)	40 (100)	17/22 (77.3)	18/22 (81.8)	17/18 (94.4)	17/18 (94.4)
Calabrese et al. 2009	72	67 (93.1)	72 (100)	n.e.	62/72 (92.5)	n.e.	1/5 (20.0)
Onali et al. 2010	25	24 (96.0)	25(100)	n.e.	25/25 (100)	n.e.	n.e.
Chatu et al. 2012	143	n.r.	86 (60.1)	n.e.	n.r. (93.0)	n.e.	n.r. (99.0)
Overall %	772	412	392 (63.3)	109/137 (79.6)	288/316 (91.1)	73/74 (98.6)	202/211 (95.7)

n.e. = not evaluated n.r. = not reported CD = Crohn's disease [a] US enteroclysis

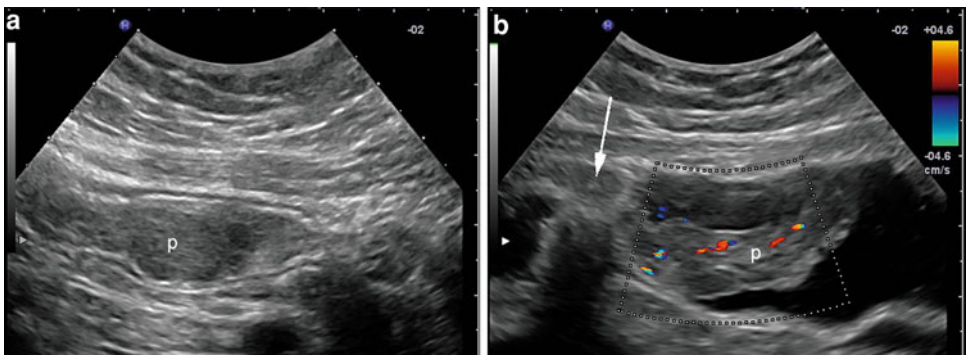

Fig. 6 **a** Conventional and **b** small intestinal contrast ultrasound of in a female patient who have had surgery for Crohn's disease presenting with intermittent bowel occlusions. Only after PEG ingestion (500 ml), the longitudinal sonogram of pre-anastomotic ileum showed a large polypoid lesion (*p*) of the ileum just before the anastomosis (arrow) between ileum and ascending colon, determining occlusions

Like these procedures, hydrocolonic sonography requires bowel preparation consisting in a laxative, following which 1500 ml of water should be instilled into the colon, after an intravenous injection of 20 mg of scopolamine-N-butyl-bromide (Buscopan, Boehringer Ingelheim, Germany) for relaxation of the colon. The amount of instilled water depends on distension of the colon, and a relaxant may be necessary to achieve optimal distension and to suppress the sense of urgency of elimination, of the patient.

The sonographic examination can be carried out after instillation of water, preferably using a 3.5–7 MHz transducer and, for detailed evaluation, 5–12 MHz transducers.

The accuracy of hydrocolonic sonography appears to depend on the indication and, therefore, on the study population.

Most studies have reported that hydrocolonic sonography was accurate in the detection of colorectal cancer, with sensitivity ranging from 70 to 97 % (mean, 89.7 %), (Düx et al. 1997; Bru et al. 2001; Chung et al. 2004; Dixit et al. 1999; Hernandez-socorro et al. 1995; Limberg 1987, 1990, 1992; Segura et al. 1999; Walter et al.1993; Elewaut and Afschrift 1995; Candia et al. 1995; Hirooka et al. 1989) albeit very negative results have also been reported (sensitivity <7 %, with a false positive rate of 19.2 %) (Chui et al. 1994) (Table 3). However, these controversial results

Table 3 Sensitivity and specificity of hydrocolonic sonography in detecting polyps and neoplastic lesions in adults (modified from Maconi et al. 2009)

		Patients with polyps			Patients with Cancer				
Author	Pts (no.)	Sensitivity TP/ TP + FN (%)	Specificity TN/ TN + FP (%)	Polyps ≥ 7 mm no. (%)[b]	Sensitivity TP/ TP + FN (%)	Specificity TN/ TN + FP (%)	T stage[a] TP/ TP + FN (%)	N stage[a] TP/ TP + FN (%)	T3-T4 no. (%)
Hirooka et al. 1989[c]	56	8/13 (61.5)	n.e.	4 (30.8)	4/4 (100)	n.e.	n.e.	n.e.	n.e.
Limberg 1992	300	41/54 (75.9)	246/246 (100)	42 (77.8)	28/29 (96.6)	271/271 (100)	23/28 (82.1)	n.e.	25 (85.7)
Walter et al. 1993	100	n.e.	n.e.	n.e.	n.e. (83.0)	n.e.	n.e.	n.e.	n.e.
Chui et al. 1995	52	2/29 (6.9)	18/23 (78.3)	8 (27.6)	0/4 (0)	43/48 (89.6)	n.e.	n.e.	n.e.
Hernandez-Socorro et al. 1995	104	n.e.	n.e.	n.e.	39/40 (97.5)	63/64 (98.4)	38/39 (97.4)	32/39 (82.0)	37 (92.5)
Elewaut and Afschrift 1995	106	9/12 (75.0)	91/94 (96.8)	n.e.	5/5 (100)	101/101 (100)	5/5 (100)	n.e.	5 (100)
Candia et al. 1995	120	40/50 (80.0)	70/70 (100)	40 (80.0)	31/32 (96.8)	88/88 (100)	n.e.	n.e.	n.e.
Dux et al. 1997	60	n.e.	n.e.	n.e.	24/34 (70.6)	n.e.	23/33 (70.0)	7/28 (25.0)	23 (69.7)
Segura et al. 1999	155	15/19 (78.9)	132/136 (97.1)	19 (100)	46/50 (92)	103/105 (98.2)	n.e.	n.e.	n.e.
Dixit et al. 1999	100	2/2 (100)	n.e.	2 (100)	15/16 (93.8)	n.e.	n.e.	n.e.	12 (75.0)
Chung et al. 2004	17	n.e.	n.e.	n.e.	n.e.	n.e.	15/17 (88.2)	4/8 (50.0)	15 (88.2)
Overall %	1170	117/179 (65.4)	557/569 (97.9)	115 (64.2)	192/214 (89.7)	669/677 (98.8)	104/122 (85.2)	43/75 (57.3)	117 (83.6)

n.e. = not evaluated; [a] Stage correctly assessed by US/All cancers staged by histology
[b] No. polyps ≥7 mm/All polyps
[c] Sono-enterocolonography with orally administered contrast

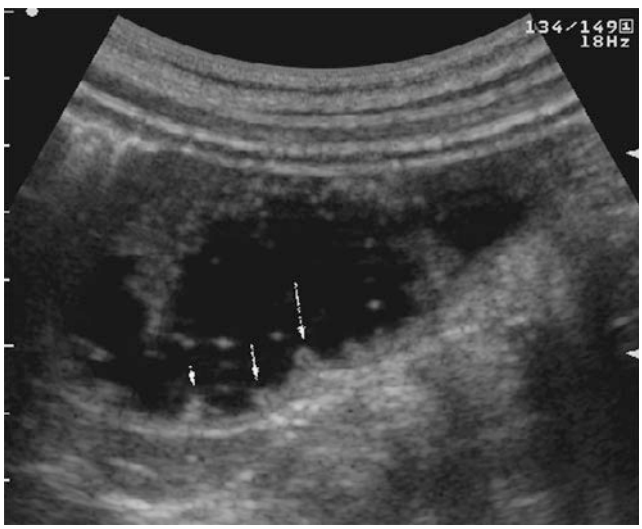

Fig. 7 Small intestinal contrast ultrasound of coeliac disease patient. Diameter of jejunal loop is significantly greater and number of Kerckring's folds (*arrows*) reduced

depend on the variable presence of overweight patients in the case series, skill of the operators, and the nature, size, stage, and site of the neoplastic lesions since a poor accuracy in detecting rectal cancer by hydrocolonic sonography has been reported, in most studies. High sensitivity has also been reported in assessing the T stage of colorectal cancer (mean, 85.2 %), even if more than 80 % of these lesions were found to be in an advanced stage (T3 or T4). On the contrary, the sensitivity of the technique in assessing *N* stage was disappointing.

Early stage neoplasms and polyps, particularly if small in size, are usually detected with lower accuracy. Detection and staging of rectal cancer are frequently underestimated and lesions located in the transverse colon and in both colonic flexures may be difficult to image properly with US (Chung et al. 2004; Dux 1999).

For these and other reasons (i.e., obviously hydrocolonic sonography does not offer the possibility/opportunity to collect biopsies or remove polyps), although less invasive and expensive than colonoscopy, the use of hydrocolonic

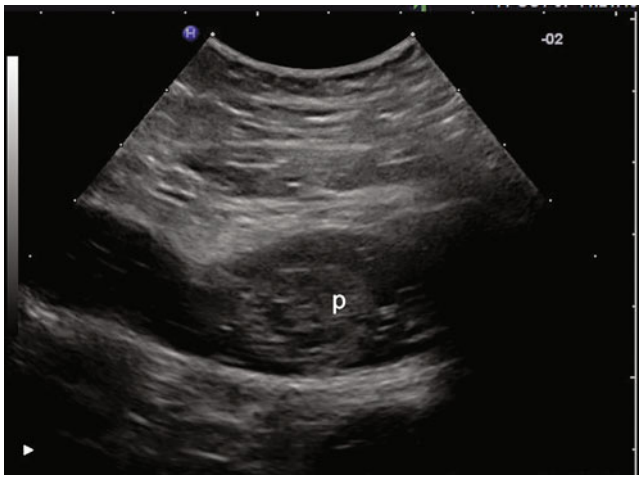

Fig. 8 Hydrocolonic sonogram showing a polypoid lesion (*p*) in the proximal sigmoid colon in a 5 year old boy. The patient presented with rectal bleeding, following a negative (incomplete) sigmoidoscopy

sonography, as a screening tool for colorectal cancer, should be evaluated with due care.

The lack of radiation exposure and limited invasiveness makes hydrocolonic sonography a useful option for the early assessment and follow-up of colonic lesions, both in pediatric and elderly patients with poor compliance with radiographic and endoscopic diagnostic procedures. However, it should also be borne in mind that in these patients, compliance may be negatively affected by the bowel preparation that is required for hydrocolonic sonography examination.

Assessment of colonic lesions by conventional sonography without preparation is likely to be less accurate than that by hydrocolonic sonography. The few comparative studies performed thus far have shown that hydrocolonic sonography is more accurate than conventional sonography in detecting colonic lesions.

However, hydrocolonic sonography has proven to be of value as an early diagnostic technique in the diagnosis of juvenile colonic polyps (Baldisserotto et al. 2002; Ling et al. 1995; Nagita et al. 1994). Nagita et al. (1994) used hydrocolonic sonography with saline enema to examine 39 children (age, 2–8 years) with rectal bleeding. Solitary juvenile colonic polyps were shown and histologically confirmed in 25 children, whereas children with no sonographic abnormalities had no further rectal bleeding, five of whom had negative colonoscopic findings. Remarkably, a significant correlation was seen between sonographic and histological features of the polyps, in that the lesions showed hypoechoic areas in more hyperechoic polyps that were shown, histologically, to be dilated glandular canals (Fig. 8).

In inflammatory lesions, hydrocolonic sonography may play a useful role in the assessment of disease extension and activity (Limberg and Osswald 1994; Bru et al. 2001). Considering its accuracy, low risk, and cost, hydrocolonic sonography can be useful in the study of disease extension in patients with incomplete colonoscopy, after confirmation of the diagnosis by histology. In patients in whom the diagnosis of inflammatory bowel disease has been established, hydrocolonic sonography may also provide an estimate of disease severity.

References

Baldisserotto M, Spolidoro JV, Bahú Mda G (2002) Graded compression sonography of the colon in the diagnosis of polyps in pediatric patients. AJR Am J Roentgenol 179:201–205

Biancone L, Calabrese E, Petruzziello C et al (2007) Wireless capsule endoscopy and small intestine contrast ultrasonography in recurrence of Crohn's disease. Inflamm Bowel Dis 13:1256–1265

Bru C, Sans M, Defelitto MM et al (2001) Hydrocolonic sonography for evaluating inflammatory bowel disease. AJR Am J Roentgenol 177:99–105

Calabrese E, La Seta F, Buccellato A et al (2005) Crohn's disease: a comparative prospective study of transabdominal ultrasonography, small intestine contrast ultrasonography, and small bowel enema. Inflamm Bowel Dis 11:139–145

Calabrese E, Petruzziello C, Onali S et al (2009) Severity of postoperative recurrence in Crohn's disease: correlation between endoscopic and sonographic findings. Inflamm Bowel Dis 15:1635–1642

Candia C, Ciacci V, Di Segni R, Santini E (1995) Hydrocolonic sonography in the study of colonic diseases: comparison with double-contrast enema [in Italian]. Radiol Med (Torino) 89:258–263

Castiglione F, Bucci L, Pesce G et al (2008) Oral contrast-enhanced sonography for the diagnosis and grading of postsurgical recurrence of Crohn's disease. Inflamm Bowel Dis 14:1240–1245

Chatu S, Pilcher J, Saxena SK, Fry DH, Pollok RC (2012) Diagnostic accuracy of small intestine ultrasonography using an oral contrast agent in Crohn's disease: comparative study from the UK. Clin Radiol 67:553–559

Chui DW, Gooding GA, McQuaid KR et al (1994) Hydrocolonic ultrasonography in the detection of colonic polyps and tumors. N Engl J Med 331:1685–1688

Chung HW, Chung JB, Park SW, Song SY, Kang JK, Park CI (2004) Comparison of hydrocolonic sonography accuracy in preoperative staging between colon and rectal cancer. World J Gastroenterol 10:1157–1161

Cittadini G, Giasotto V, Garlaschi G, de Cicco E, Gallo A, Cittadini G (2001) Transabdominal ultrasonography of the small bowel after oral administration of a non-absorbable anechoic solution: comparison with barium enteroclysis. Clin Radiol 56:225–230

Dell'Aquila P, Pietrini L, Barone M et al (2005) Small intestinal contrast ultrasonography-based scoring system: a promising approach for the diagnosis and follow-up of celiac disease. J Clin Gastroenterol 39:591–595

Dixit R, Chowdhury V, Kumar N (1999) Hydrocolonic sonography in the evaluation of colonic lesions. Abdom Imaging 24:497–505

Dux M (1999) Hydrocolonic sonography. Abdom Imaging 24:506–507

Düx M, Roeren T, Kuntz C, Richter GM, Kauffmann GW (1997) TNM staging of gastrointestinal tumors by hydrosonography: results of a histopathologically controlled study in 60 patients. Abdom Imaging 22:24–34

Elewaut AE, Afschrift M (1995) Hydrocolonic sonography: a novel screening method for the detection of colon disease? Bildgebung 62:230–234

Folvik G, Bjerke-Larssen T, Odegaard S, Hausken T, Gilja OH, Berstad A (1999) Hydrosonography of the small intestine: comparison with radiologic barium study. Scand J Gastroenterol 34:1247–1252

Futagami K, Hata J, Haruma K et al (2001) Extracorporeal ultrasound is an effective diagnostic alternative to endoscopic ultrasound for gastric submucosal tumours. Scand J Gastroenterol 36:1222–1226

Guibaud L, Fouque P, Genin G, Valette PJ, Frering V, Partensky C (1996) Case report. CT and ultrasound of gastric and duodenal duplications. J Comput Assist Tomogr 20:382–385

Harisinghani MG, Saini S, Schima W, McNicholas M, Mueller PR (1997) Simethicone coated cellulose as an oral contrast agent for ultrasound of the upper abdomen. Clin Radiol 52:224–226

Hernandez-Socorro CR, Guerra C, Hernandez-Romero J, Rey A, Lopez-Facal P, Alvares-Santullano V (1995) Colorectal carcinomas: diagnosis and preoperative staging by hydrocolonic sonography. Surgery 117:609–615

Hirooka N, Ohno T, Misonoo M et al (1989) Sono-enterocolonography by oral water administration. J Clin Ultrasound 17:585–589

Ishigami S, Yoshinaka H, Sakamoto F et al (2004) Preoperative assessment of the depth of early gastric cancer invasion by transabdominal ultrasound sonography (TUS): a comparison with endoscopic ultrasound sonography (EUS). Hepatogastroenterology 51:1202–1205

Joharjy IA, Mustafa MA, Zaidi AJ (1990) Fluid-aided sonography of the stomach and duodenum in the diagnosis of peptic ulcer disease in adult patients. J Ultrasound Med 9:77–84

Lee DH, Ko YT, Park SJ, Lim JW (2001) Comparison of hydro-US and spiral CT in the staging of gastric cancer. Clin Imaging 25:181–186

Limberg B (1987) Diagnosis of inflammatory and neoplastic colonic disease by sonography. J Clin Gastroenterol 9:607–611

Limberg B (1990) Diagnosis of large bowel tumours by colonic sonography. Lancet 335:144–146

Limberg B (1992) Diagnosis and staging of colonic tumors by conventional abdominal sonography as compared with hydrocolonic sonography. N Engl J Med 327:65–69

Limberg B, Osswald B (1994) Diagnosis and differential diagnosis of ulcerative colitis and crohn's disease by hydrocolonic sonography. Am J Gastroenterol 89:1051–1057

Ling UP, Chen JY, Hwang CJ, Lin CK, Chang MH (1995) Hydrosonography in the evaluation of colorectal polyps. Arch Dis Child 73:70–73

Lund PJ, Fritz TA, Unger EC, Hunt RK, Fuller E (1992) Cellulose as a gastrointestinal US contrast agent. Radiology 185:783–788

Maconi G, Radice E, Bareggi E, Bianchi Porro G (2009) Hydrosonography of the gastrointestinal tract. AJR Am J Roentgenol 193:700–708

Nagi B, Rana SS, Kochhar R, Bhasin DK (2006) Sonoenteroclysis: a new technique for the diagnosis of small bowel diseases. Abdom Imaging 31:417–424

Nagita A, Amemoto K, Yoden A, Yamazaki T, Mino M, Miyoshi H (1994) Ultrasonographic diagnosis of juvenile colonic polyps. J Pediatr 124:535–540

Onali S, Calabrese E, Petruzziello C, et al (2010) Endoscopic vs ultrasonographic findings related to Crohn's disease recurrence: a prospective longitudinal study at 3 years. J Crohns Colitis 4:319–328

Pallotta N, Baccini F, Corazziari E (1999a) Ultrasonography of the small bowel after oral administration of anechoic contrast solution. Lancet 353:985–986

Pallotta N, Baccini F, Corazziari E (1999b) Contrast ultrasonography of the normal small bowel. Ultrasound Med Biol 25:1335–1340

Pallotta N, Baccini F, Corazziari E (2000) Small intestine contrast ultrasonography. J Ultrasound Med 19:21–26

Pallotta N, Baccini F, Corazziari E (2001) Small intestine contrast ultrasonography (SICUS) in the diagnosis of small intestine lesions. Ultrasound Med Biol 27:335–341

Pallotta N, Tomei E, Viscido A et al (2005) Small intestine contrast ultrasonography: an alternative to radiology in the assessment of small bowel disease. Inflamm Bowel Dis 11:146–153

Pallotta N, Vincoli G, Montesani C et al (2012) Small intestine contrast ultrasonography (SICUS) for the detection of small bowel complications in crohn's disease: a prospective comparative study versus intraoperative findings. Inflamm Bowel Dis 18:74–84

Parente F, Greco S, Molteni M et al (2004) Oral contrast enhanced bowel ultrasonography in the assessment of small intestine crohn's disease. A prospective comparison with conventional ultrasound, x ray studies, and ileocolonoscopy. Gut 53:1652–1657

Polkowski M, Palucki J, Butruk E (2002) Transabdominal ultrasound for visualizing gastric submucosal tumors diagnosed by endosonography: can surveillance be simplified? Endoscopy 34:979–983

Segura JM, Olveira A, Conde P, Erdozain JC, Suárez J (1999) Hydrogastric sonography in the preoperative staging of gastric cancer. J Clin Ultrasound 27:499–504

Tiao MM, Ko SF, Hsieh CS et al (2005) Antral web associated with distal antral hypertrophy and prepyloric stenosis mimicking hypertrophic pyloric stenosis. World J Gastroenterol 11:609–611

Tsai TL, Changchien CS, Hu TH, Hsiaw CM (2000) Demonstration of gastric submucosal lesions by high-resolution transabdominal sonography. J Clin Ultrasound 28:125–132

Válek V, Kysela P, Vavríková M (2007) Crohn's disease at the small bowel imaging by the ultrasound-enteroclysis. Eur J Radiol 62:153–159

Walter DF, Govil S, William RR, Bhargava N, Chandy G (1993) Colonic sonography: preliminary observations. Clin Radiol 47:200–204

Worlicek H (1986a) Sonographic diagnosis of the fluid-filled stomach. Ultraschall Med 7:259–263

Worlicek H, Lederer P, Lux G (1986b) Ultrasonographic evaluation of the wall of the fluid-filled stomach—case report of a leiomyoblastoma. Hepatogastroenterology 33:184–186

Worlicek H, Dunz D, Engelhard K (1989) Ultrasonic examination of the wall of the fluid-filled stomach. J Clin Ultrasound 17:5–14

Functional Ultrasound of the Gastrointestinal Tract

Trygve Hausken and Odd Helge Gilja

Contents

T. Hausken · O. H. Gilja (✉)
Section of Gastroenterology, National Centre for Ultrasound in Gastroenterology, Haukeland University Hospital, Institute of Medicine, University of Bergen, Jonas Liesvei 65, 5021 Bergen, Norway
e-mail: Odd.Gilja@uib.no

Abstract

Functional ultrasound of the gastrointestinal (GI) tract includes studies of gastroduodenal and gallbladder motility and flow of luminal contents within the upper GI tract. Furthermore, it includes the effect of different meals and pharmacological intervention. Nutritional imaging comprimises ultrasound imaging to study the effects of nutrition such as fat, proteins and glucose on the function of the GI tract.

1 Introduction

Functional ultrasound of the gastrointestinal (GI) tract includes studies of the distal and proximal stomach, gastric and gallbladder emptying, gastric distribution, GI wall motility, and flow of luminal contents in healthy subjects as well as in patients. Furthermore, it includes the effect of different meals and pharmacological intervention.

It is possible to perform ultrasound of the motility in the small and large bowel. However, it is difficult to standardize and cover the entire intestine in one examination. In inflammatory bowel disease, however, it is possible to study stiffness and lack of peristalsis in bowel segments. The blood flow in the superior mesenteric artery can be evaluated by the use of duplex ultrasonography to study the effects of nutrients and the effect of balloon distension.

In the present review, we will focus on the upper part of GI motility.

Imaging methods have much to offer in the understanding of gastric mechanics, as they can be used to assess gastric wall motion and luminal diameter at the same time and the movement of luminal contents (Ehrlein 1980; Code 1979; Hausken et al. 1992; King et al. 1984; Holt et al. 1980; Bolondi et al. 1985; Hveem et al. 1996; Bateman and Whittingham 1982). Fluoroscopic imaging has been used since the turn of the last century for this purpose, but its application in humans is severely constrained by radiation exposure. Scintigraphy is, at present, the "gold standard"

G. Maconi and G. Bianchi Porro (eds.), *Ultrasound of the Gastrointestinal Tract*, Medical Radiology. Diagnostic Imaging,
DOI: 10.1007/174_2012_665, © Springer-Verlag Berlin Heidelberg 2012
Published Online: 14 August 2012

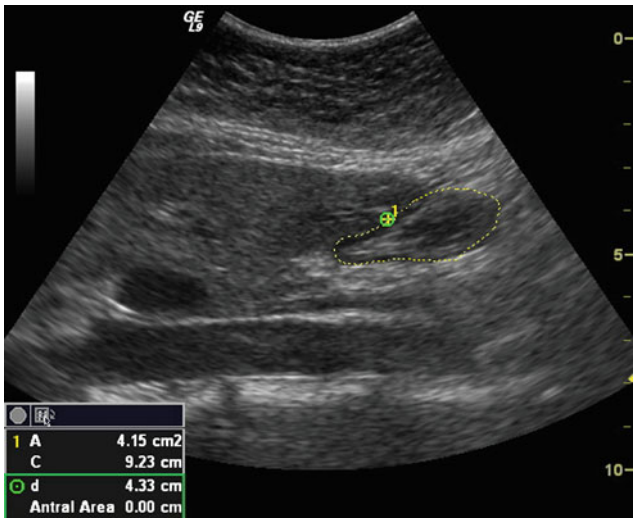

Fig. 1 Standardized section of the antrum. Antral area is outlined

for clinical measurement of gastric emptying. Recently, single photon emission computed tomography (SPECT) has been reported as a possible noninvasive alternative (Bouras et al. 2002). Radiolabeled 99mTc pertechnetate is injected intravenously and accumulates in the gastric mucosa allowing visualization of the stomach. This technique was shown to record changes in postprandial volume to a similar extent to the gastric barostat. Measurement of intra-luminal impedance changes is now used to study transport of fluids in the gut (Savoye et al. 2003; Sifrim et al. 2001). This technique involves application of a low-voltage potential difference to closely spaced electrodes on a catheter in the gut lumen and measurement of the resulting current.

Other techniques such as magnetic resonance imaging (MRI) and ultrasound imaging are attractive options, since they permit prolonged observation of the human stomach without exposure to radiation. Real-time gastric MRI has special appeal but, as yet, its full potential has not been realized due to costs and technical difficulties (Marciani et al. 2001).

Ultrasound imaging of gastroduodenal motility has mainly been performed with a transabdominal approach and until recently primarily as 2D ultrasonography (Gilja et al. 1995; Hausken et al. 1992; Ricci et al. 1993; Undeland et al. 1997). Three-dimensional ultrasound has, so far, only been applied as an investigational tool in scientific studies due to the complex and time-consuming procedure of image recording and processing (Gilja et al. 1997a, b; Berstad et al. 1994). Due to its high availability, modest costs, and lack of radiation hazard, 2D real-time ultrasonography has found its place in clinical diagnostic practice and not only as an experimental tool.

A number of motility studies have now established ultrasound as a valuable method of studying both the proximal (Gilja et al. 1995) and the distal stomach (Hveem et al. 1994; Hausken et al. 1992).

2 Distal Stomach

The width of the antral area is measured in a vertical section in which the antrum, the superior mesenteric vein, and the aorta are visualized simultaneously. The outer profile of the muscularis propria is outlined and the area is calculated automatically (Fig. 1). The values obtained of all measurements are given as the average of two successive measurements.

The relationship between the antral area as measured by ultrasound and the amount of fasting gastric content quantitated by aspiration through the gastroscope and the increment of the antral area after ingestion of graded volumes of water were highly reproducible, with small variations within 1 h and from day to day, and there was a highly significant correlation between the ultrasonographically measured antral area and the amount of fasting gastric juice and between the increase in the antral area and amounts of ingested water (Hveem et al. 1994).

Recent studies have shown that fasting and postprandial antral areas increase in patients with functional dyspepsia and diabetes mellitus compared with normal subjects (Undeland et al. 1997; Hveem et al. 1996). The antral area, and hence antral distention, is a significant determinant of postprandial fullness (Hausken et al. 1992).

3 Gastric Emptying

Scintigraphy is at present the "gold standard" for clinical measurement of gastric emptying. Scintigraphy provides quantitative information about total stomach emptying and intragastric meal distribution of both solid and liquid meals (Collins et al. 1988). With the use of a gamma-camera, the rate of gastric emptying of a standardized test meal marked with a radioisotope can be calculated. Scintigraphy requires expensive equipment that is often not readily available, is associated with a radiation burden, and cannot detect individual episodes of transpyloric flow.

Using ultrasound, gastric emptying has typically been assessed by changes in either the antral cross-sectional area or diameter (Bolondi et al. 1985; Holt et al. 1986). In order to establish ultrasound as an acceptable or even preferred method in assessing gastric emptying, studies have been conducted to compare ultrasound with scintigraphy.

In order to do so, the subjects are usually seated with their back against the gamma camera and the ultrasound transducer is positioned in the region of the umbilicus. The first measurement is performed within 1 min of meal ingestion, followed by subsequent images at intervals depending on which meal is used. Ultrasound T_{50} is defined as the time when the antral area is decreased to half its maximum (Horowitz et al. 1993).

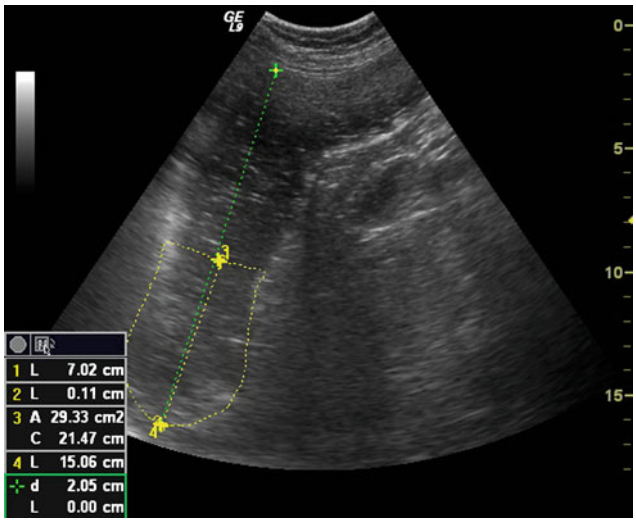

Fig. 2 A proximal gastric area in a sagittal section is outlined by tracing from the top margin of the fundus and 7 cm downward along the axis of the stomach

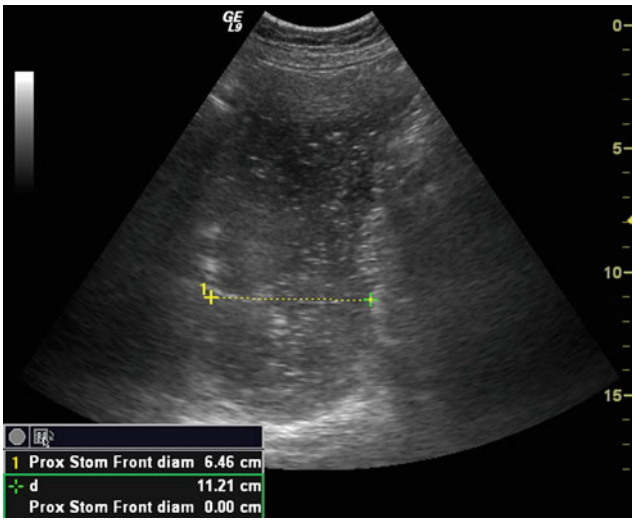

Fig. 3 A fundal diameter defined as the maximal diameter in an oblique frontal section kept within 7 cm along the axis of the proximal stomach

With a high- and low-nutrient liquid meal, scintigraphic and ultrasonographic 50 % emptying times (T_{50}'s) were comparable and longer for dextrose (300 kcal) than for meat soup (20 kcal) (dextrose 107 ± 16 min vs. 108 ± 18 min, soup 24 ± 4 min vs. 23 ± 5 min). A close correlation was found between scintigraphic and ultrasound T_{50} and the T_{50}, and the limits of agreement were good (Hveem et al. 1996).

Other comparative studies between ultrasound and scintigraphic measurements of gastric emptying have shown a very close relationship between the two methods (Bolondi et al. 1985; Holt et al. 1986). The intra–individual variation in gastric emptying of liquids in normal subjects, however, is relatively large.

4 Proximal Stomach and Gastric Accommodation

We have developed a sonographic method to monitor postprandial size of the proximal stomach. A proximal gastric area in a sagittal section (Fig. 2) is outlined by tracing from the top margin of the fundus and 7 cm downward along the axis of the stomach as described by Gilja et al. (1995). Diameter on the fundus (Fig. 3), defined as the maximal diameter in an oblique frontal section kept within 7 cm along the axis of the proximal stomach, is chosen as the second measure. The subjects are scanned in a sitting position with a 3.25-MHz transducer after ingestion of 500 ml meat soup and the measurements are performed 10 and 20 min postprandially.

The soup emptied from the proximal stomach in a linear manner with a moderate day-to-day variation, low intra- and interobserver error, and the method allowed estimation of initial emptying fractions of the proximal stomach (Gilja et al. 1995).

Ultrasound of the proximal stomach has shown that patients with functional dyspepsia and diabetes have a smaller proximal stomach than healthy subjects (Gilja et al. 1996; Undeland et al. 1998). Sublingual glyceryl trinitrate improves accommodation of the proximal stomach to a meal as measured by ultrasound and reduces postprandial symptoms in a group of patients with functional dyspepsia (Gilja et al. 1997a, b).

In reflux esophagitis patients, the sagittal area of the proximal stomach was significantly larger after a meal, and the patients experienced more epigastric fullness (Tefera et al. 2001, 2002). The findings with both 2D and 3D ultrasound methods in gastroesophageal reflux disease (GERD) patients are consistent with the results of other recently published studies. Zerbib et al. (1999) found a more pronounced relaxation of the proximal stomach in GERD patients using a barostat, and observed an inverse correlation between maximal postprandial relaxation and severity of disease. Penagini et al. (1998) found delayed recovery of proximal gastric tone after intake of a combined solid and liquid meal in GERD patients.

The "gold standard" to study gastric accommodation after a meal has been the barostat. The barostat measures gastric wall relaxation and from that one can infer gastric tone. However, introducing the barostat balloon into the gastric lumen may influence the gastric motility patterns (Moragas et al. 1993; Ropert et al. 1993), and furthermore the examination is invasive and unpleasant. Neither the barostat nor scintigraphy allows estimation of the size of the proximal stomach. On the contrary, ultrasound and SPECT scanning

can detect changes in gastric volume in a noninvasive manner. Like ultrasound, SPECT scanning is a noninvasive alternative to the barostat in evaluating gastric relaxation. However, in comparison with meal-induced volume increase, SPECT scanning failed to detect the profound gastric relaxation following glucagon infusion. These findings suggest that SPECT scanning is less suitable than the gastric barostat in detecting gastric relaxation and rather detects the volume of the intragastric contents after meal intake.

An important question is whether imaging methods, such as MRI, SPECT, or ultrasonography, can actually be compared to the measurements made by the barostat. We believe that imaging methods and the invasive barostat method do not measure the same aspects of the gastric accommodation process. Thanks to its close contact with the gastric wall, the barostat bag adjusts to changes in proximal gastric pressure by changing the intrabag volume. Thus, changes in volume are believed to reflect changes in muscle tone of the wall. However, the quantitative change in volume seen during barostat examinations is only valid during barostat studies using exactly the same equipment and positioning technique. Imaging methods, however, visualize directly the size of the gastric compartments, thus giving an indirect measure of relaxation and contraction. The volume change seen using imaging can thus be explained by additional secretion, air retention, or most probably changes in gastric emptying.

The gastric meal accommodation process has two components: passive meal distension of the gastric compartments and active muscle relaxation of the gastric wall. The first component is best measured with imaging methods, whereas the barostat is best suited for studying the second component. Imaging methods, at this stage, do not distinguish between enlargements of the stomach due to reflex relaxation or due to meal-induced distension; it just measures the totally accommodated volume. Accordingly, it may not be adequate to compare imaging methods to the barostat for validation of gastric accommodation. Gastric accommodation depends on neuromuscular factors and hence it is also a matter of evaluation of the mechanical properties of the stomach. In this sense, the barostat merely detects the existence of change in wall tone, but cannot, like imaging methods, provide data on the distribution of the volume and the normal behavior of the gastric wall. In biomechanics, it is essential to understand the geometry of the organ and the forces and deformation in different directions in order to better understand the active–passive muscle function and mechano-sensation in health and in diseases such as the functional disorders. This warrants 2D and 3D image analysis of the gastric compartments.

The different imaging methods exhibit different spatial and temporal image resolution and these factors strongly influence accuracy in volume calculation. MRI, and in particular SPECT, imaging have poor spatial and temporal resolution compared to ultrasonography. Ultrasonography can provide temporal resolution above 100 fps, if necessary, and a spatial resolution at submillimeter level. Also, the "stress-factor" of the imaging methods should be considered in this context because dyspeptic patients in general, and vagal reflexes in particular, are very sensitive to psychological stress. Anyone who has been inside a narrow, noisy MR scanner knows how frightening this can be. Naturally, the stress-factor is also substantially involved in studies using the barostat. Simply because functional disorders are so strongly associated with psychological factors, the examination should be performed in a quiet and relaxing atmosphere with a minimum of distress. Ultrasonography satisfies these criteria as it is noninvasive and does not in itself distort the physiological response in stress-responsive individuals. Moreover, due to gravity playing a central role in the propulsion of gastric content, the study of meal accommodation should preferably be performed in a "natural position" such as sitting in a chair. Therefore, methods that enable patients to be seated have an advantage over methods requiring patients to be in a supine position during the examination.

5 Antral Peristalsis

Antral contractions (3 per minute) are responsible for mixing and grinding of a solid meal into smaller particles (<5 mm) that can pass onto the duodenum. These antral contractions can easily be seen at ultrasonography. The contractions can be occlusive or nonlumen-occlusive. An antral contraction is defined as an indentation of the gastric wall greater than one antral wall thickness, which is not due to respiration, pulsation transmitted from the aorta or heart, or to movements of adjacent intestine.

A lumen-occlusive contraction is defined as a contraction in which the ultrasound image shows the gastric walls to come into apposition at some point along the imaged antrum.

Amplitude of antral contractions is measured as a fraction of relaxed area and the motility index is calculated as the amplitude multiplied by frequency.

The motility index as measured by ultrasound was reduced in patients with functional dyspepsia (FD). The effects of acute mental stress on gastric antral motility were reduced by mental stress in the healthy individuals, but not in FD patients (Hausken et al. 1993).

Manometry is the most widely used method for measuring gastric motility (Malagelada and Stanghellini 1985; Husebye 1999). Manometric studies have demonstrated that the patterns of luminal pressure waves are complex both in

the fasting and fed states. So far, only two studies assessing concurrent ultrasound and high-resolution manometry have been published.

In the study by Hausken et al. (2002), in the pre- and postprandial period, a total of 44 % of antral contractions were not detected by manometry, and only 1/5 of nonoccluding contractions.

Hveem et al. (2001) found that only 53 % of antral contractions seen ultrasonographically had a temporally associated pressure event in the manometric reference channel. The lumen-occlusive contractions had, in 69 %, an associated pressure event. Of the nonlumen-occlusive contractions, only 20 % were associated with a pressure event.

The median amplitude of the pressure events in the manometric reference channel was 16 mmHg (range 4–98 mmHg) for lumen-occlusive, and 7 mmHg (range 4–23 mmHg) for nonlumen-occlusive contractions. However, a substantial overlap exists between the two categories of contraction.

In about 50 % of antral contractions observed by ultrasound, the corresponding pressure events are not identified in the manometric reference channel. This more than indicates that the knowledge of gastric mechanics, based solely on manometry, is at the least inadequate, missing almost half of the information given by ultrasound with regard to antral contractions.

6 Flow of Luminal Contents

Information concerning movement of luminal contents in humans can be obtained by fluoroscopy, scintigraphy, MRI, impedance, and duplex sonography.

Studies based on scintigraphy and standard ultrasound of the stomach and duodenum will indirectly measure overall rates of gastric emptying, but these methods do not have the temporal resolution to assess on a second-to-second basis. However, promising new MRI methods are being developed. Echo planar imaging, an ultrafast variant of MRI, can provide excellent images of both gastric wall movements and movements of solid and liquid meals.

Ultrasonographic studies by King et al. (1984) using test meals containing bran particles showed that gastric emptying occurred in episodes lasting a few seconds in healthy subjects. The emptying period usually started immediately after relaxation of the antro-pyloro-duodenal segment and was finished before the next peristaltic contraction approached the distal antrum. A brief episode of duodenogastric reflux occurred in about 60 % of the peristaltic cycles shortly before the terminal antral contraction. A similar type of reflux was shown in dogs by Malbert and Ruckebusch (1991), who used operatively implanted electromagnetic flow meter probes. Hausken et al. (1992) showed that using pulsed Doppler combined with real-time ultrasonography (duplex sonography), it is possible to visualize antroduodenal motility and transpyloric flow simultaneously. Antegrade and retrograde transpyloric flow is visualized using bidirectional velocity curves. Most contractions of the proximal duodenal bulb precede closure of the pylorus (and the terminal antrum), and duodenal bulb contraction is often accompanied by a short burst of duodenogastric reflux occurring immediately before closure of the pylorus.

Studies of the antro-pyloro-duodenal region are performed with the ultrasound probe positioned at the level of the transpyloric plane, and the antrum, the pylorus, and the proximal duodenum are visualized simultaneously. The subjects are studied in a seated position, with a 3.5 to 5-MHz transducer.

In order to study the relation between motility and flow in detail, techniques with a high temporal and spatial resolution are required for the assessment of antro-pyloro-duodenal pressure waves and transpyloric flow. Subjects have to be intubated with a manometric assembly, which is introduced transnasally and positioned in the antro-pyloro-duodenal region using fluoroscopy. The Doppler/ultrasound and manometric recordings have to be synchronized (Hausken et al. 2002).

- First gastric emptying is defined as the first occurrence of gastric emptying after drinking of the soup is initiated. An episode of gastric emptying is defined as flow across the pylorus with a mean velocity of more than 10 cm/s lasting more than 1 s.
- Occluding peristaltic-related transpyloric emptying is defined as gastric emptying associated with contractile activity in which the ultrasound image shows an occlusion of the stomach wall. Nonoccluding peristaltic-related emptying is defined as transpyloric emptying of gastric contents associated with contractile activity of the gastric wall which does not occlude the lumen. During maximal contractions, transpyloric flow can still be seen passing back and forth through the open pylorus.
- Nonperistaltic-related transpyloric emptying is defined as transpyloric emptying of gastric contents, without contractions detected on ultrasound or manometry.

Gastric emptying of a low caloric liquid meal follows sequences of emptying-reflux-emptying pulses. About half of the sequences are peristaltic related, but both nonoccluding, peristaltic-related, and nonperistaltic-related emptying sequences occur. Nonperistaltic-related flow sequences often have more alternating emptying-reflux episodes than those associated with peristalsis, and the duration of nonperistaltic-related emptying and reflux pulses are longer. The pressure gradients for all types of emptying are low and the pressure gradients during nonperistaltic-related emptying are significantly lower than during peristaltic-related emptying.

Flow can only occur in the presence of an open pylorus. Transpyloric flow can be classified into flow associated with a local increase in the pressure gradient between antrum and duodenum (Pa–Pd) due to antral propagating pressure waves. The second type of flow is independent of peristalsis and is likely to be caused by changes in gastric tone, or by pressure changes outside the stomach such as aortic pulsation and inspiration (Hausken et al. 2002).

The method can be used to study normal physiology and pathophysiology of the gastro-pyloro-duodenal segment and to monitor the effect of medications on transpyloric flow.

Patients with functional dyspepsia often experience early satiety and discomfort after a meal. Using duplex sonography it is possible to relate timing of symptoms and early postprandial emptying in patients with functional dyspepsia (Hausken et al. 1998). Meal-related discomfort was experienced after commencement of transpyloric emptying. An inverse relationship was found between the duration of the tasting period and symptom intensity, suggesting that the time allowed for duodenal tasting might be too short in patients with functional dyspepsia.

Currently available methods for studying gastric emptying do not provide quantitative information about the movement of gastric contents. A new noninvasive method for evaluating stroke volumes using three-dimensional (3D) guided digital color Doppler imaging might help the investigator to quantify net gastric emptying and to estimate the amount of duodenogastric reflux (Hausken et al. 2001). The technique involved color Doppler digital images of transpyloric flow in which the 3D position and orientation of the images were known by using a magnetic location system. In vitro, the system was found to slightly underestimate the reference flow (by average 8.8 %). In vivo (five volunteers), stroke volume of gastric emptying episodes lasted on average only 0.69 s with a volume on average of 4.3 ml (range 1.1–7.4 ml), and duodenogastric reflux episodes on average 1.4 s with a volume of 8.3 ml (range 1.3–14.1 ml). It was concluded that with the appropriate instrument settings, orientation determined color Doppler can be used for stroke volume quantification of gastric emptying and duodenogastric reflux episodes.

7 Gastroesophageal Reflux Disease

Hirsch et al. (1996, 1997) performed a comparative study of ultrasonography (abnormal reflux or physiological reflux) with and without the use of color Doppler versus 24-h esophageal pH measurements in 84 high-risk children for suspected gastroesophageal reflux (GER). They found abnormal reflux in 60.7 % by pH-metry, in 51.2 % by B-mode ultrasonography, and in 59.5 % by color Doppler ultrasonography. There was agreement between pH-metry and B-mode ultrasonography in 87 % of patients as compared to 94 % between pH-metry and color Doppler ultrasonography, and increased sensitivity of reflux detection from 84.4 to 98 % when color Doppler was added to B-mode ultra-sonography. Similarly, Jang et al. (2001) showed that color Doppler sonography was highly sensitive and was thought to be easier to use and more acceptable to the child than pH monitoring. In this study, the two tests showed 81.5 % agreement in the detection of GERD. This modality may be clinically useful in screening children for GERD (Jang et al. 2001).

8 Gallbladder

As real-time ultrasonography is a cheap, noninvasive, relatively easy, validated, and reproducible technique, it can be repeated over time to document time-related changes of gallbladder motor function. Ultimately, functional ultrasonography estimates gallbladder shape and volume in the fasting state and in response to a test meal (liquid or mixed solid–liquid, provided there is sufficient fat content) or exogenous stimulus (e.g., i.v. cholecystokinin). Patients are scanned in the supine, right anterior oblique position. Longitudinal and axial cross-sectional images of the gallbladder in its largest dimensions are obtained in triplicate. Average measurements are used for calculation of the gallbladder volume. The volume of the gallbladder (V) is subsequently calculated using the ellipsoid method as described by Dodds et al. (1985): $V = 0.52 \times L \times W \times H$, where L is the length, W is the width, and H is the height or depth of the gallbladder. All subjects are studied in the morning after an overnight fast. Fasting volume of the gallbladder (ml) represents the mean of three volume measurements taken 5 min apart. After taking the fasting volume, gallbladder contraction is stimulated by a fatty meal. Gallbladder contraction and refilling are monitored with ultrasonography and images are taken over time to document time-related changes of gallbladder volume. The difference between the basal volume and the corresponding residual volume represents the gallbladder ejected volume (ml). The gallbladder ejection fraction [GBEF (%)] is calculated according to the formula, GBEF (%) = 1 − (residual volume/fasting volume) × 100.

Although functional ultrasonography of the gallbladder has been mainly used for research purposes in specific referral centers, its simplicity makes such a technique appealing in the clinical setting to assess gallbladder motor function both in healthy and diseased subjects (Palasciano et al. 1992). Indications include the study of healthy subjects and of patients during pathophysiologically relevant conditions; in particular when subjects are at risk for gallbladder stasis and gallstone disease or during gallstone disease when a decision concerning medical dissolution

Table 1 Ultrasound meal accommodation test. The ultrasound meal accommodation test (UMAT) was developed at Haukeland University hospital on the basis of close interaction between scientific and clinical work in patients with dyspepsia. Before entering the protocol, the patients have been carefully studied with history, physical examination, blood tests, testing for *H. pylori* and upper endoscopy. In some cases, additional examinations are performed to rule out organic causes of their symptoms. The protocol presented here is the mainstream clinical protocol. In scientific studies, other elements are often added. A 500 ml liquid meal of commercial meat soup (Toro clear meat soup, Rieber & Søn A/S, Bergen, Norway) containing 1.8 g protein, 0.9 g bovine fat, and 1.1 g carbohydrate (20 kcal) is ingested over a period of 4 min. The soup is preheated and then cooled to 37 °C to improve imaging quality by reducing the amount of air bubbles. Psychometric evaluation is also performed

Time	Protocol
Fasting	Ordinary ultrasound examination of the liver, gallbladder, biliary tract, spleen, pancreas, kidneys, and large vessels
Fasting	Evaluation of symptoms by VAS
Fasting	Assessment of motility pattern (phase 1–3) by observing the pattern of contractility in the antrum
Fasting	Measurement of area of the distal stomach (AA)
Fasting	Visualization of the proximal stomach to explore whether it has content
Meal ingestion	500 ml of preheated meat soup is ingested in 4 min at a constant speed
2 min pp.	Measurement of the sagittal area (SA), the oblique frontal diameter (OFD), and the antral area (AA)
5 min pp.	Postprandial symptom evaluation
10 min pp.	SA, OFD, and AA measurement.
20 min pp.	SA, OFD, and AA measurement
30 min pp.	SA, OFD, and AA measurement

therapy is required. A decreased emptying rate of the gallbladder has been demonstrated in patients with gallstones (Fischer et al. 1982), dyspepsia (Marzio et al. 1992), diabetes mellitus (Stone et al. 1988), obesity (Marzio et al. 1988a), and in patients operated on with Billroth type II for duodenal ulcer (Marzio et al. 1988a, b).

9 Ultrasound as a Clinical Tool to Evaluate Patients with Functional GI Disorders

Another advantage of 2D ultrasonography is its clinical applicability; it can easily be performed at the bed-side and repeated numerous times in the same subject. At Haukeland University hospital, we have used the ultrasound meal accommodation test (U-MAT) for the work-up of patients with dyspepsia (Table 1) for the past 20 years. Our mainstream clinical protocol consists of a standard soup meal (500 ml), ultrasound scanning of the proximal and distal stomach using predefined scan sections, calculation of size and volume of the gastric compartments, evaluation of symptoms, and psychological assessment. In our experience, ultrasonography used in this context adds valuable clinical information to the management of these patients.

10 Nutritional Imaging

The concept of nutritional imaging compromises ultrasound imaging to study the effects of nutrition such as fat, proteins, and glucose on the function of the GI tract. Effects of aging on gastric emptying and on splanchnic blood flow as well as information relating to the effects of different macronutrients on blood pressure (BP) are limited and inconsistent.

The blood flow in the superior mesenteric artery can be evaluated by the use of duplex ultrasonography. (i.e., B-mode and Doppler imaging). Blood flow (ml/min) is calculated using the formula: π x $r2$ x TAMV $\times$ 60, where r is the radius of the superior mesenteric artery, and TAMV is the time-averaged mean velocity. The flow in the splanchnic vessels is known to increase after both intravenous as well as after oral nutrients (Fig. 4).

To evaluate the effects of healthy aging on transpyloric flow and gastric emptying, and the relationship between the glycemic response to oral glucose and 10 healthy "young" and 8 healthy "older" subjects had simultaneous measurements of mesenteric artery blood flow, gastric emptying, and blood glucose after a 600 ml drink (75 g glucose). A postprandial hypotension occurred in the elderly. The hypotensive response to the glucose meal was assumed to be triggered by the interaction of nutrients with the small intestine (O'donovan et al. 2005).

To investigate whether this effect in elderly was caused by an oral or an intraduodenal route of administration, the magnitude of the systolic blood pressure and superior mesenteric artery (SMA) flow was measured. The fall in systolic blood pressure and rise in heart rate induced by an oral glucose load was less compared with glucose infused intraduodenally at a comparable rate, presumably reflecting the loss of "protective" factors related to gastric distension (Gentilcore et al. 2009).

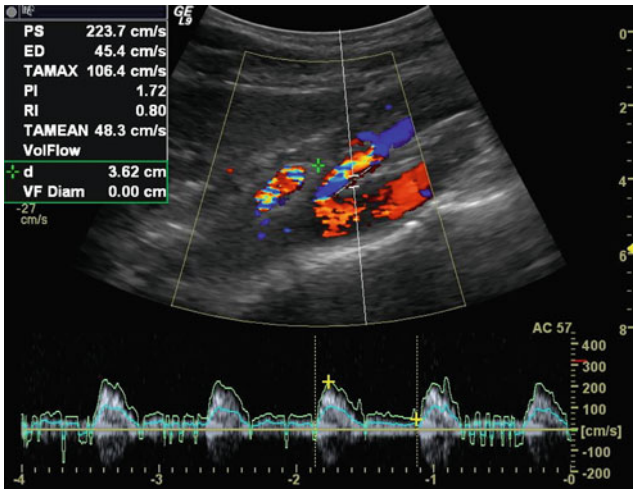

Fig. 4 Triplex ultrasonography of the superior mesenteric artery. *Upper panel* Color Doppler, *lower panel* Pulsed Doppler

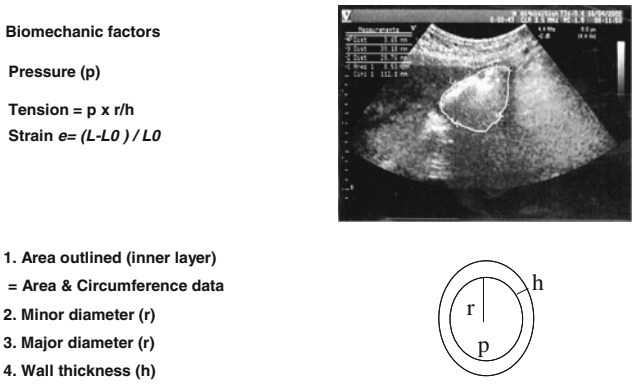

Fig. 5 Balloon distension of the antrum including biomechanical factors (*upper panel*). Schematic drawing of the antrum (*lower panel*)

Effects of gastric distension on blood pressure and SMA blood flow responses to intraduodenal glucose were then measured in eight healthy older subjects using barostat for gastric distension and duplex ultrasonography for flow measurements (Vanis et al. 2010). The results of this study were that gastric distension has the capacity to abolish the fall in blood pressure and attenuate the rise in SMA blood flow induced by intraduodenal glucose.

The effects of intraduodenal glucose, fat, and protein were also determined on blood pressure, heart rate (HR), and SMA blood flow in healthy older subjects (Gentilcore et al. 2008). The subjects received intraduodenal glucose, fat, protein, or followed by intraduodenal saline. It was found that intraduodenal glucose, fat, and protein decrease systolic blood pressure, but the onset of the hypotensive response was earlier after glucose, and the effect of protein on SMA blood flow is less than that of the other nutrients.

11 Ultrasound of a Light Hospital Breakfast

While intake of clear fluids 2–3 h before surgery is considered safe as it does not influence gastric content, it is not known if the same applies to a light breakfast meal. We therefore studied gastric emptying of a light breakfast in healthy, female volunteers without evidence of gastrointestinal motility disorders. The test meal consisted of one slice of buttered toast with jam, one cup of coffee without milk or sugar, and one glass of pulp-free orange juice taken together with a paracetamol mixture. Using ultrasonography, the stomach was identified without problems in all subjects, and gastric emptying curves using changes in gastric antral area and serum-paracetamol were obtained. Emptying of the fluid phase started immediately after intake of the meal. All subjects had solid particles in the stomach 120 min after the meal. The gastric antral area returned to fasting value significantly faster than the disappearance of solid particles. In healthy subjects, the stomach cannot be considered empty for solid particles the first 4 h after a light breakfast meal (Søreide et al. 1996).

12 Ultrasound and Antral Biomechanics

Gastric antral mechanical behavior including active and passive wall tension and stresses and distension-induced sensory-motor responses were evaluated in patients with FD and controls (C) using a special designed distension balloon located in the distal antrum under fluoroscopy. The balloon was inflated with water as ramp distension at a volume rate of 100 ml/min up to 180 ml and this volume were kept for 60 s before the pump was reversed (Fig. 5).

Concomitant measurements of pressures, the antral geometry (radius of curvature and wall thickness measured by ultrasonography), and abdominal discomfort (digitized symptom device (VAS 10 cm) were assessed continuously. The administration of the antimuscarinic drug butylscopolamine (Buscopan 20 mg iv) allowed investigation of active and passive tissue behavior.

Antral distension up to 180 ml induced more symptoms in FD than C. The administration of butylscopolamine reduced symptoms, pressures, tensions, and wall stresses in FD as measured with ultrasonography. Symptoms, however, were not related to the biomechanical properties. The sensory responses were most closely associated to the luminal circumference, indicating that the sensation during antral distension depend on deformation rather than on tension (Hausken et al. 2003).

References

Bateman DN, Whittingham TA (1982) Measurement of gastric emptying by real-time ultrasound. Gut 23:524–527

Berstad A, Hausken T, Gilja OH, Thune N, Matre K, Odegaard S (1994) Volume measurements of gastric antrum by three-dimensional ultrasonography and flow measurements through the pylorus by duplex technique. Dig Dis Sci 39(12 Suppl):97S–100S

Bolondi L, Bortolotti M, Santi V, Calletti T, Gaiani S, Labo G (1985) Measurement of gastric emptying time by real-time ultrasonography. Gastroenterology 89:752–759

Bouras EP, Delgado-Aros S, Camilleri M et al (2002) SPECT imaging of the stomach: comparison with barostat, and effects of sex, age, body mass index, and fundoplication. Gut 51:781–786

Code CF (1979) The interdigestive housekeeper of the gastrointestinal tract. Perspect Biol Med 22(2 Pt 2):S49–S55

Collins PJ, Horowitz M, Chatterton BE (1988) Proximal, distal and total stomach emptying of a digestible solid meal in normal subjects. Br J Radiol 61:12–18

Dodds WJ, Groh WJ, Darweesh RMA (1985) Sonographic measurement of gallbladder volume. Am J Radiol 145:1009–1011

Ehrlein HJ (1980) A new technique for simultaneous radiography and recording of gastrointestinal motility in unanesthetized dogs. Lab Anim Sci 30:879–884

Fischer RS, Seltzer F, Rock E, Malmud LS (1982) Abnormal gallbladder emptying in patients with gallstones. Dig Dis Sci 27:1019–1024

Gentilcore D, Hausken T, Meyer JH, Chapman IM, Horowitz M, Jones KL (2008) Effects of intraduodenal glucose, fat, and protein on blood pressure, heart rate, and splanchnic blood flow in healthy older subjects. Am J Clin Nutr 87:156–161

Gentilcore D, Nair NS, Vanis L et al (2009) Comparative effects of oral and intraduodenal glucose on blood pressure, heart rate, and splanchnic blood flow in healthy older subjects. Am J Physiol Regul Integr Comp Physiol 297:R716–R722

Gilja OH, Hausken T, Odegaard S, Berstad A (1995) Monitoring postprandial size of the proximal stomach by ultrasonography. J Ultrasound Med 14:81–89

Gilja OH, Hausken T, Ødegaard S, Berstad A (1996) Ultrasonography of the proximal stomach in patients with functional dyspepsia. Hepatogastroenterology 42:86–87

Gilja OH, Detmer PR, Jong JM, Leotta DF, Li XN, Beach KW (1997a) Intragastric distribution and gastric emptying assessed by three-dimensional ultrasonography. Gastroenterology 113:38–49

Gilja OH, Hausken T, Bang CJ, Berstad A (1997b) Effect of glyceryl trinitrate on gastric accommodation and symptoms in functional dyspepsia. Dig Dis Sci 42:2124–2131

Hausken T, Ødegaard S, Matre K, Berstad A (1992) Antroduodenal motility and movements of luminal contents studied by duplex sonography. Gastroenterology 102:1583–1590

Hausken T, Svebak S, Wilhelmsen I et al (1993) Low vagal tone and antral dysmotility in patients with functional dyspepsia. Psychosom Med 55:12–22

Hausken T, Gilja OH, Undeland KA, Berstad A (1998) Timing of postprandial dyspeptic symptoms and transpyloric passage of gastric contents. Scand J Gastroenterol 33:822–827

Hausken T, Li XN, Goldman B, Leotta D, Odegaard S, Martin RW (2001) Quantification of gastric emptying and duodenogastric reflux stroke volumes using three-dimensional guided digital color Doppler imaging. Eur J Ultrasound 13:205–213

Hausken T, Mundt M, Samsom M (2002) Low antroduodenal pressure gradients are responsible for gastric emptying of a low-caloric liquid meal in humans. Neurogastroenterol Motil 14:97–105

Hausken T, Mundt M, Lunding JA, Gilja OH, Gregersen H (2003) Abnormal perception of visceral symptoms in response to antral isovolumetric balloon distension in functional dyspepsia. Gastroenterolohy 124:S1721

Hirsch W, Kedar R, Preiss U (1996) Color Doppler in the diagnosis of the gastroesophageal reflux in children: comparison with pH measurements and B-mode ultrasound. Pediatr Radiol 26:232–235

Hirsch W, Preiss U, Kedar R (1997) Color coded Doppler ultrasound in diagnosis of gastroesophageal reflux. Klin Padiatr 209:6–10

Holt S, McDicken WN, Anderson T, Stewart IC, Heading RC (1980) Dynamic imaging of the stomach by real-time ultrasound—a method for the study of gastric motility. Gut 21:597–601

Holt S, Cervantes J, Wilkinson AA, Wallace JH (1986) Measurement of gastric emptying rate in humans by real-time ultrasound. Gastroenterology 90:918–923

Horowitz M, Edelbroek MA, Wishart JM, Straathof JW (1993) Relationship between oral glucose tolerance and gastric emptying in normal healthy subjects. Diabetologia 36:857–862

Husebye E (1999) The patterns of small bowel motility: physiology and implications in organic disease and functional disorders. Neurogastroenterol Motil 11:141–161

Hveem K, Hausken T, Berstad A (1994) Ultrasonographic assessment of fasting liquid content in the human stomach. Scand J Gastroenterol 29:786–789

Hveem K, Jones KL, Chatterton BE, Horowitz M (1996) Scintigraphic measurement of gastric emptying and ultrasonographic assessment of antral area: relation to appetite. Gut 38:816–821

Hveem K, Sun WM, Hebbard G, Horowitz M, Doran S, Dent J (2001) Relationship between ultrasonically detected phasic antral contractions and antral pressure. Am J Physiol Gastrointest Liver Physiol 281:G95–G101

Jang HS, Lee JS, Lim GY (2001) Correlation of color Doppler sonographic findings with pH measurements in gastroesophageal reflux in children. J Clin Ultrasound 29:212–217

King PM, Adam RD, Pryde A, McDicken WN, Heading RC (1984) Relationships of human antroduodenal motility and transpyloric fluid movement: non-invasive observations with real-time ultrasound. Gut 25:1384–1391

Malagelada JR, Stanghellini V (1985) Manometric evaluation of functional upper gut symptoms. Gastroenterology 88(5 Pt 1):1223–1231

Malbert CH, Ruckebusch Y (1991) Relationships between pressure and flow across the gastroduodenal junction in dogs. Am J Physiol 260:G653–G657

Marciani L, Gowland P, Fillery-Travis A et al (2001) Assessment of antral grinding of a model solid meal with echo-planar imaging. Am J Physiol Gastrointestinal Liver Physiol 280:G844–G849

Marzio L, Capone F, Neri M, Mezzetti A, DeAngelis C, Cuc-curullo F (1988a) Gallbladder kinetics in obese patients. Effect of a regular meal and a low caloric meal. Dig Dis Sci 33:4–9

Marzio L, Di Felice F, Celiberti V, DiGioacchino M, Mezzetti A, Cuccurullo F (1988b) Gallbladder emptying in duodenal ulcer patients having undergone Billroth II gastrectomy. Digestion 41:223–228

Marzio L, Di Felice F, Laico MG, Imbimbo B, Lapenna B, Cuccurullo F (1992) Gallbladder hypokinesia and normal gastric emptying of liquids in patients with dyspeptic symptoms. A double-blind placebo-controlled clinical trial with cisapride. Dig Dis Sci 37:262–267

Moragas GM, Azpiroz F, Pavia J (1993) Relation among intragastric pressure postcibal perception, and gastric emptying. Am J Physiol 264:G1112–G1117

O'Donovan D, Hausken T, Lei Y et al (2005) Effect of aging on transpyloric flow, gastric emptying, and intragastric distribution in healthy humans–impact on glycemia. Dig Dis Sci 50:671–676

Palasciano G, Serio G, Portincasa P et al (1992) Gallbladder volume in adults, and relationship to age, sex, body mass index, and

gallstones: a sonographic population study. Am J Gastroenterol 87:493–497

Penagini R, Hebbard G, Horowitz M (1998) Motor function of the proximal stomach and visceral perception in gastroesophageal reflux disease. Gut 42:251–257

Ricci R, Bontempo I, Corazziari E, La Bella A, Torsoli A (1993) Real time ultrasonography of the gastric antrum. Gut 34:173–176

Ropert A, des Varannes SB, Bizais Y (1993) Simultaneous assessment of liquid emptying and proximal gastric tone in humans. Gastroenterology 105:667–674

Savoye G, Savoye-Collet C, Oors J, Smout A (2003) Interdigestive transpyloric fluid transport assessed by intraluminal impedance recording. Am J Physiol Gastrointest Liver Physiol 284:G663–G669

Sifrim D, Holloway R, Silny J, Xin Z, Lerut A, Janssens J (2001) Acid and gas reflux in patients with gastroesophageal reflux disease during ambulatory recordings. Gastroenterology 120:1588–1598

Søreide E, Hausken T, søreide JA, Steen PA (1996) Gastric emptying of a light breakfast. A study using real-time ultrasonography. Acta Anaestesiol Scand 40:549–553

Stone BG, Gavaler JS, Belle SH et al (1988) Impairment of gallbladder emptying in diabetes mellitus. Gastroenterology 95:170–176

Tefera S, Gilja OH, Hatlebakk JG, Berstad A (2001) Gastric accommodation studied by ultrasonography in patients with reflux esophagitis. Dig Dis Sci 46:618–625

Tefera S, Gilja OH, Olafsdottir E, Hausken T, Hatlebakk JG, Berstad A (2002) Intragastric maldistribution of a liquid meal in patients with reflux esophagitis assessed by three-dimensional ultrasonography. Gut 2:153–158

Undeland KA, Hausken T, Aanderud S, Berstad A (1997) Lower postprandial gastric volume response in diabetic patients with vagal neuropathy. Neurogastroenterol Motil 9:19–24

Undeland KA, Hausken T, Gilja OH, Aanderud S, Berstad A (1998) Gastric meal accommodation and symptoms in diabetes. A placebo-controlled study of glyceryl trinitrate. Eur J Gastroenterol Hepatol 10:677–681

Vanis L, Gentilcore D, Hausken T, et al. (2010) Effects of gastric distension on blood pressure and superior mesenteric artery blood flow responses to intraduodenal glucose in healthy older subjects. Am J Physiol Regul Integr Comp Physiol. 2010

Zerbib F, des Varannes SB, Ropert A A (1999) Proximal gastric tone in gastroesophageal reflux disease. Eur J Gastroenterol Hepatol 11:511–515

Three-Dimensional Ultrasound of the Gastrointestinal Tract

Odd Helge Gilja

Contents

Abstract

Three-dimensional (3D) ultrasonographic methods have evolved as a supplement to ordinary 2D ultrasound examinations to improve volume estimation and enhance visualisation of complex structures. This chapter reviews some of the principles, methods and clinical applications in 3D ultrasonography of the gastrointestinal tract. Previously, the process of making 3D images based on ultrasonography was divided into 5 steps: Data acquisition, data digitization, data storage, data processing, and data display. However, at present real-time matrix probes have made 4D ultrasound imaging possible. 3D ultrasonography may become an important imaging modality in interventional medicine where accurate 3D display is warranted.

1 Introduction

The digital revolution has made 3D ultrasonography a natural extension of 2D ultrasound scanning. Most frequently this is made by stacking serial 2D ultrasonograms together and utilizing computerized algorithms and equipment to process and display the data. However, in recent years, 2D array matrix probes have been developed to enable real-time 3D scanning.

2 Formation of 3D Ultrasonographic Images

If the relative position in space of a series of 2D sonograms is recorded along with the image data, three-dimensional (3D) ultrasonographic images can be constructed. For most applications, the process of making 3D images based on ultrasonography is divided into five major steps: data acquisition, digitization, storage, processing, and display.

O. H. Gilja (✉)
Department of Medicine,
National Center for Ultrasound in Gastroenterology,
Haukeland University Hospital,
N-5021 Bergen, Norway
e-mail: Odd.Gilja@uib.no

G. Maconi and G. Bianchi Porro (eds.), *Ultrasound of the Gastrointestinal Tract*, Medical Radiology. Diagnostic Imaging,
DOI: 10.1007/174_2012_666, © Springer-Verlag Berlin Heidelberg 2012
Published Online: 5 August 2012

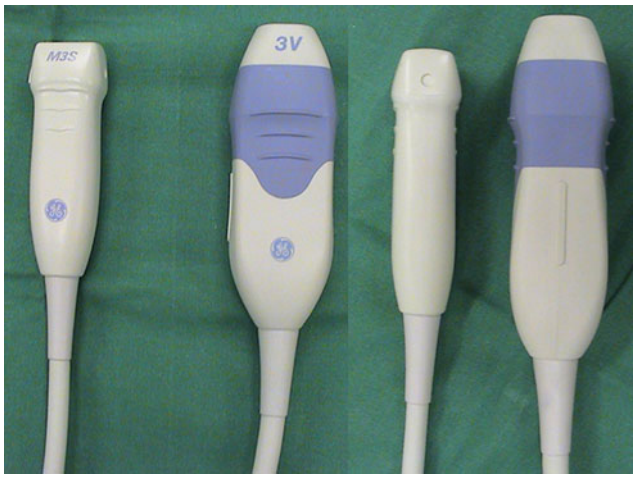

Fig. 1 Two ultrasound probes viewed from a frontal and lateral prospective. To the left of both panels an ordinary 2D phased array is shown and to the right in both panels a matrix probe that enables real-time 3D ultrasound scanning is depicted

2.1 Data Acquisition

Principally, data acquisition by 3D ultrasonography can be performed in three different ways (Salustri and Roelandt 1995). Sampling of data may be carried out either by using a 2D probe attached to a motor which moves the probe in a computer-defined way, or by a spatial localizing system connected to a 2D probe, or by electronic 3D probes with the possibility of direct volume acquisition in real time.

First, and most frequently used, are ordinary 2D probes which are inserted into motorized holders and either rotated (Ghosh et al. 1982; Roelandt et al. 1994), translated (Picot et al. 1993; Ross et al. 1993; Sackmann et al. 1994; Sehgal et al. 1994; Sohn and Grotepass 1990), or tilted (Belohlavek et al. 1993a; Hamper et al. 1994; Martin et al. 1986; Martin and Bashein 1989; Pretorius and Nelson 1995; Wagner et al. 1994; Zoller and Liess 1994) to acquire a data volume. The rotation scanning is often applied to cardiac imaging, while acquisition by tilting or translating is frequently used for transcutaneous abdominal and obstetric scanning. Pullback devices have also been constructed to aid intravascular and intraductal scanning where the transducer is positioned at a distant site in relation to the mechanical holder (Chandrasekaran et al. 1994; Mintz et al. 1993; Rosenfield et al. 1991).

Second, acquisition of ultrasonographic data can be assisted by devices that record the exact position and movements of the transducer in space. This has been obtained by utilizing mechanical arms (Whittingham and Bateman 1983; Dekker et al. 1974; Geiser et al. 1982; Nikravesh et al. 1984; Raichlen et al. 1986; Sawada et al. 1985), acoustic sensors (Handschumacher et al. 1993; King et al. 1990; King et al. 1991; Levine et al. 1989; Moritz et al. 1976), or magnetic sensors (Detmer et al. 1994; Hodges et al. 1994; Kelly et al. 1994; Leotta et al. 1995; Pretorius and Nelson 1994). A magnetic sensor, a transducer, and a magnetic field generator are depicted in Fig. 1. Furthermore, gyroscopic and optical devices can be applied to follow the position of the scanhead.

Third, true volumetric 2D array transducers have been developed (Green and Campbell 1994). These complex transducers generate a pyramidal volume of ultrasound data, enabling dynamic real-time 3D ultrasonography. The matrix probes have been validated in volume estimation and seem to perform well (Bu et al. 2005; Qin et al. 2000; Binder et al. 2000), also compared with magnetic resonance imaging (MRI) (Jenkins et al. 2004). Clinical applications of real-time 3D ultrasound include measurement of left ventricular volume (Arai et al. 2004), quantitative assessment of perfusion defects with myocardial contrast agents (Camarano et al. 2002), and detection of ischemia during dobutamine-induced stress (Ahmad et al. 2001). In pathologic fetal hearts, 3D Echocardiography (3DE) was helpful for localizing multiple cardiac tumors; estimating size and function of the right and left ventricles, and evaluating mechanism of valvular regurgitation and pulmonary obstruction (Acar et al. 2005). Several ultrasound vendors have now developed real-time 3D probes to promote clinical and interventional scanning exploiting all dimensions (Sugimoto et al. 2011; Harris et al. 2010; Foroughi et al. 2006). An example of 4D scanning is shown in Fig. 2.

2.2 Data Digitization

Ultrasound raw data are available in a digital format in most scanners; however, some of the commercially available ultrasound scanners generate analog output signals. Therefore, in order to be processed by a computer, conversion of ultrasonographic data into a digital format is necessary. Frequently, this is done by video frame grabbing using designated hardware cards in the computer or in the scanner. However, frame grabbing of video signals impairs image resolution. Therefore, preferably, raw ultrasound data is digitized directly maintaining the original resolution.

2.3 Data Storage

Following data capture and digitisation, image data is normally stored temporarily until computer processing can take place. High-resolution 3D ultrasound data give rise to large image files necessitating high-capacity storage media such as magneto-optical disks, CD/DVD, or hard disks. The ultimate goal in 3D ultrasonography is to obviate the data storage operation and perform direct data processing and

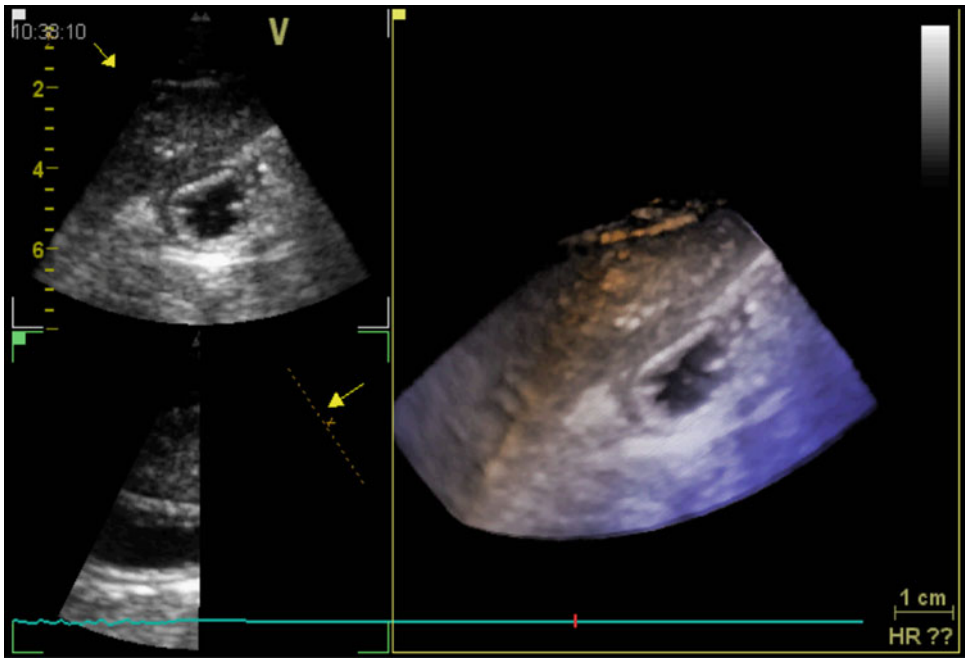

Fig. 2 Ultrasonogram of fluid-filled gastric antrum acquired by a real-time 3D matrix probe showing two 2D slices in left panels and a 3D volume in the right panel

volume estimation in real time, and subsequently store only the clinically relevant images and measurements.

2.4 Data Processing

Depending on the mode of acquisition, the image data can be prepared in different ways (Belohlavek et al. 1993b). Only the mainstream flowchart of processing will be outlined here.

First, the image data must be converted to a rectangular (Cartesian) co-ordinate system. Image points are assigned to new positions within a cuberille (regular data volume) on the basis of their pyramidal (if tilting acquisition) co-ordinates. This scan conversion is usually relatively time consuming and is performed by computer algorithms.

Second, mathematical interpolation is performed to generate values that "fill in the gaps" between 2D slices that are stacked together in the cuberille. After scan conversion and interpolation, the pixels can be treated as spatially correct 3D image elements, known as voxels.

Third, methods for image enhancement are usually applied to improve image contrast and remove artifacts. These techniques include filtering, histogram stretching and sliding, and morphological operations. This step may be important to the overall quality of the final 3D ultrasound image but may not be of great importance for volume measurement. Image enhancement represents an uncertainty because significant clinical information can be lost in the operation.

Fourth, the cube of image data is now ready for segmentation; i.e., the procedure where the object of interest is separated from the surrounding structures (Greenleaf et al. 1993). Three fundamental approaches to segmentation have been utilized in 3D ultrasonography:

(1). Extraction by visual inspection and manual outlining of contours
(2). Semi-automatic separation using visualization algorithms (Nielson and Shriver 1989) aided by operator interaction
(3). Fully automatic computer segmentation.

The latter method is capable of detecting edges with high contrast, but is subject to inaccuracies and artifact production. Therefore, automatic segmentation must be used with great care if applied to patient data. Manual segmentation of structures in the 3D data set makes accurate volume estimation and reconstruction of organs or pathology achievable. This method, which primarily supplies quantitative information, is applicable to all areas of sonographic imaging where volume calculation is indicated.

2.5 Data Display

The final step in formation of 3D ultrasound images is to display the data so that the inherent voxel information is communicated accurately. Commonly, simple rotation of the object on the computer monitor provides some 3D effects. To further enhance the 3D outcome of the images, stereoglasses have been applied (Martin et al. 1995; Nelson and Pretorius 1995). Projection of images by optical holography enables the observer to move around the object and examine the spatial relationships from different viewpoints (Baum and

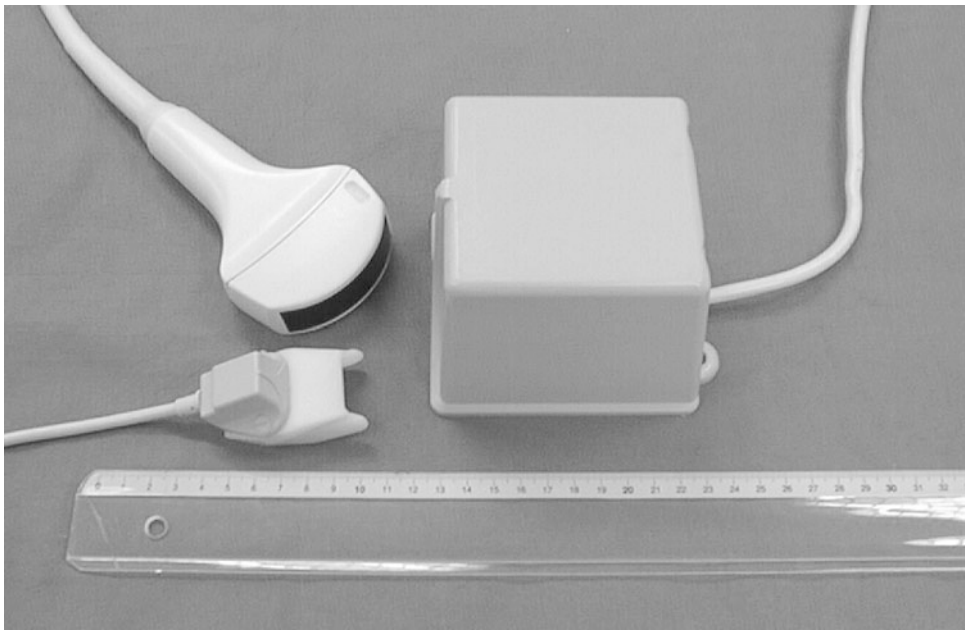

Fig. 3 A 3D ultrasound system based on magnetic Position and Orientation Measurement (POM). The Bird System (Ascension Technology Corp., Burlington, VT, USA) consists of a sensor that can be attached to the scanhead, a magnetic field generator, and a system control unit (usually hidden in the scanner)

Stroke 1975; Koivukangas et al. 1986; Redman et al. 1969). A typical setup of a 3D ultrasound system is shown in Fig. 3.

Data processing and display requires specialized computer software to handle the ultrasound images. We have developed, in collaboration with Christian Michelsen Research (Bergen, Norway) and Vingmed Sound (Horten, Norway), a software package: EchoPac3D® (Martens et al. 1997; Martens and Gilja 2004). EchoPac3D enable import of image data that are acquired both with mechanical devices and magnetic position sensors, as well as endosonographic acquisitions. Manual segmentation or semiautomatic rendering of structures in the 3D data set makes accurate volume estimation and reconstruction of organs or pathologic tissue achievable. The accuracy of volume estimation in this software package has been evaluated in several studies (Gilja et al. 1994; Gilja et al. 1995; Thune et al. 1996). A display of the EchoPac3D software is shown in Fig. 4. The 3D ultrasound system used in our lab is outlined more in depth in a previous review (Gilja et al. 1999).

Ultrasound data contains a significant amount of noise and speckle and may exhibit boundary regions several pixels wide. It is important to keep in mind that the quality of the final 3D data display strongly depends on the resolution of the raw data. Transducer frequency and lateral resolution, frame rate of the scanner, accuracy of 3D probe, speed of scanning, methods of filtering and segmentation, are all factors that influence the final image and subsequently volume measurements. Furthermore, there is no advantage in sampling over a spatial scale that is much smaller than the resolution cell of the display system. The ultrasound sampling conditions using a specific transducer is closely related to the display parameters.

3 Three-Dimensional Ultrasonography of the Stomach

Two-dimensional (2D) ultrasonography has been utilized to assess gastric emptying in patients with functional dyspepsia (Bolondi et al. 1985; Duan et al. 1993; Hou et al. 1992; Berstad and Gilja 2004), diabetes mellitus (Dorlars et al. 1994), and in infants with gastroesophageal reflux (Li Voti et al. 1992). In several studies, repeated single 2D ultrasonic sections of the antrum have been applied to measure gastric emptying rates (Desaga and Hixt 1987; Dorlars et al. 1994; Duan et al. 1993; Hou et al. 1992; Newell et al. 1993). To estimate volumes of the gastric antrum by means of 2D ultrasound, a sum-of-cylinders method (Radberg et al. 1989) and simple formulas (Bolondi et al. 1985) have been used. Volume estimation based on 2D sonograms is subject to significant error because assumptions regarding geometrical shape of the antrum need to be made before reliable volume measurements can be performed.

To overcome these limitations, a method for volume estimation of organs and tissue based on three-dimensional (3D) ultrasonography was developed (Gilja et al. 1994). Using a motor device, the transducer was tilted through an angle of 90°, capturing sequential 2D-frames before the data set was transferred to a graphic workstation for final 3D processing. This 3D ultrasound system demonstrated excellent accuracy in vitro both on phantoms (Thune et al. 1996) and on animal organs (Gilja et al. 1994), and intra- and

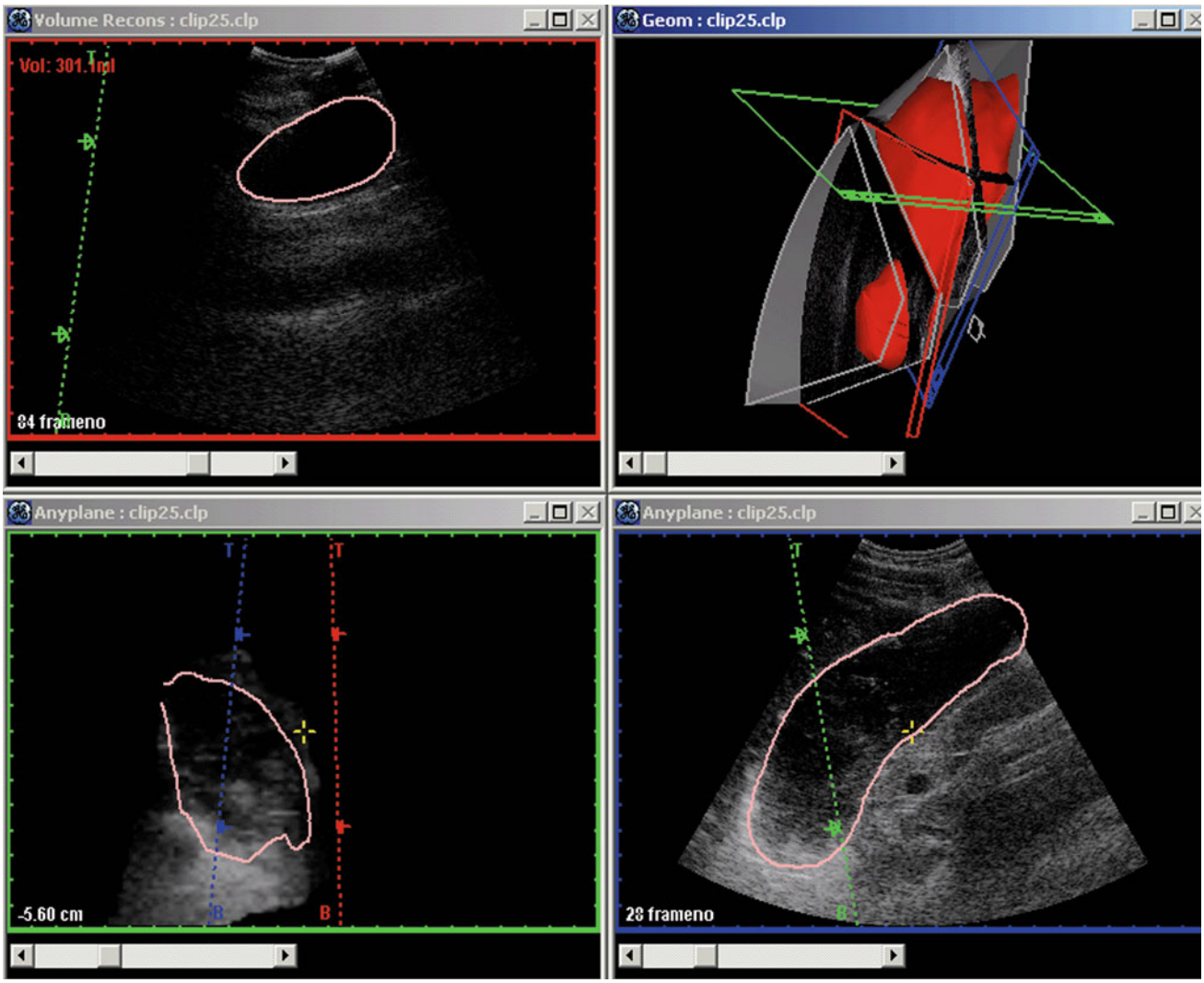

Fig. 4 A display of EchoPac3D software manufactured by GE-Vingmed Sound (Horten, Norway). In the *upper right panel*, the red volume is a reconstructed stomach shown in the geometry window. In the antrum an ultrasound section is displayed and this sagittal section is also depicted in the reconstruction window in the *upper left panel*. The visualization window, enabling application of numerous algorithms, is shown in the *lower right* and *left panels*. The software EchoPac3D® enables accurate post-processing of 3D ultrasonographic images

interobserver variation was low. When validated in vivo against MRI, this 3D ultrasound system was in good agreement and presented high precision (Gilja et al. 1995). This system has also been used to study diseases of the liver (Hokland and Hausken 1994), and to evaluate patients with functional dyspepsia (Berstad et al. 1994; Gilja et al. 1996a; Hausken et al. 1994). Despite the significant achievements with respect to accuracy in volume estimation and 3D reconstruction of tissue and organs, this 3D system could only acquire a 90° fan-like data set from a predetermined, fixed orientation of the transducer. Accordingly, although highly accurate, a mechanical acquisition system like this poses great limitations to acquisition, because only small volumes can be captured.

Random acquisition of 3D ultrasound data has been achieved by utilizing different devices to locate the exact position and orientation of the transducer in space. To enable scanning of a large organ like the fluid-filled stomach, a commercially available magnetometer-based position and orientation measurement (POM) device was interfaced to the scanner. This system for magnetic scanhead tracking (Bird, Ascencion Technology Inc., Vermont, USA) was validated both with respect to its precision in locating specific points in space (Detmer et al. 1994) and to its accuracy in volume estimation (Hodges et al. 1994; Matre et al. 1999). In these studies, the sensor system worked satisfactorily in scanning human organs, and high precision and accuracy were revealed in volume estimation.

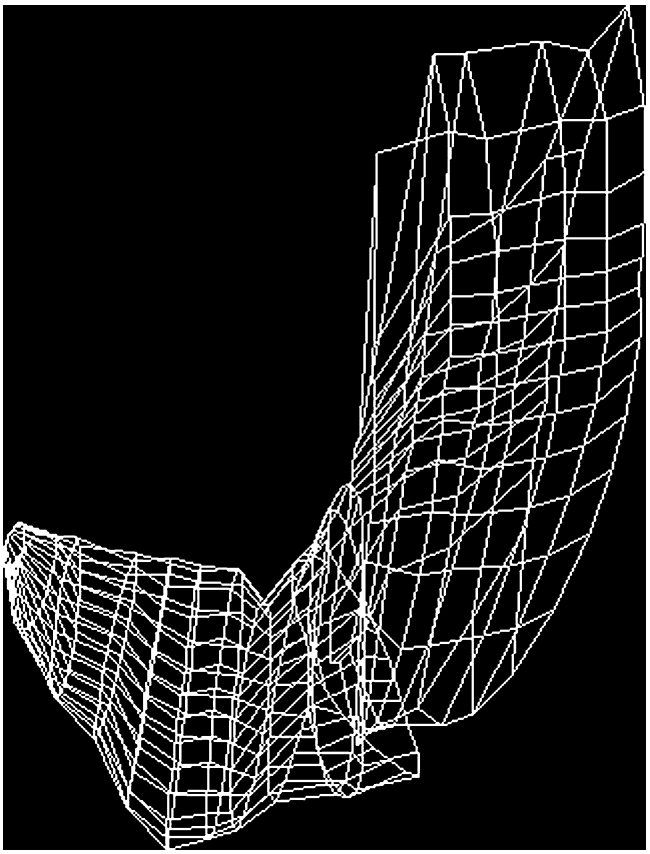

Fig. 5 A wire-frame outline of the total stomach volume after ingestion of a soup meal serving as contrast medium. The images used for 3D reconstruction are acquired by ordinary 2D ultrasonography and magnetic scanhead tracking enables precise acquisition and reconstruction of the organ

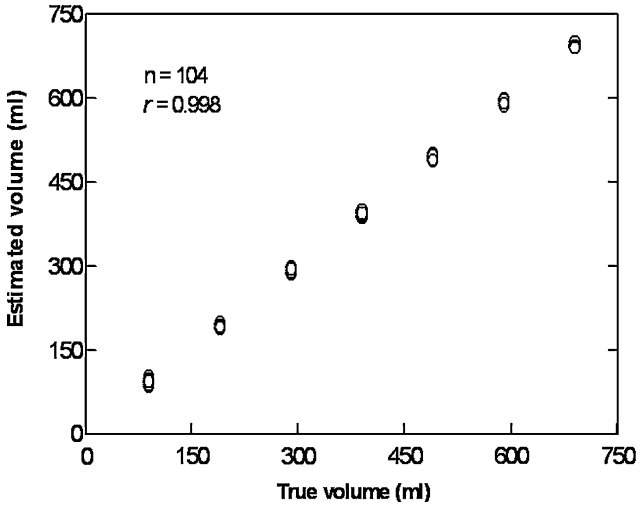

Fig. 6 Scatter plot showing the correlation between estimated and true volumes of a barostat bag positioned in the human stomach after scanning by a 3D ultrasound system. Scanning was performed with a 3.5 MHz transducer attached to a Bird system after stepwise instillation and aspiration of the test meal. The magnetic transmitter was positioned just behind the back of the examined subject and within the performance range of the sensor (60 cm)

For the first time, total gastric volumes and intragastric distribution of meals could be studied by ultrasonography (Gilja et al. 1997). In this study, the depth of scanning was adjusted to fit each individual's habitus, averaging 17.6 cm. Sagittal sections of the stomach were recorded throughout its entire length, starting in the proximal part where the transducer was positioned by the left subcostal margin and tilted cranially to image the most superior part of the stomach. After stepwise scanning of the proximal stomach angling from left to right, the transducer was moved and held to insonicate normally to the skin surface. Then the distal stomach was scanned stepwise moving distally to the gastroduodenal junction. The image data and the position and orientation data were transferred to a workstation for final processing. A 3D reconstruction of the total stomach volume based on magnetic scanhead tracking from this first study is depicted in Fig. 5.

The stomach is a large and geometrically complex organ to study by ultrasonography. Therefore, we have validated this 3D ultrasonographic method in vivo in healthy controls. A barostat bag was positioned in the proximal stomach of six healthy subjects who underwent scanning with the Bird® magnetic system. In steps of 100, up to 700 ml of meat soup was instilled into and subsequently aspirated from the barostat bag while simultaneous 3D scanning was performed. This 3D ultrasound system correlated very well to infused volumes (Fig. 6) and showed very good agreement with true volumes, as well as low interobserver variation (Tefera et al. 2002). Patients with reflux esophagitis exhibited an abnormally large volume of the proximal stomach soon after a liquid meal, concomitant with the perception of fullness. The abnormal distention of the proximal stomach may represent an important pathogenetic mechanism in reflux oesophagitis.

In functional dyspepsia, poor accommodation of the proximal stomach to a meal has been found in many studies (Ahluwalia et al. 1994; Berstad et al. 1997; Gilja et al. 1996b; Tack et al. 1998). Drinking capacity is often reduced in these patients and drink tests may therefore have a diagnostic potential. A simple drink test in combination with 3D ultrasonography was applied in a test using Toro meat soup, Nutridrink, and water (Hjelland et al. 2004). The meals were ingested at a rate of 100 mL/min until maximal drinking capacity was reached. Intragastric volume at maximal drinking capacity was determined using 3D ultrasonography (Fig. 7). Optimal discrimination between patients and controls was obtained by the combination of symptoms and intragastric volume (S/V) using meat soup as the test meal.

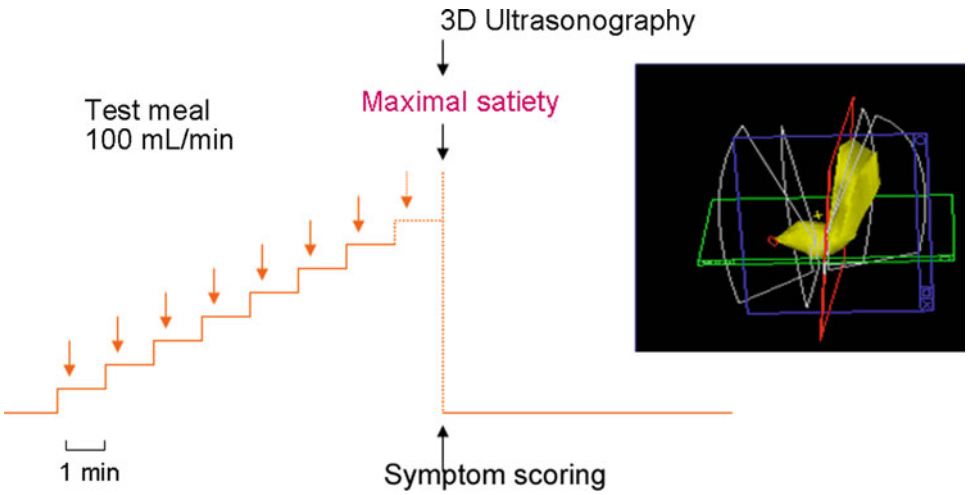

Fig. 7 The scanning protocol is shown using 3D ultrasound to determine maximal gastric volume after a meal in patients with functional dyspepsia. Interestingly, the fraction of symptoms per volume (S/V) distinguished best between patients and controls after a soup meal

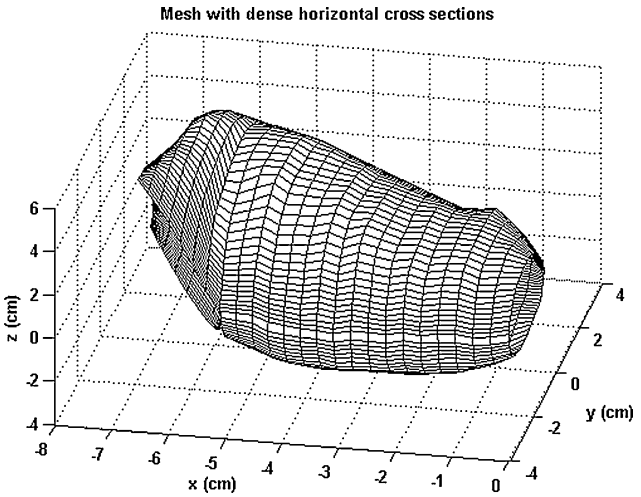

Fig. 8 A 3D gastric antrum generated by the Echopac-3D program and reconstructed in a new coordinate system. In this geometry, 3D strain can be calculated and visualized following ultrasound scanning

Impaired gastric accommodation may induce dyspeptic symptoms also in postfundoplication patients. Using 3D ultrasonography, postfundoplication patients with and without dyspeptic symptoms were scanned and symptoms were scored postprandially (Scheffer et al. 2004). Dyspeptic and nondyspeptic fundoplication patients exhibited similar total gastric volumes at 5 min postprandially compared to controls, whereas smaller total gastric volumes were observed from 15 to 60 min postprandially. Distal stomach volume was more pronounced in dyspeptic fundoplication patients and related with the increase in postprandial fullness sensations. In healthy volunteers, the sensation of fullness was also related to antral volume and area rather than proximal volume (Mundt et al. 2005).

In another study, we developed an analytical method to describe the 3D geometry of the gastric antrum, gastric fundus, and the whole stomach based 3D ultrasound acquisitions. The Fourier series method was used to simulate the organ surface geometry. The principal curvatures spatial distributions were non-homogeneous in the gastric antrum, gastric fundus, and the stomach due to their complex geometry (Fig. 8). An analytical tool for characterizing the complex 3D geometry of an organ like the human stomach reconstructed by 3D ultrasound was provided (Liao et al. 2004).

Hausken et al. developed a noninvasive method for evaluating transpyloric flow and duodenogastric reflux stroke volumes using a 3D-guided digital color Doppler imaging model (Hausken et al. 2001). They studied healthy subjects during ingestion of a soup meal and 10 min postprandially. Cross-sectional color Doppler digital images of duodenogastric reflux episodes were acquired with a 5–3 MHz phased-array transducer. The 3D position and orientation data were acquired using a magnetic sensing system. They found high intra- and interindividual variations of the stroke volumes of transpyloric flow episodes during the initial gastric emptying. The duodenogastric reflux episodes lasted on average 2.4 s with a volume of on average of 8.3 ml. This novel method minimized geometric assumptions and angular ambiguity.

4 Three-Dimensional Endoscopic Ultrasonography

Endoscopic ultrasonography (EUS) has gained acceptance as a valuable tool in obtaining diagnostic information in patients with digestive diseases, as it enables detailed visualization of small structures along the gastrointestinal tract. However, its use has been limited to a few centers, partly due to the high demands for skills in both endoscopy and ultrasound scanning. Interpretation of 2D endosonographic images can be challenging, even for experienced operators. Therefore, the applicability of new acquisition units allowing endosonographic recordings to

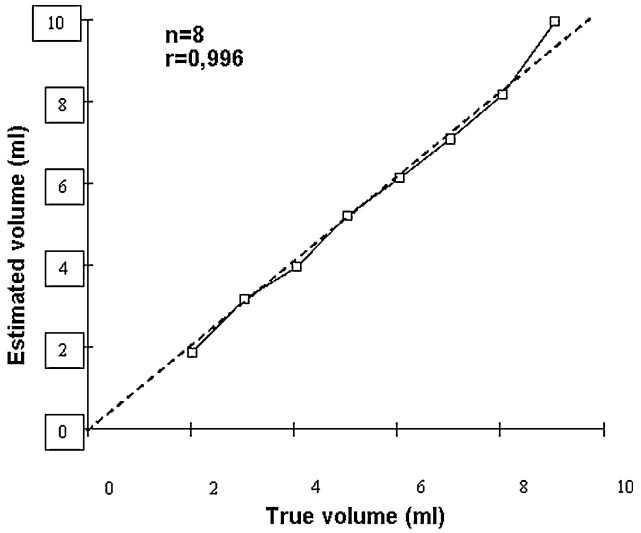

Fig. 9 The plot shows the association between estimated and true volumes after EUS scanning of a phantom in vitro. The acquisition was performed using Olympus miniprobe 12 MHz (UM-2R)

Fig. 10 A prototype acquisition unit for 3D EUS imaging that can be used both for echoendoscopes and miniprobes. The pullback system allows for a constant speed of transducer movement

be imported into the general 3D reconstruction systems was investigated (Molin et al. 1996a, b; Molin et al. 1997; Molin et al. 1999). So far, 3D endosonography has been based on sequential sampling of 2D images, mainly during pull-back of radial scanning probes. The 3D data are usually displayed in an orthogonal window or by any plane slicing. In one study, endoluminal ultrasound examinations were performed with 360° radial scanning 7.5- and 12-MHz echoendoscope and miniature probes, 8 F., 12, and 20 MHz (Olympus Co Ltd, Tokyo, Japan). Acquisition of 2D ultrasound images was achieved by connecting the probes to a computer controlled linear stepping motor device (Prototype, MKAB, Gothenburg, Sweden) with an acquisition length of 0.5–15 cm and an operating speed at 10 mm/s, resulting in a distance between serial images of 0.1 to 0.2 mm. Further post-processing was performed using EchoPac3D®. These studies demonstrated that 3D endosonography enabled accurate volume estimation of a wide range of tumors (Fig. 9), and improved global display of tumor extensions and topographic relations, thus enabling better preoperative planning (Odegaard et al. 1999; Odegaard et al. 1998). We also explored other methods of 3D acquisition by testing the performance in vitro of a miniature magnetic sensor (MiniBird, Ascension Technology Corp., Burlington, VT, USA) for endoluminal ultrasound and 3D EUS (Molin et al. 2000). The magnetic 6D position and orientation measurement system (POM) was used to track different types of radial scanning endoluminal ultrasound probes. The performance of the POM system was similar if ferric or non-ferric ultrasound endoscopes were used for EUS. Sumiyama et al. later developed a linear-array 3D EUS with a miniature position sensor attached to the tip of the echoendoscope used in freehand scanning and confirmed its applicability (Sumiyama et al. 2003).

In order to improve the image quality of the 3D data set by avoiding artifacts from pulsatile organs, ECG-triggered 3D EUS reconstructions was attempted (Molin et al. 1998). They found that ECG-triggered 3D EUS images could easily be obtained using a stepping motor device during routine examinations, resulting in a clear demonstration of the different wall layers in the longitudinal image axis (Fig. 10).

The lateral dislocation was 2.40 mm (SD 0.56) in non-ECG trigged examinations resulting in a "fuzzy" image in the axial display, compared to 0.19 mm (SD 0.23) in the ECG trigged scans ($p < 0.0027$) (Fig. 11). This resulted in higher accuracy in the evaluation of small and superficial lesions of the esophageal wall and fundic region of the stomach.

Other researchers have also assessed the clinical usefulness and problems of 3D images obtained by endosonography (Nishimura et al. 1997). Nishimura et al. (1997) studied 18 resected specimens of gastrointestinal lesions and 21 patients. In the resected specimens, the surface images were quite consistent with the macroscopic findings in 17 cases. In two esophageal cancers, 7 of 10 gastric cancers, and 2 colonic cancers the depth of tumor invasion was assessed accurately from the reconstructed images. In the in vivo study, although 3D displays had some limitations, it was

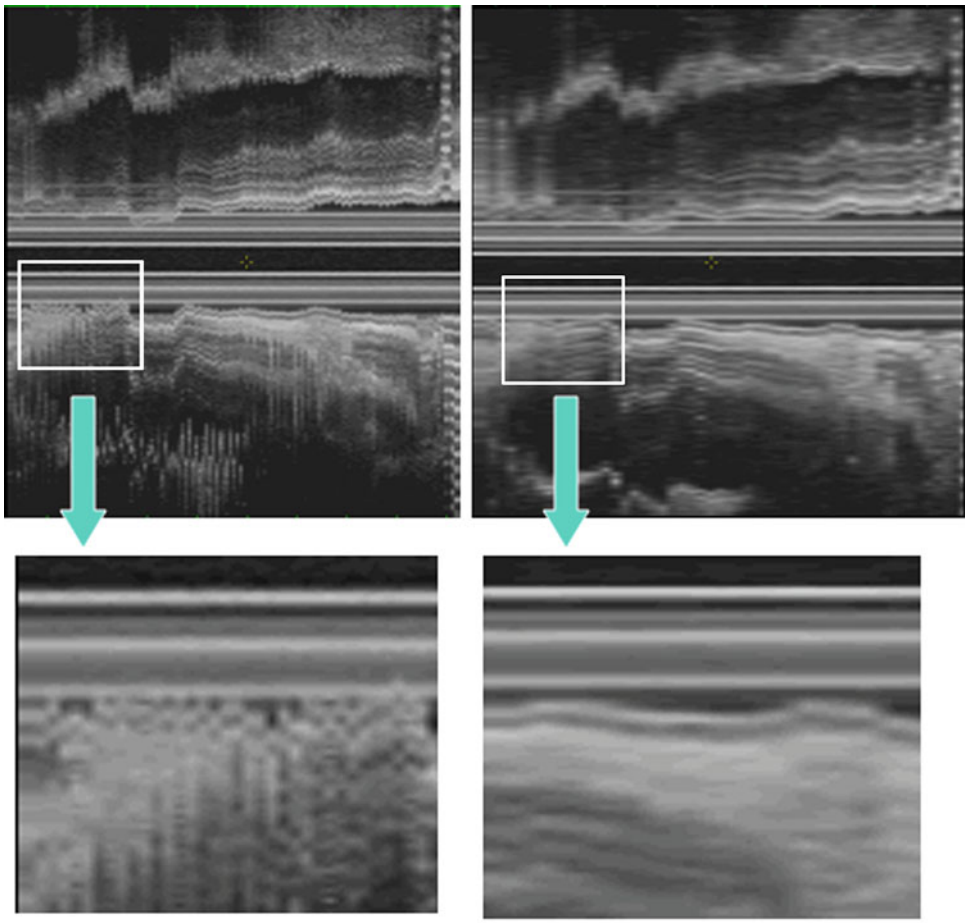

Fig. 11 The ECG-triggered 3D EUS reconstructions could be obtained during routine examinations, resulting in a clear demonstration of the different wall layers in the longitudinal image axis. In the *left panel*, a non-ECG-triggered EUS acquisition is depicted. Eight-French miniature ultrasound catheters 12–20 MHz (Olympus Optical Inc., Japan) were used. Image distortion was measured as lateral dislocation of the organ wall layers, perpendicular to the probe, in the longitudinal axis of the reconstructed ultrasound image. The lateral dislocation was 2.40 mm (SD 0.56) in non-ECG trigged examinations resulting in a "fuzzy" image in the axial display, compared to 0.19 mm (SD 0.23) in the ECG-triggered examination ($p < 0.0027$)

particularly useful for esophageal and rectal lesions. They concluded that this new diagnostic method enabled visualization of the total extent of gastrointestinal lesions and appeared to have useful clinical applications.

Another Japanese group used a system of 3D endoscopic ultrasonography to analyze the surface, the echo-density, and the echo-patterns of cross-sectional images of submucosal lesions. They evaluated the quality of the 3D image and cross-sectional images of lipomas, leiomyomas, and cysts. They stated that analysis of 3D EUS images was useful in making a diagnosis of submucosal lesions (Miyamoto et al. 1998). Tsutsui et al. (1998) evaluated the usefulness of 3D sonography using Olympus ultrasound 3D imaging system to spatially clarify digestive lesions. They converted the sequential 2D data into volume data by an image processing software (Medical Design Composer 1.0) developed by them. They found that determination of the depth and the extent of tumor invasion was more correctly viewed when arbitrary slicing was applied. However, it was difficult to obtain precise 3D images in lesions greatly influenced by heartbeats.

In another study, volume measurement using tissue characterization of 3D endoscopic ultrasonographic images was performed (Yoshino et al. 2000), showing good correlation between the volume measured with 3D EUS and the volume obtained using tissue characterization. The tissue characterization volumes were only relatively slightly larger than the volumes measured using 3D EUS, and they suggested that there is some promise for tissue characterization in 3D EUS.

Hunerbein et al. (1997) aimed at developing a technique for 3D endoscopic ultrasound of the esophagus based on standard endosonographic images. They attached a high-resolution miniprobe (360°, 12.5°MHz) to a stepping motor that enabled ECG-triggered withdrawal of the transducer for imaging of esophageal cancer patients. The system enabled the acquisition of accurate 3D ultrasound data within 30–50 s. Computed image processing allowed display of the data in transverse, longitudinal, and oblique sections, or as a 3D reconstruction. Three-dimensional imaging provided accurate visualization of the tumor and surrounding structures in all cases. Longitudinal scan planes and 3D views improved the assessment of longitudinal tumor infiltration and the spatial relation of the tumor to relevant mediastinal structures. They concluded that 3D endoscopic ultrasound of the esophagus was technically feasible and it allowed the assessment of local tumor spread in previously unattainable scan planes.

5 Three-Dimensional Ultrasonography of the Rectum

Transrectal ultrasound is the most sensitive technique for preoperative staging and follow-up of rectal cancer. Major limitations of this technique include the complexity of image interpretation and the inability to examine stenotic tumors or to identify recurrent rectal cancer. Therefore, Hunerbein and Schlag (1997) conducted a prospective study to investigate the value of 3D endosonography for staging of rectal cancer. Three-dimensional endosonography was performed in 100 patients with rectal tumors. Transrectal volume scans were obtained using a 3D multiplane transducer (7.5/10.0 MHz). Stenotic tumors were examined with a 3D front-fire transducer (5.0/7.5 MHz). The volume scans were processed and analyzed on a Combison 530 workstation (Kretztechnik, Zipf, Austria). Display of volume data in three perpendicular planes or as 3D view facilitated the interpretation of ultrasound images and enhanced the diagnostic information of the data. The accuracy of 3D endosonography in the assessment of infiltration depth was 88 compared to 82 % with the conventional technique. In the determination of lymph node involvement, 3D and 2D endosonography provided accuracy rates of 79 and 74 %, respectively. The 3D scanning allowed the visualization of obstructing tumors using reconstructed planes in front of the transducer. Correct assessment of the infiltration depth was possible in 15 out of 21 patients with obstructing tumors (accuracy 76 %). Three-dimensional endosonography displayed suspicious pararectal lesions in 30 patients. Transrectal ultrasound-guided biopsy was extremely precise (accuracy 98 %) and showed malignancy in 10 of 30 patients. They concluded that the 3D imaging and ultrasound-guided biopsy seemed capable to improve staging of rectal cancer. The same authors also investigated the value of 3D endorectal ultrasonography for staging of obstructing rectal cancer (Hunerbein et al. 1996). In this study, they concluded that this technique may improve therapy planning in advanced rectal cancer by selecting patients who require preoperative adjuvant therapy. Kim et al. (2002) performed a prospective study to verify whether 3D endorectal ultrasonography (EUS) enhances the accuracy of rectal cancer staging, as compared with conventional EUS. They scanned 33 consecutive patients and the accuracy of 3D EUS was 90.9 for pT2 and 84.8 % for pT3, whereas that of conventional EUS was 84.8 and 75.8 %, respectively. The lymph node metastasis was accurately predicted by 3D EUS in 28 patients (84.8 %), whereas conventional EUS predicted the disorder in 22 patients (66.7 %). These differences were not statistically significant, probably due to a low number of patients. The average infiltration grade of the circumference on transverse 3D EUS scans was associated closely with advancement of the TNM stage and lymph node metastasis (Kim et al. 2002).

Williams et al. (2001) used 3D endoanal sonography to determine the incidence and functional consequences of external sphincter trauma. They examined 55 women after delivery and found ultrasound evidence of postpartum trauma in 13 of 45 women who had a vaginal delivery, involving the external sphincter in five, the puboanalis in nine, and the transverse perineii in three. They concluded that coronal imaging offered by 3D ultrasonography of the external anal sphincter was a useful adjunct to the assessment of trauma. The positive influence of 3D scanning was confirmed by Christensen et al. (2005) who found that 3D anal endosonography improves diagnostic confidence in detecting damage to the anal sphincter complex. The agreement between two observers was acceptable using 2D but better when using 3D. They concluded that the 3D method may improve the selection of patients for surgical repair of the anal sphincter complex. Christensen et al. (2004) also used 3D endosonography in patients with anal carcinoma and found that detection of perirectal lymph nodes and tumor invasion were improved, compared with 2D endosonography. This may affect local tumor staging and thus planning of treatment.

West et al. (2004) determined the agreement between hydrogen peroxide-enhanced 3D endoanal ultrasonography (3D HPUS) and endoanal MRI in preoperative assessment of perianal fistulas, and assessed patient preference with regard to these techniques. The methods agreed in 88 for the primary fistula tract, in 90 for the location of the internal opening, in 78 for secondary tracts, and in 88 % for fluid collections. They concluded that 3D HPUS and endoanal MRI are equally adequate for the evaluation of perianal fistulas. Both methods are associated with similar discomfort and patients have no preference for either procedure.

6 Conclusion

The introduction of 3D ultrasonographic imaging in the field of gastroenterology seems to improve standardization of data acquisition and analysis, and this is particularly relevant for endosonographic imaging. Moreover, acquisition time during an unpleasant procedure for the patient can be reduced. The 3D imaging also makes ultrasonography less operator dependent and facilitates easier interpretation of ultrasonographic images. For volume estimation, there are several studies that demonstrate high accuracy of 3D ultrasonography. Furthermore, when conventional 2D scanning is compared with 3D ultrasonography, studies concluded that 3D ultrasonography performs better than 2D ultrasonography with respect to accuracy and precision in volume

calculation (Kyei Mensah et al. 1996; Riccabona et al. 1995; Sapin et al. 1993).

For mapping of complex anatomy, e.g. to aid surgical planning, 3D ultrasonography appears to be a promising tool (Borges et al. 1996; Trocino et al. 1996; Vannier and Marsh 1996; Vogel et al. 1995). However, there are limitations of 3D ultrasonography that need to be acknowledged. The whole process from acquisition to display of 3D images is, except for real-time 3D scanning, time consuming and requires dedicated, well-trained operators. The importance of high-quality raw data enabled by careful acquisition cannot be overestimated, as there is principally no new image data in the 3D file compared to the original 2D image.

There is a future for 3D ultrasonography as development in acquisition devices, transducer technology, and computer software and hardware will permit real-time data acquisition and image rendering. On-line display and volume calculation will enhance diagnostic value and allow smooth patient examination and work-up. Furthermore, 3D ultrasonography may become an important imaging modality in interventional medicine where accurate 3D display is warranted.

References

Acar P, Dulac Y, Taktak A, Abadir S (2005) Real-time three-dimensional fetal echocardiography using matrix probe. Prenat Diagn 25:370–375

Ahluwalia NK, Thompson DG, Barlow J, Troncon LEA, Hollis S (1994) Relaxation responses of the human proximal stomach to distension during fasting and after food. Am J Physiol 267: G166–G172

Ahmad M, Xie T, McCulloch M, Abreo G, Runge M (2001) Real-time three-dimensional dobutamine stress echocardiography in assessment stress echocardiography in assessment of ischemia: comparison with two-dimensional dobutamine stress echocardiography. J Am Coll Cardiol 37:1303–1309

Arai K, Hozumi T, Matsumura Y, Sugioka K et al (2004) Accuracy of measurement of left ventricular volume and ejection fraction by new real-time three-dimensional echocardiography in patients with wall motion abnormalities secondary to myocardial infarction. Am J Cardiol 94:552–558

Baum G, Stroke GW (1975) Optical holographic three-dimensional ultrasonography. Science 189:994–995

Belohlavek M, Foley DA, Gerber TC, Greenleaf JF, Seward JB (1993a) Three-dimensional ultrasound imaging of the atrial septum: normal and pathologic anatomy. J Am Coll Cardiol 22:1673–1678

Belohlavek M, Foley DA, Gerber TC, Kinter TM, Greenleaf JF, Seward JB (1993b) Three- and four-dimensional cardiovascular ultrasound imaging: a new era for echocardiography. Mayo Clin Proc 68:221–240

Berstad A, Gilja OH (2004) Ultrasonographic alterations in functional dyspepsia. In: Odegaard S, Gilja OH, Gregersen H (eds.) Basic and new aspects of gastrointestinal ultrasonography. World Scientific, New Jersey, pp 395–420

Berstad A, Hausken T, Gilja OH et al (1997) Gastric accommodation in functional dyspepsia. Scand J Gastroenterol 32:193–197

Berstad A, Hausken T, Gilja OH, Thune N, Matre K, Odegaard S (1994) Volume measurement of gastric antrum by 3D ultrasonography and flow measurements through the pylorus by duplex technique. Dig Dis Sci 39:97–100

Binder TM, Rosenhek R, Porenta G, Maurer G, Baumgartner H (2000) Improved assessment of mitral valve stenosis by volumetric real-time three-dimensional echocardiography. J Am Coll Cardiol 36:1355–1361

Bolondi L, Bortolotti M, Santi V, Calletti T, Gaiani S, Labo G (1985) Measurement of gastric emptying time by real-time ultrasonography. Gastroenterology 89:752–759

Borges AC, Witt C, Bartel T, Muller S, Konertz W, Baumann G (1996) Preoperative two- and three-dimensional transesophageal echocardiographic assessment of heart tumors. Ann Thorac Surg 61:1163–1167

Bu L, Munns S, Zhang H et al (2005) Rapid full volume data acquisition by real-time 3Dimensional echocardiography for assessment of left ventricular indexes in children: a validation study compared with magnetic resonance imaging. J Am Soc Echocardiogr 18:299–305

Camarano G, Jones M, Freidlin RZ, Panza JA (2002) Quantitative assessment of left ventricular perfusion defects using real-time three-dimensional myocardial contrast echocardiography. J Am Soc Echocardiogr 15:206–213

Chandrasekaran K, Sehgal CM, Hsu TL et al (1994) Three-dimensional volumetric ultrasound imaging of arterial pathology from two-dimensional intravascular ultrasound: an in vitro study. Angiology 45:253–264

Christensen AF, Nielsen MB, Engelholm SA, Roed H, Svendsen LB, Christensen H (2004) Three-dimensional anal endosonography may improve staging of anal cancer compared with two-dimensional endosonography. Dis Colon Rectum 47:341–345

Christensen AF, Nyhuus B, Nielsen MB, Christensen H (2005) Three-dimensional anal endosonography may improve diagnostic confidence of detecting damage to the anal sphincter complex. Br J Radiol 78:308–311

Dekker DL, Piziali RL, Dong E Jr (1974) A system for ultrasonically imaging the human heart in three dimensions. Comput Biomed Res 7:544–553

Desaga JF, Hixt U (1987) Sonographic determination of gastric emptying. Ultraschall Med 8:138–141

Detmer PR, Bashein G, Hodges TC et al (1994) 3D ultrasonic image feature localization based on magnetic scanhead tracking: In vitro calibration and validation. Ultrasound Med Biol 20:923–936

Dorlars D, Schilling D, Riemann JF (1994) The feasibility of ultrasonography for the evaluation of stomach motility disorders. Dtsch Med Wochenschr 119:575–580

Duan LP, Zheng ZT, Li YN (1993) A study of gastric emptying in non-ulcer dyspepsia using a new ultrasonographic method. Scand J Gastroenterol 28:355–360

Foroughi P, Abolmaesumi P, Hashtrudi-Zaad K (2006) Towards real-time registration of 4D ultrasound images. Conf Proc IEEE Eng Med Biol Soc 1:404–407

Geiser EA, Christie LGJ, Conetta DA, Conti CR, Gossman GS (1982) A mechanical arm for spatial registration of two-dimensional echocardiographic sections. Cathet Cardiovasc Diagn 8:89–101

Ghosh A, Nanda NC, Maurer G (1982) Three-dimensional reconstruction of echo-cardiographic images using the rotation method. Ultrasound Med Biol 8:655–661

Gilja OH, Detmer PR, Jong JM et al (1997) Intragastric distribution and gastric emptying assessed by 3D-ultrasonography. Gastroenterology 113:38–49

Gilja OH, Hausken T, Berstad A, Odegaard S (1999) Measurements of organ volume by ultrasonography. Proc Inst Mech Eng [H] 213:247–259

Gilja OH, Hausken T, Odegaard S, Berstad A (1996a) Three-dimensional ultrasonography of the gastric antrum in patients with functional dyspepsia. Scand J Gastroenterol 31:847–855
Gilja OH, Hausken T, Wilhelmsen I, Berstad A (1996b) Impaired accommodation of proximal stomach to a meal in functional dyspepsia. Dig Dis Sci 41:689–696
Gilja OH, Smievoll AI, Thune N et al (1995) In vivo comparison of 3D ultrasonography and magnetic resonance imaging in volume estimation of human kidneys. Ultrasound Med Biol 21:25–32
Gilja OH, Thune N, Matre K, Hausken T, Odegaard S, Berstad A (1994) In vitro evaluation of three-dimensional ultrasonography in volume estimation of abdominal organs. Ultrasound Med Biol 20:157–165
Green K, Campbell G (1994) Nitric oxide formation is involved in vagal inhibition of the stomach of the trout (Salmo gairdneri). J Auton Nerv Syst 50:221–229
Greenleaf JF, Belohlavek M, Gerber TC, Foley DA, Seward JB (1993) Multidimensional visualization in echocardiography: an introduction. Mayo Clin Proc 68:213–220
Hamper UM, Trapanotto V, Sheth S, DeJong MR, Caskey CI (1994) Three-dimensional US: preliminary clinical experience. Radiology 191:397–401
Handschumacher MD, Lethor JP, Siu SC et al (1993) A new integrated system for three-dimensional echocardiographic reconstruction: development and validation for ventricular volume with application in human subjects. J Am Coll Cardiol 21:743–753
Harris EJ, Miller NR, Bamber JC, Symonds-Tayler JR, Evans PM (2010) Speckle tracking in a phantom and feature-based tracking in liver in the presence of respiratory motion using 4D ultrasound. Phys Med Biol 55:3363–3380
Hausken T, Li X-N, Goldman B, Leotta DF, Odegaard S, Martin RW (2001) Quantification of gastric emptying and duodenogastric reflux stroke volumes using three-dimensional guided digital color Doppler imaging. Eur J Ultrasound 13(3):205–213
Hausken T, Thune N, Matre K, Gilja OH, Odegaard S, Berstad A (1994) Volume estimation of the gastric antrum and the gallbladder in patients with non-ulcer dyspepsia and erosive prepyloric changes, using three-dimensional ultrasonography. Neurogastroenterol Mot 6:263–270
Hjelland IE, Ofstad AP, Narvestad JK, Berstad A, Hausken T (2004) Drink tests in functional dyspepsia: which drink is best? Scand J Gastroenterol 39:933–937
Hodges TC, Detmer PR, Burns DH, Beach KW, JrDE Strandness (1994) Ultrasonic three-dimensional reconstruction: In vitro and in vivo volume and area measurement. Ultrasound Med Biol 20:719–729
Hokland J, Hausken T (1994) An interactive volume rendering method applied to ultrasonography of abdominal structures. IEEE Ultrason Symp Proc 3:1567–1571
Hou XH, Deng YB, Zhang JK (1992) Measurement of gastric emptying in non-ulcer dyspepsia. Chung Hua Nei Ko Tsa Chih 31(623–5):658
Hunerbein M, Below C, Schlag PM (1996) Three-dimensional endorectal ultrasonography for staging of obstructing rectal cancer. Dis Colon Rectum 39:636–642
Hunerbein M, Gretschel S, Ghadimi BM, Schlag PM (1997) Three-dimensional endoscopic ultrasound of the esophagus. Preliminary experience. Surg Endosc 11:991–994
Hunerbein M, Schlag PM (1997) Three-dimensional endosonography for staging of rectal cancer. Ann Surg 225:432–438
Jenkins C, Bricknell K, Hanekom L, Marwick TH (2004) Reproducibility and accuracy of echocardiographic measurements of left ventricular parameters using real-time three-dimensional echocardiography. J Am Coll Cardiol 44:878–886
Kelly IM, Gardener JE, Brett AD, Richards R, Lees WR (1994) Three-dimensional US of the fetus. Work in progress. Radiology 192:253–259
Kim JC, Cho YK, Kim SY, Park SK, Lee MG (2002) Comparative study of three-dimensional and conventional endorectal ultrasonography used in rectal cancer staging. Surg Endosc 16:1280–1285
King DL, King DL Jr, Shao MY (1990) Three-dimensional spatial registration and interactive display of position and orientation of real-time ultrasound images. J Ultrasound Med 9:525–532
King DL, King DL Jr, Shao MY (1991) Evaluation of in vitro measurement accuracy of a three-dimensional ultrasound scanner. J Ultrasound Med 10:77–82
Koivukangas J, Ylitalo J, Alasaarela E, Tauriainen A (1986) Three-dimensional ultrasound imaging of brain for neurosurgery. Ann Clin Res 18(Suppl 47):65–72
Kyei Mensah A, Zaidi J, Pittrof R, Shaker A, Campbell S, Tan SL (1996) Transvaginal three-dimensional ultrasound: accuracy of follicular volume measurements. Fertil Steril 65:371–376
Leotta DF, Detmer PR, Gilja OH et al. (1995) Three-dimensional ultrasound imaging using multiple magnetic tracking systems and miniature magnetic sensors. Proceedings of IEEE International Ultrasonics Symposium, Seattle WA, pp 1415–1418
Levine RA, Handschumacher MD, Sanfilippo AJ et al (1989) Three-dimensional echocardiographic reconstruction of the mitral valve, with implications for the diagnosis of mitral valve prolapse. Circulation 80:589–598
Liao D, Gregersen H, Hausken T, Gilja OH, Mundt M, Kassab G (2004) Analysis of surface geometry of the human stomach using real-time 3D ultrasonography in vivo. Neurogastroenterol Motil 16:315–324
LiVoti G, Tulone V, Bruno R et al (1992) Ultrasonography and gastric emptying: evaluation in infants with gastroesophageal reflux. J Pediatr Gastroenterol Nutr 14:397–399
Martens D, Gilja OH (2004) The EchoPAC-3D software for 3D image analysis. In: Odegaard S, Gilja OH, Gregersen H (eds) Basic and new aspects of gastrointestinal ultrasonography. World Scientific, New Jersey
Martens D, Hausken T, Gilja OH, Steen EN, Alker HJ (1997) 3D processing of ultrasound images using a novel echopac-3D software. Ultrasound Med Biol 23[S1]:136
Martin RW, Bashein G (1989) Measurement of stroke volume with three-dimensional transesophageal ultrasonic scanning: comparison with thermodilution measurement. Anesthesiology 70:470–476
Martin RW, Bashein G, Zimmer R, Sutherland J (1986) An endoscopic micromanipulator for multiplanar transesophageal imaging. Ultrasound Med Biol 12:965–975
Martin RW, Legget M, McDonald J et al (1995) Stereographic viewing of 3D ultrasound images: A novelty or a tool? Proc IEEE Int Ultrasonics Symp 2:1431–1434
Matre K, Stokke EM, Martens D, Gilja OH (1999) In vitro volume estimation of kidneys using three-dimensional ultrasonography and a position sensor. Eur J Ultrasound 10:65–73
Mintz GS, Pichard AD, Satler LF, Popma JJ, Kent KM, Leon MB (1993) Three-dimensional intravascular ultrasonography: reconstruction of endovascular stents in vitro and in vivo. J Clin Ultrasound 21:609–615
Miyamoto M, Aoyama N, Sakashita M et al (1998) Three-dimensional endoscopic ultrasonography for SMT. Digestion 59:194
Molin S, Nesje LB, Gilja OH, Hausken T, Martens D, Odegaard S (1999) 3D-endosonography in gastroenterology: methodology and clinical applications. Eur J Ultrasound 10:171–177
Molin SO, Engstrøm A, Nesje LB, Gilja OH, Odegaard S (1998) Improvement of 3D EUS using ECG- and respiratory triggered acquisition. Eur J Ultrasound 7:54
Molin SO, Jirås A, Hall-Angerås M, Falk A, Martens D, Gilja OH, Nesje LB, Odegaard S (1997) Virtual reality in surgical practice. In vitro and in vivo evaluations. In: Sieburg H, Weghorst S, Morgan K, (eds.) Studies in health technology and informatics. IOS Press and Ohmsha, pp 246–253

Molin SO, Liedman B, Lundell L et al (2000) Performance of a miniature magnetic position sensor for 3D-EUS imaging. Endoscopy 32:50

Molin SO, Nesje LB, Gilja OH, Hausken T, Odegaard S (1996a) Modalities for three-dimensional endoscopic and laparoscopic ultrasonography: in vitro and in vivo evaluation. Endoscopy 28:S38

Molin SO, Nesje LB, Gilja OH, Hausken T, Odegaard S (1996b) Adoption of conventional endosonography for 3D visualization of GI tract. Scand J Gastroenterol 31:33

Moritz WE, Shreve PL, Mace LE (1976) Analysis of an ultrasonic spatial locating system. IEEE Trans Instrum Meas 25:43–50

Mundt MW, Hausken T, Smout AJ, Samsom M (2005) Relationships between gastric accommodation and gastrointestinal sensations in healthy volunteers. A study using the barostat technique and two- and three-dimensional ultrasonography. Dig Dis Sci 50:1654–1660

Nelson TR, Pretorius DH (1995) Visualization of the fetal thoracic skeleton with three- dimensional sonography: a preliminary report. AJR Am J Roentgenol 164:1485–1488

Newell SJ, Chapman S, Booth IW (1993) Ultrasonic assessment of gastric emptying in the preterm infant. Arch Dis Child 69:32–36

Nielson GM, Shriver B (1989) Visualization in scientific computing. IEEE Computer Society Press, Los Alamitos

Nikravesh PE, Skorton DJ, Chandran KB, Attarwala YM, Pandian N, Kerber RE (1984) Computerized three-dimensional finite element reconstruction of the left ventricle from cross-sectional echocardiograms. Ultrason Imaging 6:48–59

Nishimura K, Niwa Y, Goto H, Hase S, Arisawa T, Hayakawa T (1997) Three-dimensional endoscopic ultrasonography of gastrointestinal lesions using an ultrasound probe. Scand J Gastroenterol 32:862–868

Odegaard S, Nesje LB, Gilja OH, Hausken T, Molin SO, Martens D (1998) Diseases of the gastrointestinal tract examined with 3D endoscopic ultrasonography. In: Bismuth H, Galmiche JP, Huguier M, Jaeck D (eds.) Monduzzi Editore. 8th World Congress of the Int Gastro-Surgical Club. 15 Apr 0098, pp 827–831

Odegaard S, Nesje LB, Molin SO, Gilja OH, Hausken T (1999) Three-dimensional intraluminal sonography in the evaluation of gastrointestinal diseases. Abdom Imaging 24:449–451

Picot PA, Rickey DW, Mitchell R, Rankin RN, Fenster A (1993) Three-dimensional colour Doppler imaging. Ultrasound Med Biol 19:95–104

Pretorius DH, Nelson TR (1994) Prenatal visualization of cranial sutures and fontanelles with three-dimensional ultrasonography. J Ultrasound Med 13:871–876

Pretorius DH, Nelson TR (1995) Fetal face visualization using three-dimensional ultrasonography. J Ultrasound Med 14:349–356

Qin JX, Jones M, Shiota T, Greenberg NL et al (2000) Validation of real-time three-dimensional echocardiography for quantifying left ventricular volumes in the presence of a left ventricular aneurysm: in vitro and in vivo studies. J Am Coll Cardiol 36:900–907

Radberg G, Asztely M, Cantor P et al (1989) Gastric and gallbladder emptying in relation to the secretion of cholecystokinin after a meal in late pregnancy. Digestion 42:174–180

Raichlen JS, Trivedi SS, Herman GT, St John Sutton MG, Reichek N (1986) Dynamic three-dimensional reconstruction of the left ventricle from two-dimensional echocardiograms. J Am Coll Cardiol 8:364–370

Redman JD, Walton WP, Fleming JE, Hall AM (1969) Holographic display of data from ultrasonic scanning. Ultrasonics 7:26–29

Riccabona M, Nelson TR, Pretorius DH, Davidson TE (1995) Distance and volume measurement using three-dimensional ultrasonography. J Ultrasound Med 14:881–886

Roelandt JR, ten Cate FJ, Vletter WB, Taams MA (1994) Ultrasonic dynamic three-dimensional visualization of the heart with a multiplane transesophageal imaging transducer. J Am Soc Echocardiogr 7:217–229

Rosenfield K, Losordo DW, Ramaswamy K et al (1991) Three-dimensional reconstruction of human coronary and peripheral arteries from images recorded during two-dimensional intravascular ultrasound examination. Circulation 84:1938–1956

Ross JJ Jr, D'Adamo AJ, Karalis DG, Chandrasekaran K (1993) Three-dimensional transesophageal echo imaging of the descending thoracic aorta. Am J Cardiol 71:1000–1002

Sackmann M, Pauletzki J, Zwiebel FM, Holl J (1994) Three-dimensional ultrasonography in hepatobiliary and pancreatic diseases. Bildgebung 61:100–103

Salustri A, Roelandt JR (1995) Ultrasonic three-dimensional reconstruction of the heart. Ultrasound Med Biol 21:281–293

Sapin PM, Schroeder KD, Smith MD, DeMaria AN, King DL (1993) Three-dimensional echocardiographic measurement of left ventricular volume in vitro: comparison with two-dimensional echocardiography and cineventriculography. J Am Coll Cardiol 22: 1530–1537

Sawada H, Fujii J, Aizawa T, Kato K, Onoe M, Kuno Y, Nakanishi T (1985) Three dimensional reconstruction of the human left ventricle from multiple cross-sectional echocardiograms: comparison with biplane cineventriculography using Simpson's rule. J Cardiogr 15:439–447

Scheffer RC, Gooszen HG, Wassenaar EB, Samsom M (2004) Relationship between partial gastric volumes and dyspeptic symptoms in plication patients: a 3D ultrasonographic study. Am J Gastroenterol 99:1902–1909

Sehgal CM, Broderick GA, Whittington R, Gorniak RJ, Arger PH (1994) Three-dimensional US and volumetric assessment of the prostate. Radiology 192:274–278

Sohn C, Grotepass J (1990) 3Dimensional organ image using ultrasound. Ultraschall Med 11:295–301

Sugimoto K, Moriyasu F, Shiraishi J, Yamada M, Imai Y (2011) A phantom study comparing ultrasound-guided liver tumor puncture using new real-time 3D ultrasound and conventional 2D ultrasound. AJR Am J Roentgenol 196:W753–W757

Sumiyama K, Suzuki N, Tajiri H (2003) A linear-array freehand 3D endoscopic ultrasound. Ultrasound Med Biol 29:1001–1006

Tack J, Piessevaux H, Coulie B, Caenepeel P, Janssens J (1998) Role of impaired gastric accommodation to a meal in functional dyspepsia. Gastroenterology 115:1346–1352

Tefera S, Gilja OH, Olavsdottir E, Hausken T, Hatlebakk JG, Berstad A (2002) Intragastric maldistribution of a liquid meal in patients with reflux oesophagitis assessed by three dimensional ultrasonography. Gut 50:153–158

Thune N, Hausken T, Gilja OH, Matre K (1996) A practical method for estimating enclosed volumes using 3D ultrasound. Eur J Ultrasound 3:83–92

Trocino G, Salustri A, Roelandt JR, Ansink T, van Herwerden L (1996) Three-dimensional echocardiography of a flail tricuspid valve. J Am Soc Echocardiogr 9:91–93

Tsutsuii A, Okamura S, Okita Y, Fukuda T, Hayashi S, Muguruma N, Okahisa T, Shibata H, Ito S, Umino K (1998) Usefulness of three-dimensional display of digestive lesions by endoscopic ultrasonography. Digestion 59[S3], p 194

Vannier MW, Marsh JL (1996) Three-dimensional imaging, surgical planning, and image-guided therapy. Radiol Clin North Am 34:545–563

Vogel M, Ho SY, Lincoln C, Yacoub MH, Anderson RH (1995) Three-dimensional echocardiography can simulate intraoperative visualization of congenitally malformed hearts. Ann Thorac Surg 60:1282–1288

Wagner S, Gebel M, Bleck JS, Manns MP (1994) Clinical application of three-dimensional sonography in hepatobiliary disease. Bildgebung 61:104–109

West RL, Dwarkasing S, Felt-Bersma RJ, Schouten WR, Hop WC, Hussain SM, Kuipers EJ (2004) Hydrogen peroxide-enhanced three-dimensional endoanal ultrasonography and endoanal magnetic resonance imaging in evaluating perianal fistulas: agreement and patient preference. Eur J Gastroenterol Hepatol 16:1319–1324

Whittingham TA, Bateman DN (1983) Measurement of stomach volume by real-time ultrasound. Ultrasound Med Biol Suppl 2:459–463

Williams AB, Bartram CI, Halligan S, Spencer JA, Nicholls RJ, Kmiot WA (2001) Anal sphincter damage after vaginal delivery using three-dimensional endosonography. Obstet Gynecol 97:770–775

Yoshino J, Nakazawa S, Inui K, Wakabayashi T et al (2000) Volume measurement using tissue characterization of three-dimensional endoscopic ultrasonographic images. Endoscopy 32:624–629

Zoller WG, Liess H (1994) 3D ultrasound in gastroenterology. Bildgebung 61:95–99

Imaging of Tissue Elasticity in Gastrointestinal Disorders

Roald Flesland Havre and Odd Helge Gilja

Contents

Abstract

Elastography or strain imaging are ultrasonographic methods which detect the elasticity or stiffness of a tissue providing a visual display. The basis of every strain imaging technique is to measure tissue deformation caused by an external stimulus. The derivative of the tissue displacement is called strain, and can be calculated by cross-correlating the radio-frequency data before and after compression. The strain value in each point is color-coded and displayed in an elastogram. This elastogram can then be combined with the B-mode image to display the elastic properties of the tissue to the examiner through color information. Equipment using a quasi-static method of producing strain in the tissue through external compression with the US probe is now commercially available for clinical application. The quasi-static application of elastography of the small intestine represents special difficulties, as the pressure from the US transducer can cause several changes. When adding pressure, one not only deforms the GI wall, but also displaces the luminal content and the intestine itself. With refined technology and adapted transducers, sono-elastography may become an important imaging modality to supplement B-mode ultrasonography for the assessment of gastrointestinal diseases.

1 Introduction

The use of palpation in medical examination has a long tradition, and has been part of the diagnostic approach for centuries. The limitations have been that clinicians had to touch the surface of the organ, often limited to findings within reach for the clinician close to the surface of the skin or limited areas of mocous membrane. Also, the accuracy of palpation findings has been reported to be low in several studies. Using US-based elasticity imaging, the clinician is

R. F. Havre (✉) · O. H. Gilja
Institute of Medicine, University of Bergen and National Centre for Ultrasound in Gastroenterology, Department of Medicine, Haukeland University Hospital, Jonas Lies vei 65, 5021 Bergen, Norway
e-mail: roald.flesland.havre@helse-bergen.no

G. Maconi and G. Bianchi Porro (eds.), *Ultrasound of the Gastrointestinal Tract*, Medical Radiology. Diagnostic Imaging,
DOI: 10.1007/174_2013_799,
Published Online: 16 May 2013

now able to image organs that are beyond the reach of the fingers (Ophir et al. 1991, 1999).

In order to become a reliable diagnostic imaging modality, possibly reducing the need for biopsy, some conditions have to be met. First, the elasticity of pathological tissue, i.e. malignant tumours, has to change out of the range of normal tissue. In order to allow tissue characterisation with high specificity, it is important that benign entities, such as inflammatory lesions, do not change elasticity by the same magnitude as malignant tumours. If this is the case, this may reduce the specificity of the method. The second condition is that the elastography dynamic range must correspond to the tissue elasticity dynamic range, so that changes can be detected. Ideally, the resolution of the elasticity or strain imaging modality must be good enough to produce elasticity patterns specific for the malignant and different from benign entities. The technique must also be easy to use during examinations and findings must be reproducible.

Clearly, techniques providing quantitative data are more convenient for performance evaluation and will be easier to validate. They may also be easier to relate to for clinicians with little experience with US as a clinical imaging modality. The downside of quantitative imaging is that it is often more cumbersome, and may have to be repeated a number of times to be accurate. Qualitative imaging, providing elasticity information in grey scale or colour maps may be easier to use during patient scanning. Furthermore, it adds a new tool in the ultrasound toolbox consisting of B-mode scanning, colour-Doppler, strain imaging and contrast enhanced ultrasonography.

Strain imaging:
Strain/Stress = elastic modulus (Youngs Modulus, E)
$E = L0 - L/(\text{Force}/\text{Area}) = \sigma/\varepsilon$

2 The Imaging Techniques

2.1 Sono-Elastography (Quasi-Static Elastography)

This technique uses operator induced stress or endogenous stress to create strain in the tissue under the US probe. Since the amount of stress is unknown, only the resulting tissue strain is recorded. Different varieties of this method are the most frequently applied elastography module on most high-end commercial US scanners. The method is based on different autocorrelation algorithms and requires variable amounts of force or amplitude of repetitive stress. These methods also induce variable strain artifacts hampering the elasticity assessment.

Presentation: This strain is imaged, frequently superimposed on the B-mode image, as a colour map or as a grey scale map. Changing the Elasticity dynamic range allows focus on smaller or larger elasticity contrasts in the tissue and may alter the colour map.

Quantification: If both lesion and reference tissue is imaged, a strain ratio may be calculated between the lesion and reference tissue and may be used for quantification. A strain indicator on the screen provides feedback to the operator if there is adequate strain in the region of interest. This method relies on a focal stress source being the probe or a source out of the imaging plane. The strain attenuates with increasing distance to this source. Also, as the stress is transmitted through the inhomogeneities of biological tissues, this attenuation of stress will be different in different parts of the ROI.

2.2 Shear wave imaging

$$G = (v_s)^2 \rho$$

G = Shear modulus, v_s = shear wave speed, ρ = density

There are a number of commercialised methods making use of this relation between the shear wave speed and the Shear modulus, G. The density, ρ of soft biological is close to 1. Some methods give up the shear wave speed directly; others approximate the Shear modulus in KPa by measuring the shear wave speed.

2.2.1 Transient Elastography

The Fibroscan® (Echosense, Paris), is a dedicated instrument for measuring liver tissue stiffness (Castera et al. 2005; Talwalkar et al. 2007; Rockey 2008). A patented US transducer equipped with a small piston creates a shear wave induced from the skin surface intercostally over the right liver lobe.

Presentation: This scanner does not provide a B-mode US image or a strain map. It has a simple A-mode like US image for providing quality assurance for the strain measurements. A strict algorithm requiring ten repeated liver tissue measurements of shear wave speed, within limited variation ensures quantitative measurements of good quality.

Quantification: This method provides quantitative measurements of liver tissue stiffness, but it is not an imaging method as there is no B-mode US image or strain image. The apparatus is easy to learn to use and no knowledge of US scanning is necessary. It has limitations for use in very obese patients or patients who have developed ascites.

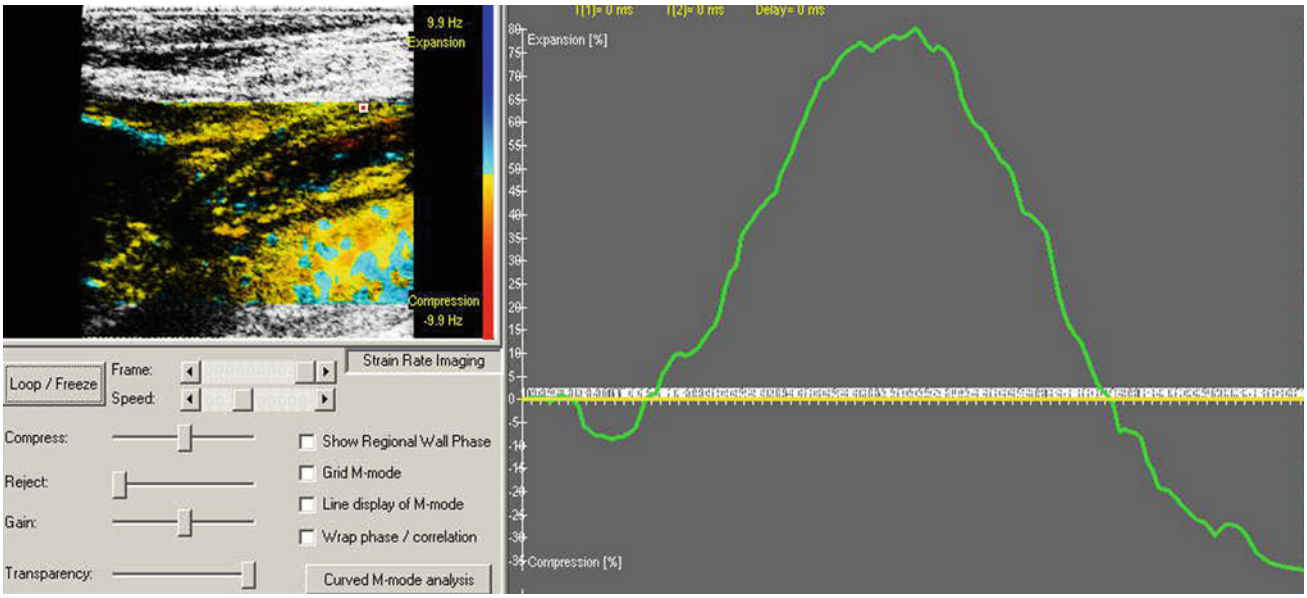

Fig. 1 Stomach: Strain rate imaging of the gastric antrum showing colour-coded doppler signals in the *left panel* superimposed onto the B-mode image with the measurement cursor located in the muscle layer. In the *right panel*, the relative strain curve shows 80 % expansion during the gastric relaxation phase

2.2.2 Acoustic Radiation Force Imaging

This method uses acoustic energy in order to create shear waves and then US is used to map the shear wave speed within a small ROI (Palmeri et al. 2005; Friedrich-Rust et al. 2009).

Presentation and quantification: The user selects an area of interest and the shear wave velocity is recorded in this space and presented in metres per second. This modality is used together with a qualitative strain imaging map covering a larger area, superimposed on the B-mode image. The shear waves are released transiently, and the observer must allow some time for the transducer too cool down after each release.

2.2.3 Supersonic Shear Imaging

This imaging of tissue elasticity is made possible by parallel US wave transmission and receiving, and very powerful data processing allowing a frame rate of 5000 frames or more per second. Combined with the tissue stress induced by several columns of circular shear waves parallel to the scanning plane forming parallel acoustic "cones" in the region of interest (Bercoff et al. 2004; Muller et al. 2009).

Presentation and quantification: The shear waves can be tracked due to the high frame rate of the scanner and local differences in shear wave speed can be mapped and tissue elasticity approximated into KPa. This technique is able to image a larger plane with quantitative elastography, as the acoustic signals create shear waves from multiple cones and thus strain attenuation have a more limited influence on the results. The elasticity image is presented as a colour-coded image, and a quantitative KPa result can be obtained from any area containing strain signal. The recording of nonlinear propagation of shear waves made possible with this technique may also be useful in describing the viscosity characteristics of soft tissues, which has not been possible before.

2.3 Strain Rate Imaging

Local tissue velocities can be estimated by using Doppler methods in an attempt to obtain information about GI wall motility (Grubb et al. 1995; Heimdal 2005). To enable differentiation between actively contracting and passively following tissue, a Doppler method based on strain rate imaging (SRI) and estimation of relative strain was developed (Heimdal 2005).

Presentation: The Doppler strain data is displayed as a colour map superimposed on a B-mode image. A ROI is selected and video-clips are analysed to calculate the relative strain of the smooth muscle contraction (Fig. 1).

Quantification: The calculation of strain by SRI is based on the relative elongation or contraction of the moving target. The accuracy of SRI was evaluated in vitro using a silicone strip phantom mimicking slowly moving tissue (Matre et al. 2003) and in measuring strain in the porcine antral wall in vitro (Ahmed et al. 2006). SRI demonstrated accurate measurement of radial strain of the antral wall and low intra- and inter-observer variation.

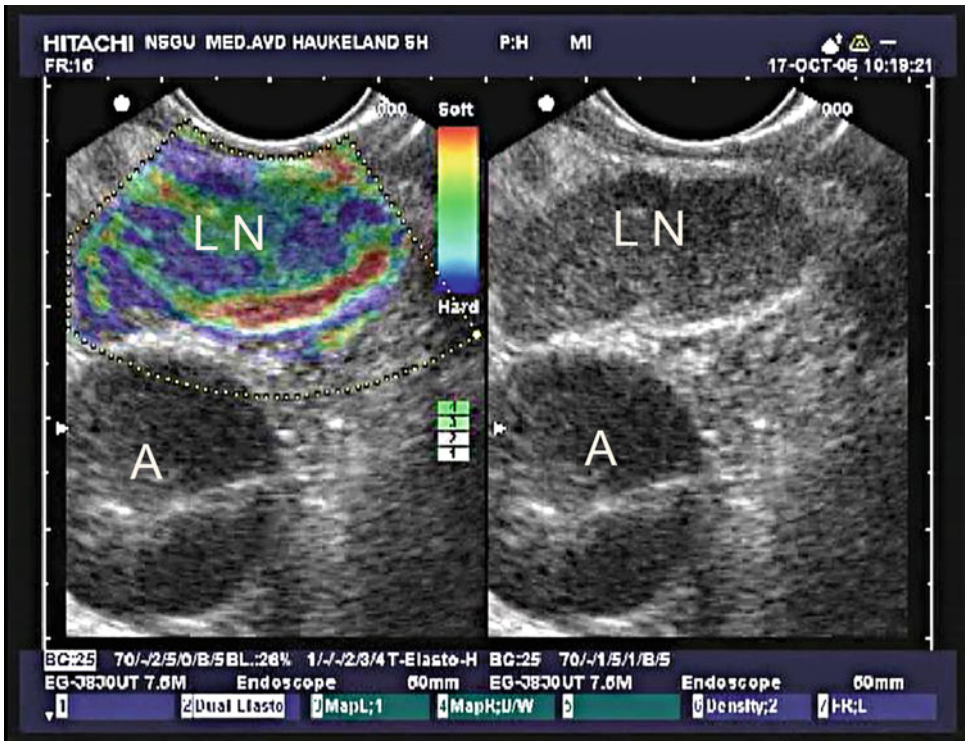

Fig. 2 Metastatic mediastinal lymph node: In the right panel the B-mode image of a mediastinal lymph node (*LN*) close to the aorta (*A*). The left panel shows an elastogram with blue and green areas indicating inhomogeneous elasticity with reproducible low-strain areas indicating harder tissue. An EUS guided FNA confirmed metastasis from a non-small cell lung carcinoma

3 Pathological Conditions

External US application:

3.1 Liver Tissue Stiffness

Measuring liver fibrosis without repeated liver biopsies is of relevance in the follow-up of patients with chronic viral hepatitis C/B, alcoholic or autoimmune hepatitis. This may be useful in order to predict disease progression and may be of value in planning for a liver transplantation. Transient elastography has in many publications shown its value for the identification of fibrosis > Metavir score 2 or higher (Fraquelli et al. 2007; Friedrich-Rust et al. 2008) and has become the reference standard for new elasticity imaging methods of liver tissue. Also ARFI (Sporea et al. 2011) and SSI have been successfully been used for this purpose (Gennisson et al. 2009; Bavu et al. 2011). The latter methods may be even more useful in patients with advanced liver disease who also have developed ascites, which is limiting the use of transient elastography. Elasticity imaging of patients at risk of liver disease may also be of value, e.g. for screening patients in general practice or i.v. drug users. This may contribute to earlier diagnosis and treatment (Gennisson et al. 2009; Moessner et al. 2011; Roulot et al. 2011).

Endoscopic US applications: Until date, only one producer of US scanners and EUS endoscopes offer elastography as part of their software. This is Hitachi Medical Corp. in co-operation with Pentax. The EUS elastography reported here is thus based on this system.

3.2 Evaluation of Lymph Nodes in the Mediastinum

Lymph nodes in the mediastinum may be enlarged in a number of diseases. For patients with malignant disease, particularly tumours in lung and breast, the finding of metastatic lymph nodes in the mediastinum leads to adjuvant chemo- or radiotherapy and may limit futile surgery by providing a more accurate N-staging. The oesophagus and the bronchial tree are excellent ways of getting access to this area. Endoscopic ultrasonographic criteria for lymph node evaluation are based on echogenicity, size, border, architecture and short- and long-diameter. Generally, enlarged, rounded, hypoechoic lymph nodes raise the suspicion of metastatic engagement, but B-mode criteria alone overlap with findings caused by benign conditions such as sarcoidosis, tuberculosis and several other inflammatory states. Endoscopic ultrasonography (EUS) combined with sonoelastography has been used in order to evaluate the nature of mediastinal lymph nodes (Fig. 2). Saftoui et al. found a sensitivity of 86.4 % and a specificity of 91.9 % for

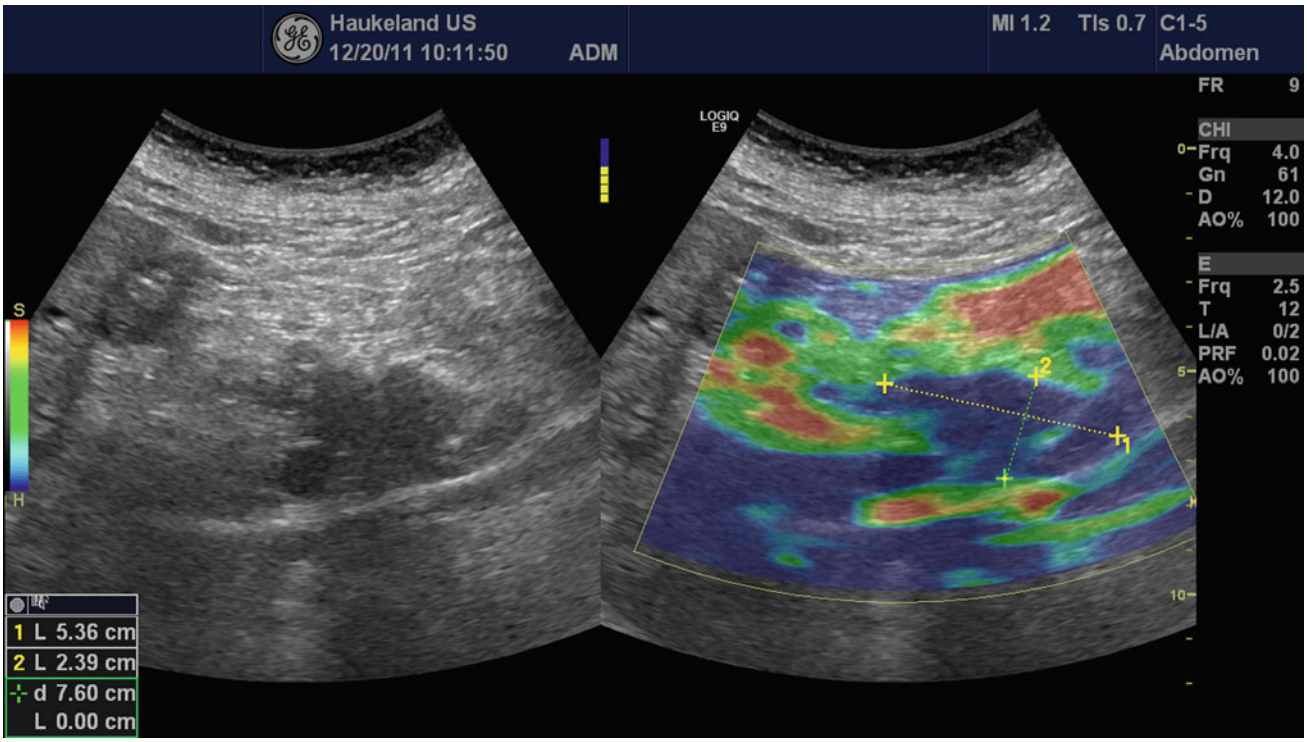

Fig. 3 Pancreas: In the *left panel*, a B-mode ultrasonogram of a hypoechoic pancreatic tumour is shown in a sagittal section of the epigastrium. In the *right panel*, colour-coded elastography is applied showing that the tumour is *blue* (hard) compared with the surrounding tissue in front and above

predicting malignancy when using a mean colour hue cut-off at 166 in 256 colour hues. Janssen et al. found an accuracy of 84.6–86.4 % among three observers using a visual evaluation of predominantly low strain (blue colour) as a sign of malignancy. The conclusion is that the results are good for a non-invasive method, but it is still inferior to the EUS-fine needle aspiration technique, which provides tissue samples.

3.3 Evaluation of Solid Focal Lesions in the Pancreas

Focal lesions in the pancreas are being described more frequently as the image quality of CT and MRI has improved. These lesions may represent malignant or benign lesions, and patients may have no symptoms at the time of diagnosis. In some cases, external elastography of the pancreas is possible attempting to evaluate tumour characteristics (Fig. 3). However, in most cases EUS is the method of choice to perform elastography. EUS elastography may improve the preoperative diagnosis of solid focal pancreatic lesions. Cystic lesions in the pancreas usually provide a characteristic artefact consisting of a blue, green, red-layered structure or no signal. Strain is not measurable in a serous fluid, however, D'Onofrio et al. have demonstrated that ARFI can be used to non-invasively differentiate between mucinous and serous cyst fluid (D'Onofrio et al. 2011). This distinction is useful because only the mucinous cysts are considered to have a malignancy potential, while serous cysts and pseudocysts do not. For solid pancreatic lesions, several studies have considered this method prospectively for the distinction between malignant and benign lesions (Figs. 4 and 5). Most studies have used visual categorical scores (Janssen et al. 2007; Hirche et al. 2008; Giovannini et al. 2009). These studies have an accuracy of 45–89 % for diagnosing malignancies. In a multicentre study including 13 European centres, Saftoiu et al. used an automated colour-hue cut-off measuring the mean colour hue in the lesion of interest over several image frames in a cine-loop. This resulted in a sensitivity of 93.4 % and a specificity of 66.0 % (Saftoiu et al. 2011). Generally, all studies end up with an acceptable sensitivity, but with a lower specificity. Cases of focal pancreatitis or microcystic adenomas may sometimes produce elastography images with low strain resembling malignant lesions, and thus make a clear cut-off between malignancies and benign lesions difficult in vivo.

3.4 Evaluation of Inflammatory Bowel Disease and Tumours in the GI Tract

For diagnostic purposes the distinction between inflammatory bowel disease (IBD) and tumours is of minor importance.

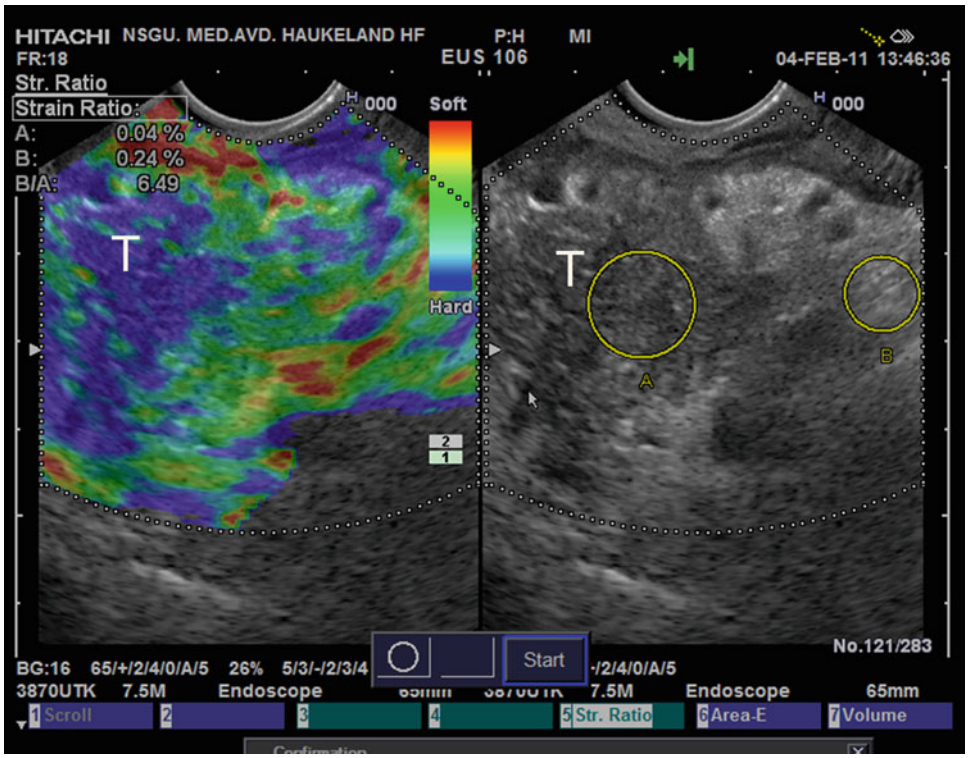

Fig. 4 Malignant tumour in the pancreas: In the *right panel*: a EUS B-mode image showing a hypoechoic tumour with irregular edges. In the *right panel* an elastogram shows low strain (*blue*) in the central parts of the tumour. A strain ratio was calculated between the reference (B) and tumour tissue (A). The strain ratio was: 6.49

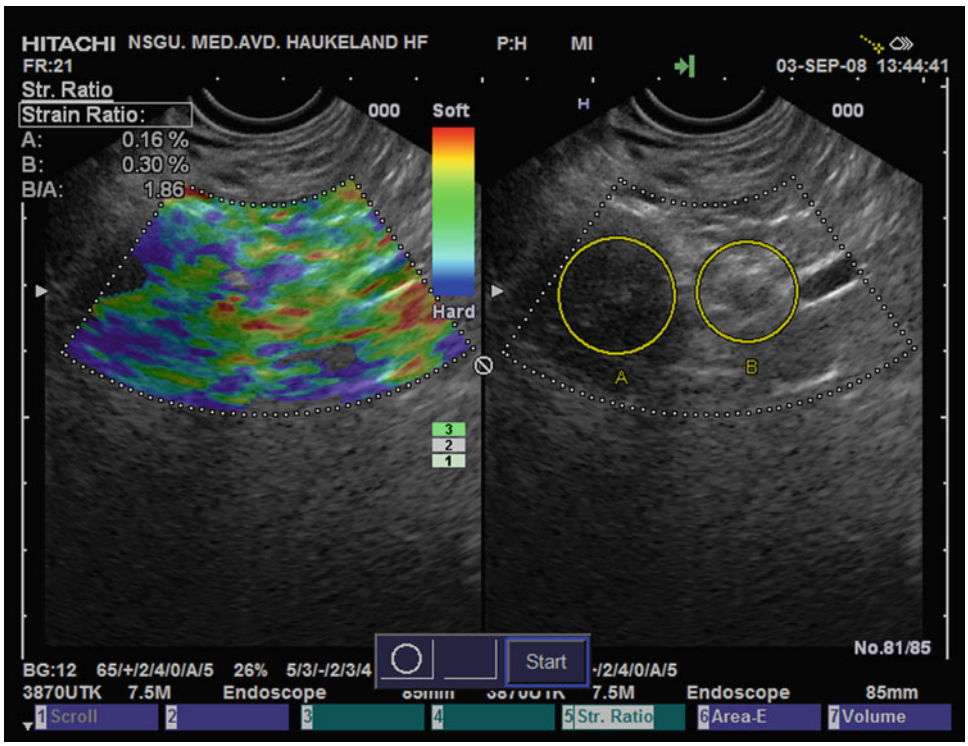

Fig. 5 Benign hypoechoic lesion in previous pancreatitis: In the *right panel*: EUS B-mode image of pancreatic tissue with a hypoechic focal lesion in a patient with previous acute pancreatitis. In *the left panel*, the hypoechoic area is imaged with predominantly *green colour*, and resembles the pancreatic reference tissue. The strain ratio was calculated between the reference tissue (B) and the tumour tissue (A) and was 1.86

The main objective for this modality in IBD is to serve as a clinical tool in follow-up, and possibly to predict relapses or enable imaging of the bowel wall providing information that can be used for treatment planning. Elastography has been used in a Crohn animal model (Kim et al. 2008) and clinically external elastography patterns have corresponded well to different classes of endoscopic disease grades (Ishikawa et al. 2011). An inflamed, thickened bowel wall in Crohn's disease may have resembling findings as neoplasias on high frequency ultrasonography, including gradual loss of the normal

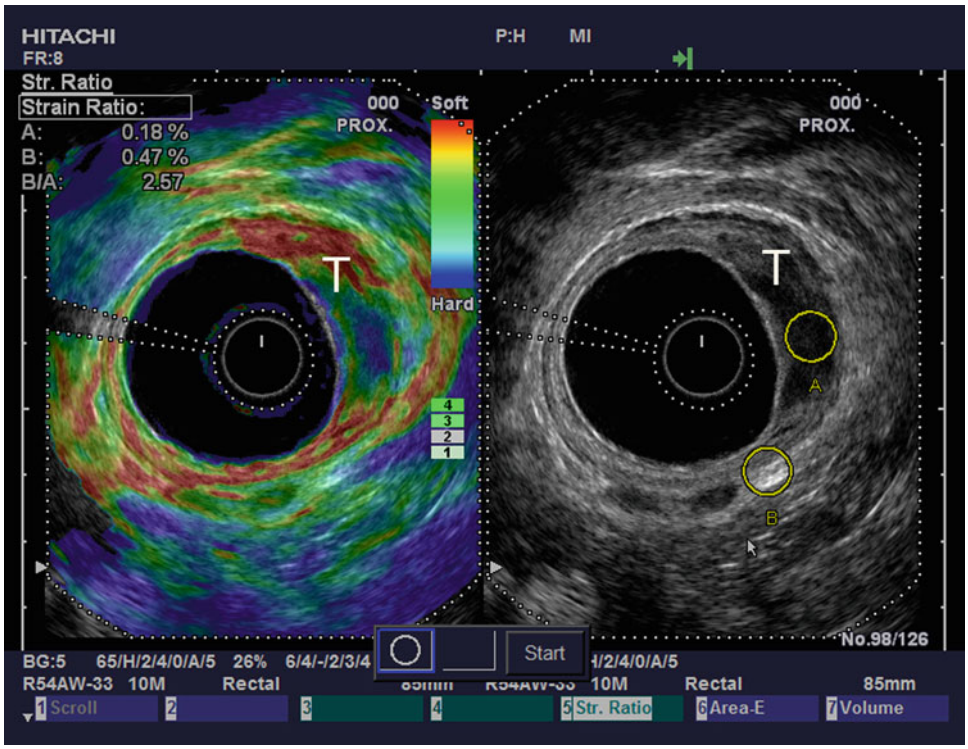

Fig. 6 Rectal cancer: A transrectal ultrasound probe is placed centrally with a water filled balloon that can exert pulsatile pressure in the rectal circumference. In the *right panel*: B-mode image with a tumour in the rectal wall (T). The normal structures of wall layers are not visible in the central part of tumour. In the *right panel*: The elastogram shows a central hard area within the tumour tissue (*blue*). A strain ratio was calculated between the reference and tumour tissue (*yellow circles B and A*): 2.57. Postoperative histology: Adenocarcinoma, tumour stage T2. (Courtesy of Dr. Jo Erling Riise Waage)

layered structure of the bowel wall. In an experimental study on strain imaging in surgical specimens from patients undergoing surgery with stricturing Crohn's disease and tumours in the bowel, we found lower strain in both malignant tumours and in Crohn's disease indicating harder tissue. There was no significant difference in strain ratio between Crohn's disease lesions and in adenocarcinomas. In a small number of benign tumours (adenomas) we found lower strain ratio (Havre et al. 2012). This finding has also been observed in vivo of adenomas and adenocarcinomas in the rectum (Waage et al. 2011).

3.5 Evaluation of Strain in the Gastric Wall

Calculation of relative strain of the muscle layer of the GI wall by Doppler ultrasonography is feasible. SRI enables detailed mapping of local strain distribution in the gastric wall. Radial strain measurements of the antrum enable distinction between the inner circular and the outer longitudinal muscle layers (Gilja et al. 2002) although it is not visible on the plain B-mode image. Strain levels in the different Migrating Motor Complex phases can be estimated by SRI. Erythromycin induces more frequent lumen-occlusive contractions both fasting and postprandially (Ahmed et al. 2009). Furthermore, ultrasound Strain Rate Imaging may discriminate between dyspepsia patients having "epigastric pain syndrome" or "postprandial distress syndrome" (Ahmed et al. 2012). Patients with "epigastric pain syndrome" have more powerful, and patients with "postprandial distress syndrome" have weaker antral contractions than healthy controls.

3.6 Evaluation of Rectal Tumours

The treatment options for rectal tumours are becoming increasingly tailored based on the tumour stage and the patient. Most rectal tumours are staged by MRI, but this method still lacks accuracy in staging rectal tumours $\leq$ T2 (Bipat et al. 2004; Tytherleigh et al. 2008). Endo Rectal ultrasonography (ERUS) with elastography is feasible to perform during an outpatient consultation preoperatively, and yields good results in distinguishing malignant tumours from adenomas (Figs. 6 and 7, Waage et al. 2011). This study of 68 consecutive patients by Waage et al. found sensitivity of ERUS with elastography of 93 %, specificity 95 % and accuracy: 94 % for detecting malignant lesions using a strain ratio cut-off of 1.25. This examination may prove to be very useful for the selection of patients to transanal microsurgery as an alternative to the standard total mesorectal excision (TME) (Worrell et al. 2004; Baatrup et al. 2007). For the lymph node evaluation there is still little data, but we have seen some cases were MRI indicated preoperative radiation therapy (N1), while ERUS with elastography correctly staged the patient as N0.

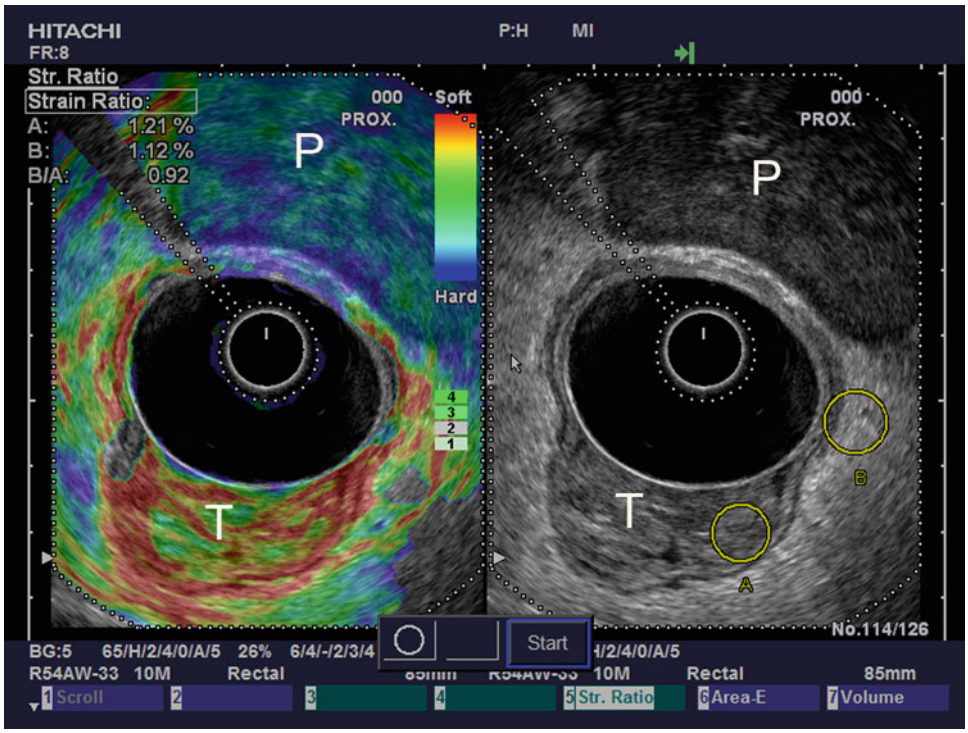

Fig. 7 Rectal adenoma: A transrectal ultrasound probe is placed centrally with a water filled balloon that can exert pulsatile pressure in the rectal circumference. In the right panel: B-mode image with a tumour within the rectal wall (T). In the *right panel*: The elastogram shows a soft representation of the whole tumour (*green and red*). A strain ratio was calculated between the reference and tumour tissue (*yellow circles B and A*): 0.92. Postoperative histology: broad-based adenoma. (Courtesy of dr. Jo Erling Riise Waage)

4 Summary and Further Reading

Strain and elasticity imaging is mainly based on either autocorrelation algorithms of echogenic elements in consecutive US frames or shear wave imaging. In gastroenterology, the imaging and measurements related to increasing liver fibrosis in chronic liver disease has been the most documented application so far. Individual patients may be followed with repeated non-invasive measurements of liver elasticity. Focal lesions along the GI tract may be imaged by transabdominal and EUS elastography. Characterisation of lymph nodes in the mediastinum and retroperitoneum has shown moderate results, inferior to the more invasive EUS-fine-needle aspiration method. For solid pancreatic lesions the method may provide additional diagnostic information. If a solid lesion is imaged with the same strain as the surrounding tissue or softer, it is an indication of a benign lesion. However, a number of benign lesions also produce low-strain lesions, so a hard lesion does not necessarily indicate malignancy. With refined technology and adapted transducers, this method may become an important imaging modality to supplement B-mode ultrasonography. In order to validate different technical solutions for clinical applications in gastroenterology, there is still a lot of research to be done.

5 Further Reading

Wells, P. N. Liang, H. D. Review: Medical ultrasound: imaging of soft tissue strain and elasticity. J R Soc Interface. 2011. Vol 8, No: 64 pages:1521–1549 (Wells and Liang 2011)

Acknowledgments We thank Dr. Jo Erling R. Waage for allowing us to include the images of Endorectal utrasound scanning with real-Time Elastography.

References

Ahmed AB, Gilja OH, Gregersen H, Odegaard S, Matre K (2006) In vitro strain measurement in the porcine antrum using ultrasound doppler strain rate imaging. Ultrasound Med Biol 32:513–522

Ahmed AB, Gilja OH, Hausken T, Gregersen H, Matre K (2009) Strain measurement during antral contractions by ultrasound strain rate imaging: influence of erythromycin. Neurogastroenterol Motil 21:170–179

Ahmed AB, Matre K, Hausken T, Gregersen H, Gilja OH (2012) Rome III subgroups of functional dyspepsia exhibit different characteristics of antral contractions measured by strain rate imaging. Ultraschall Med 134:A531

Baatrup G, Elbrond H, Hesselfeldt P, Wille-Jorgensen P, Moller P, Breum B, Qvist N (2007) Rectal adenocarcinoma and transanal endoscopic microsurgery. Diagnostic challenges, indications and short term results in 142 consecutive patients. Int J Colorectal Dis 22:1347–1352

Bavu E, Gennisson JL, Couade M, Bercoff J, Mallet V, Fink M, Badel A, Vallet-Pichard A, Nalpas B, Tanter M, Pol S (2011) Noninvasive in vivo liver fibrosis evaluation using supersonic shear imaging: a clinical study on 113 hepatitis C virus patients. Ultrasound Med Biol 37:1361–1373

Bercoff J, Tanter M, Fink M (2004) Supersonic shear imaging: a new technique for soft tissue elasticity mapping. IEEE Trans Ultrason Ferroelectr Freq Control 51:396–409

Bipat S, Glas AS, Slors FJ, Zwinderman AH, Bossuyt PM, Stoker J (2004) Rectal cancer: local staging and assessment of lymph node involvement with endoluminal US, CT, and MR imaging–a meta-analysis. Radiology 232:773–783

Castera L, Vergniol J, Foucher J, Le Bail B, Chanteloup E, Haaser M, Darriet M, Couzigou P, De Ledinghen V (2005) Prospective comparison of transient elastography, Fibrotest, APRI, and liver biopsy for the assessment of fibrosis in chronic hepatitis C. Gastroenterology 128:343–350

D'Onofrio M, Gallotti A, Salvia R, Capelli P, Mucelli RP (2011) Acoustic radiation force impulse (ARFI) ultrasound imaging of pancreatic cystic lesions. Eur J Radiol 80:241–244

Fraquelli M, Rigamonti C, Casazza G, Conte D, Donato MF, Ronchi G, Colombo M (2007) Reproducibility of transient elastography in the evaluation of liver fibrosis in patients with chronic liver disease. Gut 56:968–973

Friedrich-Rust M, Ong MF, Martens S, Sarrazin C, Bojunga J, Zeuzem S, Herrmann E (2008) Performance of transient elastography for the staging of liver fibrosis: a meta-analysis. Gastroenterology 134:960–974

Friedrich-Rust M, Wunder K, Kriener S, Sotoudeh F, Richter S, Bojunga J, Herrmann E, Poynard T, Dietrich CF, Vermehren J, Zeuzem S, Sarrazin C (2009) Liver fibrosis in viral hepatitis: noninvasive assessment with acoustic radiation force impulse imaging versus transient elastography. Radiology 252:595–604

Gennisson JL, Muller M, Deffieux T, Tanter M, Fink M (2009) Quantitative viscoelasticity mapping of human liver using supersonic shear imaging: preliminary in vivo feasability study. Ultrasound Med Biol 35:219–229

Gilja OH, Heimdal A, Hausken T, Gregersen H, Matre K, Berstad A, Odegaard S (2002) Strain during gastric contractions can be measured using Doppler ultrasonography. Ultrasound Med Biol 28:1457–1465

Giovannini M, Thomas B, Erwan B, Christian P, Fabrice C, Benjamin E, Genevieve M, Paolo A, Pierre D, Robert Y, Walter S, Hanz S, Carl S, Christoph D, Pierre E, Jean-Luc VL, Jacques D, Peter V, Andrian S (2009) Endoscopic ultrasound elastography for evaluation of lymph nodes and pancreatic masses: a multicenter study. World J Gastroenterol 15:1587–1593

Grubb NR, Fleming A, Sutherland GR, Fox KA (1995) Skeletal muscle contraction in healthy volunteers: assessment with Doppler tissue imaging. Radiology 194:837–842

Havre R, Waage JE, Leh S, Gilja OH, Ødegaard S, Baatrup G, Nesje LB (2012) Strain assessment in surgically resected inflammatory and neoplastic bowel lesions. Ultraschall in Med [Epub ahead of print:17, Nov]

Heimdal A (2005) Strain rate imaging—a new tool for studying the GI tract. In: Odegaard S, Gregersen H (eds) Basic and new aspects of gastrointestinal ultrasonography. World Scientific, Singapore, pp 243–263

Hirche TO, Ignee A, Barreiros AP, Schreiber-Dietrich D, Jungblut S, Ott M, Hirche H, Dietrich CF (2008) Indications and limitations of endoscopic ultrasound elastography for evaluation of focal pancreatic lesions. Endoscopy 40:910–917

Ishikawa D, Ando T, Watanabe O, Ishiguro K, Maeda O, Miyake N, Nakamura M, Miyahara R, Ohmiya N, Hirooka Y, El-Omar EM, Goto H (2011) Images of colonic real-time tissue sonoelastography correlate with those of colonoscopy and may predict response to therapy in patients with ulcerative colitis. BMC Gastroenterol 11:29

Janssen J, Schlorer E, Greiner L (2007) EUS elastography of the pancreas: feasibility and pattern description of the normal pancreas, chronic pancreatitis, and focal pancreatic lesions. Gastrointest Endosc 65:971–978

Kim K, Johnson LA, Jia C, Joyce JC, Rangwalla S, Higgins PD, Rubin JM (2008) Noninvasive ultrasound elasticity imaging (UEI) of Crohn's disease: animal model. Ultrasound Med Biol 34:902–912

Matre K, Ahmed AB, Gregersen H, Heimdal A, Hausken T, Odegaard S, Gilja OH (2003) In vitro evaluation of ultrasound doppler strain rate imaging: modification for measurement in a slowly moving tissue phantom. Ultrasound Med Biol 29:1725–1734

Moessner BK, Jorgensen TR, Skamling M, Vyberg M, Junker P, Pedersen C, Christensen PB (2011) Outreach screening of drug users for cirrhosis with transient elastography. Addiction 106:970–976

Muller M, Gennisson JL, Deffieux T, Tanter M, Fink M (2009) Quantitative viscoelasticity mapping of human liver using supersonic shear imaging: preliminary in vivo feasibility study. Ultrasound Med Biol 35:219–229

Ophir J, Alam SK, Garra B, Kallel F, Konofagou E, Krouskop T, Varghese T (1999) Elastography: ultrasonic estimation and imaging of the elastic properties of tissues. Proc Inst Mech Eng H 213:203–233

Ophir J, Cespedes I, Ponnekanti H, Yazdi Y, Li X (1991) Elastography: a quantitative method for imaging the elasticity of biological tissues. Ultrason Imaging 13:111–134

Palmeri ML, Frinkley KD, Zhai L, Gottfried M, Bentley RC, Ludwig K, Nightingale KR (2005) Acoustic radiation force impulse (ARFI) imaging of the gastrointestinal tract. Ultrason Imaging 27:75–88

Rockey DC (2008) Noninvasive assessment of liver fibrosis and portal hypertension with transient elastography. Gastroenterology 134:8–14

Roulot D, Costes JL, Buyck JF, Warzocha U, Gambier N, Czernichow S, Le Clesiau H, Beaugrand M (2011) Transient elastography as a screening tool for liver fibrosis and cirrhosis in a community-based population aged over 45 years. Gut 60:977–984

Saftoiu A, Vilmann P, Gorunescu F, Janssen J, Hocke M, Larsen M, Iglesias-Garcia J, Arcidiacono P, Will U, Giovannini M, Dietrich C, Havre R, Gheorghe C, McKay C, Gheonea DI, Ciurea T (2011) Accuracy of endoscopic ultrasound elastography used for differential diagnosis of focal pancreatic masses: a multicenter study. Endoscopy 43:596–603

Sporea I, Sirli RL, Deleanu A, Popescu A, Focsa M, Danila M, Tudora A (2011) Acoustic radiation force impulse elastography as compared to transient elastography and liver biopsy in patients with chronic hepatopathies. Ultraschall Med 32(Suppl 1):S46–S52

Talwalkar JA, Kurtz DM, Schoenleber SJ, West CP, Montori VM (2007) Ultrasound-based transient elastography for the detection of hepatic fibrosis: systematic review and meta-analysis. Clin Gastroenterol Hepatol 5:1214–1220

Tytherleigh MG, Ng VV, Pittathankal AA, Wilson MJ, Farouk R (2008) Preoperative staging of rectal cancer by magnetic resonance imaging remains an imprecise tool. ANZ J Surg 78:194–198

Waage JE, Havre RF, Odegaard S, Leh S, Eide GE, Baatrup G (2011) Endorectal elastography in the evaluation of rectal tumours. Colorectal Dis 13:1130–1137

Wells PN, Liang HD (2011) Medical ultrasound: imaging of soft tissue strain and elasticity. J R Soc Interface 8:1521–1549

Worrell S, Horvath K, Blakemore T, Flum D (2004) Endorectal ultrasound detection of focal carcinoma within rectal adenomas. Am J Surg 187:625–629

Transcutaneous Gastrointestinal Biopsy

Ilario de Sio, Luigi Castellano, Fulvia Terracciano, Luigi Maria Vitale, Marco Niosi, and Carmelina Loguercio

Contents

Abstract

Gastrointestinal tract lesions, both inflammatory and/ or neoplastic, may be visualized at ultrasound as "a target" or "bull's eye" lesion, or as a "pseudokidney" mass. Although the diagnosis of nature of gastrointestinal tract lesion is conventionally based on endoscopic biopsies, since 1981 many authors have reported the possibility to reach the diagnosis of gastrointestinal neoplasia by using an ultrasound-guided biopsy. This procedure has been performed using fine needles (i.e., Needles with an outer diameter <1 mm-20 gauge) of both the "cutting" or "non cutting" type and some authors have also used large (1,2 mm-18 gauge) cutting needles. Percutaneous ultrasound-guided biopsy of a gastrointestinal mass is performed when: the lesion is well visualized at ultrasound study; the lesion is endoscopically inaccessible (i.e., Small bowel lesion); the lesion is situated in the submucosa (i.e., Lymphoma) or develops in the subserosa. (i.e., Gastrointestinal stroma tumors-GIST); a previous biopsy during endoscopy is not diagnostic or only necrotic material is obtained; endoscopy cannot be performed or it is impossible to obtain an adequate biopsy sample due to presence of severe stenosis. The analysis of the literature data shows that percutaneous ultrasound-guided biopsy of gastrointestinal mass is a highly accurate procedure (80–100 %) with a very low complications rate (< 1 %).

I. de Sio (✉) · L. Castellano · L. M. Vitale
M. Niosi
Department of Internal Medicine and Gastroenterology, Ultrasonography Section, II University, Via S. Pansini, 5, 80131 Naples, Italy
e-mail: ilades@tiscalinet.it

F. Terracciano
Gastroenterology Unit, Ultrasonographic Section, Casa Sollievo della Sofferenza, S. Giovanni Rotondo, FG, Italy

C. Loguercio
Department of Internal Medicine and Gastroenterology, II University, Via S. Pansini 5, 80131 Naples, Italy

1 Introduction

Fine needle biopsies (FNBs) accomplished with ultrasound (US) and/or computed tomography (CT) guidance have been a widely accepted procedure in diagnosing abdominal and retroperitoneal space-occupying lesions (Droese et al. 1984; Memel et al. 1996). Compared with CT, US has been shown to be safer, more cost-effective and faster; moreover it does not require ionizing radiation and therefore, is not of any radiation risk to the patient or operator (Dodd et al. 1996;

G. Maconi and G. Bianchi Porro (eds.), *Ultrasound of the Gastrointestinal Tract*, Medical Radiology. Diagnostic Imaging,
DOI: 10.1007/174_2012_724,
Published Online: 22 August 2012

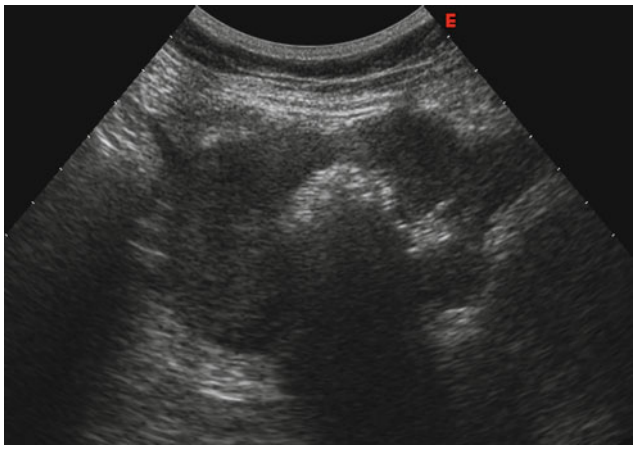

Fig. 1 The pseudo-kidney sign. The strong echogenic center (corresponding to the lumen content) is surrounded by an echo-poor rim (thickened bowel wall) in a case of colonic adenocarcinoma

Sheafor et al. 1998). Since 1975, guided FNBs have been performed mostly in solid abdominal and retroperitoneal organs such as liver, pancreas, spleen, kidney, and lymph node masses, with a high diagnostic accuracy, low complication rate (ranging from 0.05 to 0.23 % in multi-institutional and mono-institutional series, respectively) and a very low mortality rate (0.001–0.038 %). (Livraghi et al. 1983; Smith 1984, 1991; Fornari et al. 1989; Nolsoe et al. 1990).

Gastrointestinal tract lesions, both inflammatory and/or neoplastic, may be visualized by US as "a target" or "bull's eye" lesion, or as a "pseudokidney" mass (Figs. 1, 2) (Bluth et al. 1979; Fakhry and Berk 1981; Goerg et al. 1990; Lim 1996; Lutz and Petzoldt 1976; Morgan et al. 1980; Rapaccini et al. 1986; Schwerck et al. 1979). In particular, although the diagnosis of gastrointestinal tract tumor is conventionally based on biopsy performed during endoscopy, it is well known that biopsy of subserosal lesions or exophytic masses can give false negative results (Ballo and Guy 2001; Javid et al. 1999). In these cases, endoscopic ultrasound (EUS)-guided fine needle aspiration biopsy is the gold standard but this procedure is available in only few centers (Chen and Eloubeidei 2005). On the other hand, both endoscopy and EUS, when the lesion involves the colon, need adequate bowel preparation with the risk of water and electrolyte imbalance particularly in the elderly (Heriot et al. 1998). Moreover, small bowel lesions are not accessible by endoscopy and EUS and require capsule endoscopy (that does not allow biopsy) and/or double balloon enteroscopy, but both the techniques have some disadvantages (Fireman and Kapelman 2008; Ponsaing et al. 2007).

Since 1980, many authors have reported the possibility to reach the diagnosis of gastrointestinal neoplasia by using a US-guided FNB (Abbitt 1991; Allen and Irwin 1997; Ballo and Guy 2001; Bhaduri et al. 1999; Bree et al. 1991; Carson et al. 1998, Das and Pant 1994; Dodd et al. 1998; Marco-Domenech et al. 2001; Farmer et al. 2000; Green et al. 1988; Heriot et al. 1998; Ho et al. 2003; Javid et al. 1999; Ledermann et al. 2001; Shidham et al. 1998; Solbiati et al. 1986; Torp-Pedersen et al. 1984; Tudor et al. 1999). Sonographically guided fine needle aspiration biopsy of a bowel wall lesion was first performed in 1981 by Ennis and Mac Erlean (1981).

2 Indications and Contraindications

Percutaneous US-guided FNB of a gastrointestinal mass is performed mainly when:

1. The lesion is well visualized at US study;
2. The lesion is endoscopically inaccessible (i.e., localized between the ligament of Treitz and the ileocecal valve);
3. The lesion is situated in the submucosa (as frequently seen in gastrointestinal lymphoma), is intramural or develops in the subserosa (i.e., in gastrointestinal stromal tumors), and is thus not accessible by conventional endoscopic biopsy;
4. A previous biopsy during endoscopy or EUS is non-diagnostic or only necrotic material is obtained;
5. Endoscopy cannot be performed for uncooperative patients or for contraindications;
6. It is impossible to obtain an adequate biopsy sample during endoscopy due to presence of severe stenosis.

Contraindications are represented only by a severe coagulative impairment (i.e., platelet count $\leq$40000/mm^3; prothrombin time $\leq$40 %) and by distension of bowel loops.

3 Technique

Percutaneous FNBs are frequently performed under US guidance with a real-time convex transducer (3.5–5 MHz) by both a "free hand" technique and a biopsy-guide attachment. Fine needles (i.e., needles with an outer diameter <1 mm-20 gauge) of both the "cutting" or "non-cutting" type, are frequently used to obtain a cytological and/or histological diagnosis (Ballo and Guy 2001; Carson et al. 1998; Marco-Domenech et al. 2001; Ennis and Mac Erlean 1981; Green et al. 1988; Javid et al. 1999; Ledermann et al. 2001; Solbiati et al. 1986; Torp-Pedersen et al. 1984). Some authors have also used large (1.2 mm-18 gauge) cutting needles (Ballo and Guy 2001; Carson et al. 1998; Marco-Domenech et al. 2001; Farmer et al. 2000; Ledermann et al. 2001; Tudor et al. 1999). The use of large cutting needles has been experimentally demonstrated to be safe (Akan et al. 1998) and not associated to a mortality and/or morbidity increase (Marco-Domenech et al. 2001; Tudor et al. 1999). Patients must fast from the night prior to the biopsy and usually bowel preparation or

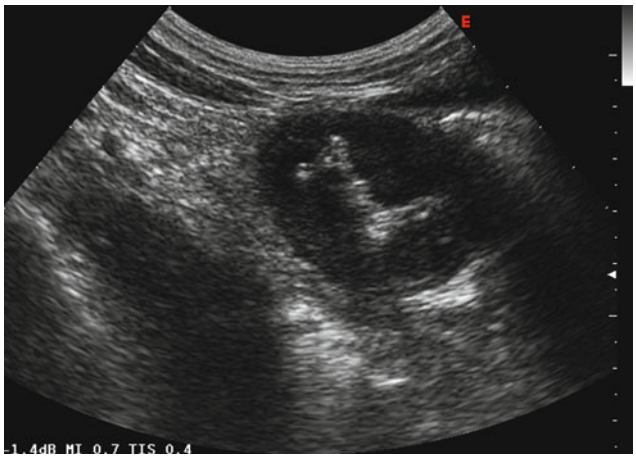

Fig. 2 The "target like" pattern in a case of small bowel lymphoma

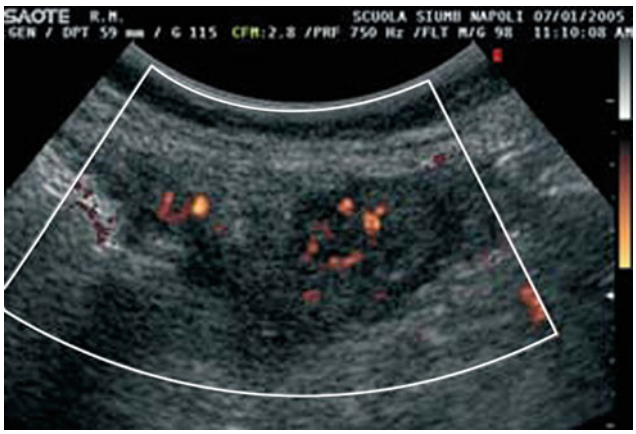

Fig. 3 Power Doppler of a diffuse thickened gastric wall shows clear vascular signals (to be avoided during biopsy)

antibiotic prophylaxis are not needed (Tudor et al. 1999). All patients sign a written informed consent. The procedure is usually performed on both an inpatient/outpatient basis (Ballo and Guy 2001) and often without local anaesthesia; however, some authors utilize local anaesthesia by infiltration of 5–10 ml of 1 % lidocaine hydrochloride into the abdominal wall by means of a 25-gauge needle (Ho et al. 2003; Tombesi et al. 2011). In many cases, color and power Doppler are useful to evaluate and avoid large vessels along the needle tract (Fig. 3) (Marco-Domenech et al. 2001; Ho et al. 2003). Briefly, percutaneous FNB is frequently performed by two operators, one holding the transducer and the second manipulating the needle. In "pseudokidney" lesions, it is important to place the needle in the hypoechoic rim, thus avoiding traversing of the echogenic center (Figs. 4, 5) which corresponds to the mucosa and the lumen of gastrointestinal loop. When a "non-cutting" needle is used, it is fitted to a 10–20 ml syringe attached to an aspiration piston, and is monitored while advancing in the lesion. When the tip of the needle (shown on the scan) is in the tumor wall, the piston is completely retracted and the needle is moved back and forth three or four times in the tumor (Torp-Pedersen et al. 1984).

When aspiration is completed, the negative pressure is equilibrated and the needle is withdrawn. After withdrawal of the needle, the syringe is disconnected, filled with air and reconnected and the material in the needle is expelled onto a glass slide and smeared. The specimen are then air-dried and fixed in ethanol; Papanicolau and May-Grunwald–Giemsa are the standard staining techniques used, while if a carcinoid tumor is suspected the Grimelius staining method is used (Solbiati et al. 1986).

When a "cutting-type" needle is used, the needle is advanced until lesion indentation is seen, then the trigger mechanism is fired and the needle is withdrawn, obtaining a histological sample (Fig. 5; Tudor et al. 1999).

Core-needle biopsy samples are fixed in formalin and embedded in paraffin wax; 3–4 μm-thick sections are cut and then stained with hematoxylin/eosin. Further immunohistochemical analysis of the material is then possible for specific indications requested. In all cases, the presence of a cytopathologist, to assess specimen adequacy during the procedure, would result in a high diagnostic outcome (Ballo and Guy 2001); however, if this is not possible, two needle punctures during the first session should be performed.

After the procedure is completed the outpatients are observed for 2 to 4 h in order to monitor eventual immediate complications such as persistent pain, fever, or bleeding at puncture site. Some authors prefer to perform an ultrasound control before discharging patients. In our Department we performed FNBs of gastrointestinal masses, with ultrasound guidance, by using a 3.5–5 MHz convex probe equipped with a biopsy device. All the procedures were performed in outpatients with no general or local anaesthesia and we used both large cutting and fine non-cutting needles (particularly in suspected lymphoma lesions in which we perform both a biopsy and cytofluorometry).

Ultrasound-guided FNBs (Ledermann et al. 2001) have been performed mostly in suspected primary or metastatic neoplastic gastrointestinal lesions, also in those patients with HIV infection (Bhaduri et al. 1999) in which gastrointestinal manifestations (such as opportunistic infections or lymphoproliferative or neoplastic disease) occur in about 50 % of the patients and endoscopic diagnosis is not possible due to the submucosal nature of the disease (Fig. 6).

4 Results

Table 1 summarizes the most important studies published on the use of FNBs of gastrointestinal wall lesions. Because of the relatively small population, and the absence of a clear gold standard in order to assess the true-negative and false-negative results, few data are available regarding sensitivity, specificity, and overall diagnostic accuracy of the procedure.

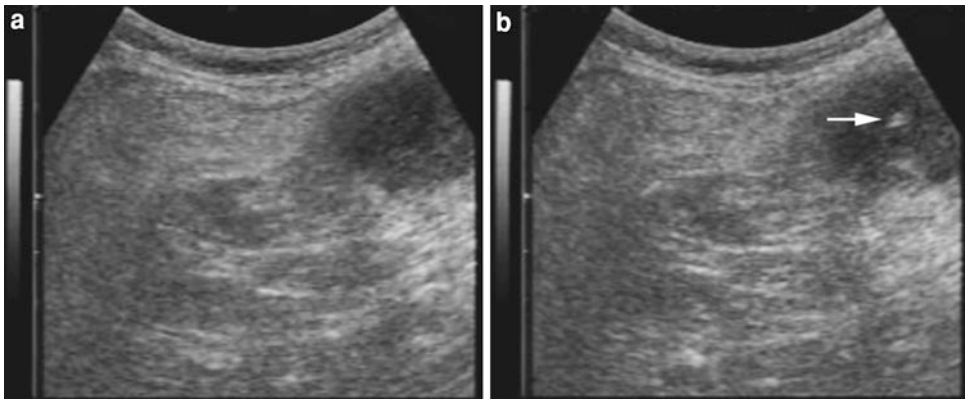

Fig. 4 **a** Transverse sonogram of abdomen showing gastric hypoechoic wall thickening. **b** Ultrasound-guided fine needle aspiration biopsy (non-cutting needle) of the lesion (*arrow* indicates the tip of the needle): cytological diagnosis of gastric adenocarcinoma

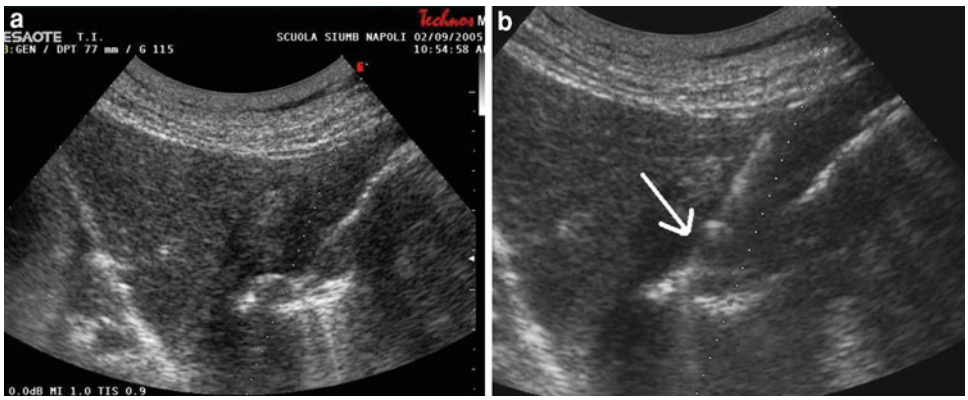

Fig. 5 **a** A diffuse thickening of the gastric wall (endoscopic biopsy resulted not diagnostic). **b** Ultrasound-guided needle biopsy with a cutting needle. The needle is well-visualized (*arrow*): histological diagnosis of undifferentiated carcinoma

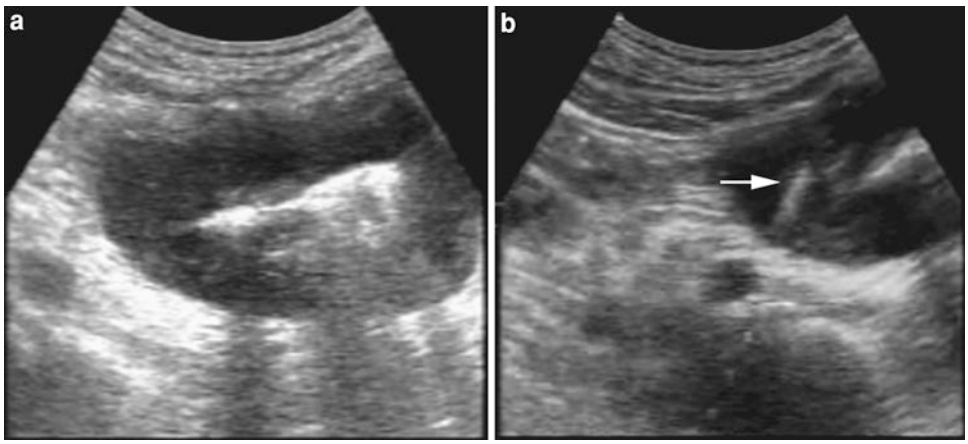

Fig. 6 **a** Small bowel wall involvement. **b** Ultrasound-guided fine needle biopsy of bowel wall involvement. The needle tip (*arrow*) is visible in the hypoechoic wall. Final diagnosis: small bowel lymphoma

When the data are reported, sensitivity, specificity, diagnostic accuracy, predictive positive value and predictive negative value are 90–91, 100 (no false-positive results), 80–100, 100, and 67 % respectively, thus equal to those obtained in other malignant abdominal diseases (Ballo and Guy 2001; Javid et al. 1999; Torp-Pedersen et al. 1984).

In a recent study by (Tombesi et al. 2011) on 45 cases, sensitivity, specificity, positive predictive value, negative predictive value, and overall diagnostic accuracy of the procedure were 97.5, 100, 100, 80, and 97.7 % respectively and, in 10 cases (22.2 %) US-guided biopsy made it possible to avoid unnecessary surgical exploration.

The procedure is well tolerated, no mortality has been reported and only five complications have been described following percutaneous US-guided FNBs of gastrointestinal tract lesions (one case of hemoperitoneum, one of sepsis, one of small parietal hematoma, one of bile peritonitis, and one of melena) (Marco-Domenech et al. 2001; Javid et al. 1999; Tudor et al. 1999; de Sio et al. 2010).

Patients with indications for percutaneous FNBs of gastrointestinal tract lesions are not commonly encountered. In fact, as reported by Solbiati et al. (1986), they represent only 1.5 % of all abdominal biopsies performed in the same period.

Table 1 Published studies on the use of percutaneous FNBs of gastrointestinal wall lesions

Reference	Number	Site	Needle type	Gauge	Complications
Ennis and Macerlean (1981)	7	B	NC		No
Torp-Pedersen et al. (1984)[a]	78	S-SB-C	NC	23	No
Solbiati et al. (1986)	24	S-SB-C	NC	22	No
Green et al. (1988)	3	S	NC	22	No
Das and Pant (1994)	78	S–C	NC		No
Carson et al. (1998)	44	S-SB-C	NC-C	18, 22	No
Tudor et al. (1999)	10	SB	C	18	Yes[d]
Bhaduri et al. (1999)	3	S-SB			No
Javid et al. (1999)[b]	50	C	NC	22	Yes[e]
Farmer et al. (2000)	12	S-SB-C	C	18	No
Marco-Domenech et al. (2000)	42	S-SB-C	C-NC	18, 21, 22	Yes[f]
Ballo and Guy (2001)[c]	20	S-SB-C	NC	18, 22	No
Ledermann et al. (2001)	7	SB-C	NC-C	18, 22	No
Tombesi et al. (2011)	45	S-SB-C	C	18, 20	No

S stomach, *SB* small bowel, *C* colon, *C* cutting type, *NC* non-cutting type

[a] Authors report a positive predictive value and a negative predictive value of FNB of 100, and 67 %, respectively

[b] Authors report a sensitivity and specificity of 91.8 and 100 %, respectively

[c] Authors report a diagnostic accuracy of 100 %

[d] One small hematoma

[e] One case of hemoperitoneum, one case of sepsis

[f] One case of bile peritonitis

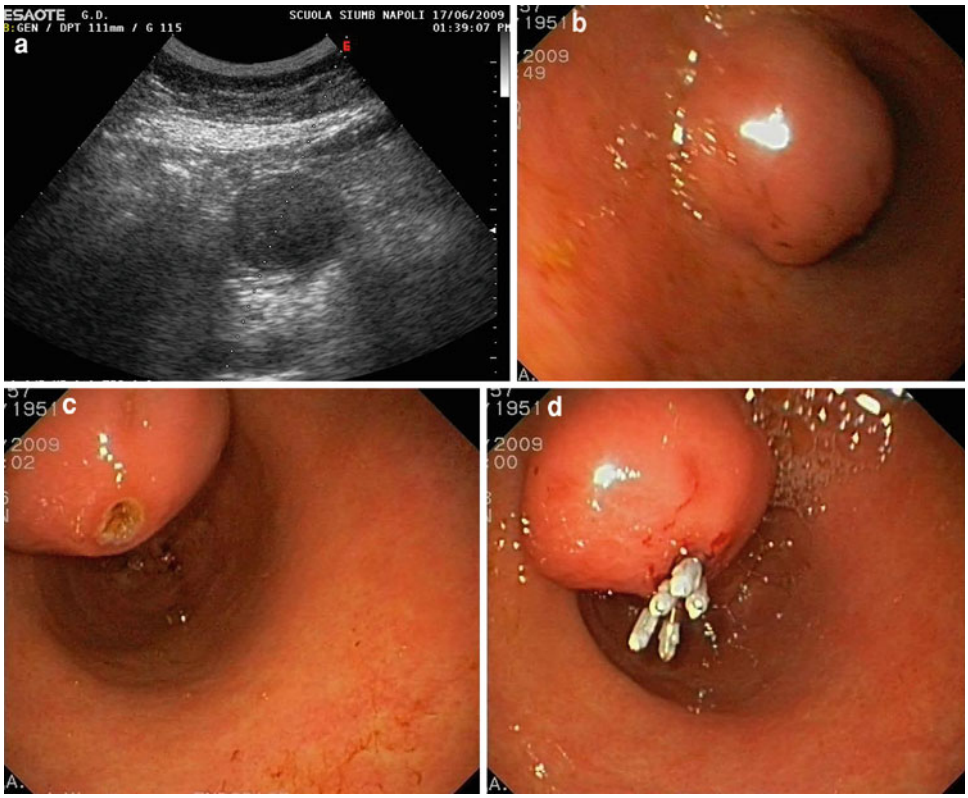

Fig. 7 **a** US appearance of gastric GIST; **b** endoscopic appearance of gastric GIST; **c** an ulcerative lesion is seen 24 h after percutaneous biopsy; **d** endoscopic treatment of the lesion with clips

Our experience is quite similar (unpublished data). In fact, US-guided FNBs of gastrointestinal masses represent only 1.7 % (114 out of 4750) of all abdominal US-guided FNBs over a 21 years period. We performed FNBs of the gastric wall in 38 cases [16 cases of gastric lymphoma, 12 cases of gastrointestinal stromal tumor (GIST), 10 cases of adenocarcinoma], of the colon-sigma in 40 cases (37 cases of adenocarcinoma, 1 case of endometriosis, 1 case of cancer-abscess, 1 case of duplication cyst) and of the small bowel in 36 cases (16 cases of lymphoma, 9 cases of GIST, 5 cases of adenocarcinoma, 5 cases of metastasis, 1 case of undifferentiated carcinoma). In all but one cases the specimen was adequate, final diagnosis was surgically confirmed in 73 cases, and complications occurred in one case (0.87 %) (melena after biopsy of a gastric GIST) (Fig. 7).

The indications to the procedure were impossibility to perform endoscopy in 28 cases, non-diagnostic endoscopic biopsies in 50 cases, and endoscopically inaccessible lesion in 36 cases. However, an alternative approach to diagnosis of gastrointestinal diseases may be needed in some cases; in particular when the lesion is clearly visible at ultrasound, US-guided FNB could be considered a simple, rapid, relatively noninvasive and accurate procedure.

References

Abbitt PL (1991) Percutaneous fine-needle aspiration of bowel wall abnormalities under ultrasonic guidance. J Clin Ultrasound 19:310–314

Akan H, Ozen N, Incesu L et al (1998) Are percutaneous transgastric biopsies using 14, 16 and 18 G Tru-Cut needles safe? An experimental study in the rabbit. Australas Radiol 42:99–101

Allen DC, Irwin ST (1997) Fine needle aspiration cytology of gastric carcinoma. Ulster Med J 66:111–114

Ballo MS, Guy CD (2001) Percutaneous fine-needle aspiration of gastrointestinal wall lesions with image guidance. Dyagn Cytopathol 24:16–20

Bhaduri S, Wiselka MJ, Rogers PM (1999) A review of ultrasound-guided percutaneous biopsy of gastrointestinal tract in HIV-infected patients. HIV Med 1:43–46

Bluth EI, Merrit CRB, Sullivan LA (1979) Ultrasonic evaluation of the stomach, small bowel and colon. Radiology 124:791–792

Bree RL, McGough MF, Schwab RE (1991) CT or US-guided fine-needle aspiration biopsy in gastric neoplasms. J Comput Assist Tomogr 15:565–569

Carson BW, Brown JA, Cooperberg PL (1998) Ultrasonographically guided percutaneous biopsy of gastric, small bowel and colonic abnormalities: efficacy and safety. J Ultrasound Med 17:739–742

Chen VK, Eloubeidei MA (2005) Endoscopic ultrasound-guided fine-needle aspiration of intramural and extraintestinal mass lesions: diagnostic accuracy, complication assessment and impact on management. Endoscopy 10:984–989

Das DK, Pant CS (1994) Fine needle aspiration cytologic diagnosis of gastrointestinal tract lesions. A study of 78 cases. Acta Cytol 38:723–729

de Sio I, Gravina AG, Federico A et al (2010) Incidental diagnosis of stromal tumor of the stomach by percutaneous ultrasound guided biopsy. J Gastrointestin Liver Dis 19:465–467

Dodd LG, Esola CC, Memel DS et al (1996) Sonography: the undiscovered jewel of interventional radiology. Radiographics 16: 1271–1288

Dodd LG, Nelson RC, Mooney EE et al (1998) Fine-needle aspiration of gastrointestinal stromal tumors. Am J Clin Pathol 109:439–443

Droese M, Altmannsberger M, Kehl A et al (1984) Ultrasound guided percutaneous fine needle aspiration biopsy of abdominal and retroperitoneal masses-accuracy of cytology in the diagnosis of malignancies, cytologic tumor typing and use of antibodies to intermediate filaments in selected cases. Acta Cytol 28:368–384

Ennis MG, Mac Erlean DP (1981) Biopsy of bowel wall pathology under ultrasound control. Gastointest Radiol 6:17–20

Fakhry JR, Berk RN (1981) The "target" pattern: characteristic sonographic feature of stomach and bowel abnormalities. AJR Am J Roentgenol 137:969–972

Farmer KD, Harries SR, Fox BM et al (2000) Core biopsy of the bowel wall: efficacy and safety in the clinical setting. AJR Am J Roentgenol 175:1627–1630

Fireman Z, Kapelman Y (2008) Small bowel capsule endoscopy: have we conquered the last frontier? Isr Med Assoc J 10:298–301

Fornari F, Civardi G, Cavanna L et al (1989) (1989) Complications of ultrasonically guided fine-needle abdominal biopsy. Scand J Gastroenterol 24:949–955

Goerg C, Schwerk WB, Goerg K (1990) Gastrointestinal lymphoma: sonographic findings in 54 patients. AJR Am J Roentgenol 155: 795–798

Green J, Katz S, Phillips G et al (1988) Percutaneous sonographic needle aspiration biopsy of endoscopically negative gastric carcinoma. Am J Gastroenterol 83:1150–1153

Heriot AG, Kurnar D, Thomas V et al (1998) Ultrasonically-guided fine needle aspiration cytology in the diagnosis of colonic lesions. Br J Surg 85:1713–1715

Ho LM, Thomas J, Fine SA et al (2003) Usefulness of sonographic guidance during percutaneous biopsy of mesenteric masses. AJR Am J Roentgenol 180:1563–1566

Javid G, Gulzar GM, Khan B et al (1999) Percutaneous sonography-guided fine needle aspiration biopsy of colonscopic biopsy negative colonic lesions. Indian J Gastroenterol 18:146–148

Ledermann HP, Binkert C, Frohlich E et al (2001) Diagnosis of symptomatic intestinal metastases using transabdominal sonography and sonographically guided puncture. AJR Am J Roentgenol 176:155–158

Lim JH (1996) Colorectal cancer: sonographic findings. AJR Am J Roentgenol 167:45–47

Livraghi T, Damascelli B, Lombardi C et al (1983) Risk in fine needle abdominal biopsy. JCU 11:77–81

Lutz H, Petzoldt R (1976) Ultrasonic patterns of space occupying lesions of stomach and intestine. Ultrasound Med Biol 133:677–680

Marco-Domenech SF, Gil-Sanchez S, Fernandez-Garcia P et al (2001) Sonographically guided percutaneous biopsy of gastrointestinal tract lesions. AJR Am J Roentgenol 176:147–151

Memel DS, Dodd GD, Esola CC (1996) Efficacy of sonography as a guidance technique for biopsy of abdominal, pelvic and retroperitoneal lymphnodes. AJR Am J Roentgenol 167:957–962

Morgan CL, Trought WS, Oddson TA et al (1980) Ultrasound patterns of disorders affecting the gastrointestinal tract. Radiology 135:129–135

Nolsoe C, Nielsen L, Torp-Pederson S et al (1990) Major complications and deaths due to interventional ultrasonography: a review of 8000 cases. J Clin Ultrasound 18:179–184

Ponsaing LG, Kiss K, Loft A et al (2007) Diagnostic procedures for submucosal tumors in the gastrointestinal tract. World J Gatroenterol 13:3301–3310

Rapaccini GL, Sabelli C, Caturelli E et al (1986) Real-time ultrasound as screening procedure in gastrointestinal tract disease. Ital J Gastroenterol 18:85–87

Schwerck W, Braun B, Dombrowsky H (1979) Real time ultrasound examination in the diagnosis of gastrointestinal tumours. J Clin Ultrasound 7:425–431

Sheafor DH, Paulson EK, Simmons CM et al (1998) Abdominal percutaneous interventional procedures: comparison of CT and US guidance. Radiology 207:705–710

Shidham VB, Weiss JP, Quinn TJ et al (1998) Fine needle aspiration cytology of gastric solitary fibrous tumor. A case report. Acta Cytol 42:1159–1166

Smith EH (1984) The hazards of fine-needle aspiration biopsy. Ultrasound Med Biol 10:629–634

Smith EH (1991) Complications of percutaneous abdominal fine-needle biopsy. Radiology 178:253–258

Solbiati L, Montali G, Croce F et al (1986) Fine-needle aspiration biopsy of bowel lesions under ultrasound guidance: indications and results. Gastointest Radiol 11:172–176

Tombesi P, Postorivo S, Catellani M et al (2011) Percutaneous ultrasonography-guided core needle biopsy of gastrointestinal lesions: what's its actual role in clinical practice? A retrospective study for safety and effectiveness. Ultraschall Med 32:S62–S67

Torp-Pedersen S, Gronval S, Holm HH (1984) Ultrasonically guided fine-needle aspiration biopsy of gastrointestinal mass lesions. J Ultrasound Med 3:65–68

Tudor GR, Rodgers PM, West KP (1999) Bowel lesions: percutaneous US-guided 18-gauge needle biopsy. Preliminary experience. Radiology 212:594–597

Part VI

Transperineal Ultrasound

Perianal Ultrasound Anatomy

Giovanni Maconi

Contents

Abstract

Transperineal is a non-invasive, simple and quick ultrasonographic procedure used for the examination of ano-rectal region. It may be performed with conventional probes, positioned directly above the anus. The absolute absence of invasiveness makes this examination well accepted by all patients, also by children and neonates. Other advantages of the procedure are the possibility to visualise perineal processes several centimetres from the rectal lumen, thus making transperineal ultrasound complementary to endoanal ultrasound to assess complex perianal fistulae. Being transperineal ultrasound a dynamic examination, it allows obtaining high-resolution images of the anal canal, the anal sphincters, pubo-rectal muscle, recto-vaginal and anovulvar septum, urinary bladder, prostate and vagina.

1 Introduction

Transperineal ultrasound has been initially proposed for the examination of ano-rectal region since 1983 in neonates with imperforate anus (Oppenhemier et al. 1983). Later, other studies have presented this procedure as a novel alternative to anal and vaginal endosonography and magnetic resonance imaging (MRI) to assess the anal canal structures, anal sphincters and perirectal space in pregnant patients (Hertzberg et al. 1991; Campbell et al. 1996) and young children (Teele et al. 1997).

It is a completely non-invasive, simple and relatively quick examination, usually performed with conventional ultrasonographic probes, and well tolerated and accepted by all patients, also by children and neonates.

Transperineal sonography shares some advantages with transanal ultrasound such as low-cost, high-resolution, multiplanar and real-time performance. However, it has also some limitations, such as inadequate visualisation of tissues

G. Maconi (✉)
Department of Gastroenterology, "L. Sacco" University Hospital, Via G. B. Grassi 74, 20157 Milano, Italy
e-mail: giovanni.maconi@unimi.it

G. Maconi and G. Bianchi Porro (eds.), *Ultrasound of the Gastrointestinal Tract*, Medical Radiology. Diagnostic Imaging,
DOI: 10.1007/174_2013_826, © Springer-Verlag Berlin Heidelberg 2013
Published Online: 21 March 2013

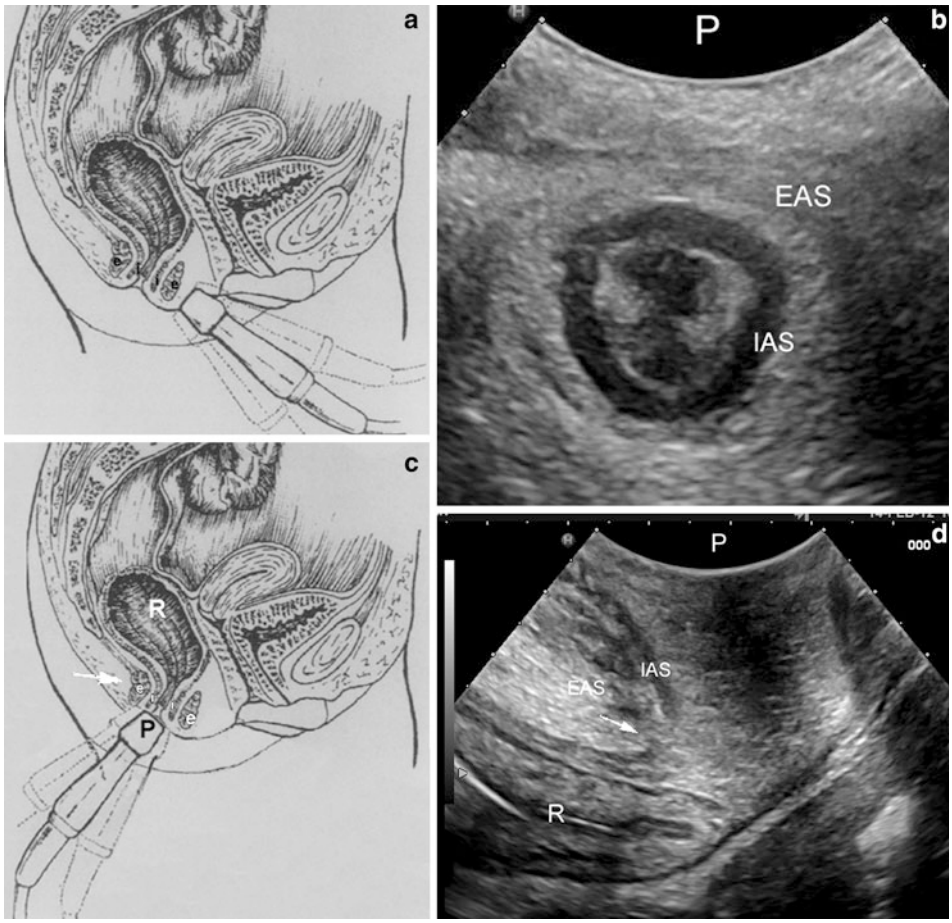

Fig. 1 Transperineal ultrasound. Technical approach (left panel; Figures a, c) and correspondent findings (right panel, Figures b, d). With patient position is dorsal or left lateral position, the transducer is placed directly on perineal body. Transducer is pressed posteriorly and angled cranially-to-caudally, to obtain a cross sectional view, mainly in women (a, b) or placed on the perineum to obtain a long axis view (c, d). In both sections, internal anal sphincter (IAS or i) and external anal sphincter (EAS or e) appears as a hypoechoic ring and as a tissue of mixed echogenicity like in anorectal ultrasound. P: probe; R: rectum; arrow: ano-rectal angle

that are far from the probe due to the limited penetration of the ultrasonic beam (usually <5–6 cm), and the potential interference of air entrapped in skin folds and skin tags, and protruding anal tumours, which hampers the quality of images. In comparison with trans-anal ultrasound, trans-perineal sonography has the advantage to visualise peri-rectal and perineal processes several centimetres from the rectal lumen (enabled by multiple windows).

Despite learning curve in performing this examination is not known, it has been recognised that most experienced abdominal sonographers achieve competency in performing transperianal ultrasound after approximately 12 patients (Stewart et al. 2001).

2 Examination Technique

Transperineal sonography may be performed using available transducers that most sonography practices already own. In particular, 3.5–7 MHz microconvenx or transvaginal arrays, but also linear, curved or sector transducers operating at the highest frequency, can be used. The probes are covered with gel and introduced into a latex examination glove or a condom, for hygienic reasons, which are covered with contact gel before the examination is performed.

The exam may be performed without specific preparation of the patients, such as enema or evacuation suppositories. However, preparation may be appropriate for dynamic evaluation when squeezing and straining are requested to the patients and in patients with faecal incontinence.

For the examination, the patient can be placed in the dorsal lithotomy position or in left lateral position, before positioning the probe directly above the anus. In patients with perianal fistulae, the probe can be also placed directly on the external orifice, to follow the fistula course up to its internal opening.

3 Perianal Ultrasound Anatomy

Standard images are obtained from axial and longitudinal viewpoints on the perineal body, above the anus. Additional oblique images and angled images are obtained as needed to outline the anatomy and pathology (Fig. 1).

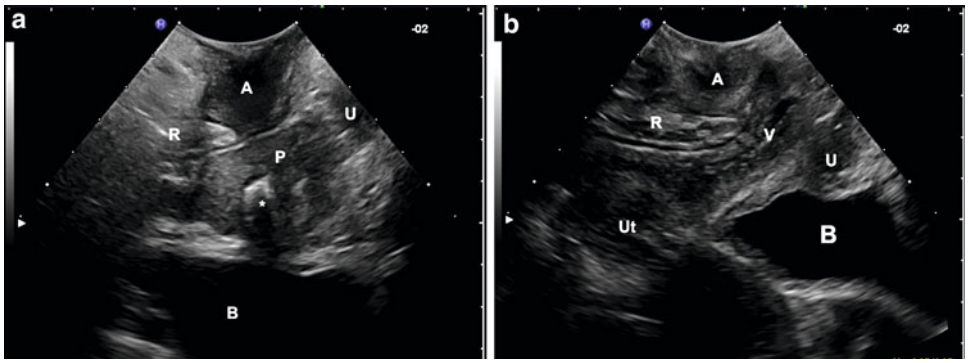

Fig. 2 Longitudinal transperineal scan allowing the simultaneous visualisation of the anus (*A*), Rectum (*R*), distal part of the urinary bladder (*B*), and prostate (*P*) and proximal art of the urethra (*U*) in men (**a**), and uterus (*Ut*), vagina (*V*) and urethra (*U*) in women (**b**). *asterisk,* prostatic calcification

In this way, it is possible to obtain high-resolution images of the anal canal, the anal sphincters, pubo-rectal muscle, recto-vaginal and anovulvar septum, urinary bladder, prostate and vagina. Internal anal sphincter is the terminal condensation of the circular rectal smooth muscle. It is seen as an approximately 3-mm thick hypoechoic symmetric band (Fig. 1) sometimes demarcated from heterogeneous subepithelial tissues medially. The surrounding mixed-echogenicity striated external sphincter is slightly thicker, extends approximately 1 cm beyond the internal anal sphincter (Fig. 1). It is a circular structure, shorter anteriorly in women. The deep part of the external anal sphincter is fused with or intimately related to the puborectalis muscle. Anteriorly it is closely related to the superficial transverse muscle of the perineum and perineal body. The external anal sphincter shows a fibrillar pattern of fine parallel hyperechoic lines in proximal third of the anal canal (deeper part of external anal sphincter) which become more homogeneous at distal third of the anal canal (superficial or subcutaneous part of external anal sphincter). Besides anal sphincter complex transperineal ultrasound allows the simultaneous visualisation of the distal part of the urinary bladder and prostate and proximal art of the urethra in men, and uterus, vagina and entire urethra in women (Fig. 2).

References

Campbell DM, Behan M, Donnelly VS et al (1996) Endosonographic assessment of postpartum anal sphincter injury using a 120 degree sector scanner. Clin Radiol 51:559–561

Hertzberg BS, Bowie ID, Weber TM et al (1991) Sonography ofthe cervix during the third trimester of pregnancy: value of the transperineal approach. Am J Roentgenol 157:73–76

Oppenheimer DA, Carroll BA, Shochat SJ (1983) Sonography of imperforate anus. Radiology 148:127–128

Stewart LK, McGee J, Wilson SR (2001) Transperineal and transvaginal sonography of perianal inflammatory disease. AJR Am J Roentgenol 177:627–632

Teele RL, Share JC (1997) Transperineal sonography in children. Am J Roentgenol 168:1263–1267

Perianal Fistulae and Abscesses

Giovanni Maconi

Contents

Abstract

Perianal fistulae and abscesses are debilitating conditions, frequently encountered in clinical practice. Perianal fistulae are classified according to their nature and their anatomical course relative to the anal sphincter complex. This is mandatory for the proper management, since incorrect or inappropriate treatment may lead to irreversible functional consequences and recurrence of the fistula. The main imaging modalities in the assessment of perianal fistulae are transanal ultrasound and magnetic resonance imaging. Transperineal ultrasound has been proposed as an alternative diagnostic tool and as a non-invasive and cheap technique to monitor perianal lesions during treatment. Perineal fistulae can be detected by transperineal ultrasound as hypoechoic tracts, sometimes with air within, between the anus or rectum and the perianal skin or vagina and are correctly classified in most patients.

1 Introduction

Perianal fistulae and abscesses are debilitating conditions, frequently encountered in clinical practice. Both these lesions share a common pathogenetic mechanism, originating from a cryptoglandular infection in the anal canal. In fact, it is believed that infection of intersphincteric glands results in an intersphincteric abscess if the draining duct is blocked by infected debris. This abscess may resolve by means spontaneously drainage into the anal canal or progress to an acute anorectal abscess that subsequently develops a perianal fistula in most cases. Abscesses may extend in perianal space and deeper in ischiorectal, intersphincteric and supraelevator spaces presenting with fever, perianal or deep-seated rectal pain, tenderness, erythema and a fluctuant mass, but normal external findings are also possible. Anorectal abscesses may result, in a perianal

G. Maconi (✉)
Department of Gastroenterology, L. Sacco University Hospital, Milan Italy, Via G. B. Grassi 74, 20157 Milan, Italy
e-mail: giovanni.maconi@unimi.it

G. Maconi and G. Bianchi Porro (eds.), *Ultrasound of the Gastrointestinal Tract*, Medical Radiology. Diagnostic Imaging,
DOI: 10.1007/174_2013_827, © Springer-Verlag Berlin Heidelberg 2013
Published Online: 16 March 2013

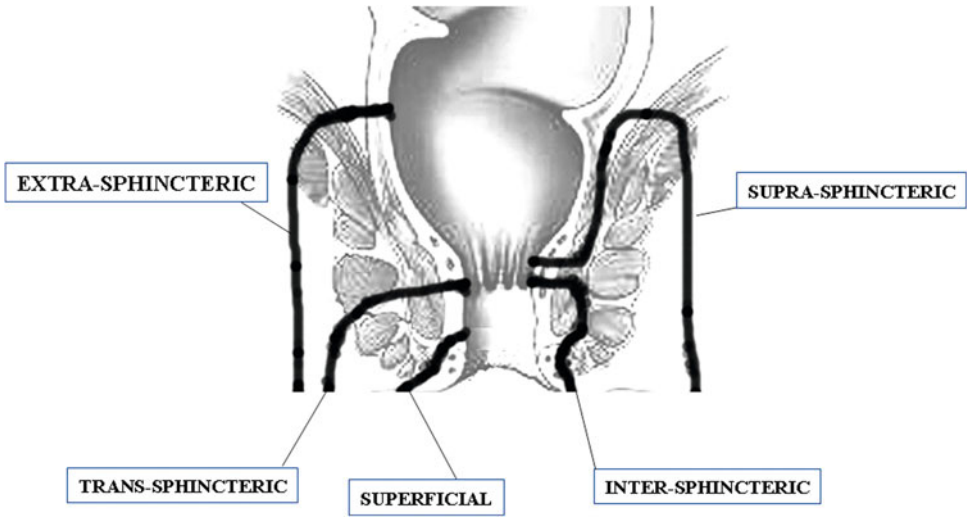

Fig. 1 Parks' classification of perianal fistulae

fistula in 30–50 % of patients. The fistula is an abnormal tract formed between the anus and perianal skin, characterised by persistent purulent drainage or intermittent perianal swelling and tenderness followed by spontaneous discharge. Perianal fistulae can be classified according to their nature and their anatomical course relative to the sphincter complex. In particular, perianal disease includes two main types of fistulae: cryptoglandular fistulae, the most common type of perianal fistula, representing up to 90 % and originating form an infection of the cryptoglandular gland and fistulae associated with inflammatory bowel disease, mainly Crohn's disease (Morgan and Thompson 1956; Parks et al. 1976; Eisenhammer 1978; Sloots et al. 2001).

According to their anatomical course, relative to the sphincter complex, perianal fistulae are classified using Parks criteria in: intersphincteric, transsphincteric, suprasphincteric, and extrasphincteric (Fig. 1) (Parks et al. 1976). However, perianal fistulae are also classified as "simple" or "complex". Simple fistulae include low transsphincteric and intersphincteric fistulae that cross < 30 % of the external sphincter. Complex fistulae include high transsphincteric fistulas with or without a high blind tract, suprasphincteric and extrasphincteric fistulae, horseshoe fistulae, and those associated with inflammatory bowel disease, radiation, malignancy, preexisting incontinence or chronic diarrhoea.

The treatment of perianal fistulae may be medical or surgical. It depends mainly on the nature and course of fistulae and the presence of abscesses. Cryptoglandular fistulae usually are primarily treated by surgery, whilst patients with Crohn's disease are treated with antibiotics, immunosuppressive agents or anti-tumour necrosis factor alpha, but after have ruled out the presence of abscesses.

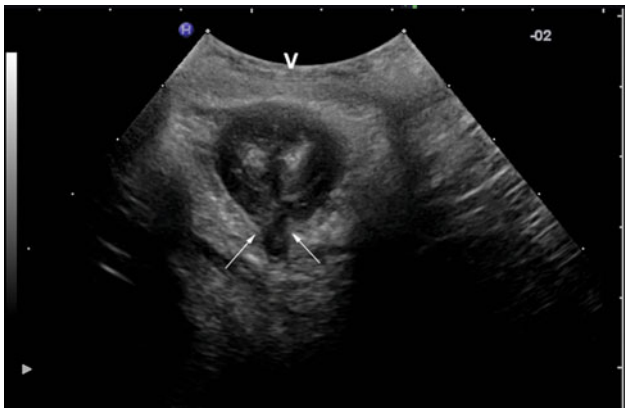

Fig. 2 Transperineal internal opening assessment. Internal opening (*arrows*) clearly appears at 6 o'clock as hypoechoic focus in the intersphincteric space that abuts the internal sphincter and crosses the submucosal layer of anal canal. *V*: vagina

Therefore, accurate diagnosis of these lesions is mandatory for the proper management, since incorrect or inappropriate treatment may lead to irreversible functional consequences and recurrence of the fistula.

To date, the main imaging modalities in the management of patients with perianal fistulae are transanal ultrasound and magnetic resonance imaging (MRI). Transperineal ultrasound has been proposed when these diagnostic tools are contraindicated, not appropriate or not available, and as a non-invasive and cheap technique to monitor perianal lesions during treatment.

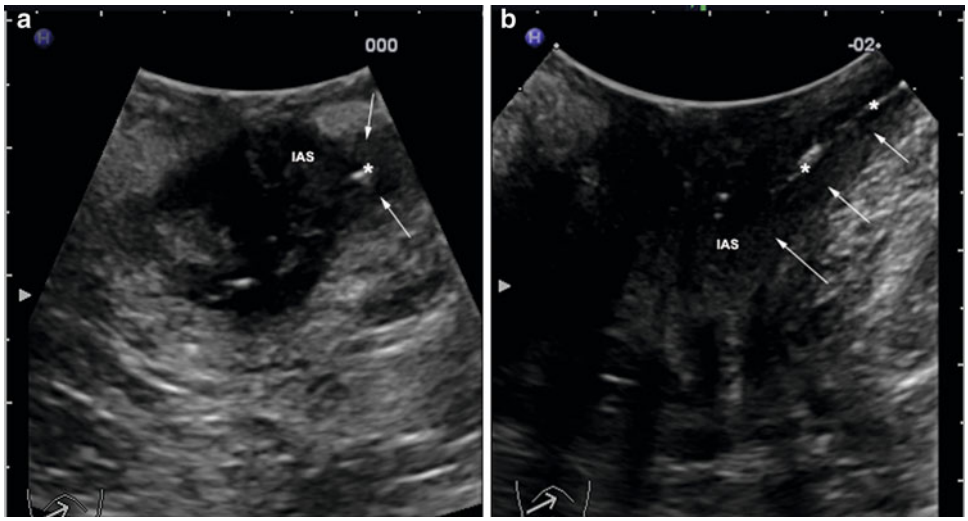

Fig. 3 Intersphincteric fistula (*arrows*) in a young woman detected by a cross sectional (**a**) and by longitudinal (**b**) transperineal scans. The fistula is visualised as hypoechoic area (**a**) or tract (**b**) containing gaseous hyperhecoic spots (*asterisks*), within or closer to internal anal sphincter (*IAS*)

2 Transperineal Ultrasound

Transperineal ultrasound is a simple, non invasive and cheap technique, to study the pelvis and perianal inflammatory diseases. It is an alternative to MRI or transanal ultrasound when, for various reasons, these are contraindicated or not appropriate, in particular in children and patients with anal strictures, painful perianal abscesses or lesions extending far from the anus and not accessible to transrectal ultrasound (e.g. in gluteus or in the scrotum). For these reasons, being perianal ultrasound performed with conventional probes, may be also used as readily available adjunct imaging procedure in patients with incomplete or dubious findings in previous examinations.

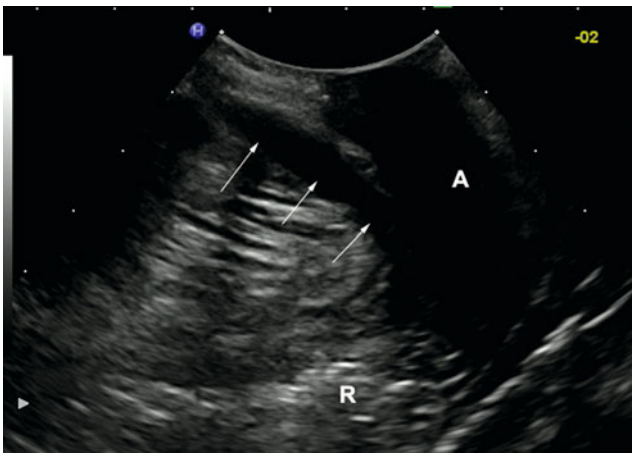

Fig. 4 Trans-sphincteric fistula detected by a longitudinal transperineal scan. The fistula, visualised as hypoechoic tract (*arrows*), arises for the posterior side of the anorectal junction and crosses the external anal sphincter. *R*, rectum; *A*, anus

2.1 Sonographic Features

Perineal fistulae can be detected by transperineal ultrasound as hypoechoic tracts, sometimes with air within, between the anus or rectum and the perianal skin or vagina (Stewart et al. 2001; Mallouhi et al. 2004; Wedemeyer et al. 2004; Zbar et al. 2006; Domkundwar and Shinagare 2007). Transperineal ultrasound also can indentify the site internal opening of the fistulae and enable a description of their anatomical course, providing a correct classification according to the Parks criteria. Internal opening may be revealed as a hypoechoic focus in the intersphincteric space that abuts the internal sphincter, often with a small corresponding defect in the internal sphincter. The site of internal opening may be assessed with a sensitivity ranging from 90 to 95 %. (Fig. 2; Wedemeyer et al. 2004; Zbar et al. 2006; Domkundwar and Shinagare 2007).

Regarding the classification of perianal fistulae, intersphincteric fistulae are visualised as hypoechoic tract within or closer to internal sphincter (Fig. 3).

Transsphincteric fistulae appear as hypoechoic tracts that cross the external sphincter (Fig. 4). Extensions of these fistulae may be revealed as hypoechoic fluid collections and intersphincteric horseshoe extension that may be imaged by transverse scan (anterior translabial scans in women) or as ovoid lesions just posterior to the anorectal junction (Fig. 5). Ischioanal or supralevator extensions and abscesses may be imaged as collection or hypoechoic extensions or masses beyond the external sphincter and elevator anii (Fig. 6). Rectovaginal or anovulvar fistulae can be imaged as hypoechoic areas or tracks between rectum or anus and vagina or vulva (Fig. 7).

Transperineal ultrasound can provide the correct classification of perianal fistulae according to the Parks criteria

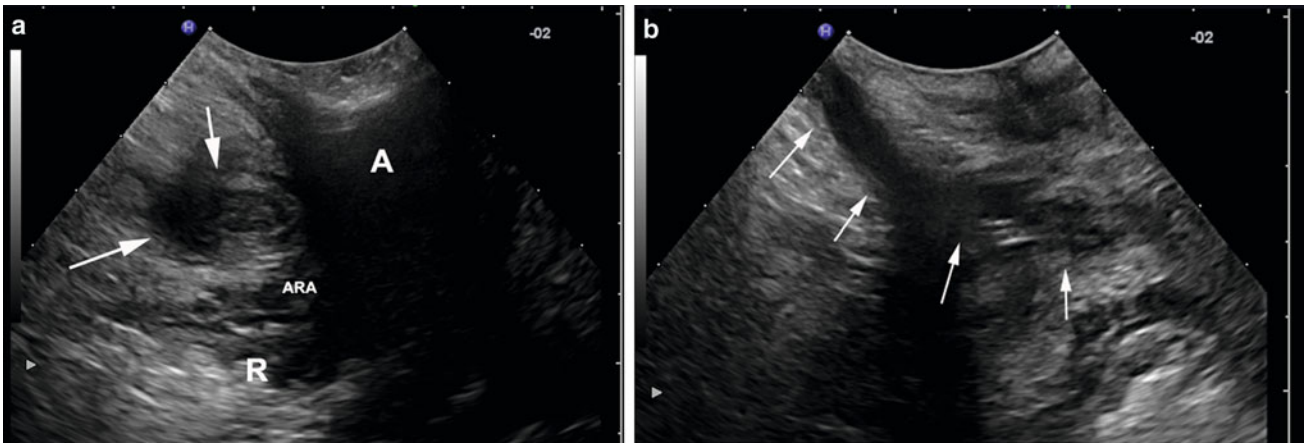

Fig. 5 Longitudinal (**a**) and transversal (**b**) perianal sonographic cross-sections of a transsphincteric fistula with left horseshoe extension (*arrows*). *A*, anus; *R*, rectum, *ARA*, anorectal angle

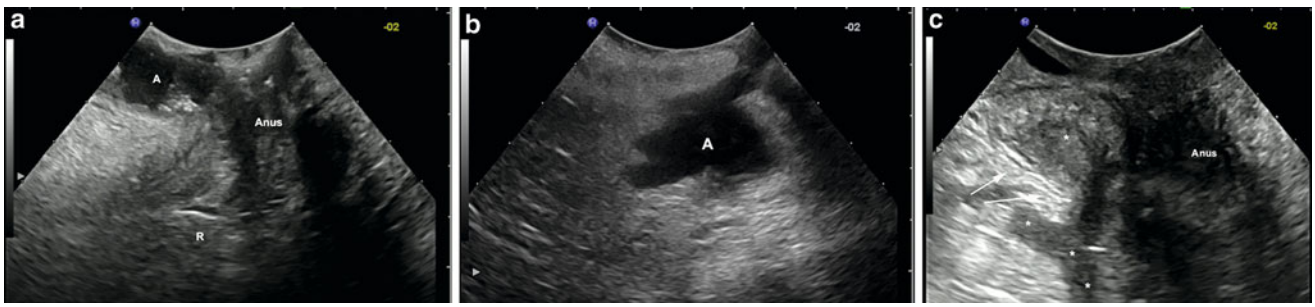

Fig. 6 Ischioanal abscesses (**a**, **b**) detected by transperineal scans as hypoechoic or anechoic areas sometimes with inhomogeneous or gaseous content (*A*) extending beyond the external sphincter. **c**, Complex perianal Crohn's disease with a large perianal abscess (*asterisks*) extending beyond the elevator anii (*arrows*)

with sensitivity greater than 85 % (Maconi et al. 2007). To enhance the fistula course and its ramifications a contrast agent, such as hydrogen peroxide, can be injected into the external orifice (Fig. 8), as already in use with endoanal ultrasound (Sloots et al. 2001).

Besides the classification of perianal fistulae and the detection of extensions and complications, transperineal ultrasound can suggest the fistulae nature. However, the possibility to distinguish cryptoglandular fistulae from those complicating inflammatory bowel diseases may be difficult and, to date, it has been mainly investigated by transanal ultrasound. In fact, the course and the sonographic appearance of cryptoglandular fistulae are different from those of Crohn's fistula (Coremans et al. 2003; Blom et al. 2011; Zawadzki et al. 2012; Zbar et al. 2012).

Cryptoglandular fistulae present more frequently with posterior external and internal openings because anal glands are more abundant in this site, and develop as a simple single primary tract (Coremans et al. 2003). However, recurrent and operated cryptoglandular fistulae may result in ramifications and extensions that branch away from the primary tract, by penetrating and involving muscles of the

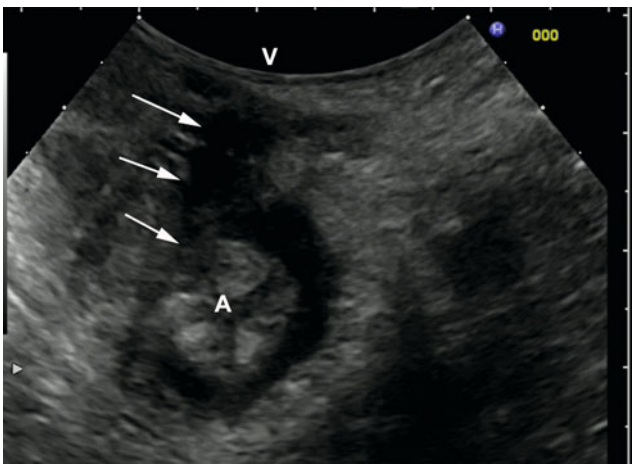

Fig. 7 Rectovaginal fistula detected by a cross-sectional, translabial, perineal scan, as a hypoechoic tract (*arrows*) between the vagina (*V*) and the anus (*A*)

anal sphincter and surrounding tissues in intersphincteric, ischioanal and pararectal or supralevator spaces, resembling those of Crohn's disease. The morphology of these

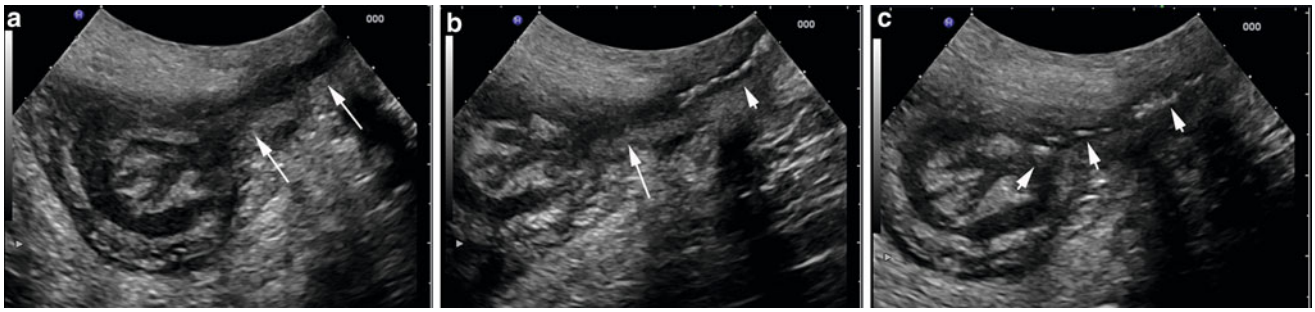

Fig. 8 Assessment of transsphincteric fistula (*long arrows*) assessed before (**a**) and after injection of contrast agent (hydrogen peroxide) into the external orifice. After hydrogen peroxide injection, the detection of contrast (*short arrows*) within the fistula (**b**) up to the anus (**c**), confirm the patency of the fistula and correctly reveals the site of the internal opening

extensions may suggest fistulous tracts or abscesses. The ischioanal fossa is the commonest site for extensions, but also the intersphincteric extension, along the horizontal plan also known as "horseshoe", is frequent (Coremans et al. 2003). On the other hand, there are fistulae in Crohn's patients that are successfully treated with means designed for ordinary cryptoglandular fistulae.

Several endoanal sonographic features of the fistulae, namely the presence of the fistulous debris or hyperechoic secretions, bifurcations and extension, cross-sectional width $\geq$ 3 mm and the presence of a hypoechogenic rim with a surrounding hyperechoic region around abscesses and fistulae, have been suggested to discriminate their Crohn's from cryptoglandular nature (Zawadzki et al. 2012; Blom et al. 2011). A recent study by Zbar et al. (2012) showed these signs are reproducible and have a high specificity but poor sensitivity, mandating endoscopy in those patients without a known diagnosis of Crohn's disease.

2.2 Assessment of Activity and Follow-up

Transperineal ultrasound may be also useful for the follow-up of perianal fistulae in Crohn's disease, in particular to assess response and occurrence of abscesses during the treatment (Rasul et al. 2003). It has been shown that sonographic appearance of perianal fistulae in Crohn's disease is correlated with clinical activity and may be assessed to evaluate the effectiveness of medical therapy with anti-tumour necrosis factor alpha (Losco et al. 2009; Rasul et al. 2003). In particular, low echogenicity of perianal fistulae is suggestive of active fistulae (Losco et al. 2009) and attenuation of echogenicity as well as the disappearance of the fistula track is associated with favourable outcome and persistent closure of fistula tracts (Rasul et al. 2003). Moreover, the regular assessment of perianal fistulae by transperineal ultrasound during treatment with infliximab may identify unsuspected fluid collections. Therefore, despite other studies should be performed on this topic, it seems that transperineal ultrasound may be used as simple, readily available and cheap tool to evaluate the behaviour of perianal fistulae during biological therapy, to stop the treatment in the event of abscess occurrence and, in patients with complete healing, it might allow to discontinue infliximab maintenance therapy with a lower risk of relapse.

References

Blom J, Nyström PO, Gunnarsson U, Strigård K (2011) Endoanal ultrasonography may distinguish Crohn's anal fistulae from cryptoglandular fistulae in patients with Crohn's disease: a cross-sectional study. Tech Coloproctol 15:327–330

Coremans G, Dockx S, Wyndaele J, Hendrickx A (2003) Do anal fistulas in Crohn's disease behave differently and defy Goodsall's rule more frequently than fistulas that are cryptoglandular in origin? Am J Gastroenterol 98:2732–2735

Domkundwar SV, Shinagare AB (2007) Role of transcutaneous perianal ultrasonography in evaluation of fistulas in ano. J Ultrasound Med 26:29–36

Eisenhammer S (1978) The final evaluation and classification of the surgical treatment of the primary anorectal cryptoglandular intermuscular (intersphinteric) fistulous abscess and fistula. Dis Colon Rectum 21:237–254

Losco A, Viganò C, Conte D et al (2009) Assessing the activity of perianal Crohn's disease: comparison of clinical indices and computer-assisted anal ultrasound. Inflamm Bowel Dis 15:742–749

Maconi G, Ardizzone S, Greco S et al (2007) Transperineal ultrasound in the detection of perianal and rectovaginal fistulae in Crohn's disease. Am J Gastroenterol 102:2214–2219

Mallouhi A, Bonatti H, Peer S et al (2004) Detection and characterization of perianal inflammatory disease: Accuracy of transperineal combined gray scale and color Doppler sonography. J Ultrasound Med 23:19–27

Morgan CN, Thompson HR (1956) Surgical anatomy of the anal canal with special reference to the surgical importance of the internal sphincter and conjoint longitudinal muscle. Ann Coll Surg Engl 19:88

Parks AG, Gordon PH, Hardcastle JD (1976) A classification of fistula-in-ano. Br J Surg 63:1–12

Rasul I, Wlson SR, MacRae H et al (2003) Clinical and radiological response after Infliximab treatment for perianal fistulizing Crohn's disease. Am J Gastroenterol 99:82–88

Sloots CE, Felt-Bersma RJ, Poen AC, Cuesta MA (2001) Assessment and classification of never operated and recurrent cryptoglandular fistulas-in-ano using hydrogen peroxide enhanced transanal ultrasound. Colorectal Dis 3:422–426

Stewart LK, McGee J, Wilson SR (2001) Transperineal and transvaginal sonography of perianal inflammatory disease. AJR Am J Roentgenol 177:627–632

Wedemeyer J, Kirchhoff T, Sellge G et al (2004) Transcutaneous perianal sonography: A sensitive method for the detection of perianal inflammatory lesions in Crohn's disease. World J Gastroenterol 10:2859–2863

Zawadzki A, Starck M, Bohe M, Thorlacius H (2012) A unique 3D endoanal ultrasound feature of perianal Crohn's fistula: the "Crohn ultrasound fistula sign". Colorectal Dis 14:e608–e611

Zbar AP, Oyetunji RO, Gill R (2006) Transperineal versus hydrogen peroxide-enhanced endoanal ultrasonography in never operated and recurrent cryptogenic fistula-in-ano: a pilot study. Tech Coloproctol 10:297–302

Zbar AP, Horesh N, Bucholtz V, Zmora O, Beer-Gabel M, Carter D (2012) Are there specific endosonographic features in Crohn's patients with perianal fistulae? J Crohns Colitis 21; [Epub ahead of print]

Index

G. Maconi and G. Bianchi Porro (eds.), *Ultrasound of the Gastrointestinal Tract*, Medical Radiology. Diagnostic Imaging,
DOI: 10.1007/978-3-642-31983-9,